International Association of Hydrogeologists

W. De Breuck
Editor-in-Chief

Hydrogeology of Salt Water Intrusion
A Selection of SWIM Papers

Volume 11
1991

Volume 11
1991

International Contributions to Hydrogeology
Series Editorial Board
G. Castany, E. Groba, E. Romijn

HEISE

HEISE

International Association of Hydrogeologists

W. De Breuck
Editor-in-Chief

Hydrogeology of Salt Water Intrusion

A Selection of SWIM Papers

A Report of the Commission on
Hydrogeology of Salt Water Intrusion
of the International Association of Hydrogeologists

Volume 11 / 1991
International Contributions to Hydrogeology
Founded by
G. Castany, E. Groba, E. Romijn
Series Editorial Board
E. Groba, M. R. Llamas, J. Marrat, J. E. Moore, I. Simmers
Verlag Heinz Heise

CIP-Titelaufnahme der Deutschen Bibliothek
Hydrogeology of salt water intrusion: a selection of SWIM papers; a report of the Commission on Hydrogeology of Salt Water Intrusion of the International Association of Hydrogeologists / International Association of Hydrogeologists.
W. De Breuck ed.-in-chief. – Hannover: Heise, 1991
(International contributions to hydrogeology; Vol. 11)
ISBN 3-922705-92-8
NE: De Breuck, W. [Hrsg.]; International Association of Hydrogeologists / Commission on Hydrogeology of Salt Water Intrusion; GT

Volume 11, 1991
International Contributions to Hydrogeology
Founded by G. Castany, E. Groba, E. Romijn
ISSN 0936-3912
ISBN 3-922705-92-8
Printed by R. van Acken GmbH, Josefstraße 35, D-4450 Lingen (Ems), Germany

P.O.B. 610407, D-3000 Hannover 61, Germany

CONTENTS

THEME 3

page

MATHEMATICAL CALCULATIONS AND MODELING 113

THEME 4

METHODS AND INSTRUMENTS 221

THEME 5

page

HYDROCHEMICAL AND SOIL-PHYSICAL INVESTIGATIONS 247

THEME 6

GEOPHYSICAL INVESTIGATIONS 359

AUTHOR'S ADDRESSES

AKKER, C. van den
National Institute for Water Supply,
The Netherlands

APPELO, C.A.J.
Institute of Earth Sciences,
Free University,
Amsterdam
The Netherlands

BARBIERI, G.
Faculty of Engineering,
University of Cagliari
Italy

BARROCU, G.
Faculty of Engineering,
University of Cagliari
Italy

BOEKELMAN, R.H.
Delft University of Technology
Department of Civil Engineering,
PO Box 5048, 2600 GA Delft
The Netherlands

BOLLE, I.
Geological Institute,
State University of Ghent
Krijgslaan 281
B-9000 Ghent
Belgium

BREUCK, W. de
Geological Institute,
State University of Ghent,
Krijgslaan 281,
B-9000 Ghent
Belgium

BRUGGEMAN, G.A., ir.
National Institute of Public Health
and Environmental Hygiene (RIVM),
PO Box 1, 3720 BA Bilthoven,
The Netherlands

COTECCHIA, V.
Istituto di Geologia Applicata e
Geotecnica,
Universita di Bari,
Via Re David 200, Bari
Italy

DAM, J.C. van
Delft University of Technology,
Department of Civil Engineering,
PO Box 5048,
2600 GA Delft
The Netherlands

EEM, J.P. van der
The Netherlands Waterworks' Testing
and Research Institute KIWA Ltd.,
Nieuwegen
The Netherlands

ERIKSSON, L.
Geological Survey of Sweden,
Uppsala
Sweden

EVANS, D.
Anglian Water Authority,
Gammar-School Walk,
Huntingdon,
Cambridgeshire PE 18 6NZ
United Kingdom

FIDELIBUS, M.D.,
Istituto di Geologia Applicata e
Geotecnica, Universita di Bari,
Via Re David 200,
Bari
Italy

FIELITZ, K.
Federal Institute for Geosciences
and Natural Resources (BGR),
Stilleweg 2
D-3000 Hannover
Federal Republic of Germany

GIESEL, W.
Federal Institute for Geosciences
and Natural Resources (BGR),
Stilleweg 2
D-3000 Hannover 51
Federal Republic of Germany

GEIRNAERT, W.
Institute of Earth Sciences,
Free University,
Amsterdam
The Netherlands

GOLDENBERG, L.C.
The Weizmann Institute of Science,
Rehovot
Israel

HAHN, J.
Niedersächsisches Landesamt für
Bodenforschung,
Stilleweg 2
D-3000 Hannover 57
Federal Republic of Germany

HOWARD, K.W.F., Dr.
University of Birmingham,
Dept. of Geol. Sciences,
P.O.B. 363,
Birmingham B 15 2TT
United Kingdom

KOOIMAN, J.W.
Amsterdam Waterworks,
Amsterdam
The Netherlands

LEBBE, L.C.
Research Associate of the
National Fund for Scientific
Research,
Geological Institute,
State University of Ghent
Krijgslaan 281,
B-9000 Ghent
Belgium

LEANDER, B.
VBB AB,
Geijersgatan 8,
S-21618 Malmoe
Sweden

LLOYD, J.W.
University of Birmingham,
Dept. of Geol. Sciences,
P.O.B. 363,
Birmingham B 15 2TT
United Kingdom

MAAS, K.
Provincial Dept. of Public Works
in Zealand,
P.O. Box 165, 4330 AD Middelburg,
The Netherlands

MEINARDI, C.R.
National Institute of Public Health and
Environmental Hygiene,
P.O.Box 1,
NL-3720 BA Bilthoven
The Netherlands

MEISER, P.
Niedersächsisches Landesamt für
Bodenforschung,
Stilleweg 2
3000 Hannover 51
Federal Republic of Germany

MOOR, G. de
Geologisch Institut,
Rijksuniversiteit Gent,
Krijgslaan 281,
B-9000 Gent
Belgium

MÜLLERN, C.-F.
Geological Survey of Sweden,
Uppsala
Sweden

NUTBROWN, D.A.
Central Water Planning Unit,
Reading
United Kingdom

PETERS, J.H.,
Netherlands Waterworks' Testing and
Research Institute KIWA Ltd.,
Nieuwegen
The Netherlands

RANIERI, G.
Faculty of Engineering,
University of Cagliari,
Italy

SCHUURMANS, R.A.
Amsterdam Waterworks
Amsterdam
The Netherlands

SENGPIEL, K.-H.
Bundesanstalt fü Geowissen-
schaften und Rohstoffe,
Stilleweg 2
D-3000 Hannover 51
Federal Republic of Germany

SOUZA, W.R.
U.S. Geological Survey
National Center, MS 432
Reston, Virginia 22092
United States of America

STUYFZAND, P.J.
The Netherlands Waterworks' Testing and
Research Insitute KIWA Ltd.
P.O.Box 1072
NL-3430 BB Nieuwegen
The Netherlands

TADOLINI, T.
Istituto di Geologia Applicata e Geotecnica
Universita di Bari
Via Re David 200
Bari
Italy

TULIPANO, L.
Istituto di Geologia Applicata e
Geotecnica, Universita di Bari,
Via Re David 200
Bari
Italy

UFFINK, G.J.M.
National Institute of Public Health
and Environmental Hygiene,
2260 AD Leidschendam
The Netherlands

VENHUIZEN, K.D., Ir.
N.V. Waterleidingsmaatschappij
voor de Provincie Groningen,
Phebensstraat 1,
Groningen
The Netherlands

VOSS, C.I.
U.S. Geological Survey
National Center, MS 432
Reston, Virginia 22092
United States of America

GENERAL INTRODUCTION

Man has always been attracted by the sea and from early times settlements have sprung up along the coasts. In Europe and in North America long stretches of coast have been urbanised.

As long as coastal settlements remained small, enough water of good quality very often could be obtained on the spot. With the rise of tourism, the establishment of harbours and the expansion of industrial activities the demand for water has risen continuously. Groundwater has been tapped in ever increasing quantities, very often overdeveloping the local resources.

In coastal aquifers the fresh water is in contact with saltwater which also intrudes along estuaries into the aquifers. The subtle equilibrium established over long periods may be disrupted by human interference. The withdrawal of large quantities of fresh water may induce a change in the groundwater flow, thus causing a landward movement of the fresh-/salt-water interface. The water management in reclaimed coastal lands has a profound influence on the position of the interface between salt and fresh water.

Although the phenomenon of salt-water intrusion in aquifers is well known the behaviour of the interface in changing conditions is far more difficult to predict. The detailed picture in ever changing hydrogeologic situations can only be understood by thorough field investigations accompanied by extensive hydrochemical analysis and mathematical modelling.

Salt-water encroachment is not just a subject for pure scientific study. The description of the phenomenon and the understanding of its evolution in time and space in natural and man-made conditions will help to optimize the management of fresh water in coastal aquifers and to safeguard it against contamination.

In the low countries, especially the Netherlands and the coastal regions of Germany the salinization of groundwater stocks has been recognized as a fundamental problem at the end of the previous century. HERZBERG in Germany and BADON GHYBEN in the Netherlands were the first to formulate a theory on the relationship between fresh and salt groundwater in an aquifer.

So it was no mere coincidence when in 1968 hydrologists of both countries, where the theory on seawater encroachment originated, joined in an informal meeting at Hannover. The activities of German researchers at that time were reviewed by the organizer of the meeting, the late Professor W. RICHTER. This meeting was to become the first of a series of biannual symposia, during which scientists interested in this field of hydrologic research exchanged their experiences. Subsequent salt-water intrusion meetings, shortened to SWIM, were held at Vogelenzang (1970), Copenhagen (1972), Ghent (1974), Medmenham (1977), Hannover (1979), Uppsala (1981), Bari (1983), Delft (1986). From 1974 on the proceedings of these

meetings were published. Except for the Hannover (1979) and the Bari (1983) SWIM's, which were edited as a volume of an internationally distributed series, these proceedings are available to only a limited number of researchers.

The International Association of Hydrogeologists (IAH) created in 1983 a commission on coastal aquifers, thus recognizing the importance of hydrogeologic investigations of coastal aquifers as a distinct field of research. This commission was to provide a forum for a worldwide audience. So as to stimulate research in coastal hydrogeology, IAH has decided to publish a selection of the earlier SWIM-proceedings. The choice of the articles has been difficult but the committee finally selected 29 papers, taken from the 4th to 9th SWIM's. The older articles may not be completely up to date but they should act as a starting point for younger researchers.

In the later SWIM's communications were gradually grouped into six themes: general description of problems and surveys, regional surveys, mathematical calculations and modelling, methods and instruments, hydrochemical and soil-physical investigations, and geophysical investigations. The selection presented here has also kept this subdivision. Each theme is introduced and discussed by a researcher who has been closely connected with the organization of the previous SWIM's.

I hope this book will encourage other scientists to work in a field of research which may not only bring scientific achievement but also contribute to the well being of man. On behalf of all my colleagues who have attended the meetings I wish to express my gratitude to the IAH for the opportunity of making our findings available to a wide audience. I also extend my thanks to all who have contributed to the preparation of this book and more especially Dr. BOEKELMAN, Dr. G.A. BRUGGEMAN, Professor V. COTECCHIA, Mr. B. LEANDER, Professor P. MEISER and Professor J. van DAM for reviewing the papers, Professor H.-R. Langguth, Mr. J.B.W. Day and Professor I. Simmers who took care of the final draft, and Dr. L. WALSCHOT, who assisted me in preparing the texts.

Prof. Dr. W. DE BREUCK
December 1987

THEME 1

GENERAL DESCRIPTION OF PROBLEMS AND SURVEYS (INCLUDING TECHNIQUES AND MANAGEMENT)

1

GENERAL DESCRIPTION OF PROBLEMS AND SURVEYS (INCLUDING TECHNIQUES AND MANAGEMENT)

1.0. INTRODUCTION

J.C. van DAM

Though there exist notes and proceedings of all previous SWIM's - this name was first introduced in the 4th SWIM, Ghent, 1974 - they have been published in different format and by different institutions. Moreover some of the older ones - just notes and small volumes - are out of stock.

Of course part of the material presented in earlier SWIM's is no longer up to date, but there are papers which are still worth reading by the present generation of geohydrologists interested in salt-water intrusion for such reasons as: being unique, originality, containing important data, description of (new) methods and techniques or even historical value.

Therefore Prof. De Breuck did a good job when he presented in 1983 his "Salt Water Intrusion Meetings 1968 - 1981, A review" - also included as an Appendix in the Proceedings of the Bari SWIM's 1983 - comprising abstracts of all papers presented in the first seven SWIM's. Thus the older papers are not lost sight of. He was the first to classify the papers in six groups, one of them being: "General descriptions of problems and surveys".

Since this review two more SWIM's have been held, the eigth in Bari (1983) and the ninth in Delft (1986). When applying the same classification in groups for the Delft SWIM we felt that some of the group titles had to be expanded somewhat in order to allow for some papers of a nature we had not seen before and which were closest to the group in which they were placed. So the title of the above mentioned group became: "General description of problems and surveys (including techniques and management)".

The very first contribution to this group was presented at the first SWIM (Hannover 1968) by its initiator the late Dr. W. Richter. His brief historical review of the investigations of the fresh-water/salt-water interface in the coastal area of Lower Saxony follows this introduction.

De BREUCK in his review included 24 papers in this group, dealing with conditions in Belgium, Denmark, Germany, Italy, India, The Netherlands, Poland, United Kingdom and Sweden. He listed them by author and characterized them in a few lines. As distinct from the comprehensive regional studies, these papers give either a review of the situation in the various countries or large parts thereof or they describe the mechanism of salt-water intrusion under

differing conditions, such as in sedimentary aquifers and in fissured-limestone aquifers, natural evolutions and the influence of man. Some authors try to explain the present situation by means of hypotheses. One paper, presented in the Hannover SWIM in 1979 dealt with coastal springs.

Among the papers presented in the Bari SWIM are another ten which could be listed in this group. Four of them deal with problems in Apulia, Catalonia, Sicily and the Vistula delta. The other six deal with coastal and submarine springs in Greece and Italy and in some of them due attention is paid to a description of the mechanism of the spring flow.

In the Delft SWIM, 1986, six papers were presented in this expanded group, all six of a different nature, varying from experiences in Italy and Spain, a spring in Italy, groundwater management in a saline environment in the Netherlands to a hypothesis on circular flow.

Clearly it must have been very difficult for the committee to make a proper choice from this group.
Besides the review of Dr. W. Richter, they selected two papers, in the first of which the authors (COTECCHIA et al.) introduce the "non-equilibrium index" to quantify the state of non-equilibrium in connection with their work in southern Italy. The second paper (MAAS, C.) deals with a technical measure to control saline seepage in an agricultural area on an island in the delta region of the Netherlands, its principles, its operation, even with a comparison of costs. It was particularly this paper which gave rise to the above mentioned expansion of the title of this group.

1.1. INVESTIGATIONS OF THE FRESH-/SALINE-WATER INTERFACE IN THE COASTAL AREAS OF LOWER SAXONY - A HISTORIC REVIEW

W. RICHTER

The groundwater is strongly saline in large parts of the coastal areas of Lower Saxony, sometimes even in those as far as 20 km from the coast. As the amount of water drawn from cisterns is not only too small, but does not comply with hygienic requirements, fresh water must be obtained from the interior, i.e. from waterworks located beyond the fresh-/saline-water interface.

The demand for drinking and industrial water, which has considerably increased since World War II, has forced the authorities to expand the already existing waterworks and to build new ones sited as closely as possible to the areas suffering from a shortage of fresh water. A geoelectrical survey was conducted by F. Hallenbach (Geological Survey of Lower Saxony, Hannover) in the Jever - Wilhelmshaven - Jadebusen area towards the end of the forties. On the basis of these data, the location of the fresh-/saline-water interface in this area was determined down to a depth of 100 m. During the fifties, these investigations were continued by the Geological Survey of Lower Saxony (H. Flathe, W. Richter, E. Blohm et al.), therefore the general location of the fresh-/saline-water interface is almost completely known from the Dutch border to the mouth of the Elbe River.

However, this could only be regarded as the beginning of the investigations of the salinization of the groundwater in the coastal areas. After initial success had thus been achieved, it was necessary to implement special investigations in order to obtain more detailed knowledge of the position and shape of the fresh-/saline-water interface, the hydrochemical conditions prevailing there, and its dynamics.

A model of the hydrochemical and genetical aspects of the salinization of coastal regions was the objective of the studies carried out within the framework of the International Hydrological Decade and subsidized by the German Science Foundation (DFG).

1.2 PHENOMENA RELATED TO THE VARIATION OF EQUILIBRIA BETWEEN FRESH AND SALT WATER IN THE COASTAL KARST-CARBONATE AQUIFER OF THE SALENTO PENINSULA (SOUTHERN ITALY)*)

V. Cotecchia, M. D. Fidelibus, L. Tulipano

Abstract

The state of saline intrusion brought about by uncontrolled abstraction from the coastal carbonate-karst aquifer in the Salento Peninsula is monitored by means of a series of observation wells scattered throughout the territory and drilled at different times during the last 20 years.
One of the methods of determining the state of non-equilibrium between fresh and salt water is based on the observation of the actual hydraulic head compared with the theoretical head that the groundwater should have, taking into account the real position of the transition zone; in this way a non-equilibrium index can be determined.
Moreover, by means of the plots of salinity against depth, it is possible to calculate the theoretical position of the salt water interface and if this is supposed to be sharp instead of a gradual transition.
The relationship between the level of the theoretical sharp interface and the actual head of fresh groundwater seems to be related to the value of the non-equilibrium index.

1. FOREWORD

In the Salento Peninsula the development of saline intrusion, brought about over many years by massive groundwater abstraction, mainly for irrigation, has been observed (TADOLINI & TULIPANO, 1970).
A range of phenomena is directly investigated by means of a network of observation wells which, although not extensive, supply data in zones considered to be particularly vulnerable to saline contamination.
The region consists of a calcareous and calcareous-dolomitic Cretaceous basement underlying, because of successive transgressive cycles, Miocene-Pliocene and Quaternary soils which are mainly derived from calcarenites with subordinate sands and clays (COTECCHIA, 1977).
Post-Cretaceous soils have little influence on the deep aquifer flow, given that a few metres above sea level, at the level of the surface, Mesozoic carbonate rocks are present.

However, post-Cretaceous soils play a role in determining the different conditions of infiltration as well as on groundwater discharge to the sea, where impermeable rocks, for instance, abut the aquifer along wide coastal stretches (COTECCHIA et al., 1973).

---

*) Work carried out within the activities of the "Centro di Studio sulle Applicazioni di Tecnologie Avanzate in Idrogeologia" of the National Council of Research.

2. Hydrogeological features

Owing to low piezometric heads, fresh groundwater in the Salento Peninsula assumes a lens-like shape, with a thickness limited to some hundred metres in the innermost parts: thicknesses decrease as, approaching the coast water heads lessen, until they become negligible along the shoreline.
The already scant freshwater reserve is further reduced because of the transition zone, located between fresh and salt water, the thickness of which changes laterally; locally the transition zone is so thick as to almost entirely exclude fresh water (TADOLINI & TULIPANO, 1977a).
Fig. 1 shows the configuration of the phreatic surface and the distribution of salinity.
As for data used to reconstruct isohalines, salinity values have had to be measured from bulked water samples taken during discharge tests in a number of drilled wells; such data are reasonably representative for such a strongly anisotropic, fissured and karstic aquifer (TADOLINI & TULIPANO, 1977b).
As can be seen from the sketch, in most cases underground waters are affected by saline intrusion.

3. Relationship between fresh water and salt water

The consequences of groundwater abstraction are reflected in the vertical distribution of underground-water salt content; the main data to evaluate the state of fresh water/salt water equilibria, that is the actual head of fresh groundwater (t_r) and the depth of intruding seawater (h_r) are best obtained by means of temperature and salinity logs, carried out periodically on the network of observation wells (Fig. 2) (TADOLINI & TULIPANO, 1981).
The theoretical head (t_t) that at any point should balance the underlying salt column h_r (Fig. 3), may be determined by the depth at which salt water occurs. Of course this involves consideration of the actual distribution of densities, thus allowing the weight average density δ_f relative to the whole column including fresh groundwater and the transition zone to be calculated; it is therefore possible to obtain coefficient K by also considering the actual density of salt water δ_s.
Densities may be derived from the relationship with salinity (Fig. 4), experimentally determined.
On the other hand it is important to remember that the whole water column consisting of the transition zone and fresh groundwater all overlying intrusive sea water, is the result of mixing between this last and fresh waters.
On this assumption, and further assuming a salinity value equal to 0,5 g/l for fresh water, and a realistic value for underground sea waters, from time to time determined by means of salinity logs, one can determine the

theoretical head h_t attained by intruding seawater, on the hypothesis of a sharp interface.
Fluctuations in the level of the transition zone in time, together with variations in the concentration of salt contamination of overlying "fresh" groundwaters, may then be regarded as variations in level of the theoretical sharp interface. Fig. 2 shows the positions of the theoretical interface for the observation wells considered: in this way easier comparisons, referring to different observation periods, may be carried out.
The relationship between depth below sea level of this theoretical interface and the actual head of fresh groundwater at same point, determines the relationship between fresh water and salt water.

Thus, in a different way, another coefficient K' may be determined; this last being closely comparable to the coefficient K previously calculated on the basis of the actual density distribution as a function of salinity throughout the water column in the observation wells (table 1).
Such K' values, derived for different observation wells and for different observation periods, appear to correlate with the differences found between actual and theoretical (calculated) heads (Fig. 5).

4. Concluding observations and examples

Some further observations may be made. The theoretical heads t_t evidently represent the levels that the phreatic surface of fresh groundwater should reach to enable a theoretical balance between the underlying saline water and the depth at which it is found. However, coefficient K' determines the relationships between the actual head and the depth, below sea level, at which a sharp interface should be located; thus, the real relationship between fresh and salt water heads are determined.
Fig. 5 demonstrates that the observation wells considered behave in different ways.
Markedly negative Δt values correspond with very low K' values; conversely, markedly positive Δt values correspond to high K' values. An example is given by well TA; during both periods, there is no equilibrium condition, since the actual head is insufficient to account for the level of the transition zone (or for the calculated depth of the sharp interface).

Original conditions of equilibrium are likely to be restored if, by reducing water abstraction, the fresh water head were to rise as high as the theoretical calculated value; otherwise the existing abstraction conditions will result in an expansion of the transition zone and salinization of overlying fresh groundwaters. This corresponds to a rise of the theoretical sharp

interface, that is a decrease of h_t. Wells NC3 and NC4 represent a peculiar situation: the very low K' values relate to markedly negative Δt values. However, the depth of the sharp interface calculated is not consistent with the actual measured head.

Such wells have been drilled recently, in an area particularly subjected to massive abstraction for irrigation purposes during long periods owing to the particularly dry climate of the region and to the type of water-demand for particular crops.

If the configuration of the water table in the neighbourhood of the above wells is considered, drawn on the basis of the yearly average groundwater level, it will be seen that the hydraulic heads which normally characterize the wells are far lower than those found during the periods (e. g. January), when abstraction is not in progress.

We may fairly assume, then, that the effects of annual recharge during a short period cause an increase in groundwater level; thus seawater maintains a (lower) level controlled by values of (higher) fresh groundwater levels which are in turn controlled by water abstraction.

REFERENCES

COTECCHIA, V. (1977). Studies and Investigations on Apulian Groundwaters and Intruding Seawaters (Salento Peninsula). Qud. Ist. Ricerca sulle Acque. 20, 462 p., (Consiglio Nazionale delle Ricerche, Roma.

COTECCHIA, V., TADOLINI, T., TAZIOLI, G.S. & TULIPANO, L. (1973). Studio idrogeologico della zona della sorgente Chidro (Taranto). In: 2nd International Symposium on groundwater, 1973, Palermo, p. 523-535.

TADOLINI, T. & TULIPANO, L. (1970). Primi risultati delle ricerche sulla zona di diffusione della falda profonda della Penisola Salentina (Puglia). In: 1st International Symposium on ground-water, 1970, Palermo, p. 633-638.

TADOLINI, T. & TULIPANO, L. (1977 a). The conditions of the dynamic equilibrium of groundwater as related to encroaching sea water. In: Symposium on Hydrodynamic diffusion and dispersion in porous media, 1977, Pavia, p. 173-185.

TADOLINI, T. & TULIPANO, L. (1977 b). Identification by means of discharge tests of water-bearing layers in fractured and karstic aquifer through the analysis of the chemico-physical properties of pumped waters. In: Symposium on Hydrodynamic diffusion and dispersion in porous media, 1977, Pavia, p. 159-171.

TADOLINI, T. & TULIPANO, L. (1981). The evolution of fresh-water(salt-water equilibrium in connection with withdrawals from the coastal carbonate and karstic aquifer of the Salentine Peninsula (Southern Italy). In: Sixth Salt Water Intrusion Meeting, 1979, Hannover, p. 69-85.

FIGURES

Fig. 1: Phreatic surface and distribution of salinity.

Fig. 2: Temperature and salinity logs in the periodically measured observation wells.

Fig. 3: Theoretical pressure heads balancing the underlying salt column.

Fig. 4: Density versus salinity (TDS).

Fig. 5: Correlation of K' values versus the differences between measured and calculated heads.

TABLE

Table 1: Values of the theoretical and real parameters for each observation well.

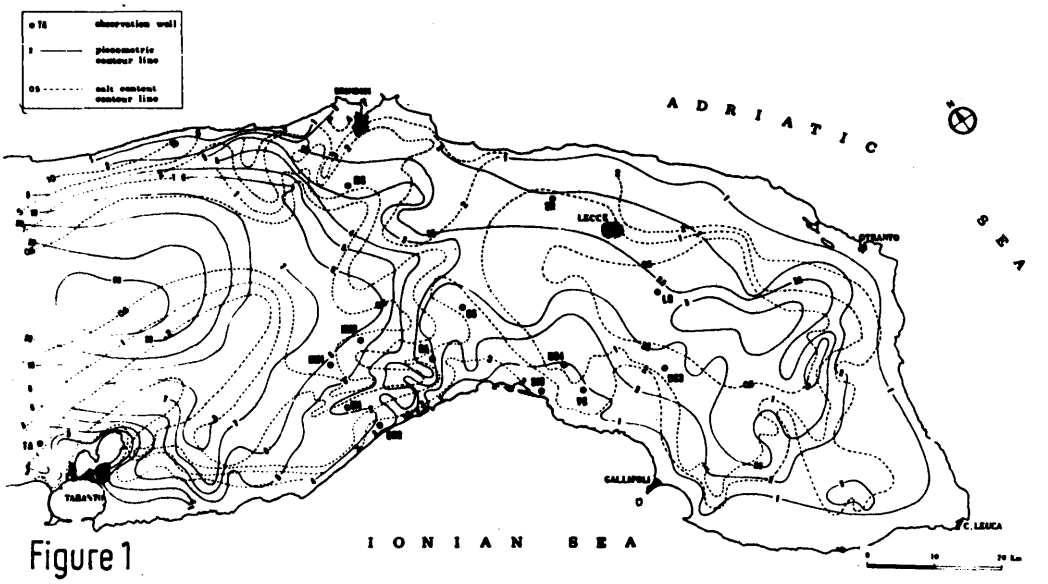

Figure 1

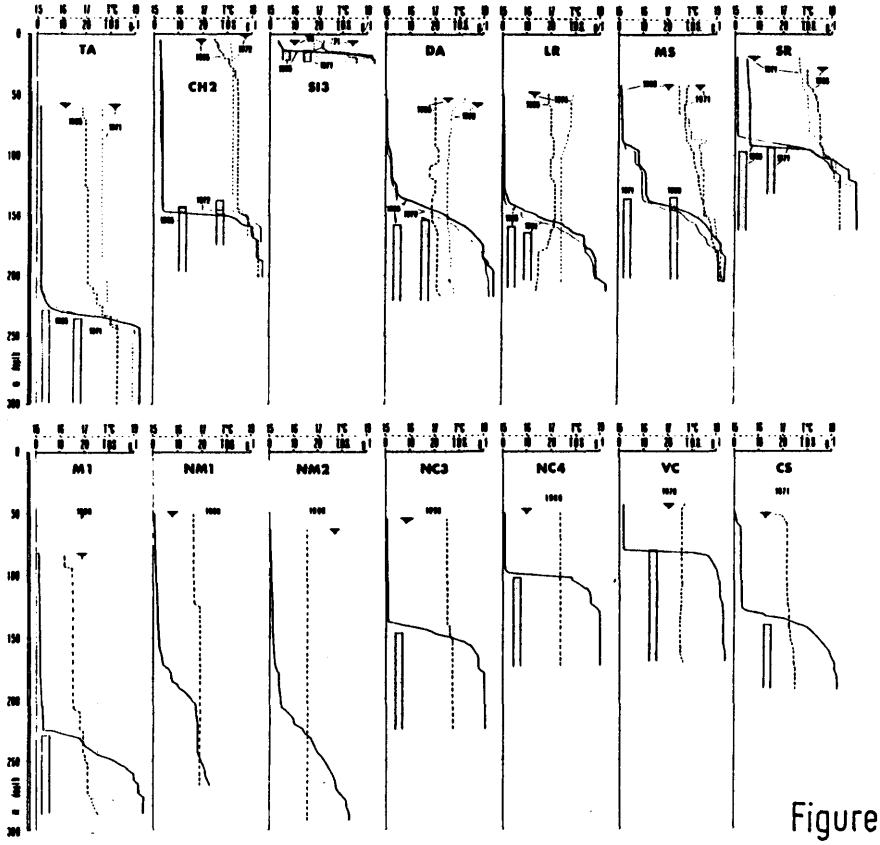

Figure 2

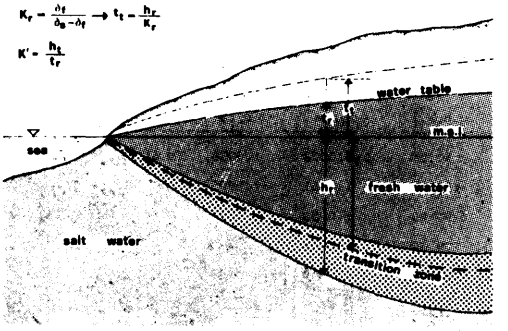

Figure 3

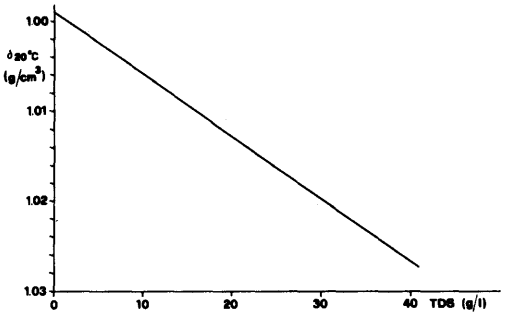

Figure 4

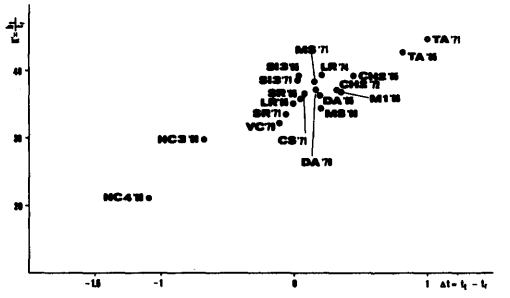

Figure 5

Table 1. Values of the theoretical and real parameters for each observation well.

date	O.W.	ground l.	t_r	h_r	δ_f	δ_s	$K=\frac{\delta_f}{\delta_s-\delta_f}$	$t_t=\frac{h_r}{K}$	$\Delta t=t_t-t_r$	h_t	$K'=\frac{h_t}{t_r}$
		m a.s.l.	m a.s.l.	m b.s.l.	g/cm^3	g/cm^3		m a.s.l.	m	m b.s.l.	
6/71	MS	44.76	2.37	130.24	1.0073	1.0268	51.66	2.52	+0.15	91.25	38.50
7/80	MS	44.76	2.58	135.24	1.0091	1.0295	52.01	2.60	+0.20	88.65	34.36
4/71	SR	29.402	2.06	90.60	1.0080	1.0282	45.31	2.00	-0.06	68.64	33.32
3/85	SR	29.402	1.80	79.60	1.0044	1.0278	42.92	1.85	+0.05	64.43	35.79
6/74	LR	51.78	2.77	158.22	1.0078	1.0268	53.04	2.98	+0.21	108.80	39.28
4/85	LR	51.78	2.98	150.82	1.0078	1.0277	50.64	2.98	0.0	104.34	35.01
1/86	MC4	50.027	2.43	77.97	1.0082	1.0256	57.94	1.34	-1.09	51.19	21.06
9/79	VC	43.023	1.16	76.98	1.0136	1.0275	72.92	1.05	-0.11	37.19	32.06
1/86	MC3	55.525	3.02	119.47	1.0056	1.0254	50.79	2.35	-0.67	89.59	29.66
11/71	SI3	5.628	0.20	12.37	1.0097	1.0275	56.72	0.22	+0.02	7.70	38.5
12/85	SI3	5.628	0.20	12.37	1.0091	1.0278	53.96	0.23	+0.03	7.84	39.2
1/71	CS	52.73	2.23	127.27	1.0092	1.0275	55.15	2.31	+0.08	81.43	36.51
9/79	DA	58.72	2.47	156.28	1.0108	1.0278	59.46	2.63	+0.16	91.83	37.18
4/85	DA	58.72	2.62	136.28	1.0079	1.0287	48.46	2.81	+0.19	95.07	36.29
1/86	M1	87.425	4.12	191.57	1.0051	1.0285	42.95	4.46	+0.34	151.85	36.86
3/72	CH2	7.423	3.45	150.58	1.0034	1.0285	39.98	3.77	+0.32	128.24	37.17
4/85	CH2	7.423	3.32	174.58	1.0063	1.0280	46.37	3.76	+0.44	138.28	39.24
12/71	TA	61.559	3.74	183.44	1.0016	1.0275	38.67	4.74	+1.00	167.51	44.79
12/85	TA	61.559	3.81	176.44	1.0014	1.0276	38.22	4.62	+0.81	162.39	42.62

1.3. A SEEPAGE BARRIER AGAINST SALT-WATER INTRUSION

K. MAAS

ABSTRACT

Seepage of brackish groundwater is one of the main causes of salinization in the southwest of The Netherlands. Especially in the province of Zealand the water of ditches and channels has become useless for agricultural purposes. Flushing is the usual way to compensate for salt-water intrusion. During investigations into the possibilities of fresh-water supply of the island Schouwen-Duiveland it was found that the amount of fresh water needed for flushing surpasses the agricultural demand by a factor two and a half. It seems to be natural to ask whether it is possible, instead of flushing, to control salt-water intrusion right at the source. The answer to this question is the subject of this paper. Design formulas are presented for a seepage barrier, consisting of a line of wells that intercept intruding saline groundwater.

1. INTRODUCTION

In the western part of The Netherlands, where phreatic groundwater levels are generally well below mean sea level, seepage of brackish groundwater is one of the main causes of salinization. This applies especially to the deltaic area of the rivers Rhine and Scheldt, known as Zealand. The vast majority of the canals and ditches in this region carries brackish or even saline water, rendering them useless for agricultural purposes. Fresh water may be obtained from the lower branches of the Rhine by pipeline or by open channels, but the costs are considerable and until now no water-supply system has been realized in Zealand. Since the dry summer of 1976, however, the demand for fresh water for sprinkling is ever increasing. At present investigations are being conducted into the costs and benefits of a supply system for the most promising areas. One of them is the isle of Schouwen-Duiveland (Fig. 1).

A team of agricultural and hydrological researchers estimated that once in ten years the fresh-water deficiency of the crop on Schouwen-Duiveland surpasses 2,1 m^3/s. Since the island suffers severely from salinization, a substantial quantity of flushing water will be required in addition. Numerical-modelling studies indicate that this quantity amounts to 5,1 m^3/s at the start of the growing season, even after excluding the saltiest areas from suppletion (WERKGROEP LANDBOUW GZZ, 1982). It may be clear that the excessive need for flushing water badly reduces the attractiveness of a water-supply system. The prospects might improve considerably when it would be possible to reduce the rate of seepage of brackish groundwater. This train of thought led the investigators to the concept of a seepage barrier, being the subject of this paper. In the sequel the hydrological and technical aspects of the seepage barrier will be discussed and the financial benefits will be indicated for the isle of Schouwen-Duiveland.

2. HYDROLOGICAL CONDITIONS AT SCHOUWEN-DUIVELAND

Schouwen-Duiveland has an area of about 250 km^2. Roughly speaking there are two or three semi-confined aquifers, except for the western dune area. Lying very low and being completely surrounded by the sea the island is constantly intruded by seawater. As a part of the investigations into the possibilities of fresh-water supply a numerical model was formulated in order to simulate the transient seepage of brackish groundwater (Van BOHEEMEN et al., 1983). Fig. 2 shows the areal distribution of the computed mean chloride load of the surface waters, during the first two months of the growing season of 1976.

Although the inflow of seawater is more or less a stationary process, the outflow of brackish groundwater to ditches and channels turns out to fluctuate wildly. This is illustrated by fig. 3.
As might be expected, the chloride load is maximum in the winter and minimum at the end of the summer. Based on experience elsewhere in The Netherlands the initial expectation was that raising ditch-water levels would completely suppress seepage during the growing season, and consequently no water would be required for flushing. The modelling study pointed out that experience with fresh-water supply cannot be transferred without a thorough understanding of hydrological processes. As the dotted area in fig. 3 indicates, raising ditch-water levels surely diminishes the salt charge, but only by some forty percent. Moreover, when the water supplied is used for sprinkling, the beneficial effect is partly cancelled.

3. PRINCIPLE AND DESIGN OF A SEEPAGE BARRIER

Flushing is the usual means to compensate for salt-water intrusion. It was indicated already in the introduction (par. 1) that in the case of Schouwen-Duiveland the amount of additional flushing water would be 5,1 m^3/s whereas the fresh-water demand of the crop is only 2,1 m^3/s. So the supply system should have a capacity of 7,2 m^3/s. It is natural to ask wether it would be possible, instead of flushing, to control the intrusion of seawater right at the source. The answer is in the affirmative. Making use of the age-old principle of the artesian well, seawater can be captured at a certain distance from the shore, before it reaches the fresh-water supply system. Hydraulics of wells being one of the most elaborate branches of hydrology, all the theory needed is readily available.
The principle is illuminated by the fis. 4a and 4b.

A screen of wells parallel to the coast discharges freely (i.e. without pumping) into a salt-water channel. It stands to reason that this channel is to be separated from the fresh water. this channel conveys the saline water to the existing pumping stations. As no moving parts are involved the wells operate at minimal costs and maintenance is hardly required.
Suppose that at the beginning of the growing season, when sprinkling is to be applied for the first time, the phreatic-groundwater level is lower than the water

level in the ditches of the supply system. The discharge q by the screen of wells is then easily shown to satisfy the relation:

$$q < \frac{T\varphi_o}{\lambda} \frac{1}{\sinh(L/\lambda)} \qquad (1)$$

where

q	= discharge per meter,	$[L^2T^{-1}]$
L	= distance from the wells to the coast,	$[L]$
φ_o	= mean sea level with respect to the water level in the ditches,	$[L]$
λ	= $\sqrt{Tc}$,	$[L]$
T	= transmissivity of the aquifer,	$[L^2T^{-1}]$
c	= resistance of the aquifer.	$[T]$

Behind the wells the hydraulic head φ of the aquifer is lower than the water level in the ditches, so seepage is eliminated there. The wells can be said to act as a barrier against seepage.
It is to be noticed that the total amount of seawater intruding the island increases under the influence of the seepage barrier by a factor

$$f < \coth(L/\lambda). \qquad (2)$$

So far, is has been tacitly assumed that the flow to the screen of wells is one-dimensional. In actual practice there will be radial flow in the vicinity of the individual wells, thus introducing a radial resistance to flow. In order to compensate for this the level in the salt-water discharge channel should be lowered as compared with the level in the fresh-water supply system by an amount Δ_1 which in a first approach can be set equal to

$$\Delta_1 = \frac{1}{2\pi} \frac{qa}{T} \ln \frac{R}{\lambda} \qquad (3)$$

where

Δ_1	= required lowering of the level of the salt-water discharge channel as compared with the water level in the fresh-water supply system in order to compensate for radial flow,	$[L]$
a	= distance between the individual wells of the seepage barrier,	$[L]$
R	= radius of the wells.	$[L]$

In deriving (3) it is assumed that a << L. An additional lowering of Δ_2 is required when the wells are not fully penetrating. Using a well known formula for partially penetrating wells (Anonymus, 1964, p. 92) Δ_2 is found to be given by

$$\Delta_2 = \frac{1}{2\pi} \frac{qa}{T} \left(1 - \frac{D}{l}\right) \ln \frac{\alpha l}{R} \qquad (4)$$

where

$$\alpha = (\frac{1}{2}\pi)^{\frac{D}{D-1}} (0.5525\ \frac{1}{D})^{\frac{1}{D-1}}$$

Δ_2 = required additional lowering of the level in the salt-water discharge channel in order to compensate for partial penetration, [L]

D = thickness of the aquifer, [L]

1 = depth of penetration. [L]

Finally the level of the salt-water discharge channel should be chosen so as to compensate for frictional losses inside and around the wells.

These losses are to be estimated by the formula (KRUIJTZER, 1971).

$$\Delta_3 = (\frac{qa}{\pi R^2})^2 \frac{1}{2g} (\frac{\mu_1 l_1}{6R} + 2 + \frac{\mu_2 l_2}{2R}) \qquad (5)$$

where

g = gravitational constant, $[L^2T^{-1}]$

μ_1 = coefficient of friction in the perforated part of the well, [-]

μ_2 = id. in the non-perforated part, [-]

l_1 = length of the perforated part, [L]

l_2 = id. of the non-perforated part [L]

Generally the coefficients $\mu_{1,2}$ will be of the order 10^{-2}. Frictional losses may become significant for small values of R, but they decrease very rapidly when R increases.

Formulas (1) through (5) suffice for a first orientation on the feasibility of a seepage barrier. The design parameters are seen to be

- the distance L from the seepage barrier to the coast;
- the distance a between the individual wells;
- the radius R of the wells;
- the depth of penetration 1 of the wells into the aquifer;
- the level $\Delta_1 + \Delta_2 + \Delta_3$ of the salt-water discharge channel with respect to the level to be maintained in the fresh-water supply system.

All parameters having a distinct effect on costs, the final choice should be the outcome of an optimization study, whereby linear programming will prove to be an effective tool.

Besides the design parameters, which have to be chosen judiciously, the formulas contain the hydrological parameters T and λ. The transmissivity T of the aquifer can be obtained by well known hydrological methods. The available methods to obtain λ, however, are not unambiguous. Therefore, let us consider the hydrological scheme shown in fig. 5.

Here, as in actual practice, the covering aquitard is provided with drains and with ditches having a fixed level. It is supposed that the phreatic-groundwater level is higher than the drains. Taking the water level of the ditches as a reference, the hydraulic head φ of the aquifer can be written as

$$\varphi = (\varphi_o - A)\, e^{-x/\nu} + A \qquad (6)$$

where

φ = hydraulic head of the aquifer, [L]
φ_o = mean sea level, [L]
x = variable of place [L]

(cf. appendix 1). The parameters A and ν are to be obtained from field observations (where at least two piezometers are needed). The problem is now to calculate λ from A and ν. It turns out that A depends on the rate of precipitation. Selecting a period with little rain (but with the phreatic-groundwater level still higher than the drains) it can be argued that

$$\lambda^2 \approx \varphi_{dr} \frac{\nu^2}{A} \qquad (7)$$

where

φ_{dr} = height of the drains above the water level of the ditches. [L]

As the hydrological schematization underlying the design formulas is rather crude, additional modelling (both analytical and numerical) is to be recommended in order to improve the design once the feasibility has been assessed. Some formulas for more complicated hydrological situations are presented in appendix 2.

4. APPLICATION TO SCHOUWEN-DUIVELAND

The effect of a seepage barrier on the chloride load of the surface waters of Schouwen-Duiveland has been simulated with a numerical model. The result is shown in fig. 6, which has to be compared with fig. 2. The distances between the wells of the seepage barrier are written along the dashed line around the island. Technically speaking it is possible to completely prevent the seawater from reaching the fresh-water supply system. For economical reasons, however, some salinization has to be accepted in the case of Schouwen-Duiveland.

Fig. 7 displays the effect of the seepage barrier as a function of time. It is seen from this graph that the barrier along the southern coast is much more effective than the northern barrier.

Table 1 finally shows the costs of a fresh-water supply system with and without a seepage barrier. The first alternative is seen to save more than 6 million guilders (about 2,4 million U.S. dollars).

Table 1. A comparison of costs of fresh water supply with and without a seepage barrier.

	without barrier	with barrier
internal supply system	$24,3 * 10^6$	$15,5 * 10^6$
fresh-water pipeline	$20 * 10^6$	$15 * 10^6$
seepage barrier	-	$7,4 * 10^6$
total (Dutch guilders)	$44,3 * 10^6$	$37,9 * 10^6$

In the case of Schouwen-Duiveland there are a number of additional benefits of the seepage barrier that have still to be quantified:

- some areas that were initially excluded from fresh-water supply because of serious salinization can now also benefit from the new approach;
- due to the seepage barrier the water quality in the supply system will be better during most of the growing season, yielding agricultural products of higher quality;
- in the vicinity of the seepage barrier dewatering of agricultural land improves considerably;
- the fresh water, originating from the river Rhine, is contaminated by heavy metals and p.c.b.'s. From an environmental point of view as little Rhine water as possible should be imported;
- the water required for flushing has to be discharged on the Eastern Scheldt. This estuary being of extreme ecological value, the Dutch government spent more than Dfl $2,7 * 10^9$ (about U$ $1,1 * 10^9$) for its protection. Discharge of fresh and contaminated Rhine water on this seawater basin is undesirable.

5. TEST SET UP ON A ONE-TO-ONE SCALE

A field test has been conducted on a one-to-one scale, involving 10 wells with a spacing of 50 meters, at a distance of about 400 meters from the coast. Hydrological measurements completely confirmed the theory (which of course, is not surprising at all as it is merely the classical theory of flow to wells in a semi-confined aquifer).
A secondary effect was the improvement in the dewatering of agricultural land. This improvement was so manifest that the farmers concerned requested the investigators not to terminate the test. It is finally mentioned that no clogging of wells has been encountered so it is expected that the maintenance costs will turn out to be low.

REFERENCES

ANONYMOUS (1964). Steady flow of groundwater towards wells. Proceedings and Informations, Committee for Hydrogeological Research TNO, The Hague, 10.

BOHEEMEN, P.J.M. van, KUSSE, P.J., MAAS, C. & WESSELING, J.W. (1983). Effects of fresh water supply on agriculture. Neth. J. Agric. Sci. 31, 269-278.

KRUIJTZER, G.F.J. (1971). Stijghoogteverliezen in en rond putfilters. Head losses in and around well screens). H_2O 14, nr. 8, 162-171.

FIGURES

Fig. 1: Situation of Schouwen-Duiveland in the south-western part of The Netherlands.

Fig. 2: Computed areal distribution of the chloride load of the surface water (April/May 1976).

Fig. 3: Computed temporal fluctuation of the chloride load of the surface water in 1976.

Fig. 4: a. Present situation; b. Attainable situation with seepage barrier.

Fig. 5: Simplified geohydrological profile of Schouwen-Duiveland.

Fig. 6: Computed areal distribution of the chloride load of the surface water in the presence of a seepage barrier (April/May 1976).

Fig. 7: Computed temporal fluctuation of the chloride load of the surface water in 1976, in the presence of a seepage barrier.

Fig. 8: Seepage barrier in a multiple aquifer system.

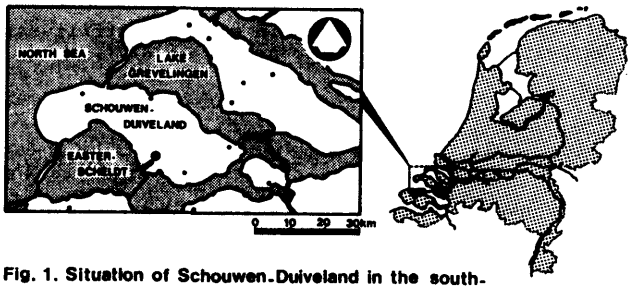

Fig. 1. Situation of Schouwen-Duiveland in the south-western part of the Netherlands.

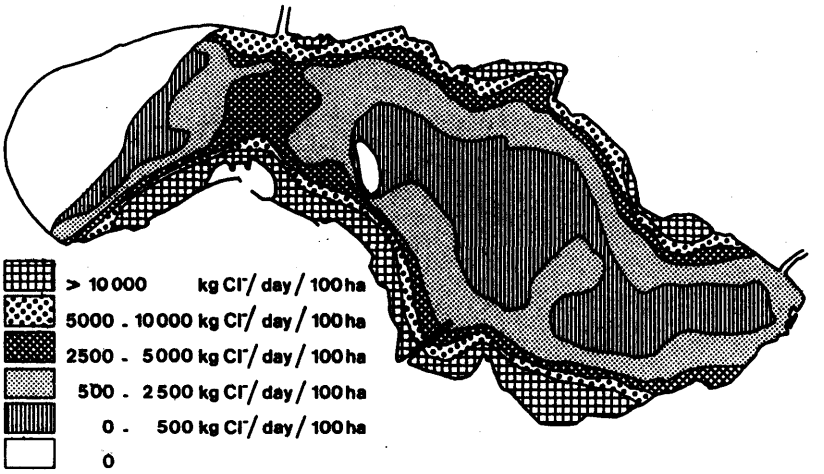

Fig. 2. Computed areal distribution of the chloride load of the surface water (april/may 1976)

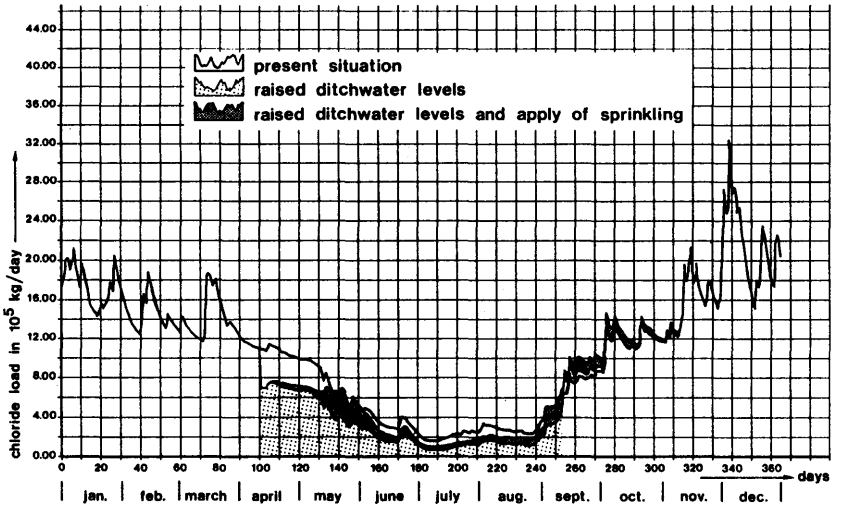

Fig. 3. Computed temporal fluctuation of the chloride load of the surface water in 1976.

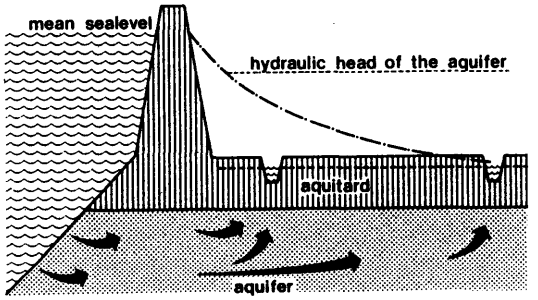

Fig. 4a . Present situation.

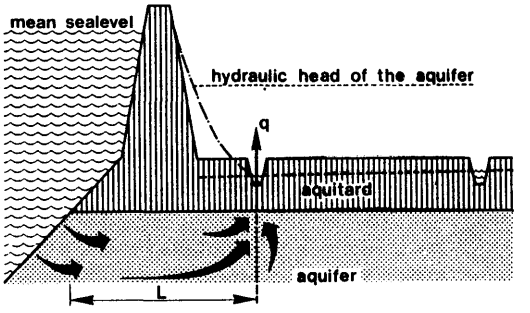

Fig. 4b. Attainable situation with seepage barrier.

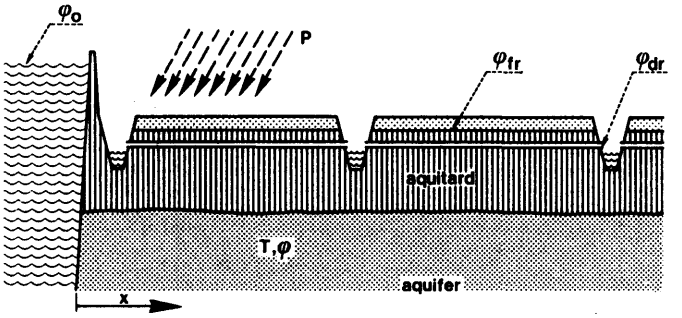

Fig. 5. Simplified geohydrological profile of Schouwen Duiveland.

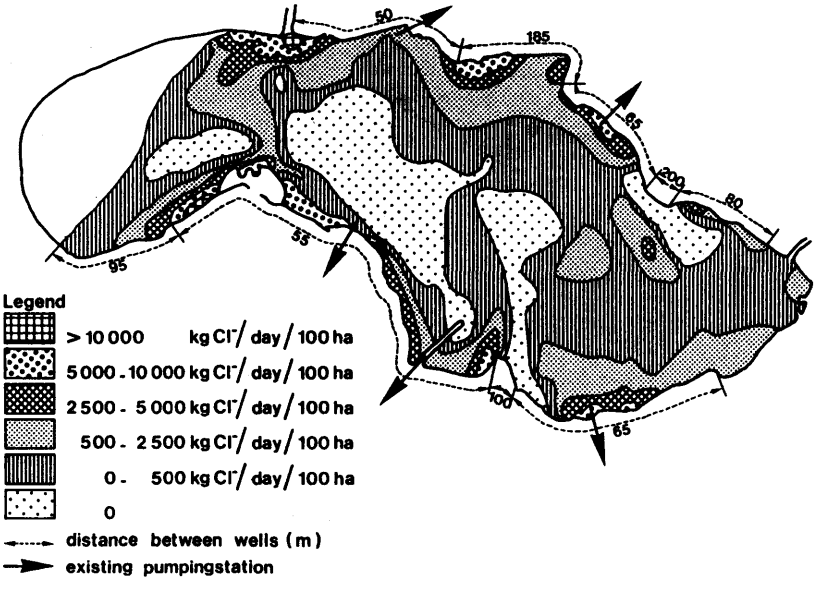

Fig. 6. Computed areal distribution of the chloride load of the surface water in the presence of a seepage barrier (april/may 1976)

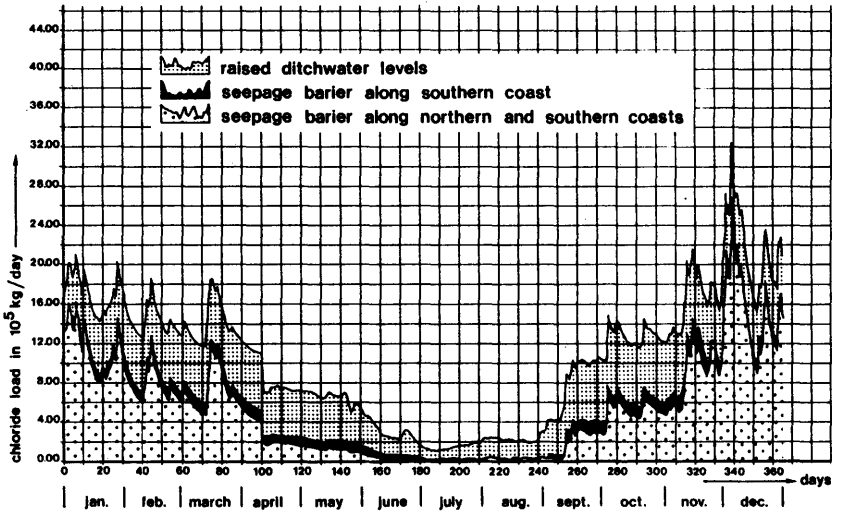

Fig. 7. Computed temporal fluctuation of the chloride load of the surface water in 1976, in the presence of a seepage barrier.

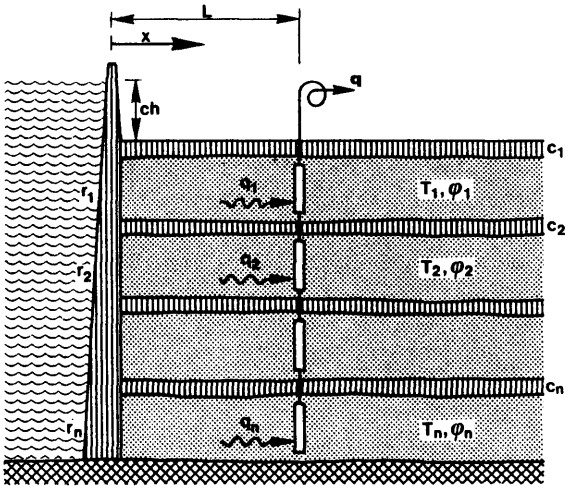

Fig. 8. Seepage barrier in a multiple aquifer system.

APPENDIX 1 - OBTAINING λ FROM FIELD OBSERVATIONS

The hydrological parameter $\lambda = \sqrt{Tc}$ occurring in formulas 1, 2 and 3 can be calculated from field observations performed in the wet season. Consider the hydrological scheme shown in fig. 5. The covering aquitard is provided with drains and with ditches, the latter having a fixed level. Taking this level as a reference, the hydraulic head in the aquifer is given by

$$T \frac{d^2\varphi}{dx^2} - \varphi\left(\frac{1}{c_d} + \frac{1}{c}\right) = - \frac{\varphi_f}{c} \qquad (a1)$$

$$\frac{\varphi_f - \varphi_{dr}}{c_{dr}} = \frac{\varphi - \varphi_f}{c} + P \qquad (a2)$$

$$\varphi(0) = \varphi_o \qquad (a3)$$

$$\frac{d\varphi}{dx}\ (x \to \infty) = 0 \qquad (a4)$$

Here

T	= transmissivity of the aquifer,	$[L]$
c	= resistance of the aquitard,	$[T]$
c_d	= resistance of the ditches,	$[T]$
c_{dr}	= resistance of the drains,	$[T]$
φ	= hydraulic head in the aquifer,	$[L^2T^{-1}]$
φ_o	= mean sea level,	$[L]$
φ_f	= phreatic-groundwater head,	$[L]$
φ_{dr}	= height of the drains above the water level in the ditches,	$[L]$
P	= precipitation,	$[L^2T^{-1}]$
x	= variable of place.	$[L]$

It follows from (a2) that

$$\varphi_f = \frac{\varphi_{dr}c + \varphi c_{dr} + Pc_{dr}c}{c + c_{dr}} \qquad (a2')$$

Notice that φ_f depends on φ and consequently is not a constant with respect to x. Elimination of φ_f from (a1) yields

$$\frac{d^2\varphi}{dx^2} - \frac{\varphi}{\nu^2} = - \frac{A}{\nu^2} \qquad (a5)$$

where

$$A = \frac{\varphi_{dr} + Pc_{dr}}{T(c + c_{dr})} \cdot \nu^2$$

and

$$\frac{1}{\nu^2} = \frac{1}{T}\left(\frac{1}{d_d} + \frac{1}{c + c_{dr}}\right)$$

Solving (a5) under the conditions (a3) and (a4) it is found that

$$\varphi = (\varphi_o - A)\, e^{-x/\nu} + A \qquad \text{(a6)}$$

which is identical to eq(6), par. 3. The parameters A and ν can be calculated from field observations of φ, using at least two piezometers. The problem that remains to be solved is to derive $\lambda = \sqrt{Tc}$ from A and ν. As in practice $c_{dr} << c$ it can be seen that

$$A \approx (\varphi_{dr} + Pc_{dr}) \cdot \frac{\nu^2}{\lambda^2}$$

Choosing a period with little precipitation, but with φ_f still higher than the drains, A can be approximated by

$$A \approx \varphi_{dr} \frac{\nu^2}{\lambda^2} \qquad \text{(a7)}$$

which is a convenient expression to calculate λ.

APPENDIX 2 - FLOW TO A SEEPAGE BARRIER IN A MULTIPLE AQUIFER SYSTEM

Is was stated in par. 2 that at Schouwen-Duiveland there are two or three semi-confined aquifers. As multiplicity of aquifers is the rule rather than the exception, formulas for multiple aquifer flow to a seepage barrier are of practical interest. Consider the geohydrological scheme shown in fig. 8. Formula (1), par. 3, is easily extended to this case. Using matrix notation it can be shown that

$$q < T \sqrt{A}\, \sinh^{-1}\{L \sqrt{A}\}\, \varphi(0) \qquad \text{(a8)}$$

where

q	= discharge vector of the seepage barrier,	$[L^2T^{-1}]$
T	= transmissivity matrix of the system,	$[L^2T^{-1}]$
A	= system matrix of steady multiple aquifer flow,	$[L^{-1}]$
$\varphi(0)$	= hydraulic head vector at x = 0.	$[L]$

Defining an entrance resistance R at x = 0 by

$$q(0) = R\{h - \varphi(0)\}$$

it is found that

$$\varphi(0) = (RT\sqrt{A}\coth\{L\sqrt{A}\} + I)^{-1}h \qquad (a10)$$

where h = h times the unit vector and h represents mean sea level with respect to the water level in the fresh-water supply system. More details on the use of matrix calculus in problems of multiple aquifer flow are presented by MAAS (1986).

REFERENCES

MAAS, K. (1986). The use of matrix functions in problems of multiple aquifer flow. Submitted for publication to the Journal of Hydrology.

THEME 2

REGIONAL SURVEYS

2

GENERAL SURVEYS

2.0 INTRODUCTION

B. LEANDER

Perhaps the most interesting aspect of work on saline intrusion is to put theory into practice. Thanks to the development of a wide range of theoretical principles it is now possible to prepare practical measures to solve particular water supply problems in regions subject to salt-water intrusion.

During the nine SWIM's some 40 papers have been presented which could be included under the theme "Regional Surveys". Most of them describe the region, the aims of the study, the criteria for the solution of a model (as well as estimating the reliability of data) and how the results of the surveys were utilised. From these papers five have been chosen for presentation here.

The first paper (DE BREUCK & DE MOOR) presents the hydrogeological research in the coastal area of Belgium that has been undertaken since 1958 and a working hypothesis concerning the evolution of the aquifer.

The second paper (VENHUIZEN) presents a theoretical calculation of the shape of the fresh-water pocket in the dune area under different conditions. The Amsterdam Water Works have extracted raw water from the dune area near the North Sea for more than 130 years.

The third paper (NUTBROWN) deals with the technique to modify the aquifer pumping regime in order to reduce the extent of saline intrusion in a chalk aquifer in the south of England.

The fourth paper (EVANS et al.) presents a 3-year multidisciplinary study that has broken new ground in hydrogeological techniques and culminated in a mathematical model, which can be used to guide management and planning decisions to meet demands in the area.

The fifth paper (TADOLINI & TULIPANO) presents the surveys that have been made during more than a decade in order to explain the influence of salt-water in the aquifer and the observed changes of equilibrium between salt- and fresh-water.

These five examples give a good idea of the state-of-the-art in the context of this theme.

2.1. THE EVOLUTION OF THE COASTAL AQUIFER OF BELGIUM

W. DE BREUCK & G. DE MOOR

ABSTRACT

In the unconfined aquifer below the coastal area of Belgium salt water occurs under a fresh-water layer at depths that vary from 2 to more than 25 m. Radiocarbon dating of groundwater samples set the seawater encroachment in the deep parts of the aquifer back at least in the Subboreal period. A working hypothesis concerning the evolution of the aquifer is formulated.

1. INTRODUCTION

The North Sea coast of Belgium is 64 km long. Behind the dune belt, the width of which varies from 50 m to 2,5 km, a flat polder landscape extends for about 10 km inland except at the IJzer basin where it forms a deep embayment. Elevations vary between +2 and +5.*) The polder area behind these dunes is almost flat, elevations varying between 2 and 5 m.

The water-table aquifer is formed mainly by Quaternary sediments (W. DE BREUCK & G. DE MOOR, 1969), which attain a maximum thickness of 35 m (fig. 1). The Tertiary substratum consists of bedded clay and sand of Eocene age dipping gently in a north-easterly direction (fig. 2).

The deepest Quaternary deposit is formed by coarse sand of Eemian age (fig. 3) and remnants of Saalian sediments (G. DE MOOR & I. HEYSE, 1974). It is covered by sediments, mostly sandy, which are of Weichselian age. These are locally overlain by sandy tidal-flat deposits of Atlantic age. At the end of the Atlantic period peat bogs developed and continued to grow during the succeeding Subboreal period until the Dunkirk transgressions flooded the coastal area. These transgressions caused the deposition of a superficial cover of clays and sands, the distribution of which and later the influence of man have shaped the present topography of the polder landscape (J. AMERYCKX, 1959; R. TAVERNIER et al., 1970).

2. HYDROGEOLOGICAL INVESTIGATIONS

A systematic geo-electric survey (W. DE BREUCK & G. DE MOOR, 1969, 1972) of more than 1700 resistivity soundings has revealed the presence of saline water (up to 30.000 ppm) all over the aquifer at depths that vary from less than 2 m to more than 25 m (fig. 4). The saline-water layer extends to the southernmost margin of the coastal area and even into its narrowest ramifications at 20 km from the seashore.

*) All levels are expressed in meters versus Ostend ordnance datum level (Zéro du dépôt de la guerre, National Geographical Institute).

Several tens of borings have been made to check the resistivity survey and to provide the water samples for analysis. In each of the drill holes 3 or 4 independent screens of 1 m length have been installed at different depths. These depths were chosen so as to have part of the screens above and part of them below the fresh-/salt-water interface. Water analyses and well logging have shown that the interface is rather sharp (fig. 5), the transition from fresh to salt water being limited to a zone of a few meters (W. DE BREUCK & G. DE MOOR, 1972). The vertical and horizontal distribution of the different water types in the aquifer shed a light upon its origin and evolution, which is related to the recent Quaternary history of the area.

The present active seawater encroachment is determined by the nature of the Tertiary substratum and by the relief and the dimensions of the dune belt; it seems to be confined to a very narrow zone along the coast extending not farther than 2 km landwards. The canals also influence, in a minor way though, the general pattern.

3. SAMPLING SITES FOR GROUNDWATER DATING

Two sampling sites have been selected in areas where apparently no active seawater encroachment it taking place. Pumping was performed at a very low yield so as to obtain water solely from a very restricted zone in the aquifer. The pump was of a peristaltic type. The suction pipe was lowered to the screen level so that mixture with other water or air would be minimal. Two samples of 50 liters were pumped from the well after a conductivity test showed no more variation.

Samples were taken on two different occasions at Vlissegem from a depth of 23 m (fig. 4). The well is situated at approximately 6 km from the seashore. This part of the coastal area shows a typical inversion relief, the former creeks now forming the elevated parts within the lower clay-on-peat areas (J.B. AMERYCKX, 1959).

The well has been drilled on a creek ridge where the fresh-/salt-water interface lies deeper than under the adjacent lowlands. The bore log (fig. 6) shows a top layer 3,5 m thick of loamy sand and clay on a sandy column resting at 30 m depth upon Tertiary clay. Screens have been installed between 5 and 6 m, 12 and 13 m, 16 and 17 m and 23 and 24 m. The interface between fresh and salt water has been located by a geo-electric sounding at 22 m. Analyses of water samples from the four screens have been reported in a Piper diagram. The water of the deepest screen, situated below the fresh-/salt-water interface contains more than 25.000 mg/l of dissolved solids, with a relative ion distribution which is very similar to that of seawater. Water samples from the three other screens are nearly fresh and have a very different ion distribution.

4. LABORATORY RESULTS

The water samples have been submitted to an extensive analysis. Some of the results are shown in table 1. A recent analysis of a seawater sample has been included for comparison. The three waters show a dissolved-solids content very similar to that of the present seawater, although the total ion content is somewhat smaller. This may be due to the admixture of fresh water.

The radiocarbon dating has been performed at the "Institut Royal du Patrimoine Artistique" (I.R.P.A.) of Brussels (M. DAUCHOT-DEHON & J. HEYLEN, 1973).

The carbondioxide of the water has been transformed into methane, which has been counted in a proportional counter by anticoincidence (HOUTERMANS-OESCHGER). The results of the radiocarbon measurements are given in table 2.

Table 2. Radiocarbon dating of water samples (I.R.P.A.).

Sample	Depth	Age (years BP)	Age (years BP)
		T = 5570 years	T = 5730 years
124DB14WAD1	23	3880 ± 180	4000 ± 180
124DB14WAD2	23	3720 ± 152	3920 ± 150
193DB1WAD1	28	3476 ± 224	3580 ± 160

5. DISCUSSION

No data on the stable-isotope composition of the waters are available at the present time, so that the first series of ages must be interpreted with the greatest care. Nonetheless they provide new evidence for an earlier advanced hypothesis on the evolution of the hydrologic conditions in this area (W. DE BREUCK & G. DE MOOR, 1969).

Although the Vlissegem well is situated on a creek ridge, in areas which have been inundated by the Dunkirk-2 transgression, and the Adinkerke well in a non-covered tidal-flats area, the water of both sites show comparable ages. The fact that the former is situated at 6 km from the sea as compared to 3 km for the latter may be a mere coincidence rather than explaining any difference in age. On the other hand the total ion content at Vlissedem is approximately 80 % of that of present-day seawater while the latter amounts to only 63 %. This could mean that at both sites the seawater was fixed at approximately the same time.

Since both sampling sites are located in areas where present seawater cannot penetrate it had formerly been assumed that the deeper salt-water layer has been introduced during the Subatlantic Dunkirk transgressions (J. DE PAEPE &

W. DE BREUCK, 1958). The radiocarbon measurements set the date of the seawater encroachment further back into the Subboreal period.

Both wells have their screens installed in Eemian deposits. It is easily understood that the subsequent lowering of the sea level during the last glaciation has resulted in a complete flushing of the salt pore water. The ensuing rise of the sea level during the postglacial period has caused the Flandrian transgression and the salinization of the older deposits. Opinions diverge (J.R. CURRAY, 1965; S. JELGERSMA, 1966; A.L. BLOOM, 1971) about the pace of rise to its present level. Some maintain that the sea reached its present level 3000 to 5000 years ago, others proclaim that there has been a slow and continuous rise until very recently. The rising sea level and the tidal movements (H.H. COOPER et al., 1964) must have created a continuous subterranean inflow of salt groundwater.

From the chemical analysis it seems obvious to consider the samples as seawater, although slightly mixed with fresh water. The fresh-water supply may have occurred in the Subboreal period or later. When contemporaneous with the intrusion of the seawater the radiocarbon measurements indicate approximately the true age. Whenever the fresh-water supply was more recent the dating of the water gives too young an age for the seawater encroachment. The seawater would then have been entrapped at an earlier stage in the Subboreal or even in the Atlantic period. One may also consider the possibility of a mixture of older Weichselian fresh water with Atlantic seawater.

Since at present we have no evidence either for a younger or an older fresh-water supply one can assume that the seawater was entrapped sometime in the Subboreal period, when the area was already covered by peat bogs.

This could be explained by two facts. The coastal dune belt had not grown high enough yet to develop a fresh-water lens that could inhibit the subterranean seawater flow, and the sea still had access to the coastal plain during spring and storm tides through existing creeks which also drained the runoff from the higher peat bogs and the back land. In the end the expanding dune-water lens curtailed and finally stopped the salt-groundwater movement (fig. 6). The creeks gradually drained fresher water, thus flushing the salt groundwater in their immediate vicinity. The salt water beneath the peat-bog areas, though, was not expelled since almost all of the precipitation was retained by the peat or immediately drained by the creek system.

A large part of this creek system probably served for the drainage of the areas when the sea flooded the coastal plain during the Dunkirk transgressions. The beaches were probably cut through the dune belt at its lowest parts, where the creeks debouched into the sea. Some areas, especially around the breaches, may have been eroded by the force of the in and out flowing water currents. When finally the sea retreated the water in the creeks became fresh again. Underneath them the brackish water was expelled.

The creek system was gradually filled up by sandy deposits, while on the higher peat bogs only clay was deposited. When the region was reclaimed the dewatering resulted in a differential settling of the clay-covered peat areas and the sandy creeks, the latter becoming the higher parts. Due to their higher elevation and their composition the creek ridges developed a fresh-water lens beneath them.

The rainwater barely penetrated into the clay-covered peat areas and was almost continuously evacuated through ditches and canals. Hence the saline water beneath these areas was not replaced.

The relatively old age of the waters furthermore suggests that the deeper groundwater in the unconfined aquifer moves at an extremely slow speed or does not move at all. This is probably the case for large parts of the coastal region. From the present data it can be assumed that the salinization effect of the Dunkirk transgression has been restricted to the top layers.

6. CONCLUSIONS

The radiocarbon dating of the deep saline water in the coastal aquifer of Belgium indicates that the seawater encroachment in large parts of the coastal area dates back at least from the Subboreal period. These measurements also suggest that movement in the deeper parts in the aquifer, if any takes place, is extremely slow. These preliminary findings are to be confirmed by a more detailed investigation which includes determination of the stable isotopes.

REFERENCES

AMERYCKX, J. (1958). Verklarende tekst bij het kaartblad Houtave 22E. Gent: Centrum voor Bodemkartering (Bodemkaart van Belgie).

AMERYCKX, J.B. (1959). De ontstaangeschiedenis van de Zeepolders. Biekorf 60, 377-400.

BLOOM, A.L. (1963). Late-Pleistocene fluctuation of sea-level and post-glacial crustal rebound in coastal Maine. Amer. J. Sci. 261, 862-879.

COOPER, H.H. Jr., KOHOUT, F.A., HENRY, H.R. & GLOVER, R.E. (1964). Sea water in coastal aquifers. U.S. Geol. Surv. Wat. Supply Pap. 1613-C.

CURRAY, J.R. (1965). Late Quaternary History. Continental Shelves of the U.S., In: The Quaternary of the U.S. (eds. H.E. Wright & D.G. Frey), 723-735. Princeton: University Press.

DAUCHOT-DEHON, M. & HEYLEN, J. (1973). Institut Royal du Patrimoine Artistique Radiocarbon Dates IV. Radiocarbon 15, 303-306.

DE BREUCK, W. & DE MOOR, G. (1969). The water-table aquifer in the Eastern Coastal Area of Belgium. Bull. Int. Ass. Sci. Hydrol. 14, 137-155.

DE BREUCK, W. & DE MOOR, G. (1972). The Salinization of the Quaternary sediments in the Coastal Area in Belgium. Expert Meeting SWIM, Copenhagen, 6-19.

DE MOOR, G. & HEYSE, I. (1974). Lithostratigrafie van de kwartaire afzettingen in de overgangszone tussen de kustvlakte en de Vlaamse Vallei in Noordwest-Belgie. Natuurwet. Tijdschr. 56, 85-103.

DE PAEPE, J. & DE BREUCK, W. (1958). De drinkwatervoorziening van de landbouw-bedrijven in West-Vlaanderen. (Brugge, Provincie West-Vlaanderen). (Ekonomische monografieen).

JELGERSMA, S. (1966). Sea-level changes during the last 10,000 years. In: World Climate from 8000 to 0 B.C., 54-71. London: Royal Meteorological Society.

MOORMANN, F.R. & T'JONCK, G. (1960). Verklarende tekst bij het kaartblad De Moeren 50W. Gent: Centrum voor Bodemkartering. (Bodemkaart van Belgie).

TAVERNIER, R., AMERYCKX, J., SNACKEN, F. & FARASYN, D. (1970). Kust, duinen, polders. Brussel: Nationaal Comité voor Geografie, 32 p., (Atlas van Belgie, bl. 17).

FIGURES

Fig. 1: Thickness of the Quaternary in the coastal area.

Fig. 2: The Tertiary substratum in the coastal area.

Fig. 3: South-north section from Varsenare to Blankenberge.

Fig. 4: Depth of the fresh-/salt-water interface and sampling sites for radiocarbon dating (Vlissegem, Adinkerke).

Fig. 5: Variation with depth of the resistivity and the conductivity of the groundwater at well site 48DB8.

Fig. 6: Logs and data at well site 124DB14.

Fig. 7: Evolution of the hydrochemistry of the groundwater and morphology in the coastal plain.

TABLES

Table 1: Water analyses.

MAP Depth of the fresh-salt water interface in the unconfined aquifer of the belgian coastal area (1963-73) . See annexe I

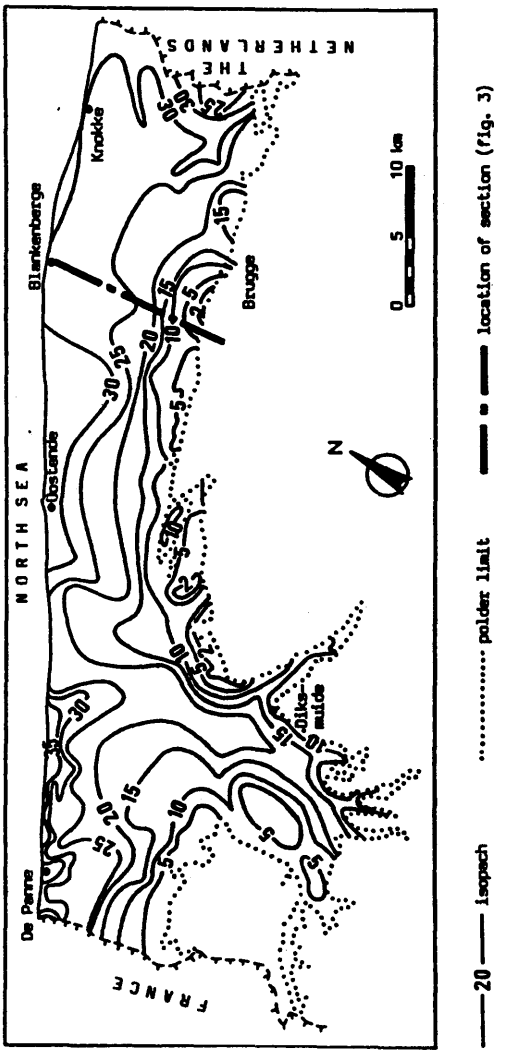
NETHERLANDS
THE
NORTH SEA
FRANCE
De Panne
Oostende
Blankenberge
Knokke
Brugge
Oiks-
muide
N
0
5
10 km
20 —— isopach
polder limit
location of section (fig. 3)

Figure 1

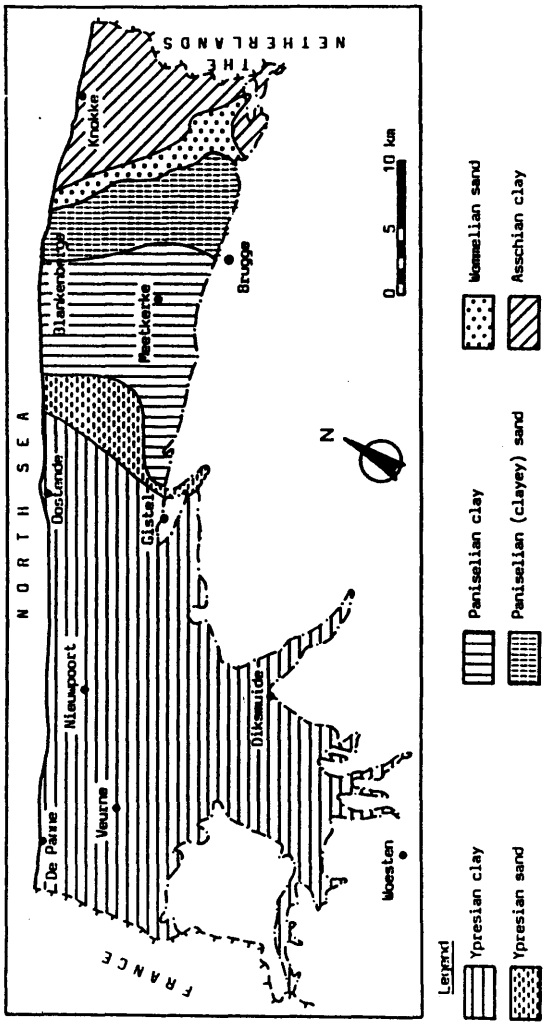
NETHERLANDS
THE
NORTH SEA
FRANCE
Knokke
Blankenberge
Brugge
Oostende
Gistel
Nieuwpoort
Veurne
De Panne
Diksmuide
Koesten
N
0 5 10 km
Legend
Ypresian clay
Ypresian sand
Paniselian clay
Paniselian (clayey) sand
Wemmelian sand
Asschian clay

Figure 2

N
S
Blankenberge
Uitkerke
Zuienkerke
Pentuerke
Quaternary
level (m)
+10
+8
+6
+4
+2
0
-2
-4
-6
-8
-10
-12
-14
-16
-18
-20
-22
-24
0
2000
4000
6000
8000
10000
12000
m
Pentuerke (Pic)
Pentuerke (Pie)
Ypresian (Ya)
Pentuerke (Pie)
Pentuerke (Pic)
sand
clay
gravel
shells
peat
excavated peat bog
fresh-/salt-water interface
well screens

Figure 3

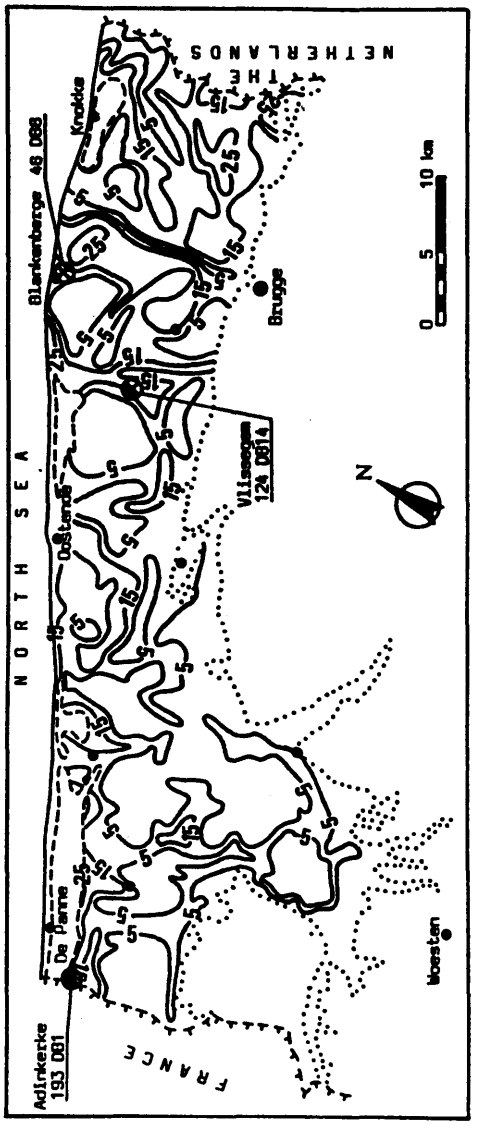
NETHERLANDS
THE
NORTH SEA
FRANCE
Blankenberge 48 088
Knokke
Bruges
Oostende
Vlissingen
124 0814
De Panne
Adinkerke
193 081
Maastam
0 5 10 km
N

Figure 4

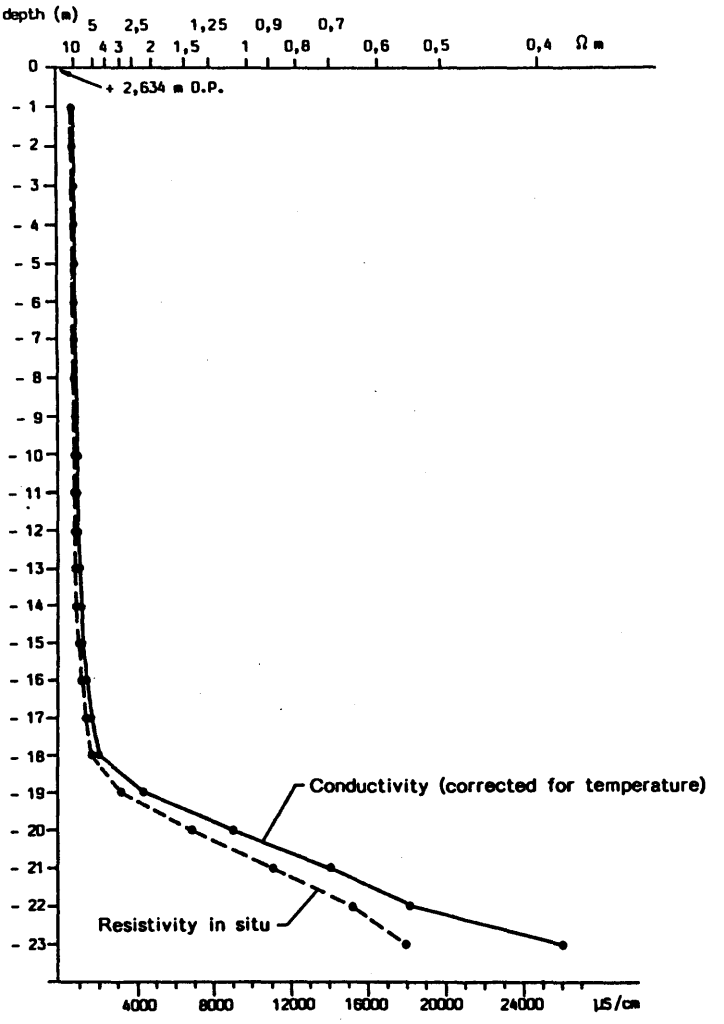
depth (m)
5
2,5
1,25
0,9
0,7
10
4
3
2
1,5
1
0,8
0,6
0,5
0,4
Ω m
0
+ 2,634 m O.P.
- 1
- 2
- 3
- 4
- 5
- 6
- 7
- 8
- 9
- 10
- 11
- 12
- 13
- 14
- 15
- 16
- 17
- 18
- 19
- 20
- 21
- 22
- 23
Conductivity (corrected for temperature)
Resistivity in situ
4000
8000
12000
16000
20000
24000
µS/cm

Figure 5

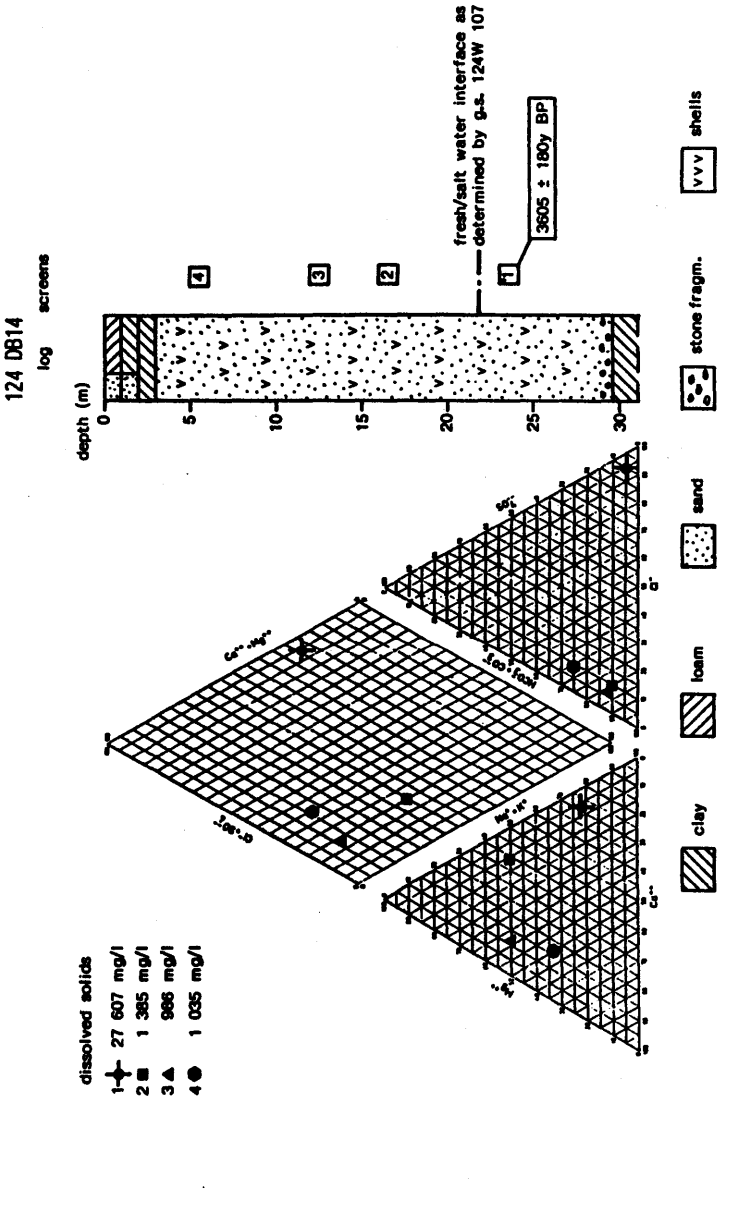
124 DB14
log screens
depth (m)
0
5
10
15
20
25
30
4
3
2
1
fresh/salt water interface as
determined by g.s. 124W 107
3605 ± 180y BP
dissolved solids
1 27 607 mg/l
2 1 385 mg/l
3 986 mg/l
4 1 035 mg/l
clay
loam
sand
stone fragm.
shells

Figure 6

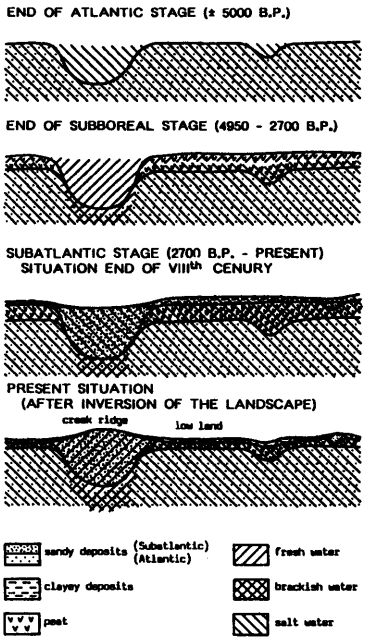

Figure 7

Table 1:

Sample	124DB14WAD1	124DB14WAD2	193DB1WAD1	seawater	
Depth	23	23	28	0	m
Conduct.18°C	33696	34492	28150	36115	$\mu S\ cm^{-1}$
Dis.solids	28305	27733	21958	34794	mg/l
cations	477.9	460.7	377.8	604.9	meq/l
Na^+	365.3	336.2	285.5	462.5	meq/l
K^+	7.2	7.3	6.1	9.9	meq/l
Ca^{++}	22.4	28.1	22.2	23.1	meq/l
Mg^{++}	80.2	87.6	62.7	109.4	meq/l
$Fe^{++} + Fe^{+++}$	1.1	1.0	0.9	0.0	meq/l
anions	483.5	470.5	370.1	602.3	meq/l
Cl^-	434.5	420.2	322.9	586.3	meq/l
SO_4^{--}	18.1	18.1	31.2	42.4	meq/l
HCO_3^-	30.7	32.1	15.8	2.7	meq/l
SAR	51	44	44	57	

2.2. THE SHAPE OF THE FRESH-WATER POCKET UNDER THE DUNE-WATER CATCHMENT AREA OF AMSTERDAM

K.D. VENHUIZEN

ABSTRACT

The evolution of the shape of the fresh dune-water lens is given, first in natural conditions and then under conditions influenced by water extraction and recharge. The dimensions of the fresh-water lens are computed for the case of a constant piezometric head in the salt water and for the case of a landward flow in the salt water.

1. INTRODUCTION

The theoretical shape characteristics of the fresh-water pocket under the dune-water catchment area of Amsterdam has been studied for a long time. During an infinite series of years the infiltrated rainfall on the dune strip along the Dutch coastline has built a fresh-water pocket, partly situated above a more or less developed clay layer, but for a more important part situated below that clay layer. This fresh-water pocket is "floating" on the salt water at depth.

The size and the shape of this fresh-water pocket depend on a series of factors of natural and artificial character mentioned below.

1) Before 1850, when the Haarlemmermeerpolder (in which the airport Schiphol is situated) was not yet in existence and the supply of drinking water for the city of Amsterdam had not yet started, there must have been a stationary final shape of the fresh-water pocket, which in shape and extent can have been dependent only on the possible variation in effective precipitation throughout the centuries. As there is no important potential difference between the average sea-level and the fresh-water potential under land, it may be assumed that there has not been a flow of salt water underneath the fresh-water pocket. This situation has been indicated in the calculations and the drawings of section 2, to which reference should be made. The cases 1 - 4 indicate for an effective precipitation of respectively 66, 125, 199 and 388 mm/year the size of the fresh-water pocket.
2) After the reclamation of the Haarlemmermeer in the middle of the last century a potential difference of 5 m was caused between the average sea-level and the water level of the new polder. This started a landward flow of salt water. The influence of this flow on the shape and size of the fresh-water pocket has for the stationary final situation been given in figs. 1 and 2.
3) In 1853 began the withdrawal of water from the dunes on behalf of the water supply of Amsterdam. Until 1903 these increasing extractions took place in the upper dune section above the clay layer by means of a system of open canals. After 1903 the additional extraction of deep dune water below the clay layer

was started by means of wells. The influence of the extraction of water from the upper dune on the shape of the fresh-water pocket can be illustrated in figs. 3 and 4.

The influence of the deep dune-water extraction on the shape of the fresh-water pocket is naturally far more direct and has - by the strong increase of the consumption of water - led to a considerable rise of the boundary plane between fresh and salt water, which could only be stopped in 1957 when the recharge works with prepurified water from the river Rhine came into use.

4) The infiltration of the dunes with prepurified river water has considerably raised the potential of the upper dune pocket. Through that and because of diminishing extraction of deep water, the fresh-water pocket under the dunes is increasing again.

The influence of the infiltration works on the stationary final situation of the fresh-water pocket is shown in figs. 1 - 4.

5) The resistence of the clay layer has an important influence on the shape of the fresh-water pocket. This is especially the case for the tongue under the sea, which in figs. 3 and 4 is much shorter than in fig. 1. Because the chosen variation of the c-value of fig. 3 and 4 is very acceptable, it may be assumed that the tongue under the sea is rather short.

2. THE SHAPE OF THE FRESH-WATER POCKET UNDER THE DUNE-WATER CATCHMENT AREA OF AMSTERDAM WITH CONSTANT PIEZOMETRIC LEVEL IN THE SALT WATER

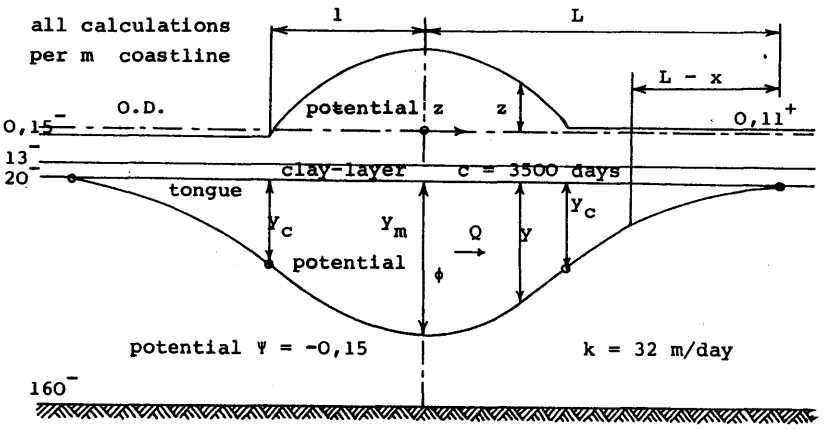

k = the coefficient of permeability

0,15⁻ O.D. = mean sea-level

specific gravity: fresh water 1000 kg/m^3

salt water 1020 kg/m^3

l = 3000 m

TONGUE

Darcy: $$Q = - k.y. \frac{d\varphi}{dx} \qquad (1)$$

Continuity: $$\frac{dQ}{dx} = \frac{\varphi - 0,11}{c} \qquad (2)$$

Equilibrium at the boundary-plane between fresh and salt water:

$$(\varphi + y + 20) \cdot 1000 = (\varphi + y + 20) \cdot 1020 \quad \text{with} \quad = -0,15$$

$$\text{so} \quad \varphi = 0,02 \cdot y + 0,25 \qquad (3)$$

Multiplying (1) and (2) gives with (3):

$$Q^2 = \frac{0,0008 \cdot k}{c} \cdot (\frac{y^3}{3} + 3,5 \cdot y^2) + C'$$

Boundary condition at the end of the tongue

$$y = 0 \qquad Q = 0 \qquad C' = 0$$

$$Q^2 = \frac{0,0008 \cdot k}{c} \cdot (\frac{y^3}{3} + 3,5 \cdot y^2) \qquad (4)$$

With (1), (3) and (4):

$$Q = \sqrt{\frac{0,0008 \cdot k}{c}} \cdot (\frac{y^3}{3} + 3,5 \cdot y^2) = - k \cdot y \cdot 0,02 \cdot \frac{dy}{dx}$$

$$dx = -5 \cdot \sqrt{0,06 \cdot kc} \cdot \frac{dy}{\sqrt{(y + 10,5)}}$$

$$x = - \sqrt{6 \cdot kc} \cdot \sqrt{(y + 10,5)} + C''$$

Boundary condition $x = L \qquad y = 0 \qquad C'' = L + \sqrt{63 \cdot kc}$

$$L - x = \sqrt{kc} \cdot [\sqrt{6 \cdot y + 63} - \sqrt{63}] \qquad (5)$$

(tongue formula)

Length of the tongue: boundary condition $x = 1 \quad y = y_c$

$$L - 1 = \sqrt{kc} \cdot [\sqrt{(6 \cdot y_c + 63)} - \sqrt{63}] \qquad (6)$$

If y_c is known, the length of the tongue is known.

With (5) and $\sqrt{kc} = 334,664$:

$$6 \cdot y + 63 = [\frac{L - x}{334,664} + 7,937]^2 \qquad (7)$$

The form of the tongue in co-ordinates

(L - x) in m	y in m	$\varphi = 0{,}02 \cdot y + 0{,}25$ m
0	0	0,250
1000	9,394	0,438
2000	21,764	0,685
3000	37,110	0,992
4000	55,432	1,359
5000	76,731	1,785
6000	101,006	2,270
7000	128,256	2,815

WATER POCKET BETWEEN THE TONGUES

Darcy: $$Q = -k \cdot y \cdot \frac{d\varphi}{dx} \qquad (8)$$

Continuity: $$\frac{dQ}{dx} = \frac{\varphi - z}{c} \qquad (9)$$

$$z = f(x)$$

$$\varphi = 0{,}02 \cdot y + 0{,}25 \qquad (10)$$

Determination of $z = f(x)$

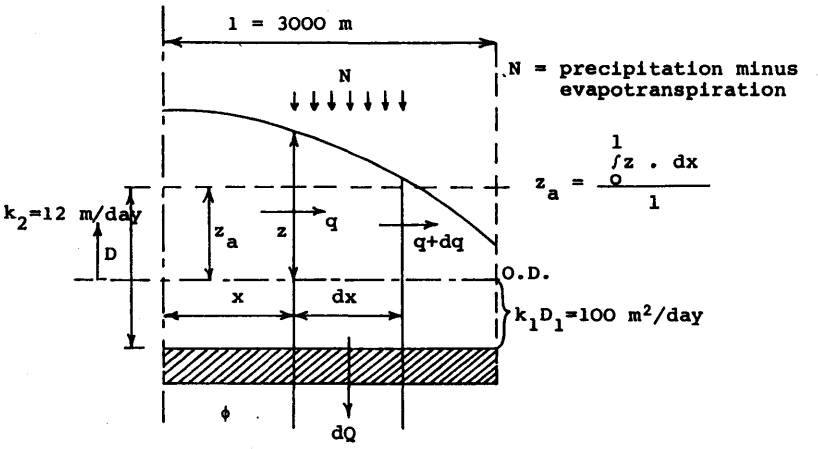

Infiltration through the clay layer: $dQ = \frac{z - \varphi}{c} dx$

Continuity: $q + N \cdot dx - q - dq - \frac{z - \varphi}{c} dx = 0$ so

$$\frac{dq}{dx} = N - \frac{z - \varphi}{c} \qquad (11)$$

Darcy: $$q = k \cdot D \cdot \frac{dz}{dx} \qquad (12)$$

in which $$kD = 100 + 12 \cdot z_a = \text{constant} \qquad (13)$$

[In reality kD is a function of z, but then it is not possible to solve the differential-equation.]

With (11) and (12):

$$\frac{dq}{dx} = -kD \cdot \frac{d^2z}{dx^2} = N - \frac{z - \varphi}{c} \qquad \text{or}$$

$$\frac{d^2z}{dx^2} - \frac{z}{kD \cdot c} + \frac{N}{kD} + \frac{\varphi}{kD \cdot c} = 0 \qquad \text{or with } \sqrt{kD \cdot c} = \lambda$$

$$\frac{d^2z}{dx^2} - \frac{z}{\lambda^2} + \frac{N \cdot c + \varphi}{\lambda^2} = 0 \tag{14}$$

This differential-equation is solvable when $\frac{d^2\varphi}{dx^2} = 0$

[possibilities: φ = constant and $\varphi = m \cdot x + n$]

A simple approximation is:

$$\varphi = \varphi_a = \frac{\int_0^1 \varphi \cdot dx}{1} = \text{constant}$$

$$\frac{d^2z}{dx^2} - \frac{z}{\lambda^2} + \frac{N \cdot c + \varphi_a}{\lambda^2} = 0 \tag{15}$$

A special solution is $z = N \cdot c + \varphi_a$

The general solution of $\frac{d^2z}{dx^2} - \frac{z}{\lambda^2} = 0$ is

$$z = C_1' \cdot e^{-\frac{x}{\lambda}} + C_2' \cdot e^{+\frac{x}{\lambda}} \quad \text{so the total solution is}$$

$$z = C_1' \cdot e^{-\frac{x}{\lambda}} + C_2' \cdot e^{+\frac{x}{\lambda}} + N \cdot c + \varphi_a$$

With the boundary condition $x = 0 \quad \frac{dz}{dx} = 0 \qquad C_1' = C_2' = C_0$

$$z = 2 \cdot C_0 \cdot \cosh \frac{x}{\lambda} + N \cdot c + \varphi_a \tag{16}$$

With this function of z however, it is not possible to solve y = f(x). Therefore an attempt is made to find a good approximation of z = f(x) that gives the possibility to find y = f(x). This is possible with:

$$z = \varphi + \alpha + \gamma \cdot x^4 \tag{17}$$

With (9) $z - \varphi = \alpha + \gamma \cdot x^4 = c \cdot \frac{dQ}{dx}$

$$cQ = \alpha x + 1/5 \cdot \gamma x^5 + C_1$$

boundary condition $x = 0$ $\quad Q = 0$ $\quad C_1 = 0$ $\quad$ so

$$cQ = \alpha x + 1/5 \cdot \gamma x^5 \tag{18}$$

With (8) and (10) $\alpha \cdot x + 1/5\ \gamma \cdot x^5 = - kc \cdot y \cdot 0{,}02 \cdot \frac{dy}{dx}$ $\quad$ or

$$1/2\ \alpha \cdot x^2 + 1/30\ \gamma \cdot x^6 + C_2 = - 0{,}01 \cdot kc \cdot y^2 \tag{19}$$

With the boundary condition $x = 0 \quad y = y_m$ it is possible to solve C_2.

x	y_m in m	C_2	$10^{-6} \cdot C_2$ (kc = 112 000)	case
0	50	- 25 kc	- 2,8	1
	75	- 56,25 kc	- 6,3	2
	100	- 100 kc	- 11,2	3
	150	- 225 kc	- 25,2	4

At the point $x = 1 = 3000$ there are two other boundary conditions:

$x = 3000 \quad z = + 0{,}11$ $\quad$ and
$x = 3000 \quad y = y_c$ $\quad$ (chosen)

With (17) and (10):

$$0{,}11 = 0{,}02 \cdot y_c + 0{,}25 + \alpha + \gamma \cdot 3000^4 \qquad \text{With } 10^{12}\ \gamma = \theta$$

$$\alpha + 81 \cdot \theta = - 0{,}14 - 0{,}02 \cdot y_c \tag{20}$$

With (19) and kc = 112000

$$1/2\ \alpha \cdot 3000^2 + 1/30\ \gamma \cdot 3000^6 + C_2 = - 1120 \cdot y_c^2$$

with $10^{12}\ \gamma = \theta$

$$4{,}5\ \alpha + 24{,}3\ \theta = - 10^{-6} \cdot C_2 - 1120\ y_c^2 \cdot 10^{-6} \tag{21}$$

with (20) and (21)

$$340{,}2\ \theta = 1120\ y_c^2 \cdot 10^{-6} - 0{,}09\ y_c + 10^{-6} \cdot C_2 - 0{,}63 \tag{22}$$

and $\qquad \alpha = - 81\ \theta - 0{,}14 - 0{,}02\ y_c \tag{23}$

For a definite y_m and a chosen y_c it is possible to solve α and θ so γ.

With (18) it is possible to solve Q_1 as follows:

$$3500\ Q_1 = 3000\ \alpha + 1/5 \cdot 3000^5 \cdot \gamma \qquad \text{With } 10^{12}\ \gamma = \theta$$

$$Q_1 = \frac{3\ \alpha + 48{,}6\ \theta}{3{,}5} \tag{24}$$

For a chosen y_c it is possible too, to calculate Q_{tongue} with (4), k = 32 m/day and c = 3500 days.

$$Q_{tongue} = \sqrt{\frac{0{,}0256\ y_c^2 \cdot (y_c + 10{,}5)}{10500}} \tag{25}$$

The third boundary condition at the point x = 1 is

$$Q_1 = Q_{tongue} \quad \text{or} \quad Q_1 - Q_{tongue} = \Delta Q = 0$$

Case 1 $y_m = 50$ m $\quad 10^{-6} \cdot C_2 = -2{,}8$ (see previous table and fig. 5)

(22) $340{,}2\ \theta = 1120\ y_c^2 \cdot 10^{-6} - 0{,}09\ y_c - 3{,}43$

(23) $\alpha = -81\ \theta - 0{,}14 - 0{,}02\ y_c$

y_c	α	$\theta = 10^{12} \cdot \gamma$	Q_1 (24)	Q_{tongue} (25)	$\Delta Q = Q_1 - Q_{tongue}$
0	0,67667	- 0,01008	0,44000	0	0,44000
10	0,66429	- 0,01240	0,39722	0,07070	0,32653
20	0,59857	- 0,01406	0,31788	0,17247	0,14541
30	0,47952	- 0,01506	0,20196	0,29811	- 0,09615

$\Delta Q = 0$ between $y_c = 20$ m and $y_c = 30$ m.

After repeated interpolation it appears that:

$$y_c = 26{,}300 \text{ m.}$$
$$\alpha = 0{,}52979$$
$$\gamma = -0{,}01476 \cdot 10^{-12}$$

With (19)

$$-1120\ y^2 = 0{,}26490 \cdot x^2 - 0{,}00049 \cdot 10^{-12} \cdot x^6 - 2{,}8 \cdot 10^6 \quad \text{or}$$

$$1120\ y^2 = 490 \cdot 10^{-18} \cdot x^6 - 264900 \cdot 10^{-6} \cdot x^2 + 2{,}8 \cdot 10^6$$

x	y in m	φ in m	z in m
0	50,000	1,250	1,780
500	49,405	1,238	1,767
1000	47,581	1,202	1,717
1500	44,417	1,138	1,593
2000	39,775	1,046	1,339
2500	33,601	0,922	0,875
3000	26,300	0,776	0,110

$$\varphi = 0{,}02\ y + 0{,}25 \qquad (10)$$

$$z = \varphi + 0{,}52979 + - 0{,}01476 \cdot 10^{-12}\ x^4 \qquad (17)$$

With (6) and y_c = 26,300 m the length of the tongue L - 1 = 2316,561 m so L = 5316,561 m.
With table (fig. 5) it is possible to draw the curves of y, φ and z.
In the same way the shape of the water-pocket can be calculated for:

Case 2 y_m = 75 m and $10^{-6} \cdot C_2 = -\ 6{,}3$ (fig. 6).

Case 3 y_m = 100 m and $10^{-6} \cdot C_2 = -\ 11{,}2$ (fig. 7).

Case 4 y_m = 150 m and $10^{-6} \cdot C_2 = -\ 25{,}2$ (fig. 8).

The values of N are in case 1 66 mm/year
case 2 125 mm/year
case 3 199 mm/year
case 4 388 mm/year.

Moreover it is possible to calculate the shape of the water-pocket with the boundary condition at x = 1 and ΔQ ≠ 0 = a chosen extraction of water.

3. THE SHAPE OF THE FRESH-WATER POCKET UNDER THE DUNE-WATER CATCHMENT AREA OF AMSTERDAM WITH A LANDWARD FLOW IN THE SALT WATER

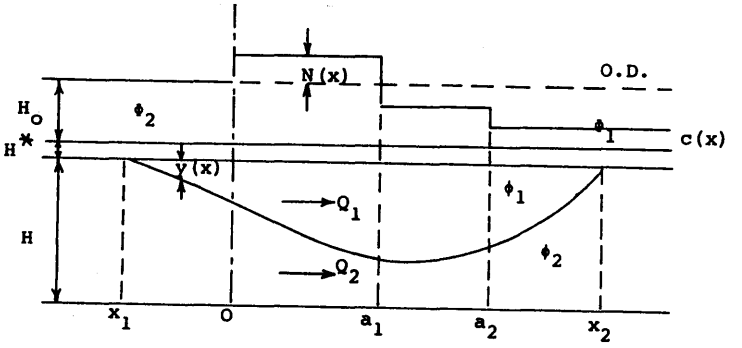

Used symbols

O.D.	mean sea-level,
$N(x)$	height of the upper water-level above O.D.,
$y(x)$	depth of the interface under the clay layer,
x_1, x_2	ends of the interface,
H_0	distance between O.D. and the top of the clay layer,
H^*	thickness of the clay layer,
H	thickness of the aquifer,
k	coefficient of permeability,
$c(x)$	resistance of the clay layer,
φ_1	fresh-water potential under the clay layer,
φ_2	salt-water potential under the clay layer,
Φ_1	potential above the clay layer in m fresh water,
Φ_2	potential above the clay layer in m salt water,
$\gamma^*(x)$	specific gravity of the upper water,
γ	specific gravity of the salt water,
Q_1	fresh-water discharge,
Q_2	salt-water discharge.

Equations

$$\Phi_1 = \gamma^* \cdot N + (\gamma^* - 1) \cdot H_0$$

$$\gamma\Phi_2 = \gamma^* \cdot N + (\gamma^* - \gamma) \cdot H_0$$

For $x < x_1$ and $x > x_2$ is

$$\frac{dQ_2}{dx} = \frac{\Phi_2 - \varphi_2}{c} \quad \text{and} \quad -k \cdot H \frac{d\varphi_2}{dx} = Q_2$$

For $x_1 < x < x_2$ is $Q_2 = Q_{20}$ = constant so

$$-k\,(H - y)\frac{d\varphi_2}{dx} = Q_{20} \quad \text{and} \quad -k \cdot y \frac{d\varphi_1}{dx} = Q_1$$

$$\frac{dQ_1}{dx} = \frac{\Phi_1 - \varphi_1}{c} \quad \text{and} \quad \varphi_1 - \gamma\varphi_2 = (\gamma - 1)\,(H_0 + H^* + y).$$

Boundary conditions

$x = \pm\infty \quad Q_2 = 0 \quad \varphi_2 = \Phi_2$

$x = x_1$ and $x_2 \quad y = 0 \quad Q_1 = 0$

φ_2 and Q_2 are continuous.

Condition for the existence of the tongue under the sea is the impossibility of an inflow of salt water; so

$$\Phi_1(x_1) - \varphi_1(x_1) \leq 0$$

This system of equations and boundary conditions was solved in 1956 by the Mathematical Centre in Amsterdam and made suitable for computer processing. It will not be mentioned how these very complicated equations were reduced. The following cases were calculated, in which the stationary final position of the shape of the water pocket is represented. The fixed values were as follows:

H_0 = 12,85 m H* = 7,00 m H = 140 m k = 32 m/day

γ = 1,02 a_1 = 5000 m $a_2 - a_1$ = 3000 m

The values of N(x) and c(x) are variable.

FIGURES

Fig. 1: In this case c = c(x) = 3500 days, and N(x) is successively 3,15 m, -0,45 m and -4,85 m. The very long tongue under the sea is remarkable.

Fig. 2: In this case c = c(x) = 3500 days, and N(x) is successively 3,15 m, -0,45 m and -2,00 m. The comparison of figures 1 and 2 gives the possibility of checking the influence of the water level in the Haarlemmermeerpolder on the shape of the fresh-water pocket. Striking in fig. 2 are the considerably smaller dimensions of the water pocket and the much shorter tongue under the sea.

Fig. 3: In this case the c(x)-value is not constant but successively 700, 3500 and 7000 days. the value of N(x) is successively 3,15 m, -0,45 m and -4,85 m. In comparison with fig. 1 the shape of the fresh-water pocket is much more compact. The tongue under the sea is rather short and the tongue under the land is somewhat longer.

Fig. 4: In this case the c(x)-values are the same as in fig. 3 but now the n(x)-values are successively 4,15 m, -0,45 m and -4,85 m. In comparison with fig. 3 the depth of the fresh-water pocket has become bigger, the tongue under the sea is still shorter and the tongue under the land is still longer.

Figures 5 to 8:

Different shapes of the fresh-water pocket calculated for different depths of the interface under the clay layer and heights of the upper water-level

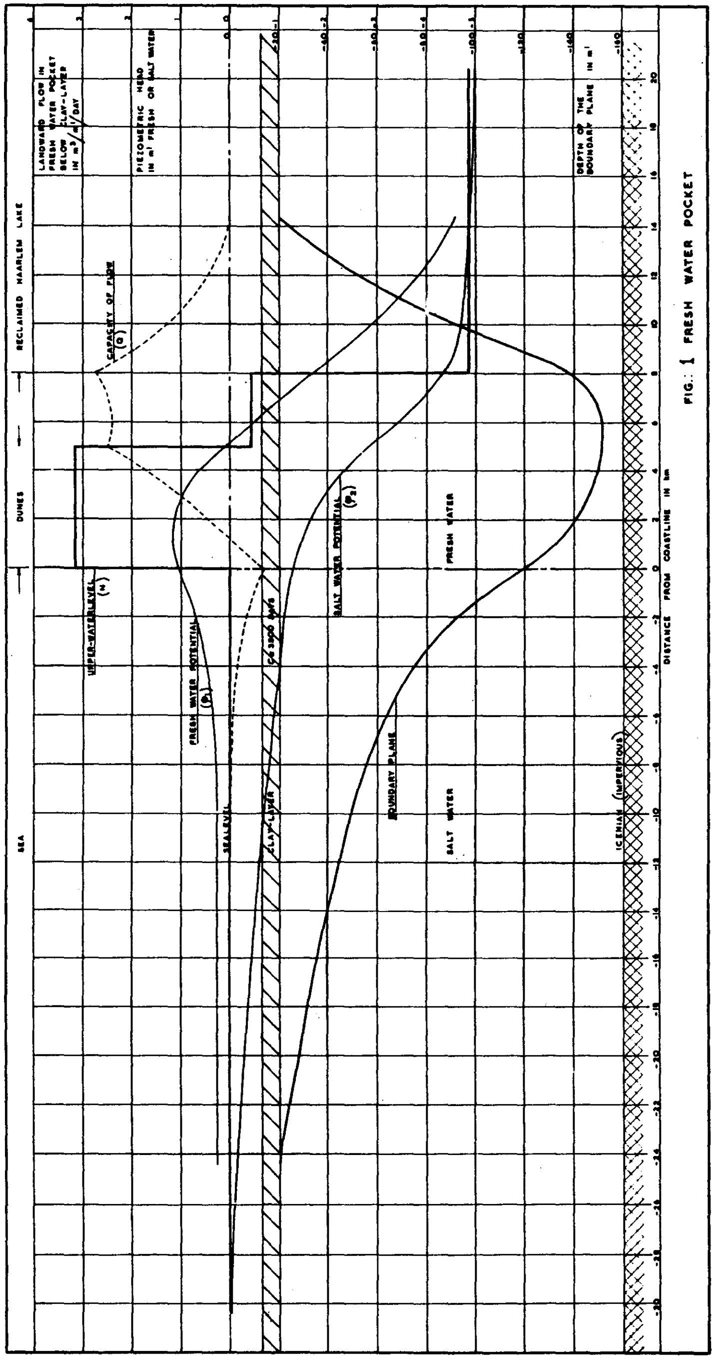
SEA
DUNES
RECLAIMED HAARLEM LAKE
LANDWARD FLOW IN FRESH WATER POCKET BELOW CLAY-LAYER IN m³/m¹/DAY
PIEZOMETRIC HEAD IN m¹ FRESH OR SALT WATER
DEPTH OF THE BOUNDARY PLANE IN m¹
CAPACITY OF FLOW (Q)
UPPER-WATERLEVEL (H)
FRESH WATER POTENTIAL (P₁)
SALT WATER POTENTIAL (P₂)
SEALEVEL
CLAY-LAYER
C=3000 DAYS
BOUNDARY PLANE
FRESH WATER
SALT WATER
ICENIAN (IMPERVIOUS)
DISTANCE FROM COASTLINE IN km
FIG.: 1 FRESH WATER POCKET

Figure 1

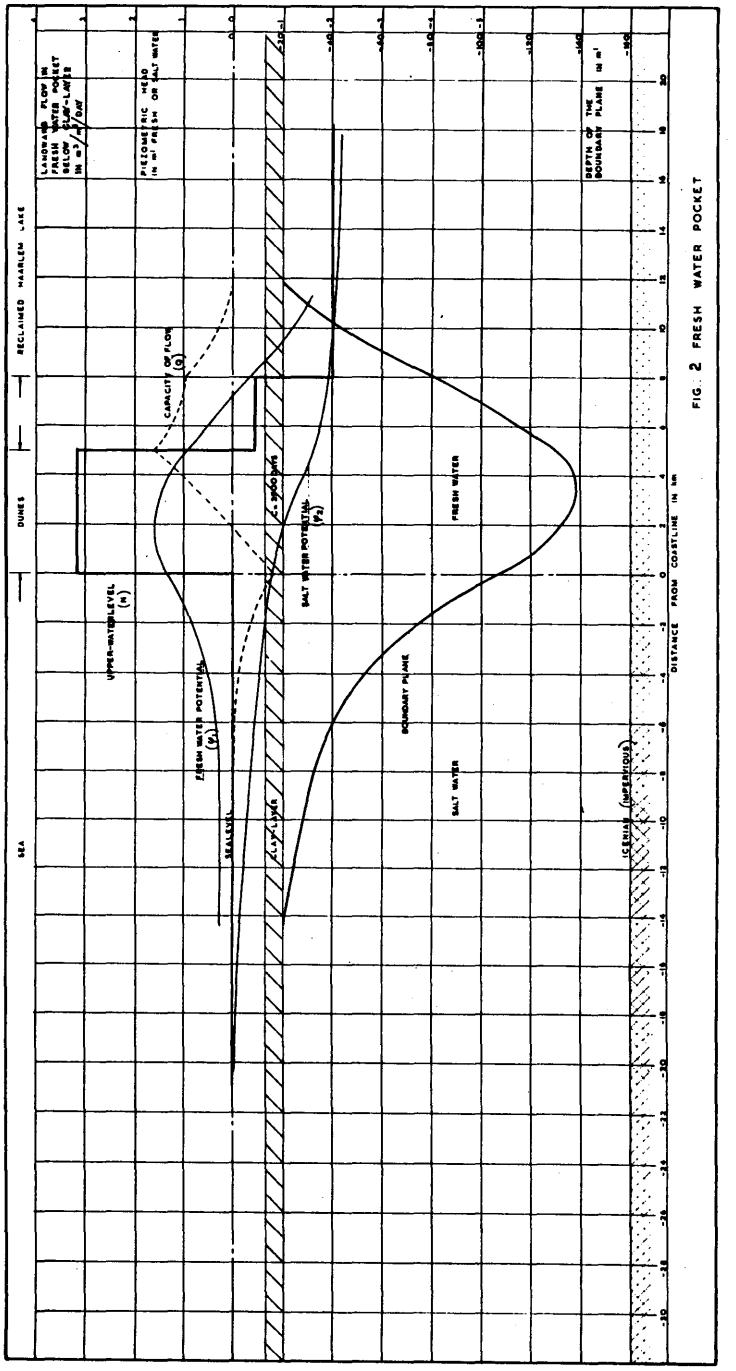
SEA
DUNES
RECLAIMED HAARLEM LAKE
LANDWARD FLOW IN FRESH WATER POCKET BELOW SEA-LEVEL IN m³/d/m COAST
PIEZOMETRIC HEAD IN m FRESH OR SALT WATER
DEPTH OF THE BOUNDARY PLANE IN m
UPPER-WATERLEVEL (h)
CAPACITY OF FLOW (k)
FRESH WATER POTENTIAL (P1)
SEALEVEL
CLAY LAYER
SALT WATER POTENTIAL (P2)
BOUNDARY PLANE
FRESH WATER
SALT WATER
ICE AGE (IMPERVIOUS)
DISTANCE FROM COASTLINE IN km
FIG. 2 FRESH WATER POCKET

Figure 2

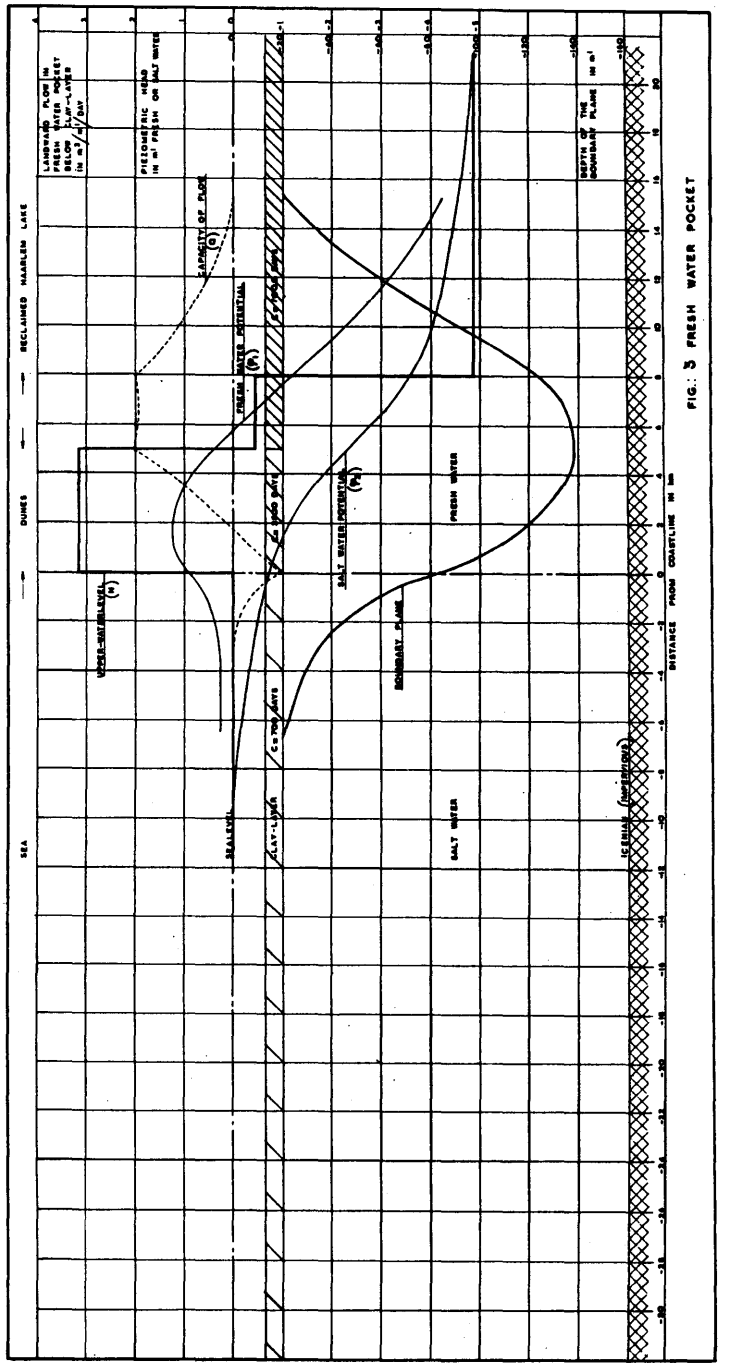

FIG.: 3 FRESH WATER POCKET

Figure 3

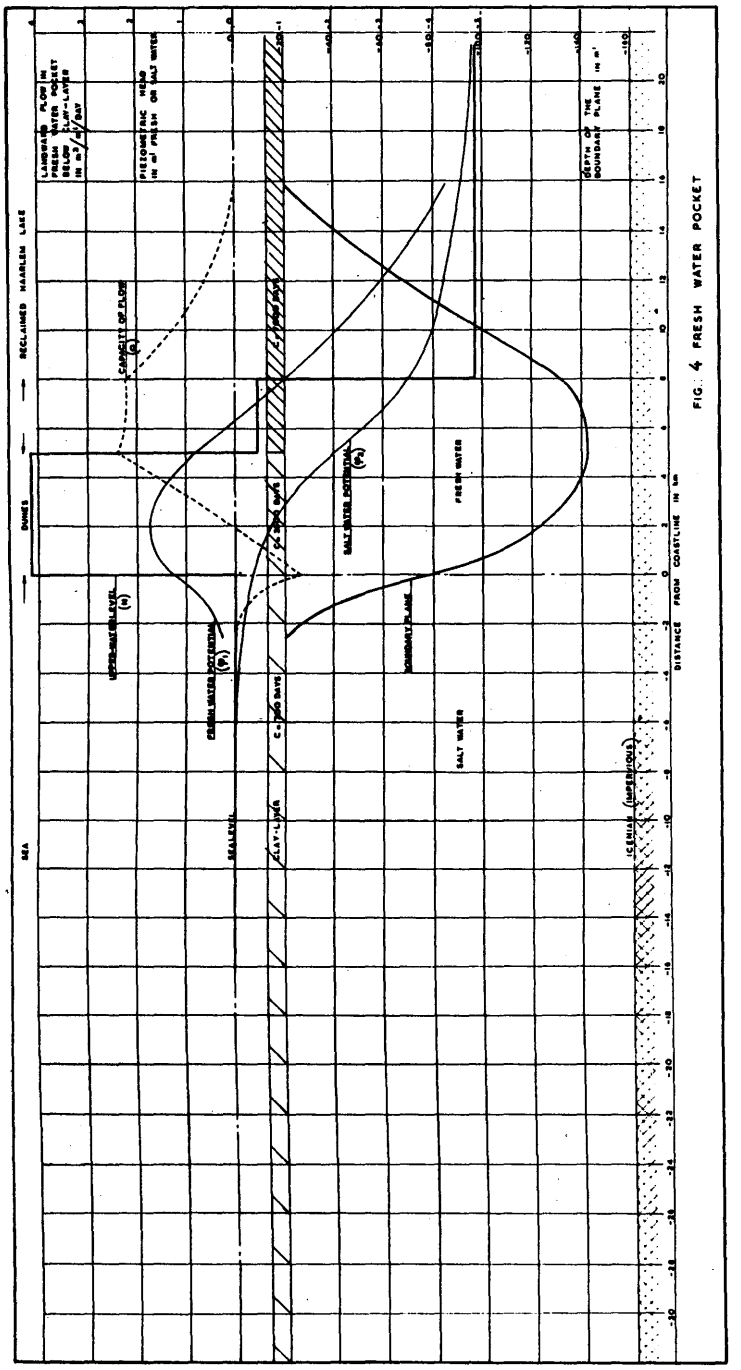

FIG. 4 FRESH WATER POCKET

Figure 4

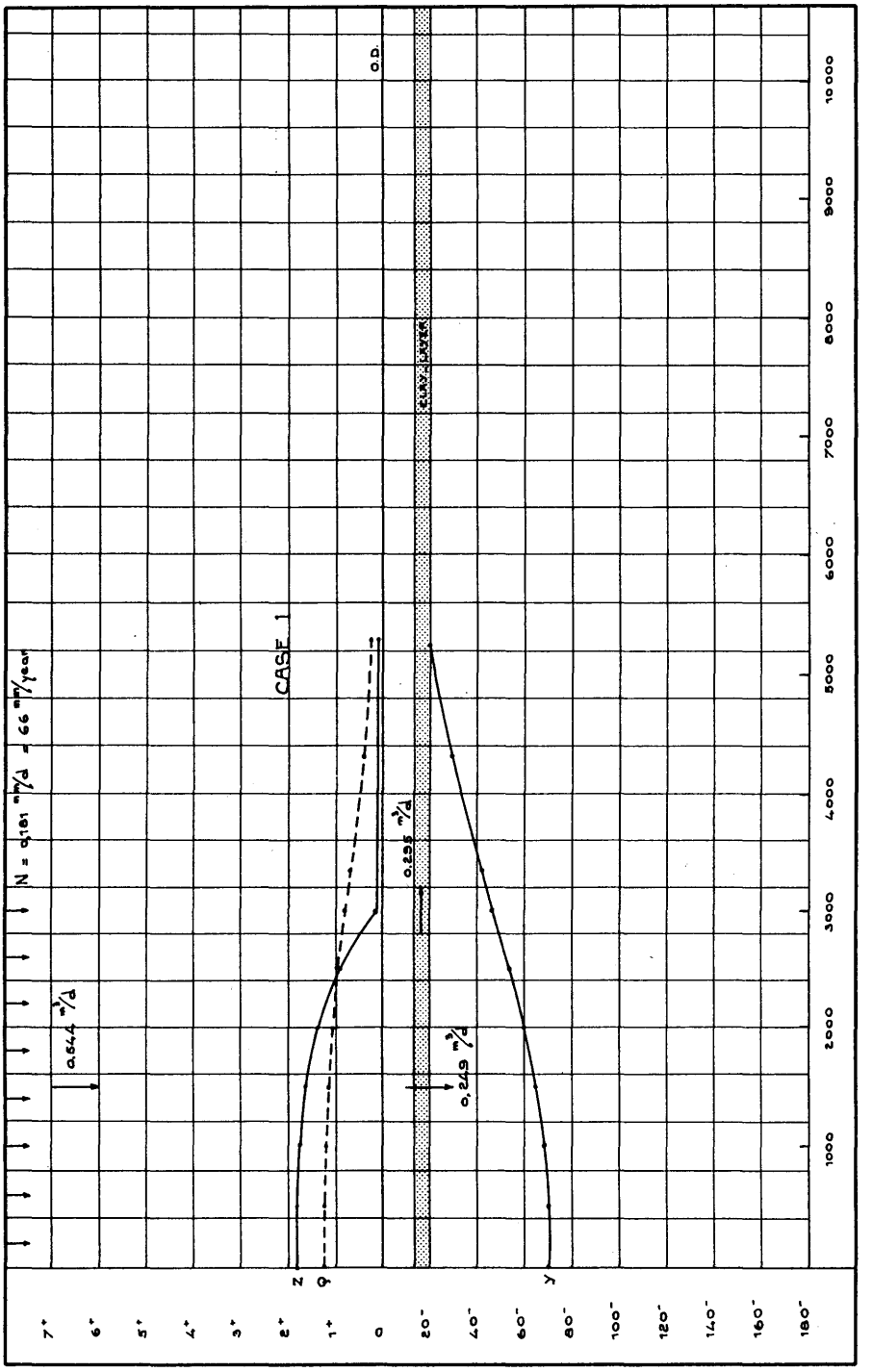
N = q181 m³/d = 66 m³/year
0.544 m³/d
CASE 1
O.D.
clay layer
0.295 m³/d
0.279 m³/d
z
q
y
7+
6+
5+
4+
3+
2+
1+
0
20-
40-
60-
80-
100-
120-
140-
160-
180-
1000
2000
3000
4000
5000
6000
7000
8000
9000
10000

Figure 5

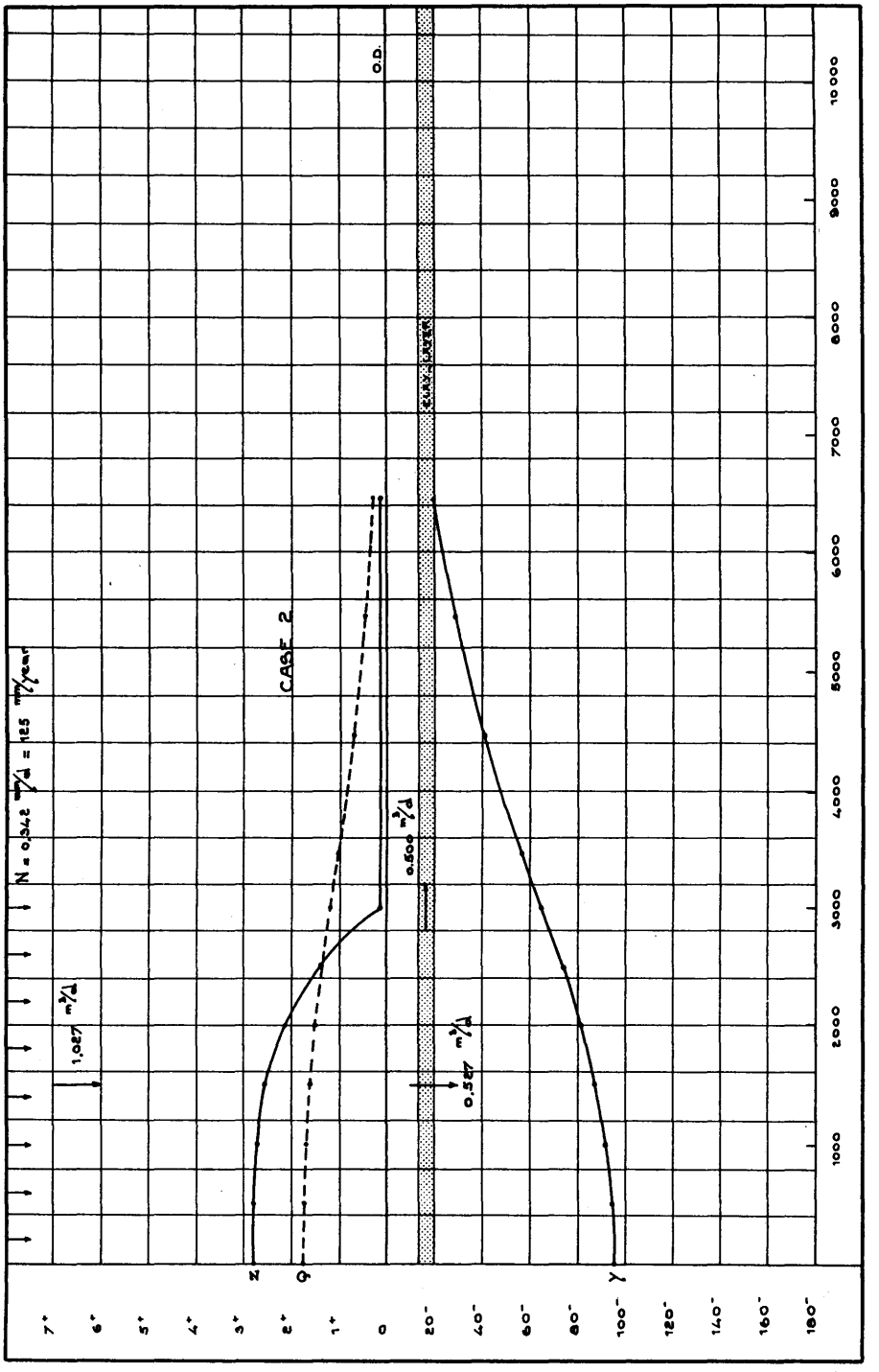
N = 0.342 m³/d = 125 m³/year
CASE 2
1.027 m³/d
0.500 m³/d
0.527 m³/d
CLAY LAYER
O.D.
N
Q
Y
7+
6+
5+
4+
3+
2+
1+
0
20-
40-
60-
80-
100-
120-
140-
160-
180-
1000
2000
3000
4000
5000
6000
7000
8000
9000
10000

Figure 6

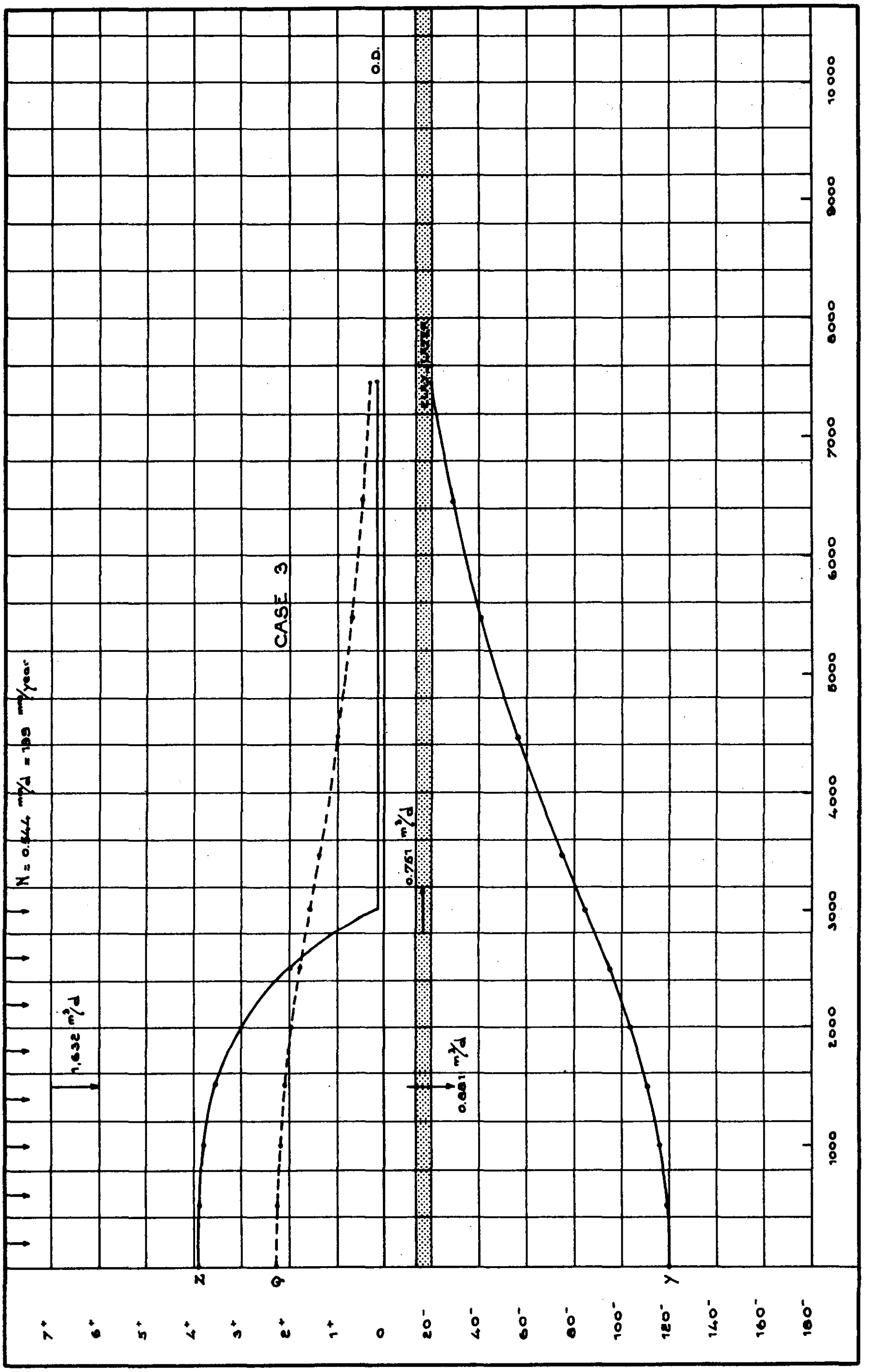

Figure 7

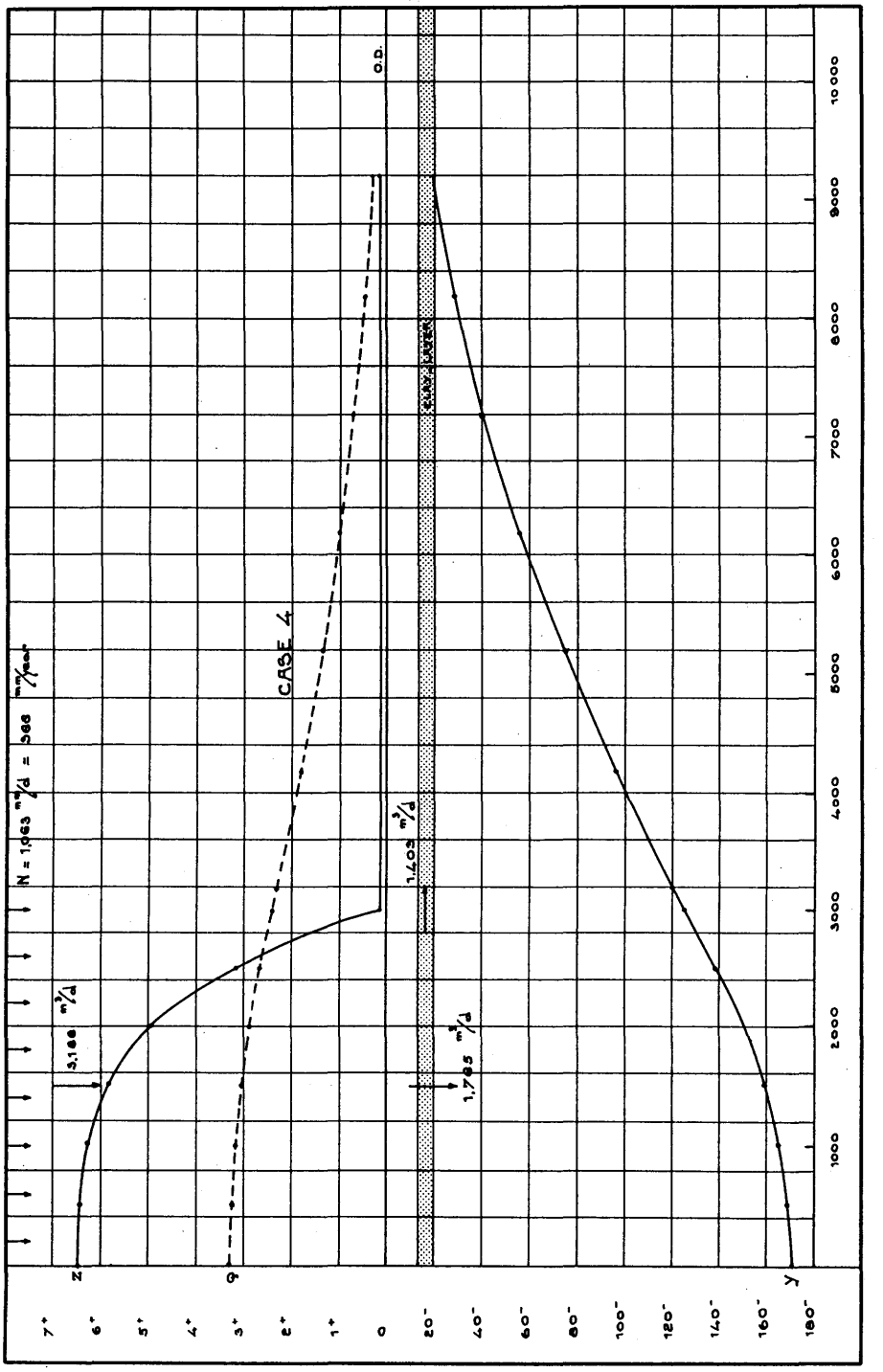
CASE 4
N = 1.963 m³/d = 368 mm/year
3.166 m³/d
1.403 m³/d
1.785 m³/d
CLAY LAYER
O.D.
z
q
y
7+
6+
5+
4+
3+
2+
1+
0
20-
40-
60-
80-
100-
120-
140-
160-
180-
1000
2000
3000
4000
5000
6000
7000
8000
9000
10000

Figure 8

2.3. AQUIFER MANAGEMENT IN THE CONTEXT OF SALINE INTRUSION

D.A. NUTBROWN

ABSTRACT

An approach to the problem of saline intrusion is to modify the aquifer pumping regime to reduce the extent of saline intrusion. This has been studied on a regional scale for the Chalk aquifer of the South Downs, England (which covers an area of 700 km²) using a novel mathematical approach. Exploitation of the entire aquifer to the same level of development has been examined and possesses considerable benefits over local, more intensive development as at present. However, pipe-line links between different parts of the aquifer would be necessary to facilitate the movement of water. This new approach, which has wide applicability, allows sensitivity analysis to be carried out economically.

As demands for water increase, so does the necessity for wide-ranging and comprehensive methods of developing water resources to meet this meed. A time comes when a collection of different sources, possibly used as isolated units satisfying local demands for water, ought to be considered for development in a unified way. Thus the problem facing the resource planner is to determine the best way of developing a collection of different sources within the variety of constraints to which the water resource system may be subject. Of particular interest in coastal regions where groundwater is a major resource is the limit to full development which can result from the problem of saline intrusion.

This paper describes a study which has been carried out on the water resources of the South Downs, England, employing a numerical description of the behaviour of the system to analyse various development options. The systems approach to planning will not be described in any detail but a schematic representation is given in fig. 1 - the "flow" in this diagram is downwards, with data being fed in at the top and results finally appearing at the bottom. Fig. 2 shows a map of the region under consideration, with a regular five-kilometre mesh, used in the quantitative analysis, superimposed. This region, with an area of approximately 3.000 km² is dominated both geologically and in resource terms by the Chalk in the south.

The exposed area of the Chalk is over 700 km² and extends 90 km along the coast westwards from Eastbourne. Geophysical logging in boreholes along the coast suggests that the effective thickness of saturated flow in the aquifer is about 100 m, with flow taking place predominantly through fissures. The Chalk is intersected by four main rivers running in a north-south direction, which are the rivers Cuckmere, Ouse, Adur and Arun. These rivers, which are tidal to points north of the Chalk, together with a groundwater divide in the west, allow definition of five Chalk 'blocks'. From east to west, using the major local demand centres as labels, these blocks will be referred to as the Eastbourne, Seaford, Brighton, Worthing and Chichester blocks, as shown in fig. 3. Under the hydrogeological conditions which prevail in the study area, these blocks

are effectively independent water resource units. The two western blocks are partially covered by Tertiary sands and clays lying in the Chichester Syncline.

The average annual rainfall in the area varies from 900 mm in the west to about 700 mm in the east, around Hastings. Some care must be taken in assessing the proportion of precipitation that infiltrates into the Chalk. Generally, conditions are such that in the summer months evaporation allows no effective infiltration, and natural recharge takes place only during the winter months. On the demand side, the public water supply sector is by far the largest - the industrial and agricultural sectors being comparatively small. The present population of the area is in excess of one million, of which 60 per cent live in urban complexes along the coastal margin. In the future the size and distribution of population, and therefore of demand, will change due to variations in the local rates of growth. Predicting the precise nature of these changes is extremely difficult but, in any case, is outside the scope of this study. For the present investigation, estimates were obtained on the likely future levels of demand in a number of sub-regions within the study area from an analysis of trends in public water supplies. For example, with reference to demand centres situated on the Chalk, demand is estimated to rise from about 70 million m^3/year in 1975 to 100 million m^3/year in 1995. In addition there is also a marked fluctuation of demand throughout the year, rising to a peak in the summer months, especially in the coastal resorts.

Given that the coastal resources should be used mainly for the benefit of the coastal demand centres, the study examined the ways in which the five independent sources (namely the Chalk blocks) might be developed in the future, subject to the limitations imposed by saline intrusion. There has not been a unified development policy for the five blocks because, until recently, each area was supplied by a separate undertaking. Instead, the quantity of groundwater pumped from each block has been used to satisfy local demand, resulting in relatively small transfers between blocks. Moreover, since about 45 per cent of the population of the Chalk is concentrated in Brighton and its environs, this pattern of abstraction had led to widely different degrees of exploitation of the individual blocks. From the planning viewpoint it is important to determine the effects on groundwater levels of pursuing the alternative 'policies' of:

a. continued exploitation of the Chalk to a degree governed by local demand levels, and

b. exploitation of all blocks to the same level (as a fraction of average annual recharge), necessitating the construction of inter-block links.

The considerations which lie behind these alternative schemes concern, on the one hand, intense development in certain blocks, possibly leading to problems of saline intrusion, and, on the other hand, the operation of all five blocks as a single water resource unit, switching abstraction from east to west and vice versa as the hydrogeological conditions dictate.

Having identified the sources of water under study, collected the relevant data and decided on suitable mathematical descriptions of their behaviour, the next stage involved their calibration and validation. Two of the major blocks (Brighton and Worthing) have already been the subject of more detailed studies (NUTBROWN, DOWNING & MONKHOUSE, 1975). These detailed models have been calibrated and validated using data pertaining to the two-year period October 1971 to October 1973. Using monthly computed distributions of infiltration (taken as precipitation less potential evaporation less soil moisture deficit), pumping rates at the various public supply wells (monthly figures furnished by the water undertakings concerned) and the corresponding water-level fluctuations, an automatic method of calculating both storage coefficient and transmissivity was used to perform the calibration (NUTBROWN, 1975). These values were transferred to the less refined models used in this study by a process of averaging. A similar approach, not however, utilising the automatic method, was adopted to calibrate and validate the models of the remaining blocks. These blocks are relatively unexploited and the present water levels are considered to be closer to their natural values.

Several simulation runs were then performed, both to assess the effects of different development strategies, and to test the sensitivity of the more important output parameters to variations in the system constants. In analysing a water-resource system to estimate its optimum safe yield, some form of critical drought sequence must be employed. Based on records of well levels extending back 100 years at Chilgrove in the Chichester block, it was assumed that infiltration values pertaining to the winters of 1971/72 and 1972/73 constituted a 2-year drought period with a 1 in 50 likelihood of occurrence. Extrapolating these values to the other blocks implied that, during the test drought, infiltration was reduced to 45 per cent and 30 per cent of the corresponding average values in the first and second winters respectively. Of course, the assessed likelihood of occurrence of this test drought could well change in the light of the very dry conditions experienced subsequently but the principles of the approach remain unaffected.

As far as the demand values are concerned, the system could be tested at any level, without reference to the year in which such a level might be attained. However, for planning purposes, it was necessary to include a prediction of the growth rate of demand in the region. The figures used were compiled within the Central Water Planning Unit and pertained to demand levels in the years 1976, 1986 and 1996. These figures, originally broken down into the previous statutory water undertaking areas, were further sub-divided into separate demand centres on the five-km mesh according to the present spread and estimated local growth rate of population. This resulted in total demand levels of 71,4, 87,5 and 103,8 million m^3/year in the three years. These figures were further distributed over twelve months according to the observed fluctuation of demand in the Brighton and Worthing areas, with peaks in the summer months. For comparison, the estimated average total recharge of the Chalk aquifer is 285,6 million m^3/year. The problem is, of course, to decide how much of this can be safely exploited, without inducing significant saline intrusion.

The first simulations with the five Chalk blocks involved their future development under the two choices already outlined. In the 'local' policy, each demand centre was supplied water, under average conditions, only from the block on which it was situated. This policy was pursued until, during the drought years, the outflow from any block was reduced to a level where saline intrusion was likely to occur. At these lower levels, water was taken from neighbouring blocks. Thus, particularly at the higher levels of development even the local policy required some inter-block transfers to be established. Although this policy does not reflect precisely the present use of the blocks, the general philosophy is mirrored. On the other hand, the 'unit' policy treated all five blocks as a single unit and developed them solely on the basis of their potential. Since, under the local policy, the Eastbourne, Brighton and Worthing blocks are more fully exploited than the others, in the unit policy the Seaford and Chichester blocks are typically exporters of water. However, in practice, some caution must be exercised in the fuller development of the Chichester block, where certain local and amenity considerations must be taken into account. A few major streams in the block, particularly the Lavant, are dependent on the Chalk aquifer for their flow - for example there are approximately 2 million m^3/year licenced for watercress cultivation, coming from springs and artesian boreholes in the block. Whereas this represents only about 2 per cent of the annual recharge of the Chichester block, such interests must be protected in some suitable way.

Fig. 4 shows the main results of these simulations. It gives the storage above sea level in October of the relevant year, as a fraction of the corresponding natural values (computed using the same method), for each block in the years 1976, 1986 and 1996. The values relating to each type of development are shown. The upper unbroken lines give the October storage value corresponding to average infiltration conditions, and the lower broken lines give the October value at the end of the test drought. Thus the uneven development pattern of the blocks can be seen in the upper graphs, whereas the lower graphs, corresponding to the unit 'policy', show the more uniform pattern. Unfortunately, judging by the experience gained with more refined groundwater models, the present analysis is not able to detect all occurrences of saline encroachment due to its rather coarse mesh. In the more detailed models, when intrusion did occur, it was only over fronts of 1 or 2 km. The five-kilometre grid of the present study therefore necessitates some interpretation of the results in fig. 4. In fact, in the more detailed models it was noted that the occurrence of saline intrusion set a limit to the development of both the Brighton and Worthing blocks when storage of groundwater above sea level in October of the final drought year was about 30 per cent of the natural value in each case.

The saline intrusion limit to storage decline is also shown in fig. 4. It is noticeable that, under the local policy, the storage values in the Eastbourne, Brighton and Worthing blocks all fall below this critical value at the end of the test drought before the 1986 demand level is reached. However, under the unit philosophy, only the Seaford block apparently suffers from saline encroachment problems up to the 1996 level. Even this problem may be removed by slightly

modifying the distribution of pumping from each block. Since, under the unit 'policy', the greatest volume of water is taken from the Chichester block and the least from the Seaford, it is in fact possible (though not necessary) to remove all pumping from the Seaford block and increase the exploitation of the Chichester block by a corresponding amount. With this modified approach, the value of groundwater storage above sea level at the end of the test drought would still exceed 40 per cent of the natural value at the 1996 development level.

These simulations provide a great deal of quantitative information about, inter alia, the number and position of well sites required at each level of development, details of optimum pumping regimes and the magnitudes of transfers necessary between each block. The general conclusion to be drawn from them is that, if the Chalk of the South Downs is to be exploited to its full potential, the levels of development of the separate blocks must be more uniform than at present. If substantial inter-block links were established, the Chalk could provide water to centres on the catchment, without inducing saline intrusion on a marked scale, at least until the year 1996 (based on current demand forecasts). To achieve this, taking the most extreme case, at the end of the test drought at the 1996 level, the Chichester block would be required to export at least 85 Ml/day, half to Worthing and half to Brighton demand centres. This figure reduces to about 70 Ml/day under average conditions. As with all predictions, these results must be viewed with some caution. Fortunately, within the systems approach, it is possible to estimate the sensitivity of such results to variations in the system constants, some of which may not be close to their true values.

Sensitivity analyses were carried out, centred on the 1986 development level, under average conditions and adopting the unit policy. Ten per cent variations were imposed on the values of natural recharge, storage coefficient, transmissivity and total demand. For the first three, only the overall scale was changed and no attempt was made to increase or decrease values at particular locations. In the case of total demand some allowance was made for the different population growth rates over the region. These four variables might be termed the 'explicit' variables (that is those whose values were changed at the start of the sensitivity study). The 'implicit' variables (that is those whose sensitivities to changes in the explicit variables were examined at the end of the study) were:

a. a linkage cost variable, related to the magnitude of inter-block transers,

b. a pumping cost variable, related to the energy cost of pumping from the water table to the ground surface in an average year, and

c. a storage variable, equal to the total amount of groundwater storage above sea level at the end of the summer period.

Fig. 5 shows the results of this exercise and some interesting points can be noted:

a. Linkage costs appear to depend only on the level of demand, nearly proportionately, and are relatively independent of the other explicit variables.

b. Pumping costs show, more or less, the expected dependencies, except perhaps for the case of storage coefficient. In fact it can be demonstrated that the lack of dependence of average pumping costs on storage coefficient is a general feature of unconfined aquifer systems. Although it will not be shown in detail in this paper, it follows from the groundwater-flow equations and the recurring nature of water levels under average conditions.

c. The final implicit variable, the total storage above sea level at the end of the summer period, is the most important one in an aquifer susceptible to saline intrusion. Again the dependencies are roughly as expected, with variations in natural recharge, storage coefficient and transmissivity being most important. Clearly, secure predictions of optimum development levels cannot be made without reliable estimates of these variables.

REFERENCES

NUTBROWN, D.A. (1975). Identification of Parameters in a Linear Equation of Groundwater Flow. Wat. Resour. Res. 11, 581-588.

NUTBROWN, D.A., DOWNING, R.A. & MONKHOUSE, R.A. (1975). The Use of a Digital Model in the Management of the Chalk Aquifer in the South Downs, England. J. Hydrol. 27, 127-142.

FIGURES

Fig. 1: Schematic representation of the systems approach to planning.

Fig. 2: Study area with mesh.

Fig. 3: The five Chalk blocks and the associated demand centres.

Fig. 4: Results of the comparison between two development policies.

Fig. 5: Results of the sensitivity exercise.

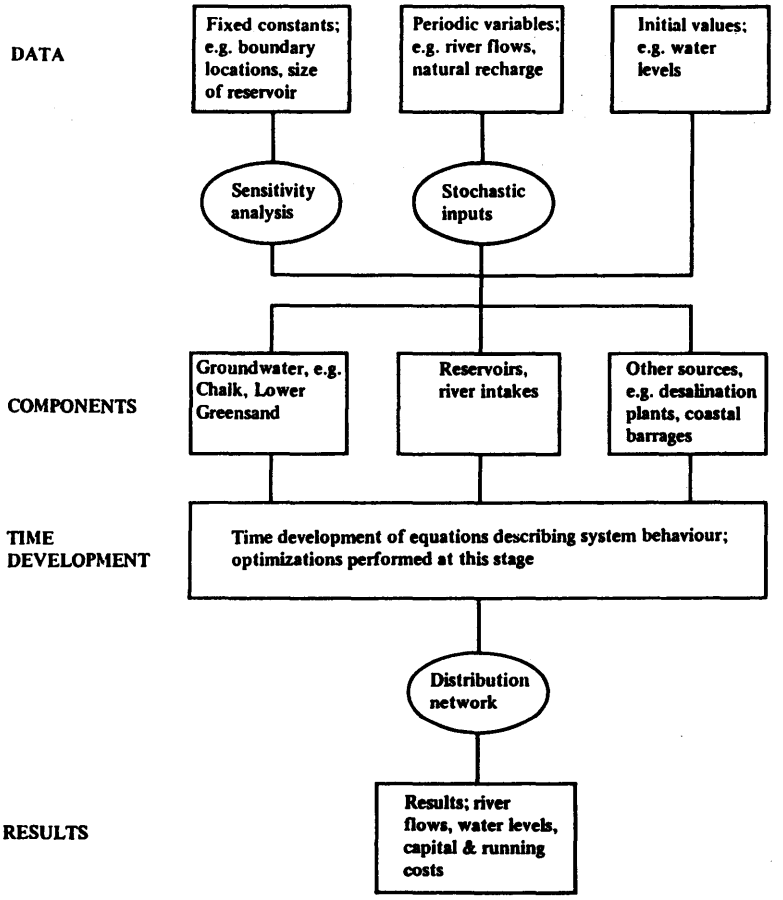
DATA
Fixed constants; e.g. boundary locations, size of reservoir
Periodic variables; e.g. river flows, natural recharge
Initial values; e.g. water levels
Sensitivity analysis
Stochastic inputs
COMPONENTS
Groundwater, e.g. Chalk, Lower Greensand
Reservoirs, river intakes
Other sources, e.g. desalination plants, coastal barrages
TIME DEVELOPMENT
Time development of equations describing system behaviour; optimizations performed at this stage
Distribution network
RESULTS
Results; river flows, water levels, capital & running costs

Figure 1

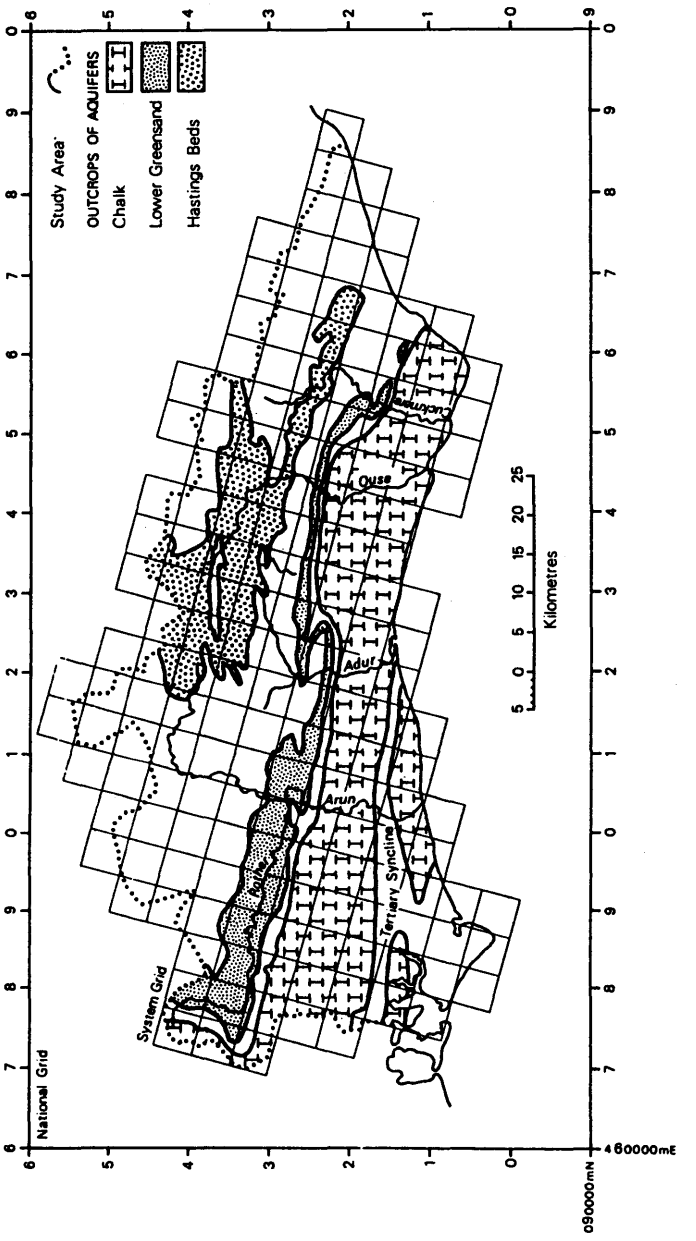
Study Area
OUTCROPS OF AQUIFERS
Chalk
Lower Greensand
Hastings Beds
Ouse
Adur
Arun
Tertiary Syncline
Kilometres
5 0 5 10 15 20 25
National Grid
System Grid
460000mE
090000mN

Figure 2

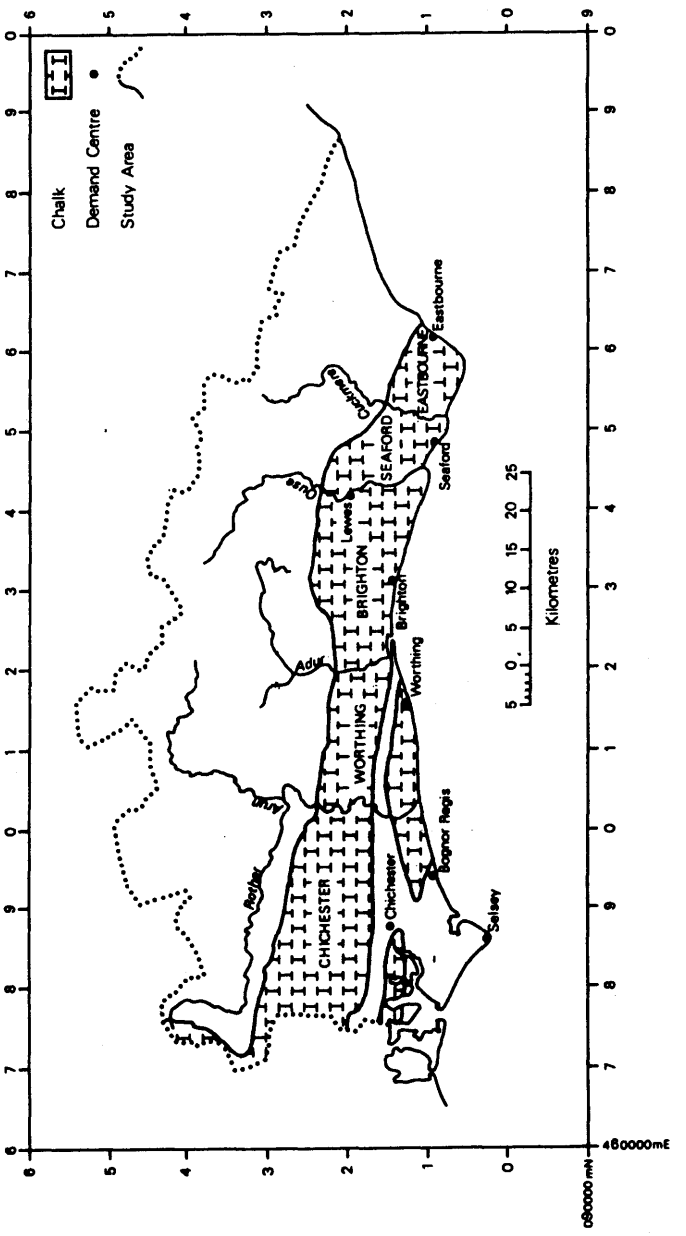
Chalk
Demand Centre
Study Area
Eastbourne
Seaford
Lewes
Brighton
Worthing
Bognor Regis
Chichester
Selsey
EASTBOURNE
SEAFORD
BRIGHTON
WORTHING
CHICHESTER
Ouse
Adur
Arun
Ryther
Kilometres
460000mE
060000 mN

Figure 3

Figure 4

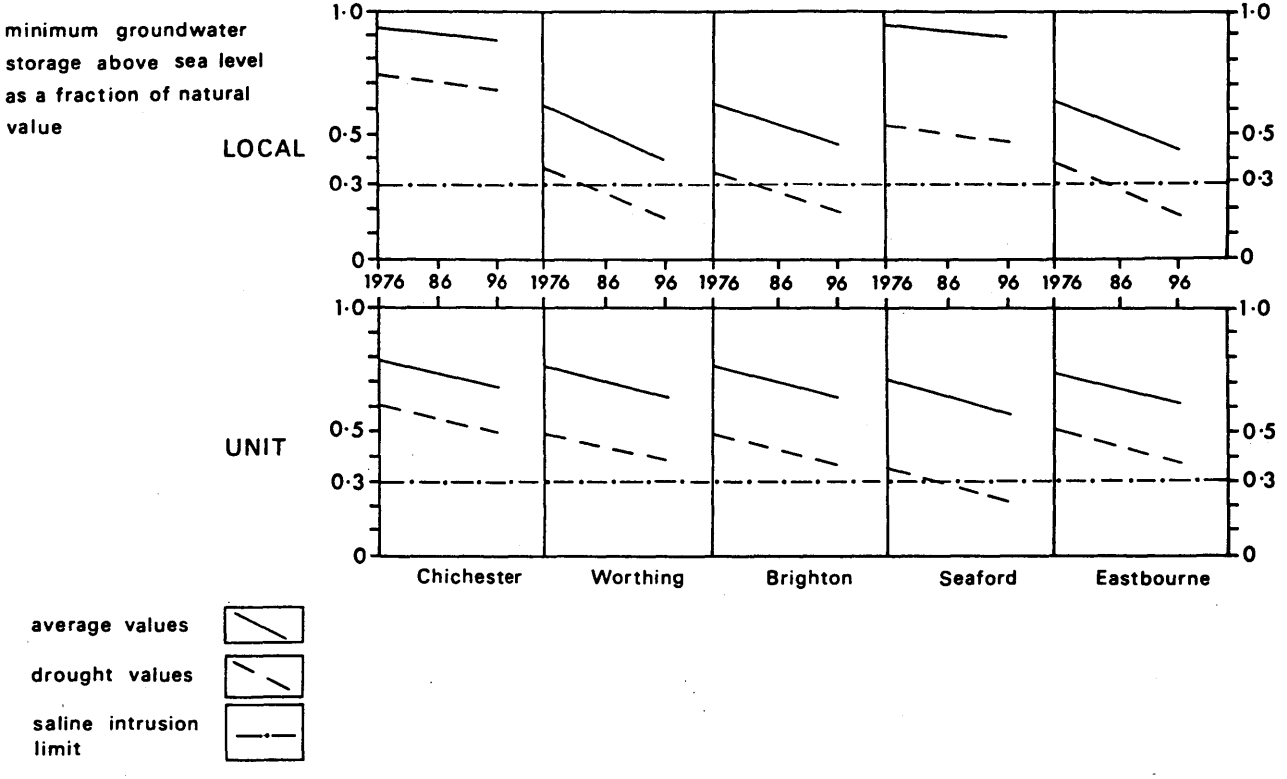
minimum groundwater storage above sea level as a fraction of natural value
LOCAL
UNIT
1·0
0·5
0·3
0
1976
86
96
Chichester
Worthing
Brighton
Seaford
Eastbourne
average values
drought values
saline intrusion limit

Linkage costs
Pumping costs
Storage values
Implicit variable sensitivities
Explicit variable perturbations
10%
0%
-10%
D
R
S
T
demand perturbations
recharge perturbations
storage coeff. perturbations
transmissivity perturbations

Figure 5

2.4. A STUDY OF SALINE INTRUSION AND THE INFLUENCE ON GROUNDWATER MANAGEMENT IN THE LINCOLNSHIRE CHALK (ENGLAND)

D. EVANS, J.W. LLOYD & K.W.F. HOWARD

ABSTRACT

The Lincolnshire Chalk yields high quality water for the industrial areas of Grimsby and South Humberside. Over-exploitation has led to falling water levels and saline intrusion from the Humber Estuary. Because of rising demands and limited alternative resources it is vital to make best use of this aquifer, and for this a 3-year multi-disciplinary study has been carried out by the Birmingham University and the Anglian Water Authority. The study has clarified the salinity problem and in doing so has broken new ground in hydrogeological techniques, which included geophysics, major and minor ion hydrochemistry and the use of environmental isotopes. The work culminated in a mathematical model of the aquifer which is being used (circumspectly) to guide management and planning decisions to meet demands in the Humberside area.

1. INTRODUCTION

The Lincolnshire Chalk provides some 170 tcmd*) of high-quality water for domestic and industrial supplies in Grimsby and South Humberside (fig. 1). Water has been pumped from the aquifer at an increasing rate for many years, and recently abstractions have exceeded the safe yield, particularly in the Grimsby area. As a result, saline water has been drawn in from the adjacent Humber Estuary.

The aquifer is physically complex and the evidence of saline intrusion in the late 1960's and early 1970's was unclear. The Anglian Water Authority (AWA) therefore commissioned Birmingham University to study the problem. That study, the South Humberside Salinity Research Project, took place from 1975 to 1978 and involved geophysics, hydrogeology, hydrochemistry and groundwater-modelling techniques. The study was first introduced at the previous SWIM Conference at Medmenham in 1977 (LLOYD et al., 1977).

This paper describes the aquifer and its significance to regional water resources, the completed salinity study and its results, and the value of those results to aquifer management and to regional water resource planning.

2. THE LINCOLNSHIRE CHALK AQUIFER

The Lincolnshire Chalk is a fissured aquifer partly confined by glacial tills. Its outcrop is shown in fig. 1; fig. 2 shows the study area in more detail. The aquifer dips to the north-east and extends at depth under the North Sea. The wetted thickness of the aquifer is of the order of 100 m. Estuarial saline water

*) tcmd = thousands of cubic metres per day = Ml/d.

has been encountered near the coast whilst at greater depth there are zones of connate saline waters. The objectives of the study included definition of the geometry of the Chalk and the confining layers, and of the various saline zones.

The effective rainfall on the outcrop is some 160 mm/year, most of which infiltrates to the aquifer. Under natural conditions this would emerge as spring flow at the confining boundary and from 'blow wells' (artesian overflows) nearer the coast. However, most of these natural overflows are now reduced as a result of abstraction.

The mean natural recharge to the aquifer, as defined in the study, is some 219 tcmd. Allowing for spring flows and various other 'losses' this implies that the safe steady abstraction rate may be of the order of 170 tcmd. Abstractions exceeded this rate for much of the 1960's, reaching a peak of 192 tcmd in 1970.

3. SIGNIFICANCE OF THE AQUIFER TO WATER-RESOURCE PLANNING

South Humberside has a population of some 300.000 people, with a higher growth rate than most parts of Britain. During the 1960's and early 1970's there was rapid expansion of heavy industry, particularly along the Humberbank (fig. 1). Much of this industry is water-intensive and there is scope for much further expansion.

The Chalk aquifer is the 'natural' local water resource, both for public supply and for direct abstraction by industry. However, it is inadequate to meet the full demand, and therefore two surface water schemes have been implemented:

a. The Covenham Scheme:
   a reservoir at Covenham (fig. 1), pump-filled from the Louth Canal and the River Great Eau, was constructed in the 1960's specifically to meet the rising industrial demands. Its safe yield is some 64 tcmd.

b. The Trent-Witham-Ancholme Scheme (T-W-A):
   a river transfer scheme, initially providing some 60 tcmd to the Grimsby area. This yield could be substantially increased, but because the main source is the River Trent which carries large volumes of effluent from the industrial Midlands, this source is non-potable. Despite expensive treatment, the water is also less acceptable to industry on other quality grounds, notably high dissolved solids.

There are no other local options for potable supplies of reasonable cost and public acceptability. Therefore the strategy for meeting growth in demand is to progressively increase the supply of T-W-A water to those industries which can use it. This releases potable water for the public supply and for industries, such as food processing, which cannot accept T-W-A water.

However, there is a limit to the amount of potable water that can be released in this way, and eventually some further potable resource will be required. This will be very expensive and will have implications elsewhere in the region. Making best use of the Chalk water is therefore important to keep down short-term operating costs, to defer costly new investment and to provide the best quality water to customers.

One way in which better use might be made of the aquifer is to use it conjunctively with the Covenham Scheme. This scheme has insufficient storage and additional storage, used only occasionally in dry years, could increase its yield. The Chalk could provide such storage, but the potential for doing so is limited by the risks of saline intrusion.

A full understanding of the recharge to, storage in and other properties of the aquifer, and of the salinity problem is therefore vital, not only for day-to-day management but also for longer term resource planning decisions.

4. SOUTH HUMBERSIDE SALINITY RESEARCH PROJECT

4.1. Organisation

The project was carried out by the staff of the Departments of Geological Sciences and Civil Engineering of the University of Birmingham with the support of staff of the Anglian Water Authority as a research contract between the Authority and the University. The project was controlled by a steering committee and a larger technical working group involving university staff, operational and planning staff of the Water Authority and representatives of local industrial abstractors and outside bodies concerned with water resources. Though apparently cumbersome, this approach succeeded well in combining the academic skills with practical knowledge and so ensuring that the end project was of maximum practical value.

4.2. Objectives

The overall objective of the project was to understand the relationship between good quality exploitable groundwater and the various poor-quality saline groundwater bodies in the Chalk. This necessitated a complete hydrogeological study of the groundwater conditions with the following complementary objectives:

- to establish the detailed geological sequence and stratigraphical distributions to obtain the basis for the aquifer geometry;
- to classify and locate the hydrochemical types of groundwater and their relationship to groundwater-flow controls;
- to determine the origin of the saline groundwater bodies, their response to historical abstraction and the influence of origin on response;

- to determine the range and distribution of aquifer characteristics and to delineate aquifer boundaries;
- to estimate recharge to the aquifer and to collate natural discharges and groundwater abstraction data from the aquifer;
- to examine groundwater head fluctuations at observation wells;
- to construct an aquifer-simulation model to represent the recent history of the aquifer with particular reference to the saline groundwaters;
- to operate the aquifer model to explore the likely response of the aquifer and saline groundwater to changes in abstraction patterns or locations.

4.3. Results of the Project

The study revealed the complex hydrogeology depicted in fig. 3. A detailed geological picture of the area was established from surface information, drilling logs and surface and borehole geophysics. The main aquifer unit was defined as the upper part (approximately 50 m) of the Chalk, which has developed a fissure system irrespective of stratigraphy. Various other aquifer units were defined below the Chalk such as the Carstone and Roach and certain sandstones. Hydrochemical evidence confirmed that these lower units are in limited hydraulic continuity with the Chalk through faulting and natural fissure development.

In the western part of the area the Chalk-aquifer unit is unconfined; in the east, towards the coast, drift 'boulder clays' are present and the aquifer system becomes confined. Because of the presence of the saline groundwater bodies in the Chalk in the coastal areas, particular attention was paid to the lithologies of the drift and it was found that significant sand and gravel deposits (up to 15 m thick) exist particularly in the western part of the drift (fig. 4). The sands and gravels rest directly upon the Chalk, their deposition having been controlled by a Pleistocene cliff-line.

Hydrochemically the groundwaters were divided into four types based on a DUROV subdivision of major ions. The saline (NaCl) groundwaters were subdivided further using minor ions as shown in fig. 5. Three different saline bodies have been recognized and have been dated using tritium and radiocarbon methods. They are defined as:

- a saline zone east of Louth probably resulting from an Ipswichian saline intrusion entrapped beneath boulder clays;
- a saline zone in the north-east of the area dating from a Flandrian saline intrusion;
- limited modern saline intrusions in the vicinity of Immingham.

To substantiate the hydrochemical findings off-shore geophysical date were obtained from the Institute of Geological Sciences, and it was found that only limited possibilities of leakage between the aquifer and Humber estuary exist.

The geometry of the saline bodies was determined by surface resistivity methods. The resistivity survey was one of the most thorough ever conducted in the United Kingdom and a new technique, to allow one-man operation, was developed to speed the work.

The geological, geophysical and hydrochemical phase of the project proved two fundamental hydrogeological factors about the area over and above the general definition of the environment. These were:

- the significant extension of the aquifer storage by sands and gravels which provide groundwater to the Chalk during nonrecharge periods and thus retard potential westerly movement of the saline waters, and
- the important evidence that the bulk of the saline water is ancient and that only limited modern saline intrusion is possible.

Recharge to the aquifer system was calculated using the classical PENMAN evaporation-soil moisture balance (PENMAN, 1949). The recharge was examined on a digital model of the aquifer and it was found that, to reproduce the recorded well hydrographs, it was necessary to allow 15 % of effective precipitation to enter directly into the aquifer (RUSHTON & WARD, 1979; HOWARD & LLOYD, 1979).

4.4. The Aquifer Model

For modelling purposes both analogue and digital methods were adopted. The analogue approach was particularly useful in the early stages of analysis when various initial and boundary conditions were investigated. However, the digital computer solution, which used a backward difference time approximation (RUSHTON, 1974) was eventually found to be more useful when detailed numerical values were required. The model was constructed on a 2 km² grid and used a monthly time-step for 1961 - 1977. Transmissivities and storages used in the aquifer model were based on radial-flow model solution of pumping tests (RUSHTON, 1978). Results of the simulation obtained are shown in fig. 6 and 7. In fig. 7 it will be seen that the flow distribution has been modelled to produce minimal flow in the ancient saline-groundwater areas. Modern saline intrusion was modelled using leakage coefficients obtained by trial and error. Fig. 7 also clearly shows that the principal groundwater flows are to the major abstraction area of Grimsby and to certain spring outlets.

Abstraction variations were considered on the model as follows:

1. Constant abstractions of 145, 170 and 210 tcmd.
2. Abstraction as 50 % average during the winter and 15 % average during the summer months.
3. Certain industrial abstractions moved 5,7 km inland.
4. The possibility of conjunctive use with the Great Eau surface water scheme.

In considering the influence of saline waters in these modelled abstractions, reversals of groundwater head in the east were identified and translated into flows. Some of the results of option (1) are depicted in fig. 8 and clearly show that little additional water can be drawn from the aquifer under safe yield criteria. It was found that the redistribution of abstraction with time (2) was unacceptable but that the re-location of certain industrial abstractions (3) could be beneficial and reduce the westerly movement of saline water during low recharge periods. Conjunctive use studies (4) showed that additional water can be abstracted with such a scheme. In low recharge periods it was found that significant inflows of saline water would occur at Grimsby but that recovery would be rapid.

5. CONCLUSIONS

The problem of saline intrusion in the North Lincolnshire Chalk led to a three-year multi-disciplinary study. The integrated use of geophysical, hydrochemical and groundwater modelling techniques enabled a far clearer understanding to be reached of this complex aquifer, in particular:

- hydrochemistry was used to define hydraulic inter-continuity between the Chalk and the lower aquifers, and to define the principal flow mechanisms (LLOYD et al., 1977);
- minor ion chemistry was used to distinguish between saline groundwaters. These were subsequently dated, using carbon-14 and environmental isotope (tritium) technique (LLOYD & HOWARD, 1978); HOWARD & LLOYD, 1978), showing that two were ancient and one of recent origin;
- integrated surface and borehole geophysics were used to define the geometry of the aquifer and the overlying strata, and of the saline bodies of water (LLOYD et al., 1977; UNIV. BIRM., 1978);
- groundwater modelling was used to bring all the data together and in particular to refine estimates of recharge to the aquifer (RUSHTON, HOWARD & LLOYD, 1979).

The study culminated in a digital model of the aquifer which is being used to guide management and planning decisions on:

- the optimum rate of abstraction;
- possible re-location of abstraction to minimise risk of saline intrusions; and
- possible conjunctive use with surface resources, to increase total potable resources.

No such study, or model, can be perfect. The results obtained will be applied circumspectly and the aquifer model progressively refined in the light of practical experience.

6. ACKNOWLEDGEMENTS

Acknowledgements are due to the Anglian Water Authority for permission to present this paper. The views expressed are those of the authors and not necessarily shared by the Anglian Water Authority.

REFERENCES

HOWARD, K.W.F. & LLOYD, J.W. (1978). Iodide enrichment in the groundwaters of the Chalk aquifer, Lincolnshire, England. Int. Symp. Hydrochemistry of Mineralized Waters, Int. Assoc. Hydrogeologists; Cieplice Spa, Poland.

HOWARD, K.W.F. & LLOYD, J.W. (1979). The sensitivity of parameters in the PENMAN evaporation equations and direct recharge balance. J. Hydrol. 41, 329-344.

LLOYD, J.W. & HOWARD, K.W.F. (1978). Environmental isotope studies related to groundwater flow and saline encroachment in the Chalk aquifer of Lincolnshire, England. Isotope Hydrology 1, 311-325, IAEA-SM-228/18.

LLOYD, J.W., RUSHTON, K.R., TAYLOR, H.R., BARKER, R.D. & HOWARD, K.W.F. (1977). Saline groundwater studies in the Chalk of northern Lincolnshire. 5th Salt Water Intrusion Meeting, W.R.C.; Reading.

PENMAN, H.L. (1949). The dependence of transpiration on weather and soil conditions. J. Soil Sci. 1, 74-89.

RUSHTON, K.R. (1974). Aquifer analysis using backward difference methods. J. Hydrol. 22, 253-269.

RUSHTON, K.R. (1978). Estimating transmissivity and storage coefficient from abstraction well data. Ground Water 16, 81-85.

RUSHTON, K.R. & WARD, K. (1979). Estimation of ground water recharge. J. Hydrol. 41, 345.

UNIVERSITY OF BIRMINGHAM (1978). South Humberside Salinity Research Project. Final Report of the Anglian Water Authority.

FIGURES

Fig. 1: Location of major resources and major elements of regional transfer network.

Fig. 2: Location map of the study area.

Fig. 3: Hydrogeological features of the Chalk-aquifer system.

Fig. 4: Distribution of drift deposits.

Fig. 5: Characterization of the saline waters using the relationship between I^- and Cl^- ions.

Fig. 6: Comparison of actual and modelled water levels.

Fig. 7: Modelled groundwater-flow distributions.

Fig. 8 a: Response of the aquifer to alternative abstraction rates (head).

Fig. 8 b: Response of the aquifer to alternative abstraction rates (flow).

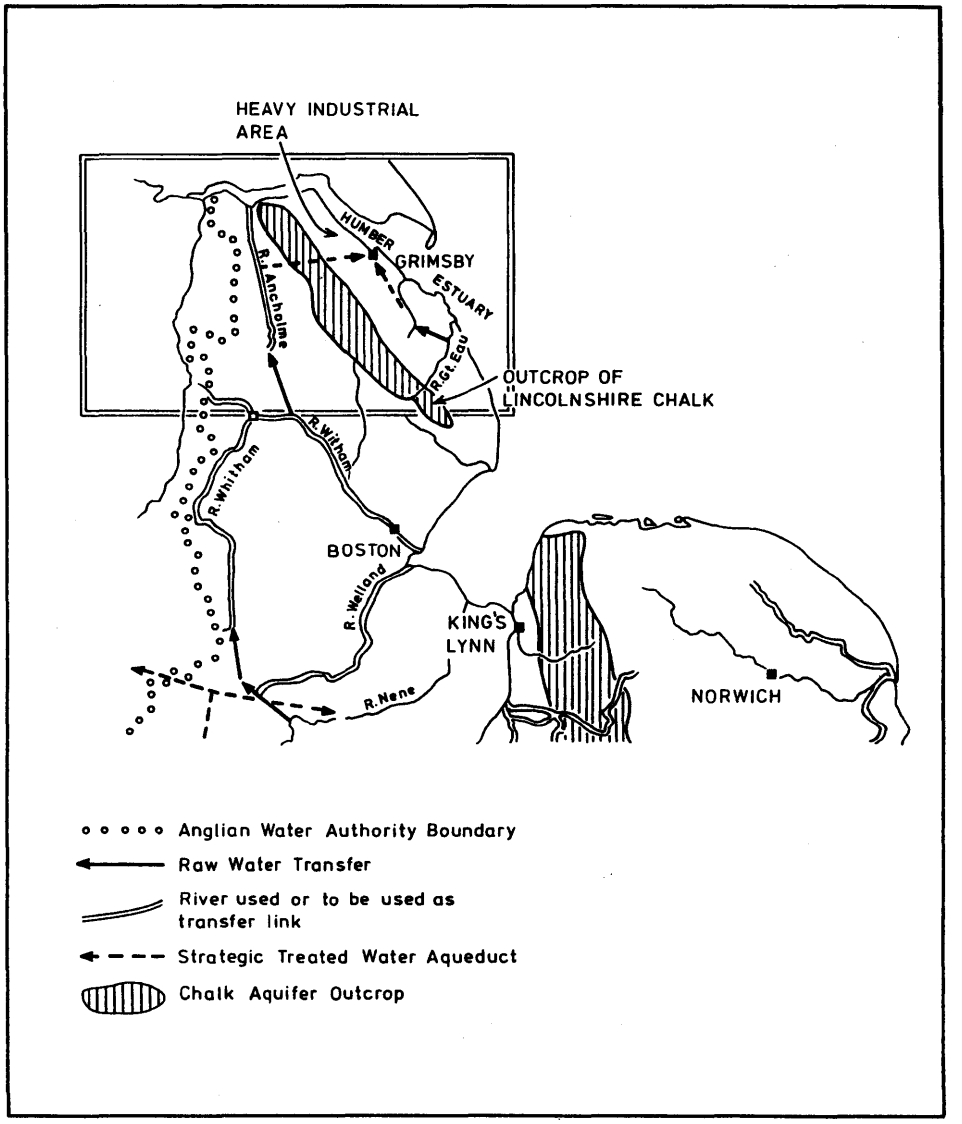

ANGLIAN WATER RESOURCE NETWORK IN STUDY AREA.

Figure 1

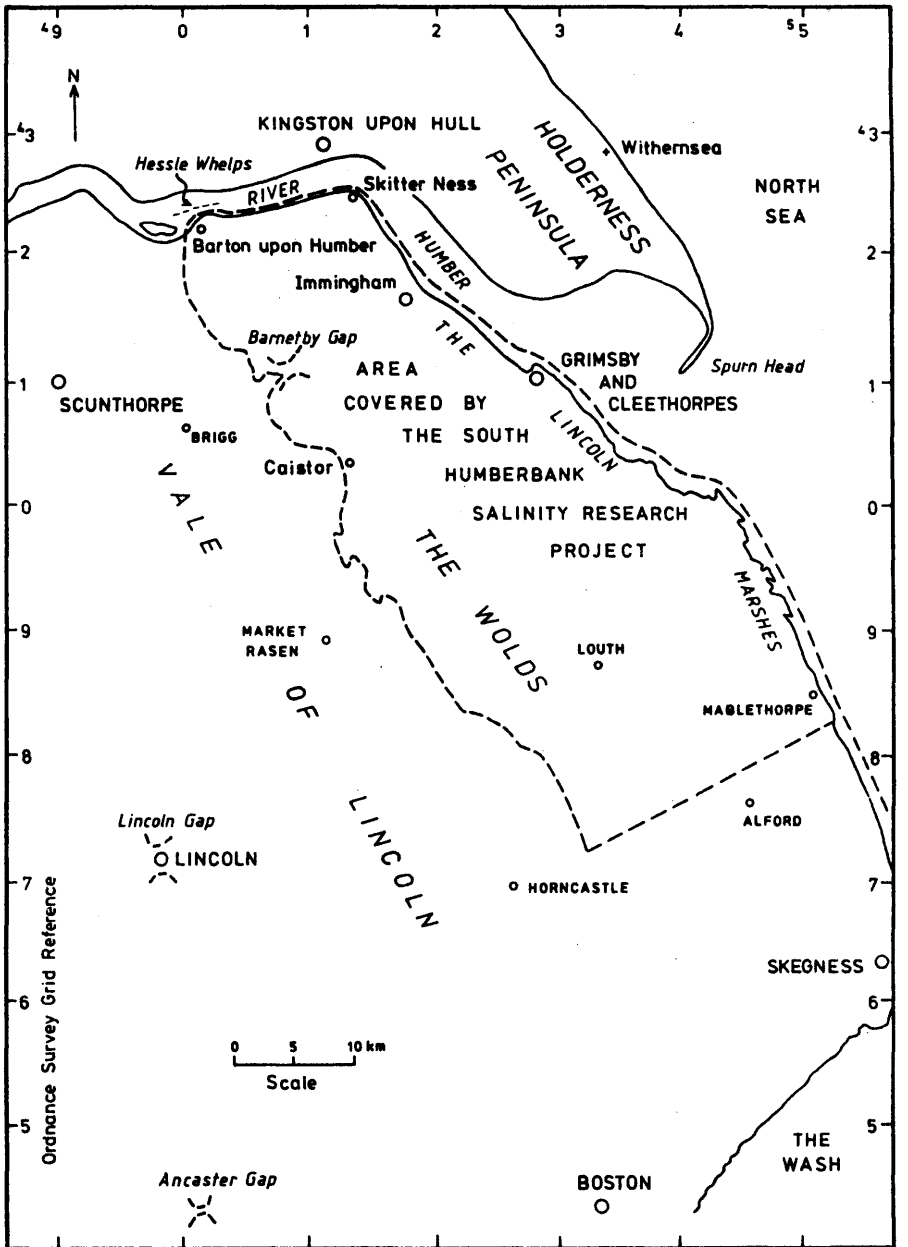

LOCATION MAP OF THE STUDY AREA FIGURE 2

Figure 3

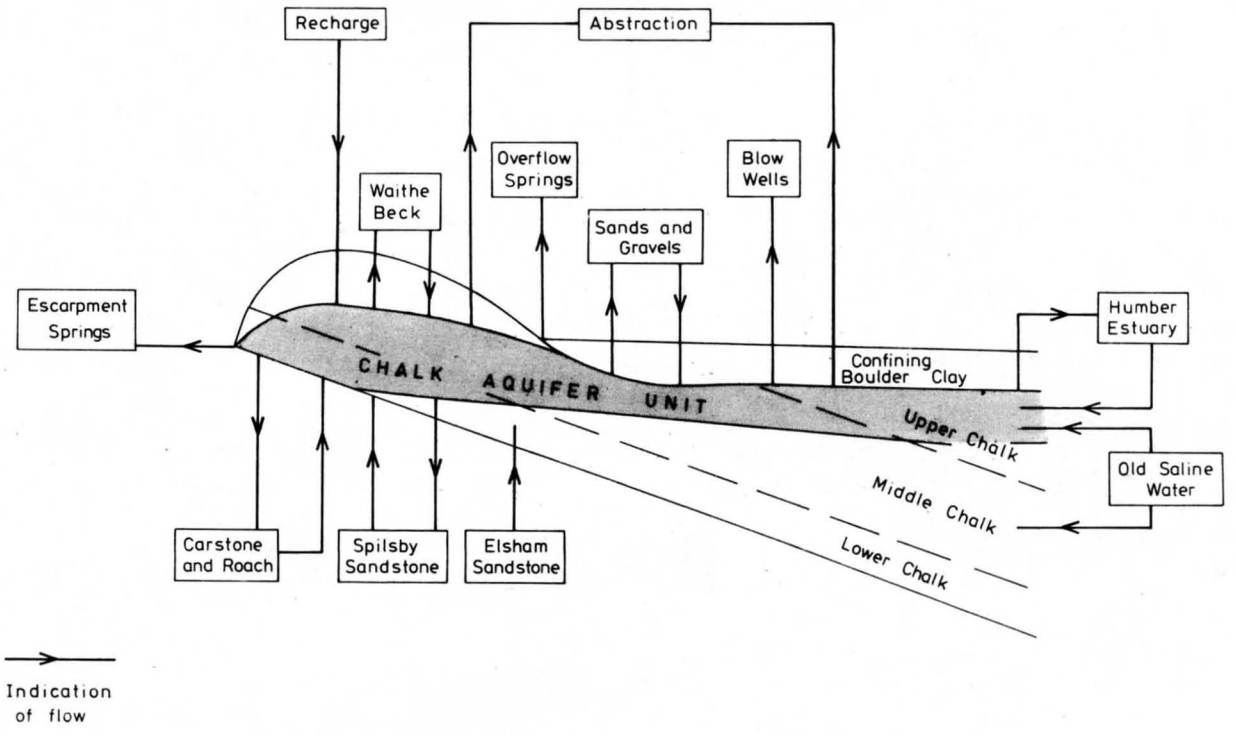

HYDROGEOLOGICAL FEATURES OF THE CHALK AQUIFER SYSTEM

FIGURE 3

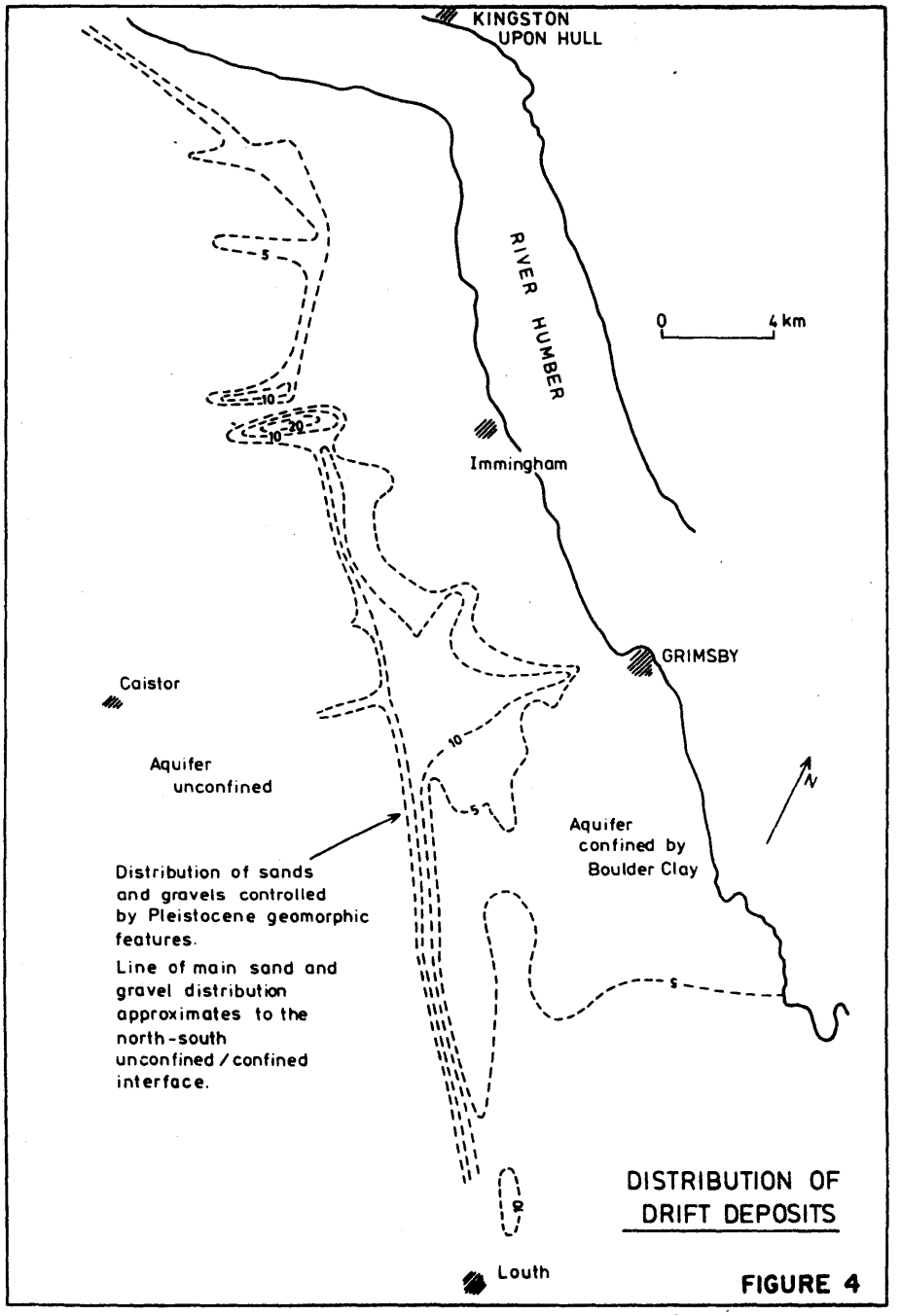
KINGSTON
UPON HULL
RIVER HUMBER
0
4 km
Immingham
GRIMSBY
Caistor
Aquifer
unconfined
Aquifer
confined by
Boulder Clay
N
Distribution of sands
and gravels controlled
by Pleistocene geomorphic
features.
Line of main sand and
gravel distribution
approximates to the
north-south
unconfined / confined
interface.
5
10
20
Louth
DISTRIBUTION OF
DRIFT DEPOSITS

FIGURE 4

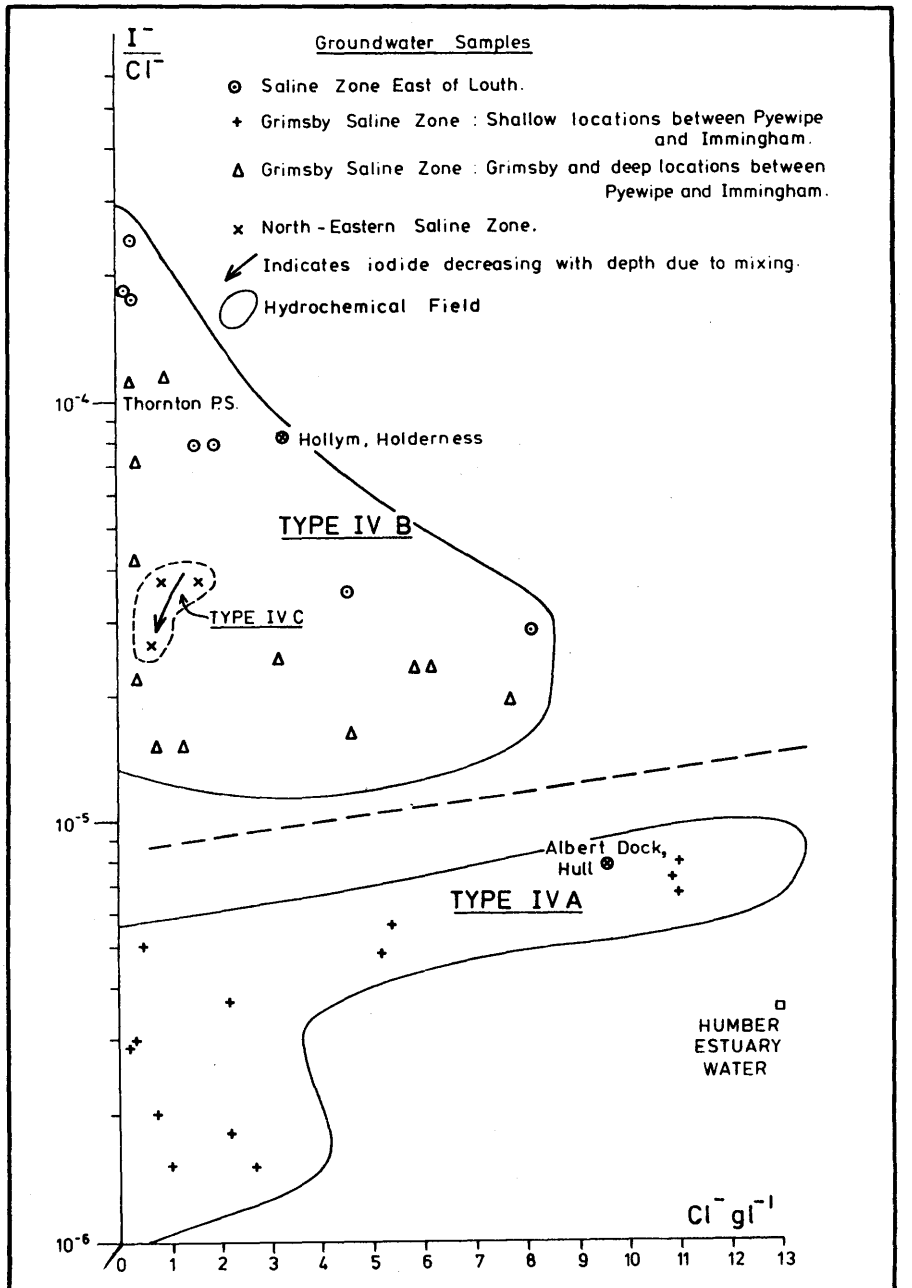

CHARACTERIZATION OF THE SALINE WATERS USING THE RELATIONSHIP BETWEEN I^- AND CL^- IONS.

Figure 5

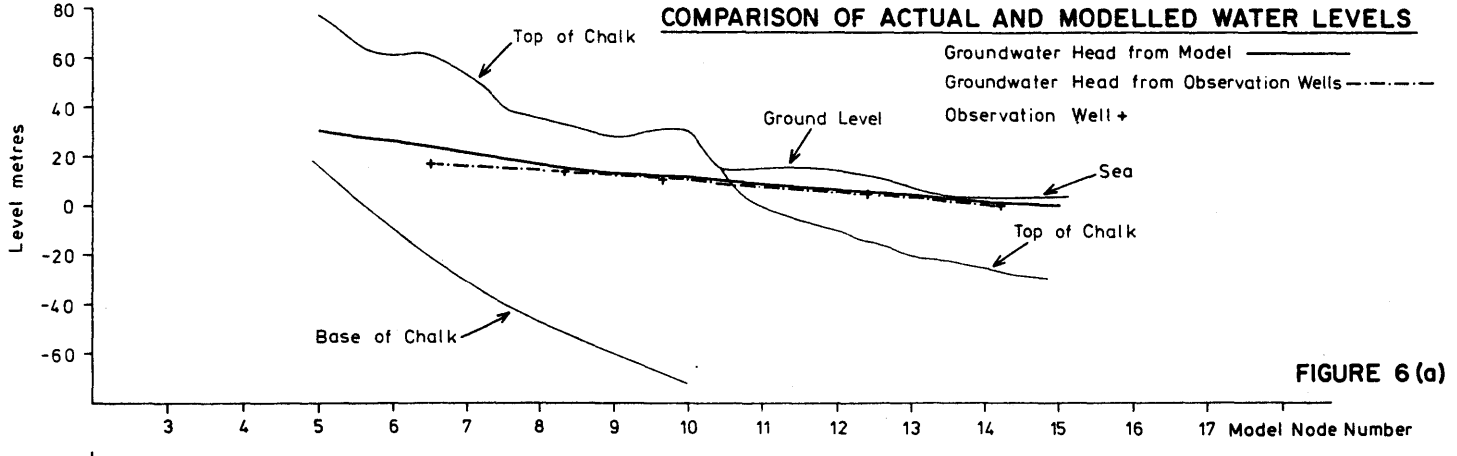

FIGURE 6(a)

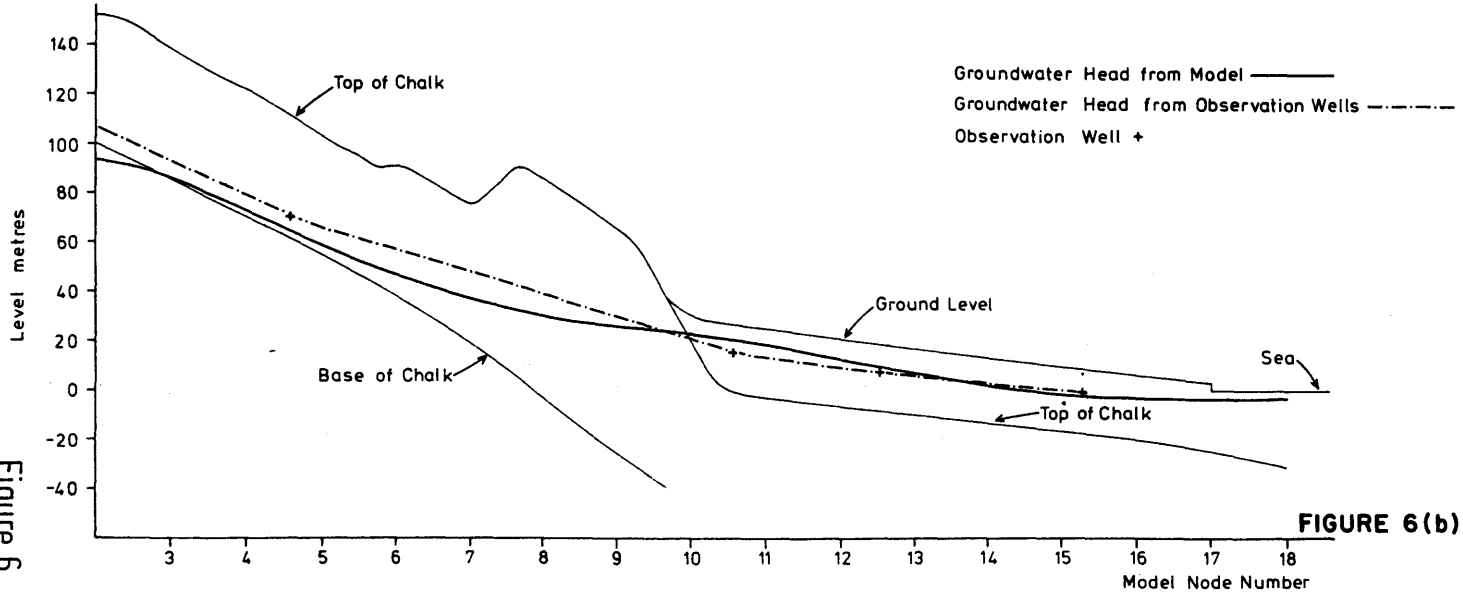

FIGURE 6(b)

Figure 6

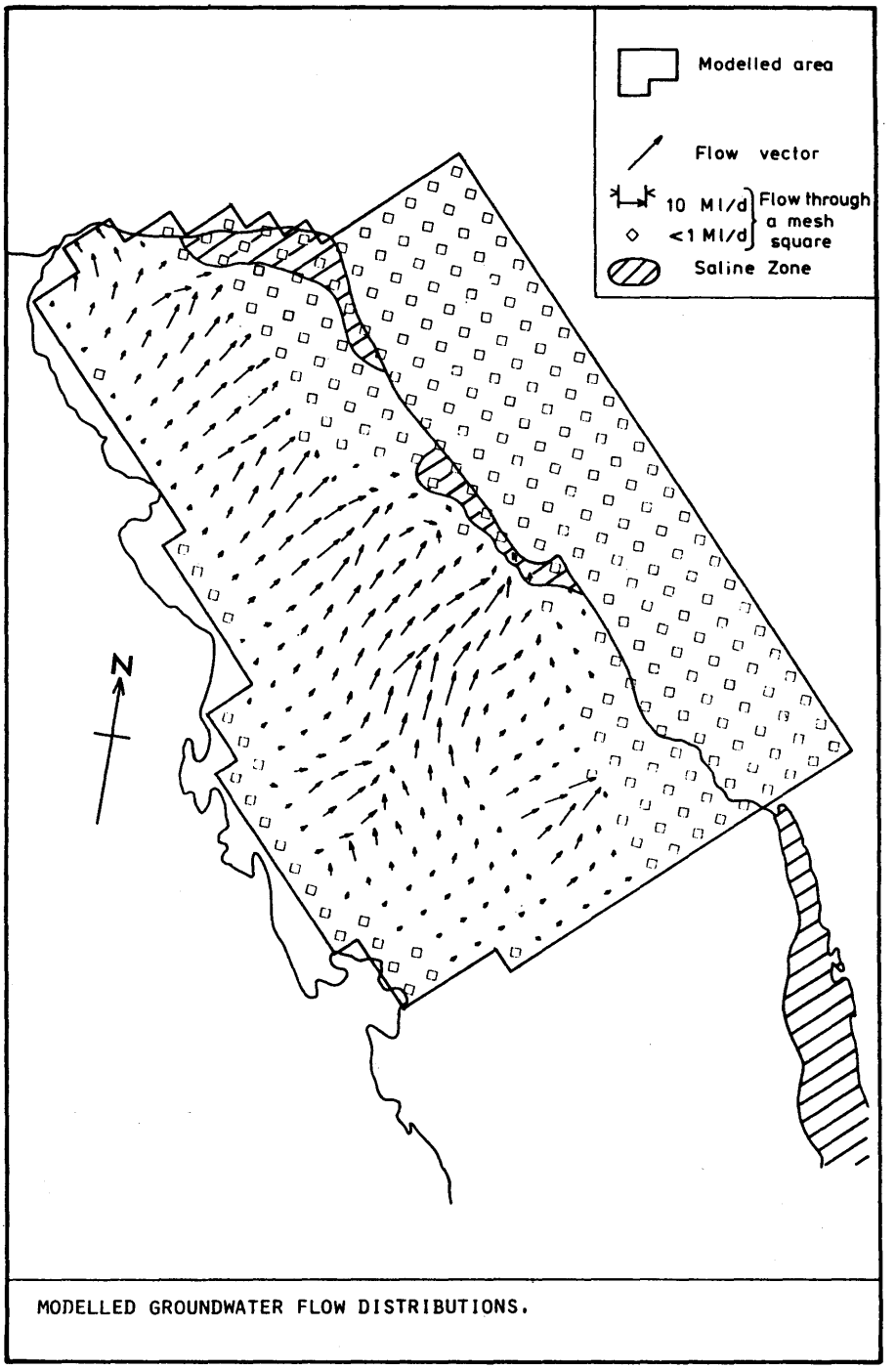

MODELLED GROUNDWATER FLOW DISTRIBUTIONS.

Figure 7

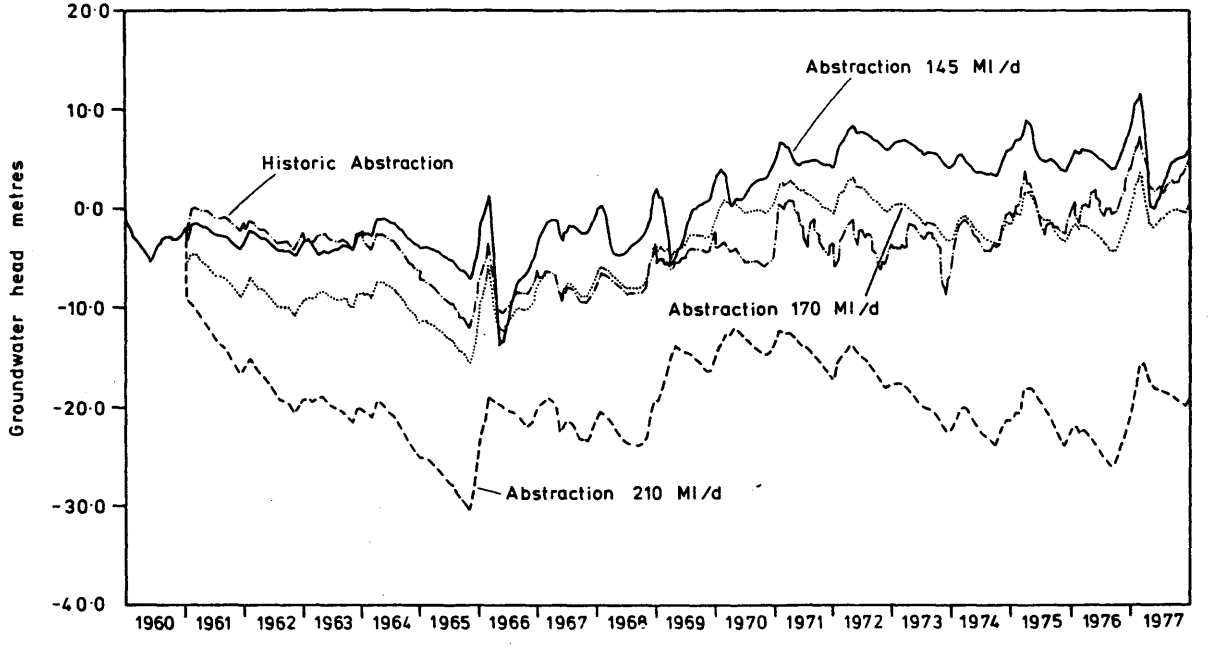

RESPONSE OF THE AQUIFER TO ALTERNATIVE ABSTRACTION RATES (HEAD)

FIGURE 8(a)

Figure 8(a)

Figure 8(b)

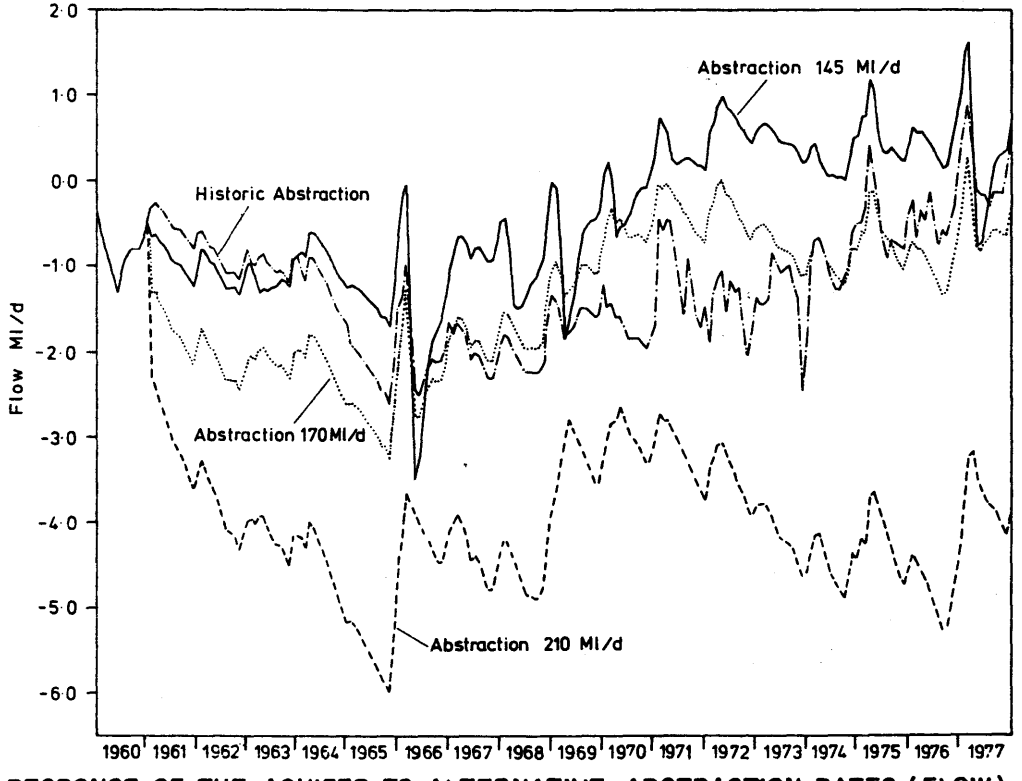

RESPONSE OF THE AQUIFER TO ALTERNATIVE ABSTRACTION RATES (FLOW) FIGURE 8(b)

2.5. THE EVOLUTION OF FRESH-WATER/SALT-WATER EQUILIBRIUM IN CONNECTION WITH WITHDRAWALS FROM THE COASTAL CARBONATE AND KARSTIC AQUIFER OF THE SALENTINE PENINSULA (SOUTHERN ITALY)

T. TADOLINI & L. TULIPANO

ABSTRACT

The Mesozoic carbonate rocks of the Salentine Peninsula, in which permeability results from fractures and karst action, contains a huge mass of groundwaster floating over continental intrusions of seawater with the sea horizon as its base level.

The phenomena that govern the influence of salt water on fresh water in the aquifer have been studied for over ten years by experimental surveys made in observation wells penetrating the seawater intrusions. At present the conditions of equilibrium between the two types of water are undergoing a change.

This fact can only be ascribed to water withdrawals which have been greatly intensified during these past ten years, and is mainly revealed by the changing depth and thickness of the transition zone between the two types of water and by a general increase in the average salt content of fresh groundwater.

1. INTRODUCTION

The Salentine Peninsula provides a typical example of a fractured and karstic coastal aquifer. Its geological rock basement is formed by Cretaceous limestones, dolomitic limestones and dolomites that are usually permeable owing to fractures and karstification.

A huge aquifer is embedded in these rocks. Groundwater is supplied to the aquifer by a certain amount of the autumn and winter rains falling on the region (COTECCHIA et al., 1973 b; TADOLINI et al., 1976). Inside the aquifer, fresh groundwater floats on continental intrusions of seawater, with the sea horizon as its base level (COTECCHIA et al., 1973 a).

Piezometric heads are usually low: about 3 m above mean sea level at most. Hence, saline water is encountered underlying fresh groundwater at ccmparatively shallow depths. This strongly limits the possibility of using the aquifer as a water resource since there is always a danger that the equilibrium between fresh and saline groundwater will be greatly disturbed resulting in salt contamination.

Our studies were started about ten years ago with the aim to investigate in what way fresh groundwater is influenced by the underlying water of marine origin. Essentially, the work was based on surveys made by means of observation wells which had been sunk low enough to penetrate the seawater encroaching into the mainland. This work was supported all along by conventional hydrogeological surveys performed on a region a scale.

As a general rule, our findings always revealed that the fresh-groundwater saline-groundwater relationship is greatly affected by the peculiar anisotropy of the aquifer.

This work is especially concerned with certain specific aspects of the influence exerted by seawater upon fresh groundwater. Specifically, the conditions of equilibrium between the two types of water in the various parts of the peninsula and their evolution with time following continuous withdrawal are discussed.

Another point of interest is the possibility of identifying the "preferential flow levels" at which water is drawn during the pumping tests. This can be done using the salt content of pumped water as a natural tracer.

In connection with this latter point, the real discharge capacity of the well is discussed in connection with the presence of such "preferential flow levels".

2. SPECIFIC ASPECTS OF GROUNDWATER FLOW

Before we analyse the subject phenomena in detail, it may prove useful to describe briefly some of the specific characteristics of groundwater flow by which such phenomena may be strongly affected.

In the Salentine Peninsula, the genesis and development of karstification are essentially related to the paleogeographic history of the area and especially to the glacio-eustatic fluctuations of the mean sea level (COTECCHIA et al., 1969).

It is an accepted fact that the karstic dissolution of carbonate rocks is governed not only by the different rates of karstification of the different lithotypes making up the formation, but also by the different modes of groundwater travel through the various parts of the aquifer (COTECCHIA et al., 1975). The presence of CO_2 and certain ions in the water may favour the dissolution process. Sufficient concentrations for this depend, among other things, on the mobility of the water within the aquifer.

With respect to the glacio-eustatic fluctuations of the sea level, karstic dissolution occurs - all other conditions being equal - when the hydrological and hydrochemical conditions stay unchanged over sufficiently long geological periods of time.

It is obvious that a change in the depth of the base of the groundwater flow causes new levels to undergo karstic dissolution, just as it may happen that previously karstified levels will become fossilized. Add to this the vertical sequence inside the aquifer of scarcely karstifiable or unkarstifiable (COTECCHIA et al., 1973 b; GRASSI, 1974) and of highly karstifiable layers, and it will soon become apparent that in reality water slows at present along

subhorizontal levels that are characterized by a high rate of permeability and are interbedded by scarcely pervious, if not practically impervious, rock horizons (TADOLINI & TULIPANO, 1977 a).

Because of this, vertical flow often occurs in wells drilled into an aquifer. This flow usually results from the water levels being crossed by wells having different heads (COTECCHIA et al., 1973 a).

The fact that groundwater rests on water of marine origin at its base has produced a true vertical stratification of the salinity of the water in the aquifer. The increase in salinity with depth is very low within the fresh groundwater compared to the much faster increase near the water of marine origin - which reveals the presence of a transitional zone (TADOLINI & TULIPANO, 1970). In practice, the aquifer contains clearly differing salt concentrations at different depths which appear to correspond to the changing mobility of water within the aquifer, hence to the distribution of the "preferential flow pathways" mentioned earlier.

The above findings were also obtained from direct measurements of the distribution of filtration velocity by means of radioactive tracers, as well as by analysing the distribution of groundwater temperature, which can be adequately used as an environmental tracer. Temperature changes along a vertical column in the aquifer are correlated to the different rates of water mobility along the water levels that make up the aquifer (COTECCHIA et al., 1973).

By the same measurements it was also determined that the seawater encroachment into the peninsula is practically at a stillstand, with the exception of the areas closest to the coast. Consequently, the temperature gradient at the transition from fresh water to salt water was found to be positive and high.

3. THE EQUILIBRIUM BETWEEN FRESH GROUNDWATER AND SALINE GROUNDWATER AND ITS CHANGES WITH TIME

Just as in any other coastal aquifer the changeover from fresh water to salt water - as already stated above - is marked by the presence of a transition zone in which water salinity increases more or less rapidly with increasing depth.

The thickness of the transition zone varies considerably at different sites, but is generally greater in most of the inland areas, and drops down to a few decimetres further towards the coast (fig. 1, 2). Far from being stable, this transition zone is subject to changes in both depth and thickness. These changes can be correlated with the mode of groundwater recharge as well as to the withdrawals which are a common practice in the region, particularly for irrigation purposes (COTECCHIA et al., 1974).

Until a few years ago, when the amount of pumping from the aquifer was compatible with the actual rate of annual recharge, vertical movements in the transition zone were practically comparable to fluctuation wells in line with the annual recharge cycles.

These vertical displacements are especially evident at the interface between the transition zone and the seawater intrusion.

Fig. 3 shows the behaviour of the transition zone since 1974 in the most representative observation wells.

It will be observed that some of the wells already show a tendency for the seawater to rise. The most striking evidence of such phenomena is observed in wells SR, LR and TA, whereas no seawater rise was recorded in wells CH2, ST1 and CS. CS, however, already shows a tendency for the seawater to behave as in the other wells since the 3 g/l isohaline has moved upwards and since this displacement occurred in no more than one and a half years.

The equilibrium conditions which govern the co-existence of fresh water and brackish water result from (a) a merely static equilibrium due to a less dense water simply floating over one of higher density, (b) the dynamic conditions of groundwater flow, (c) groundwater recharge, (d) water drafts, (e) the effects of changing atmospheric pressures on the level of the water table, (f) periodic and non-periodic fluctuations of the sea level, and (g) the effects of possible difference between the mean levels of the two seas bordering the Salentine Peninsula even for long stretches of time (TADOLINI & TULIPANO, 1974, 1977 b).

Clearly, the dominant phenomenon is that of less dense fresh water floating on salt water of higher density.

Since we can use a number of observation wells scattered all over the Salentine Peninsula (fig. 1), it may be useful to note the real conditions of equilibrium in the aquifer with respect to the actual depths of the encroaching seawater, the vertical distribution of salinity, and the measured water heads.

The density of water is a function of its salt content and temperature. By measuring in the laboratory, on a precision hydrostatic scale, the density of a large number of water samples and by determining total salt content by means of chemical analyses, linear relationships between salt content and water density were obtained at the various temperatures that are typical of the groundwater in the Salentine Peninsula (fig. 4).

Thus, for each determination in the well, the weighted average densities of the entire water column above seawater were determined, including the transition zone. Table 1 reproduces the resulting data for each of the different wells.

Starting from the exact measurement of the head $\underline{t}$ in each well at the time the survey was made, and considering the real densities of the water columns present in each well, one can determine the theoretical depth (H_t) of the bottom of the transition zone from the sea level. This depth seems to correspond to conditions of purely static equilibrium. In practice, this is equivalent to applying the well-known Ghyben-Herzberg law, since the calculated coefficient is $K = d_f/(d_m-d_f)$, except that here the real densities of all the water in the aquifer are considered namely, the overlying fresh water, that of the transition zone, and the underlying seawater having a density of 1,02750 g/cm³.

Fig. 3 shows, along with the representation of the trends of equal salt content versus time in the transition zone, the theoretical depths at which seawater is encountered in each well. It will be noted that the two depths - the theoretical and the observed depths - differ little in a few cases, but that the difference is much greater as a general rule.

With regard to the hydrogeology of the region at large, especially in connection with the evolution of pumping practices, it will be realized that, wherever there is an equilibrium between withdrawal and supplies, the differences between the data given in the tables are quite low. Conversely, the largest differences are observed in the observation wells in the area where demand for water is steadily growing and is met, even to this day, by drawing indiscriminately upon the aquifer.

By way of example, we shall describe the situation at well TA, which used to be in equilibrium until a few years ago. The difference between the theoretical and the observed values of the depth at which seawater used to be found was about one metre. Today, this difference is already in the order of some 50 m. The most striking consequences are the tendency for seawater to rise and a salinization, however mild, of the entire water column above, which causes the average density of the water to increase due to the fact that the whole aquifer is now seeking a new equilibrium.

Well MS represents a special case: if the levels of the isohalines observed in the well are compared with the calculated theoretical depth of the encroaching seawater, it will be noted that until at least 1976 differences from the real depth of seawater are not very marked.

For sake of precision, it should be pointed out, in this connection, that well MS cannot be regarded as a perfect observation well because it does not penetrate deep enough into the seawater. Since the overall conditions of the area, within which the well is located, are known, and considering the remarkable thickness of the transition zone, one might conclude that the present vertical distribution of salinity reflects an earlier condition of marked disequilibrium which has now been offset by a strong upward expansion of the transition zone, which now occupies almost the entire thickness of the aquifer.

Nevertheless, if the water samples drawn in 1979 are examined, it would appear that a new process of disequilibrium is setting in at present. Very likely, this will result in a further expansion of the transition zone, a marked rise of seawater, and a further considerable increase in the average salt content of the whole water column. Future surveys will be also aimed at investigating this possible development.

In conclusion, our study of the present conditions of equilibrium between fresh groundwater and seawater suggests that what can be considered to be the only locally available water resource is being severely curtailed. Judging by the comparatively slow rate at which this phenomenon is developing, it should be concluded that ideal conditions of equilibrium can be restored only in the long term and only if groundwater withdrawals are immediately brought under careful control so that they will become strictly compatible with the rate of groundwater recharge.

4. IDENTIFICATION OF PREFERENTIAL FLOW PATHWAYS THROUGH PUMPING TESTS

The preceding paragraphs are a description of current phenomena at a regional scale. We think it worthwhile to describe what goes on in a single well when it drains water from an aquifer of this kind.

One of the main problems in connection with the withdrawal of groundwater from coastal aquifers is that it is extremely difficult to decide what would be the ideal "working" discharge, given the need to avoid, or to reduce to a bare minimum, local upward flow of brackish or even saline water.

While a problem like this can be easily solved on mathematical grounds when dealing with a homogeneous and isotropic aquifer, it becomes extremely complex in the case of highly heterogeneous aquifers such as those of the Salentine Peninsula.

It might therefore be useful to describe a methodology applicable to individual wells and thus to offer an indication about what a "safe" pumped discharge would be.

It has already been mentioned that the Salentine aquifer actually consists of a vertical sequence of water-bearing layers along which water tends to find its way out. It is further recalled that thermosalinometric logs reveal any significant changes, however small, of the characteristics of temperature and salinity of the waters corresponding to the occurrence of one or more such layers along the vertical column in a well.

If these measurements are taken before a pumping test is made, it will be easily realized that the water removed by pumping will be drained by one or more such pathways, depending on the rate of withdrawal. This can be obtained by comparing

the salt stratification in the well at rest and the continuous recording of the salt content of the pumped water.

Figs. 5 and 6 show the trends of discharges and the corresponding drawdown with time, as observed through a series of trials. Salinity of water withdrawn by pumping is plotted against time. In the diagram, these trends are correlated to the saline stratification observed in the wells before the trials.

By means of this kind of representation in graph form, one can easily recognize the depth from which the water pumped at specific discharge values is derived - a fact which is irrespective of the position of the pump along the vertical column in the well.

The diagrams show the most characteristic situations revealed by the study.

Generally speaking, it was observed that pumping initiates flow from "preferential flow levels" which may be only a few decimetres or as much as several metres thick.

In some instances it was also observed that pumping removes water from levels that are obviously lower than the depth tapped by the well, since in such cases the salt content of pumped water is greater than that shown by logs made in a well at rest.

Moreover in only a few instances does the salinity of the water removed by pumping increase with time. Quite often such changes are independent of the withdrawal rate.

The observations described above have also been checked by means of specially arranged pumping tests of long duration. In one instance, this was done simultaneously for a group of three neighbouring wells to monitor any possible mutual interference.

In the average, the duration of the test was 10 days during which hydrological and hydrochemical surveys were also made in wells near the observation wells, whenever this was feasible (fig. 7 and 8).

A rather peculiar situation is shown by the test made in well No. 40 (fig. 6). The well has the following characteristics: static head 1,74 m at test time; penetration into the aquifer approx. 40 m. With regard to the measurements taken at observation well DA, about 4 km away from the test well, it could be concluded that the encroaching seawater was about 100 m below mean sea level, whereas the top of the transition zone must be quite close to the bottom of the well.

The test was carried out for 52 hours and the peak discharge obtained was 50 l/s with the corresponding dynamic drawndown being approx. 6 m. The salinity of the pumped water remained constant around 0,4 g/l for any rate of withdrawal, showing

that the water was drawn from a water-bearing layer in about the top five metres of the aquifer. As soon as the test was completed, another thermosalinometric log was taken. The corresponding diagram shows that the upper portion of the transition zone has risen while, as already stated, it must have initially been quite close to the bottom of the well. Despite this fact, no increase was noticed in the salt content of the water pumped from the well.

It is also interesting to note that a further thermosalinometric log, performed a few days later, showed that exactly the same conditions existing prior to the trials had been restored along the entire water column in the well.

During the same test it was also found that pumping affected the levels of two wells located about 1300 m apart and that well lowering was limited, in this case, to just 4 cm compared to the 6 m observed in the test well.

On the basis of all the results obtained in our study, it can be concluded that whenever a well crosses a series of "preferential flow pathways", the first pumped water is drawn from the layer having the highest permeability. Later on, when the pumped discharge is more than the potential capacity of this first layer, water is gradually drawn from the other levels in the series.

By observing the salinity trend of pumped water as related to the withdrawal rate, it is possible to get at least some indication about the potential capacity of the various water levels.

It is worth pointing out that, at least as long as the tests are under way, there is no indication of changes in the salt content which would be strong enough to suggest that an intrusion cone of salt water has been formed, not even in those instances in which dynamic lowering was remarkably strong and in any case sufficient to produce an intrusion cone of salt water if the test medium had been a hypothetical homogeneous and isotropic aquifer.

Our conclusion is that this study seems to provide the means needed to decide what should be the discharges that can be safely drawn from individual wells without any danger of contamination.

Obviously, the major problem is to find ways and means of implementing a co-ordinated and general policy for the management of groundwater in an aquifer of this kind, so that the total sum of discharges drawn from it will be in harmony with its hydrological equilibrium.

A distribution of groundwater flow along several preferential flow pathways can be regarded as a favourable short-term condition with respect to salt contamination produced by pumping. However, there are also long-term effects when groundwater withdrawals are greater than the aquifer's overall potential recharge. This danger has been revealed with sufficient clarity by the investigations carried out to date and by the conclusions on the present conditions of equilibrium described in this paper.

REFERENCES

COTECCHIA, V. (1955). Influenza dell'acqua marina sulle falde acquifere in zone costiere, con particolare riferimento alle ricerche di acqua sotterranea in Puglia. Geotecnica, 3.

COTECCHIA, V., DAI PRA, G. & MAGRI, G. (1969). Oscillazioni tirreniane ed oloceniche del livello mare nel golfo di Tatanto, corredate da datazioni col metodo del radiocarbonio. Geol. Appl. e Idrogeol, (Bari), 4.

COTECCHIA, V., TADOLINI, T., TAZIOLI, G.S. & TULIPANO, L. (1973 a). Studio idrogeologico della zone della sorgente Chidro (Taranto). 2° Conv. intern. sulle Acque Sott; Palermo.

COTECCHIA, V., TADOLINI, T. & TITTOZZI, P. (1973 b). Precipitazioni secche in Puglia e loro influenza sul chimismo delle acque alimentanti la falda sotterranea. Geol. Appl. e Idrogeol. (Bari), 8.

COTECCHIA, V., TADOLINI, T. & TULIPANO, L. (1974). The results of researches carried out on diffusion zone between fresh water and sea water intruding the land mass of Salentine Peninsula (Southern Italy). Intern. Symp. Hydrol. volcanic Rocks; Lanzarote, Canary Island, Spain.

COTECCHIA, V., TADOLINI, T. & TULIPANO, L. (1978). Ground water temperature in the Murgia karst aquifer (Puglia - Southern Italy). Intern. Symp. Karst Hydrology; Budapest.

COTECCHIA, V., TADOLINI, T. & TITTOZZI, P. (1975). Geochimica delle acque della Peninsola Salentina (Italia Meridionale) in relazione ai processi di dissoluzione carsica in zona satura. Conv. intern. sulle Acque Sott.; Palermo.

GRASSI, D. (1974). Il carstismo della Purgia (Puglia) e sua influenza sull' idrogeologia della regione. Geol. Appl. e Idrogeol. (Bari), 9.

TADOLINI, T. & TULIPANO, L. (1970). Primi risultati delle ricerche sulla zone di diffusione della "falda profonda" della Penisola Salentina (Puglia). 1° Conv. intern. sulle Acque Sott.; Palermo.

TADOLINI, T. & TULIPANO, L. (1974). Differenze di livello tra mare Adriatico e mare Ionio e considerazioni sui riflessi sulla circolazione idrica sotterranea della Penisola Salentina (Puglia). Geol. Appl. e Idrogeol. (Bari), 9.

TADOLINI, T. & TULIPANO, L. (1977). Identification by means of discharge tests of water-bearing layers in fractured and karstic aquifers through the analysis of the chemico-physical properties of pumped waters. Symp. "Hydrodynamic diffusion and dispersion in porous media"; Pavia.

TADOLINI, T. & TULIPANO, L. (1976). The conditions of the dynamic equilibrium of ground water as related to encroaching sea water. Symp. "Hydrodynamic diffusion and dispersion in porous media"; Pavia.

TADOLINI, T., TULIPANO, L. & ZANFRAMUNDO, P. (1976). La falda idrica della zone compresa tra Vico del Gargano ed Ischitelle (Puglia): caralleristiche ed equilibrio idrologico. Giornale del Genio Civile 10, 11, 12.

ZEZZA, F. (1975). Le facies carbonatiche della Puglia e il fenomeno carsico ipogeo. Geol. Appl. e Idrogeol. (Bari), 10.

FIGURES

Fig. 1: Location of observation wells (1) and pumping test wells (2).

Fig. 2: Salinity and temperature logs in observation wells.

Fig. 3: Variations in time of the trend of salinity stratification within the transition zone. The grey bands represent the theoretical elevation of the salt water.

Fig. 4: Groundwater salinity (TDS in g/l) vs. density (in g/cm^3).

Fig. 5: Discharge and drawndown vs. time (solid line and hyphenated line) in the upper portion of the diagrams; saline stratification (solid line) in the lower diagram drawn against the depth scale, and salinity trend of pumped waters (hyphenated line in the lower diagram) drawn against the time scale. The section level of the pump is marked on the depth scale.

Fig. 6: Discharge test of medium duration carried out in well nos. 40, 71, 29 and 82. On the right side discharge (Q) drawndown (Δh) and salinity trend (TDS) of pumped water vs. time. On the left side saline stratification of the water column of the well before (unbroken line) and after (hyphenated line) the pumping test.

Fig. 7: Discharge test of long duration carried out in well 50 and saline stratifications in the same well and in the adjacent wells 48, 49 and 51 before and after the test: saline stratification remained constant in wells 49 and 51.

Fig. 8: Discharge test of long duration carried out at the same time in wells 16 (solid line), 6 (dotted-hyphenated line) and 7 (hyphenated line). In the upper part saline stratifications before (solid line) and after (hyphenated line) the pumping test.

TABLES

Tab. 1: Real head t (m), weighted average densities (δ_f) of the entire water column above seawater, calculated coefficient $K = \delta_f/(\delta_s-\delta_f)$, real ($H_t$) and theoretical ($H_t$) depth of the bottom of the transition zone from the sea level. Values for each observation well.

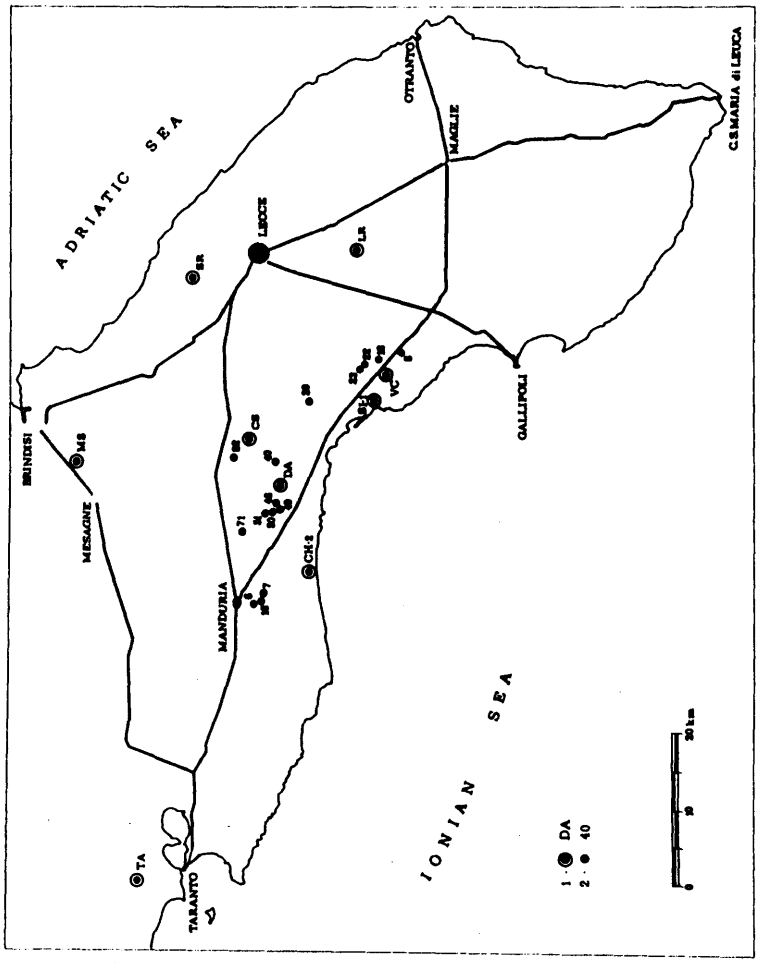
ADRIATIC SEA
IONIAN SEA
BRINDISI
MESAGNE
MANDURIA
TARANTO
LECCE
OTRANTO
MAGLIE
GALLIPOLI
C.S.MARIA di LEUCA
1 - DA
2 - 40
30 km

Figure 1

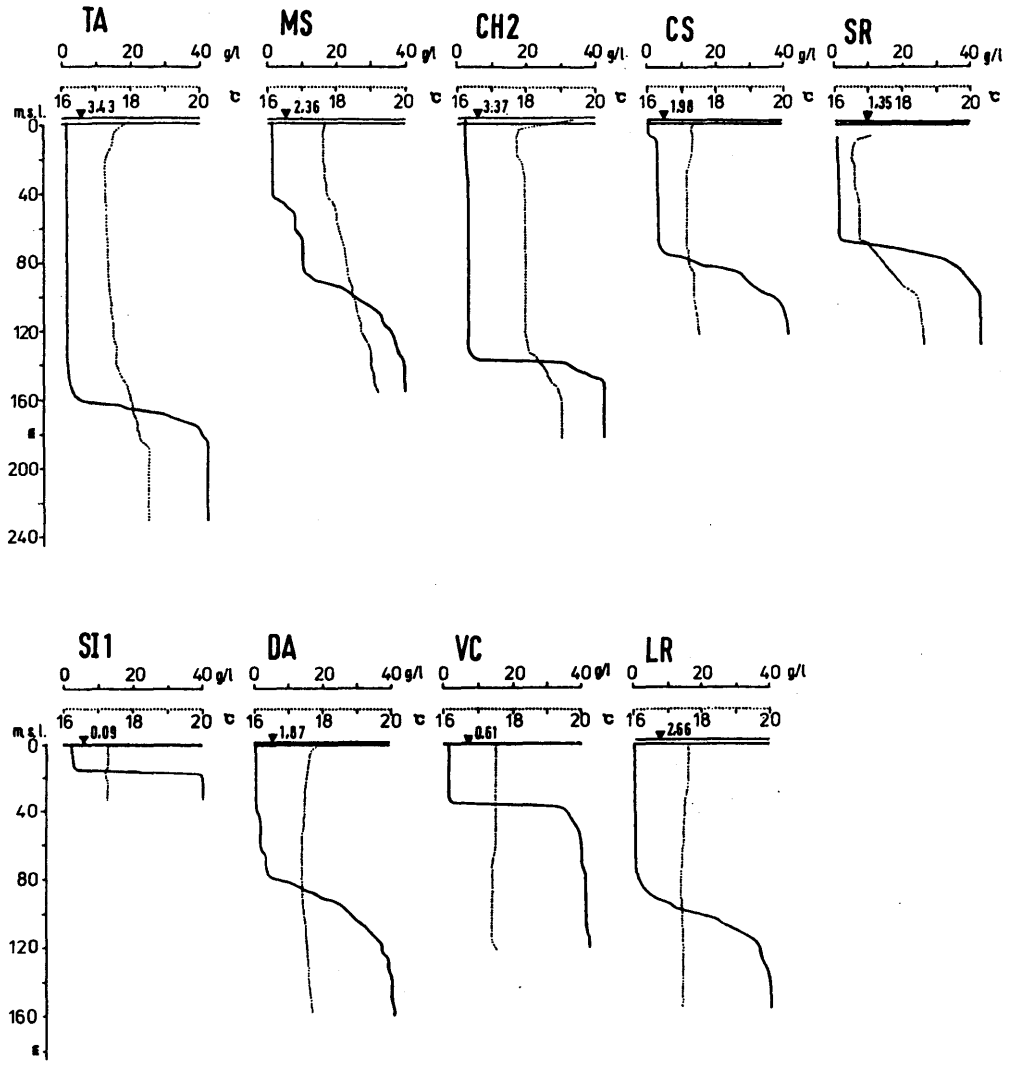
TA
MS
CH2
CS
SR
SI1
DA
VC
LR
0 20 40 g/l
16 18 20 °C
m s.l.
0
40
80
120
160
200
240
3.43
2.36
3.37
1.98
1.35
0.09
1.87
0.61
2.66

Figure 2

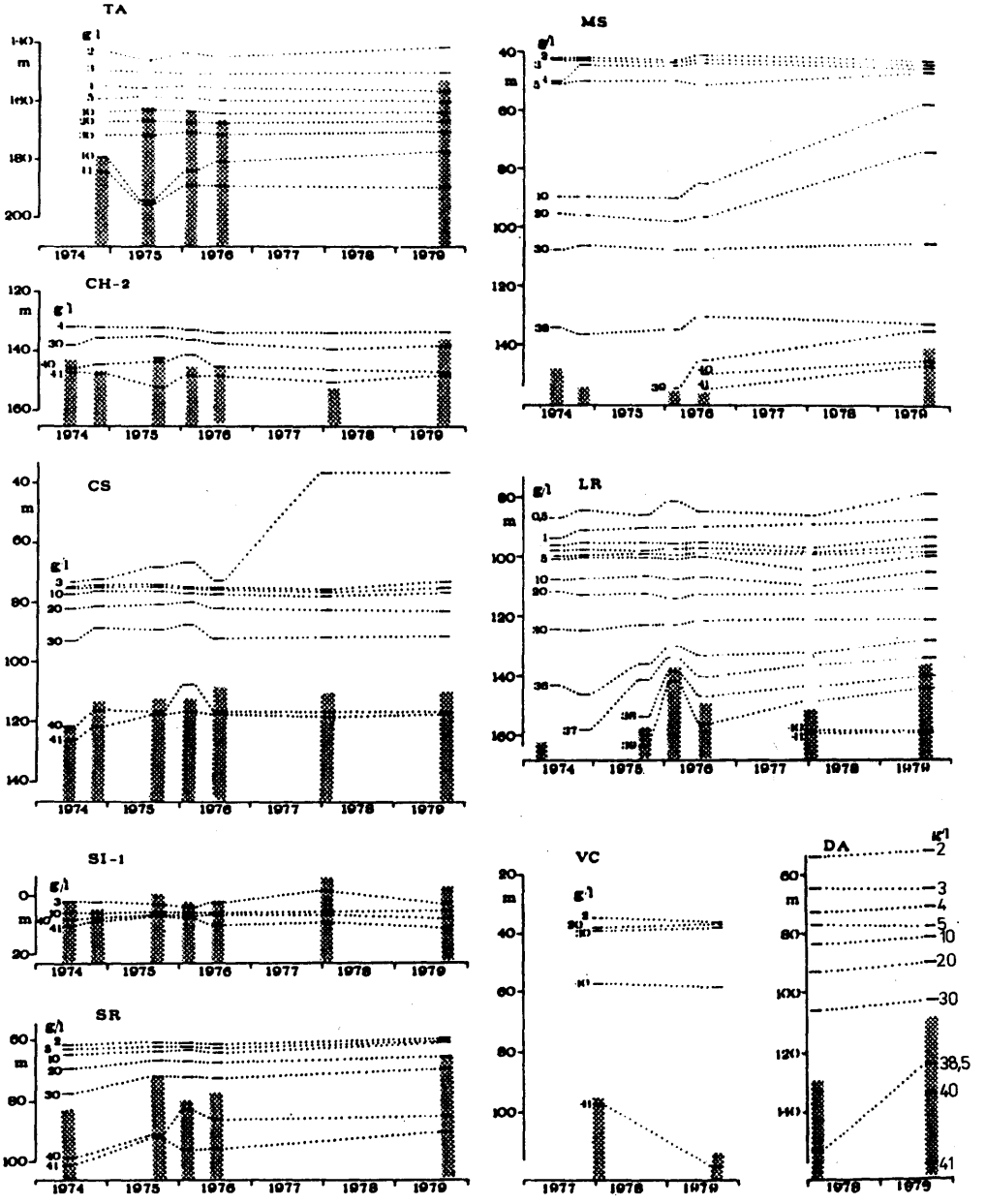

Figure 3

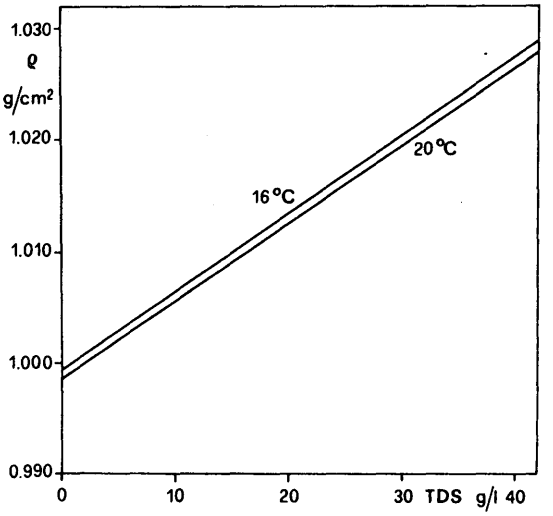

Figure 4

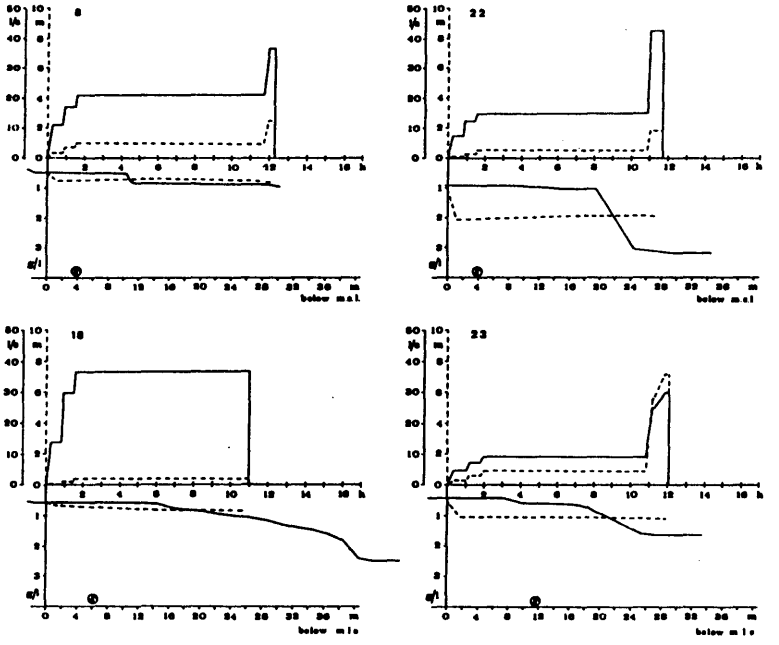

Figure 5

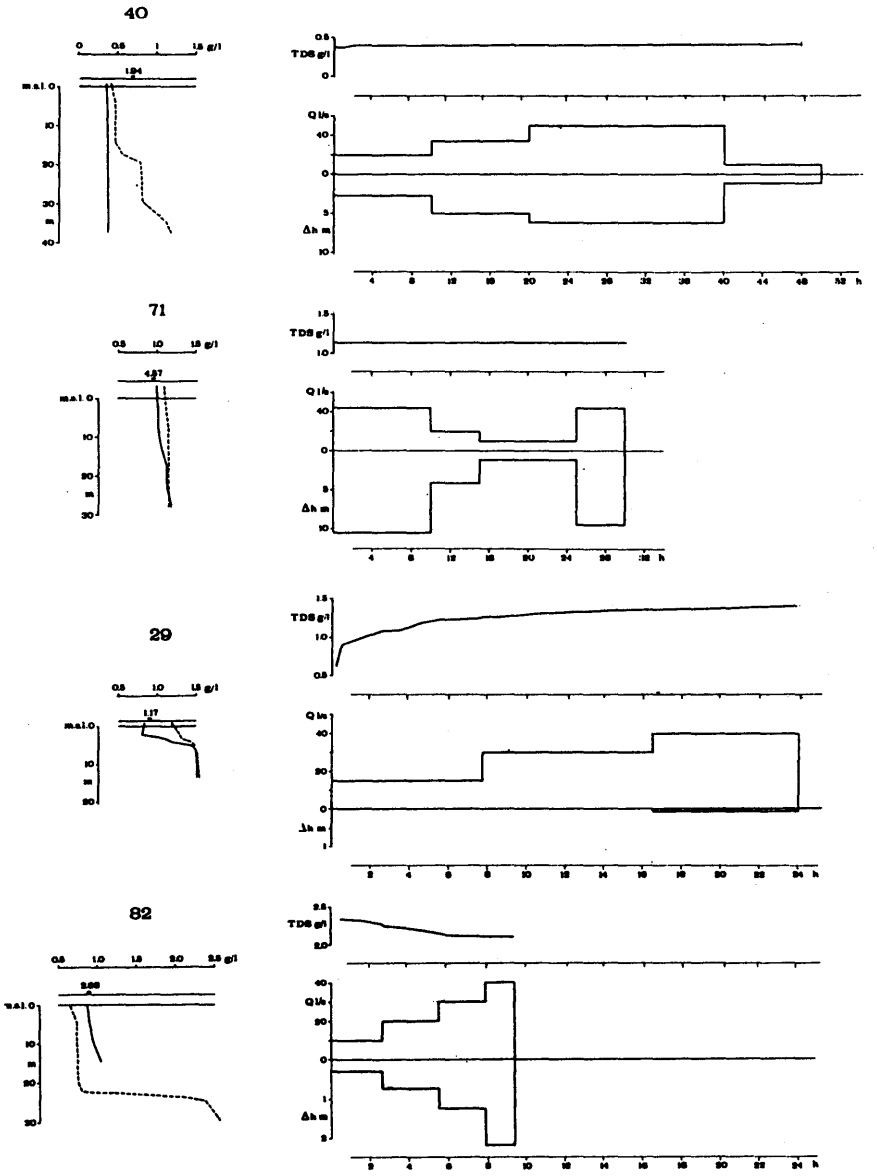

Figure 6

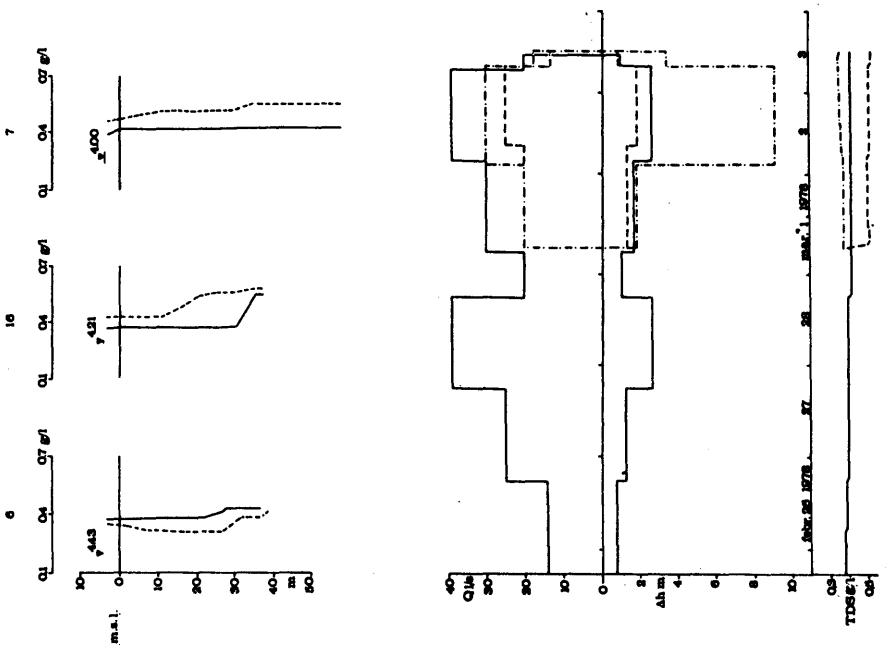

Figure 8

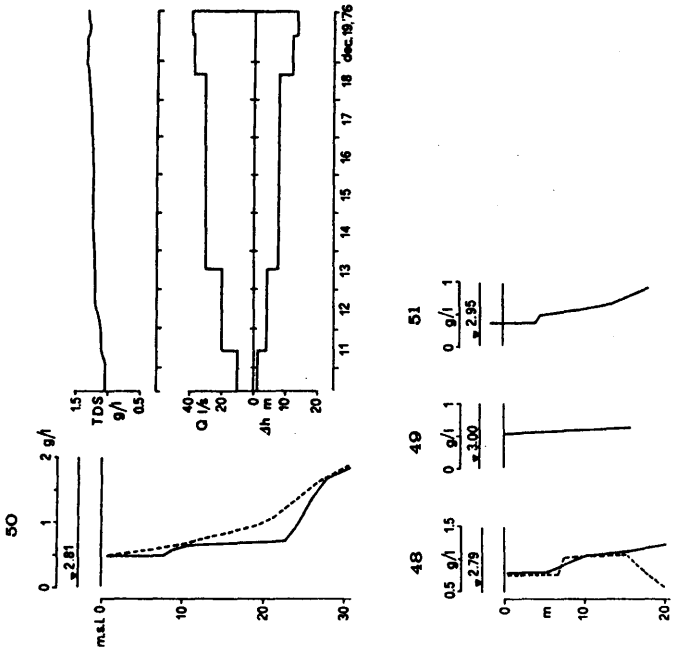

Figure 7

Table 1:

WELL	DATE	t	δ_f g/cm³	K	H_r	H_t
TA	NOV. 74	4.41	1.002550	40.18	183.74	177.16
	JUL. 75	3.81	1.003564	41.93	193.74	159.70
	FEB. 76	3.94	1.003188	41.25	188.74	162.48
	JUL. 76	4.00	1.003139	41.18	188.74	164.60
	SEP. 79	3.43	1.003342	41.53	188.74	142.41
CH-2	JUN. 74	3.52	1.002667	40.38	147.58	142.25
	NOV. 74	3.58	1.002811	40.62	147.58	145.53
	JAN. 75	3.36	1.003836	42.42	152.58	142.66
	FEB. 76	3.52	1.003033	40.99	148.58	144.43
	JUL. 76	3.54	1.002838	40.66	148.58	144.07
	FEB. 78	3.72	1.003017	40.97	150.58	152.52
	SEP. 79	3.37	1.002538	40.16	148.58	135.47
CS	JUN. 74	2.30	1.008438	52.90	127.27	121.68
	NOV. 74	2.20	1.007711	50.92	117.27	112.03
	SEP. 75	2.23	1.007547	50.49	117.27	112.61
	FEB. 76	2.13	1.007981	51.64	117.27	109.99
	JUL. 76	2.16	1.007144	49.48	117.27	106.87
	JAN. 78	2.14	1.007894	51.41	122.27	110.01
	SEP. 79	1.98	1.002834	40.66	92.26	80.50
SI-1	JUN. 74	0.25	1.006127	47.07	19.91	11.58
	NOV. 74	0.33	1.002823	40.64	16.91	13.25
	SEP. 75	0.19	1.002640	40.33	16.91	7.50
	FEB. 76	0.16	1.009359	55.67	22.91	8.68
	JUL. 76	0.21	1.006231	55.24	22.91	11.38
	JAN. 78	0.09	1.002640	40.33	16.14	3.47
	SEP. 79	0.09	1.008991	54.48	22.91	4.69
SR	JUN. 74	1.64	1.007053	49.25	100.90	80.73
	SEP. 75	1.53	1.005911	46.59	90.90	71.38
	FEB. 76	1.58	1.007190	49.59	95.90	78.45
	JUL. 76	1.55	1.007239	49.71	95.90	77.17
	SEP. 79	1.35	1.006564	48.08	90.90	65.00
MS	JUN. 74	2.80	1.008331	52.60	140.24	147.29
	NOV. 74	2.89	1.008750	53.80	145.24	155.48
	FEB. 76	2.71	1.010151	58.22	155.24	157.79
	JUL. 76	2.68	1.010195	58.37	155.24	156.45
	SEP. 79	2.36	1.010706	60.18	155.24	142.04
LR	JUN. 74	3.15	1.006554	48.05	147.84	151.37
	NOV. 74		1.007092	49.35	152.84	
	SEP. 75	2.90	1.007554	50.51	153.18	146.49
	FEB. 76	2.83	1.004994	44.65	133.18	126.37
	JUL. 76	2.82	1.007015	49.16	148.18	138.63
	JAN. 78	2.82	1.007229	49.69	148.18	140.12
	SEP. 79	2.66	1.007490	50.35	148.18	133.93
DA	FEB. 78	2.19	1.009932	57.49	156.88	125.90
	SEP. 79	1.87	1.009943	57.52	141.88	107.57
VC	JAN. 78	1.01	1.016688	94.03	96.84	94.79
	SEP. 79	0.61	1.018244	110.01	117.53	110.67

THEME 3

MATHEMATICAL CALCULATIONS AND MODELING

3

MATHEMATICAL CALCULATIONS AND MODELING

3.0. INTRODUCTION

G.A. BRUGGEMAN

Salt, brackish and fresh water belong to the category of miscible liquids, which means that the fluids are completely soluble in each other and will mix together. In theory an abrupt interface between fresh and salt water is not possible because of the phenomenon of hydrodynamic dispersion (and diffusion as a part of it) which creates a transition zone (mixing zone) where the chlorine content gradually changes from that of salt water via brackish to fresh water. Besides dispersion also the variation in density of the groundwater in salt-fresh water problems may play an important role. So in the most general case if both dispersion and differences in density of the groundwater have to be taken into account, calculation methods for salt-fresh water problems must be based on simultaneous solution of the differential equations for density flow and for dispersion together with the initial and boundary values for the transport and flow processes.

If conditions are such that to neglect the dispersion is acceptable from a point of view of accuracy, this will simplify the calculations considerably. In the case of a small transition zone this is done in many investigations by introducing an abrupt interface between fresh and salt water, thus considering fresh and salt water as mutually immiscible. The assumption then is made that changes of the hydrological regime, for instance due to human activities, will result in a new equilibrium of the interface without an appreciable transition zone as well.

Thus two main calculation methods for solving fresh-salt water problems may be distinguished: studies dealing with a transition zone, caused by dispersion and studies with a sharp interface, without dispersion.

This distinction is also applicable to the chosen eight highlights of SWIM, belonging to the category of mathematical calculations and modelling.

1. STUDIES DEALING WITH A TRANSITION ZONE

Two dimensional problems in dune areas are studied by LEBBE (3.4.) and by KOOIMAN, PETERS & v.d. EEM (3.8.). Both papers describe the use and results of a modified Konikow-Bredehoeft model in which also density differences are taken into account.

UFFINK (3.6.) describes the development of a transition zone in two dimensional flow, starting from a known sharp interface. For calculating the velocity distribution he uses a similarity between the boundary layer problem in hydrodynamics and the flow of groundwater near an interface. From this velocity distribution the dispersion is determined by means of the random walk method.

A narrow transition zone is simulated by means of a finite-element model of two dimensional density flow by VOSS & SOUZA (3.7.) that is based on a consistent velocity approximation. BRUGGEMAN (3.5.) describes a general method for calculating a transition zone in three dimensional flow, making use of so called pressure generators.

2. STUDIES WITH A SHARP INTERFACE

The finite-element method is a powerful tool for solving salt-fresh water problems with a sharp interface, according to VERRUYT (3.1.). Complicated boundary conditions, non-homogeneity and anisotropy of the soil yield no severe problems and even generalizations to non-steady flow is relatively simple.

VAN DAM (3.2.) introduces so called reduced variables in determining the possible shapes of the interface between fresh and salt water in a three dimensional axial symmetric leaky aquifer.
Movement of fresh water bubbles in saline aquifers is treated by PETERS (3.3.) using vortex theory for a three dimensional axial symmetrical sharp interface. This study provides a theoretical basis for research aimed at storage possibilities of fresh water in saline water.

3.1. ANALYSIS OF INTERFACE PROBLEMS BY THE FINITE-ELEMENT METHOD

A. VERRUIJT

ABSTRACT

The finite element method can take a free surface or a fresh-/salt-water interface into account. The method presents several advantages: 1° a solution for soil bodies of arbitrary geometrical shape can be found; 2° boundary conditions may be complicated, 3° non-homogeneity of the soil can be taken into account, 4° anisotropy presents only a small complication, 5° generalization to non-steady flow is relatively simple. As disadvantages can be cited: 1° the abstract theoretical basis (variational principle), 2° a complicated computer programme, 3° complicated conditions may surpass the limits of economic feasibility.

Some examples demonstrate the advantage of the finite element solution over the analytical one.

1. INTRODUCTION

In recent years the finite-element method has been found to be a powerful tool for the solution of groundwater-flow problems; see for instance ZIENKIEWICZ & CHEUNG (1967). In this method an approximate solution is determined in the form of values of the groundwater head in a great (but finite) number of points. These values are calculated by means of a computer program which in general solves a system of linear algebraic equations. As the construction of the system of equations is also performed within the computer program, the finite element method enables the solution of complicated problems, such as problems for anisotropic, non-homogeneous aquifers of arbitrary shape. The occurrence of a free surface or a salt-water interface can be taken into account in a relatively simple way.

Advantages of the finite element method are

1. Solution possible for soil bodies of arbitrary geometrical shape.
2. Boundary conditions may be complicated (infiltration, leakage, free surface, interface).
3. Non-homogeneity of the soil is easily taken into account.
4. Anisotropy is only a very small complication.
5. Generalization to non-steady flow is relatively simple.

Disadvantages of the method are

1. The theoretical foundation is somewhat abstract (variational principle).
2. The computer program is fairly complicated (this is the price that one has to pay for generality and flexibility).
3. For problems involving many points and complicated boundary conditions the requirements on the computer's memory and time may surpass the limits of economic feasibility.

2. DESCRIPTION OF THE FINITE ELEMENT METHOD

For a detailed derivation of the mathematical equations involved in the finite element method the reader is referred to the literature, for instance ZIENKIEWICZ & CHEUNG (1967), VERRUIJT (1970, 1972). Here only a general description is presented. Restriction is made to flow in a plane (fig. 1).

The plane is covered by a network of triangles, and it is assumed that within each triangle the variation of the head is linear (fig. 2).

This means that the function $\varphi = \varphi(x,y)$ is approximated by a piecewise differentiable function, represented by a surface of facets. The values of the groundwater head φ in each node are considered as unknowns. Thus the continuous variable $\varphi(x,y)$ is replaced by a great number (say 100 or 200, or 1000) of unknowns $\varphi_k (k = 1,2,\ldots,n)$. Instead of the differential equation governing the function $\varphi(x,y)$ one now uses a system of linear algebraic equations that is supposed to be equivalent to the differential equation. These equations are derived by requiring that the approximate solution on the average approximates the true solution as well as possible. The system of equations can be set up by a computer program that uses the following data as input:

1. the co-ordinates of each node,
2. the structure of each element,
3. the transmissibility in each element,
4. an initial estimation of the head,
5. for non-steady flow: the storage coefficient, and the values of time steps.

The computer then calculates the coefficients of the algebraic equations, and determines the solution, for instance by an iterative method similar to the usual relaxation process.

The occurrence of a free surface or an interface leads to a complication that can be overcome fairly easily, although a considerable increase in computer time has then to be accepted. The principle of the procedure can best be explained by means of a simple example (fig. 3).

The flow region at a certain moment (say $t = t_o$) is subdivided into triangles. It is assumed that at all times the salt-water head in the salt water is constant (a more refined technique would involve a network of triangles in the salt water also; this is possible, but has not yet been executed). Then, since at both sides of the interface the fluid pressure must be the same, the fresh-water head along CDE is known. Suppose that along AB the head is constant, and let AE and BC be sufficiently far away to assume that along AE and BC the head is constant. Then along the entire boundary the head is given. The finite element procedure then enables one to calculate the values of head in interior points, and the velocities in each point. The velocities in the points on the interface multiplied by Δt yield the displacements of these points during the interval Δt. This then enables calculation of the co-ordinates of the nodal points along CDE at the end of

the time interval. On the basis of these new co-ordinates the computer can next calculate the new values of the coefficients of the linear equations, solve the system, etc..

3. EXAMPLES

Some examples are given below, in the form of graphical representations of solutions.
The first example, taken from VERRUIJT (1970), refers to non-steady flow with a free surface in a rectangular dam. The response of the free surface to a sinusoidal variation of the head on the left side is shown in fig. 4. The results have been compared with other approximate solutions, and with results of tests in a Hele-Shaw model. It appears that a sufficient accuracy can be obtained provided that the time steps are taken small enough.

The second example refers to steady flow with an interface between fresh and salt water (fig. 5). The fresh water is flowing from a fresh-water reservoir (or a high land area) towards the sea. The salt water is supposed to be stationary. The theoretical solution for this problem was obtained by STRACK (1971), with the aid of complex variables. In this theoretical solution the upper boundary was schematized to a straight potential line. At great distances from the sea the depth of the interface is, of course, determined by the Ghyben-Herzberg formula. The numerical solution by means of the finite element method was obtained by KONO (1972). The final mesh of triangles is shown in fig. 5. The dashed line represents the theoretical position of the interface as calculated by means of the exact complex variable method.

The advantage of a finite element solution as compared to an analytical solution is that it is easier to generalize the finite-element technique. It is a relatively simple matter to include non-homogeneities in the soil permeability, etc.. As an example some results for the same situation as in fig. 5, with a sink or a source in the field, are represented in fig. 6.

The dashed line is the position of the interface in case of a source, and the dotted line is the interface in case of a sink. The program to calculate the interface was written by KONO (1972). Although this problem admits a theoretical solution no comparisons were made as yet. It might be mentioned, in conclusion, that in general the location of the nodes changes during the iterative determination of the position of the interface. One may specify, for instance, that on certain vertical lines 6 nodes are located between the fixed upper boundary and the lower boundary, the interface, the position of which changes during the calculation procedure. Thus at every stage of the calculations the interface consists of the lowest nodal points.

REFERENCES

KONO, I. (1972). Analysis of Interface Problems in Groundwater Flow by Finite Element Method. Delft: University Soil Mechanics Laboratory Report.

STRACK, O.D.L. (1971). Some cases of Interface Flow towards Drains. Delft: University Soil Mechanics Laboratory Report.

VERRUIJT, A. (1970). Theory of Groundwater Flow. London: Macmillan.

VERRUIJT, A. (1972). A Finite Element Approach to Plane Groundwater Flow Problems with Storage, Infiltration and Leakage. Delft: University Soil Mechanics Laboratory Report.

ZIENKIEWICZ, O.C. & CHEUNG, Y.K. (1967). The Finite Element Method in Structural and Continuum Mechanics. London: McGraw-Hill.

FIGURES

Fig. 1: Network of triangles in a plane.

Fig. 2: Linear variation of the head within the triangles.

Fig. 3: Example for explaining the principle of the computer simulation by occurrence of a free surface or an interface.

Fig. 4: Response of the free surface to a sinusoidal variation of the head on one side.

Fig. 5: Steady flow with an interface between fresh and salt water.

Fig. 6: Like figure 5, with a sink or a source in the field.

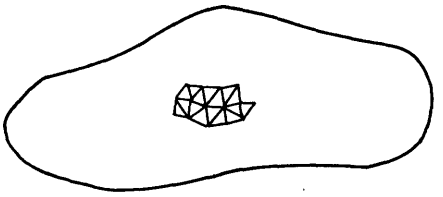

Figure 1

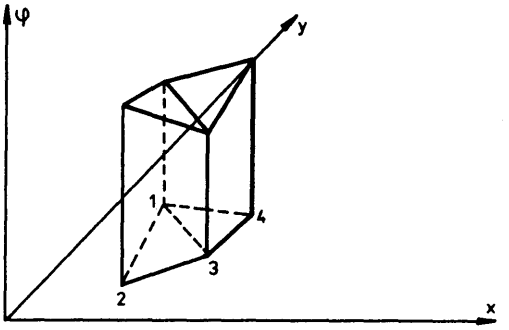

Figure 2

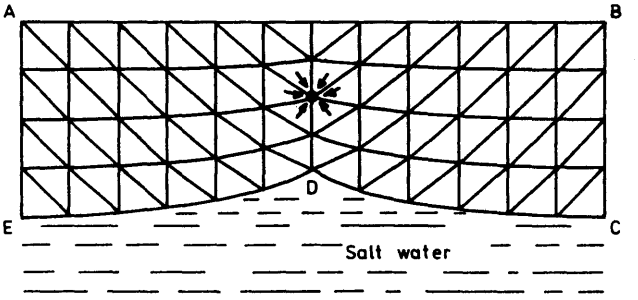

Figure 3

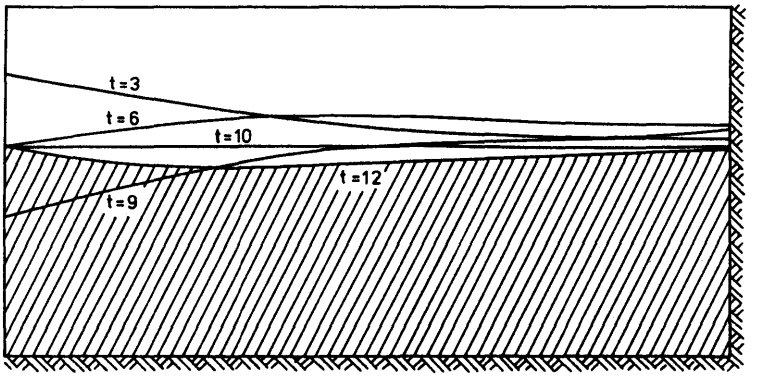

Figure 4

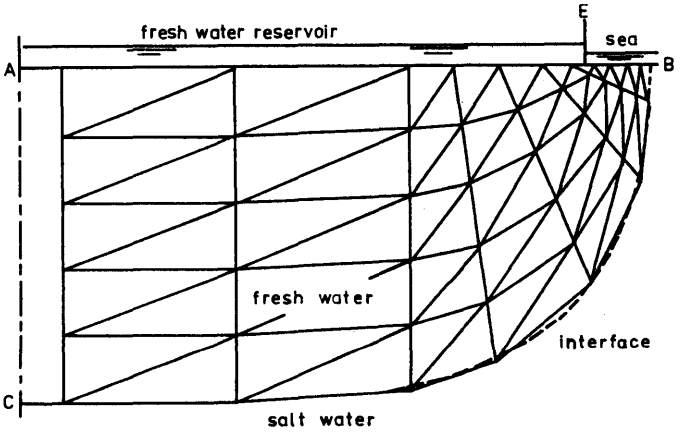

Figure 5

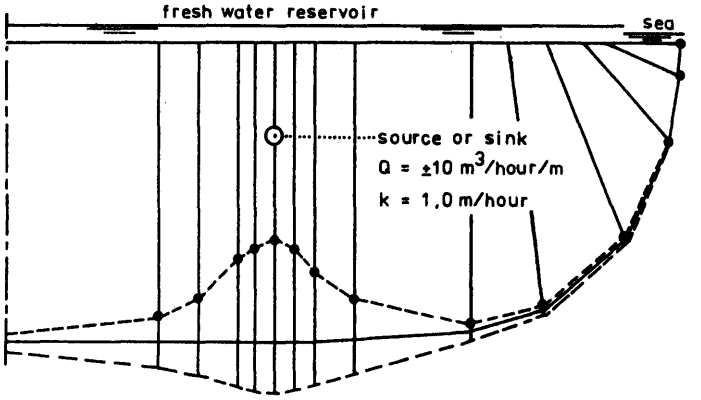

Figure 6

3.2. ANALYSIS OF THE POSSIBLE SHAPES OF THE FRESH-/SALT-WATER INTERFACE IN A SEMI-CONFINED AQUIFER WITH AXIAL-SYMMETRIC BOUNDARY CONDITIONS

J.C. van DAM

ABSTRACT

The paper comprises:

- derivation of the differential equation describing the problem mentioned in the title in the case of stagnant saline water;
- introduction of dimensionless reduced variables;
- a numerical solution method for the differential equation in terms of the reduced variables;
- presentation of the complete results obtained for all possible axial-symmetric cases, i.e. a catalogue of possible shapes of the interface.

The paper is the follow-up of a similar paper for the one-dimensional case presented in the 6th SWIM-meeting in Hannover 1979.

1. INTRODUCTION

This paper is the follow-up of the author's paper presented at the 6th Salt Water Intrusion Meeting, Hannover 1979 (van DAM, 1981). Like the previous paper the present paper deals with the flow of fresh groundwater above stagnant saline groundwater in a semi-confined aquifer. The previous paper dealt with the case of one-dimensional horizontal flow in the aquifer. The present paper describes the case of horizontal axial-symmetric flow in the aquifer. The subject of the previous paper has since been worked out in more detail in two companion papers (SIKKEMA & van DAM, 1982; van DAM & SIKKEMA, 1982) concentrating respectively on the analytical solutions and on an approximate solution method of the relevant differential equation. The paper by van DAM & SIKKEMA contains practical examples and an analysis of the accuracy of the results of the approximate solution method. The reader of the present paper may profit from reading the previous papers as well for two more reasons. The reduced variables used in the present paper were first introduced and discussed in the previous papers (van DAM, 1981; van DAM & SIKKEMA, 1982). The 13 different curves obtained by analytical solution of the one-dimensional case (SIKKEMA & van DAM, 1982) can be seen as limit-cases of the curves described in the present paper.

2. PROBLEM FORMULATION

This paper deals with the axial-symmetric geohydrologic profile of fig. 1. The vertical axis of rotation is at r = 0. The following assumptions were made:

- the aquifer is homogeneous; not necessarily isotropic as only horizontal flow in the aquifer is considered;
- the semi-permeable layer is homogeneous; not necessarily isotropic as only vertical flow in this layer is considered;

- the interface between fresh and saline groundwater is sharp; diffusion and dispersion are ignored;
- both the fresh and the saline groundwater are homogeneous (i.e. of constant densities);
- the saline groundwater is stagnant; this implies that the fresh water flows in steady state;
- the phreatic-groundwater table is horizontal.

The depth D is not relevant for the mathematical formulation of the problem, except as a boundary. Yet - for practical reasons - D is chosen equal to the aquifer thickness (van DAM, 1981; van DAM & SIKKEMA, 1982).

The Dupuit approach of describing the flow in the aquifer as horizontal flow can be justified as long as the slope of the interface is not too steep (e.g. < 0,02 to 0,05). This is often the case in large-scale problems. Similarly the flow in the semi-permeable top layer is described as vertical flow, which is mostly justified because the permeability of this layer is often so much smaller than that of the aquifer.

The meaning and dimension of the symbols, most of which occur in fig. 1, are:

- geohydrological constants:
  - k = aquifer permeability [LT^{-1}]
  - c = hydraulic resistance of the semi-permeable layer [T]
  - D = thickness of the aquifer [L]
  - α = $(\rho_s - \rho_f)\rho_f$ [-]
  - ρ_s = density of the saline groundwater [ML^{-3}]
  - ρ_f = density of the fresh groundwater [ML^{-3}]
- boundary conditions:
  - p = elevation of the phreatic groundwater table, horizontal, above reference level*) [L]
  - h_s = piezometric level of the stagnant saline groundwater, above reference level*) [L]
  - E = equilibrium depth, see expression (5) [L]
- variables:
  - h_f = piezometric level of the flowing fresh water in the aquifer, above reference level*) [L]
  - H = thickness of the fresh water in the aquifer [L]
  - Q = flow of fresh groundwater in the aquifer through a cylindrical surface of radius r [L^3T^{-1}]
  - r = distance from the centre [L]

*) The reference level has been chosen as the top of the aquifer.

3. EQUATIONS

The problem is described by the following three equations:

Darcy's law: $$Q = - 2\pi r H k \frac{dh_f}{dr} \qquad (1)$$

continuity equation: $$\frac{dQ}{dr} = - 2\pi r \frac{h_f - p}{c} \qquad (2)$$

Badon-Ghijben/ Herzberg's principle: $$h_f - h_s = \alpha(h_s + H) \qquad (3)$$

The three basic equations (1), (2) and (3) contain three unknowns Q, H and h_f, variables of the independent variable r. When eliminating the variables Q and h_f one easily arrives at the following differential equation in H:

$$rH \frac{d^2H}{dr^2} + r\left(\frac{dH}{dr}\right)^2 + H \frac{dH}{dr} - r \frac{H-E}{kc} = 0 \ , \qquad (4)$$

where $$E = \frac{p - (1 + \alpha)h_s}{\alpha} \ , \qquad (5)$$

E is a function of p, h_s and α. The constants p, h_s and α occur in the differential equation in the term E only. E is called the equilibrium depth because it is that particular value of H for which the corresponding value of the piezometric level of the fresh groundwater h_f equals p, so that no vertical flow occurs in the semi-permeable layers.

So far, the author knows only two particular solutions of differential equation (4), viz.:

$$H = E \qquad (6)$$

$$H = 2E + \frac{r^2}{8kc} \ . \qquad (7)$$

A general solution has, to the best of his knowledge, not yet been found. In order to overcome this difficulty a good approximation can be formulated by replacing the continuity equation (2) by:

$$\frac{dQ}{dr} = - 2\pi r \frac{\overline{h_f} - p}{c} \ , \qquad (8)$$

where $\overline{h_f}$ is the average value of the variable h_f over a small reach of r.

Integration of (8) yields:

$$Q = Q_o - \pi(r^2 - r_o^2) \frac{\overline{h_f} - p}{c} \ . \qquad (9)$$

The unknown Q can be eliminated by combination of the equations (1) and (9):

$$- 2\pi r H k \frac{dh_f}{dr} = Q_o - \pi(r^2 - r_o^2) \frac{\overline{h_f} - p}{c} \ . \qquad (10)$$

h_f and $\overline{h_f}$ can be eliminated from (10) when using equation (3) and the corresponding equation:

$$\overline{h_f} - h_s = \alpha(h_s + \bar{H}) \ , \tag{11}$$

where $\bar{H}$ is the average value of the variable H over that same reach.

After this elimination and introduction of the equilibrium depth E the following differential equation is found:

$$rH\frac{dH}{dr} - (r^2 - r_o^2)\frac{\bar{H} - E}{2kc} + \frac{Q_o}{2\pi k\alpha} = 0. \tag{12}$$

This differential equation describes the variable H as a function of r over a small reach of r starting from $r = r_o$. In $r = r_o$, $Q = Q_o$ and $\bar{H}$ is the estimated average value of H over the considered reach. The estimated value $\bar{H}$ is subject to revision after each calculation of H.

4. REDUCED DIMENSIONLESS VARIABLES

For convenience it is attractive to introduce the following reduced, dimensionless, variables

$$y = H/D \tag{13}$$

$$u = r/\lambda \ , \text{ where } \lambda = \sqrt{kDc} \tag{14}$$

$$q = Q/\pi k\alpha D^2 \tag{15}$$

and the reduced, dimensionless, constant

$$\varepsilon = E/D. \tag{16}$$

Differential equation (4) then reduces to:

$$uyy'' + u(y')^2 + yy' - u(y - \varepsilon) = 0. \tag{17}$$

Differential equation (12) then reduces to:

$$uyy' - 1/2(u^2 - u_o^2)(\bar{y} - \varepsilon) + 1/2q_o = 0. \tag{18}$$

Equation (9) then reduces to:

$$q = q_o - (u^2 - u_o^2)(\bar{y} - \varepsilon). \tag{19}$$

5. SOLUTION

The solution of differential equation (18) was first found by van der MOLEN (van der MOLEN, about 1975). In a somewhat modified denotation his solution is:

$$y = \pm \sqrt{(1/2(\bar{y}-\varepsilon)(u^2-u_o^2) - \{(\bar{y}-\varepsilon)u_o^2 + q_o\} \ln u/u_o + y_o^2)} , \tag{20}$$

where y_o is the value of y at $u = u_o$.
The estimated value of $\bar{y}$ can now be checked by

$$\bar{y} = (y + y_o)/2 \tag{21}$$

and, if necessary, revised. This iterative procedure can be avoided when substituting (21) in expression (20):

$$y = \pm \sqrt{\{\frac{y+y_o-2\varepsilon}{4} (u^2-u_o^2) - \{(\frac{y+y_o-2\varepsilon}{2}) u_o^2 + q_o\} \ln \frac{u}{u_o} + y_o^2\}} \tag{22}$$

or:

$$y^2-(\frac{u^2-u_o^2}{4} - \frac{u_o^2}{2} \ln \frac{u}{u_o})y- [\frac{y_o-2\varepsilon}{4} (u^2-u_o^2)-\{u_o^2(\frac{y_o-2\varepsilon}{2}) + q_o\} \ln \frac{u}{u_o} + y_o^2] 0 =. \tag{23}$$

This is a quadratic equation. The explicit solution for y is:

$$y = \frac{- B \pm \sqrt{(B^2 - 4C)}}{2} \tag{24}$$

where $$B = - (\frac{u^2 - u_o^2}{4} - \frac{u_o^2}{2} \ln \frac{u}{u_o}) \tag{25}$$

and $$C = - [\frac{y_o-2\varepsilon}{4} (u^2 - u_o^2) - \{u_o^2(\frac{y_o-2\varepsilon}{2}) + q_o\} \ln \frac{u}{u_o} + y_o^2] . \tag{26}$$

This enables us to proceed directly from $u = u_o$, where $y = y_o$ and $q = q_o$, to $u = u$. For the next step a new value of y_o and a new value of q_o is needed; y_o for the next step is the y found with (24) for the present step and q_o for the next step is the q at $u = u_o$ found with (19) after substitution of (21):

$$q = q_o - (u^2 - u_o^2) (\frac{y+y_o}{2} - \varepsilon) , \tag{27}$$

where y_o and y respectively are the values at the beginning and the end of the present step.

6. RESULTS

Calculations have been made with a programmable pocket calculator HP67 using the expressions (24) and (27) for y and q. Some details of the programme will be dealt with later, together with the tricks applied to overcome some numerical

problems for the calculator. After gaining some experience with the programme a survey was made of the possible shapes of the curves.

On account of the results obtained for the one-dimensional case (van DAM, 1981; SIKKEMA & van DAM, 1982; van DAM & SIKKEMA, 1982) and of understanding of the geohydrological problem it may be taken that each possible curve has q = 0 for at least one value of u. So one may expect to find all possible shapes when taking q = 0 respectively at:

u = 0
u = small, e.g. u = 1.
u = great, e.g. u = 100.

This holds for each of the three classes $\varepsilon > 0, \varepsilon = 0$ and $\varepsilon < 0$. So nine different cases occur as in the table below.

	q = 0 at u = 0	q = 0 at u = 1	q = 0 at u = 100
$\varepsilon > 0$	figure 2	figure 3	see van DAM (1981)
$\varepsilon = 0$	figure 4	figure 5	and SIKKEMA and
$\varepsilon < 0$	figure 6	figure 7	van DAM (1982)

Three of them, namely those for q = 0 at u = 100 are practically the same as for the one-dimensional cases described in previous papers (van DAM, 1981; SIKKEMA & van DAM, 1982). This is obvious because for the large values of u the curvature of the cylinder is negligibly small. The numerical results of the calculations confirmed this. Therefore in the present paper only the remaining 6 cases are dealt with. A survey of the possible shapes in each of these six cases is given in the six figures 2 through 7, the numbers of which have been indicated in the table.

A discussion of the curves in each of these six figures now follows. The description of the curve types is chosen in accordance with the terminology chosen for the one-dimensional case by van DAM & SIKKEMA (1982).

Figure 2. $\varepsilon > 0$ is chosen at $\varepsilon = + 0.4$.
q = 0 at u = 0 for respectively $y_{q=0} = + 1,0; + 0,8; + 0,5; + 0,35; - 0,2; - 0,5$ and - 1,0. The first three of these curves ($y_{q=0} > \varepsilon$) are of a mutually similar shape, the reverse U-type. The same holds for the last three curves ($y_{q=0} < 0$), the S-type. The curve with $y_{q=0} = + 0,35$ is one of the U-type which occurs for $0 < y_{q=0} < \varepsilon$. The curve with $y_{q=0} = + 0,8$ is the particular solution, the parabola.

Figure 3. $\varepsilon > 0$ is chosen at $\varepsilon = + 0,4$.
q = 0 at u = 1 for respectively $y_{q=0} = + 0,6; + 0,35; - 0,2; - 0,228$ and - 0,3. The curve with $y_{q=0} = + 0,6$ is one of the reverse U-type wich is found for $y_{q=0} > \varepsilon$. The curves with $y_{q=0} = + 0,35$ and - 0,2 are both of the U-type which

is found for $-0{,}228 < y_{q=0} < \varepsilon$. The curve with $y_{q=0} = -0{,}228$ is a particular one; the upper asymptotic type, as it goes asymptotically to $y = \varepsilon$. A lower asymptotic type curve is also drawn in this figure. It goes from below to that same asymptote. The upper and lower asymptotic type curves have been found by trial and error; the starting conditions were iteratively changed until the asymptotic behaviour was reached. the curve with $y_{q=0} = -0{,}3$ is one of the S-type which occurs for $y_{q=0} < -0{,}228$.

Figure 4. $\varepsilon = 0$.
$q = 0$ at $u = 0$ for respectively $y_{q=0} = +0{,}4$; 0 and $-0{,}4$. Only two curve-types were found, namely the reverse U-type for $y_{q=0} \geq 0$ and the S-type for $y_{q=0} < 0$.

Figure 5. $\varepsilon = 0$.
$q = 0$ at $u = 1$ for respectively $y_{q=0} = +0{,}4$; $+0{,}05$ and $-0{,}4$. Only two curve-types were found, namely the reverse U-type for $y_{q=0} \geq 0$ and the S-type for $y_{q=0} < 0$.

Figure 6. $\varepsilon < 0$ is chosen at $\varepsilon = -0{,}4$.
$q = 0$ at $u = 0$ for respectively $y_{q=0} = +0{,}4$; 0; $-0{,}2$; $-0{,}6$; $-0{,}8$; 1,0 and $-1{,}2$. The curves with $y_{q=0} = 0$ and $y_{q=0} = -0{,}8$, the parabola, are of the intersecting type, separating the three types for which:

$0 < y_{q=0}$ reverse U-type
$2\varepsilon < y_{q=0} < 0$ oscillating type (new term)
and $y_{q=0} < 2\varepsilon$ S-type.

Figure 7. $\varepsilon < 0$ is chosen at $\varepsilon = -0{,}4$.
$q = 0$ at $u = 1$ for respectively $y_{q=0} = +0{,}4$; 0; $-0{,}2$; $-0{,}4$; $-0{,}708$ and $-1{,}0$. The curves with $y_{q=0} = 0$ and $y_{q=0} = -0{,}708$ are particular ones separating the three types:

$0 < y_{q=0}$ reverse U-type
$-0{,}708 < y_{q=0} < 0$ oscillating type
and $y_{q=0} < -0{,}708$ S-type.

The value $y_{q=0} = -0{,}708$ was found by trial and error until that particular curve was found for which the intersection of the horizontal axis (at $u > 1$) was with a finite gradient ($q = 0$).

The reader may have observed that in all six figures the parts of the curves for $y < 0$ have been drawn in dotted lines and the parts for $y > 0$ in continuous lines. This is because only the parts for $y > 0$ make sense for the geohydrological problem considered in this paper.

The steeper parts of the continuous lines, though mathematically correct, must also be rejected from the geohydrological point of view for two reasons. First of all the Dupuit approach of only horizontal flow in the aquifer is not justified for the steeper parts. Moreover, where the curves intersect the horizontal axis (top of the aquifer) vertically the water velocities would be infinite which is physically impossible. Among the curves that intersect the horizontal axis only those particular ones which intersect with a small angle are geohydrologically acceptable.

The reader will recognize parts of the continuous curves which can serve as solutions or parts thereof for such cases as: abstraction or injection wells in the centre or in a circle around the centre of a polder, a circular polder bounded by one or several annular polders surrounded by another polder extending to infinity or by open water.

7. SOME REMARKS ON THE PROGRAMME AND ITS IMPLEMENTATION

The programme requires the following input data: u_o, $\Delta u (= u - u_o)$, y_o, q_o and ε and gives for each step Δu: u, y and q. These values enter automatically as u_o, y_o and q_o for the next step. It is of course also possible to change these values before starting the run of the next step. This can be useful for Δu, q_o and ε. A change in q_o corresponds to the input of an abstraction or injection at u_o (in reality a change in Q_o at x_o). A change in ε corresponds to the passage of a boundary (at r_o) between two polders with different polder levels p. The step size Δu can always be adapted to the required degree of accuracy (related to the values of y and y') and the desired speed of operation. In many cases a step size $\Delta u = \pm 0{,}2$ gave very accurate results. This statement is based on a test with the only curve which is exactly known, the parabola. Mostly a step size of $\pm 0{,}1$ or $\pm 0{,}05$ was applied. In the steeper parts of the curves even smaller values of $|\Delta u|$ have been used. For the curves with vertical passage of the horizontal axis too great values of $|\Delta u|$ gave "error" because the curve does not exist there as in expression (24) $B^2 - 4C < 0$. In such cases the step size $|\Delta u|$ was automatically reduced to half its original value until $B^2 - 4C > 0$. At the vertical passage of the horizontal axis it was always necessary to reverse the direction of progress i.e. to change the sign of Δu. This change is made automatically in the programme, not only for the sign of Δu, but also for the sign of y, once the value of $|y|$ is smaller than a prescribed small value (0,02 was chosen). The value of q_o remains unchanged in these reversals.

In some cases tricks had to be applied to run the programme. For example, at $u_o = 0$ the term $\ln u/u_o$, which occurs in expression (23), would become ∞. Therefore, instead of $u_o = 0$ a very small value, as $u = 10^{-99}$, was applied. It was already mentioned that for the greater values of u the results must be approximately equal to those obtained in the one-dimensional case. This was confirmed indeed by the numerical results obtained when starting with $u_o = 100$ (better than $u_o = 10$). For values of u_o in the order of 10^3 to 10^6, where the curvature of the cylinder is even smaller, the results were worse because the values of $\ln u/u_o$ in expression (23) became very small e.g. $\ln \frac{10^6 + 10^{-1}}{10^6} = \ln 1.0000001$, which led to loss of accuracy.

8. CONCLUSIONS

There exists a great variety of possible shapes for the interface between flowing fresh water above stagnant saline water in a semi-confined aquifer. For various

practical problems sections of different curves can be used and interconnected so as to satisfy boundary conditions and connection conditions.

The one-dimensional case, presented earlier, can be seen as a special case of the axial-symmetric case.

A programme for an HP67 pocket calculator has been developed, and is available, for rapid straight forward calculation of interfaces. It starts from given or assumed values for the interface depth and the flow of fresh groundwater at one end and continues even over discontinuities, such as differences in polder level, abstractions and injections. In case certain conditions must be met at the other end the calculation must be repeated with other assumed values at the beginning (shooting) until the required conditions at both ends are met.

REFERENCES

DAM, J.C. van (1981). The shape of the fresh water - salt water interface in a semi-confined aquifer. Proceedings of the 6th SWIM-Hannover, 1979.

DAM, J.C. van & SIKKEMA, P.C. (1982). Approximate solution of the problem of the shape of the interface in a semi-confined aquifer. Journ. Hydrol. 56, 221-237.

MOLEN, W.H. van der (about 1975). Personal Communication.

SIKKEMA, P.C. & DAM, J.C. van (1982). Analytical formulae for the shape of the interface in a semi-confined aquifer. Journ. Hydrol. 56, 201-220.

FIGURES

Fig. 1: Geohydrologic profile.

Fig. 2: Curves for $\varepsilon = +0{,}4$ with $q = 0$ at $u = 0$.

Fig. 3: Curves for $\varepsilon = +0{,}4$ with $q = 0$ at $u = 1$ and with $q = 0$ at $u = \infty$, $y = \varepsilon$.

Fig. 4: Curves vor $\varepsilon = 0$ with $q = 0$ at $u = 0$.

Fig. 5: Curves vor $\varepsilon = 0$ with $q = 0$ at $u = 1$.

Fig. 6: Curves for $\varepsilon = -0{,}4$ with $q = 0$ at $u = 0$.

Fig. 7: Curves for $\varepsilon = -0{,}4$ with $q = 0$ at $u = 1$.

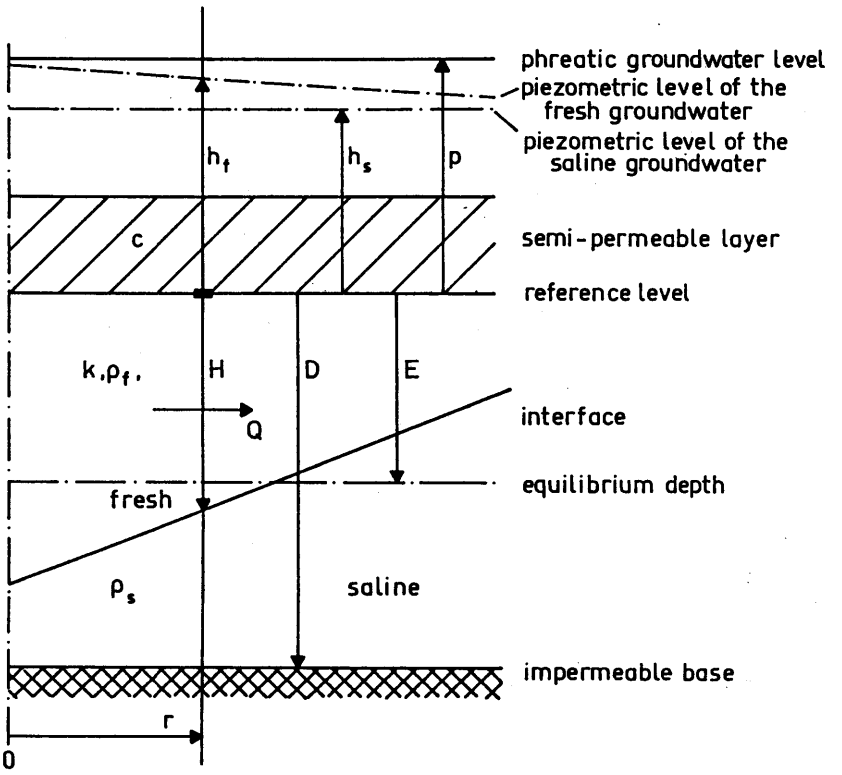
phreatic groundwater level
piezometric level of the fresh groundwater
piezometric level of the saline groundwater
h_f
h_s
p
c
semi-permeable layer
reference level
$k, \rho_f,$
H
D
E
Q
interface
equilibrium depth
fresh
ρ_s
saline
impermeable base
r
0

Figure 1

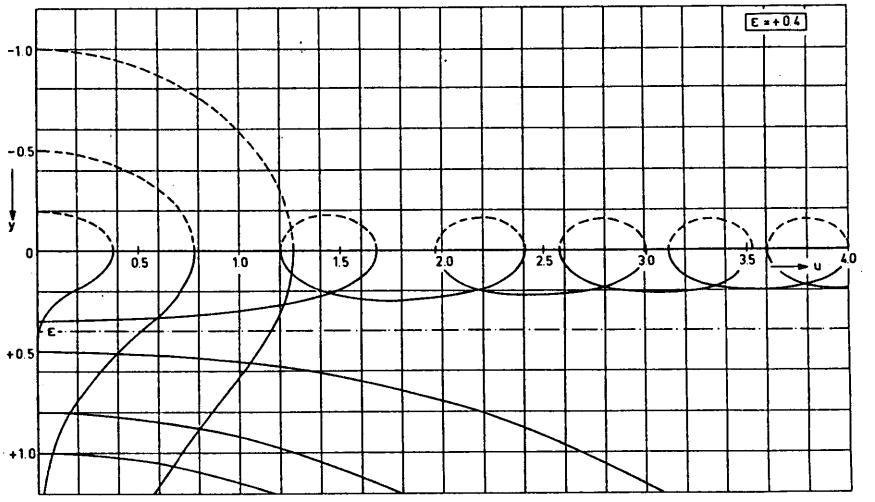

Figure 2

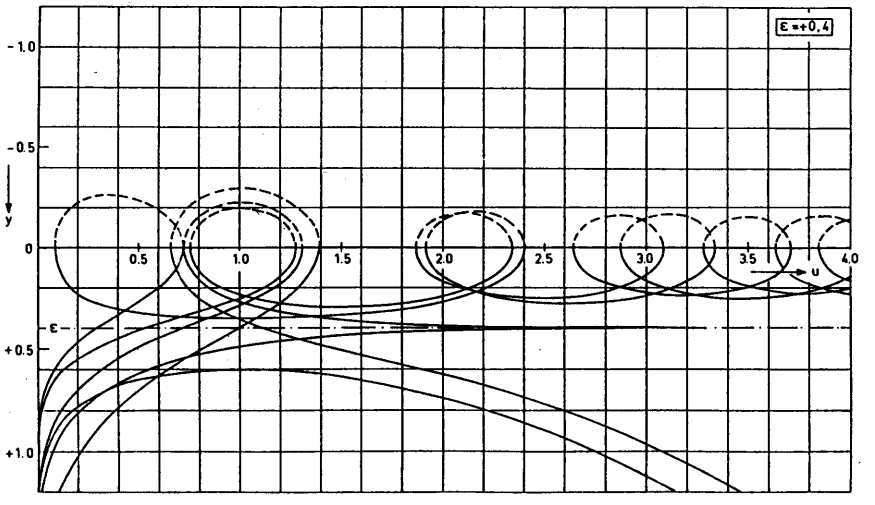

Figure 3

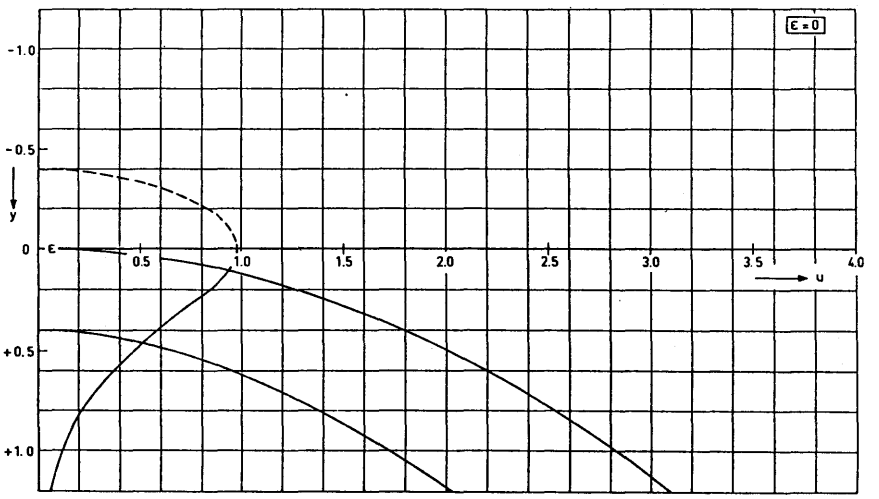

Figure 4

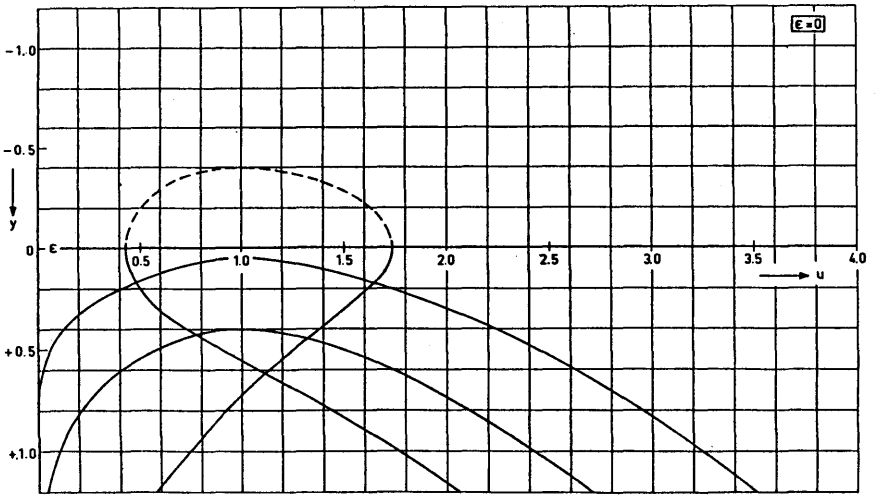

Figure 5

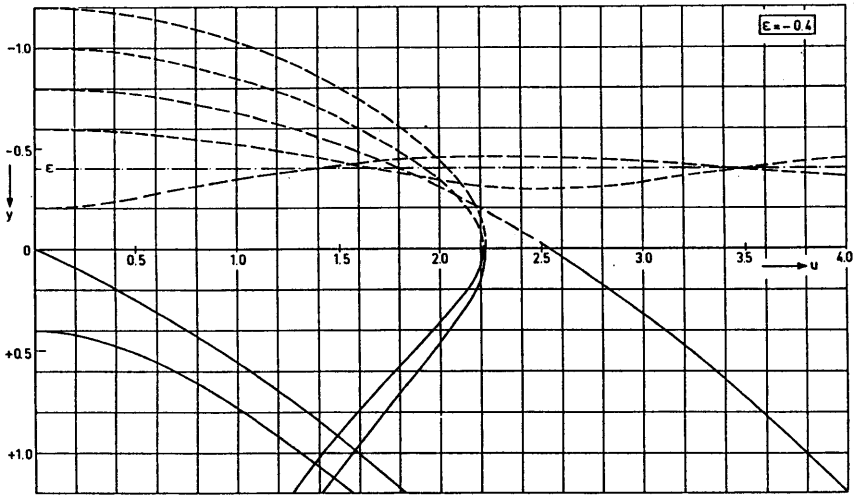

Figure 6

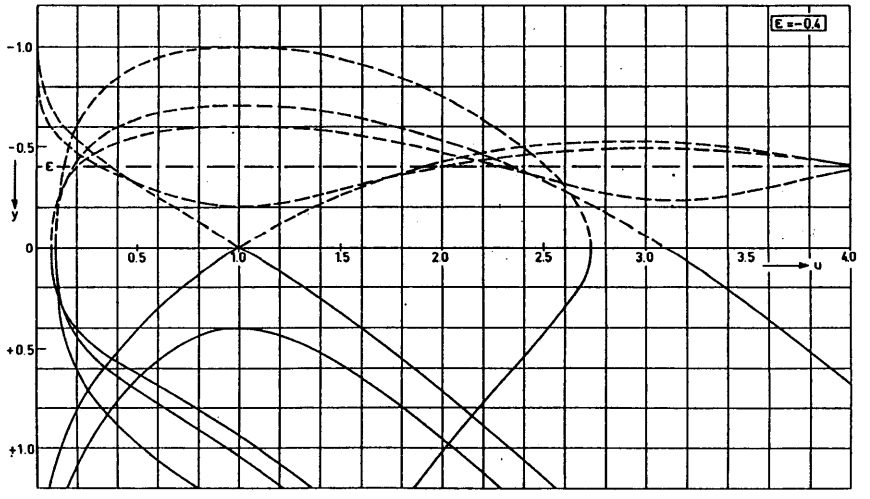

Figure 7

3.3. THE MOVEMENT OF FRESH WATER INJECTED IN SALAQUIFERS

J.H. PETERS

SUMMARY

The storage of fresh water in a significant quantity is not only possible in surface water reservoirs or phreatic aquifers but also in aquifers that are (partially) saline or brackish. When these aquifers are located at greater depth, injection can only be accomplished with wells.

The present study will provide a theoretical basis for predicting the movement of bubbles of fresh water injected in saline aquifers. In the modelling, use is made of vortex-theory to simulate the flows of the liquids with different densities. Factors that affect recovery efficiency will be reviewed.

1. INTRODUCTION

When surface water is the sole source for supply of drinking and industrial water, there must be a storage in order to guarantee an uninterrupted supply. Spin-off advantages from storage are that by selective intake plus the decomposition and mixing processes that occur the quality of the water can be further improved. Storage in times of ample river flow of sufficient quality can be provided by open reservoirs or by recharge of groundwater. This paper deals with storage facilities that can be created underground by displacing salt water. Before this can be applied in practice on an operational scale a number of questions must be answered. Among these are recovery results and the extent to which formation of brackish water is likely to occur. Irregularities in soil structure play an important part in this connection. This is why several Dutch waterworks use field tests to study this phenomenon. Investigation of the parameters governing displacement of one fluid by the other includes resort to calculation methods for simultaneous flows of fluids with different densities.

2. REVIEW OF WORK BY OTHERS

Possibilities for using saline aquifers to store fresh water have been studied extensively both with field tests and laboratory experiments. DE JOSSELIN DE JONG (1960) computed the rate of tilting of an interface in a confined aquifer using vortex distributions. The results were verified by a parallel plate model and an electrical resistance model.

GARDNER et al. (1962) studied static gravity segregation of miscible fluids in linear horizontal models. ESMAIL & KIMBLER (1967) did the same in synthetic sandstone models. The results of these experiments were used in a computer-program to calculate recovery efficiencies in hypothetical aquifers. Computed recoveries of fresh water ranging from 25 to 85 % are reported. KIMBLER (1970) described flow studies in artificial sandstone models that have been used to test the above mentioned computational technique for predicting the recovery

efficiencies. MOULDER (1970) reviewed factors that affect recovery of fresh water stored in saline aquifers and compared recovery results of several field tests. Efficiencies ranged from 0 to 50 %. Efficiency is defined as the percentage of injected water recovered before a detectable amount of native water was observed. Recoveries obtained experimentally in artificially consolidated models constructed by KUMAR & KIMBLER (1970) ranged from 8,5 to 87,6 %.

So far all investigations have been for single-well radial systems. WHITEHEAD (1974) however extended it to well fields and KIMBLER et al. (1975) studied a method to counteract the effects of pre-existing groundwater movement.

Most of the above mentioned investigations deal with rather thin aquifers, fully penetrating wells and small density differences thus leading to favourable conditions for high recovery efficiencies. The aim of this paper is to discuss cases of convective currents in rather thick aquifers. Those currents can be significant if density differences and permeabilities are large.

3. VORTEX THEORY

To calculate the transient and simultaneous flows of fresh and salt groundwater only those models that consider both horizontal and vertical flow components of all fluids can be used. The computer program BUBBLE that is developed for this study uses vortex-theory, the principle of which will be described below.

It was first recognized by DE JOSSELIN DE JONG (1960) that density differences create rotations in the flow. This rotation can be modelled with singularity or vortex distributions whose action is such that interfaces are tilted (back) to a horizontal position. The concept of vortex theory is to replace all fluids with different densities by one hypothetical fluid and then to introduce singularities at those places where the densities of the actual fluids change. The vortices generate the effect of varying density. By applying the principle of superposition the resulting flow can be computed. It consists of two parts. One of them is accounting for the effects of the density differences, the other for the flow of the hypothetical fluid.

Vortex distributions were first implemented in computer programs for two-dimensional groundwater flow by HAITJEMA (1977). Later on he elaborated the velocity components for the flow resulting from vortex rings for use in axial-symmetric models. Stability criteria for vortex computer programs have been derived by PETERS (1980). All this is used in the computer program BUBBLE. Results and possibilities will be discussed in the next few paragraphs.

4. BUBBLES IN INFINITE MEDIA

Bouyancy effects of spherical foreign fluid substances in infinite aquifers with both a different viscosity and density can be calculated directly by solving the Laplace equation (1980). In case of a sphere and when only the density of foreign and native fluids differ, down- or upward velocity of the bubble turns out to equal 2/3 times α. In this connection α is defined as a constant of gravitational segregation (L/T).

$$\alpha = \frac{k}{n} \frac{\Delta\rho}{\rho} = \frac{\varkappa g}{n\mu} \Delta\rho$$

(Used notations are explained at the end of the text.

This result can also be elaborated by introducing vortex rings between the both fluids (fig. 1).

To check the computer program BUBBLE some tests have been carried out. The velocity field that exists when heavy foreign fluids sink through infinite aquifers is presented in fig. 2 and 3.

Agreement with mathematically obtained results is exact. The foreign fluid (if an ellipsoid) moves as a rigid body slowly displacing the native fluid. Noteworthy in this connection is the problem of undeterminacy. Most researchers are familiar with the phenomenon of interfingering instability. When a fluid is displaced by a less viscous one the interface is not stable. Irregularities will grow. This and other viscosity effects can be significant when injecting surface water with varying temperatures, especially close to wells where flow velocities can be large. In our analysis, however, viscosity differences are ignored.

Other undeterminacy phenomena exist when heavy fluids lie on top of lighter ones. Any irregularity of the interface will grow because of interface instability. In fact it is impossible to model this kind of displacement because time steps for which the movement is stable cannot be found. The movement is dominated by whatever small irregularity that may exist both in nature and in the computer model, leading to unpredictable or incorrect interface positions.

Another test is the calculation of a time-dependent motion of a bubble of fresh water rising in a saline aquifer when it encounters an impermeable boundary. With the passage of time the upward movement of the lighter fluid is retarded. Eventually the fresh water spreads laterally along the top of the aquifer. The movement is plotted in fig. 4 as a function of t* defined as α times t. Values of t* are in metres. At t* = 0 the bubble is assumed spherical.

5. WELL RECHARGE IN SEMI-INFINITE SALTY MEDIA

To calculate the motion of fresh water that is injected with wells the flow velocity components due to this injection are implemented in the axial-symmetric computer program. It is assumed that along the filter screen the discharge is constant and equals Q/2L.

VAN DEN AKKER (1982) elaborated the flow components in r and z direction by taking the derivative of the groundwater head for injection in a filter screen with length 2L. Another possibility is to write down the flow components for both directions due to a point source and then to integrate over the total filter-screen length. This leads to the following less intricate formula (saving computer processing costs)

$$v_r = ((L + z)/a + (L - z)/b) \cdot c/r$$

$$v_z = (1/b - 1/a) \cdot c$$

with

$$a = \text{SQRT}\ (r^2 + (z + L)^2)$$

$$b = \text{SQRT}\ (r^2 + (z - L)^2)$$

$$c = Q\ /\ (8\pi Ln).$$

Using methods of images (to account for the impermeable boundary) and superposition the movement of fresh water injected in saline aquifers can now be calculated. To test the model, computed displacement is compared with the observed displacement of salt water as reported by e.g. SCHUURMANS & VAN DEN AKKER (1981). They described a field test with injection of fresh water in a completely saline aquifer bounded at the top by a rather impervious layer at a depth of 90 m. Injection discharge was 480 m^3/day in a filter of 15 m starting at a depth of 101 m. Permeability for fresh water is estimated at 40 m/day, porosity with respect to flow 38 % and density difference 25 kg/m^3. Calculated is the motion of the interface if fresh water is injected for 60 days. When injection stops density effects cause the infiltrated bubble to rise with such velocity that within 3 weeks almost the complete filter screen is in saline water again (fig. 6).

The model BUBBLE yields a result that shows acceptable agreement with the experiment described by SCHUURMANS & VAN DEN AKKER. Of course it should be kept in mind that sediment heterogeneity and dispersion are the principal factors to take into consideration when comparing both results.

It can be concluded that it turns out to be impossible to store water in thick saline aquifers if both permeability and density difference are large because subsequent attempts of recovery (with the same well) and storage times will lead to almost immediate entrance of native waters to the well.

6. FACTORS AFFECTING RECOVERY EFFICIENCY

Any plan to store water as described in this study should start with field tests, geologic investigations and use of predictive models to get an impression of recovery results. Exact values of recovery efficiency certainly depend on its definition. Recovery efficiency is the fraction of total injected water that can be abstracted before native water can be detected in the pumped water or as long as the quality meets standards for use. In literature various factors influencing recovery results are mentioned. These will be reviewed in short.

Mixing due to the fact that some of the liquid is not displaced as fast as the rest will cause a blurred transition zone between injected and native waters. This will also happen in the case of dead-end-pores where transport of salts can only take place by diffusion and not by flow or in the case of secondary permeability and porosity when fissure flow will occur. The extent to which this hydrodynamic dispersion is likely to cause brackish water is an important question which must be answered. Irregularites (inhomogeneities) play an important part in this connection. Gravitational segregation (reshaping or laydown of interface) occurs when two fluids with different density are in contact. With the passage of time the lighter fluid tends to rise compared to the heavier one. This effect is influenced by the density difference and by permeability. In this connection stratification and anisotropy seriously reducing vertical permeability should be mentioned. Pre-existing groundwater flow - sometimes called salt water flux - is unfavourable since it displaces the injected water so that (part of) it cannot be retrieved. Aquifer dip can reduce recovery efficiency. A density difference will then cause the injected bubble to move in a "horizontal" direction. Injection rates do influence recovery results. If injection is large other unfavourable convective effects will be less harmful. However if storage times are large effects of density difference, aquifer dip and hydraulic gradients can again be serious. Other variables that do affect recoveries are aquifer thickness, cross flow over the upper and lower boundaries of the target-aquifer and chemical reactions between injected water and sediments. Various experiments subsequent to each other can also increase recovery efficiency ("multicycle operation").

7. CONCLUSIONS

Many reported laboratory results indicate that it is feasible to store fresh water in saline aquifers. However it should be kept in mind that actual field conditions that depart from idealized model assumptions can seriously reduce recovery results. Many field experiments show that dispersion in nature is much larger than in laboratory models. Calculations presented in this paper, however, indicate that density effects can be a much more important cause of poor freshwater recovery results than is dispersion. It can be concluded that before storage build-up in practice can be applied, a number of questions remain to be answered. Geologic and hydrogeologic investigations should lead to a profound knowledge of subsurface environment. Analytic models can quickly give an

impression of recovery efficiencies. Use of numerical models that can take into account inhomogeneity and dispersion should only then be considered.

With some modifications the results of this study can also be applied to other research projects. Among these are injection of fluid waste or treated sewage and percolate flow near disposal sites. Vortex theory can enable us to predict behaviour of injected fluids in target - formations with low permeabilities or hydraulic gradients. Attention should then be centred on possible impact on the environment.

ACKNOWLEDGEMENTS

This work is a result of a project "Hydrology of Recharge Well Systems" sponsored by the VEWIN-research program. VEWIN is the Association of Waterworks in the Netherlands.

Discussions with Prof. G. de Josselin de Jong and the assistance of Mr. W. Boerhout in preparing some of the computer plots, are gratefully acknowledged.

NOTATIONS

g	acceleration of gravity (L/T^2)
Q	strength of injection (L^3/T)
k	hydraulic permeability (L/T)
L	half the length of filter screen or dimension of length
M	dimension of mass
n	porosity with respect to flow (-)
r	distance to axis of symmetry (L)
T	dimension of time
t	(time (T)
t^*	α times t (L)
v_r	actual velocity component in r-direction (L/T)
v_z	actual velocity component in z-direction (L/T)
z	vertical coordinate (L)
α	constant of gravitational segregation (L/T)
$\varkappa$	intrinsic permeability of sediments (L^2)
μ	dynamic viscosity of fluid ($M/L/T$)
ρ	density of fluid (M/L^3)
$\Delta\rho$	density difference (M/L^3).

REFERENCES

AKKER VAN DEN, C. (1982). Numerical analysis of the streamfunction in plane groundwater flow. Ph. D. Thesis, Delft.

ESMAIL, O.J. & KIMBLER, O.K. (1967). Investigations of the technical feasibility of storing fresh water in saline aquifers. Water Res. Res. 3, p. 683-695.

GARDNER, G.H.F., DOWNIE, J. & KENDALL, H.A. (1962). Gravity segregation of miscible fluids in linear models. Trans. SPE of AIME 225, pt. II, p. 95-104.

HAITJEMA, H.M. (1977). Numerical application of vortices to multiple fluid flow in porous media. Delft Progr. Rep. 2, p. 237-248.

HAITJEMA, H.M. (1980). The use of vortex rings for modelling salt water upconing. Communications of Lab. Soil Mech., Delft 11, nr. 2.

JOSSELIN DE JONG, G., de (1960). Singularity distributions for the analysis of multiple fluid flow through porous media. J. Geoph. Res. 65, p. 3739-3758.

KIMBLER, O.K. (1970). Fluid model studies of the storage of fresh water in saline aquifers. Water Res. Res. 6, p. 1522-1527.

KIMBLER, O.K., KAZMANN, R.G. & WHITEHEAD, W.R. (1975). Cyclic storage of fresh water in saline aquifers. Louisiana Water Res. Res. Inst., bull. 10, (Louisiana State University, Baton Rouge).

KRUIJTZER, G.H.F. (1980). The downward penetration of a spherical foreign fluid substance in an aquifer. Communications of Lab. Soil Mech. Delft 11, nr. 2, p. 153-159.

KUMAR, A. & KIMBLER, O.K. (1970). Effect of dispersion, gravitational segregation and formation stratification on the recovery of fresh water stored in saline aquifers. Water Res. Res., p. 1689-1700.

MOULDER, E.A. (1970). Fresh water bubbles: A possibility for using saline aquifers to store water. Water Res. Res. 6, p. 1528-1531.

PETERS, J.H. (1983). De stroming van zoet en zout grondwater in een "confined aquifer". KIWA-report SWE-83002.

SCHUURMANS, R.A. & VAN DEN AKKER, C. (1981). Artificial removal of intruded saline water in a deep aquifer. Sveriges Geologiska Undersökning, Rapporter och Meddelanden 27 (Proc. of SWIM 17, Uppsala Sweden).

WHITEHEAD, W.R. (1974). Storage of fresh water in saline aquifers using a well field. Louisiana Water Res. Res. Inst., Ph.D. Thesis, Louisiana State University, Baton Rouge.

FIGURES

Fig. 1: A distribution of vortex rings.

Fig. 2: Velocity fields when heavy fluids sink through infinite aquifers.

Fig. 3: Maximum downward velocity related to velocity of native fluid turns out to be α. Velocities depend solely on shape of bubble, not on dimensions.

Fig. 4: Motion of a fresh-water bubble rising in a semi-infinite salty aquifer with impervious boundary at $z = 0$. Constant t^* is defined as α times t.

Fig. 5: Velocity components of flow due to well recharge or abstraction.

Fig. 6: Motion of interface if fresh water is injected for 60 days.

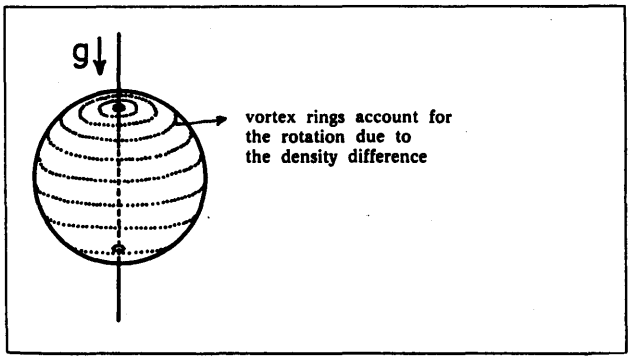

Figure 1

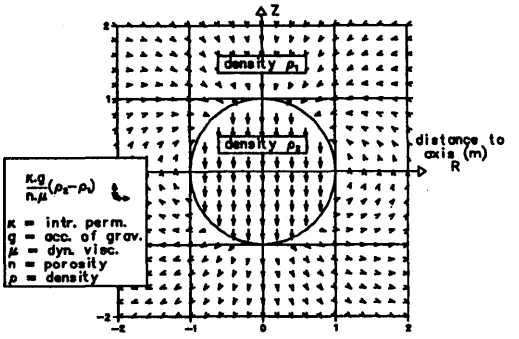

Figure 2

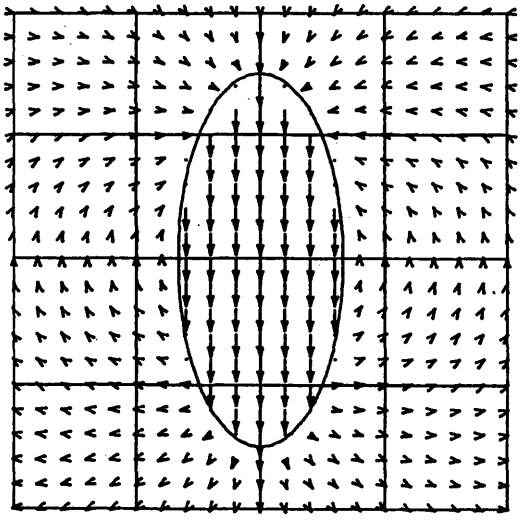

Figure 3

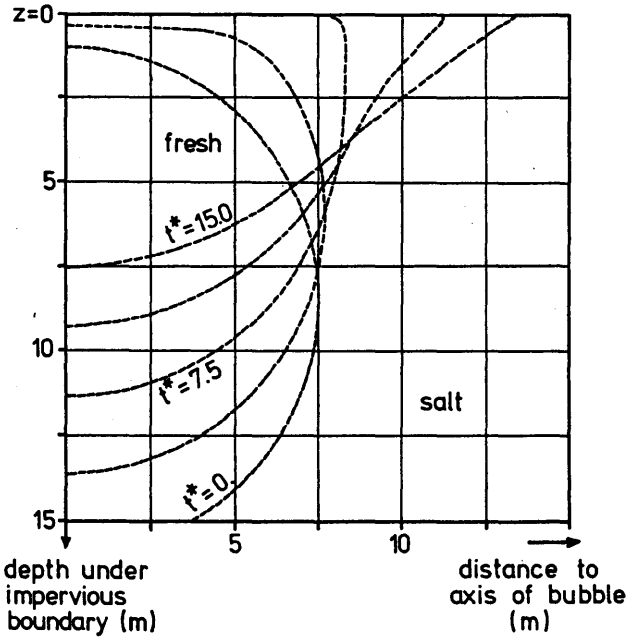

Figure 4

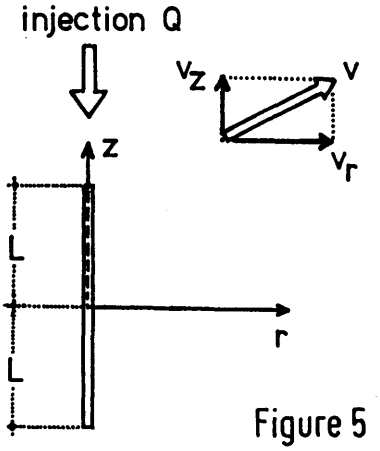

Figure 5

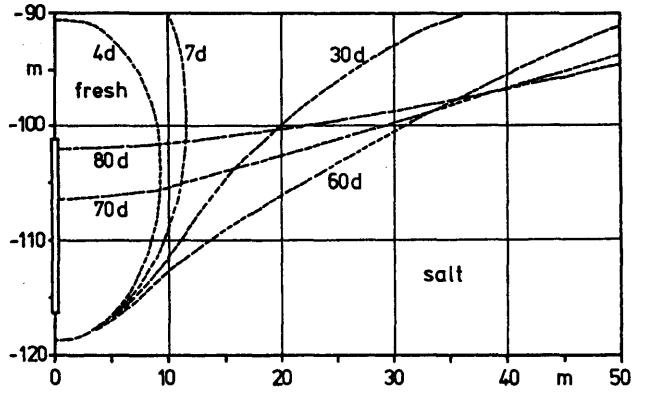

Figure 6

3.4. A MATHEMATICAL MODEL OF THE EVOLUTION OF THE FRESH WATER LENS UNDER THE DUNES AND BEACH WITH SEMI-DIURNAL TIDES

L.C. LEBBE

ABSTRACT

The mathematical model of solute transport and dispersion of KONIKOW & BREDEHOEFT (1978) has been modified so that density-difference effects can be taken into account. With this two-dimensional model the evolution of the fresh-water lens under the dunes and under the shore was studied in a vertical cross-section. At initial time the whole aquifer is supposed to be filled with salt water. A constant infiltration rate of fresh water in the dunes and a constant hydraulic head under the dunes as a function of the semi-diurnal tides is assumed. The vertical boundary under the sea is a constant-hydraulic-head boundary; the one under the dunes is a non-horizontal-flow boundary. The results are compared with field measurements. The hydraulic parameters which have an influence on the distribution of salts will be treated. Finally the effect of water withdrawal in the dunes on the salt distribution can be estimated by the mathematical model.

1. INTRODUCTION

In a former study the subterranean flow of fresh and salt water underneath the western Belgian beach has been described (LEBBE, 1981). For this study thirty borings were drilled on the gently sloping runnel and ridge beach through the unconfined aquifer (fig. 1). In each of the boreholes a resistively logging was performed. Five resistivity profiles perpendicular to the shore line were drawn (fig. 2). These profiles provide a fairly good idea of fresh-, brackish- and salt-water distribution underneath the beach. At one of these profiles the hydraulic-head pattern has been measured continuously in the upper and the lower part of the aquifer. From these piezometers groundwater has been sampled for chemical analysis. Based on these data a mathematical model was developed. This two-dimensional mathematical model treated the steady-state flow of fresh and salt water with a sharp interface. It also took the density-difference effect into account. Thus the most important feature of the different fresh-/salt-water distribution can be explained.

Several examples were treated of different amounts of fresh-water flow from the dunes towards the sea. The results are represented in fig. 3 where the lines of equal fresh-water head are shown together with the stream lines in the vertical plane of the two-dimensional model. The constant-flow-boundary conditions are indicated by the letter Q for the horizontal fresh-water flow of the dunes in the direction of the sea and the letter N for the vertical fresh-water flow, namely the infiltration rate in the dune area. The constant-head-boundary conditions are represented by the value of the constant fresh-water head. The inflow and outflow through the permeable boundaries of the mathematically treated area are calculated and represented near these boundaries. The stream lines have been drawn in such a way that they begin at a cell boundary and at a permeable boundary where an inflow of fresh or salt water occurs. The arrows on the stream lines

indicated the end of the even years a water particle had travelled from the boundary of the area considered. For the last calculation a water-conducting porosity of 0,30 is taken into account.

A first example was given with a considerable seaward fresh-water flow (fig. 3). Because of this flow a horizontal hydraulic gradient towards the sea underneath the dune area exists. Underneath the backshore and the upper part of the foreshore salt water infiltrates. It flows upon the fresh dune water. On the larger part of the foreshore the salt-water flow is directed vertically upwards resulting in an outflow at the beach surface. The fresh water only flows out beneath the sea.

When the horizontal fresh-water flow through the vertical boundary is reduced the infiltration of salt water on the backshore and upper part of the foreshore is enlarged. Consequently the upper salt-water lens is enlarged in depth as well as in width. The fresh-water outflow is further offshore on the seabottom. The zone of fresh-water flow becomes narrower. The lower salt-water tongue retreats towards the sea.

In the last example treated (fig. 4) the fresh-water flow through the vertical boundary under the dunes is reversed. Nearly all the infiltrating fresh water in the dune area is flowing towards this boundary. Only a small part of the infiltrating fresh water still flows towards the sea. On the backshore and upper part of the foreshore the infiltration of salt water becomes so large that the salt-water lens fills the whole aquifer under the shore. In spite of the very small fresh-water flow towards the sea there still is a tongue of fresh water underneath the backshore.

In this mathematical model the process of hydrodynamic dispersion was not incorporated. It was also not possible to explain how much time it takes to evolve from one steady state to another and which intermediate states can occur. Therefore the mathematical model of solute transport and dispersion of KONIKOW & BREDEHOEFT (1978) has been applied to this problem. Since in this mathematical model the hydraulic-head gradients were the only significant driving mechanism for the fluid flow it was first necessary to incorporate the effect of fluid density on the velocity distribution.

2. PROFILES OF FRESH-WATER PERCENTAGE

The five resistivity profiles enable us also to draw profiles of fresh-water percentage. This percentage of fresh water can be calculated if the salinity of the water in a point i of the groundwater reservoir is known together with the salinities of the fresh and salt water.

$$P_{fi} = 100\ F_{fi} = 100\ \left(\frac{c_s - c_i}{c_s - c_f}\right) \qquad (1)$$

where P_{fi} is the fresh-water percentage in a point i
F_{fi} is the fresh-water fraction in a point i
c_i is the salinity of the water in a point i
c_s is the salinity of the salt water
c_f is the salinity of the fresh water.

The salinity can be measured as the total dissolved solids, the chloride or electrical conductivity if we accept the simple linear relation between these parameters (LEBBE et al., 1983). Considering the relation between the total dissolved solids and the resistivity of the water and a formation factor of 2,7 one obtains a relation between the resistivity of a sediment ρ_t, and the total dissolved solids TDS of the pore water.

$$\rho_{ti} = 32.400/TDS_i \qquad (2)$$

where ρ_{ti} is the resistivity of the sediments at a point i in Ωm.

TDS_i is the total dissolved solids of the pore water at that point i in mg/l.
The total dissolved solids of native dune water (fresh water) is 450 mg/l and of seawater (salt water) is 34.500 mg/l.
The resistivity of sediments filled by fresh water following equation (2) is 72 Ωm.

The resistivity of sediments filled by salt water equals 0,95 Ωm. Combining equation (1) and (2) one finds the relation between the fresh-water percentage P_{fi} at a point i and the resistivity of the sediments ρ_{ti} at this point.

$$P_{fi} = 100 \cdot \left(\frac{\rho_{ti} \cdot \rho_{tf} - \rho_{tf} \cdot \rho_{ts}}{\rho_{ti} \cdot \rho_{tf} - \rho_{ti} \cdot \rho_{ts}}\right) \qquad (3)$$

The salt-water percentage is the complement of the fresh-water percentage.

$$P_{si} = 100 - P_{fi} \qquad (4)$$

The salt-water percentage can also be expressed in terms of salinities.

$$P_{si} = 100 \left(\frac{c_i - c_f}{c_s - c_f}\right) \qquad (5)$$

This salt-water percentage is also called the relative salinity S_R (TODD, 1980). Combining equation (2) and (5) results in a relation between the salt-water percentage P_{si} and the resistivity of the sediments ρ_{ti}.

$$P_{si} = 100 \cdot \left(\frac{\rho_{tf} \cdot \rho_{ts} - \rho_{ti} \cdot \rho_{ts}}{\rho_{ti} \cdot \rho_{tf} - \rho_{ti} \cdot \rho_{ts}}\right). \qquad (6)$$

It is clear that the resistivity varies significantly when a small amount of salt water is mixed with fresh water (fig. 5). The contrary is not true. As a consequence one can easily detect differences in admixtures of small amounts of salt water in fresh water. It is more difficult to detect differences in admixtures of small amounts of fresh water in salt water. Consequently the lines of equal fresh-water percentage are accurately drawn for large values. For smaller values of fresh-water percentage these lines cannot be drawn accurately.

The profiles of fresh-water percentage allow one to compare the field observations with the results of the mathematical model of solute transport and dispersion.

3. MATHEMATICAL MODEL

3.1. Theoretical background and numerical technique

The mathematical model of solute transport and dispersion in groundwater of KONIKOW & BREDEHOEFT (1978) has been applied. This model calculates the transient changes in concentration of a non-reactive solute in flowing groundwater. The computer program solves simultaneously two partial differential equations. One equation is the groundwater-flow equation, which describes the head distribution in the aquifer. The second is the solute-transport equation, which describes the chemical concentration in the system.

The computer program is modified so that density-difference effects can be taken into account. For this purpose the groundwater-flow equation has been adjusted. The horizontal and vertical Darcian velocity in a point i of the groundwater reservoir was deduced from equations (1) and (2).

$$q_{hi} = k_{hi} \frac{\rho_f}{\rho_i} \frac{\delta \Psi_{if}}{\delta x} \qquad (7)$$

$$q_{vi} = k_{vi} \frac{\rho_f}{\rho_i} \left(\frac{\delta \Psi_{if}}{\delta z} + \frac{\rho_i - \rho_f}{\rho_f} \right) \qquad (8)$$

where q_{hi} is the horizontal Darcian velocity (LT^{-1})
k_{hi} the horizontal hydraulic conductivity (LT^{-1})
ρ_f the density of the water (ML^{-3})
ρ_i the density of water at point i (ML^{-3})
$\delta \Psi_{if}/\delta x$ the horizontal fresh-water head gradient (dimensionless)
q_{vi} the vertical Darcian velocity (LT^{-1})
k_{vi} the vertical hydraulic conductivity (LT^{-1})
$\delta \Psi_{if}/\delta z$ the vertical fresh-water head gradient (dimensionless)
$(\rho_i - \rho_f)/\rho_f$ the buoyancy at point i (dimensionless).

The buoyancy is deduced from the chemical concentration or salinity which results from the solute-transport equation. A simple linear relation is assumed between the salinity at a point i and the density at this point. The contribution of higher degree terms in this relation can be ignored as well as the influence of the temperature and the pressure on this relation. Of course this is within the limiting values of salinity, temperature and pressure which can occur in the studied area.

The density of the fresh water having a salinity c_f (TDS = 450 mg/l) is taken as ρ_f(= 1 g/cm³) and the density of salt water having a salinity c_s (TDS = 34.500 mg/l) is taken as ρ_s(= 1,025 g/cm³). The linear relation between a density ρ_i and a salinity c_i and passing through the points ρ_f, c_f and ρ_s, c_s can be expressed as:

$$\rho_i = (c_i \cdot (\rho_s-\rho_f) + \rho_f c_s - \rho_s c_f)/(c_s-c_f). \qquad (9)$$

The buoyancy can be expressed as a function of the salinity by means of equation (9):

$$(\rho_i-\rho_f)/\rho_f = (c_i-c_f) \cdot (\rho_s-\rho_f)/(c_s-c_f). \qquad (10)$$

Substitution of equation (5) into equation (10) results in a simple relation between the buoyancy and the salt-water percentage or the relative salinity.

$$(\rho_i-\rho_f)/\rho_f = P_{si} \cdot (\rho_s-\rho_f)/(\rho_f \cdot 100). \qquad (11)$$

The digital computer program uses an alternating-direction implicit procedure to solve a finite-difference approximation of the groundwater-flow equation and it uses the method of characteristics to solve the solute-transport equation. The latter uses a particle-tracking procedure to represent convective transport and a two-step explicit procedure to solve a finite-difference equation that describes the effect of hydrodynamic dispersion, fluid sources and sinks and divergence of velocity.

3.2. Initial and boundary conditions

At the initial time an unconfined aquifer is supposed to be completely filled with salt water. During the simulation period we suppose that the boundary conditions do not change.

The aquifer is bounded below by an impermeable layer. The landward vertical boundary is assumed to be the water-divide line or in the mathematical model a non-horizontal-flow boundary. The upper boundary of the aquifer is partially located under the dunes and partially under the beach and the sea. Under the dunes we assume a constant-vertical-flow boundary. This vertical flow rate is equal to the infiltration rate of fresh water in the dune area. Beneath the

beach and the sea a constant hydraulic-head boundary is assumed. The values of these hydraulic heads were deduced from measurements on the beach (LEBBE, 1981). Where a downward vertical flow occurs on the beach there is an infiltration of salt water. The seaward vertical boundary is a constant-hydraulic-head boundary. The salt-water head is the same over the whole depth. The density or salinity of the water flowing through this boundary depends on the calculated flow direction. When the flow is towards the studied area salt water enters.

3.3. Sequences of calculations

Because we assume at the initial time an unconfined aquifer completely filled with salt water the buoyancies between the nodal points are equal. With the given boundary conditions and the known buoyancies between the nodal points the fresh-water head at each nodal point is derived for the first time step. With the fresh-water-head differences and the buoyancies between the nodal points the velocity components between these nodal points are calculated by equations (7) and (8). By using these components the solute transport equation is solved by applying the method of characteristics. From these results the chemical concentrations or salinities are deduced between the nodal points, and calculated using equation (11). They are used for the calculation of the fresh-water heads and velocity components for the second time period. By the method of characteristics the salinity is calculated after the second time step, after which the buoyancies can again be calculated for the next time step.

3.4. Input

In the two-dimensional model the aquifer is considered in a vertical plane. The aquifer is subdivided in ten layers with a thickness of three metres and thirty-eight columns with a width of thirty metres. Eighteen columns are located under the dunes, fourteen under the beach and six under the sea. In this case the water-divide was assumed to be at 540 m from the high-high-water line and the low-low-water line at 420 m from the high-high-water line. The offshore is considered over a width of 180 m. The mean infiltration rate of fresh water under the dunes is $7{,}39 \cdot 10^{-4}$ m/d. The horizontal hydraulic conductivity is held constant over the considered aquifer at a value of 10 m/d, the vertical hydraulic conductivity is also held constant at a value of 0,2 m/d. By the application of the method of characteristics nine traceable particles, where a concentration is assigned, are used in each cell of the finite-difference grid. The maximum cell distance per movement of the particles has been chosen at 0,85. The longitudinal dispersivity of the porous medium, α_L, is 0,15 m. The ratio of the transverse dispersivity to the longitudinal dispersivity, α_T/α_L, is 0,3. The effective or water-conducting porosity, ε, is 0,3. After each time step of five years the buoyancy was deduced from the calculated concentration and a new fresh-water head and groundwater-velocity configuration were recalculated.

First the evolution of the fresh-water lens under the dunes and beach was simulated during a period of five hundred years. Finally the effect of fresh-water withdrawal in the dunes was simulated. In the eighteen nodal points indicated in fig. 6 there was a water withdrawal. During the first five years the total amount of water pumped was 0,10 m^2/d. The second five years this amount becomes 0,21 m^2/d and finally stays equal to 0,42 m^2/d during a period of thirty years. This last total amount of water pumped exceeds the total amount of infiltration of fresh water in the dune area i.e. 0,40 m^2/d.

3.5. Output

For every nodal point the fresh-water head and the groundwater-flow velocities are obtained for every time step, the chemical concentration after every time step. These output data for the different time steps can be represented in a vertical cross-section through the aquifer. In this cross-section the vertical axis is exaggerated with respect to the horizontal axis. The fresh-water heads during the time step are represented by lines of equal fresh-water head. These lines are found by a linear interpolation between the values of the nodal points. The groundwater-flow velocities during the time step are represented by vectors. These vectors are obtained by calculating the horizontal and vertical components at the nodal points. These components are found by the multiplication of the horizontal or vertical velocities with a time increment. This time increment was chosen in fig. 6 and fig. 7 as one half year. The vectors are plotted at all nodal points taking the units of the horizontal and vertical axis into account. The concentration at the end of every time step is represented by linear interpolation between the concentrations at the nodal points.

3.6. Discussion of results

With the two-dimensional model, which treats the steady-state flow of fresh and salt water with a sharp interface and takes the density difference into account, only the stable fresh-salt-water distribution could be explained. Such a stable salt-fresh-water distribution occurs at the Belgian-French border.There the natural groundwater flow towards the sea is the least affected. It was already more difficult to explain the fresh-salt-water distribution before the urban area of De Panne. This was in particular the case for the occurrence of the isolated lens of brackish water under the lower part of the foreshore (K3 and K4 in fig. 2).

Through the application of the two-dimensional model of solute transport and dispersion which takes density difference into account one notices intermediate states in the evolution from one steady state to another. Looking at the results of our first run represented in fig. 6 and fig. 7 we can already explain more features of water-quality distribution.

To obtain the water-quality distribution under dunes, beach and sea one has first to simulate the evolution for a sufficiently long period until the changes are no

longer meaningfull. At the initial time the aquifer was supposed to be filled with salt water. From this time point on the sea did not inundate the young dune ridge and the water starts to infiltrate through the unsaturated zone.

The salt water is driven out and a fresh-water lens starts to form. During the first years a large transition zone exists between this fresh-water lens and the salt water. Already at the beginning of the formation of the fresh-water lens a brackish-water tongue starts to form in the upper part of the aquifer. In course of time the fresh-water lens grows and the brackish tongue becomes larger, less mineralized and sinks. The washout of the last salt particles near the impermeable substratum occurs first, with the most under the back shore and last and least under the water-divide in the dunes. Finally the brackish tongue becomes fresh although the wash-out is very slow.

Under the sea the salt-water flow is considerable, principally horizontal and in the seaward direction during the first years. When time goes on the salt water becomes less mineralized and the flow diminishes continuously. In the lower part of the aquifer this flow inverts and the water again becomes more mineralized. In the upper part of the aquifer this flow stays in the seaward direction. A very slow flow of salt water develops from the lower to the upper part of the aquifer as was already discribed by COOPER et al. (1964).

After five hundred years of simulation the hydraulic-head and water-quality distribution under dunes, beach and sea does not meaningfully change further. The hydraulic-head and water-quality distribution are now used as initial values for the simulation of the evolution of the water-quality distribution during pumping in the dunes. After ten years of pumping the total pumping, Q_{tot}, is held at 105 % of the total infiltration of fresh water, N_{tot}^{fresh}. During the first five years the total pumping is a quarter of the total pumping after ten years while it is a half during the second five years. This simulation is run to study the effect of over-pumping of fresh water in the dunes.

From the moment that the pumping starts the salt-water lens in the upper part under the shore extends. This happens especially under the foreshore. The fresh-water tongue under the beach becomes narrower and more mineralized. When over-pumping starts, two important developments take place in the water-quality distribution. The first takes place under the boundary of dunes and beach, the second under the foreshore and the sea. Under the boundary of the dunes and the beach salt water starts to flow landwards. A vertical transition zone develops. When over-pumping goes on the developing salt-water encroachment under the dunes sinks until it reaches the lower part ot the aquifer. Finally the salt-water encroachment advances in the lower part of the aquifer. The fresh water which is less mineralized rises from the proximity of the impermeable substratum to the water catchment. Under the foreshore and the sea the fresh-water tongue becomes more mineralized and the salt-water lens sinks especially under the foreshore so that an isolated brackish lens is squeezed out of the tongue. When time goes on this brackish lens becomes more and more mineralized and moves upwards and in

the direction of the sea. This explains the existence of the brackish lenses under the lower part of the offshore before the urban area of De Panne.

From the above given description it is clear that models give an insight into the evolution of salt-water encroachment and can help to take measures against this danger. Although these models can be applied, field data stay indispensible to calibrate them. Only a good combination of accurate field data, like hydraulic heads, water-conducting properties of the sediments and water-quality distribution for the models can help us to attain the above mentioned goals. As KONIKOW (1981) mentioned the model does not replace field data, but it does offer a feedback mechanism that can help to guide the design of more effective and more efficient data-collection programs.

Finally accurate hydrogeological field data and the use of models of solute transport and dispersion can help us to check some proposed geological and geomorphological evolution of some parts of the coastal plain. This help will rather be in the exclusion of some possibilities. A direct deduction of the evolution is rather difficult although not wholly excluded in some cases. For the simulation of the evolution of the water quality under the coastal plain during geological times a good knowledge of the evolution of the topography, and the type, amplitude and mean level of the tidal movement are necessary together with the estimates of the infiltration rates of fresh water during this time.

The calibration of models of solute transport and dispersion in groundwater is interesting because one can easily collect accurate data about the water-quality distribution by means of resistivity logging. This is in particular true for low salt-water percentages (or low relative salinities).

The above described simulation was only a first run. The calibration of the model should be prolonged. By sensitivity analysis we get insight into the effect of the change of the different parameters. The calibration must first take place on the measured hydraulic heads and later on the water-quality distribution. So we hope to obtain more insight in the solute transport and dispersion processes.

4. CONCLUSIONS

Resistivity logging enables us to draw profiles of fresh-water percentage. When fresh-water percentage is high the resistivity varies significantly with change of fresh-water percentage. As a consequence it is easy to detect differences in mixtures of small amounts of salt water in fresh water. In the profiles of fresh-water percentage the lines of equal percentage of fresh-water are drawn for the values 1, 50, 84, 95, 99. In this way the field observation of water quality can easily be compared with the results of the mathematical model of solute transport and dispersion.

The mathematical model of solute transport and dispersion of KONIKOW & BREDEHOEFT (1978) has been modified so that density-difference effects can be taken into

account. With this two-dimensional model the evolution of the fresh-water lens under dunes and beach was simulated for five hundred years. This results in a fresh-water head and water-quality distribution which have been used as initial values for the simulation of the evolution of the fresh-water lens under the dunes during pumping.

Field data such as hydraulic-head measurements and resistivity logging enables us to calibrate this model. The result of the model help us to plan collection of field data. The model calibrated to the field data can be a helpful tool in the control of the fresh-water supply of the dunes of the western coastal plain. The collection of other field data such as porosity and hydraulic conductivies is advisable.

ACKNOWLEDGEMENT

The author would like to thank the National Fund of Scientific Research (Belgium) under whose auspices the study was carried out. He also wishes to express his gratitude to L.K. Konikow, U.S. Geological Survey, Reston, USA, for placing the computer model of two dimensional solute transport and dispersion in ground water at his disposal. Last but not least he thanks Prof. Dr. W. De Breuck for the help in obtaining the field data.

REFERENCES

COOPER, H.H., KOHOUT, F.A., HENRY, H.R. & GLOVER, R.E. (1964). Seawater in coastal aquifers. U.S. Geol. Surv. Wat. Sup. Pap. 1613-C, 1-84.

KONIKOW, L.F. (1981). Role of numerical simulation in analysis of groundwater quality problems. The Science of the Total Environment, 21, 299-312.

KONIKOW, L.F. & BREDEHOEFT, J.D. (1978). Computer model of two-dimensional solute transport and dispersion in ground-water. U.S. Geological Survey Techniques of Water-Resources Inv., Book 7, Chap. C2, 90 pp.

LEBBE, L.C. (1981). The subterranean flow of fresh and salt water underneath the western Belgian beach. In: Proceedings of 7th Salt Water Intrusion Meeting, Uppsala, Sver. Geolog. Unders. Rap. Meddel. 27, 193-219.

LEBBE, L.D., De BREUCK, W. & BOLLE, I. (1983). Salt-water encroachment in the western Belgian coastal plain. Proceedings of 8th Salt Water Intrusion Meeting, Bari.

TODD, D.K. (1980). Groundwater Hydrology, 2nd edition, 535 p., New York: John Wiley & Sons.

FIGURES

Fig. 1: Situation of the hydrogeological study in the Westhoek area with calculated lines of equal hydraulic head and of the resistivity logging profiles.

Fig. 2: Resistivity profiles perpendicular to the shore line of the Westhoek area.

Fig. 3: Flow of salt and fresh water and the lines of equal fresh-water head with a seaward fresh-water flow of 0,25 · m^2/d.

Fig. 4: Flow of salt and fresh water and the lines of equal fresh-water head with a landward fresh-water flow of 0,09 m^2/d.

Fig. 5: Profiles of fresh-water percentage.

Fig. 6: Evolution of fresh-water lens under dunes, beach and sea.

Fig. 7: Evolution of fresh-water lens during pumping in dunes.

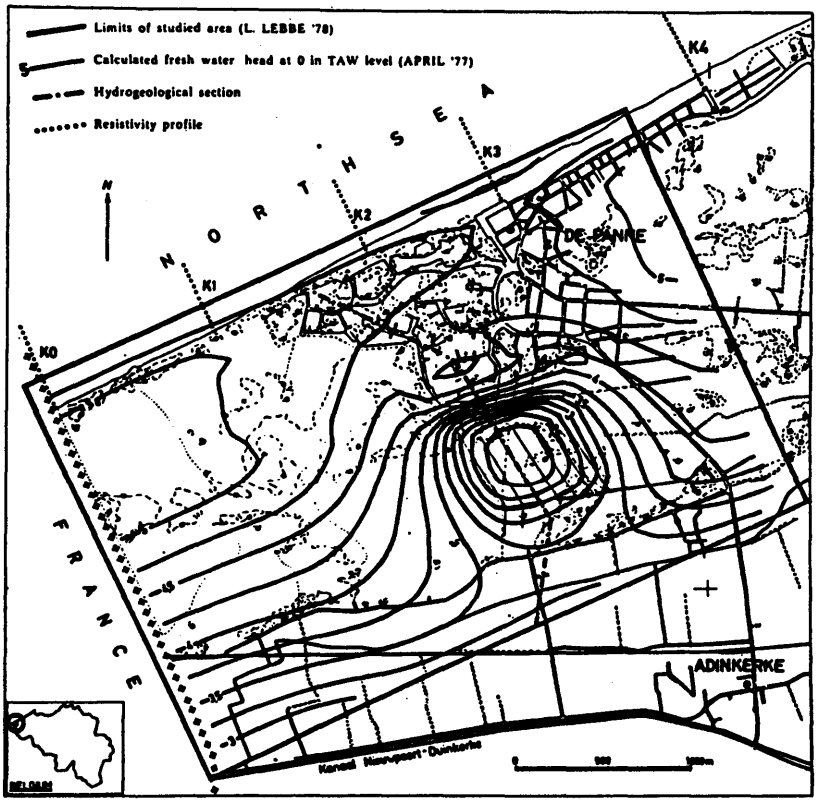

Figure 1

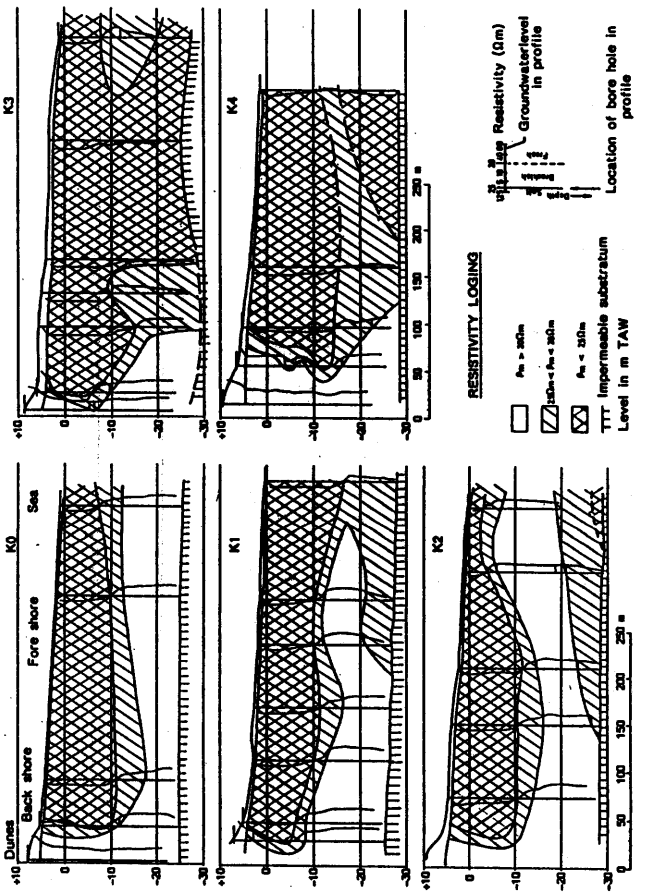
K3
K4
K0
K1
K2
Dunes
Back shore
Fore shore
Sea
RESISTIVITY LOGGING
Resistivity (Ωm)
Groundwaterlevel in profile
Location of bore hole in profile
Impermeable substratum
Level in m TAW

Figure 2

q_h (10 mm/d)
q_v (10 mm/d)
2.865
2.940
3.015
3.090
3.165
3.240
3.315
3.390
600 m
450
300
150
0
low low tide line
high high tide line
fresh water
salt water
impermeable substratum
q_h (10 mm/d)

Figure 3

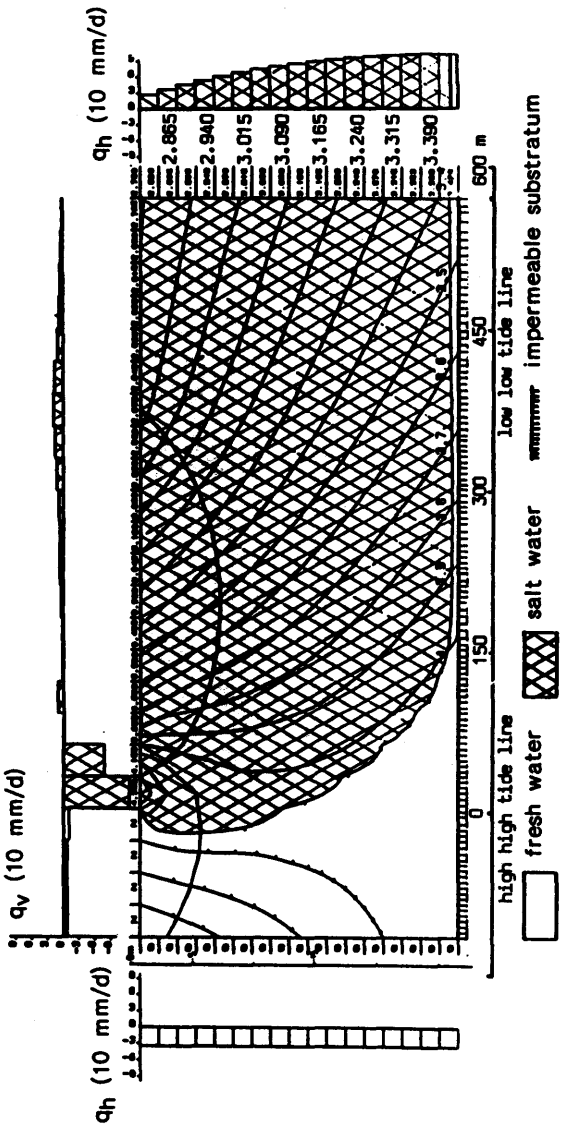
qh (10 mm/d)
2.865
2.940
3.015
3.090
3.165
3.240
3.315
3.390
600 m
450
300
150
0
low low tide line
high high tide line
qv (10 mm/d)
qh (10 mm/d)
fresh water
salt water
impermeable substratum

Figure 4

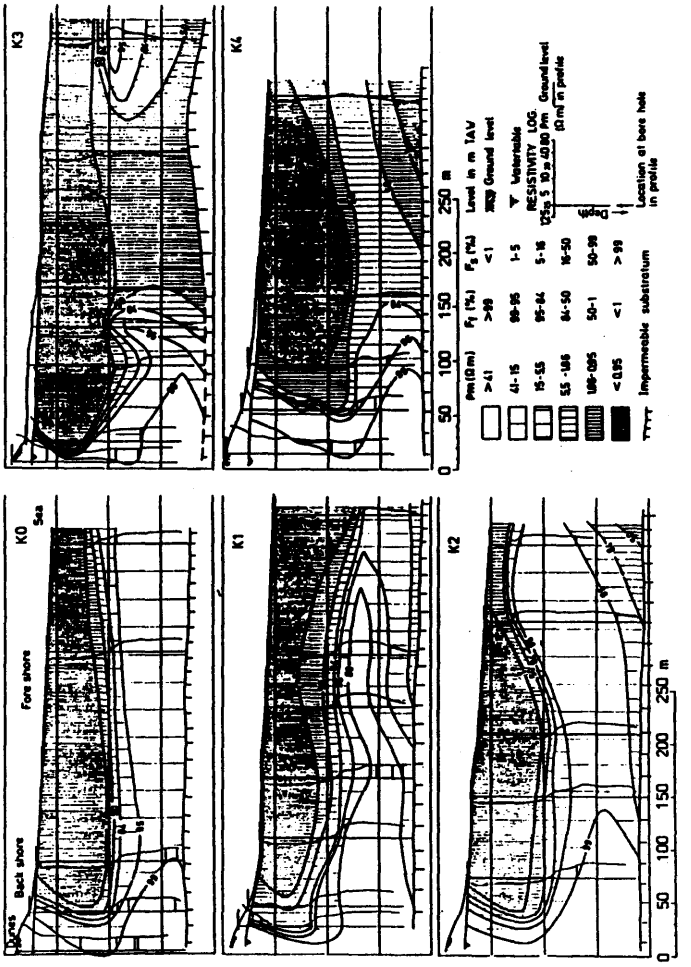
K3
K4
K0
K1
K2
Sea
Fore shore
Back shore
Dunes
0
50
100
150
200
250 m
Level in m TAV
Ground level
Watertable
Location of bore hole in profile
Impermeable substratum

Figure 5

DUNES
SHORE
SEA
after 5 years
after 10 years
after 20 years
after 40 years
after 80 years
after 160 years
after 320 years
after 500 years
0
5
10
15
20
25
m
-450
-300
-150
0
150
300
450
600 m
99
95
84
50
P_f 99%
99% P_f 95%
95% P_f 84%
84% P_f 50%
50% P_f 1%
P_f 1%

Figure 6

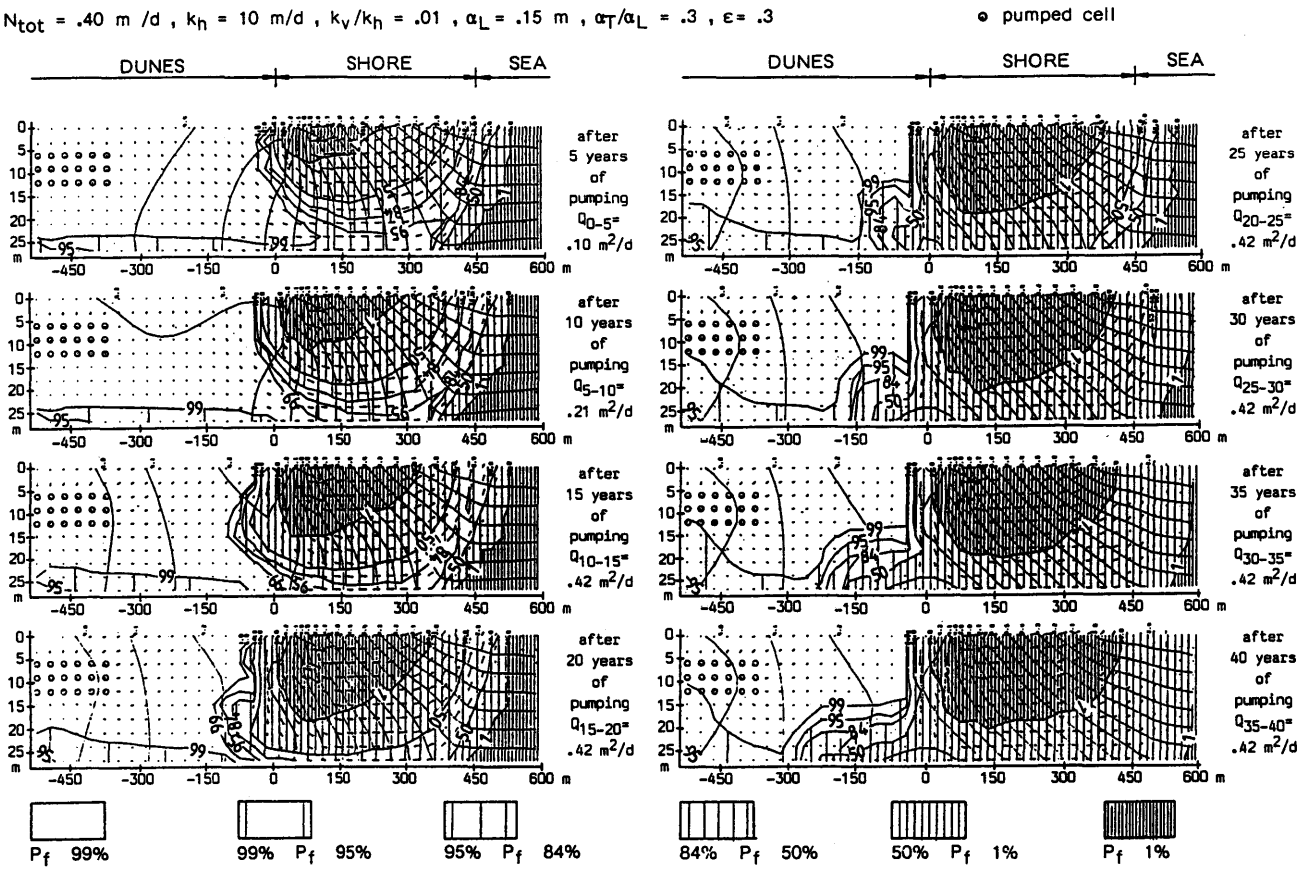
N_{tot} = .40 m /d , k_h = 10 m/d , k_v/k_h = .01 , α_L = .15 m , α_T/α_L = .3 , ε = .3
pumped cell
DUNES
SHORE
SEA
after 5 years of pumping Q_{0-5}= .10 m^2/d
after 10 years of pumping Q_{5-10}= .21 m^2/d
after 15 years of pumping Q_{10-15}= .42 m^2/d
after 20 years of pumping Q_{15-20}= .42 m^2/d
after 25 years of pumping Q_{20-25}= .42 m^2/d
after 30 years of pumping Q_{25-30}= .42 m^2/d
after 35 years of pumping Q_{30-35}= .42 m^2/d
after 40 years of pumping Q_{35-40}= .42 m^2/d
-450 -300 -150 0 150 300 450 600 m
0 5 10 15 20 25 m
99 95 84 50
P_f 99%
99% P_f 95%
95% P_f 84%
84% P_f 50%
50% P_f 1%
P_f 1%

Figure 7

3.5. THE USE OF PRESSURE GENERATORS IN SOLVING THREE-DIMENSIONAL SALT-/FRESH-GROUNDWATER PROBLEMS

G.A. BRUGGEMAN

ABSTRACT

A calculation method for the flow of groundwater of varying densities, e.g. at a salt-/fresh-water interface, is discussed. A three-dimensional flow is calculated by means of pressure functions and generators.

The following calculation method is in a way comparable to the well-known vortex theory, which treats a two-dimensional flow by means of stream functions and vortices (DE JOSSELIN DE JONG, 1977; VAN DEN AKKER, 1982). The present paper considers a three-dimensional flow with the aid of pressure functions and generators.

Considering confined or semi-confined aquifers in coastal regions the following assumption are made.

1. The soil is homogeneous and isotropic, so the intrinsic permeability is constant in all directions.
2. The viscosity μ of the fluid is constant.
3. The density ρ of the fluid is related to the concentration of a solute and is a function of place and time.
4. The soil skeleton and the fluid are incompressible, so the elastic storage will be zero.

It follows from these assumptions that the density is not a function of pressure, but of the concentration of a solute.

Making use of a control volume having the form of a box with sides dx, dy and dz, the general continuity equation for the flux of groundwater that contains a solute, such as salt or chlorine, can be written as:

$$\operatorname{div}(\rho\vec{v}) + \frac{\partial(\rho n)}{\partial t} = 0 \quad \text{or}$$

$$\frac{\partial}{\partial x}(\rho v_x) + \frac{\partial}{\partial y}(\rho v_y) + \frac{\partial}{\partial z}(\rho v_z) + \frac{\partial(\rho n)}{\partial t} = 0 \qquad (1)$$

in which ρ = density, $\vec{v}$ = bulk velocity or Darcy velocity or specific discharge and n = porosity. We can reduce these equations to

$$\rho \operatorname{div} \vec{v} + \vec{v} \cdot \operatorname{grad} \rho + n \frac{\partial \rho}{\partial t} = 0 \qquad (2)$$

bearing in mind that the soil was assumed incompressible (n = constant, so $\frac{\partial n}{\partial t} = 0$).

As the water is incompressible (assumption 4), an increase of the solute concentration in the control volume only results in a change of the density and not of the volume of the groundwater. Therefore it is permissable to apply the continuity equation for the volume, which means:

$$\text{div } \vec{v} = 0 \quad \text{or} \quad \frac{\partial v_x}{\partial x} + \frac{\partial v_y}{\partial z} + \frac{\partial v_z}{\partial z} = 0 \ . \tag{3}$$

The continuity equation (2) can be divided into two equations, one for the groundwater and one for the solute:

$$\text{div } \vec{v} = 0$$

$$\text{and } \vec{v} \cdot \text{grad } \rho + n \frac{\rho \partial}{\partial t} = 0. \tag{4}$$

The density $\rho = \rho(c)$ is a function of the concentration of the solute (chlorine content in salt-/fresh-water problems). So, as the density is not a constant, the general form of Darcy's law must be chosen for the equation of motion:

$$\vec{v} = - \frac{k}{\mu} (\text{grad } p + \rho g \text{ grad } z) \text{ or}$$

$$v_x = - \frac{k}{\mu} \frac{\partial p}{\partial x} \quad v_y = - \frac{k}{\mu} \frac{\partial p}{\partial y} \quad v_z = - \frac{k}{\mu} (\frac{\partial p}{\partial z} + \gamma) \tag{5}$$

in which p = pressure of the groundwater, k = intrinsic permeability g = gravity acceleration and $\gamma = \rho g$ = specific weight of the groundwater = $\gamma(c)$, a function of the concentration of the solute.

It has no sense to introduce some kind of potential function instead of pressure in this case, because in density flow the velocity vector is no longer simply proportional to the gradient of a potential function: the flow is rotational and not potential.

Combining the equation of motion (5) with the two continuity equations (4) the following two differential equations for three-dimensional density flow are found:

$$\frac{\partial^2 p}{\partial x^2} + \frac{\partial^2 p}{\partial y^2} + \frac{\partial^2 p}{\partial z^2} + \frac{\partial \gamma}{\partial z} = 0 \text{ and}$$

$$\frac{k}{\mu} (\frac{\partial p}{\partial x} \cdot \frac{\partial \gamma}{\partial x} + \frac{\partial p}{\partial y} \cdot \frac{\partial \gamma}{\partial y} + \frac{\partial p}{\partial z} \cdot \frac{\partial \gamma}{\partial z} + \frac{\partial \gamma}{\partial z}) = n \frac{\partial \gamma}{\partial t} \tag{6}$$

or in vector notation: $\nabla^2 p + \frac{\partial \gamma}{\partial z} = 0$

and $\frac{k}{\mu} (\text{grad } p \cdot \text{grad } \gamma + \gamma \frac{\partial \gamma}{\partial z}) = n \frac{\partial \gamma}{\partial t}$.

These two differential equations are mutually dependent and have to be solved simultaneously for p(x, y, z, t) and γ(x, y, z, t). Although both water and soil are assumed to be incompressible, the flow nevertheless is non-steady as a result of the varying density of the groundwater.

Only if $\vec{v} \cdot \text{grad } \rho = 0$, as can be seen from (4), may the density flow become steady ; that is if the streamlines everywhere are tangential to the surface ρ = constant.

Now the basic principle of the calculation method lies in the fact that it is possible to separate the original differential equation (2) into the two equations (6), of which the first is steady (no derivative with respect to time):

$$\frac{\partial^2 p}{\partial x^2} + \frac{\partial^2 p}{\partial y^2} + \frac{\partial^2 p}{\partial z^2} + \frac{\partial \gamma}{\partial z} = 0 \ . \qquad (7)$$

This is a differential equation of the Poisson type, which may be solved with the aid of a so called singularity integral, as follows.

$$\frac{\partial^2 p}{\partial x^2} + \frac{\partial^2 p}{\partial y^2} + \frac{\partial^2 p}{\partial z^2} = = \qquad (8)$$

but where in any point where $\frac{\partial \gamma}{\partial z} \neq 0$, a so called "pressure discharge" is introduced with a strength that equals the value of $\frac{\partial \gamma}{\partial z}$ at that point.

Such a pressure generator at a point causes a small pressure change everywhere in the field, in the same way as an abstraction or injection of water at a point gives changes of head everywhere in the flow field.

That change of pressure is, besides on the strength of the generator, also dependent on the boundary values of the flow problem, expressed this time in pressures or pressure gradients. The total contribution of the pressure generators situated at all points of the field where $\frac{\partial \gamma}{\partial z} \neq 0$, to the value of the pressure p at an arbitrary point (x_o, y_o, z_o) of the field, then gives the solution of the first differential equation.

This means, that starting from an initial known distribution of the density or specific weight of the groundwater, the initial pressure distribution all over the field can be determined by solving the Poisson equation (7) with the aid of pressure generators, thus reducing non-potential flow to potential flow. This may also be done for complicated three-dimensional problems, as potential flow does not yield severe difficulties for a good computer.

As soon as the pressure distribution is known, the velocity distribution, related to it by means of Darcy's law, can also be determined.

Next consider a small time interval Δt. During that time the water particles will move according to the calculated velocity distribution.

Assuming that a certain particle always maintains the same solute concentration (dispersion is neglected; this will be discussed later) the density distribution will have been changed according to the displacement of the water particles, which can be calculated; computer programs are available for this purpose. With the new density distribution the Poisson equation (7) can again be solved and the corresponding new pressure distribution, and also the related new velocity distribution, can be determined.

In this way the non-steady density flow can be calculated iteratively determining the concentration of a solute as a function of place and time as a result of any natural or human interference on the groundwater system.

Primarily the influence of one pressure generator with a constant intensity η on the pressures in an infinite field will be determined.
Consider a sphere with radius R in an infinite field.

Assume that the flow inside the sphere satisfies a Poisson equation of the form

$$\nabla^2 p_1 = \eta \text{ for } r \leq R \tag{9}$$

while outside the sphere a potential flow exists:

$$\nabla^2 p_2 = 0 \text{ for } r \leq R, \tag{10}$$

the problem thus being pure spherical.

Inside the sphere, ($r \leq R$) using spherical co-ordinates (9) becomes:

$$\text{for } r \leq R: \frac{1}{r^2} \frac{d}{dr} \left(r^2 \frac{dp_1}{dr}\right) = \eta \tag{11}$$

with solution: $p_1 = \frac{1}{6} \eta r^2 - \frac{A}{r} + B$

with A and B arbitrary constants.

As $\frac{dp_1}{dr}(o) = 0$ the constant A becomes zero, so

$$p_1 = \frac{1}{6} \eta r^2 + B \text{ and } \frac{dp_1}{dr} = \frac{1}{3} \eta r.$$

Outside the sphere ($r \geq R$) equation (10) in spherical co-ordinates becomes:

$$\text{for } r \geq R: \frac{d}{dr} \left(r^2 \frac{dp_2}{dr}\right) = 0$$

$$\text{wit solution } p_2 = -\frac{C}{r} + D.$$

The constant D vanishes, with the condition that for $r \to \infty$ p_2 becomes zero.

$$\text{So } p_2 = -\frac{C}{r} \text{ and } \frac{dp_2}{dr} = \frac{C}{r^2}$$

Continuity at the sphere surface requires that both $p_1(R) = p_2(R)$ and

$$\frac{dp_1}{dr}(R) = \frac{dp_2}{dr}(R).$$

The last condition gives $\frac{1}{3}\eta R = \frac{C}{R^2}$ from which $C = \frac{1}{3}\eta R^3$, while the first condition yields:

$$\frac{1}{6}\eta R^2 + B = -\frac{1}{3}\eta R^2 \text{ and thus } B = -\frac{1}{2}\eta R^2.$$

The complete solution is:

$$r \leq R: \; p_1 = -\frac{1}{6}\eta (3R^2 - r^2) \tag{12}$$

$$r \geq R: \; p_2 = -\frac{1}{3}\eta \frac{R^3}{r}. \tag{13}$$

According to (13), a spherical pressure generator with intensity η and strength ηV_R, with V_R = volume of the sphere = $\frac{4}{3}\pi R^3$ gives a change in pressure in an infinite field, which is inversely proportional to the distance from the centre of the sphere:

$$p = -\frac{\eta}{4\pi r} V_R, \tag{14}$$

The dimension of $\eta = [FL^{-4}]$ and of strength $\eta V_R = [FL^{-1}]$.

The magnitude of the volume V_R in (14) is immaterial for the foregoing analysis; so the region of generator strength can be reduced to a volume as small as pleased, such that V_R becomes the infinitesimal small volume dV. The spherical pressure generator becomes a point generator that gives a small pressure change everywhere in the field according to:

$$dp = -\frac{\eta \, dV}{4\pi r}. \tag{15}$$

If η is a function of place: $\eta = \eta(x,y,z)$ in some region R, then the total contribution of the infinite pressure generators in that region to the pressure in the field becomes:

$$p = -\frac{1}{4\pi} \iiint_V \frac{\eta(x_o,y_o,z_o) \, dx_o dy_o dz_o}{\sqrt{\{(x-x_o)^2 + (y-y_o)^2 + (z-z_o)^2\}}}.$$

According to (7), $\eta(x_o,y_o,z_o) = -\frac{\partial \gamma}{\partial z}(x_o,y_o,z_o)$.

The solution of the Poisson differential equation (7) now can be found as the solution of the Laplace differential equation (8) with initial and boundary conditions for the same problem, assuming the groundwater is homogeneous (constant γ) with an added pressure distribution caused by an infinite number of infinitely small pressure generators with strength $-\frac{\partial \gamma}{\partial z}$ at those points, where the density varies in the z-direction.

For an infinite field this pressure distribution becomes:

$$p_1 = \frac{1}{4\pi} \iiint_V \frac{1}{r} \frac{\partial \gamma}{\partial z} (x_o, y_o, z_o) dx_o, dy_o, dz_o \qquad (16)$$

$$\text{with} \quad r = \sqrt{\{(x-x_o)^2 + (y-y_o)^2 + (z-z_o)^2\}}$$

in which the volume integral has to be taken over the region where $\frac{\partial \gamma}{\partial z} \neq 0$.

As p_1 is the solution in an infinite field, a second solution p_2 must be found, such that $\nabla^2 p_2 = 0$ and $p_1 + p_2$ satisfies the initial and boundary conditions. The sum $p = p_1 + p_2$ then represents the pressure distribution caused by the pressure generators.

The integral in equation (16) is called a singularity integral, because of the fact that a rotational flow is transformed into a potential flow by means of introducing pressure generators in an infinite number of singular points.

A particular case of the singularity integral (16) originates from a sharp interface S between two fluids of different densities ρ_1 and ρ_2.

Assume initially for instance the equation of the interface (t = 0):

$$z_i = z_i(x_i, y_i)$$

where i denotes interface. If we consider a strip between the two surfaces z_i and $z_i + dz_i$ then $\frac{\partial \gamma}{\partial z}$ becomes $\frac{\gamma_1 - \gamma_2}{dz_i}$ and integration in (16) in the z-direction becomes $\frac{\gamma_1 - \gamma_2}{r}$

where: $$r = \sqrt{\{(x-x_i)^2 + (y-y_i)^2 + z-z_i\ (x_i, y_i)^{\ 2}\}} \ .$$

So the singularity integral in an infinite field in the case of a sharp interface $z_i = z_i(x_i, y_i)$ become:

$$p_1 = \frac{\gamma_1 - \gamma_2}{4\pi} \iint_{S_{xy}} \frac{dx_i\ dy_i}{r} \qquad (17)$$

with r defined above.

The integration must be performed over S_{xy}, the projection of the interface S on the xy-plane; r is the distance between a small element dS on the interface with projection $dx_i dy_i$ and the arbitrary point P(x,y,z), where pressure changes take place in an infinite field as a result of an infinite number of pressure generators with intensity $\gamma_1 - \gamma_2$, located on the interface S.

Along an interface a so called shear flow exists, which means that there are differences in velocity, tangential to the interface, of the fluids with different density at both sides of the interface.
This can be shown as follows:

Assume that the interface separates fresh water with specific weight γ_f from underlying salt water with specific weight γ_s.

Equilibrium considerations require that at points of the interface the pressures p_f and p_s for the fresh and the salt water are equal ($p_f = p_s = p_i$).

The piezometric heads at points of the interface become:

$$\phi_{if} = \frac{p_i}{\gamma_f} + z_i \quad \text{and} \quad \phi_{is} = \frac{p_i}{\gamma_s} + z_i$$

respectively. Elimination of p_i gives:

$$\gamma_f(\phi_{if} - z_i) = \gamma_s(\phi_{is} - z_i) \tag{18}$$

at the interface.

Differentiation of (18) with respect to x_i gives:

$$\gamma_f\left(\frac{\partial \phi_{if}}{x_i} + \frac{\partial \phi_{if}}{\partial z_i} \cdot \frac{\partial z_i}{\partial x_i} - \frac{\partial z_i}{\partial x_i}\right) = \gamma_s\left(\frac{\partial \phi_{is}}{\partial x_i} + \frac{\partial \phi_{is}}{\partial z_i} \cdot \frac{\partial z_i}{\partial x_i} - \frac{\partial z_i}{\partial x_i}\right) . \tag{19}$$

Within each region on both sides of the interface, Darcy's law for potential flow is applicable separately, though with different permeabilities:

$$v_{xf} = - K_f \frac{\partial \phi_f}{\partial x} = - \frac{k\gamma_f}{\mu} \frac{\partial \phi_f}{\partial x}, v_{xs} = - K_s \frac{\partial \phi_s}{\partial x} = \frac{k\gamma_s}{\mu} \frac{\partial \phi_s}{\partial x}$$

assuming $\mu_f = \mu_s = \mu$ (equal viscosities).

Thus at the interface we get with (19) a first relation between the differences of the Darcy velocities for the fluids on both sides of the interface:

$$(v_{xf} - v_{xs}) + (v_{zf} - v_{zs}) \frac{\partial z_i}{\partial x_i} = \frac{k}{\mu} (\gamma_s - \gamma_f) \frac{\partial z_i}{\partial x_i} . \tag{20}$$

In the same way differentiating (18) with respect to y we find a second relation:

$$(v_{yf} - v_{ys}) + (v_{zf} - v_{zs}) \frac{\partial z_i}{\partial y_i} = \frac{k}{\mu} (\gamma_s - \gamma_f) \frac{\partial z_i}{\partial y_i} . \qquad (21)$$

The interface is in general non-steady and may be represented by $z_i = z_i (x_i, y_i, t)$.

At every point of this moving interface the following expression holds

$$\frac{dz_i}{dt} = \frac{\partial z_i}{\partial x_i} \frac{dx_i}{dt} + \frac{\partial z_i}{\partial y_i} \cdot \frac{dy_i}{dt} + \frac{\partial z_i}{\partial t} . \qquad (22)$$

As $\frac{dx_i}{dt}$ represents both the real velocity component in the x-direction for fresh and the salt water, at points of the interface, and also $\frac{dy_i}{dt}$ and $\frac{dz_i}{dt}$ the real velocity components in y- and z-directions, respectively, we get in terms of Darcy velocities:

$$\frac{\partial z_i}{\partial z_i} v_{xf} + \frac{\partial z_i}{\partial y_i} v_{yf} - v_{zf} + n_e \frac{\partial z_i}{\partial t} = 0$$

and

$$\frac{\partial z_i}{\partial x_i} v_{xs} + \frac{\partial z_i}{\partial y_i} v_{ys} - v_{zs} + n_e \frac{\partial z_i}{\partial t} = 0 .$$

Subtraction of these two equations gives the third relation between the differences of the Darcy velocities in the three co-ordinate directions on both sides of the interface at points of the interface:

$$(v_{xf} - v_{xs}) \frac{\partial z_i}{\partial x_i} + (v_{yf} - v_{ys}) \frac{\partial z_i}{\partial y_i} - (v_{zf} - v_{zs}) = 0. \qquad (23)$$

Denoting $v_{xf} - v_{xs}$ by d, (d = difference) and $v_{yf} - v_{ys} = d_y$ and $v_{zf} - v_{zs} = d_z$ the equations may be solved for d_x, d_y and d_z:

$$d_x = v_{xf} - v_{xs} = \frac{k}{\mu} (\gamma_s - \gamma_f) \frac{\frac{\partial z_i}{\partial x}}{1 + (\frac{\partial z_i}{\partial x})^2 + (\frac{\partial z_i}{\partial y})^2}$$

$$d_y = v_{yf} - v_{ys} = \frac{k}{\mu} (\gamma_s - \gamma_f) \frac{\frac{\partial z_i}{dx}}{1 + (\frac{\partial z_i}{\partial x})^2 + (\frac{\partial z_i}{\partial y})^2} \qquad (24)$$

$$d_z = v_{zf} - v_{zs} = \frac{k}{\mu} (\gamma_s - \gamma_f) \frac{(\frac{\partial z_i}{\partial x})^2 + (\frac{\partial z_i}{\partial y})^2}{1 + (\frac{\partial z_i}{\partial x})^2 + (\frac{\partial z_i}{\partial y})^2} . \quad (24)$$

These velocity differences may be considered as the components of a vector $\vec{d}$ (d_x, d_y, d_z).

The vector n, normal to the interface at a point on the interface, is, if we write the interface as:

$$f_i = z_i - z_i (x_i, y_i) = 0:$$

$$\vec{n} = \text{grad } f_i = (-\frac{\partial z_i}{\partial x}, -\frac{\partial z_i}{\partial y}, 1).$$

It can easily be seen that $\vec{d}$ and $\vec{n}$ are orthogonal vectors and the scalar product equals zero:

$$\vec{d} \cdot \vec{n} = 0.$$

The absolute value of the velocity difference vector is, if $K^* = \frac{k}{\eta} (\gamma_s - \gamma_f)$:

$$|\vec{d}|^2 = d_y^2 + d_y^2 + d_z^2 = K^* d_z$$

as can be shown easily.

Conclusion: the velocity difference vector $\vec{d}$ at a point of an abrupt interface between two homogeneous fluids of different density is directed along the interface (lies in the plane tangent to the interface at that point) and is called shear flow; the absolute value amounts to:

$$|\vec{d}| = \sqrt{K^* d_z}.$$

It follows that in the direction normal to the interface the velocity difference equals zero and the flow is continuous in that direction, as might be expected.

In two-dimensional flow, for example flow only in the x- and z-directions, $\frac{\partial z}{\partial y} = 0$, $\frac{\partial z}{\partial x} = \text{tg } \beta$; equations (24) then become:

$$d_x = K^* \sin \beta \cos \quad \text{and } d_z = K^* \sin^2 \beta$$

and

$$|\vec{d}| = K^* \sin \beta$$

in which β = the angle between the tangent at a point of the interface line and the positive x-axis.

As soon as transport of a solute in groundwater takes place, as in the case of density flow, we encounter the phenomenon of dispersion.

However, the differential equations that describe the transport may be considered as additional to the here described differential equations and need not be neglected; instead of equations (6) we get:

$$\nabla^2 p + \frac{\partial \gamma}{\partial z} = 0 \qquad (26)$$

$$\text{and } n \frac{\partial}{\partial_i} (D_{ij} \cdot \frac{\partial \rho}{\partial_i}) + \frac{k}{\mu} (\text{grad } p \cdot \text{grad } \rho + \rho g \frac{\partial \rho}{\partial z}) = n \frac{\partial \rho}{\partial t}$$

if the density ρ is a linear function of the concentration of the solute. The dispersion terms are written according to the Einstein convention with i,j = x,y,z:

$$\frac{\partial}{\partial i} (D_{ij} \frac{\partial \rho}{\partial j}) = \frac{\partial}{\partial x} (D_{xx} \frac{\partial \rho}{\partial x} + D_{xy} \frac{\partial \rho}{\partial y} + D_{xz} \frac{\partial \rho}{\partial z})$$

$$+ \frac{\partial}{\partial y} (D_{yx} \frac{\partial \rho}{\partial x} + D_{yy} \frac{\partial \rho}{\partial y} + D_{yz} \frac{\partial \rho}{\partial z})$$

$$+ \frac{\partial}{\partial z} (D_{zx} \frac{\partial \rho}{\partial x} + D_{zy} \frac{\partial \rho}{\partial y} + D_{zz} \frac{\partial \rho}{\partial z}) \ .$$

REFERENCES

DE JOSSELIN DE JONG, G. (1977). Review of vortex theory for multiple fluid flow. Delft Progress Report 2, 225-236.

VAN DEN AKKER, C. (1982). Numerical analysis of the stream function in plane groundwater flow. PhD Thesis Technical University Delft, Holland.

3.6. A RANDOM-WALK SIMULATION OF DISPERSION AT AN INTERFACE BETWEEN FRESH AND SALINE GROUNDWATER

G.J.M. UFFINK

ABSTRACT

Simulation techniques for fresh- and saline-groundwater flow are usually based on the assumption that fresh and saline water do not mix. However, due to dispersion mixing occurs and a zone with brackish water is formed. Modelling of the brackish zone is important for management of the fresh-water reservoir in the deep aquifers along the coast in Holland.

In principle convective-flow models may be extended with a dispersive component using a random-walk method. With this method solutions for sharp interfaces could be used to study the width of the brackish zone, if additionally the velocity distribution and dispersion coefficients near the interface are known and the amount of salt entering the brackish zone. In the paper the velocity distribution in the brackish zone has been found with a boundary layer analysis. The analysis also gives an expression for the total amount of salt flowing into the brackish zone. An example of a random-walk simulation is included, using the information from the boundary-layer analysis.

1. INTRODUCTION

The fresh groundwater lying under the dunes along the coast forms an important source for the drinking-water supply in the west part of the Netherlands. Artificial recharge with ponds is applied in the upper aquifer to increase the fresh-water reservoir. Experiments with infiltration wells are carried out in the deep aquifer where both fresh and saline water occur (KOOIMAN & UFFINK, 1986). Management of a future fresh-water reservoir in the deep aquifers requires a simulation technique. This concerns not only the position of the interface, but the growth of a brackish transition zone as well.

Problems with fresh and saline groundwater are usually studied with a sharp interface assumption, while mixing by dispersion is neglected. These purely convective-flow models may be combined with a random-walk method to include the effect of dispersion (UFFINK, 1985). So far this technique has not been used in sharp interface problems, since information on the amount of salt flowing into the brackish zone is missing and a detailed description of the velocity (and the dispersion coefficient) in the transition zone is not available. In this paper the flow in the brackish transition zone is studied in detail and the required information is derived from a boundary-layer approximation. A set of first-order boundary-layer equations is given and reduced to a single non-linear ordinary differential equation by introducing Lagrange's stream function and a similarity transformation. This equation has been integrated numerically with a Runge-Kutta method. The solution is given in terms of the stream function, so stream lines in the brackish zone can easily be plotted. The flow pattern shows a convective flow of saline water perpendicular to the original interface. This flow is an important source of salt entering the brackish zone, and in most cases much more

important than transport by diffusion. An expression for the flux of salt into the brackish zone is given. All data required for a random-walk simulation may be derived from this boundary-layer solution. The solution is also applicable to a curvilinear interface. In the last section an example is given, in which an analytical solution for a sharp interface (STRACK, 1973) is chosen and particle tracking is applied using the random walk to simulate dispersion in and outside the brackish zone.

2. THE PROBLEM

Consider an interface between fresh and saline groundwater under steady-flow conditions. If it is assumed that fresh and saline groundwater do not mix, the fluid density shows a discontinuity at the interface. For physical reasons, however, a continuous-pressure distribution is required. EDELMAN (1940) has shown that this requirement leads to a shear flow along the interface (fig. 1).

$$q_{x_2} - q_{x_1} = - \frac{k}{\mu} [\rho_2 - \rho_1] g \sin \beta \qquad (1)$$

Here q_x is the specific discharge in the x-direction, μ the dynamic viscosity and ρ the density of the fluid. k is the intrinsic permeability of the aquifer, β is the angle of interface with the horizontal and g is the constant of gravity. When mixing of fresh and saline water is taken into account, a sharp interface no longer occurs. Due to dispersion a brackish transition zone will be formed, where density and specific discharge vary continuously. As a first approximation one may assume that the density in the brackish zone is described by a function of y only: $\rho = \rho(y)$. If also parallel stream lines are assumed (fig. 2), EDELMAN's formula could be rewritten as:

$$q_x(y) = q_{x_1} - \frac{k}{\mu} [\rho(y) - \rho_1] g \sin \beta. \qquad (2)$$

It will be shown that in the boundary-layer approximation this expression holds, even if stream lines are not exactly parallel.

To determine the velocity and density distribution around the original sharp interface, dispersion has to be taken into account. However, the dispersion coefficient in turn depends on the velocity, so obviously the problem leads to a system of coupled equations. VERRUIJT (1971) treated the problem assuming a layer between the fresh and saline water, with a resistance to solute transport. VERRUIJT's solution, however, does take into account the effect of density differences on the flow pattern. For the one-dimensional case de JOSSELIN, de JONG & VAN DUIJN (1986) recently published a non-steady solution, in which density variations have been taken into account (also VAN DUIJN, 1986).
The problem studied in this paper is illustrated in fig. 3.
At the left hand side of point 0 saline and fresh water are supposed to be separated by an impermeable sheet, while at the right hand side mixing of fresh and saline water starts to take place. The problem is described in two dimensions and is considered to be in a steady state.

3. BASIC EQUATIONS

The equation of continuity is:

$$\frac{\partial u}{\partial x} + \frac{\partial v}{\partial y} = 0. \tag{3}$$

Here u is written for q_x/ε, and v for q_y/ε, ε being effective porosity. A mass balance for salt leads to:

$$u \frac{\partial c}{\partial x} + v \frac{\partial c}{\partial y} = \nabla \cdot (D\nabla c) \tag{4}$$

where c is the salt concentration and D the dispersion tensor. Darcy's law gives:

$$u = - \frac{k}{\mu\varepsilon} [\frac{\partial p}{\partial x} + \rho g \sin \beta] \tag{5}$$

$$v = - \frac{k}{\mu\varepsilon} [\frac{\partial p}{\partial y} + \rho g \cos \beta] \tag{6}$$

where p denotes the pressure. In these four equations five unknown variables occur (ρ,c,u,v,p). A 5th equation follows from a relation between ρ and c. If it is assumed that the presence of salt molecules does not influence the spatial distribution of the water molecules, one may write:

$$\rho = \rho_2 + c. \tag{7}$$

The pressure p may be eliminated by cross differentiation of (5) and (6). Eliminating density as well with (7), the set of equations becomes:

$$\frac{\partial u}{\partial x} + \frac{\partial v}{\partial y} = 0 \tag{8}$$

$$u \frac{\partial c}{\partial x} + v \frac{\partial c}{\partial y} = \nabla \cdot (D\nabla c) \tag{9}$$

$$\frac{\partial u}{\partial y} - \frac{\partial v}{\partial x} = - \frac{kg}{\mu\varepsilon} [\frac{\partial c}{\partial y} \sin \beta + \frac{\partial c}{\partial x} \cos \beta]. \tag{10}$$

Note that (10) expresses the vorticity rot(q/ε). Dimensionless variables are now introduced, given by:

$$[U,V,X,Y,\bar{D},K,C] = [\frac{u}{u_2}, \frac{v}{u_2}, \frac{x}{L}, \frac{y}{L}, \frac{D}{\alpha_T u_2}, \frac{k\rho_2 g}{\mu\varepsilon u_2}, \frac{c}{c_o}] \tag{11}$$

where α_T is transversal dispersivity, L a characteristic length of the problem in a x-direction and u_2 the original fresh-water velocity. The concentration of the pure saline water c_o is given by:

$$c_o = \rho_1 - \rho_2. \tag{12}$$

Next, a quantity δ is introduced, defined by:

$$\delta^2 = \frac{\alpha_T}{L} \tag{13}$$

and a parameter Γ by:

$$\Gamma = \frac{\rho_1 - \rho_2}{\rho_2} . \tag{14}$$

In dimensionless form (8), (9) and (10) may finally be written as:

$$\frac{\partial U}{\partial X} + \frac{\partial V}{\partial Y} = 0 \tag{15}$$

$$U \frac{\partial C}{\partial X} + V \frac{\partial C}{\partial Y} = \delta^2 \nabla \cdot (D \nabla C) \tag{16}$$

$$\frac{\partial U}{\partial Y} - \frac{\partial V}{\partial X} = - \Gamma K [\frac{\partial C}{\partial Y} \sin \beta + \frac{\partial C}{\partial X} \cos \beta]. \tag{17}$$

4. BOUNDARY LAYER EQUATIONS

In hydrodynamics the description of the viscous friction at the surface of a streamlined body forms a classical problem (SCHLICHTING, 1978). A solution based on the full Navier-Stokes equation does not exist. Approximate solutions are known, based on a boundary-layer approach. In this approach viscosity is taken into account only in the vicinity of the surface (the boundary layer), where high-velocity gradients exist. Outside the boundary layer viscous forces are neglected.

The problem encountered here is similar. High concentration gradients occur locally near the interface, while in the hydrodynamical problem high-velocity gradients are found near the surface of the body. Outside the brackish zone density differences are so small that effects on the flow pattern may be neglected, as is done outside the boundary layer with respect to viscous forces. The groundwater problem differs from the hydrodynamical problem with respect to the transport parameter. The dispersion coefficient is a space-dependent variable, while in hydrodynamics viscosity is a constant parameter.

The boundary-layer technique is described in more general terms in perturbation theory (COLE, 1968; VAN DYKE, 1975). In equation (16) the dispersion term is considered to be a perturbation. Here the order of the differential equation is determined by the perturbation term, which is known as a singular perturbation. In such a case the solution consists of two parts, an inner solution that holds in the domain where the perturbation term dominates, and an outer solution that is valid only in the domain where the perturbation term is neglectable. The inner-region corresponds with the boundary layer and in the hydrological problem it corresponds with the brackish zone. Equations for the inner-region are obtained by co-ordinate transformations, such that the perturbation term itself

does not vanish if Δ approaches zero. The transformed variables (inner-variables), denoted with $\tilde{}$, are:

$$[\tilde{U},\tilde{V},\tilde{X},\tilde{Y},\tilde{C}] = [U, \frac{V}{\delta}, X, \frac{Y}{\delta}, C]. \tag{18}$$

With (18) equations (15), (16) and (17) are rewritten as:

$$\frac{\partial\tilde{U}}{\partial\tilde{X}} + \frac{\partial\tilde{V}}{\partial\tilde{Y}} = 0 \tag{19}$$

$$\tilde{U}\frac{\partial\tilde{C}}{\partial\tilde{X}} + \tilde{V}\frac{\partial\tilde{C}}{\partial\tilde{Y}} = \nabla\cdot(\tilde{D}\nabla\tilde{C}) \tag{20}$$

$$\frac{\partial\tilde{U}}{\partial\tilde{Y}} - \delta^2\frac{\partial\tilde{V}}{\partial\tilde{X}} = -\Gamma K[\frac{\partial\tilde{C}}{\partial\tilde{Y}}\sin\beta + \delta\frac{\partial\tilde{C}}{\partial\tilde{X}}\cos\beta]. \tag{21}$$

First-order boundary-layer equations are obtained neglecting terms of order δ and δ^2.
Evaluating all terms of the dispersion-tensor (BEAR, 1972) at the right-hand side of (20), writing molecular diffusion separately and dropping the term of order δ and δ^2 yields:

$$\nabla\cdot(\tilde{D}\nabla\tilde{C}) = \frac{\partial}{\partial\tilde{Y}}(\tilde{U}\frac{\partial\tilde{C}}{\partial\tilde{Y}}) + \lambda\frac{\partial^2\tilde{C}}{\partial\tilde{Y}^2} \tag{22}$$

where λ denotes the ratio between molecular diffusion and dispersion:

$$\lambda = \frac{\nu}{\alpha_T u_2}. \tag{23}$$

Here ν is the diffusion constant for salt. Letting δ approach zero, equation (21) reduces to:

$$\frac{\partial\tilde{U}}{\partial\tilde{Y}} = -\Gamma K\frac{\partial\tilde{C}}{\partial\tilde{Y}}\sin\beta. \tag{24}$$

This equation can be integrated with respect to $\tilde{Y}$, giving:

$$\tilde{U} = A(x) - \Gamma K\tilde{C}\sin\beta. \tag{25}$$

A(x) is obtained from the boundary condition:

$$\tilde{U} = \tilde{U}_2, \qquad \text{for } \tilde{Y}\to\infty \tag{26}$$
$$\tilde{C} = 0.$$

Therefore $A(x) = \tilde{U}_2 = 1$ and (25) can be written as:

$$\tilde{U} = \tilde{U}_2 - \Gamma K\tilde{C}\sin\beta. \tag{27}$$

In fact this is equation (2) in dimensionless form, which means that the distribution of the flow component parallel to the original interface is equal to this 'generalized' EDELMAN equation, even though in the boundary-layer approximation no parallel stream lines are assumed. In the next section it will be shown that in the boundary-layer approximation there is still a flow perpendicular to the original interface.
The second boundary equation:

$$\tilde{U} = \tilde{U}_1, \qquad \text{for } \tilde{U} \to -\infty \tag{28}$$
$$\tilde{C} = 1$$

is satisfied if

$$\tilde{U}_2 - \tilde{U}_1 = \Gamma K \sin\beta. \tag{29}$$

This is EDELMAN's original expression (1) in dimensionless form. This equation is always satisfied, since the inner solution should match an outer solution, based on a sharp interface assumption. Note that in the inner-region y-co-ordinates are stretched due to transformation (18), so, if Y goes to infinity, the y-co-ordinate itself remains finite and in fact will be quite small. The first-order equations now become:

$$\frac{\partial \tilde{U}}{\partial \tilde{X}} + \frac{\partial \tilde{V}}{\partial \tilde{Y}} = 0 \tag{30}$$

$$\tilde{U}\frac{\partial \tilde{C}}{\partial \tilde{X}} + \tilde{V}\frac{\partial \tilde{C}}{\partial \tilde{Y}} = \frac{\partial}{\partial \tilde{Y}}\left(\tilde{U}\frac{\partial \tilde{C}}{\partial \tilde{Y}}\right) + \lambda\frac{\partial^2 \tilde{C}}{\partial \tilde{Y}^2} \tag{31}$$

$$\tilde{U} = \tilde{U}_2 - \Gamma K \tilde{C} \sin\beta. \tag{32}$$

5. STREAM FUNCTION

Because of (30) a stream function exists for which (VERRUIJT, 1970):

$$\tilde{U} = \frac{\partial \tilde{\Psi}}{\partial \tilde{Y}} \quad \text{and} \quad \tilde{V} = -\frac{\partial \tilde{\Psi}}{\partial \tilde{X}}. \tag{33}$$

If $\tilde{C}$ is eliminated from (31) and (32) the equations may be reduced to a single partial differential equation:

$$\frac{\partial \tilde{\Psi}}{\partial \tilde{Y}}\frac{\partial^2 \tilde{\Psi}}{\partial \tilde{X}\partial \tilde{Y}} - \frac{\partial \tilde{\Psi}}{\partial \tilde{X}}\frac{\partial^2 \tilde{\Psi}}{\partial \tilde{Y}^2} = \left[\frac{\partial^2 \tilde{\Psi}}{\partial \tilde{Y}^2}\right]^2 + \frac{\partial \tilde{\Psi}}{\partial \tilde{Y}}\frac{\partial^3 \tilde{\Psi}}{\partial \tilde{Y}^3} + \lambda\frac{\partial^3 \tilde{\Psi}}{\partial \tilde{Y}^3}. \tag{34}$$

6. SIMILARITY TRANSFORMATION

In many boundary-layer problems a similarity transformation is used, given by:

$$\eta = \frac{\tilde{Y}}{\sqrt{\tilde{X}}} \tag{35}$$

and

$$f(\eta) = \frac{\Psi}{\sqrt{\tilde{X}}} \tag{36}$$

so

$$\frac{\partial \Psi}{\partial \tilde{Y}} = f' \quad , \quad \frac{\partial \Psi}{\partial \tilde{X}} = -\frac{\eta f' - f}{2\sqrt{\tilde{X}}}$$

$$\frac{\partial^2 \Psi}{\partial \tilde{Y}^2} = \frac{f''}{\sqrt{\tilde{X}}} \quad , \quad \frac{\partial^2 \Psi}{\partial \tilde{X} \partial \tilde{Y}} = -\frac{\eta f''}{2\tilde{X}} \tag{37}$$

$$\frac{\partial^3 \Psi}{\partial \tilde{Y}^3} = \frac{f'''}{\tilde{X}}$$

where $f'(\eta)$ stands for $df(d\eta$.
This transformation reduces (34) to the following ordinary non-linear differential equation:

$$f''' [2f' + 2\lambda] + f'' [f + 2f''] = 0 \tag{38}$$

7. NUMERICAL INTEGRATION

If

$$h_1 = f$$

$$h_2 = f' \tag{39}$$

$$h_3 = f''$$

a set of three first-order ordinary differential equations equivalent to (38) is obtained:

$$h_1' = h_2$$

$$h_2' = h_3 \tag{40}$$

$$h_3' = -\frac{h_3(h_1 + 2h_3)}{2h_3 + 2\lambda} \, .$$

This set of equations has been integrated numerically with a Runge-Kutta method, using the boundary conditions for the case, where the saline water has no flow component in the $\tilde{X}$ direction, so $\tilde{U}_1 = 0$:

$$f' = \tilde{U}_1 = 0$$

$$f'' = 0 \quad , \quad \text{for } \eta \to -\infty \tag{41}$$

we also have

$$f \dashrightarrow \infty$$

$$f' \dashrightarrow 1 \qquad \text{for } \eta \to +\infty \tag{42}$$

To perform the integration a set of starting values (η_o, f_o, f_o', f_o'') is required.

Starting values

As far as η_o is concerned, it is observed that (38) is autonomous, which means that if $f(\eta)$ is a solution, $f(\eta - b)$ is also a solution, b being an arbitrary constant. The choice of b influences the position of the stream line $\Psi = 0$ (or $f = 0$), since b corresponds to a shift of the whole solution on the Ψ-axis. In this paper we have chosen b such that the line $\Psi = 0$, representing the original interface, coincides with the line $\tilde{Y} = 0$, so in fact:

$$f(0) = 0. \tag{43}$$

A full discussion on this aspect of the problem cannot be given here because of the length of the paper. A starting value f_o is not available, but may be determined with the "shooting method" using the boundary condition $f' \to 1$ for $\eta \to \infty$ as an aim "to shoot at". The shooting method results in the following starting values η_o and f_o.

λ	f_o	η_o
0,5	-1,1209	-7,5125
0,2	-0,8953	-5,0355
0,1	-0,8050	-3,8414
0,05	-0,7554	-3,0855
0,02	-0,7238	-2,5336
0,01	-0,7196	-2,3184
0,005	-0,7074	-2,1990
0,002	-0,7041	-2,1201
0,001	-0,0730	-2,0912

The case $\lambda = 0{,}02$ has been investigated in detail. Fig. 4 gives the velocity components $\tilde{U}$ and $\tilde{V}$, while in fig. 5 stream lines are plotted.
The value of the stream function in the saline water is:

$$\Psi_s = f_o \sqrt{\tilde{X}}. \tag{44}$$

From table 1 it follows that this value is always negative. With increasing $\tilde{X}$, Ψ_s decreases further. Physically it means that the amount of water flowing in the $\tilde{X}$ direction increases compared to the original amount of fresh-water flowing along the impermeable sheet. An explanation is shown in fig. 5, where stream lines are coming "upward" from the saline water adding water (and salt) to the brackish zone. This transverse-flow component is equal to

$$\tilde{V} = \frac{\eta f' - f}{2\sqrt{\tilde{X}}} \tag{45}$$

Substitution of $f'(\eta_o) = 0$ and $f(\eta_o) = f_o$ leads to:

$$\tilde{V}(\eta_o) = -\frac{f_o}{2\sqrt{\tilde{X}}}. \tag{46}$$

It is noted that this result does not depend on the value chosen for η_o. The salt flux along the interface is given by:

$$C_o \, V(\eta_o) = c_o \, u_2 \, f_o \sqrt{\alpha_T x} \tag{47}$$

8. CURVILINEAR CO-ORDINATES

The analysis above may also be carried out for a curvilinear interface. In that case curvilinear co-ordinates are also used as shown in fig. 6.

In this case the angle of elevation β is a function of s : $\beta = \beta(s)$.
Using a transformation:

$$\xi = \frac{1}{L} \int_o^s \sin^2\beta(s) \, ds \quad \text{and} \quad \tau = \frac{\eta}{\delta L} \tag{48}$$

and neglecting transport by diffusion ($\lambda = 0$) the problem can be handled in the same manner as shown before, leading to the equation:

$$f'' \, [f + 2 f''] + 2 f''' f' = 0 \tag{49}$$

which is equation (38) for $\lambda = 0$. In this case however

$$f = \frac{\Psi}{\sqrt{\xi}} \tag{50}$$

$$\eta = \frac{\tau \sin \beta}{\sqrt{\xi}} \tag{51}$$

The salt flux along the interface is given this time by:

$$c_o \, V(\eta_o) = c_o \, u_2 \, f_o \, \sqrt{a_T \xi} \, . \qquad (52)$$

9. RANDOM WALK

The principle of the method proposed in this paper is illustrated by an example based on an analytical solution for a (sharp) interface in the case of a drain infiltrating fresh water above a body of stagnant saline water. The upper boundary consists of an equipotential line. This solution, given by STRACK (1973), will not be discussed here. From the solution the convective-flow components are derived and particle tracking has been applied using the random-walk approach (UFFINK, 1985) to take dispersion into account (fig. 7). The convective flow of the particles close to the interface is corrected using the velocity distribution found by the boundary-layer approximation (fig. 4). In the brackish zone particles are followed as they flow along the interface. They are traced as well when they leave the transition zone. Further work will be done to study upconing. Upconing problems treated with a sharp interface may answer such questions as when the pure saline groundwater enters the pumping well. However, long before that moment the water will already be unsuitable as a source for drinking water. It may be expected that with random walk techniques questions like this may be answered in a more detailed sense e.g., at what pumping rate the upper part of the brackish zone starts entering the well.

REFERENCES

BEAR, J. (1979). Hydraulics of Groundwater. New York: McGraw-Hill.

COLE, J. (1968). Perturbation Methods in Applied Mathematics. Waltham (Massachusetts: Blaisdell.

de JOSSELIN, de JONG, G. & VAN DUIJN, C.J. (1986). Transverse dispersion from an orginally sharp fresh-salt interface caused by shear flow. J. Hydrol. 84, 55-79.

EDELMAN, J.H. (1940). Strooming van zoet en zout water. Rapport inzake de watervoorziening van Amsterdam, Bijlage 2, 8-14.

KOOIMAN, J.W. & UFFINK, G.J.M. (1986). Deep-well infiltration in the dune area of Amsterdam waterworks and modeling of the moving interface. Proceedings of the 9th Salt Water Intrusion Meeting, Delft.

SCHLICHTING, H. (1978). Boundary Layer Theory. New York: McGraw-Hill.

STRACK, O.D.L. (1973). Many-valuedness Encountered in Groundwater Flow. Delft: PhD Thesis.

UFFINK, G.J.M. (1985). A random-walk method for the simulation of macrodispersion in a stratified aquifer. Relation of Groundwater Quality and Quantity. IAHS-Publication 146, 103-114 (Proceedings of the Hamburg Symposium, August 1983).

VAN DYKE, M. (1975). Perturbation Methods in Fluid Mechanics. New York: Academic Press.

VAN DUIJN, C.J. (1986). A mathematical analysis of density dependent dispersion in fresh-salt groundwater flow. Proceedings of the 9th Salt Water Intrusion Meeting, Delft.

VERRUIJT, A. (1970). Theory of Groundwater Flow. London: MacMillan.

VERRUIJT, A. (1971). Steady dispersion across an interface in a porous medium. J. Hydrol. 14, 337-347.

FIGURES

Fig. 1: **Shear flow along the interface between fresh and saline groundwater without mixing.**

Fig. 2: **Approximation of stream lines under assumption of a brackish zone.**

Fig. 3: **Synopsis of figure 1 and figure 2.**

Fig. 4: **Velocity distributions of $\hat{U}$ and $\hat{V}$ for λ=0,02 .**

Fig. 5: **Plot of stream lines added to figure 4**

Fig. 6: **Analysis of a curvilinear interface**

Fig. 7: **Convective flow of particles close to the interface**

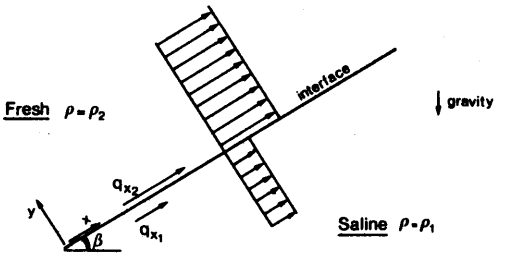

Figure 1

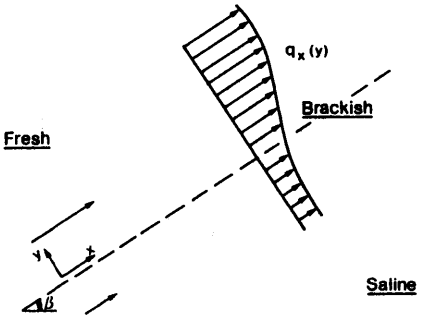

Figure 2

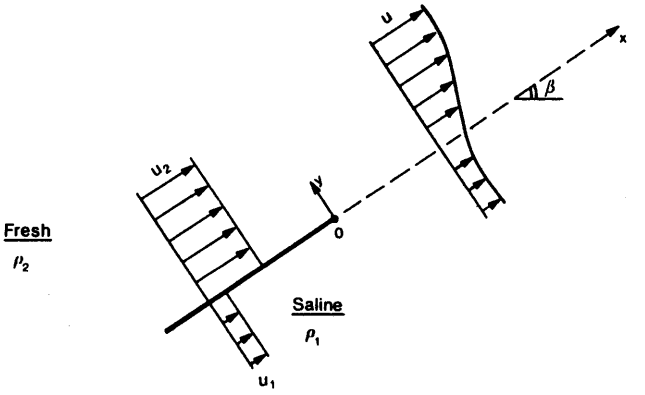

Figure 3

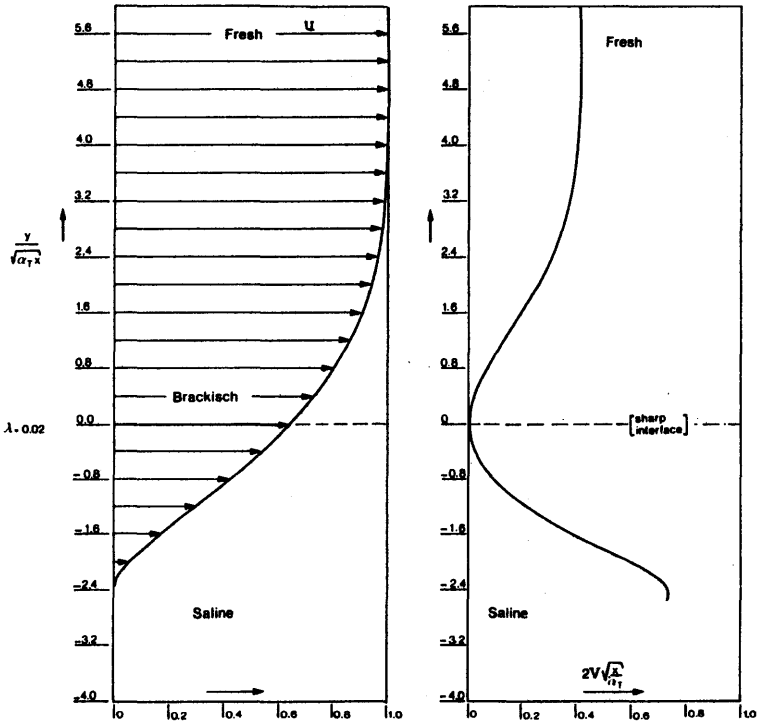
Fresh
U
Brackisch
Saline
Fresh
sharp interface
Saline
λ = 0.02

Figure 4

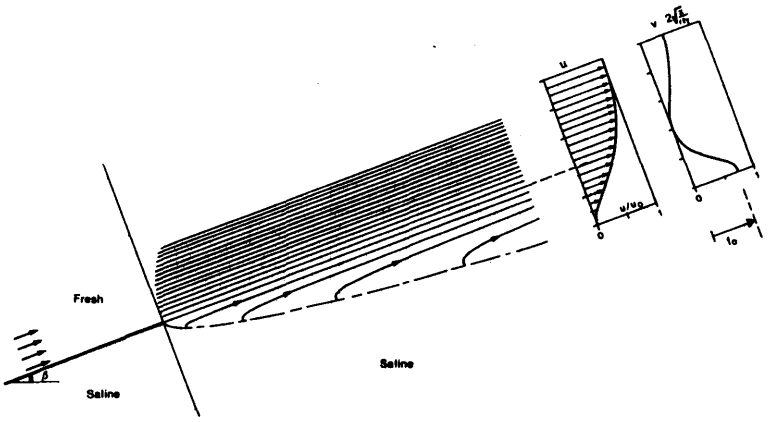

Figure 5

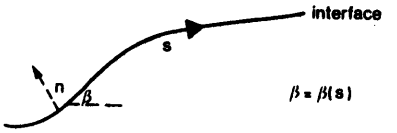

Figure 6

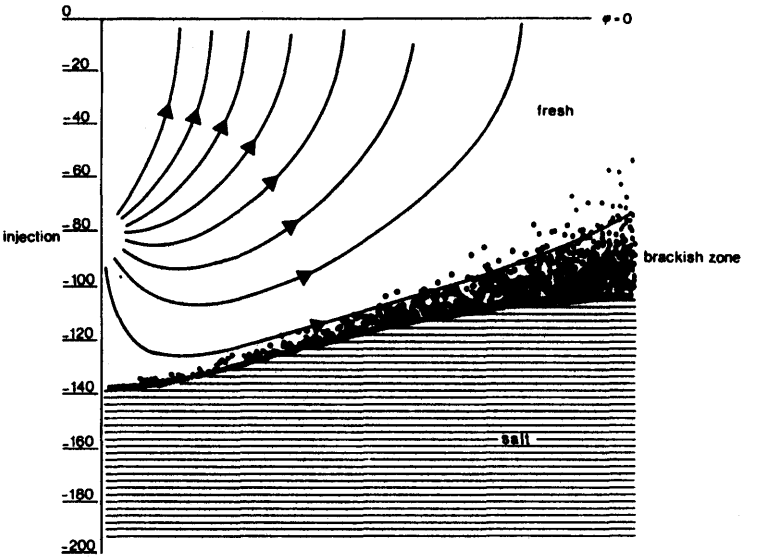

Figure 7

3.7. MODELING A REGIONAL AQUIFER CONTAINING A NARROW TRANSITION BETWEEN FRESH WATER AND SALT WATER USING SOLUTE-TRANSPORT SIMULATION. PART 1 - THEORY AND METHODS

C.I. VOSS & W.R. SOUZA

ABSTRACT

Methodology based on a consistent approximation for calculating vertical velocity in a variable-density fluid is required to successfully simulate narrow transition zones between fresh water and salt water with a solute-transport model. The need for local fluid density and numerical vertical-pressure gradient to be accurate and consistent with one another in order to avoid artificial velocities in regions of high-density gradients applies to finite-element and finite-difference models as well. Classically, only cases involving wide transition zones have been simulated with transport models. Moreover, adequate spatial discretization is required to allow simulation of the low transverse dispersivity related to flow in both isotropic and anisotropic aquifers. The available tests for the correctness of density-dependent transport simulators are inadequate to check for consistency of the approximations and the accuracy of density-driven flow. Additional tests are suggested by the analysis.

The flow of fresh and saline groundwater in the layered-basalt aquifer of Southern Oahu, Hawaii, is simulated in cross section with the USGS-SUTRA finite-element model of two-dimensional, density-dependent flow and transport that is based on a consistent velocity approximation and that satisfies the complete series of tests. This simulation has the unique aspect that not only is a transport model applied to a complete regional flow system, but results are obtained for the difficult but common case where the transition zone is broadly dispersed near the discharge or pumping area, and is very narrow elsewhere. Simulation with an inconsistent velocity approximation gives incorrect results for this system. The hydrologic analysis of Southern Oahu based on this simulation is described in a paper of the 9th SWIM proceedings.

1. INTRODUCTION

The problem in analysing a regional aquifer system containing a narrow transition zone between fresh water and salt water with a density-dependent fluid flow and dissolved-solids transport model is two-fold: (1) The adequacy of the dispersion theory is not certain and values of dispersion parameters are neither well known nor may they be directly measured at the regional scale. Clearly, the transport simulation must be successful before a study of the adequacy of old and new dispersion models and the determination of field parameter values can be undertaken. Further, investigation of the physical reasons for the structure of a particular transition zone may be done only after careful fitting of model hydraulics to the field conditions. (2) Transport codes have considerable difficulty simulating the movement of narrow concentration fronts on a regional scale. The difficulties are: a) instabilities in the numerical solution when tracking a narrow front, b) inability to maintain the sharpness of a front due to insufficient discretization, and c) significant numerical errors in calculating fluid velocity within narrow transition zones causing broadening of the zones.

Classically, the problems inherent in transport simulation of systems containing narrow portions of transition zones are skirted by basing analysis on a variety of sharp interface approximations. The various areal and cross-sectional approaches are reviewed by REILLY & GOODMAN (1985). While not minimizing the great value of such approaches in representing fundamental aspects of aquifer-system dynamics, they do not account for the often significant effect of the mixing process on the structure and position of the transition zone, nor do they allow prediction of the concentration of seawater arriving at water-supply wells. The impact of these limitations is clear when considering that water of potable quality contains less than about one percent seawater. On the other hand, regional scale analysis based on transport simulation is capable of representing system dynamics including the effects of mixing, as founded on current theories of dispersion in aquifers, and is capable of making predictions of concentration. However, transport simulations have typically dealt with transition zones that are quite broad on the regional scale (in the order of aquifer thickness). These include analyses reported by LEE & CHENG (1979), SEGOL & PINDER (1976), VOLKER & RUSHTON (1982), FRIND (1982 b) and LEBBE (1983). While some authors (VOLKER, 1980, and FRIND, 1982 a) have shown results for narrower transition zones, it may be questioned whether broad transition zones are typically chosen as candidates for transport-simulation analysis to avoid the numerical problems in representing narrow zones, or whether inaccuracies in variable-density transport models give broad transition results that are accepted for lack of definitive field data that shows otherwise. Often in regional aquifers, the transition zone is quite narrow except in areas that undergo pumping or recharge, discharge and tidal stresses. The ability to simultaneously simulate the dynamics of both narrow and broad portions of the transition zone is vital to hydrologic analysis and water-supply prediction in such cases.

This paper describes a numerical modeling approach that deals with the problems inherent in the representaton of fresh water and salt water systems. The approach guarantees a regional-scale transport simulation of narrow transition zones with minimal numerical dispersion. Through application of the modeling approach to the Southern Oahu aquifer, Oahu, Hawaii, it is demonstrated that successful transport simulation combined with a parsimonious fit of hydraulic parameters to field conditions provides an excellent tool for hydraulic investigations.

2. THEORY

The solute-mass balance per unit aquifer volume at a point in the aquifer is given by:

$$\varepsilon\rho \frac{\partial C}{\partial t} + \varepsilon\rho \underline{v} \cdot \underline{\nabla} C - \underline{\nabla} \cdot [\varepsilon\rho(D_m \underline{\underline{I}} + \underline{\underline{D}}) \cdot \underline{\nabla} C] = Q_p(C^* - C) \qquad (1)$$

where:

$C(x,z,t)$ is solute concentration as a mass fraction, (mass solute/mass fluid) in units $[M_s/M]$, where $[M_s]$ are units of solute mass and $[M]$ are units of fluid mass,

$\varepsilon(x,z)$ is aquifer volumetric porosity, [1],

$\underline{v}(x,z,t)$ is fluid velocity, in units [L/T], where [L] are length units and [T] are time units,

D_m is molecular diffusivity of solute in pure fluid including aquifer material tortuosity effects, in $[L^2/T]$ units,

$\underline{\underline{I}}$ is the identity tensor [1],

$\underline{\underline{D}}(x,z,t)$ is the dispersion tensor, in $[L^2/T]$,

$Q_p(x,z,t)$ is a fluid-mass source, (mass fluid/aquifer volume/time), in units of $[M/L^3 \cdot T]$,

$C^*(x,z,t)$ is concentration of solute as a mass fraction in the source fluid, $[M_s/M]$,

$\rho(x,z,t)$ is fluid density in units $[M/L_f^3]$ where $[L_f^3]$ is fluid volume,

and density is given as a linear function of concentration:

$$\rho = \rho_o + \frac{\partial \rho}{\partial C} (C - C_o) \tag{2}$$

where:

ρ_o is fluid density where $C = C_o$,

C_o is a base solute concentration, and

$\partial\rho/\partial C$ is a constant coefficient of density variability.

Darcy's law gives the mass-average fluid velocity as:

$$\underline{v} = - \left[\frac{\underline{\underline{k}}}{\varepsilon \mu}\right] \cdot (\underline{\nabla} p - \rho \underline{g}) \tag{3}$$

where:

$\underline{\underline{k}}(x,z)$ is the permeability tensor, in units [L]

μ is fluid viscosity, in units $[M/L \cdot T]$ and

$\underline{g}$ is the gravity vector, in units $[L/T^2]$

$p(x,z,t)$ is the fluid pressure in units $[M/L \cdot T^2]$.

The mass balance of fluid per unit aquifer volume at a point in the aquifer, assuming the contribution of solute dispersion to the mass-average flux of fluid is negligible, is given by:

$$\left[\frac{S_y}{b|g|} + \rho S_{op}\right] \frac{\partial p}{\partial t} + \varepsilon \frac{\partial \rho}{\partial C} \frac{\partial C}{t} + \underline{\nabla} \cdot (\varepsilon \rho \underline{v}) = Q_p. \tag{4}$$

Substitution of Darcy's law (2) for mass-average velocity in the fluid-mass balance (4) gives:

$$[\frac{S_y}{b|g|} + \rho S_{op}] \frac{\partial p}{\partial t} + \varepsilon \frac{\partial \rho}{\partial C} \frac{\partial p}{\partial t} - \underline{v} \cdot [[\frac{\underline{\underline{k}}\rho}{\mu}] \cdot (\underline{\nabla} p - \rho \underline{g})] = Q_p \qquad (5)$$

This form of the fluid-mass balance allows a cross-sectional model to include both fluid storage at the water table (S_y term) and compressive fluid storage

where:

$S_y(x,z)$ is the water-table specific yield [(volume fluid released/aquifer volume) for unit drop in hydraulic head] in units [L],

$b(x,z)$ is the effective thickness of the water-table aquifer in units [L],

$|g|$ is the magnitude of gravitional acceleration in units $[L/T^2]$,

where:

S_{op} is the specific pressure storativity in units of $[M/(L \cdot T^2)]^{-1}$

and
$$S_{op} = (1 - \varepsilon)\alpha + \varepsilon\beta \qquad (6)$$

where:

α is porous matrix compressibility in units $[M/(L \cdot T)]$ and

β is fluid compressibility in units $[M/(L \cdot T^2)]^{-1}$.

The water table is modelled as a finite thickness layer (of height b(x)) that is superposed at the top of an aquifer modelled in cross-section, in which S_y is non-zero. The dispersion tensor in two spatial dimensions is given by:

$$\underline{\underline{D}} = \begin{bmatrix} D_{xx} & D_{xz} \\ D_{xx} & D_{zz} \end{bmatrix} \qquad (7)$$

where:

$$D_{xx} = [\frac{1}{v^2}][d_L v_x^2 + d_T v_z^2] \qquad (8)$$

$$D_{zz} = [\frac{1}{v^2}][d_T v_x^2 + d_L v_z^2] \qquad (9)$$

$$D_{xz} = [\frac{1}{v^2}][d_L - d_T][v_x v_z] \qquad (10)$$

where:
$$d_L = \alpha_L v \qquad (11)$$

$$d_T = \alpha_T v \qquad (12)$$

v is the magnitude of velocity and:

$\alpha_L(x,z,t)$ is longitudinal dispersivity in units [L], and

$\alpha_T(x,z)$ is transverse dispersivity in units [L].

3. CONSISTENT VELOCITIES

When the governing equations are solved by a numerical method, velocities must be evaluated at points within the modelled region to calculate the solute advective term and the velocity-dependent dispersion tensor.

A contradiction in approximation of velocity arises in the Galerkin finite-element method and sometimes in a finite-difference method. The contradiction gives rise to artificial vertical velocities in the case where both pressure and density are allowed to vary linearly (or have the same order in space) in the vertical direction across an element or cell of the spatial grid. This contradiction may be the reason for previous difficulties with simulators solving for pressure and concentration which employ velocities that are discontinuous for an element (SEGOL et al., 1975). This contradiction may also cause problems in simulators based on other hydraulic variables such as equivalent fresh-water head, or a quasi-stream function. The contradiction is most clearly demonstrated by consideration of hydrostatic conditions for an element in which pressure and concentration are allowed to vary linearly from the top to bottom of the element. If the pressure at the top of an element with height, H, is zero, then the bottom pressure, under hydrostatic conditions, is given by $p_B = \rho_{AVG} \cdot |g|H$, where ρ_{AVG} is the average density of fluid in the element. If linear relation (2) holds between density and concentration, then when the concentration varies linearly from top to bottom, the density does as well. If the density changes linearly, the pressure must change quadratically in order to maintain hydrostatic equilibrium. However, the discretization for pressure allows only a linear change across the element and a linear constant pressure change exists only under conditions of constant fluid density. Combining a linear change in density with a linear change in pressure in relation (29) would result in an upward velocity calculated at points in the upper half of the example element and in a downward velocity in the lower half. A zero velocity exists at the element centroid, however, as the density and pressure gradient are consistent at this point. The artificial velocities calculated within a finite element because of inconsistent discretization of pressure gradient and density would disperse a sharp transition zone even under hydrostatic conditions. Only employing ρ_{AVG} at all points in the element, in lieu of $\rho(C)$, would yield a calculated value of zero vertical velocity throughout the element. Artificial velocities of hundreds of meters per year easily arise as shown in the subsequent discussion related to model verification.

An artificial velocity would be calculated in any numerical method whenever allowed spatial variability of pressure gradient and density are not consistent.

This discrepancy arises both in the Darcy's Law terms of the fluid mass balance, (5), and in evaluation of fluid velocity, and it generates artificial velocity-dependent dispersion coefficients (11) and (12). If density is allowed to vary spatially in the vertical directions as an (N)th power polynomial, then pressure must be allowed to vary as an (N + 1)th power polynomial in order that the pressure gradient be consistent and vary to the (N)th power. For finite elements and a linear density-concentration relationship, this would be satisfied by a choice of linear basis-function discretization for concentration and quadratic basic-function discretization for pressure. Quadratic basic functions, however, significantly increase computational expense and another approach is preferable.

Another approach may be found for finite elements by observing that strictly the requirement of consistency governs the choice of discretization only in the co-ordinate direction parallel to the direction of gravity. In other directions the density-gravity term drops out of both the fluid-mass balance, (5), and the velocity calculation based on (3). Thus, within an element, a higher-order approximation for density may be employed horizontally than vertically. Such an approach is described in VOSS (1984).

4. DENSITY-DEPENDENT MODEL VERIFICATION

Density-dependent transport models are typically verified by comparison with the HENRY (1964) approximate analytic solution for steady-state salt-water intrusion. No model to date has successfully matched the Henry solution even for simulation times which approach steady state. However, a number of numerical models based on significantly different methods give simulated results nearly identical to one another for the Henry problem. These include a particle tracking model by PINDER & COOPER (1970), finite-element models by SEGOL et al., (1975), HUYAKORN & TAYLOR (1977), DESAI & CONTRACTOR (1977) and FRIND (1982 a), a finite-difference model by INTERA (1979), and the USGS finite-element/integrated-finite-difference model, SUTRA (VOSS, 1984). This evidence indicates some inaccuracy in Henry's results that may be due to missing higher-order terms which were originally dropped by Henry for the sake of reducing computation time. A more accurate semi-analytic calculation would now be practical to carry out on high-speed computers. While verification of a model by exact comparison with Henry's results is not possible, some confidence in the accuracy of a particular model may be gained if it matches the results of the above listed suite of models.

The Henry problem involves fresh water in a confined aquifer discharging to a vertical open-sea boundary over a diffuse wedge of salt water that has intruded the aquifer. Fig. 1 describes the physical system. Dispersion is approximated in the simulations by using a large constant value of molecular diffusivity and zero dispersivity. The comparison between various models and the Henry solution must be shown in a few figures as some authors have published either a different representation of the solution or have used different parameter values. The

parameters chosen to match Henry's dimensionless values and the other simulations are:

$\varepsilon = 0,35$ $\quad k = 1,020408 \times 10^{-9} [m^2]$ (based on $K = 1,0 \times 10^{-2}$ [m/s])

$C_s = 0,0357 \left[\frac{\text{kg(dissolved solids)}}{\text{kg(seawater)}}\right]$ $\quad |\underline{g}| = 9,8 [m/s^2]$

$\rho_s = 1025 \cdot [kg/m^3]$ = sea water density $\quad \alpha_L = \alpha_T = 0,0$

$\frac{\partial \rho}{\partial C} = 700 \cdot \left[\frac{\text{kg(seawater)}^2}{\text{(kg dissolved solids} \cdot m^2)}\right]$ $\quad B = 1,0 [m]$

$\rho_o = 1000 \cdot [kg/m^3]$ $\quad D_m = \begin{matrix} 6,6 \times 10 [m^2/s] \\ 18,8571 \times 10^{-6} [m^2/s] \end{matrix}$ two cases

$Q_{IN} = 6,6 \times 10^{-2} [kg/s]$ $\quad C_{IN} = 0,0$

The total fresh-water recharge is chosen as $6,6 \times 10^{-5}$ (m^3/s) per meter of cross-section thickness. Two different values of a total dispersion coefficient have been used by the various authors. For the chosen total-recharge rate, and Henry's non-dimensional factor of total dispersivity divided by recharge equal to 0,1, the total dispersivity must be $6,6 \times 10^{-6}$ (m^2/s). Because total dispersivity for the SUTRA model, (relation (1)) in the case of no velocity-dependent dispersion, is given by a product of porosity and the molecular-diffusion coefficient, the diffusion coefficient should be set to $18,8571 \times 10^{-6}$ (m^2/s) when the porosity is 0,35. This gives a simulated result for the concentration at the bottom of the aquifer after 100 minutes (essentially steady state) as shown in fig. 2, where a comparison is made with steady-state results from three different models of HUYAKORN & TAYLOR (1977).

The same parameters give a concentration distribution in space as shown in fig. 3. Here, the Henry solution for the 0,5 isochlor is compared with results of SEGOL et al. (1975), and results from new simulations using SUTRA and the INTERA (1979) transport code. Mesh blocks were 0,1 (m) by 0,1 (m) for both the SUTRA finite-element solution and the INTERA solution which was done with both centreed-in-time and centreed-in-space finite-difference approximations. SUTRA and INTERA results are nearly identical but do not compare well with SEGOL and HENRY. Moreover, the SUTRA results do not approach the Henry solution even for simulations lasting thousands of minutes. Assigning a value of $6,6 \times 10^{-6}$ (m^2/s) to the molecular diffusivity would give a total dispersivity of $2,31 \times 10^{-6}$ (m^2/s) when the porosity is 0,35. This diffusivity value, rather than that which Henry used appears to have been employed by PINDER & COOPER (1970), SEGOL et al. (1975), DESAI & CONTRACTOR (1977) and FRIND (1982 a). Published results for these models and SUTRA using the molecular diffusivity value $6,6 \times 10^{-6}$ (m^2/s) are compared to the Henry solution in fig. 4. Simulated results are nearly identical including those of DESAI & CONTRACTOR (1977) who employed a coarser mesh than the others. None of these solutions compare well with Henry's.

Through the preponderance of simulators that have identically matched results for the Pinder-Cooper version of the Henry problem, this has become the standard test for all density-dependent transport models. However, because of the unrealistically large amount of dispersion introduced in the solution by the constant total-dispersion coefficient (required to make the analytical solution converge), this test does not check whether a model is consistent, nor does it check whether a model is accurate in the more realistic field situations with relatively narrow transition zones. In fact, experiments show that Henry-problem results are the same for both non-consistent and consistent discretization of the terms involved in the velocity calculation. Thus, when the transition zone is broadly dispersed and concentration gradients are low, the artificial velocities created by the non-consistent approach are insignificant compared with the field velocities, and the artificially-generated velocity-dependent dispersion due to the artificial velocities is small relative to the total dispersion.

In the case where the transition zone is narrow, artificial velocities do have a significant effect on the transport solution. This is especially true for long term or steady-state simulations in which very small velocities can strongly affect the solution. The magnitude of artificial velocity at the top of an element may be calculated to be $v = (1/2)(k|g|\Delta\rho/\varepsilon\mu)$, where $\Delta\rho$ is the difference in density from top to bottom of the element. For example, when permeability corresponds to that of silty sand, $k = 10^{-11}$ m^2 with porosity $\varepsilon = 1$, and an element changes from fresh water at the top to sea water at the bottom ($\Delta\rho = 25 \cdot (kg/m^3)$), the artificial velocity is about $380 \cdot (m/yr)$. In simulating such a system with the non-consistent method, the particularly sharp transition zone initially contained in one element would artificially begin to broaden at a rate of $760 \cdot (m/yr)$, even when no other natural velocities were superimposed on the system. Moreover, the velocity-dependent dispersion coefficients, relations (7) to (12), take on large non-zero values based on the artificial velocities, and further disperse the sharp transition zone. This is clearly unacceptable for steady-state simulation, and, depending on the geometry and scale of the system, would cause significant errors in simulations of a month or more.

Two additional tests are suggested in order to test for consistency: first, steady-state simulation of a completely closed horizontal aquifer containing a horizontal layer of fresh water above a layer of salt water; and second, steady-state simulation of the same system with open vertical sides and perfectly uniform horizontal flow. (1) The first additional test simply checks for consistency under hydrostatic conditions with a stable density configuration and no flow allowed across any boundaries. The choice of geometric scale and hydraulic parameters is not important because the system goes to steady state. Longitudinal and transverse dispersivities should be set to values equivalent to the length of the largest finite element; diffusivity should be set to zero. The correct solution is obtained only if the pressure gradient and density-gravity terms are consistent and is uninteresting to view as the transition zone should remain fixed in one row of elements. (2) The second additional test checks for consistency in a system where flow is perfectly parallel to the transition zone

and to the mesh. The simulation should be carried out with a longitudinal dispersivity of half the horizontal mesh spacing and a zero transverse dispersivity. The correct steady-state solution is also uninteresting to see as the transition zone should remain in the same single row of elements. Inconsistent approximations would result in spreading of the sharp interface in both cases.

The numerical results of ELDER (1967) for a problem of natural convection make up a useful basis for a test to check transport simulators in the case of flow driven purely by fluid-density differences. While ELDER (1967) dealt with thermally-driven convection, the solute analog to this 'long-heater problem' is a closed rectangular box, modelled in cross-section, with a source of solute at the top implemented as a specified concentration-boundary condition (fig. 5), and concentration specified as zero along the entire base. Solute enters the initially pure water by diffusion, increases its density, and thereby begins a circulation process. A zero value of pressure is specified at each upper corner. The following data are used to match Elder's dimensionless results:

$\varepsilon = 0{,}1$	$\lvert g \rvert = 9{,}81$ (m/s)
$k = 4{,}845 \times 10^{-13}$ (m^2)	$D_m = 3{,}565 \times 10^{-6}$ (m^2/s)
$\mu = 1{,}0 \times 10^{-3}$ (kg/m·s)	$\alpha_L = \alpha_T = 0$
$\rho = 1000 \cdot (kg/m^3) + 200)\ C$	$C_{initial} = 0$

Note: $\rho_{max}\ (C - C_{max}) = \rho(C = 1) = 1200\ (kg/m^3)$.

Fig. 6 compares results of simulation with SUTRA (mesh: 44 elements horizontally, 25 elements vertically) to those of ELDER (1967) for solute concentrations. The results compare very well, spatially and through time, showing that both numerical solutions give like representation of the complex density-driven flow and solute-transport behaviour. As with the Henry problem, comparison of simulation results with other numerical solutions (such as Elder's) gives confidence in the accuracy of the simulation.

5. EXAMPLE - SOUTHERN OAHU, HAWAII

The USGS finite-element/integrated-finite-difference model, SUTRA (VOSS, 1984), with consistent velocity terms is applied for simulation of flow and salt-water movement in the Southern Oahu aquifer near Honolulu, Hawaii. The simulation problem is difficult, as the transition between fresh water and salt water is expected to be extremely narrow inland, although it is broad near the coast. Because important hydraulic boundaries are relatively close to areas of interest near pumping centres, the entire aquifer must be simulated, including both narrow and broad portions of the transition zone. In a hydrologic model of the Southern Oahu aquifer, a consistent-velocity approximation is a vital factor in successful simulation. A more comprehensive description of the hydrologic modelling of what follows is given in a paper in the 9th SWIM proceedings by SOUZA & VOSS (1986).

The Southern Oahu basaltic aquifer is composed of thinly-bedded lava and rubble layers. Regionally the aquifer is very thick and quite permeable. The aquifer fabric may be expected to have anisotropic permeability between 10:1 and 1000:1 due to the layered structure, although the regional anisotropy value is not yet well established. Near the coast, and below the sea, the basalt is semi-confined by a wedge of interlaced sediment and coral formations, referred to as the 'caprock' (fig. 7). Primary recharge occurs over the Koolau mountains where significant intrusions of vertical dike walls into the horizontal beds make horizontal flow difficult. The dike-intruded region is considered a no-flow boundary that contributes a large specified recharge to the basalt aquifer. Discharge in the undeveloped section of the aquifer occurs primarily at springs along the inland edge of the caprock. Some diffuse discharge is expected as upward leakage through the caprock into the sea. A cross-sectional model is highly appropriate for representation of system behaviour because of the region-wide nearly uniform flow field.

The finite-element mesh for the cross-section consists of a region of very fine vertical discretization (15,24 m) in the region of the aquifer where the transition zone between fresh-water and salt-water is expected to reside. This allows sufficient discretization to represent the thin portion of the transition zone. Below this region, concentrations, velocities and pressures change very slowly in space and coarse discretization is sufficient. Pressure changes and converging high fluid velocities occur near the edge of the caprock; thus, horizontal discretization is increased in this region to a horizontal spacing of 304,8 m. Although regional longitudinal dispersivity is expected to be less than 100 m, horizontal spacing may greatly exceed the stability limit (400 m), based on a mesh Peclet number of four, because lines of constant concentration will, for the most part, parallel the flow directions. All boundaries of the mesh are closed to flow except where fresh-water recharge is specified at the back of the aquifer. The mesh boundary is also open where pressure is specified to be zero below the sea, and at hydrostatic pressure where the mesh is arbitrarily cut off on the seaward end. Based on the results of a parsimonious model identification (SOUZA & VOSS, 1986), the following parameters define the one-meter thick representation of the system.

Q inflow = 0,404 kg/s

K horizontal = 457,2 m/day

K_s = (K horizontal)(10^{-2})

K caprock = (K horizontal)(10^{-4})

ε = 0,04

ρ_o = 1000 (kg/m^3)

$\partial\rho/\partial C$ = 700 (kg/m^3)

S_y = 0,04

α = 2,5 x 10^{-9} (kg/m·s^2)$^{-1}$

β = 4,47 x 10^{-10} (kg/m·s^2)$^{-1}$

μ = 1,0 x 10^{-3} (kg/m·s)

α_L = 76 m

α_T = 0,25 m

C seawater = 0,0357

ρ seawater = 1024,99 (kg/m^3)

where K is hydraulic conductivity, and C is the dissolved solids concentration as a mass fraction, and K_s is the hydraulic conductivity of the vertical seaward boundary in the basalt aquifer.

The simulated concentration distribution (for anisotropy value of horizontal divided by vertical conductivity, $K_h/K_v = 200$) for predevelopment steady-state conditions is shown in fig. 8 to scale and in fig. 9 with vertical exaggeration. The transition zone is extremely sharp inland, as expected, and gradually broadens near the caprock. These solutions are impossible to obtain with an inconsistent velocity approximation (standard Galerkin method). Experiments show that neither low values of dispersivity nor high anisotropy (K_h/K_v) allow a relatively narrow transition zone to be simulated. The artificial velocity and resultant dispersion generated by the inconsistent approximation give highly incorrect results. However, an accurate simulator based on a consistent velocity approximation provides a fundamental tool for hydrologic analysis of the system as described in the companion paper (SOUZA & VOSS, 1986).

6. DISCUSSION

The problem of cross-sectional transport-simulation analysis of a fresh-water/salt-water aquifer system including a relatively narrow transition zone has not previously been approached. Most published analyses either deal directly with the case where data indicate a broad transition zone, or give simulation results that imply a broad zone in the absence of data. The question must be asked whether these analyses have accurately represented the transverse dispersion process (albeit given by the standard dispersion model) that is the primary force which creates a narrow or broad structure of the transition zone in such systems. A narrow transition zone amplifies any inconsistencies, inaccuracies or instabilities inherent in a given simulation model. The likely sources of simulation error are three-fold: (1) Vertical discretization is typically too coarse for the desired level of transverse dispersion. (2) Inconsistent approximations of terms involved in the fluid velocity calculation can lead to large artificial velocity and dispersion components in a simulation. (3) The process of flow driven by density differences in the fluid may not be accurately represented by the simulation. Tests typically used to verify such models do not verify that a given model is free of the above sources of error.

The following modelling approach rectifies these difficulties: (1) Vertical discretization must be in the order of the transverse dispersivity value when flow is predominantly horizontal. Transport simulation studies should always begin with a steady-state simulation for the case of zero transverse dispersion to check for the sharpest transition zone possible with a given mesh and flow field. (2) A numerical method that gives a consistent velocity approximation must be employed. The standard Galerkin finite-element method gives an inconsistent velocity approximation that can generate overwhelming artificial velocities in a simulation. Finite-difference methods may or may not be consistent

depending on the particular approach used. (3) Two new model tests for consistency of the velocity approximation are suggested. These simulate a simple system with a sharp interface that should remain sharp for all time. (4) The HENRY (1964) seawater-intrusion problem serves only as a most simple basis for verifying a variable-density transport code. The test does not check for consistency. Because of the unrealistically high level of dispersion in this problem, the Henry problem does not serve as a sufficient verification of the accuracy of a transport simulator for typical field systems. (5) The ELDER (1967) natural-convection problem is suggested as a test for verification of the accuracy of simulation of flow driven purely by density differences in the fluid. While an analytic solution of this problem is not available, the Elder test serves to build confidence in a simulator by comparison with results of other simulators.

A variable density flow and solute transport simulator based on a consistent velocity approximation, when verified with the before-mentioned tests, and when used with proper spatial discretization is a state-of-the-art tool that can give excellent results for a range of difficult problems at various scales of analysis. An interesting case in point is the simulation analysis of the regional aquifer of Southern Oahu, Hawaii, that contains both narrow and broad sections of a transition zone. This analysis is described in a companion paper: SOUZA & VOSS (1986).

ACKNOWLEDGEMENT

The authors wish to gratefully acknowledge E. Buctow and colleagues, Technical University of Berlin, for suggesting the Elder problem as a test case.

REFERENCES

DESAI, C.S. & CONTRACTOR, D.N. (1977). Finite element analysis of flow, diffusion and salt water intrusion in porous media. In: Formulation and Computational Algorithms in Finite Element Analysis. K.J. BATHE et al. (eds.), 958-983, Cambridge (Mass.): MIT.

ELDER, J.W. (1967). Transient convection in a porous medium, J.Fluid Mech. 27(3), 609-623.

FRIND, E.O. (1982 a). Simulation of long-term transient density-dependent transport in groundwater. Adv. Water Resources 5, 73-78.

FRIND, E.O. (1982 b). Seawater intrusion in continuous coastal aquifer-aquitard systems. Adv. Water Resources 5, 73-78.

HENRY, H.R. (1964). Effects of dispersion on salt encroachment in coastal aquifers. In: Sea Water in Coastal Aquifers, U.S. Geological Survey Water-Supply Paper 1613-C, C71-C84.

HUYAKORN, P.S. & TAYLOR, C. (1976). Finite element models for coupled groundwater flow and convective dispersion. In: Finite Elements in Water Resources (GRAY et al. (eds.), 1.131-1.151. London: Penteck Press.

INTERA (1979). Revision of the documentation for a model for calculating effects of liquid waste disposal in deep saline aquifers. U.S. Geological Survey Water-Resources Investigations Report 79-96, 73 p.

LEBBE, L.C. (1983). Mathematical model of the evolution of the fresh water lens under the dune and beach with semi-diurnal tides. Proceedings of the 8th Salt Water Intrusion Meeting, Geologia Applicata e Idrogeologia, 18(2), 211-266.

LEE, C.-H. & CHENG, R.T. (1974). On seawater encroachment in coastal aquifers. Wat. Resour. Res. 10(5), 1039-1043.

MINK, J.F. (1980). State of the Groundwater Resources of Southern Oahu, Board of Water Supply, City and Country of Honolulu, Hawaii, 83 p.

PINDER, G.F. & COOPER, H.H. (1970). A numerical technique for calculating the transient position of the saltwater front. Wat. Resour. Res. 6(3), 875-882.

REILLY, T.E. & GOODMAN, A.S. (1985). Quantitative analysis of saltwater-freshwater relationships in groundwater systems - a historical perspective. J. Hydrology 80, 125.160.

SEGOL, G., PINDER, G.F. & GRAY, W.G. (1975). A Galerkin finite element technique for calculating the transient position of the saltwater front. Wat. Resour. Res. 11(2), 343-347.

SEGOL, G. & PINDER, G.F. (1976). Transient simulation of saltwater intrusion in southeastern Florida. Wat. Resour. Res. 12(1), 65-70.

SOUZA, W.R. & VOSS, C.I. (1986). Modeling a regional aquifer containing a narrow transition between freshwater and saltwater using solute transport simulation: Part II - Analysis of a coastal aquifer system. 9th SWIM Proceedings.

VOLKER, R.E. (1980). Comparison of immiscible and miscible fluid models for sea water intrusion in aquifers. 7th Australian Hydraulics and Fluid Mechanics Conference, Brisbane, Qld., 23-26.

VOLKER, R.E. & RUSHTON, K.R. (1982). An assessment of the importance of some parameters for seawater intrusion in aquifers and a comparison of dispersive and sharp-interface modelling approaches. J. Hydrology 56, 239-250.

VOSS, C.I. (1984). SUTRA: A finite-element simulation model for saturated-unsaturated fluid-density-dependent groundwater flow with energy transport or chemically-reactive single-species solute transport. U.S. Geological Survey Water-Resources Investigations Report 84-4369, 409 p.

FIGURES

Fig. 1: Boundary conditions and finite-element mesh for HENRY (1964) solution.

Fig. 2: Match of isochlors along bottom of aquifer for numerical results of HUYAKORN & TAYLOR (1976) and SUTRA.

Fig. 3: Match of isochlor contours for Henry-analytical solution (for 0,50 isochlor) (long dashes), INTERA code solution (short dashes) SEGOL et al. (1975) (dotted line), SUTRA solution (solid line).

Fig. 4: Match of 0,50 isochlor contours for Henry problem with simulated results for D_m = 6,6 x 10^{-9} (m^2/s) of PINDER & COOPER (1970), (short dashes), SEGOL et al. (1975) (dotted line), FRIND (1982) (long and short dashes), DESAI & CONTRACTOR (1977) (long dashes). SUTRA results at isochlors (0,25, 0,50, 0,75) (solid line). HENRY (1964) solution for D_m = 18,8571 x 10^{-9} (m^2/s), (0,50 isochlor, dash-dot).

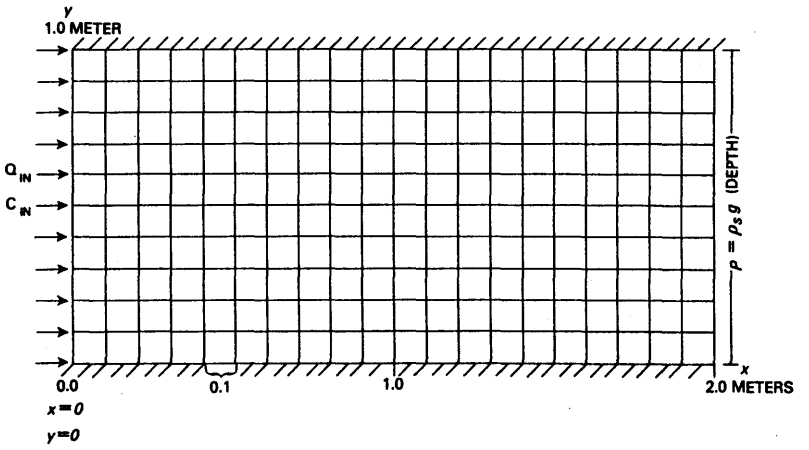

Figure 1

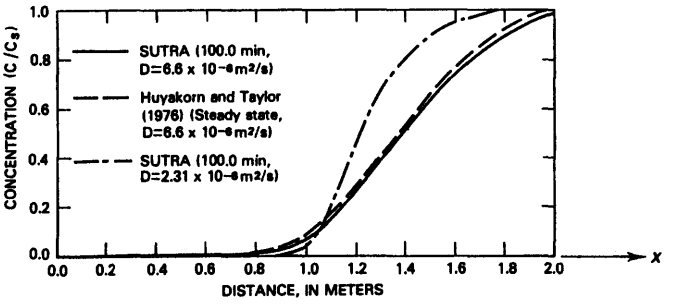

Figure 2

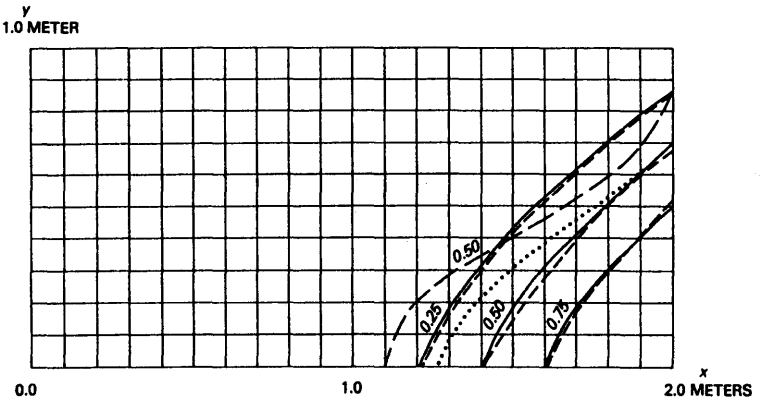

Figure 3

Figure 4

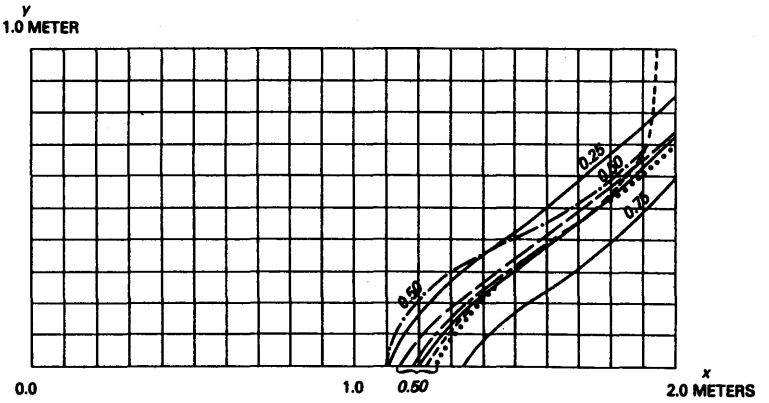

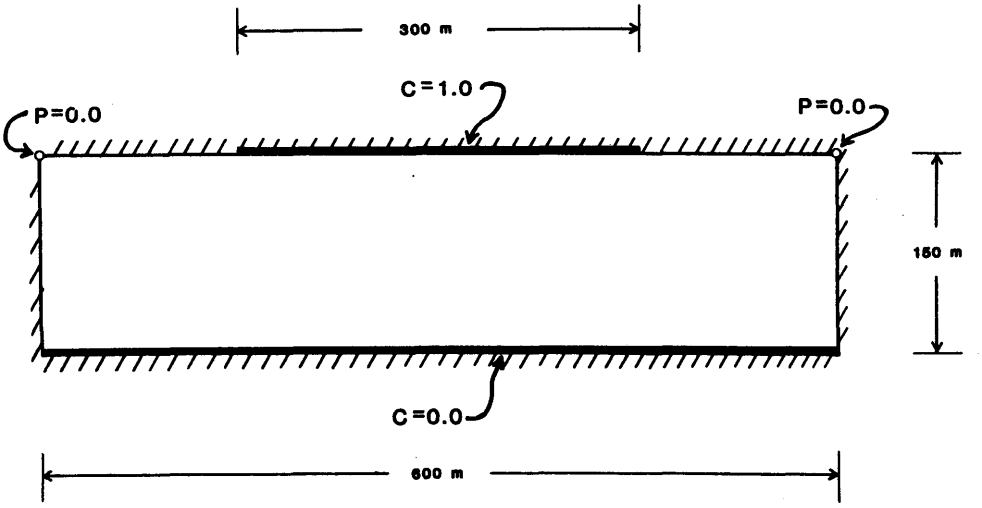

Figure 5

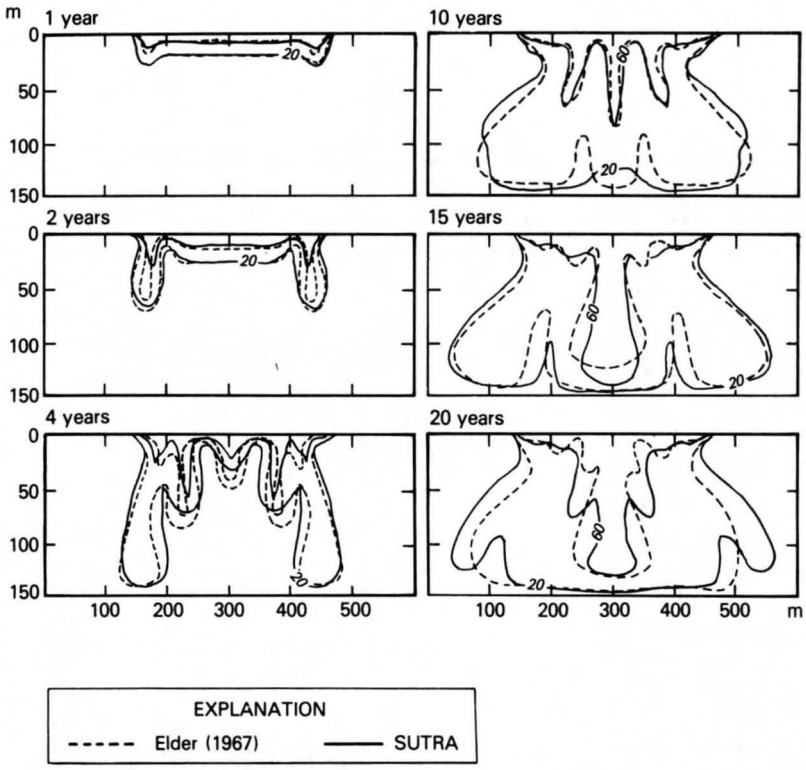

Figure 6

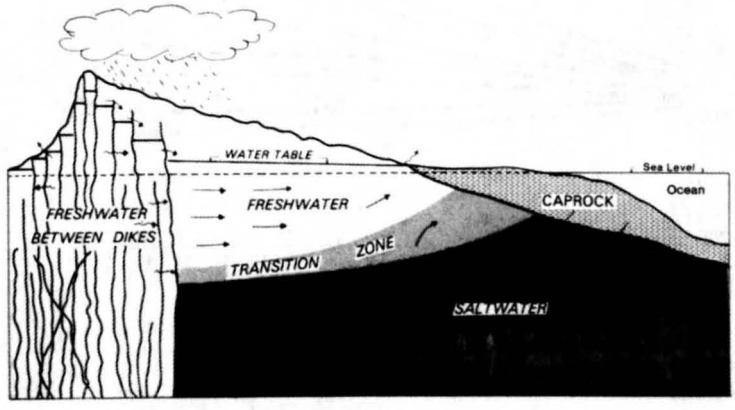

Figure 7

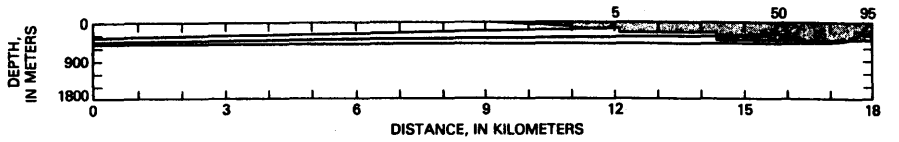

Figure 8

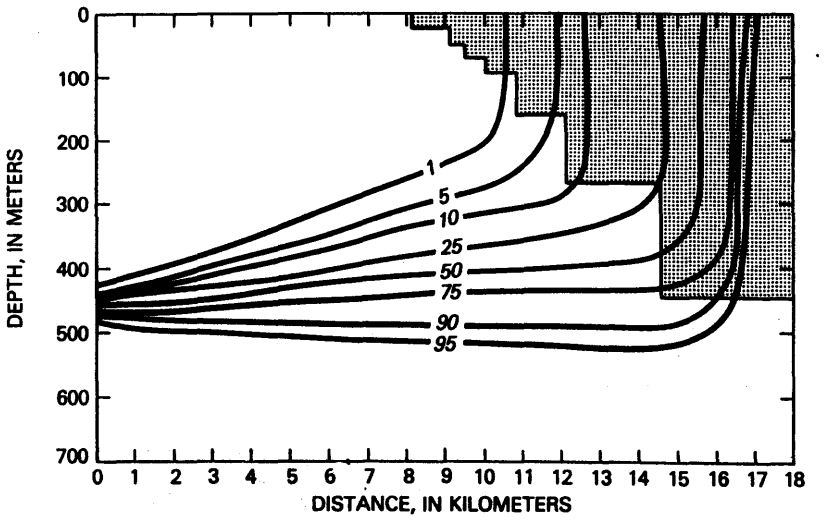

Figure 9

3.8. UPCONING OF BRACKISH AND SALT WATER IN THE DUNE AREA OF THE AMSTERDAM WATERWORKS AND MODELING WITH THE KONIKOW-BREDEHOEFT PROGRAM

J.W. KOOIMAN, J.H. PETERS and J.P. van der EEM

ABSTRACT

For the water supply of Amsterdam, groundwater is abstracted from the dune area near the North Sea; since 1853 from the phreatic aquifer by means of canals, and since 1903 also from the deep aquifers. From 1957 the upper aquifer is artificially recharged with river water which has higher chloride contents than the original dune water.

The Boogkanaal, in the northern part of the dune-water catchment area, is important because of the low chloride content of the abstracted water. As a result of the continuous abstraction a heavy intrusion and upconing of brackish and salt water occurred. Therefore, in 1978, the deep-well abstraction was terminated. Before taking these wells into use again research has to be done, by computer modeling, to assess the consequences for the fresh-water pocket.

A supplementary version of the two-dimensional groundwater contaminant transport program Konikow-Bredehoeft, as presented by LEBBE (1983, 1984), is suited for the calculations mentioned. The program calculates the transport of solutes in the saturated zone. In an adaption to the original version the effects of differences in density are taken into account.

The model was calibrated with the available data. The consequences of different groundwater-abstraction policies on the chloride content of the abstracted water can be computed.

1. INTRODUCTION

Amsterdam Waterworks is in charge of the drinking-water supply for more than 1.000.000 citizens. Three production units are used:

1. Dune waterworks $83 \cdot 10^6$ m^3/a (72 %)
2. Lake waterworks $30 \cdot 10^6$ m^3/a (26 %)
3. Hilversum Pumping Station $2 \cdot 10^6$ m^3/a (2 %)

The dune-water catchment area is a very important unit, not only quantitatively but also qualitatively: it is the property of Amsterdam Waterworks and so groundwater quality can be protected effectively against pollution by agriculture, industry or waste disposal.

On the other hand there is the continuous threat of salt-water intrusion and upconing of brackish and salt water. Especially in the last decades this presents problems in water production. To minimize these problems the optimum distribution of total capacity over the different abstraction units in the dune area, especially those in the deep aquifer, has to be determined.

2. DUNE-WATER CATCHMENT AREA

The dune-water catchment area of the Amsterdam Waterworks is situated along the Dutch North Sea coast, south of Haarlem (fig. 1).

Withdrawal of water in this area - some 36 sq. km - started as early as 1853, by the simple method of draining a system of excavated canals. In this way, water was abstracted from the phreatic aquifer, and it was not until many years later that the presence of a vast stock of semiconfined water of good quality was discovered deeper in the subsurface.

In the catchment area, the subsurface at greater depth is saturated with salt water. The fresh water is limited to a fresh-water pocket, or lens, under the dunes. Since 1903 water has been abstracted from the deep aquifer by a system of wells.

Over the years the volume withdrawn from the dune area increased gradually. From the early twenties the total water production exceeded the natural replenishment by effective precipitation. A heavy salt-water intrusion occurred in the deep aquifer, resulting in an increasing number of wells contaminated with salt water (ROEBERT, 1972).

To stop this process of intrusion, from 1957 a part of the upper aquifer is artificially recharged with pretreated water from the river Rhine. The water abstraction from the deeper aquifer at that time decreased to a low level.

There remains, however, a vast stock of groundwater of good quality which is used for quality reasons and during periods when the river-water intake has to be interrupted. To avoid continuous salt-water intrusion and upconing the deep abstraction is limited (SCHUURMANS, 1983).
Nowadays the total water production of the entire dune area varies between 55 and 60 million m^3/yr. Some 10 million m^3/yr is natural dune-water.

3. PRODUCTION UNIT BOOGKANAAL

The Boogkanaal in the northern part of the dune-water catchment area has a length of 1000 meter, more or less parallel to the coast at a distance of 2,5 km (fig. 1). The geohydrological situation in a cross-section perpendicular to the Boogkanaal is given in fig. 2.

Abstraction from the Boogkanaal started in 1887. By artificially maintaining a low water level (N.A.P. - 1,70 m; N.A.P. is approximately mean sea level), the canal abstracts water from the upper aquifer in an amount which varies between 1 and 1,5 million m^3/yr (fig. 3). In 1903 withdrawal from the upper part of the deep aquifer started (table 1). Because of the increasing chloride

content of the abstracted water the abstraction of deep groundwater was terminated in 1978 (fig. 4).

For the quality of the abstracted water from the dune area it is desirable that the total installed capacity at the Boogkanaal can be used. In the direct surroundings of the canal there is no artificial recharge, so the abstracted water has a very low chloride content (40 mg/l). Therefore it is used mainly for mixing purposes in order to lower the chloride content of the supplied water. If, as a result of the deep abstraction, the chloride content increases to 90 - 100 mg/l, which was the case in the early seventies, the Boogkanaal will lose this important function. Nowadays the amount of 1 to 1,5 million m^3/yr is only 2 % of the total water production of the dune area, including the infiltrated river water, but it is 10 - 15 % of the total amount of abstracted natural water. Regarding the fact that a substantial part of this natural water is mixed with the infiltrated water, the importance of the Boogkanaal for the water supply is obvious.

Table 1. Deep-well abstraction from the Boogkanaal.

Period	Number of wells	Maximum abstraction 10^6 m^3/a	Remarks
1903 - 1909	40	1,4	Along north-west side of canal
1909 - 1929	55	3,7	Extension to the south with 15 wells
1929 - 1954	79	3,6	24 extra wells along south-east side
1954 - 1978	20	2,9	20 new artesian wells along canal
1978 - now	20	0,0	No deep abstraction

The movement of the salt, brackish and fresh water until 1970 has been studied by ROEBERT (1972) as a result of the continuous abstraction. He used the observations of three boreholes located on a line perpendicular to the centre of the Boogkanaal (fig. 1): no. 31 (just near the canal), no. 48 (500 meter to the west) and no. 257 (500 meter east of the canal).

In table 2 and 3 the developments from 1920 until 1985 are presented, which, for a good understanding, have to be compared with the abstraction amounts as presented in fig. 3 and 4.
From these tables one can see the rise of the 100 mg/l isochlor at a rate of 1,5 m/yr in the years 1920 - 1950 at the site of observation well 31. Due to the increasing abstractions in the years between 1950 and 1960, from the Boogkanaal as well as from other abstraction units south, east and north at distances of 500 to 750 meter, the rate of rise increased to some 3 m/yr. After the start of the artificial recharge in 1957 and the decrease in the

abstractions the rate reduced to 1 m/yr. The period 1968 - 1978 is characterized by a stabilization of the situation, whereas in the last period the ending of the deep-well abstraction in 1978 resulted in a displacement in the opposite direction.

Table 2. Average rate of rise (m/yr) of the 100 mg/l and 10.000 mg/l isochlors in wells 48, 31 and 257.

Period	100 mg/l			10.000 mg/l		
	48	31	257	48	31	257
1920 - 1930	1,0	1,5	1,5	0,5	0,5	0,5
1930 - 1940	0,5	1,5	1,0	0,5	0,5	0,6
1940 - 1950	0,4	1,5	1,5	0,4	0,5	0,8
1950 - 1955	1,2	3,0	1,5	0,2	0,5	1,4
1955 - 1960	2,4	1,5	2,0	0,1	0,5	0,0
1960 - 1968	1,0	1,0	1,0	0,0	0,5	0,0
1968 - 1978	0,0	0,0	- 0,8	0,0	- 0,5	- 0,4
1978 - 1985	0,0	- 1,0	- 0,7	0,0	- 0,7	- 0,5

Table 3. Position of the 100 mg/l and 10.000 mg/l isochlors in meters below N.A.P. (Mean Sea Level) in wells 48, 31 and 257.

Year	100 mg/l			10.000 mg/l		
	48	31	257	48	31	257
1920	- 116	- 108	- 112	- 124	- 116	- 120
1968	- 71	- 33	- 46	- 105	- 92	- 94
1985	- 71	- 40	- 60	- 109	- 102	- 102

4. COMPUTER PROGRAMS FOR SALT-/FRESH-WATER

To manage fresh-groundwater resources that are in contact with saline water it is essential to obtain quantitative understanding of the pattern of movement and mixing between fresh and saline water. Recently REILLY & GOODMAN (1985) amply reviewed the factors that determine the appropriate methods to be used. They considered three major factors:

- assumptions about the physics of the mixing process,
- characteristics of the aquifer system under study and
- desired scale and detail of the resulting analysis.

In practice problems are often presented by the movement of slightly brackish water. This is why an approach with sharp interfaces between finite numbers of (immiscible) fluids is instructive but academic. It is more appropriate to model the behaviour of just one fluid with differences in concentrations of dissolved solids (transport models). These differences bring about gradients in density that can influence the flow pattern.

All aquifers are inhomogeneous. In practice an approach with homogeneous flow systems might suffice, most of the time it does not. In that case resort to numerical models - that can account for differences in characteristics of the aquifer - is essential. Once the flow problem is solved, transport of solutes due to both advection and dispersion has to be determined. Well-known are the problems that go along with this. Solutions sometimes contain errors - due to numerical dispersion - which invalidate the solution. Numerical dispersion can be minimized when the method of characteristics (MOC) is used. The two-dimensional model as documented by KONIKOW & BREDEHOEFT (1978) is a numerical transport model that uses MOC. In the case that is presented in this paper, flow predominantly occurs in two directions (vertical and horizontal). An approach with a two-dimensional flow system can be justified. However, it is essential to adapt the original version of the model to account for the flow induced by density differences.

5. GROUNDWATER-CONTAMINANT TRANSPORT MODEL KONIKOW-BREDEHOEFT

The Konikow-Bredehoeft model has been developed by the U.S. Geological Survey and is based upon the finite difference method (for solution of the flow equation) together with the method of characteristics (for solution of the solute transport equation). The model requires that the aquifer in the area of interest is divided by a regular grid into a number of blocks. The purpose of the model is to compute heads and concentrations at any specified time and place (in the centre of a block, 'block-centred grid').

To account for density-induced flow the model has been adapted as described by LEBBE (1983, 1984). Water pressures are computed as fresh-water heads. Vertical-flow components are adjusted for relative densities. Further information on the program and adaptions can be found in the reference list (KONIKOW & BREDEHOEFT, 1978; LEBBE, 1983, 1984).

Some practical problems were encountered when running the program:

- The program first computes the head distribution. With this information the velocities (and dispersion coefficients) on cell boundaries are determined. These velocities depend on the average density in a cell. With these velocities so-called tracer particles are moved within the flow field. After the displacement of the tracer particles and the calculation of the dispersion the new average density in a cell is computed. Then the process restarts with the computation of the head distribution.

It was found that instabilities arise when the displacement of tracer particles within one time step, without recalculation of the pressure head, becomes too large. This can be explained by the following example (rather) exaggerated!): Under an abstraction well with limited capacity a sharp interface is found. Salt particles under the well will have a velocity component in an upward direction. If such a salt particle is allowed a large displacement it can move upward beyond the equilibrium position of the interface. Then recalculation of heads takesplace. A large vertical velocity downward will be computed (because of the extreme upconing). The particle can now move.
The remedy for the problem is clear: the displacement of particles between two successive computations of the pressure-head distribution should not be too large.

- Especially when abstractions are limited, the calculation of the pressure head has to be done very accurately. A tolerance of 0,00001 m was used.
- The water pressure in the model is expressed in fresh-water heads. If the solute content along the boundary is not constant, the fresh-water head will not be constant either, even if there is no vertical flow. To eliminate boundary 'rotations' the pressure head has to fit the chloride content along the boundary. In our case the heads had to be accurately given in millimeters.

6. SCHEMATIZATION AND CALIBRATION

Computations are made in a vertical plane perpendicular to the Boogkanaal. The cross section contains several observation wells. Three of them are measured for chloride content (wells 48, 31 and 257; fig. 1 and 2). The west boundary is located at well 48, the east boundary at 257. With the computer model an attempt is made to describe chloride content at the middle observation well 31, just near the Boogkanaal (calibration).

The input for the model is extensive. As with all groundwater-flow models the characteristics of the flow domain have to be given, i.e. the spatial distribution of hydraulic conductivities in a horizontal and vertical direction, porosity and storage coefficients. Because a solute-transport model is used, information is also needed on the behaviour of the solute. Furthermore, initial and boundary conditions have to be described for heads and concentrations.

The schematization of the subsoil is straightforward as shown in fig. 2, i.e. three aquifers separated by semi-permeable clay and loam layers. The hydrological base is situated at 155 m below mean sea level. The quantitative data are based on a pumping-test analysis and borehole information. The vertical hydraulic conductivities are chosen to be ten times smaller than the horizontal conductivities throughout the system (anisotropy).

Chloride is a non-reactive (decay equals zero) and non-adsorbing solute. Introduction of dispersion deals with the process of mixing of fresh and salt water. It should be noted that actually it is not justified to model hydrodynamic dispersion in non-isotropic media with longitudinal and transversal components (BEAR, 1979).
Very small dispersivities showed the best results (dispersion is the product of dispersivity and velocity). A longitudinal dispersivity of 0,02 m is used. The transversal dispersivity is smaller by a factor 10. LEE et al. (1980) found comparable values.
In literature, laboratory tests show very small dispersivities indeed (see for example LI & LAI, 1966). Field studies indicate larger values for the dispersivity (several researchers reported about the scale-dependency of dispersion (MOLZ et al., 1983; GILHAM et al., 1984)). Sometimes these values are found at locations where tidal movement is important. In our case tidal influence is small, which might explain the low dispersivity. It should be emphasized here that in the case of a predominantly horizontal flow the solute transport in a vertical direction is mainly caused by transversal or lateral dispersion (dispersion perpendicular to the flow).
The relative density difference amounts to 2,5 % for a chloride content of 18630 mg/l.

Boundary conditions are taken from observation wells 48 and 257. A sharp interface between fresh and salt water is chosen as initial condition. The salt-water layer extends over the lower 30 m of the lower aquifer (horizontal interface). Because no storativity effects are taken into account initial values of heads are not necessary.
The groundwater suppletion by effective precipitation is taken constant at 0,465 $m^3/m^2/yr$..

The finite difference grid consists of rectangular blocks of 40 m · 10 m. The number of blocks in the horizontal direction is 27 and in the vertical 16. In each cell initially five tracer particles are placed. A period of 80 years is simulated, starting in 1903, coinciding with the start of deep groundwater abstraction. For periods of five years groundwater abstractions and boundary conditions are defined. Pressure heads and the position of tracer particles are computed in time steps of one month. The time steps are this small to avoid the maximum displacement of tracer particles exceeding 30 m.
The abstractions of phreatic and deep groundwater have to be computed as an abstraction per meter. It is not sufficient to simply divide the total abstraction by the length of the abstraction means. Because of the finite length of Boogkanaal and the line of deep wells the abstraction will not be equally distributed. Right in the middle of the Boogkanaal, where the vertical cross-section is made, the abstraction will be a factor R smaller than the average. For the phreatic and deep-water abstractions this factor was fixed at respectively 0,75 and 0,70 (HUISMAN, 1972).

7. RESULTS

The measured chloride content in time is compared with the calculated chloride content for three filters of observation well 31 (fig. 5, 6 and 7; for a location of the filters see fig. 2). The peaks and dips in the figures are caused by the discretization of the solute in space (only five tracer particles in each grid). Despite the simplifications (two-dimensional flow, little spatial variability in aquifer characteristics, no storativity, constant dispersivities etc.) the chloride content in time can be satisfactorily simulated with the model. The largest deviations are found for filter 6. This can be explained partly because small absolute deviations here are relatively large and partly because filter 6 is located at distance from the chloride-source, i.e. the salt-water body. Furthermore, as we look at the spatial distribution of the chloride content (fig. 8), we can see an upconing of brackish water on the east side of the abstractions. This is caused by natural groundwater flow from west to east. When we slightly overestimate this natural groundwater flow the cone of brackish water is displaced too far to the east. This might be another cause of the observed deviations in filter 6.

With the model the chloride content of the abstracted water is predicted for 25 years. Deep water abstraction is assumed 0,5 Mm^3/yr and the phreatic abstraction is fixed at 1,0 Mm^3/yr. The initial concentration profile is the generated chloride-content at the end of the simulation period of 80 years. Boundary conditions are kept constant.
During the prediction period no serious increase in chloride-content of the abstracted water is found. From analysis of the head distribution it become clear that a stagnation point occurs just east of the deep-well abstractions. This stagnation point causes the brackish cone to more or less stabilize at its current position.
It can be concluded that a deep-well abstraction of e.g. 0,4 Mm^3/yr might be safe. Additional observation wells at the east side of the Boogkanaal are necessary to trace the movement of the brackish cone under the renewed withdrawal.

8. GENERAL CONCLUSIONS AND RECOMMENDATIONS

With the computer model of two-dimensional solute transport in groundwater, as documented by KONIKOW & BREDEHOEFT and adapted for density-induced flow by LEBBE, a good insight can be obtained in the formation and behaviour of the brackish water. However, predictions on whether an abstraction will show a chloride-content of 100 mg/l or 200 mg/l, a relevant difference if the water is used for production of drinking water, cannot be given accurately enough. Yet, the model can indicate whether problems with brackish water can be expected. Furthermore it can be used as an effective tool in developing a system for monitoring the brackish water.

The reasons for obtaining rather small dispersivities are not clearly understood. For the sake of future investigations research on actual values for the dispersion parameters should be carried out.

9. ACKNOWLEDGEMENT

Adaption of the model (provided by the National Institute of Public Health and Environment), testing, schematization and calculations have been performed within projects on recharge wells that are part of the research program of KIWA under contract from VEWIN, the Association of Waterworks in the Netherlands. The research projects are partly funded by the Ministry of Housing, Country Planning and Environment in the Netherlands. Discussions with Dr. L. Lebbe when adapting the model are gratefully acknowledged.

REFERENCES

BEAR, J. (1979). Hydraulics of groundwater. 567 p., London: McGraw-Hill.

GILLHAM, R.W., SUDICKY, E.A., CHERRY, J.A. & FRIND, E.D. (1984). An advection-diffusion concept for solute transport in heterogeneous unconsolidated geological deposits. Water Resources Research 20, 369-378.

HUISMAN, L. (1972). Groundwater recovery, 336 p., London: MacMillan.

KINZELBACH, W. (1986). Groundwater modelling. 333 p., Amsterdam: Elsevier. (Developments in water science 25).

KONIKOW, L.F. & BREDEHOEFT, J.D. (1978). Chapter C2: Computer model of two-dimensional solute transport and dispersion in groundwater. In: Book 7: Automated data processing and computations, Techniques of water-resources investigations of the United States Geological Survey, 90 p., Washington: U.S. Government printing office.

LEBBE, L. (1983). Mathematical model of the evolution of the fresh water lens under the dunes and beach with semi-diurnal tides. Proceedings of the 8th Salt Water Intrusion Meeting, Bari, 25-29 May 1983, 211-226.

LEBBE, L. (1984). Numerische simulatie van grondwaterkwaliteitsproblemen als hulp bij het beheer van de watervooraden in het vlaamse kustgebied. Tijdschrift Becewa 76, 67-88.

LEE, D.R., CHERRY, J.A. & PICKENS, J.F. (1980). Groundwater transport of a salt tracer through a sandy lakebed. Limnol. Oceanogr. 25, 45-61.

LI, W.H. & LAI, F.H. (1966). Experiments on lateral dispersion in porous media. J. of the Hydraulics Division, Proc. of ASCE, HY 6, 141-149.

MOLZ, F.J., GÜVEN, O. & MELVILLE, J.G. (1983). An examination of scale-dependent dispersion coefficients. Groundwater 21, 715-725.

REILLY, T.E. & GOODMAN, A.S. (1985). Quantitative analysis of salt-water - fresh-water relationships in groundwater systems - a historical perspective. J. of Hydrology 80, 125-160.

ROEBERT, A.J. (1972). Fresh water winning and salt water encroachment in the Amsterdam dune water catchment area. Geologie en Mijnbouw 51, 35-44.

SCHUURMANS, R.A. (1983). Restoring a briny catchment area. Proceedings of the 8th Salt Water Intrusion Meeting, Bari, 25-29 May 1983, 169-182.

FIGURES

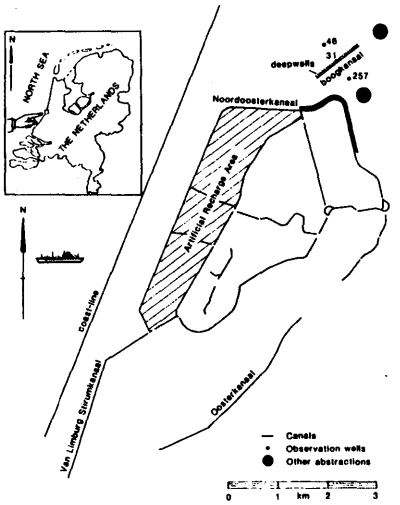

Figure 1

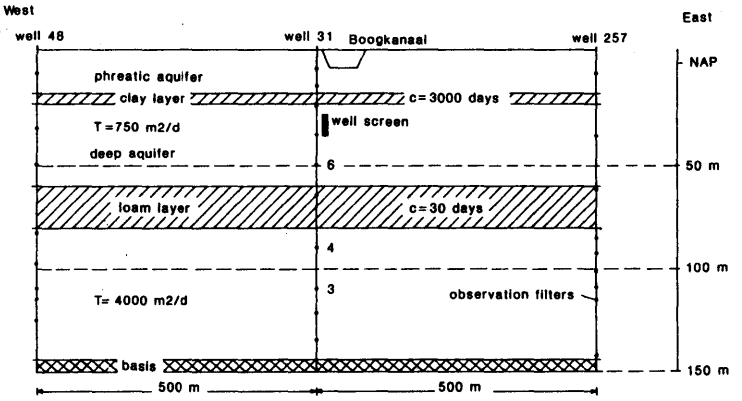

Figure 2

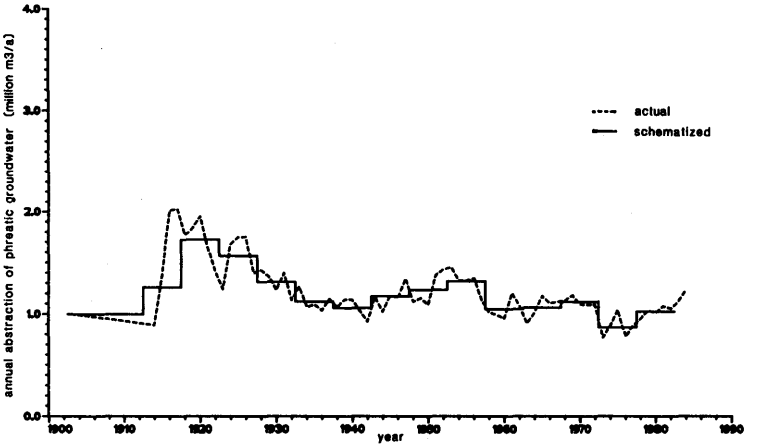

Figure 3

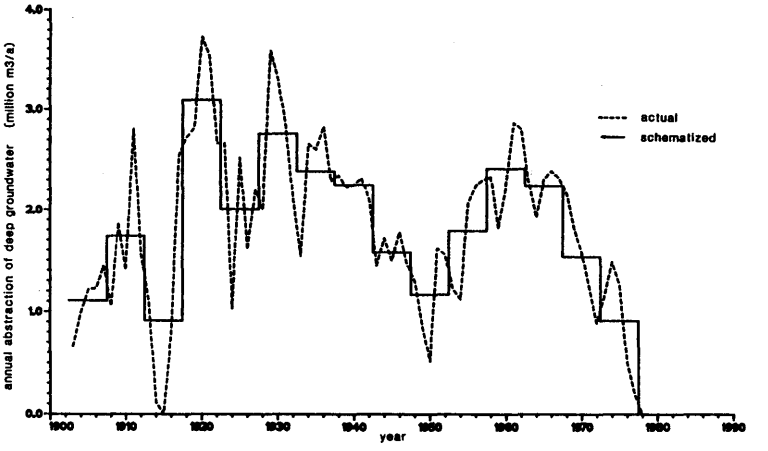

Figure 4

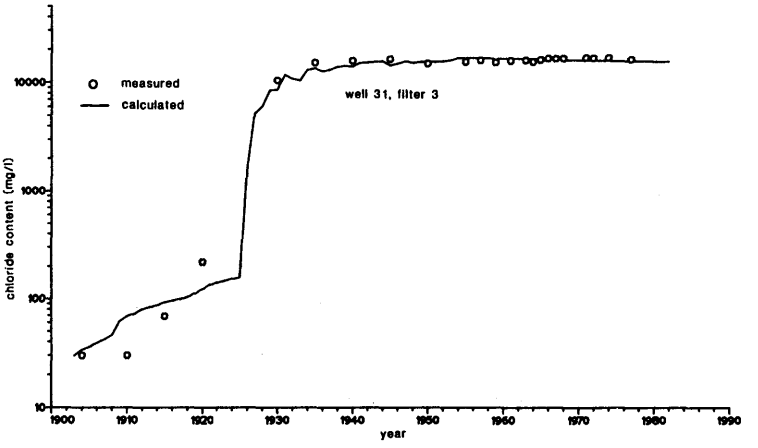

Figure 5

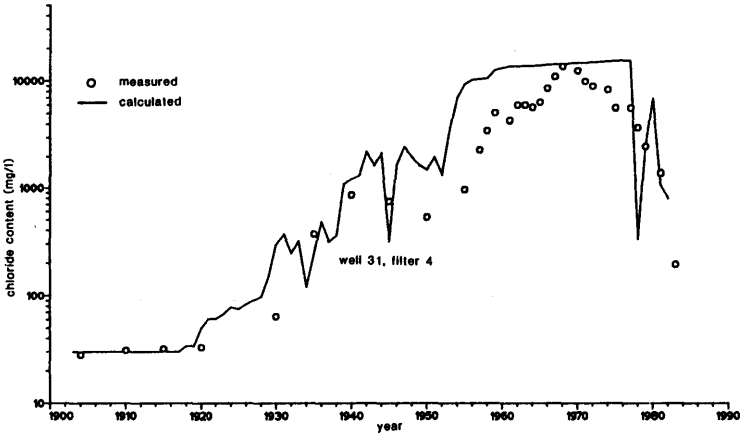

Figure 6

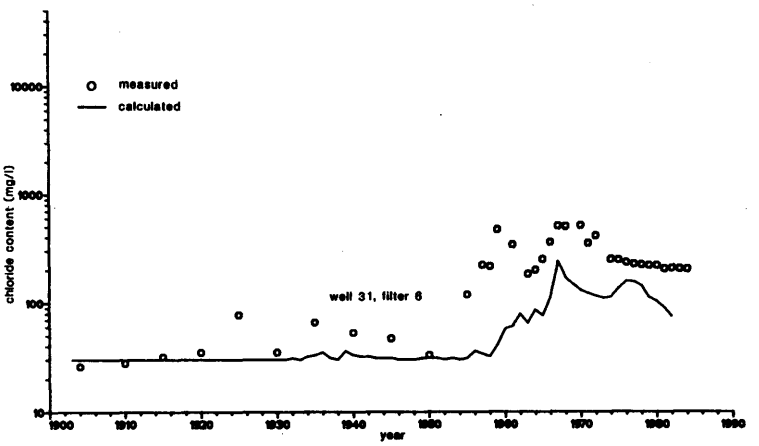

Figure 7

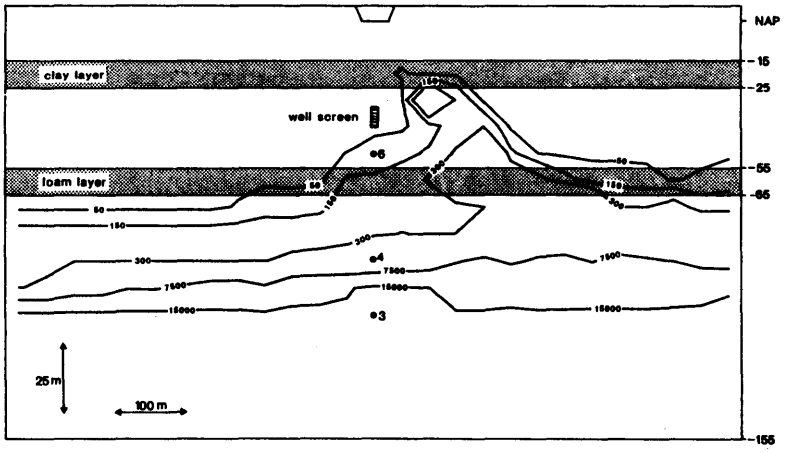

Figure 8

THEME 4

METHODS AND INSTRUMENTS

4

METHODS AND INSTRUMENTS

4.0. INTRODUCTION

R.H. BOEKELMAN

When reviewing past research on groundwater in coastal areas and more particularly the methods and instruments used in order to determine salt-water intrusion, considerable changes become evident.

In the late sixties, the emphasis was laid upon borings for chemical analysis of groundwater samples and determination of flow patterns based on piezometric levels. Later the use of geophysical methods became more important, as faster drilling techniques (rotary drilling) required additional information.

In the last decade isotope techniques, dating and research in the field of physico-chemical processes have become more and more important, as have the development of methods to prevent salt-water intrusion by infiltrating fresh water.

In fact the investigations of salt-water intrusion developed from hydrogeological into multi-disciplinary research.

Today there are a great variety of methods available, all of which have their place. For instance well logging; vertical electric, electro-magnetic and Very Low Frequency (VLF) resistivity measurements; dating, isotope techniques and chemical analysis of groundwater samples, sometimes using trace elements; classification of groundwater; research into the interaction between aquifer matrix and groundwater etc..

Much attention is paid to numerical modelling for simulation and/or prediction of salt-water intrusion, especially for non-steady cases and with varying salt concentrations. Too often calibration of these models appears to be cumbersome, due to a lack of data, particularly if time series are needed or due to a poor knowledge of the system and the processes involved. Looking into the future, when three-dimensional models will be available, knowledge of systems processes and the collection of data will become even more important.

This leads to the conclusion that, although field research is very laborious and the results achieved may seem to be limited, it remains very important and should be intensified.

An inter-disciplinary approach to salt-water intrusion problems and integration of the results of the different methods and instruments will prove to be essential to an achievement of a better understanding of the systems and processes involved and will lead to better modelling results.

From the contributions, as presented during previous SWIM's in the group "Methods and instruments", two papers were selected:
In the first, by MUELLER & ERIKSSON, the application of the VLF method is tested to locate saline groundwater in different situations and from different origin.

The second paper, by SCHUURMANS & VAN DEN AKKER, deals with the effects of infiltration of fresh water in a saline aquifer in order to store a volume of fresh water as a reserve for public water supply.

4.1. TESTING VLF-RESISTIVITY MEASUREMENTS IN ORDER TO LOCATE SALINE GROUNDWATER

C.-F. MÜLLERN & L. ERIKSSON

ABSTRACT

VLF-resistivity measurements are being tested as a rather cheap and rapid tool for making rough estimations of the occurrence of saline groundwater. In this study the method has been tested in order to: 1. locate fossil saline groundwater in a Pleistocene esker (sand and gravel) aquifer, 2. locate fossil saline groundwater in the Precambrian crystalline basement, 3. locate the saline-water/freshwater boundary on the coast of the Bothnian Sea, 4. outline the boundary of pollution from storage of salt used for de-iceing and dust prevention on roads. The results of these tests are presented and discussed.

1. INTRODUCTION

During the last few years VLF-measurements have been used to locate groundwater-bearing fracture zones. This method has in many cases been successful and many geological consultants, and others, in Sweden have acquired this kind of equipment. Since it is also possible to make at least approximate resistivity measurements with this kind of equipment, preferably in single- and two-layer cases, it was thought worthwhile to test it in connection with problems concerning saline groundwater. Under favourable geological conditions, the measurements are not very complicated, quickly made and inexpensive. It must be pointed out, however, that the results of this study are the first obtained in Sweden in order to locate saline groundwater, and some of the results are not yet properly verified. The different sites where the measurements of this study were carried out are shown in fig. 1.

2. THE VLF-RESISTIVITY TECHNIQUE

The VLF-instrument, including the attached resistivity device, is mainly a radio receiver measuring the ratio and phase angle between the horizontal electric and magnetic fields of very low frequency radiowaves (15 - 20 kHz) transmitted from distant stations. The instrument is calibrated to read the resistivity directly. If the earth is of constant electrical conductivity down to the depth of penetration the phase angle is 45°. If in a two-layer case the top layer has lower resistivity than the bottom layer, the phase angle is less than 45°. If the situation is reversed, the phase angle is more than 45°. The penetration depth depends on the measured resistivity and can be determined from a graph, supplied with the instrument. From other graphs the thickness of the upper layer, the resistivity of that layer and of the lower layer can be determined. One of these three parameters must however be known (or almost correctly inferred).

3. FOSSIL SALINE GROUNDWATER IN A PLEISTOCENE ESKER

During the uplift of land after the latest glaciation, saline seawater has been trapped in different aquifers under varying geological and morphological conditions.

About 70 km west of Stockholm a row of small islands in lake Mälaren constitutes a part of the Enköping esker. On one of the islands (Tallholmen) drilling for groundwater was undertaken by a Swedish consulting company (AIB). It was found that underneath a fresh-groundwater layer, about 10 m thick, there is saline groundwater. This is shown in fig. 2.

The resistivity values of the sand and gravel above the groundwater table were obtained from Beam Slingram readings.*) The resistivity values below the groundwater table have been calculated from the chemical analyses of the groundwater. In the left part of fig. 2 the geological setting constitutes a rather clear-cut two-layer case, with fresh groundwater on top of saline down to penetration depth. In this part the high phase angles indicate low resistivities below high resistivities, and the interpreted depths to the saline groundwater are in rather good agreement with the actual depths. In the right part of fig. 2 the geological setting constitutes a multi-layer case. Down to penetration depth the geological sequence is, from top: 1. dry sand and gravel, 2. sand and gravel with fresh groundwater, 3. ditto with saline groundwater, 4. Precambrian crystalline bedrock, probably with saline groundwater (not shown in fig. 2). It can be seen that the more pronounced the multi-layer case, the more difficult it is to make correct interpretations from the measured data. (At the right-most part of fig. 2, the interpreted depth to the saline groundwater is more likely the depth to the fresh-groundwater table.)

4. FOSSIL SALINE GROUNDWATER IN THE PRECAMBRIAN CRYSTALLINE BASEMENT

At Östervåla, about 100 km north-north-west of Stockholm and about 40 km inland from the coast of the Bothnian Sea, two wells were drilled into the Precambrian basement for the supply of water to the municipality. One well 79 m deep yields fresh water and the other 69 m deep yields saline water. The wells are 1 km apart and are drilled in two different, almost parallel fracture zones. The geological setting at the two well sites is almost identical (see fig. 3).

Calculations made from the resistivity readings at A show that the resistivity ρ^2 of the second layer, the granite with fresh groundwater, is 30 000 ohm m. At A the resistivity of the granite with saline groundwater is only 1 000 ohm m. Due to this large contrast in resistivity it is probably possible to roughly outline the borders of the saline groundwater body.

---

*) A moving electromagnetic source receiver instrument (9,8 kHz) calibrated for direct resistivity reading.

In this context it can be mentioned that the total output from the two wells over a ten year period is about 1 000 000 m^3 of saline groundwater and 1 500 000 m^3 of fresh groundwater, respectively. The chloride concentration has been almost constant in the two wells over this period of time. This indicates that the body of trapped saline groundwater is rather large.

5. THE SALINE-/FRESH-WATER BOUNDARY ON THE COAST OF THE BOTHNIAN SEA

In order to test the VLF-resistivity method in connection with salt-water intrusion, a profile was measured from the shore of the Bothnian Sea to 20 km inland. This was done in the vicinity of Forsmark about 120 km north of Stockholm. The results of these measurements are shown in fig. 4.

The geological setting is the same in all the measured points: 1 - 3 m of till on top of the Precambrian basement consisting of granites and metamorphic volcanics. In fig. 4 it can be seen that the resistivity rises from 100 ohm m close to the shore to roughly 5 000 ohm m a few hundred metres inland (except for two peaks and one low). The high phase angles (more than 45°) close to the shore indicate the occurrence of saline groundwater within the depth of penetration. Somewhere around 200 m inland there is a sudden change in phase angle, where the values turn from high to low. This means that further inland there is no saline groundwater within the depth of penetration along this profile, and that contact with saline groundwater is lost at about 175 m depth. Obviously this does not exclude saline groundwater at greater depth.

Fig. 5 shows a map of Slingram (horizontal-loop electromagnetic survey, 18 kHz) measurements, from the area corresponding to the first 1 000 m in fig. 4. On this map the influence of the seawater can be seen to generally reach between 100 and 150 m inland except in certain north-south and northwest-southeast trending zones, probably related to minor fracture zones. The penetration depth of the Slingram instrument is in this case about 80 m.

Measurements with the Beam Slingram instrument recorded an influence of the seawater between 25 and 50 m from the shore. The penetration depth of this instrument is usually about 6 m (perhaps in some cases about 10 m).

Using these data the slope of the interface between saline and fresh groundwater can be roughly calculated to be something like that shown in fig. 6. However, the interface can be expected to be rather irregular due to the nature of the different fractures in this kind of aquifer.

6. POLLUTION OF GROUNDWATER FROM A STORAGE OF SALT

At Rasbo, about 70 km north of Stockholm, salt (NaCl and $CaCl_2$) used for deicing and dust prevention on roads has been stored for a few decades. The geological setting is shown in fig. 7 a and b.

Concerning the pollution of the wells, the two dug wells had a very high content of cloride (between 1 800 and 1 900 mg/l Cl^-) for some time before they were abandoned. Today only the drilled wells are being used. As a consequence of this, the most northern of the dug wells no longer yields saline groundwater but is now in an area of fresh-groundwater flow towards the drilled wells. The salinity of this well is now 96 mg/l Cl^-, while the salinity of the southernmost dug well is still 1 800 mg/l Cl^- and still in an area of polluted-groundwater flow. The drilled wells are somewhat polluted, but the main part of the groundwater probably derives from deeper and larger fractures conducting fresh groundwater (see fig. 7 a).

The VLF-resistivity readings are shown in fig. 7 b. Resistivity values lower than 4 000 ohm m can in this case be considered to be influenced by salt pollution. It can be seen that the polluted area is something like 200 by 300 m (although the distribution of polluted groundwater below the southern clay area is uncertain. The phase angle readings are not very helpful in this case since this is a multi-layer case down to penetration depths, ranging from 45 to ca. 200 m within the polluted area.

In fig. 7 c the Beam Slingram resistivity readings are shown. Since the penetration depth of the Beam Slingram is of the same order as the thickness of the till and the clay, and, this overburden being more polluted than the bedrock, the readings of the Beam Slingram measurements can be expected to be more accurate for outlining the borders of the salt pollution. Resistivities lower than 800 ohm m measured with this instrument in the till area can be considered to be influenced by salt pollution. Comparing fig. 7 b and c one can see that the polluted area shown by the Beam Slingram measurements is somewhat larger than that shown by VLF-resistivity measurements.

7. CONCLUSIONS

This study has shown that when the VLF-resistivity technique is used it is necessary to have some knowledge of the geology including groundwater conditions in the measured area down to penetration depth, in order to make correct interpretations of the readings. Supporting information can be rather easily gained by other electromagnetic measurements in the same frequency interval (10 - 20 kHz). The obtained depth and resistivity values are often not completely exact due to the geological conditions not being as uniform and simple as one often tends to think they are. But mostly they are good enough for approximate estimations.

The VLF-resistivity measurements are more useful in pure one- or two-layer cases, but important information on the apparent resistivity in multi-layer cases can often be obtained.

REFERENCES

Allmänna Ingenjörsbyrån AB (AIB) (1974). Report (in Swedish) on groundwater prospecting for the municipality of Enköping. Not published.

DE GEER, J. (1981). Personal communication on the Östervåla case.

ERIKSSON, L. (1974). Elektriska och magnetiska metoder för påvisande av svaghetszoner i berg. Stiftelsen bergteknisk forskning. Bergmekanikdag.

MÜLLERN, C.-F. (1979). Grundvattenprospektering med radiovågor - VLF - och Rama-mätningar. Vannet i Norden 1; also in SGU Rapporter och meddelanden 14.

MÜLLERN, C.-F. & ERIKSSON, L. (1979). VLF-mätningar för prospektering efter grundvatten i berg. STU-rapport 78-3694.

MÜLLERN, C.-F. (1980). Airborne geophysical measurements used for hydrogeological mapping. 6th Nordic Hydrologic Conference.

FIGURES

Fig. 1: Geographical positions of the sites where VLF-resistivity measurements of this study were carried out.

Fig. 2: VLF-resistivity measurements were carried out in order to determine the depth to the interface between fresh and saline groundwater on an island constituting a part of the Enköping esker in lake Mälaren.

Fig. 3: Two wells supplying drinking water to the municipality of Östervåla. One well with low salinity, another with high. The resistivity of the granite aquifer was in the first case normally found to be high, in the second case definitely lower than normal.

Fig. 4: A VLF-resistivity profile was measured from the shore of the Bothnian Sea to 20 km inland. Both resistivity and phase angle readings incicate saline groundwater a few hundred metres inland.

Fig. 5: Slingram measurements have earlier been carried out in this area, corresponding to the first 1 000 m in fig. 4. These measurements recorded saline groundwater generally 100 - 150 m inland except in certain north-south and northwest-southest trending zones, probably related to fractures.

Fig. 6: A rough estimate of the slope of the fresh-water/saline-water interface, interpreted from VLF-resistivity, Slingram and Beam Slingram readings.

Fig. 7 a: Section showing the geology and position of wells at a storage of salt at Rasbo. The salt has polluted the groundwater.

Fig. 7 b: VLF-resistivity and phase angle readings at the storage of salt at Rasbo.

Fig. 7 c: Beam Slingram readings at the storage of salt at Rasbo.

Figure 1

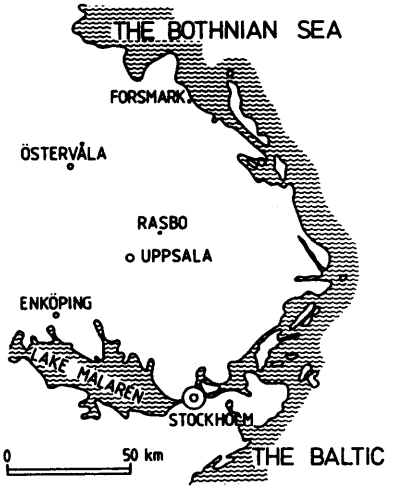

Figure 2

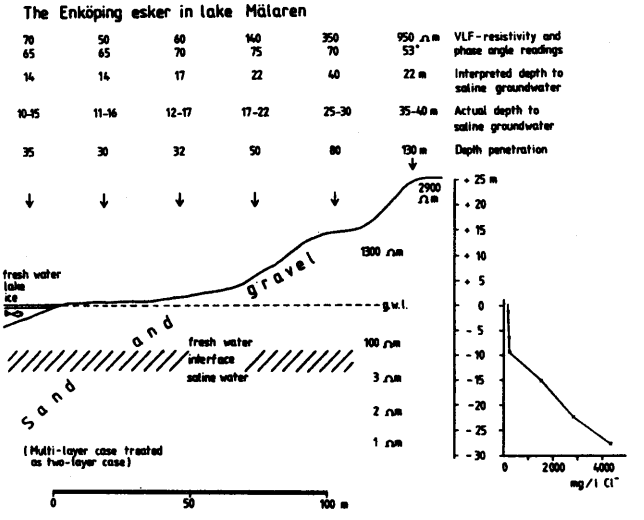

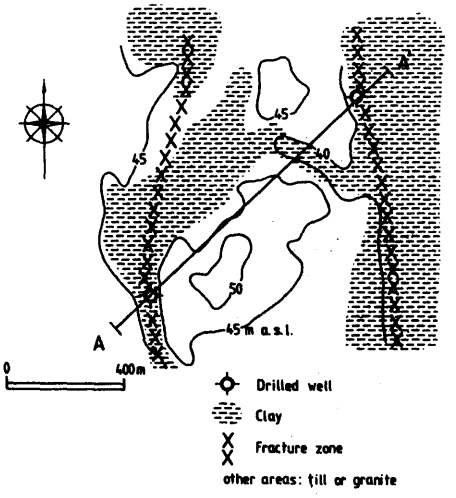
45
45
40
50
A
A
45 m a.s.l.
0
400m
Drilled well
Clay
Fracture zone
other areas: till or granite

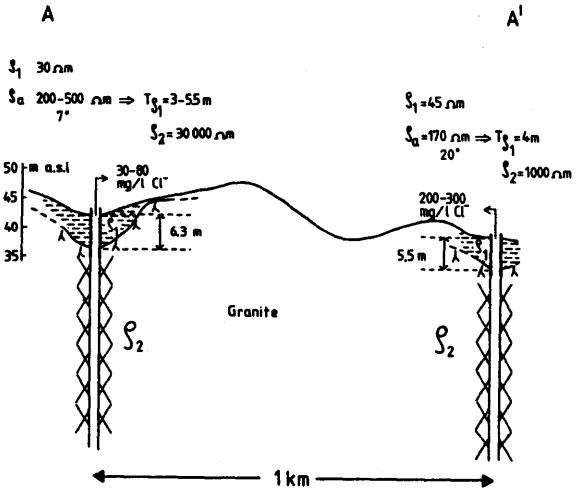
A
A'
ρ1 30 Ωm
ρa 200-500 Ωm ⇒ Tρ1=3-5.5m
7°
ρ2= 30 000 Ωm
ρ1=45 Ωm
ρa=170 Ωm ⇒ Tρ1=4m
20°
ρ2=1000 Ωm
50 m a.s.l
45
40
35
30-80 mg/l Cl⁻
6.3 m
200-300 mg/l Cl⁻
5.5 m
Granite
ρ2
ρ2
1 km

Figure 3

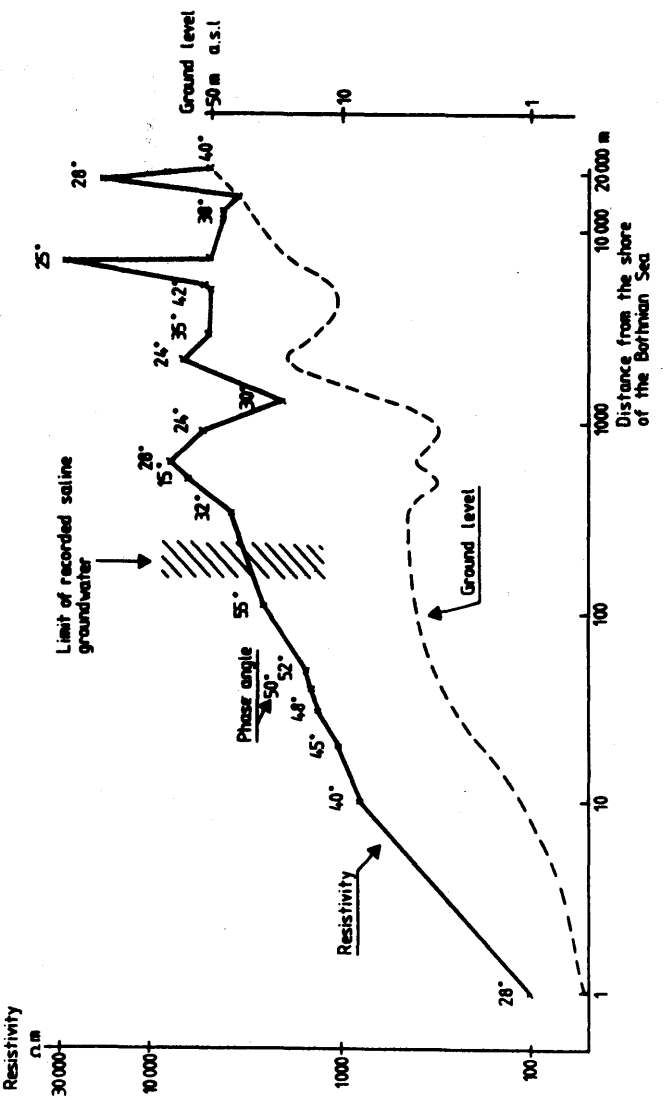
Resistivity
Ω.m
30 000
10 000
1000
100
Limit of recorded saline groundwater
Phase angle
Resistivity
Ground level
Ground level
50 m a.s.l
10
1
1
10
100
1000
10 000
20 000 m
Distance from the shore of the Bothnian Sea

Figure 4

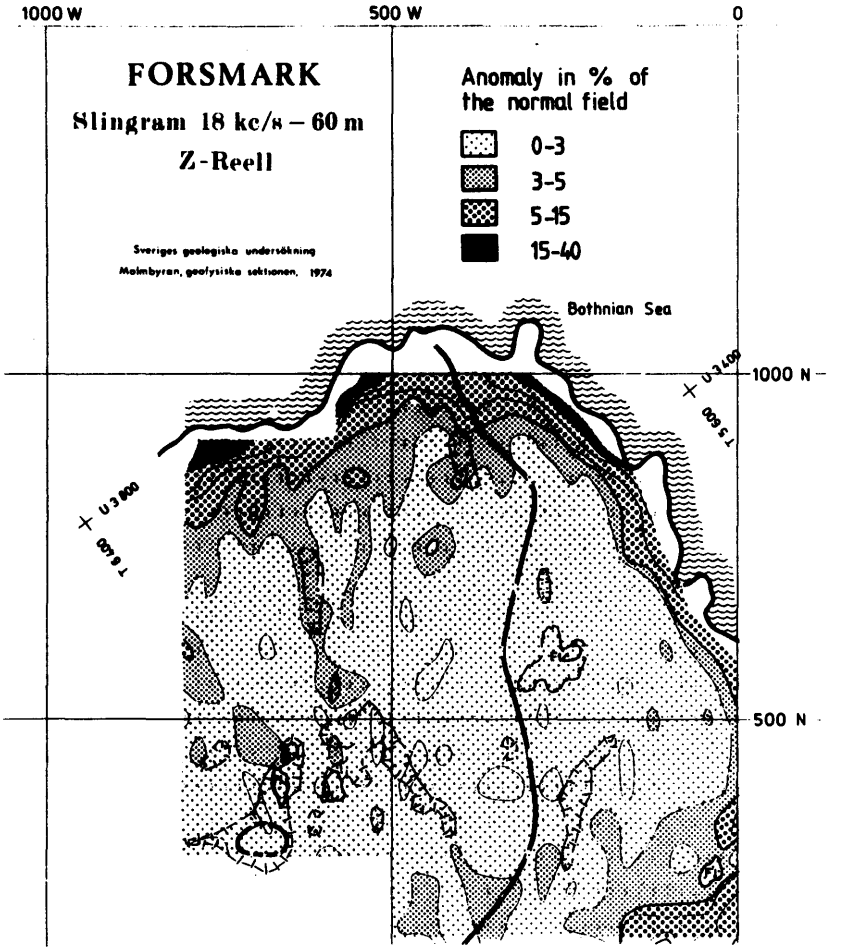
1000 W
500 W
0
FORSMARK
Slingram 18 kc/s – 60 m
Z-Reell
Sveriges geologiska undersökning
Malmbyran, geofysiska sektionen, 1974
Anomaly in % of the normal field
0-3
3-5
5-15
15-40
Bothnian Sea
1000 N
500 N
U 3 400
T 5 600
U 3 800
T 6 600

Figure 5

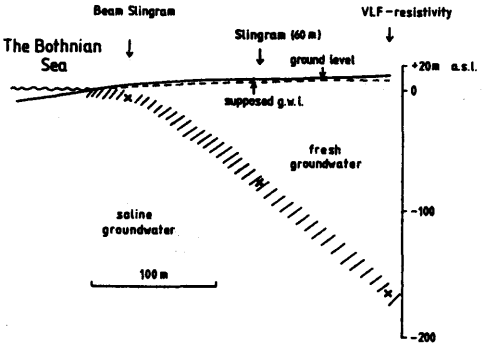

Figure 6

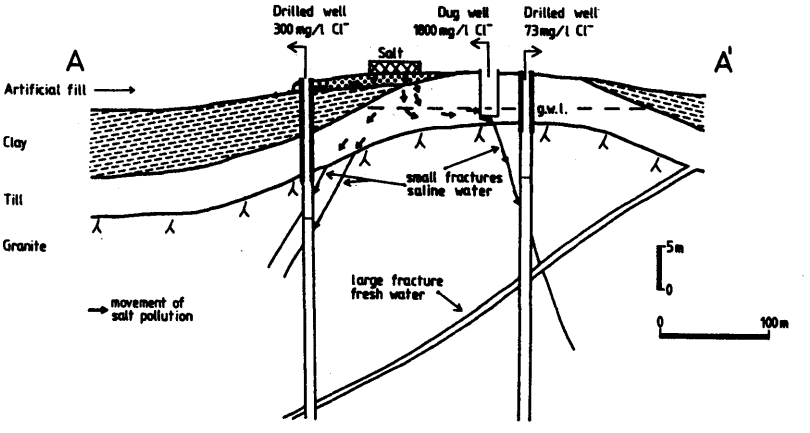

Figure 7a

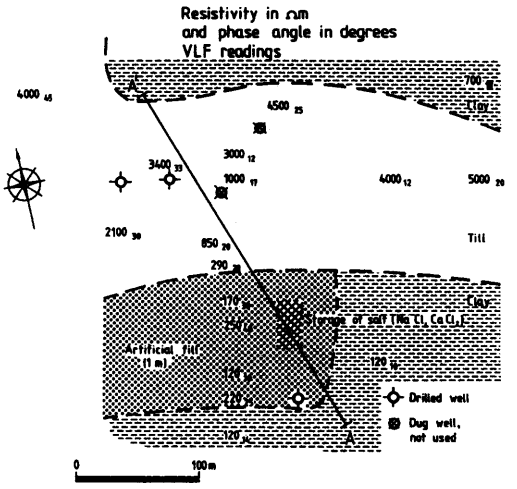

Figure 7 b

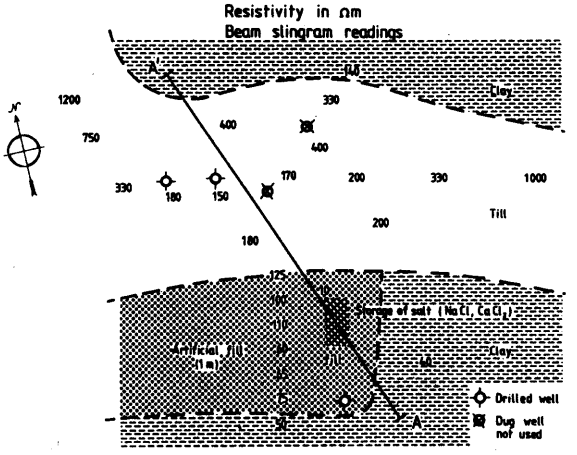

Figure 7 c

4.2. ARTIFICIAL REMOVAL OF INTRUDED SALINE WATER IN A DEEP AQUIFER

R.A. SCHUURMANS & C. VAN DEN AKKER

ABSTRACT

For the water supply of Amsterdam groundwater is extracted from the dune area near the North Sea, since 1903 also from a deep aquifer. Severe salt-water intrusion has occurred.

After 1957 the situation stabilized because the infiltration of river water at the surface of the area strongly diminished the deep extraction. The remaining fresh-water pocket is considered as a storage that can be used to improve or to replace the river water during pollution periods.

Because of the increasing production of drinking water and the worsening of the situation around the river Rhine (quality and accidents) the storage in the dune water catchment area should be enlarged. As no works are allowed at the surface, the deep aquifers with salt water are investigated in order to create a storage of fresh water by means of deep-well infiltration.

1. INTRODUCTION

Amsterdam Waterworks is charged with the drinking water supply for more than 1.000.000 people. The production now amounts to about 90.10^6 m^3/yr. The company has three sources:

a) East of the town:
   1. Lake Waterworks: Capacity 30.10^6 m^3/yr
   2. Hilversum Pumping-Station: Capacity 2.10^6 m^3/yr

b) West of the town:
   3. Dune Waterworks: Capacity 83.10^6 m^3/yr

The total installed capacity (115.10^6 m^3/yr) appears to be large in comparison with the demand. Even when one adds a certain percentage to the demand for safety reasons (in Holland 10 - 20 %) there is still about 10.10^6 m^3/yr extra-capacity available.

But there are reasons why the situation is worse than it seems. The dune water-works get the raw material for the production of drinking-water from:

1. effective rainfall, average 13.10^6 m^3/yr,
2. river water from the Rhine.

The river water is infiltrated in the dune area by shallow canals and collected by drains and by deep canals around the infiltration area. The system was started in 1957 and is still very effective. One of the properties of the system is that an increasing demand on the capacity of the infiltration works asks for lower levels in the deep canals around the area. This measure affects the storage in the first aquifer with phreatic water and the proportion of storage and real production decreased during the years 1957 - 1980. In fact the period of full

production, when the intake of river water has to be stopped, was reduced from about 60 days to 30 days.

In the meantime the condition of the river Rhine grew worse. In general the quality became bad and the number of shipping-disasters, in which dangerous and poisonous loads are involved, increased. Therefore the chance that the intake of river water should be stopped increased as well. However, there is little insight as to how long such a calamity could continue and the period of 30 days is considered possible.

The storage in the dune water catchment area now limits the capacity to 70.10^6 m^3/yr, while the production plant has a capacity of 83.10^6 m^3/yr.

Measures have to be taken to change this situation. The problems of the river Rhine could not so far be solved and another source is not available. This makes it necessary to enlarge the storage in the dune area. The phreatic first aquifer is not available for this anymore. Nowadays the area has the big interest of nature conservation and it is impossible to make new infiltration and storage works. Attention is thus turned to the deep aquifers.

2. GEOHYDROLOGICAL SITUATION

The deep aquifers are situated between 20 and 160 m below O.D. (= Mean Sea Level) and are separated from the first aquifer by a clay layer, which has an average hydraulic resistance of 12 years or 4400 days. At 160 m depth layers of fine sand with silt and clay layers start.

The deep aquifer itself can be divided into three important layers: two aquifers separated by a semi-pervious layer from about 60 until 90 m below O.D. This layer has a resistance varying from 500 days in the north-east to 5 days in the south of the area.

The second aquifer extends from 20 to 60 m below O.D. It consists of rather coarse sand with a total transmissivity of 1000 m^2/d. The third aquifer, from 90 until 160 m, has layers of very coarse sand. The transmissivity is about 3000 m^2/d. Most of the aquifer always contained salt water; the fresh-water pocket originally had a maximum depth of about 110 m on the east side of the area. On the west side the depth was 70 m. The thickness of the brackish zone varied from 20 m (east side) to 10 m (west side).

The second aquifer was originally filled with fresh water. In this layer pumping by deep wells started in 1903. The pumping increased until 1957 to an amount of 20.10^6 m^3/yr. The leakage from the first aquifer is about 7.10^6 m^3/yr. This led to intrusion and upconing of brackish water followed by an alarming situation during and after the second world war. This was stopped by the artificial infiltration of river water in 1957.

Since then the fresh water in the second aquifer has been reserved, for quality reasons, for periods when the river water intake has to be stopped. It is considered as a deep safe storage. To use this storage 290 deep wells are now available with a total capacity of 3000 m^3/h. Reconstruction of the well-system is going on in order to restore the original and allowed capacity of 4000 m^3/h. This is about 40 % of the required capacity for the catchment area.

The use of this capacity in time of calamities on the river Rhine is limited, in the first place, from the point of view of the water balance. In about 60 days the total input per year of the second aquifer by leakage would be abstracted. Secondly, there would be an immense salt-water intrusion, especially by upconing from the third aquifer.

Something therefore has to be done about this upconing of salt water. The solution may be to create a new fresh-water pocket below the semi-pervious layer between the second and third aquifer. The artificial storage of fresh water in the salty third aquifer requires the technical science of deep-well infiltration. If knowledge and experience prove the validity of the operational system, extraction of the existing 4000 m^1/h can perhaps be increased. In that case, the safety of the water supply of Amsterdam is ensured.

3. DEEP-WELL INFILTRATION

The technique of deep-well infiltration has been used for many years in the Netherlands. Operational systems exist for discharge of waste water, for cooling and for temporary drainage by deep wells. To keep the wells in operation for a long time special precautionary measures are required. If the wells get clogged they are cleaned in a mechanical or chemical way. After some time the well may often have to be abandoned because the clogging cannot be removed from the surrounding material.

Drinking-water supply makes special demands on deep-well infiltration. The amount of water is generally rather high and the system must be in operation for a long time. The infiltration water has to be conditioned in a rather simple way and preferably without chemical measures. If there is some clogging of the wells there must be a good method for cleaning. This method should also not be chemical but mechanical or hydraulic. Besides, the system has to be feasible from an economic point of view. In the Netherlands some research has been done on the economic feasibility of injection wells.

The mentioned technical construction of the well and the conditioning of the infiltration water have been tested previously by Amsterdam Waterworks in a special well that was situated in the second aquifer to the east of the area. The water available for infiltration is river water. This water is pretreated at the intake station by coagulation, sedimentation and rapid sand filtration. The experimental well was clogged by the river water because sometimes the water had

not the right properties. An important property is represented by the MFI (Modified Fouling Index), a test of the water by membrane-passage. A low index, e.g. drinking-water with number 1, works excellently; the pretreated river water with sometimes 6 to 12 clogged the well. The important conclusion from the test well was that the river water needed a better treatment.

During this period of tests the spreading of the infiltrated water was observed intensively. The difference in quality parameters for the river water and the groundwater showed the shape of the recharged waterbody with rather sharp interfaces. A fairly good agreement was obtained between a numerical calculation with a finite element technique and the observations from the test. In this case both liquids had the same density.

4. SALT-WATER REMOVAL

After the preliminary experiments a new deep well for infiltration was designed. The objective in this case was to infiltrate fresh water with low density into the third aquifer, containing salt water with a high density. This well must confirm that the system also works in the new circumstances, being the deep aquifer near the sea. An extra-treatment of the river water should improve the infiltration condition of the river water. Most of all, however, the proof was wanted that the fresh water would stay in a lens with rather sharp interfaces and without too much mixing with the salt water. Water supply has no use for brackish water.

The pretreatment of the river water was extended with a type of slow sand filtration. This was achieved by drains at a depth of 0,5 m below the bottom of existing infiltration canals. The value of MFI up to now was decreased to below 3.

The construction of the well did not change much. The head of water in the third aquifer was about 5 m below ground level and the level of the infiltration canal was sufficient to achieve a flow of about 20 m^3/h. The diameter of the screen is 230 mm, the depth of the screen is from 101 m to 116 m below O.D.

In the surroundings of the injection well three observation wells were sited at distances of 5 m, 15 m and 40 m. In the wells many small screens were placed at different levels; geohm cables were installed for measuring the electrical resistance at many points. A processor registers several parameters. These can be telemetered to the office over a distance of 4 km. Here a second processor takes over the data for handling, printing and plotting.

The test started on January 26, 1981, and measured data until about August 14 are presented here. Over a period of about 200 days a volume of nearly 100.000 m^3 river water has been recharged to the deep aquifer.

The objectives of the injection well test can be summarized as follows:

- to investigate the possibility of infiltrating pretreated river water in the deep aquifer of the dune water catchment area;
- to investigate the salt-/fresh-water interaction in the deep aquifers, where problems such as hydrodynamic dispersion, unsteady recharge by the injection well, inhomogeneous and anisotropic soils and the extraction of the infiltrated water play an important role;
- to investigate the possibility of monitoring and controlling the storage in the deep aquifer by means of observation wells with filters and geohm cables. Here also the automatic processing of data with the help of a computer is essential;
- to find out the basic design rules for a recharge/recovery system.

5. THE RESULTS OF THE TEST

At this moment (September 1981) the injection well is almost 8 months into operation. Of course this period is too short to deal adequately with the questions and problems as stated in the previous chapter. However, with the data and the experience already obtained, some interesting results can be presented. Furthermore it is important for the investigations to hear the opinion of specialists on salt-/fresh-water problems with respect to such tests as described here. One should keep in mind that tests like these take several years in order to obtain the maximum information on the groundwater movement and salt-/fresh-water interaction.
Therefore a discussion with colleagues and suggestions would be a great help in obtaining the maximum results from tests like these.

However, the tests with the well will continue; already it can be established that the main objective of the pilot plant has been achieved, namely the proof that in the local aquifer, filled with salt water, storage of fresh water can be created.

From the different measurements it is easy to infer the shape of the fresh-water body at a certain point in time. Moreover the plot of the measurements makes clear that the extension of the fresh-water body has the following characteristics:

a) there is a brackish zone at the bottom of the fresh-water body with an order of magnitude thickness of 5 m;

b) the quick extension of the fresh-water body in the most coarse layer of the aquifer does not cause a very large amount of brackish water, in spite of the high velocity;

c) on the top of the fresh-water body the present salt and brackish water is displaced slowly.

6. THE BRACKISH ZONE

Until now it is calculated that about 50 % of the infiltrated fresh water is present in the fresh-water body, if this body has a regular circular shape. This will be monitored by new observation wells in several directions at a distance of about 100 m from the infiltration well.

This rather high loss of fresh water is largely because the screen of the infiltration well is about 15 m below the semi-pervious layer. This depth is chosen because between the mentioned layer and the screen there is brackish water. Moreover, the very coarse layer in the aquifer between depths of 95 m and 125 m should be used to observe the phenomenon under conditions of high velocity. The present well is therefore not representative for a pilot plant investigating a system with operational characteristics.

Within the period of 200 days the thickness of the brackish zone is relatively small in comparison with the natural situation in the aquifer. The brackish zone below the dune water catchment area was originally 10 to 20 m thick, but is now only about 5 m. Very near to the injection well the thickness is even less.

It is not known if the several small silt or clay layers in the aquifer have a large influence on the amount of brackish water. These layers will cause dispersion. The inhomogeneous properties of the aquifer, as a result of the sedimentology, should be studied in a more fundamental way. Tests at laboratory-scale should be carried out to evaluate the influence of sedimentary properties on dispersion.

7. CONCLUSIONS

During the first 200 days of the test with the injection well it was been shown that:

a) the quality of the available river water can be improved by a simple drainage method with a long effective life;

b) the construction of the well is satisfactory;

c) storage of fresh water can be achieved in a saline aquifer. It seems that dispersion stays within predictable limits.

8. FUTURE AIMS

The well will be in use for many years. During at least 1 year there will be observations of the increasing body of fresh and brackish water. These observations will mainly concern the periphery of the body, the bottom and also the top. In the long term it is expected that the brackish water on the top of the fresh-water body will be displaced beneath the semi-pervious layer. The infiltration capacity may have to be increased from 20 to 30 m^3/h.

If the brackish water is removed, a second phase can start. A pumping well will be installed with a screen at a short distance above the semi-pervious layer. The influence of the extraction by this well on the fresh-water body can be studied. A combination of abstraction and infiltration is also possible. In this phase of the investigations it must be made clear if the losses of fresh water can be kept within acceptable limits. If so, the next step might be to install a new deep well, specially designed to investigate the possibilities of deep storage for operational purposes; or , the capacity-increasing effect and the influence on quality resulting from the choice of travel and residence time distributions in the system.

It is clear that in this case the pumping cannot be from the same well. Extraction from this well, situated so near the brackish and salt water, would immediately cause upconing of salt water. A dual-purpose well would be inappropriate.

Instead, extraction by many small wells in the second aquifer above the semi-pervious layer would make it possible to utilize the leakage from storage in the third aquifer.

REFERENCES

BRIEMEN, W.A. van (1978). De verbreiding van met een persput geinjekteerd water in een gelaagd watervoerend pakket met semi-spanningswater. T.H. Delft: Afdeling Civiele Techniek.

STEINMETZ, J.J. (1978). Technische Opbouw van de Persput te Leiduin. Mededeling KIWA 56.

STUYFZAND, P.J. (1977). Hydrochemical aspects of drinking water injection by a deep well in a semi-confined aquifer at Leiduin pumpingstation near Zandvoort, North-Holland.

FIGURES

Fig. 1: The aquifer system, the salt-water intrusion and the situation of the infiltration well.

Fig. 2: Examples of measuring the electrical resistance in two points of the Geohm cable. In this case the cable is situated 5 metres from the infiltration well.
In about 10 hours the front passes the point and the surrounding water turns from salt into fresh.

Fig. 3: The spreading of the infiltrated fresh water with time. Fresh-, brackish- and salt-water zones are measured by Geohm cables, water samples from filters and by temperature-logging in the wells.

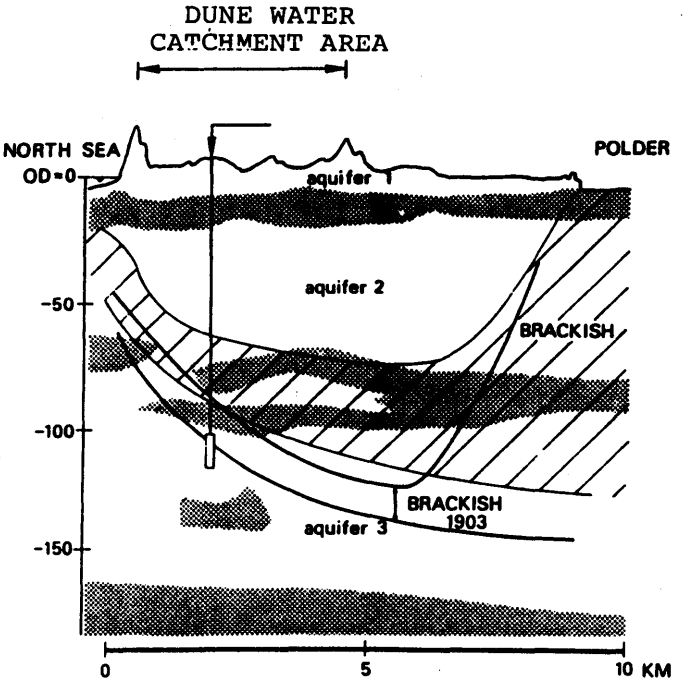

Figure 1

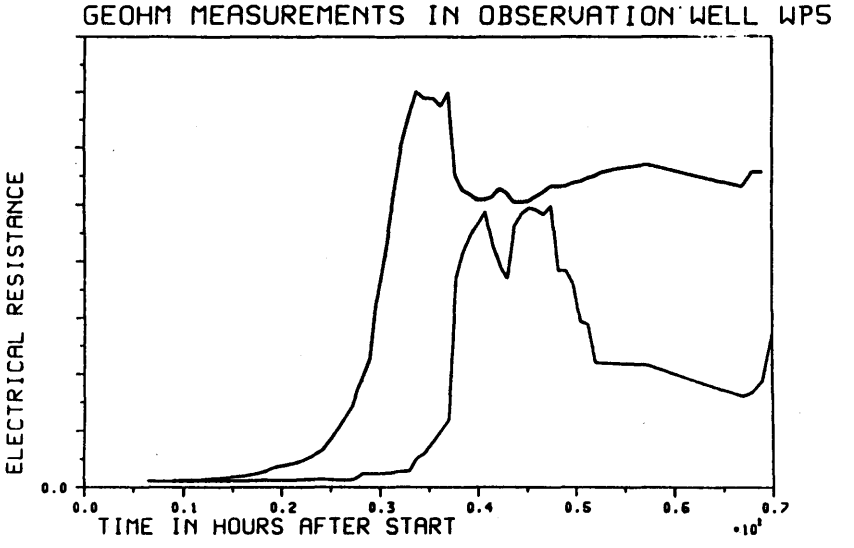

Figure 2

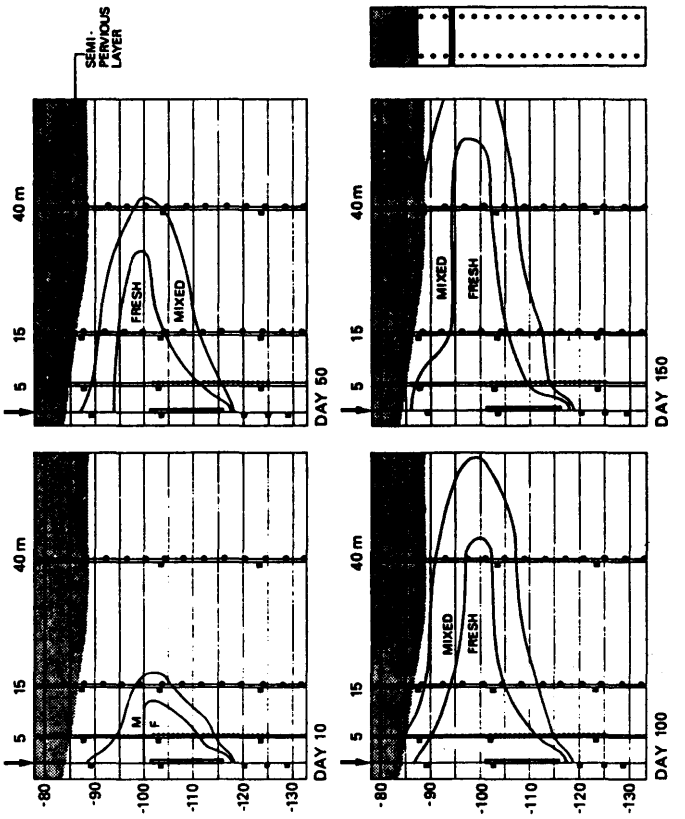
SEMI-PERVIOUS LAYER
40 m
15
5
FRESH
MIXED
DAY 50
M
F
DAY 10
MIXED
FRESH
DAY 150
MIXED
FRESH
DAY 100
-80
-90
-100
-110
-120
-130

Figure 3

THEME 5

HYDROCHEMICAL AND SOIL-PHYSICAL INVESTIGATIONS

5

HYDROCHEMICAL AND SOIL-PHYSICAL INVESTIGATIONS

5.0. INTRODUCTION

V. COTECCHIA

Today the extensive usage of chemical and isotopic methods in hydrogeology is taken for granted.

But just looking through the stages in the progress of the Salt-Water Intrusion Meetings we can realize that only recently have these methods of investigation become important.

From being only a complementary source of information on the quality, age and provenance of fresh, salt and mixed waters, chemical and isotopic methods have today acquired a fundamental role. They are now essential in the study of a wide range of problems, including hydrogeological research of coastal areas. In reality, in a particular environment, the presence of both fresh and salt water of different origin and age, interacting with aquifers often overexploited, and having different geological characteristics, creates complex conditions not easily interpretable without the help of these methods.

Several different statements can be made on the present state and future developments in the field of hydrochemical and isotopic studies, particularly in research on sea-water intrusion.

On the one hand isotope methods can be viewed as well established. The attainable targets are clear and the method of application well outlined.

Rightly research continues in several directions: testing new fields of application within hydrogeological studies of coastal areas for the great number of available enrivonmental isotopes, especially where remarkable water-soil interactions are present: tracing back the original characteristics of the recharge, starting from groundwaters having an isotope content profoundly changed by salt contamination and by their entire hydrogeological history; identifying salt-contamination processes different from sea-water intrusion; recognizing the involvement of salt waters of progressively deeper origin in the contamination of groundwater resources as a result of overexploitation.

On the other hand hydrochemical methods show ever increasing potential. As the technology advancement leads to faster and more reliable determination, the application horizons become larger and larger.

For instance, in addition to accomplishing its main role, hydrochemistry is today being used to solve problems which have previously been studied exclusively with the help of environmental isotopes.

In some cases the results obtained during the hydrochemical study of sea-water intrusion have interesting implications for other important areas of applied geology. Not only do they allow the interpretation of the history and evolution of waters, but also of the rocks in which these circulate. It may be redundant to underline the importance of all this when we think for example of soils whose present geomechanical characteristics are linked to their geological and hydrogeological history.

Just this is enough for encouraging research aimed at a better understanding of the complex phenomena of water-soil interaction.

In the history of SWIM one can trace signs of the continuous progress in hydrochemistry; this is proof that this science will play an even more important role in the future studies of sea water intrusion.

5.1. ASPECTS OF GROUNDWATER SALINIZATION IN THE WITTMUND (EAST FRIESLAND) COASTAL AREA

J. HAHN

ABSTRACT

The dynamics of sea-water intrusion phenomena has been investigated in the East Frisian coastal aquifers near Wittmund by taking water samples at depths of between 5 and 300 m, i.e. above and below the fresh-water/saline-water interface. Full analyses were carried out and oxygen and sulphur isotope ratios and ^{14}C were also determined. Interpretation of these analyses and geothermal measurements carried out in the wells showed that within the area affected by sea-water intrusion at least three different saline water bodies can be distinguished which intruded at different times. Apparently a correlation exists between the age relations within the salinization front and the large-scale climatic history of the last 7000 years.

The salinization of near-shore inland aquifers by infiltrating sea-water represents a worldwide phenomenon of considerable practical consequence. It is the result of a disturbance of the equilibrium between inland fresh groundwater and heavy sea-water due to fluctuations of the sea level and/or the groundwater level.

To acquire more detailed knowledge on the occurrence and dynamics of this type of "salinization of the groundwater of coastal areas", special boreholes were drilled to depths of between 5 and 300 m in the coastal region near Wittmund both seaward and landward of the saline-/fresh-water interface (fig. 1 and 2); 46 groundwater samples were taken. The mineral composition was analyzed (figs. 4 to 8) and the oxygen and sulphur isotope ratios (figs. 11 and 12) as well as the radiocarbon concentration were determined. Additionally, the dynamics of the salinization processes (fig. 15) was studied using geothermal measurements and special calculation methods.

The location of the interface between fresh groundwater and infiltrated sea-water, as determined by geoelectrical methods, in general follows the contour lines of the outcrops of sandy geest sediments. It depends on the distribution and thickness of nearly impermeable sediments in salt marsh and sandy geest areas (fig. 2, 3).

A hydrochemical section through the saline-/fresh-water interface shows that in the study area the groundwater is salinized by infiltrated sea-water as far as 16 km landward from the present coastline and down to a depth of 250 m in unconsolidated sediments of both high and low permeability (fig. 13).

Beyond this depth, the groundwater is increasingly salinized by highly mineralized deep-seated groundwater which is relatively rich in lithium. In the transition zone to fresh water, sodium bicarbonate water sometimes occurs (fig. 4, 10).

The interface between fresh water and infiltrated sea-water is not a gently dipping plane, but is made up of a number of interlocking strata filled with fresh water and saline water such that highly saline water may be underlain by fresh water (fig. 13). The main reason for this is that the salinization of the groundwater in the coastal area of Wittmund is not due to uniform infiltration of sea-water with respect to time but that the infiltrated sea-water consists of water of differing compositions that infiltrated at different times (fig. 16), as demonstrated also by ^{14}C dating.

Of prime importance for the fluctuations in the chemical composition of the infiltrated waters were the type and sequence of events with respect to the individual cases of infiltration, which were influenced by time-dependent factors, e.g. climate, vegetation, rate of infiltration, length of the path of migration, and type of the sediment through which the water flowed.

On closer examination of an individual infiltration event, it becomes evident that in spite of certain common chemical properties of the water that intruded at different times, the chemical composition varies considerably. In addition to differences in the concentrations of landward and seaward zones due to the mixing of water of differing compositions, the differences in the chemical composition of water from the margins and those of the center of the infiltration body (fig. 10) are primarily caused by differences in the extent of cation exchange in the sediment.

On the basis of hydrochemical and ^{14}C studies, a minimum of three saline water bodies can be delineated within the zone salinized by infiltrated sea-water. These zones are characterized by differences in chemical composition and must have been infiltrated at different times.

The initial reason for the salinization of the groundwater in the Wittmund coastal region was a groundwater-pressure gradient towards the inland area caused by a general rise in the sealevel due to climatic eustatic changes.

In the course of this development the North Sea reached the present East Frisian coast during the early to middle Atlantic period. Frequent inundations led to the levelling of a coastal region of varying width and to the deposition of marine mud (formation of salt marshes). The extent of groundwater salinization in these coastal regions which occurred as a consequence of these processes was much the same during the middle Atlantic period as today. Since then, freshening took place only very gradually because the original hydrodynamic conditions changed markedly due to the deposition of almost impermeable mud layers and to a lowering of the groundwater gradient.

Fig. 16 shows the history of the salinization of the groundwater in the coastal area around Wittmund. The oldest water infiltrated during the middle Atlantic period and is now found only as relics in deep, almost impermeable zones or zones near the sea.

Although the comparatively thin mud layers of the initial inundation maxima impeded the infiltration of precipitation and thus lowered the pressure of the fresh groundwater flowing towards the sea, they did not impede the subsequent gradual freshening of parts of the saline-water-filled zones. This process must probably be regarded in connection with the humid climate (increased precipitation) during the Atlantic period. Only in the course of further inundations, which reached their peak during the Subboreal, did the mud layers increase so much in extent and thickness that groundwater recharge in the catchment area markedly decreased and newly infiltrating sea-water could no longer be replaced or freshened. It must be assumed that the extent of the Subboreal salinization of the groundwater in coastal areas was significantly influenced by the lower rate of precipitation and groundwater recharge during the comparatively dry Subboreal. Only during the rainy, early Subatlantic period did freshening apparently take place again. Due to the low difference in pressure, however, only the permeable near-surface layers were affected.

During the last salinization phase, another groundwater body was formed. This was probably due to the formation of Harle Bay, which took place during the 12th Century and which caused serious alterations in terms of the equilibrium between fresh inland groundwater and sea-water and which resulted in the rapid infiltration of recent sea-water into the near-surface aquifers. While the area was gradually diked the permeable near-surface aquifers were again freshened, a process which has probably not yet been concluded.

FIGURES

Fig. 1: Salinization of groundwater in East Frisia

Fig. 2: Salinization of groundwater in the Wittmund study area

Fig. 3: Salinization of groundwater in the Wittmund area

Fig. 4: Anion-cation-diagram - well I

Fig. 5: Anion-cation-diagram - well II

Fig. 6: Anion-cation-diagram - well III

Fig. 7: Anion-cation-diagram - well IV

Fig. 8: Anion-cation-diagram - well V

Fig. 9: Saline water differentiated by lithium and chloride content

Fig. 10: Effects of ion exchange on the Ca and Mg concentration in infiltrated sea-water from the Wittmund area (wells II, III, IV, VI)

Fig. 11: Sulphur isotope analyses of groundwater from the Wittmund area

Fig. 12: Salinization of groundwater in the Wittmund area

Fig. 13: Salinization of groundwater in the Wittmund area

Fig. 14: Borehole logging in the Wittmund area (East Frisia)

Fig. 15: Salinization of groundwater in the Wittmund area

Fig. 16: Probable phases of salinization of groundwater in the Wittmund coastal area .

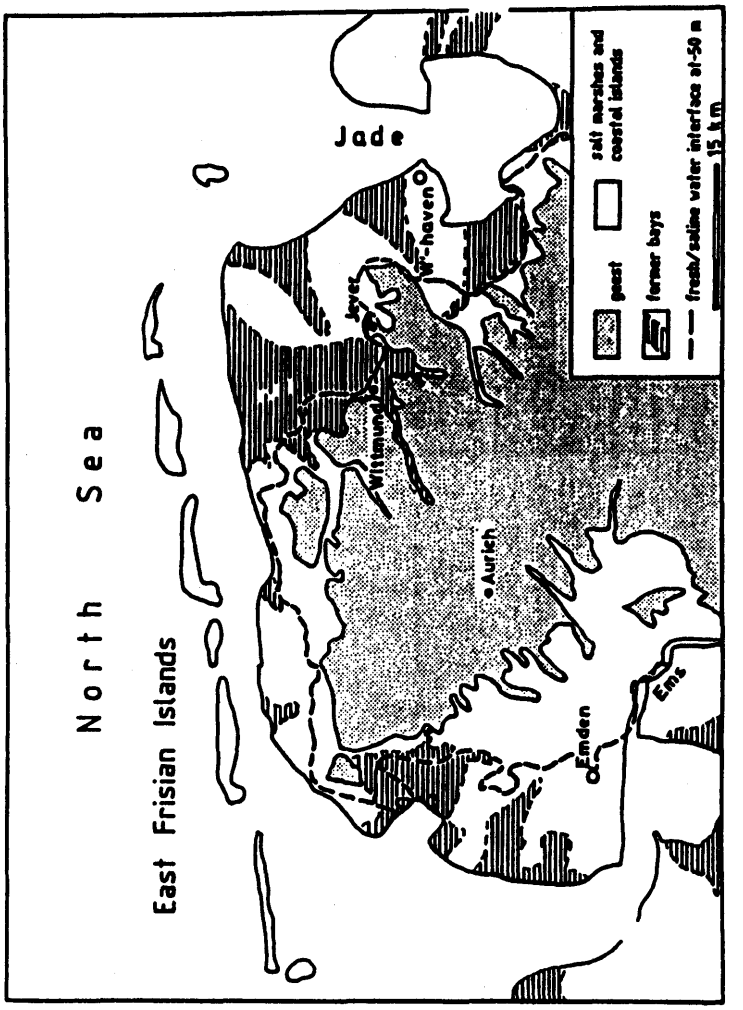

Fig. 1 Salinization of the groundwater in East Frisia

Figure 1

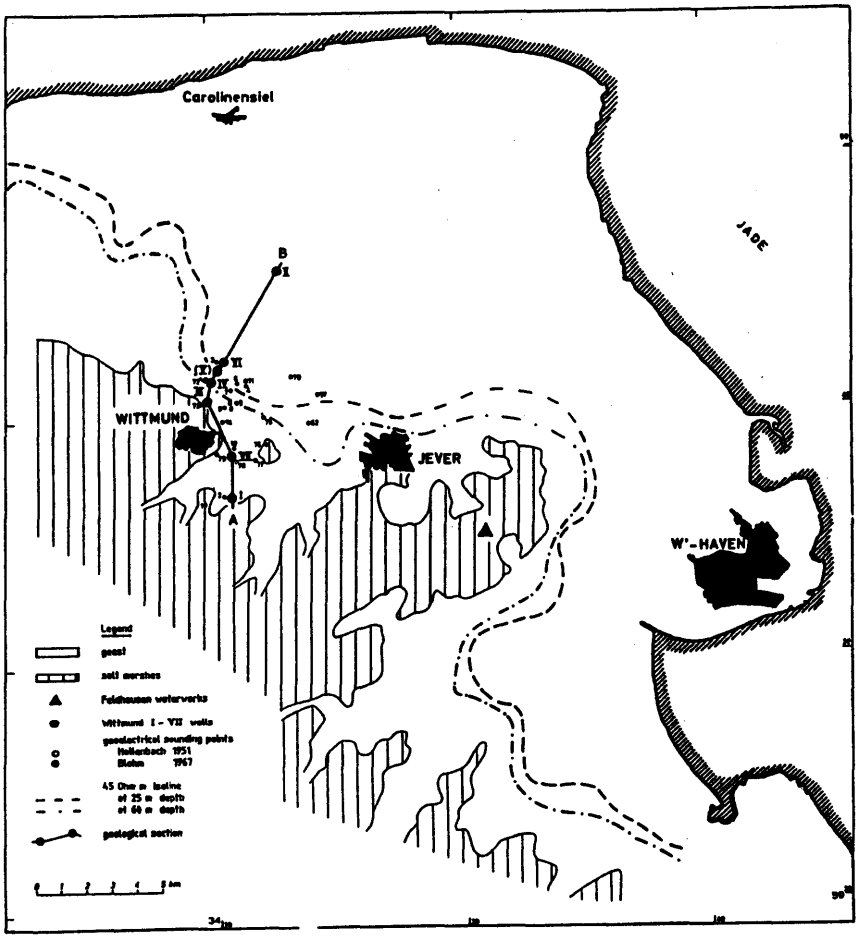

Salinization of the Groundwater in the Wittmund area
Location of the study area

Figure 2

Figure 3

Salinization of the Groundwater in the Wittmund area

Geoelectrical survey by E. Blohm

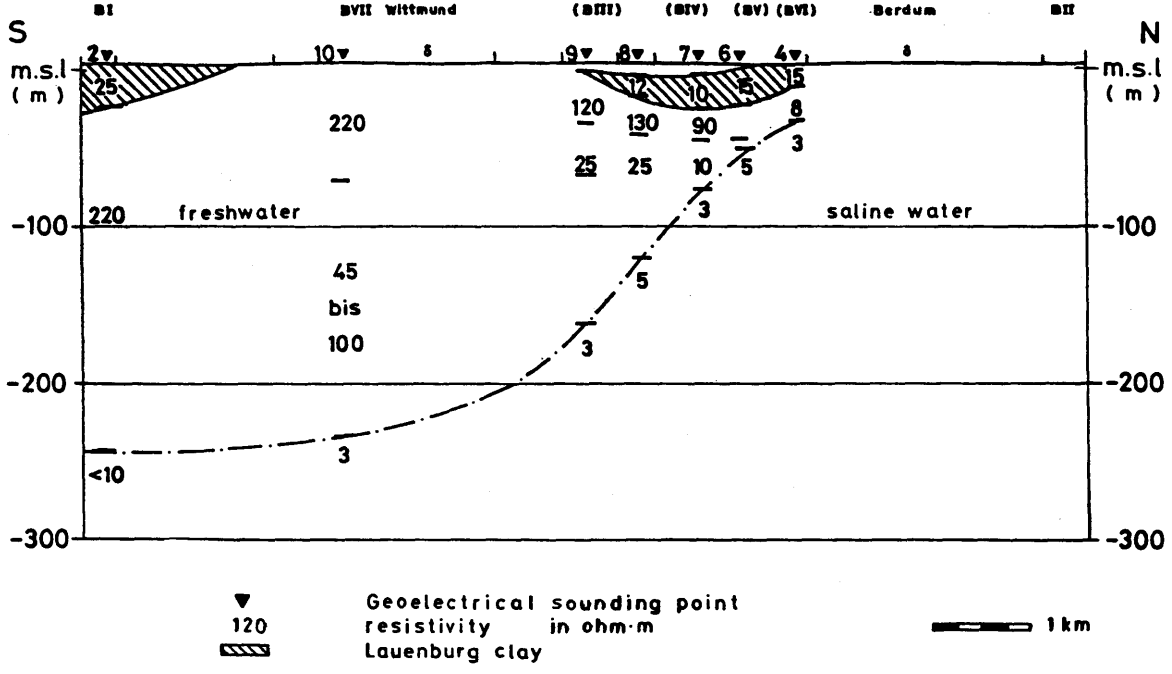

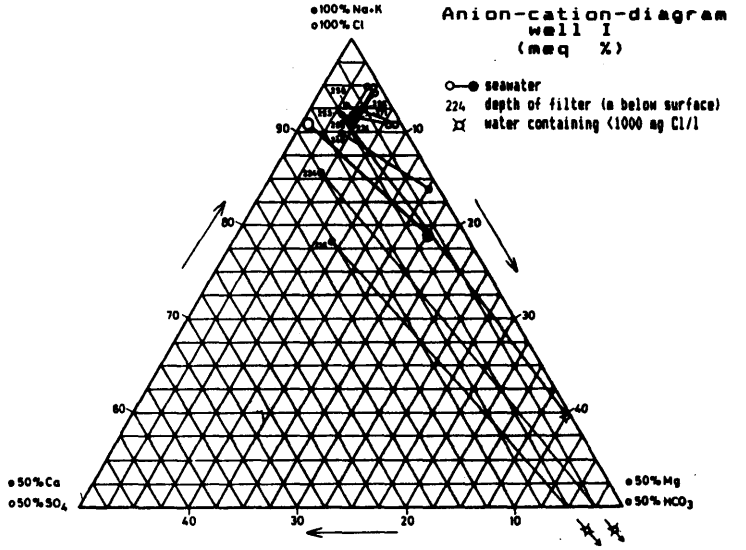

Results well I

No. (depth of filter)		216	224	231	248	253	258	271	288	296
pH		8.7	7.4	7.9	7.3	7.8	7.5	8.0	7.2	7.3
conductivity	µSiem	490	710	1200	3500	7100	6300	15000	22500	24000
lithium	mg/l	48	55	64	170	250	250	490	820	900
potassium	mg/l	5.44	10	9.6	22.4	32.5	33.4	68	93.5	108
sodium	mg/l	98	154	265	745	1550	1570	3475	5200	5475
magnesium	mg/l	4.62	3.6	3.6	13.7	23.1	24.3	63.2	113	131
calcium	mg/l	15.22	15.2	12.5	37.1	53.1	52.1	127.5	187	224
strontium	mg/l	0.6	0.5	0.6	2.2	1.7	3.0	5.8	15.2	15.6
chloride	mg/l	45.4	103	253	1134	2400	2590	5014	8370	8366
bromide	mg/l	0.11	0.15	0.3	1.13	2.05	2.0	4.13	7.05	8.1
iodide	mg/l	<0.05	<0.1	<0.1	0.21	0.3	0.5	0.66	1.4	1.1
sulfate	mg/l	4.2	<2.0	<5.0	3.0	<8.0	<5.0	<5.0	32.3	40.5
bicarbonate	mg/l	265	293	305	316	370	400	480	555	608
nitrate	mg/l	<0.5	<0.5	13.8	3.3	4.5	<0.5	7.4	<0.5	<0.5
iron	mg/l	1.44	4.56	0.82	4.4	2.0	1.44	2.98	2.4	1.94
manganese	mg/l	<0.05	0.1	0.05	<0.05	0.07	0.07	<0.05	<0.05	0.04
copper	µg/l	10	20	20	20	16	90	900	90	900
lead	µg/l	<6.0	20	<6.0	<6.0	<6.0	<6.0	<6.0	<6.0	<6.0
zinc	µg/l	180	800	350	700	600	600	750	900	750
boron	mg/l	0.2	0.4	0.4	0.8	2.4	2.4	2.2	4.3	3.3
silicic acid	mg/l	11.1	11.1	11.4	10	12.3	12.5	11.6	15.2	17.7

Figure 4

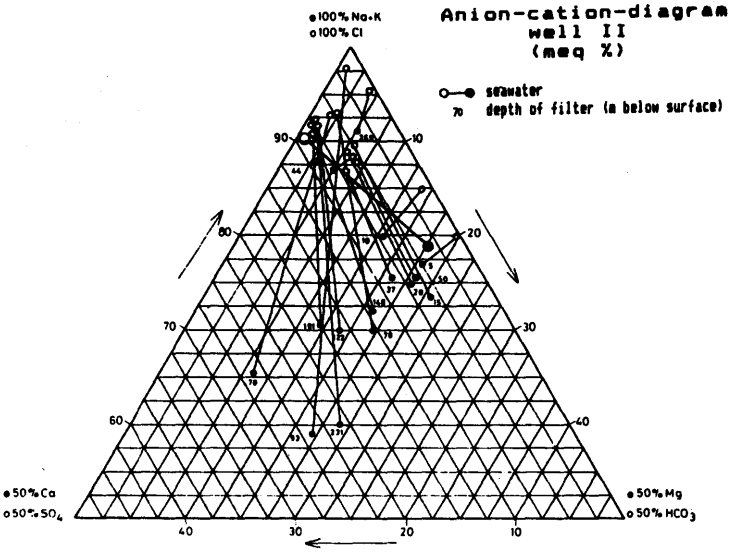

Results well II

No. (depth of filter)		5	10	15	20	37	44	50	70	78	93	122	148	191	231	276
pH		7.7	7.0	6.8	6.7	6.8	6.8	6.9	6.2	6.2	5.5	5.8	5.9	6.6	6.2	7.4
conductivity	uSiem	13000	15000	15000	17000	18000	20000	20000	6300	7500	13000	19000	21000	20000	19000	11000
lithium	mg/l	102	75	48	26	33	42	36	13	22	102	150	170	500	440	530
potassium	mg/l	206	236	221	256	276	310	314	49	83	118	82	92	92	177	97
sodium	mg/l	3475	4125	3800	4350	4875	6000	5475	1270	1620	2400	4750	5300	4975	3700	3750
magnesium	mg/l	432	377	578	547	572	185	607	80.2	215	359	511	572	450	699	94.8
calcium	mg/l	170	321	291	321	431	385	401	477	241	822	982	711	1162	1453	134
strontium	mg/l	2.2	2.9	4.0	4.0	4.1	4.2	4.2	3.0	2.2	4.1	9.0	7.8	43	46.8	12.2
chloride	mg/l	6026	7019	7550	8295	9075	10130	10299	3013	3546	6319	10351	11060	10472	9855	6132
bromide	mg/l	5.9	10.4	17.1	8.3	7.5	16.1	6.7	8.68	10.2	13.2	0.0	0.68	23.5	21.2	3.36
iodide	mg/l	0.33	0.32	0.68	0.11	0.3	0.63	0.13	0.11	0.13	0.25	0.53	0.63	0.34	0.32	0.21
sulfate	mg/l	42	45.7	560	744	947.3	827	997.5	184	238	89.3	1068	1233	1277	1063	31.7
bicarbonate	mg/l	2593	1861	848	796	915	1196	1220	120	159	23.2	74.4	48.8	192.8	61	393
nitrate	mg/l	<0.5	46.8	22.4	14.4	14.4	23.6	23.6	2.8	0.7	<0.5	<0.5	<0.5	7.2	0.5	1.8
iron	mg/l	<0.05	<0.05	0.05	<0.05	<0.05	0.05	<0.05	35.8	15.7	157	152	98	12.7	18.4	3.8
manganese	mg/l	0.05	0.44	0.68	0.86	0.44	0.84	1.0	0.94	0.34	4.54	2.8	1.0	0.36	0.54	0.09
copper	µg/l	<1.0	<1.0	<1.0	<1.0	<1.0	1.0	<1.0	1.0	8.0	<1.0	4.0	<1.0	<1.0	<1.0	4.0
lead	µg/l	<6.0	<6.0	<6.0	<6.0	<6.0	<6.0	<6.0	<6.0	<6.0	<6.0	<6.0	<6.0	<6.0	<6.0	<6.0
zinc	µg/l	12	140	700	250	12	8.0	720	8.0	500	16	500	1600	<8.0	16	800
boron	mg/l	2.3	1.5	1.2	1.3	1.3	1.7	1.7	0.5	0.15				0.03	0.04	2.4
silicic acid	mg/l	10	3.0	21	16.6	11.8	23.2	18.8	12.8	16.2	15.4	13	18	14.2	9.0	18.2

Figure 5

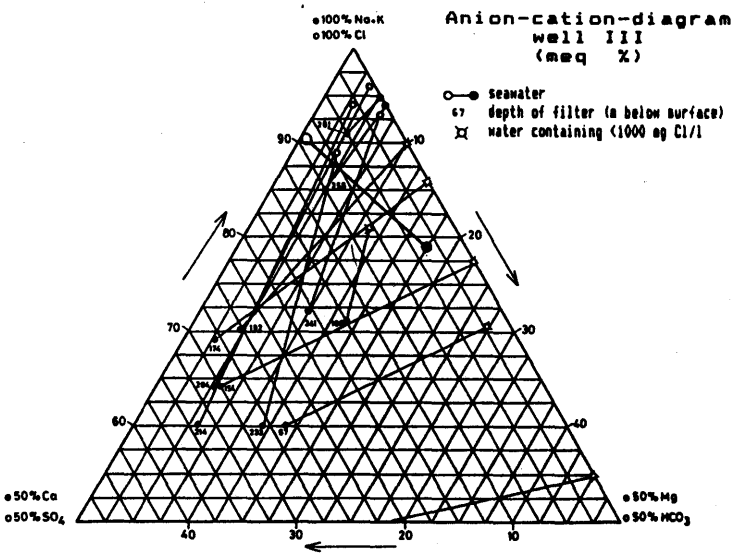

Results well III

No. (depth of filter)		63	96	118	148	172	190	200	212	230	239	256	278
pH		6.7	6.9	7.3	6.9	8.3	7.2	7.0	6.8	7.2	7.5	7.6	7.4
conductivity	µSiem	900	2300	450	900	1400	2100	4400	6000	8500	4800	4500	10000
lithium	mg/l	12	15	8	8.4	17	37	65	410	320	220	230	390
potassium	mg/l	9.4	22	2.8	6.8	9	12.4	19.6	34.5	54	34.5	35	66
sodium	mg/l	143	400	48.5	159	288	443	860	1200	1800	1050	1200	3050
magnesium	mg/l	18.24	43.8	6.1	5.47	5.47	15.8	30.4	67	170	73	35.3	68
calcium	mg/l	58	78.2	50	63	100	134	373	591	701	232	92	120
strontium	mg/l	0.56	0.73	0.42	0.5	0.94	1.2	2.8	5.6	12.7	4.2	4.1	6.4
chloride	mg/l	291	759	106	312	580	921	2127	3119	4397	2197	2127	5104
bromide	mg/l	0.49	1.6	0.2	0.27	0.8	1	3.1	4.1	6.9	2.4	1.86	4.33
iodide	mg/l	<0.05	<0.05	<0.05	<0.05	0.08	0.13	0.2	0.6	0.2	<0.05	<0.05	0.13
sulfate	mg/l	24	100	<5	<5	<5	<5	19.1	178	472	18.1	<5	<5
bicarbonate	mg/l	171	173	147	161	159	154	134	144	251	212	247	398
nitrate	mg/l	<0.5	1	<0.5	1.7	<0.5	<0.5	1.9	4.4	11.5	10.8	3.9	10.6
iron	mg/l	4.84	8.9	11.6	5.3	2.1	1.9	4.1	3.8	5.7	1.02	0.96	1.46
manganese	mg/l	0.05	0.05	0.44	0.44	<0.05	<0.05	0.09	<0.05	0.22	0.09	<0.05	<0.05
copper	µg/l	<4	<4	<4	<4	<4	4	<4	<4	<4	<4	<4	<4
lead	µg/l	<4	<4	<4	<4	<4	<4	<4	<4	<4	<4	<4	<4
zinc	µg/l	600	250	250	350	100	60	100	10000	9000	2500	600	7000
boron	mg/l		0.16	0.02	0.02	0.04	0.10	0.16	1.8	0.09	0.22	0.98	1.8
silicic acid	mg/l	26.8	24.7	24.7	21.2	18.6	16.2	15.4	13.3	11.8	12	1.5	11

Figure 6

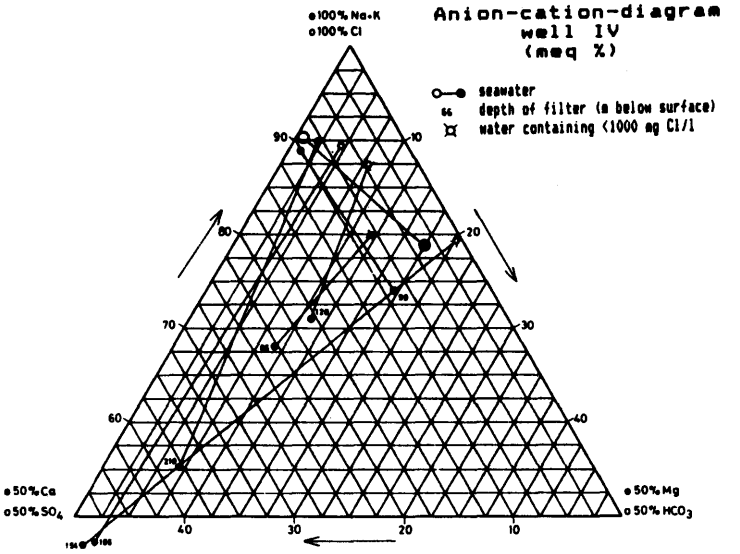

Results well IV

No. (depth of filter)		81	96	117	153	182	204
pH		6.5	6.1	6.6	6.9	6.7	6.6
conductivity	µSiem	1300	17500	2300	970	6200	10000
lithium	mg/l	9	45	12	9	39	115
potassium	mg/l	9.6	212	26.4	5.88	28.4	51
sodium	mg/l	283	4475	480	96	830	2075
magnesium	mg/l	17.6	552	38.3	15.2	75.4	122
calcium	mg/l	85.2	473	104	145	954	1271
strontium	mg/l	0.76	4	0.94	1.1	5	7.9
chloride	mg/l	549	8833	922	379	3119	5672
bromide	mg/l	1.5	17.1	2.44	1.1	6.5	8.8
iodide	mg/l	0.08	0.23	0.08	<0.05	0.2	0.13
sulfate	mg/l	68.3	1407	95.9	6.4	217	617
bicarbonate	mg/l	137	170	142	154	137	198
nitrate	mg/l	<0.5	<0.5	<0.5	<0.5	2.7	<0.5
iron	mg/l	23.4	112	14.4	7.6	14.7	23.2
manganese	mg/l	0.18	2.09	0.16	0.05	0.34	0.16
copper	µg/l	<4	<4	<4	<4	<4	<4
lead	µg/l	<6	<6	<6	<6	16	<6
zinc	µg/l	700	400	4000	180	8000	2500
boron	mg/l	0.18		0.02	0.1	0.54	0.1
silicic acid	mg/l	23	23	18	21.2	13	9.4

Figure 7

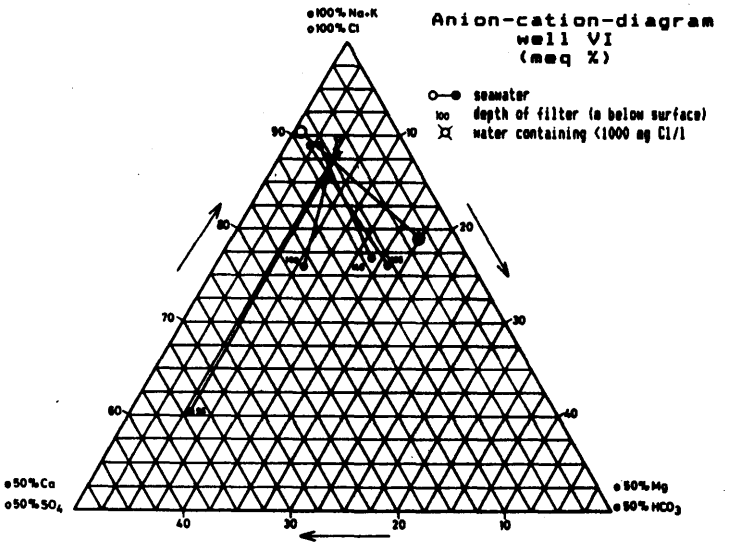

Results well VI

No.(depth of filter)		52	94	144	189
pH		6.1	6.1	6.2	7.0
conductivity	µSiem	2400	4300	11000	14000
lithium	mg/l	17	22	26	45
potassium	mg/l	12.8	26	150	170
sodium	mg/l	375	810	2760	3425
magnesium	mg/l	18.2	42.6	216	494
calcium	mg/l	184	150	220	277
strontium	mg/l	0.93	0.56	1.1	3.8
chloride	mg/l	893	1524	4537	6948
bromide	mg/l	1.3	2.9	8.95	10.4
iodide	mg/l	0.15	0.15	0.3	0.32
sulfate	mg/l	92.2	128.4	566	933
bicarbonate	mg/l	85.4	97.6	237	212
nitrate	mg/l	1.8	2.5	<0.5	<0.5
iron	mg/l	40.4	39.8	40.4	48
manganese	mg/l	1.0	0.68	0.94	1.0
copper	µg/l	<6	<6	<6	<6
lead	µg/l	<6	<6	<6	<6
zinc	µg/l	72	48	40	1500
boron	mg/l	0.02	0.2		1.1
silicic acid	mg/l	15.7	19.4	23.3	25.6

Figure 8

Figure 9

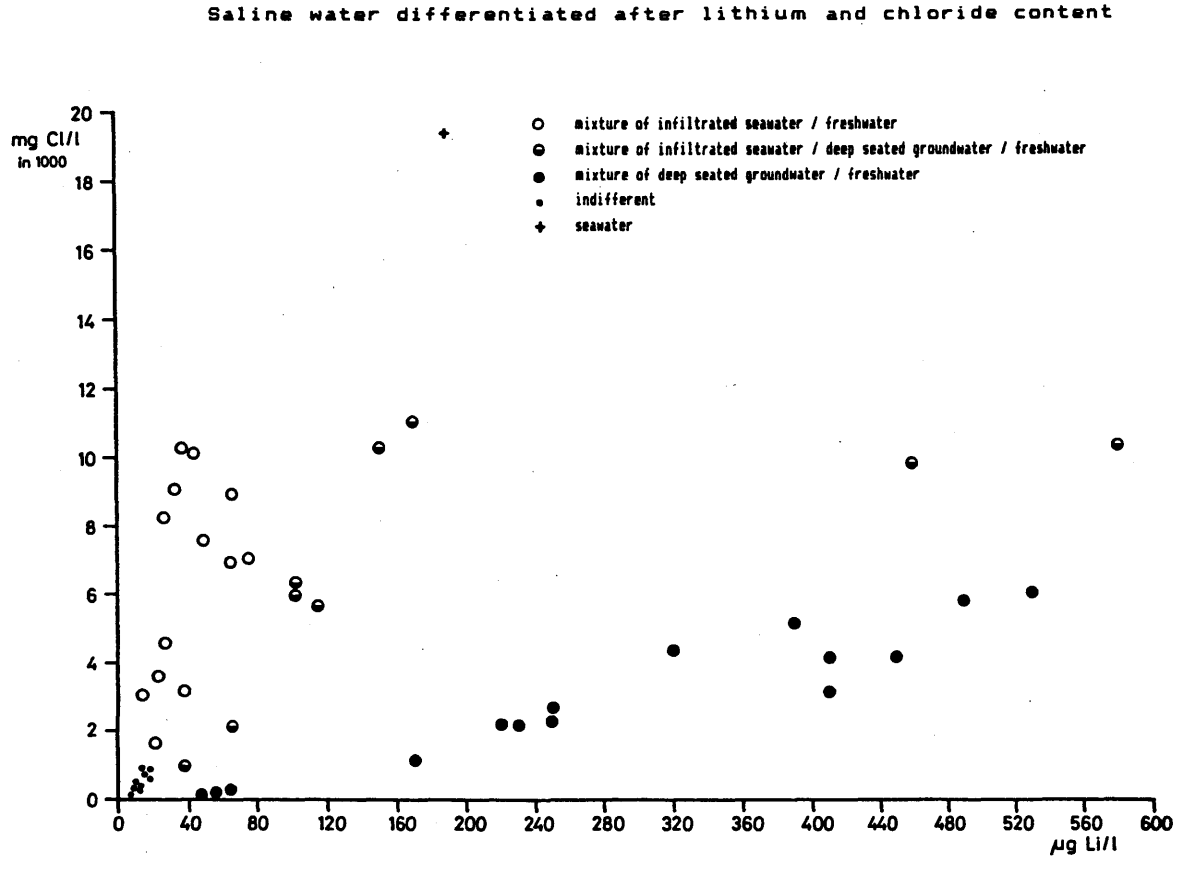
Saline water differentiated after lithium and chloride content
mg Cl/l
in 1000
20
18
16
14
12
10
8
6
4
2
0
0
40
80
120
160
200
240
280
320
360
400
440
480
520
560
600
µg Li/l
mixture of infiltrated seawater / freshwater
mixture of infiltrated seawater / deep seated groundwater / freshwater
mixture of deep seated groundwater / freshwater
indifferent
seawater

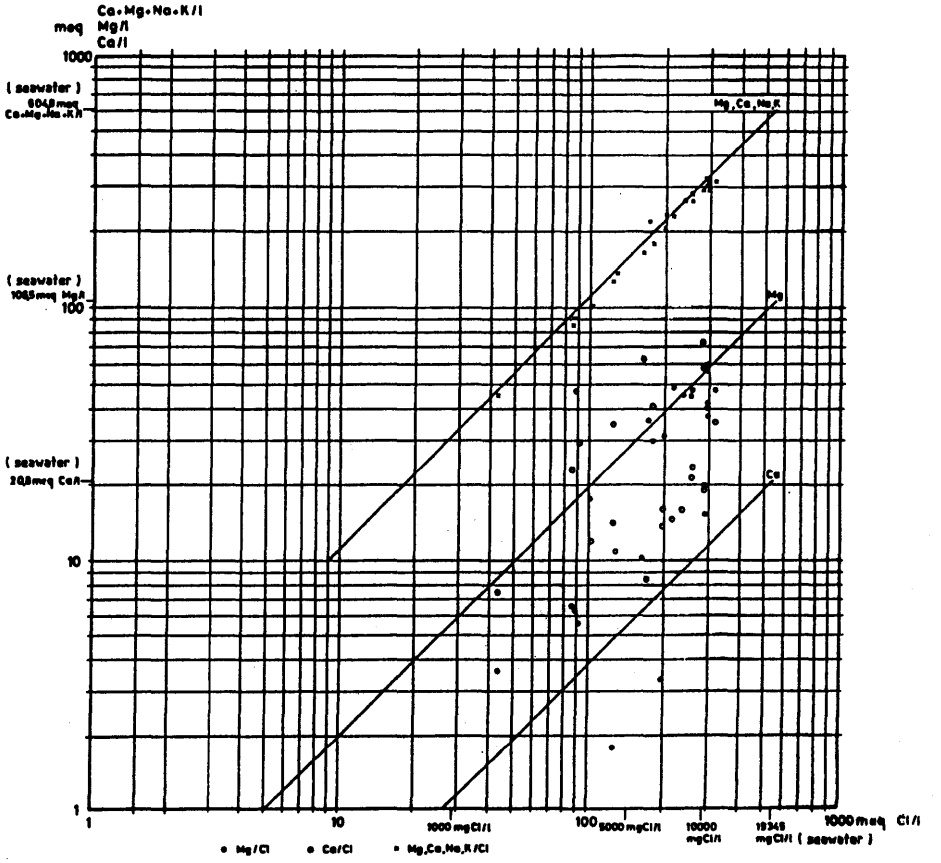

Effects of ion exchange on Ca and Mg concentration in infiltrated seawater from the Wittmund area (wells II,III,IV,VI)

Figure 10

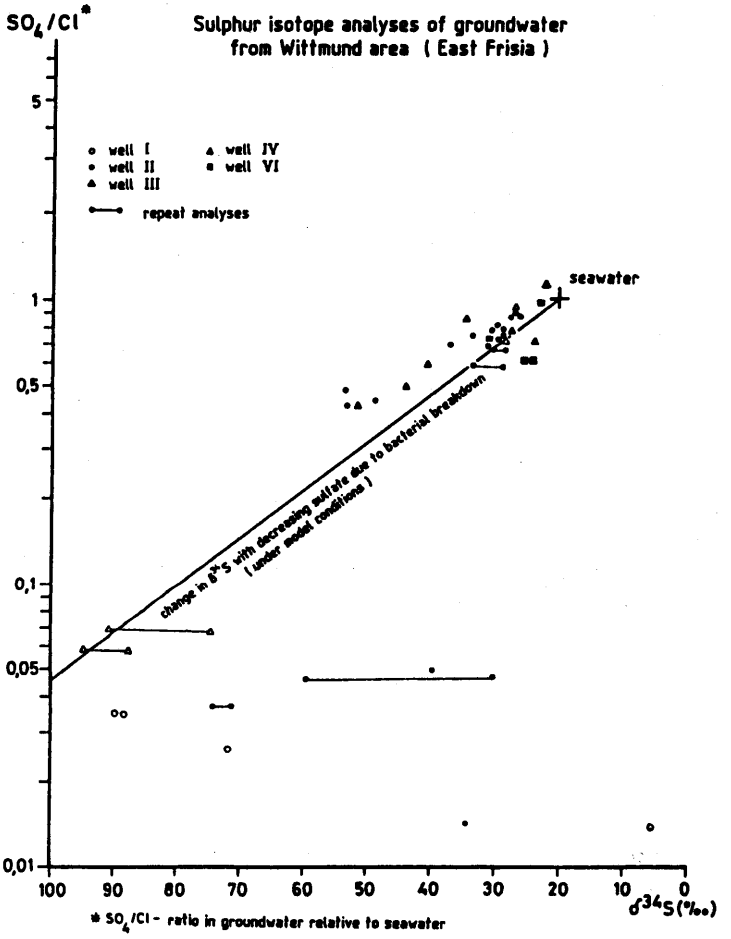

after Nielsen

Figure 11

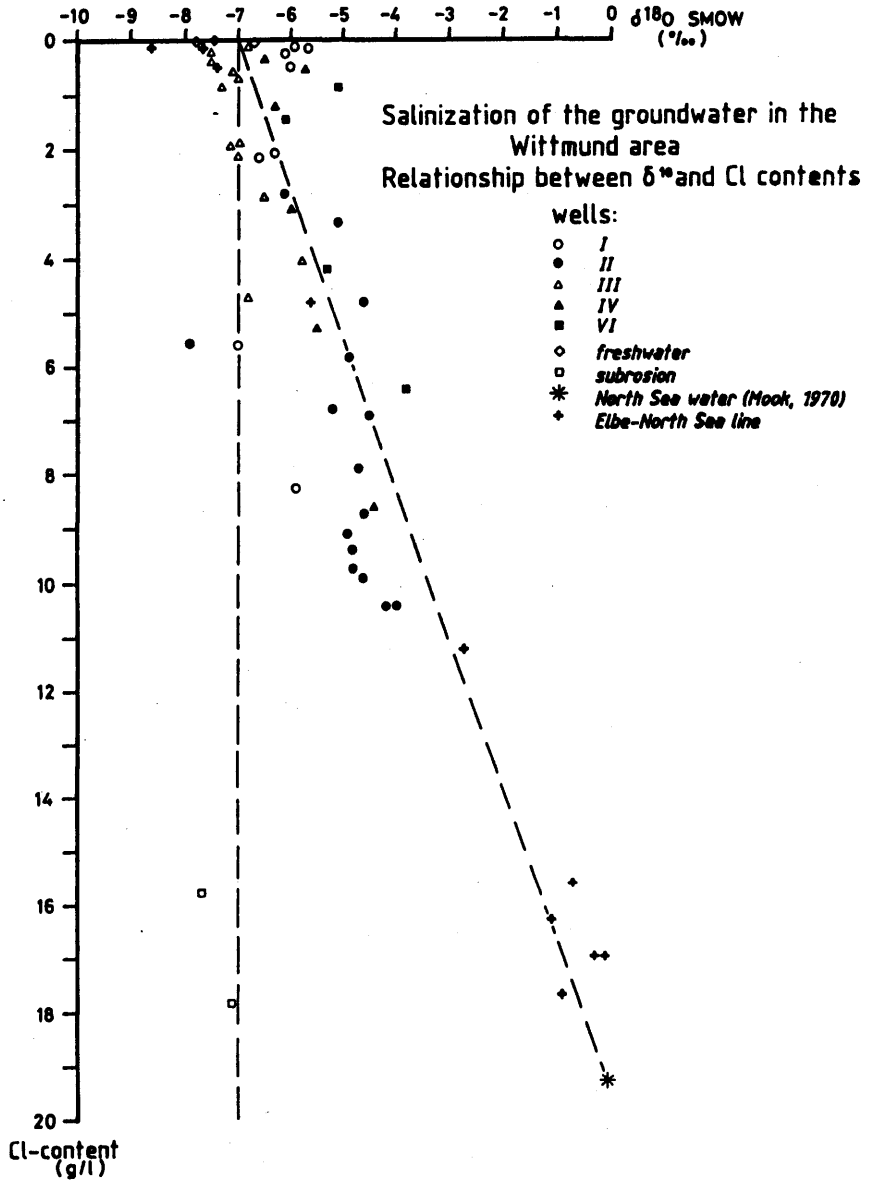
-10 -9 -8 -7 -6 -5 -4 -3 -2 -1 0 δ18O SMOW (‰)
0
2
4
6
8
10
12
14
16
18
20
Cl-content (g/l)
Salinization of the groundwater in the Wittmund area
Relationship between δ18 and Cl contents
wells:
I
II
III
IV
VI
freshwater
subrosion
North Sea water (Mook, 1970)
Elbe-North Sea line
after Stahl

Figure 12

Salinization of the Grourdwater in the Wittmund area
Distribution of groundwater ages
and extent of salinization caused by infiltrated sea water
S
N
m.s.l.
(m)
I
VII
III
IV
V
VI
Bd.2
II
fresh -
water
sea -
water
-100
-200
-300
1000
2500 - 3500
15000
6000 - 7000
30000
limit of zone of influence
of deep-seated saline groundwater
100 - 1000 mg Cl/l
1000 - 5000 mg Cl/l
5000 - 10000 mg Cl/l
> 10000 mg Cl/l
saline, Cl-concentration unknown
1000 14C - model ages in years
10 km to the east
1 km

Figure 13

Borehole logging in the Wittmund area (East Frisia)

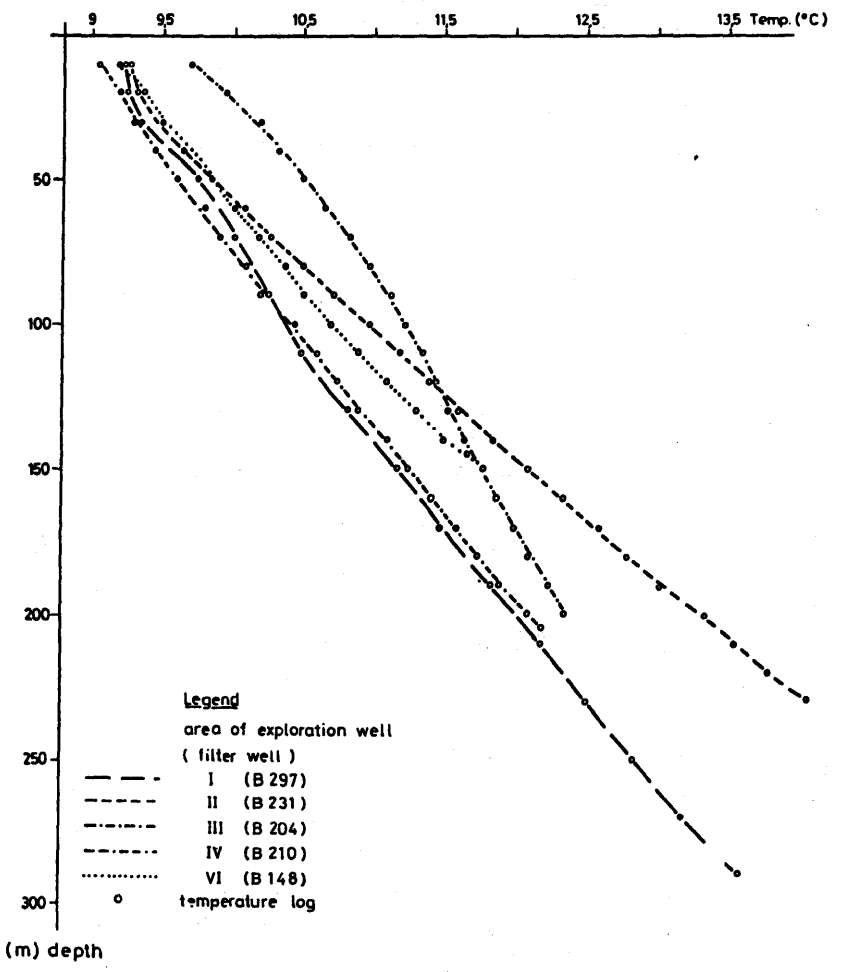

after R. Hänel

Figure 14

Salinization of the Groundwater in the Wittmund area
Groundwater movement
S
N
m.s.l. (m)
fresh-
water
sea-
water
-100
-200
-300
I
III
VI
II
9°C
14°C
groundwater movement on the basis
of geothermal measurements
of water level measurements
--- rise of temperature in the well
--- freshwater / seawater interface
1 km

Figure 15

Probable phases of salinization of the groundwater in the Wittmund coastal area

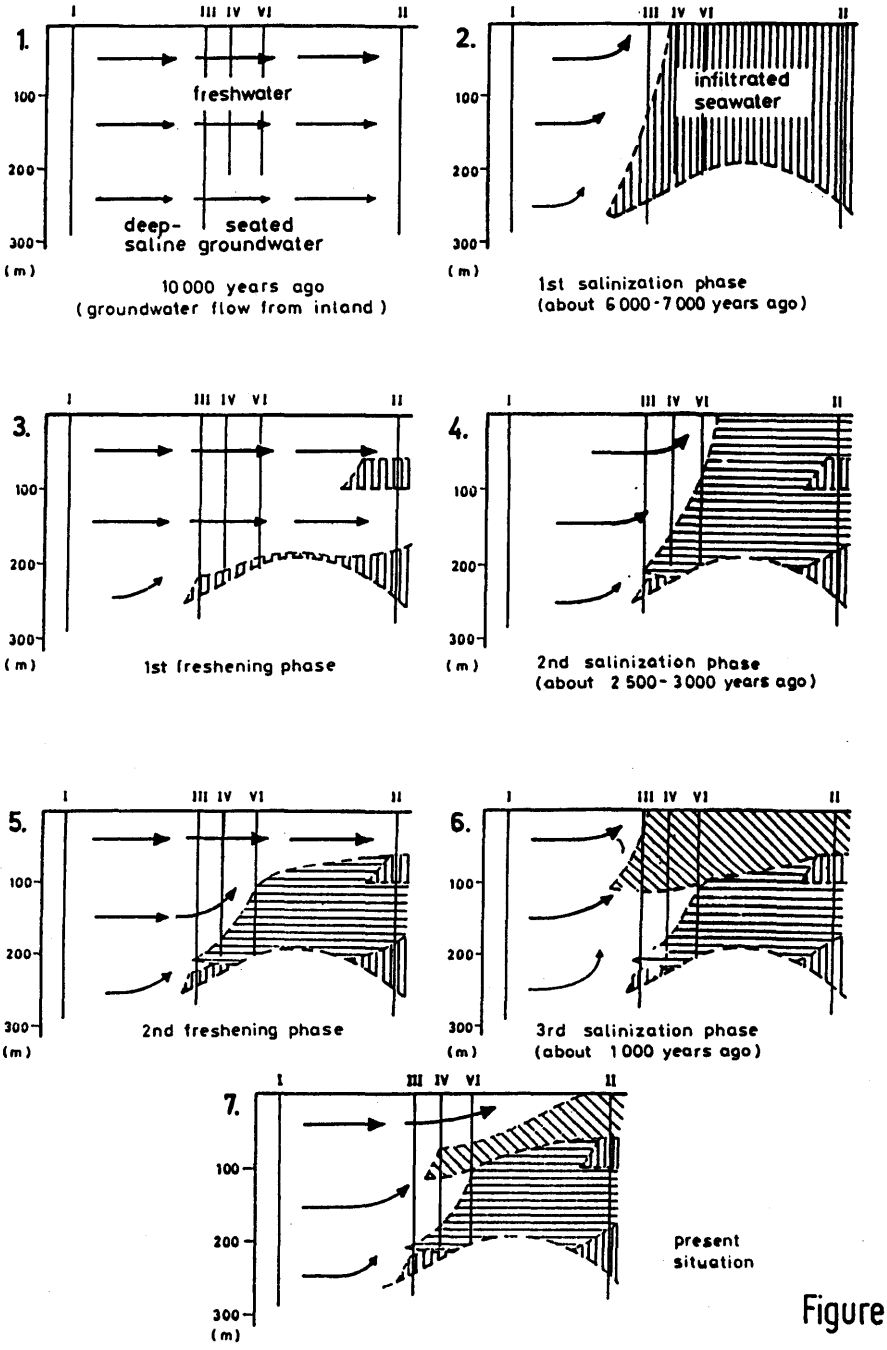

Figure 16

5.2. THE ORIGIN OF BRACKISH GROUNDWATER IN THE LOWER PARTS OF THE NETHERLANDS

C.R. MEINARDI

ABSTRACT

In the sandy aquifers of the Netherlands brackish groundwater can be found even far inland. In the coastal region it may reach the surface. As the upper parts of these aquifers are of fluviatile origin, the salt must have been brought there afterwards. Existing theories about the transport mechanism do not always stand a critical review. The occurrence of brackish groundwater can only partly be explained by recent (Holocene) transgressions of the sea. In sea-covered areas chlorine ions are transported into the underground mainly by molecular diffusion. Another source is formed by the deep-lying marine sediments of Early Pleistocene and Tertiary Age. The salt may be transported upwards by hydrodynamic dispersion. Brackish-groundwater bodies have changed after the creation of polders, which strongly influence groundwater flow.

1. GENERAL SCOPE

A hydrological problem of practical interest for the public water supply in the Netherlands is the occurrence of brackish groundwater in aquifers suitable for groundwater recovery. Pumping stations can be mentioned where the recovered groundwater has continuously grown more brackish, resulting in a forced reduction of the capacity, or even in abandonment of certain wells in the well-field. This phenomenon has to be faced in many parts of the Netherlands, but particularly in the lower regions (the polder area), where only a few places bear fresh groundwater. In this area the brackish groundwater is even interfering with agriculture.

A general and satisfactory theory to explain the occurrence of the brackish groundwater has not yet been published. This is probably due to the fact that in the course of geological history the Netherlands have repeatedly been invaded by the sea, making it possible for scientists to find partial explanations, each of them related to such a transgression of the sea. Furthermore the transport mechanism of the chlorine ions may adopt different forms. Therefore, these partial theories, sometimes being correct for the particular area of investigation, may prove to be wrong if extended to other areas. Research was also hampered by the fact that not enough data were available for a general view. Only recently geoelectrical investigations made it possible to obtain - at least roughly - the interface between fresh and brackish groundwater in large parts of The Netherlands.

In this paper the validity of some of the existing theories will be reconsidered, the number of possible transport mechanisms for the chlorine ions will be extended by one, and a general review will be given on the origin of the brackish-groundwater bodies, describing the phenomena which gave them their actual shape.

2. VOLKER'S THEORY

The reclamation of the former Zuiderzee (now IJsselmeer) led to extensive geo-hydrological investigations in that area, some of them also concerning the quality of the groundwater. Theories were developed by MAZURE (1940) and VOLKER (1961) on the different chloride contents of the groundwater of the upper and the lower layers. They stated that transport of the chlorine ions has almost exclusively been accomplished by molecular diffusion.

The general differential equation describing molecular diffusion for the one-dimensional case is:

$$D \frac{d^2c}{dh^2} - \frac{dc}{dt} = 0$$

where,

c = chloride concentration in ppm;
h = depth in m;
t = time in days;
D = the diffusion factor for diffusion through pores in granular sediments in m^2 per day.

The solution of this equation is dependent on the boundary conditions. MAZURE and VOLKER having found an analytical solution satisfying the boundary conditions in their case, were able to calculate the chloride concentration in the upper 15 m of the underground of the IJsselmeer as a result of diffusion of chloride from the sea-water into the underground during the existence of the Zuiderzee (between about A.D. 1300 and 1932) and a reverse process after the enclosure (when Zuider Sea became IJssel Lake). For the calculation, a value of the diffusion factor D had to be determined by laboratory experiments; surprisingly D turned out to be equal for both sandy and (not too heavy) clayey layers, a mean value being 0,015 m^2 per year. The calculated chloride concentration at different depths appeared to be in close agreement with measured values. VOLKER repeated certain measurements, thus making it possible to follow the process of molecular diffusion in the course of time. In this case too, the measured values were in accordance with theory. As molecular diffusion is effective under all circumstances, groundwater moving or not, the existence of an additional transport mechanism of chlorine ions e.g. by infiltration of sea-water, is not likely. So theories trying to explain the chloride concentration in the upper layers of the underground of the IJsselmeer from other phenomena than diffusion are probably not correct.

The success of this explanation for the upper layers led VOLKER to a similar hypothesis for the deeper layers. The chloride concentration of the groundwater in the deeper layers (which are of fluviatile origin from NAP -20 m to NAP -200 à 300 m*)) is characterized by a continuous increase with depth; at great depth

*) NAP is the national reference level, approximately mean sea-level.

a mighty reservoir of chloride is available in thick marine layers of Early Pleistocene and Tertiary Age. In the absence of groundwater flow during at least the Pleistocene period following the Saalian glaciation (about 200.000 years ago) measured chloride concentrations at different depths can be explained by molecular diffusion. Against this second part of the theory a couple of arguments can be raised.

a) If the diffusion factor D is the same for lithologically different layers and geological history being essentially the same for the whole western part of the Netherlands, chloride-concentration profiles with depth should be the same everywhere. That this is not the case can be deduced from fig. 1, and from the values VOLKER (1961) gives.

   VOLKER's argument that this irregular distribution pattern is due to recent Pleistocene transgressions (the Holsteinian and the Eemian Sea) does not sound very convincing.

b) The assumption that no groundwater flow occurred during the last part of the Pleistocene Age might very well not be true. This proposition however is an essential feature, because molecular diffusion needs a very long time to become effective over such a depth as the thickness of the fluviatile Pleistocene layers. There is a good chance that, at least at the end of the Pleistocene and in the beginning of the Holocene Age, groundwater flow has occurred. At that time the land surface in the west and the northwest of the present Netherlands had a slope of about 5 m over 25 km as can be seen from fig. 2 (note that fig. 2 does not represent the level at that time, the land having subsided since; the slope however will be about correct). Permafrost conditions, prevailing during the last part of the Pleistocene Age, will have been absent or reduced at the beginning of the Holocene Age. The river system of that time is thought to have been composed of braided rivers. Considering all this, the slope of the land surface might very well have been representative for the slope in groundwater level. Assuming a permeablity of 30 m per day for the coarse fluviatile sediments, the actual velocity of the corresponding groundwater flow was about 10 m/year, according to Darcy's law. The groundwater in and under the ice-pushed ridges of the Veluwe and the Utrecht Hills may presumably have become fresh, shortly after the formation of these ridges (see fig. 1 and 2). All the groundwater between these ridges and the coast may, according to the above calculated velocity, very well have been replaced, the present groundwater not being older than some 10.000 years (the duration of the Holocene Age).

3. SOME POPULAR OPINIONS ABOUT BRACKISH GROUNDWATER

Two of the aforementioned partial explanations need some further comment, not because of their intrinsic importance but because of their widespread use by engineers and geologists.

The first is that salt water from the actual North Sea is intruding the underground of the Dutch polders, polder levels lying in general a few metres under mean sea level. Undeniably, an inward directed groundwater flow has been created by the drainage of the polders. Its effect however is small, as will be shown. Let us take the example of the Haarlemmermeerpolder (fig. 8), lying a relatively short distance, about 10 km, from the coast and having a polder level of about NAP -6 m. Taking Darcy's law the actual velocity of the eastward directed groundwater flow can be estimated to be 15 m per year. The polder having been reclaimed 100 years ago, the front of the salt groundwater has moved only 1,5 km in that lapse of time. Most polders are older, yet the age of the deep ones very often does not exceed 300 years (the time windmills came into common use). The inward flow of sea-water could therefore have intruded somewhat further than 1,5 km; nevertheless, the vast amount of brackish groundwater in the fluviatile sediments of the Dutch underground cannot be explained by this theory.

The secound theory states that during recent transgressions of the sea (the Eemian Sea and different stages of the Holocene North Sea, see fig. 3) seawater infiltrated from above into the until then fresh fluviatile sediments, the driving force being the difference in density between fresh and salt water.

Development of salt-water wedges might be responsible for a horizontal spreading of the brackish groundwater towards areas not having been covered by the sea. The groundwater will not obtain the chloride concentration of sea-water due to mixing with the original fresh groundwater. Moreover, after retreat of the sea a reinstalled fresh-groundwater flow dilutes the brackish groundwater.

The validity of this theory is questionable for the following reasons.

1. No quantitative proof has ever been given to support the infiltration theory. However, MAZURE and VOLKER gave convincing evidence that the intrusion of chlorine ions from the Zuiderzee into the underground followed the laws of molecular diffusion (note that various types of seafloor, both sandy and clayey have been researched). It is difficult to understand why salt intrusion during earlier transgressions or in other regions, but showing essentially the same general features, should follow another path. Due to local differences concentrations of chloride may vary, but the transport mechanism will have been the same.

2. Some of the observed phenomena in nature do not easily fit the infiltration theory. Should infiltration and subsequent mixing with fresh groundwater have occurred, then a continuous increase of chloride concentration with depth should not be expected, but just the opposite. Furthermore, brackish groundwater has been observed in fluviatile sediments at a distance of 10 km and more from any recent coastline (fig. 1 and 3). Salt wedges of such extent are not very plausible.

3. Groundwater flow in sea-covered areas will generally be absent or very weak, as it can only be initiated by small differences in density.

It may be concluded that recent transgressions of the sea most certainly will have influenced the groundwater in the invaded areas, though molecular diffusion should be cited as the cause of this influence.

4. TRANSPORT OF CHLORIDE BY HYDRODYNAMIC DISPERSION

In constructing a theory on the occurrence of brackish groundwater, attention should be paid to groundwater flow. Assuming groundwater flow and taking into account the existence of a large reservoir of chloride in the deep-lying marine sediments of Early Pleistocene and Tertiary Age, it is worthwile to consider chloride transport by hydrodynamic dispersion. Hydrodynamic dispersion is the combined action of molecular diffusion and movement of groundwater. When flowing, groundwater has to find its way through the inhomogeneities of the subsurface. Hereby, groundwater coming from a deeper and more brackish part of the aquifer may contact groundwater from a more fresh part. During the time of contact, interchange of chlorine ions is possible by molecular diffusion, tending to level the concentration differences. The steady-state situation of hydrodynamic dispersion, being dependent on molecular diffusion and groundwater flow (rate and direction), is reached much quicker than that of molecular diffusion alone.

Groundwater flow is a component of the hydrological situation. The present hydrological conditions for the lower parts of the Netherlands can be described sufficiently, but one must bear in mind that the creation of the polders (begun at about A.D. 1200) has significantly changed the hydrological regime of the polder area. As groundwater is generally moving at a very slow rate, one should expect that the basic form of the brackish-groundwater bodies already existed before A.D. 1200. This means that ancient hydrological conditions have to be estimated. A few postulations are necessary:

1. In most of the geological periods after the Saalian Ice Age a certain groundwater flow will have occurred. This is obvious for the Eemian Interstage; climate being more or less comparable to today's, one may certainly expect groundwater flow in areas not covered by the Eemian Sea. The situation is less clear for the Weichselian Age. During this period the subsoil of the Netherlands will most probably have been frozen permanently (permafrost). Nevertheless, the permafrost layer will in all likelihood not have reached the base of the aquifer system, at a depth of several hundreds of metres. Moreover, permafrost layers often contain unfrozen parts through which discharge and recharge of groundwater can happen (as can be concluded from research in actual permafrost areas). So even in Weichselian times groundwater flow is likely to have occurred.

Groundwater flow at the beginning of the Holocene Age has been discussed already. In the rest of the Holocene Age groundwater flow will have been rather weak; the growth of big peat layers in that period indicates a flat country with slowly moving or stagnant water. Yet, as the drainage systems of the fen areas were linked with the big rivers passing through, there may have been a weak slope in the land surface, generally directed towards the coast. This would mean that a gradient in groundwater level and consequently a certain groundwater flow have existed.

2. The general direction of groundwater flow resembled at any time the general direction of the surface water (= the direction of the big rivers). One may take it for granted that before the construction of the dikes the Dutch rivers were draining rivers. The rate of groundwater flow is not known.

3. An assumption pertaining to the properties of chloride is that no chemical changes have affected the chlorine ions, not even in the long term.

Literature on hydrodynamic dispersion is becoming extensive. For the present paper use has been made of VERRUIJT's mathematical treatment of steady-state dispersion across an interface (VERRUIJT, 1971). An approximate solution is given for two cases of steady-state dispersion by uniform flow in an isotropic porous medium, the first one concerning polluted (salt) and non-polluted (fresh) water moving with the same velocity parallel to the interface, whereas in the second one the salt water is at rest. For this last problem the following solution is given:

$$C = 1 - \operatorname{erf}\left(\frac{Y}{2\sqrt{X}}\right) - \frac{Y}{\sqrt{\pi X}} \exp.\left(-\frac{Y^2}{4X}\right).$$

The symbols used represent the following dimensionless variables:

$C = c/c_o$ the concentration at (x, y) divided by the concentration in the salt water, which is assumed to be constant,

$y = y/((\lambda + 2\mu)\ \lambda)^{1/2}$,

$X = x/(\lambda + 2\mu)$,

y = the co-ordinate perpendicular to the interface heading towards the fresh water,

x = the co-ordinate in the direction of the groundwater flow,

λ and μ are constants giving the relation between the components of the velocity vector and the dispersion tensor. They are of the same order of magnitude as the inhomogeneities in the underground (e.g. the grain size) and have the same dimension as x and y.

The term $\frac{V}{\sqrt{\pi X}} \exp.\left(-\frac{Y^2}{4X}\right)$, containing the velocity of the groundwater flow will not be discussed further as it may be omitted. This term is only of importance for small values of x (small-scale problems). However, the occurrence of brackish groundwater is a regional-scale problem.

At many points, similarity exists between VERRUIJT's theoretical case and the groundwater-flow situation in the lower parts of the Netherlands (the region between the outcropping of the Pleistocene layers and the coast, see fig. 1 and 2). Let us take in fig. 2 the lowest point of the fresh-water pocket under the Utrecht Hills as the point (x = o, y = o), x heading horizontally towards the coast and y vertically upwards. This deepest point, the location of which is not exactly known, but which may be estimated to lie at a depth of about NAP -350 m, may be situated in Tertiary clay layers of great extent and thickness (marine Miocene and older). Groundwater flow under the interface (x > o, y < o) will be practically zero and chlorine ions will be transported by molecular diffusion from the deeper layers containing salt water at rest. At (x = o, y > o) a fresh-groundwater flow towards the coast begins. This flow is not exactly uniform, but may be taken as such. As groundwater flow in the above sense is likely to have occurred since the Saalian Ice Age, dispersion will have reached a practically steady-state situation.

Difficulties arise when one has to estimate the size of the inhomogeneities to be taken into account. For small-scale problems one may probably take - as VERRUIJT suggests - the grain size. In the present case it is more likely that the size of the inhomogeneities is in the order of magnitude of the thickness of clay layers or may be even of geological formations (in the range of 0,5 m to several metres). At this point we should also note that the subsurface is far from being an isotropic porous medium.

In fig. 5 some computed lines of equal chloride concentration are shown. They are based on VERRUIJT's equation, and his suggestion on the relation between the size d of the inhomogeneities and the constants λ and μ. The value C = 0,01 is thought to represent C_o = 15 000 mg per litre (supposed to be the chloride concentration in the deep Tertiary layers) and C = 150 mg/l (the concentration at the salt-fresh interface in fig. 1).

For a size d of the inhomogeneities of the order of magnitude of 1 m, a reasonable fit exists between the measured and the computed line. A perfect fit is not obtained, due to local circumstances (polders) and also due to the fact that in the western part recent (Holocene) transgressions have salted the upper layers.

In fig. 5, 6 and 7 the vertical chloride distributions at different distances from the origin are given for different values of d. They are compared with measurements in the IJsselmeer area (where deep borings have been made and where disturbances by polders have been absent until recently). The origin of the fresh-groundwater flow, defining x, might in this case be situated in the central area of the Veluwe. Again the measured values of the chloride concentration are in agreement with computed values for inhomogeneities of the order of magnitude of 1 m. As could be expected a perfect match cannot be obtained; the somewhat more complicated groundwater-flow pattern and the irregularities in the underground found in nature, cannot be taken into account.

Conclusion: transport of chloride from the deep brackish layers into the originally fresh fluviatile layers by hydrodynamical dispersion can explain the following observed phenomena.

1. The increase in chloride concentration with depth at any place in the lower western part of the country.

2. The increase in chloride concentration at a given depth towards the coast (being generally also the direction of the groundwater flow).

Local singularities, e.g. deviations from the general rule expressed under 1), are not constraining this theory, as they might in many cases be explained by a locally more complicated groundwater-flow pattern or by varying sizes of the inhomogeneities in the underground.

5. THE GROUNDWATER-FLOW PATTERN AFTER A.D. 1200

Groundwater flow before A.D. 1200 can be discussed in a general way (as has been done in the previous chapter). This is not possible with respect to the groundwater movement after that time, as since then the hydrological regime in the lower parts of The Netherlands has been thoroughly changed by activities of man. The big rivers (Rhine and Meuse) passing The Netherlands, have been endiked and the areas in between became polders. Former lakes were reclaimed, after 1600 even the deeper ones. As a result, a complicated pattern of different surface-water levels and consequently different groundwater levels even within small areas was formed. In general, highest groundwater levels can be found near or at the big rivers or former river branches. In these regions groundwater is recharged and they form the present starting point for groundwater flow. The deepest polders, often being reclaimed lakes, are attracting groundwater and discharging it. Consequently, near the rivers the interface between fresh and brackish groundwater is lying deeper than under the deep polders (GEIRNAERT, 1973), where it sometimes reaches the surface.

This may be illustrated by two maps, compiled at the Institute for Land and Water Management Research (VAN REES VELLINGA et al., 1972) and showing the chloride concentration of the groundwater at two different levels. These maps concern the upper part of the fluviatile layers. This means that first the influence of the Holocene transgressions should be researched.

At a depth of NAP -15 m to -25 m (fig. 8), some distinct areas with groundwater containing a high chloride concentration can be seen. Of them the Westland area near Rotterdam Waterway has to be related to the recent Dunkirk transgression, when the sea invaded it at about A.D. 1000. The chlorine ions may have penetrated into the underground in the same way as happened in the Zuiderzee area. The same holds for two areas along the former Rhine branch "Oude Rijn". These two regions do not coincide with the area invaded by the

Dunkirk Sea. It looks as if the invaded area was split into two parts, one having moved north and the other one south. The reason for this can be found in the actual groundwater-flow pattern. River water and rainfall are continuously recharging the groundwater under the Oude Rijn and the shallow adjacent polders. The shallow layers once having been brackish, are being flushed by fresh water, while the brackish groundwater is driven both to the north and to the south. The other areas containing groundwater with a high chloride concentration are all situated in very low polders which are now the centres of groundwater discharge (this means that locally even important vertical components in groundwater flow may occur). The attracted brackish groundwater may be partly of Holocene origin but another part will have been derived from the much older brackish groundwater at greater depth.

At the level of NAP -15 m to -25 m no clear traces can be found of the earlier Holocene period of transgressions, called the Calais Age (about 4000 years ago). The chloride being brought into this layer will have been removed (by diffusion) during the long period of regression after the retreat of the Calais Sea.

Yet, at the level of NAP -45 m to -55 m (fig. 9) part of the chloride which penetrated the underground during the Calais transgressions is still present. This can be concluded from the fact that the areas where groundwater with a chloride concentration of more than 200 mg/l (and even more than 1000 mg/l) predominates closely agree with the areas covered by Calais sediments (compare figs. 3 and 9). This is in accordance with VOLKER's theory that at this depth a certain amount of chloride diffused during the Calais Age may still be found.

However, from figs. 4, 5 and 6 it may be concluded that part of the chloride at the NAP -45 m to -55 m level originates from dispersion from the brackish water in the marine Early Pleistocene and Tertiary layers. At increasing depth, the chloride of Calais Age will lose its dominance in favour of the chloride being transported by means of dispersion from below.

6. CONCLUSIONS

Major sources of brackish groundwater in the fluviatile sediments in the subsurface of the lower parts of The Netherlands are:

6.1. DISPERSION

Chlorine ions are transported by hydrodynamic dispersion from deep-lying marine sediments of Early Pleistocene and Tertiary Age into the fluviatile layers. This has resulted in a desalination of the marine layers near the starting point of the groundwater flow, situated under the ice-pushed ridges of Utrecht and Gelderland and in a salting-up of the lower parts of the fluviatile layers, beginning at a certain distance from the starting point and increasing in the direction of the groundwater flow and with depth.

6.2. MOLECULAR DIFFUSION

In or near areas where, during Holocene transgressions, the sea invaded the present area of The Netherlands, brackish groundwater can be found in the upper part of the fluviatile sediments. Presumably, the chlorine ions have been transported downwards by molecular diffusion in the same way as has been shown by MAZURE and VOLKER for the chloride of the Zuiderzee.

Desalination of the groundwater in these areas will have occurred in periods of regression, partly by molecular diffusion and partly by flushing with fresh groundwater.

6.3. RECLAMATION

After the reclamation, groundwater flow has grown to be more intense and more diversely directed. This has caused a change in the brackish-groundwater bodies in the sense that the interface between fresh and brackish groundwater has gone down under the big rivers and shallow polders and has risen in the subsurface of the deep polders.

Intrusion of brackish groundwater from the recent North Sea by a landward directed groundwater flow is only of minor importance, this phenomenon being restricted to a narrow zone along the coast.

The different origins of the brackish groundwater in the lower parts of The Netherlands are shown schematically in fig. 10.

REFERENCES

BREEUWER, J.B. & JELGERSMA, S. (1973). An East-West geohydrological section across the Netherlands. Verh. K. Ned. Geol. Mijnb. Gen. 29, 105-106.

GEIRNAERT, W. (1973). The hydrology and hydrochemistry of the lower Rhine fluvial plain. Leidse Geol. Meded. 49, 59-84.

JELGERSMA, S., de JONG, J., ZAGWIJN, W.H. & van REGTEREN ALTENA, J.F. (1970). The coastal dunes of the Western Netherlands; geology, vegetational history and archeology. Meded. Rijks Geol. Dienst N.S. 21, 93-167.

MAZURE, J. (1940). Bijlage IX van het Rapport van de Commissie Drinkwatervoorziening Westen des Lands.

PONS, L.J., JELGERSMA; S., WIGGERS, A.J. & De JONG, J.D. (1963). Evolution of the Netherlands coastal area during the Holocene. Verh. K. Ned. Geol. Mijnb. Gen. 21-2, 197-208.

van REES VELLINGA, E., TOUSSAINT, C.G. & van GILS, J.B.H.M. (1972). Het chloridegehalte van het grondwater in midden-west Nederland. I.C.W. Nota 695.

VERRUIJT, A. (1971). Steady dispersion across an interface in a porous medium. J. Hydrol. 14, 337-347.

VOLKER, A. (1961). Source of brackish groundwater in Pleistocene formations beneath the Dutch polderland. Econ. Geol. 56, 1045-1057.

ZONNEVELD, J.I.S. (1958). Litho-stratigraphische eenheden in het Nederlandse Pleistoceen. Meded. Geol. Sticht. N.S. 12, 31-64.

FIGURES

Fig. 1: West-East geohydrological section (schematic) through the central-western part of the Netherlands

Fig. 2: The top of the pleistocene sediments

Fig. 3: The extent of recent transgressions

Fig. 4: The chloride concentration of 150 mg/l resulting from steady dispersion across an interface as a function of depth, distance and size of the inhomogeneities.

Fig. 5: Chloride concentration versus depth for x = 50 km and different values of d (steady dispersion across an interface).

Fig. 6: Chloride concentration versus depth for x = 65 km and different values of d (steady dispersion across an interface).

Fig. 7: Chloride concentration versus depth for x = 100 km and different values of d (steady dispersion across an interface).

Fig. 8: Chloride concentration for a depth of mean sea level -15 to -25 m.

Fig. 9: Chloride concentration for a depth of mean sea level -45 to -55 m.

Fig. 10: Brackish-groundwater bodies in the course of geological time in the central western part of the Netherlands.

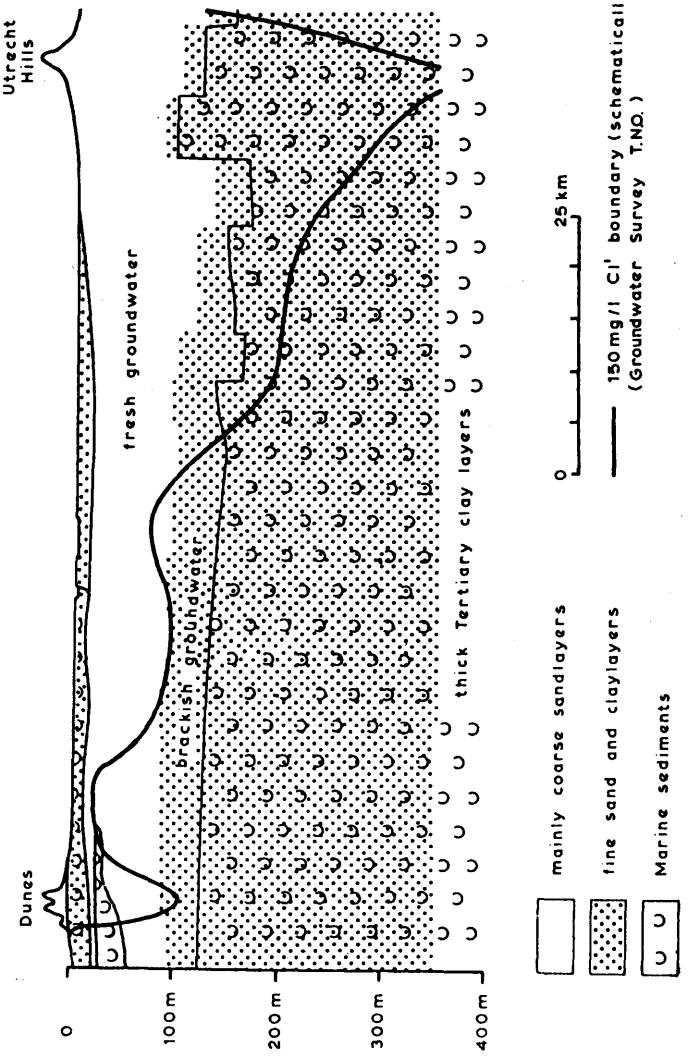
Utrecht Hills
Dunes
fresh groundwater
brackish groundwater
thick Tertiary clay layers
0
100 m
200 m
300 m
400 m
mainly coarse sandlayers
fine sand and claylayers
Marine sediments
0
25 km
150 mg/l Cl' boundary (schematically)
(Groundwater Survey T.NO.)

Figure 1

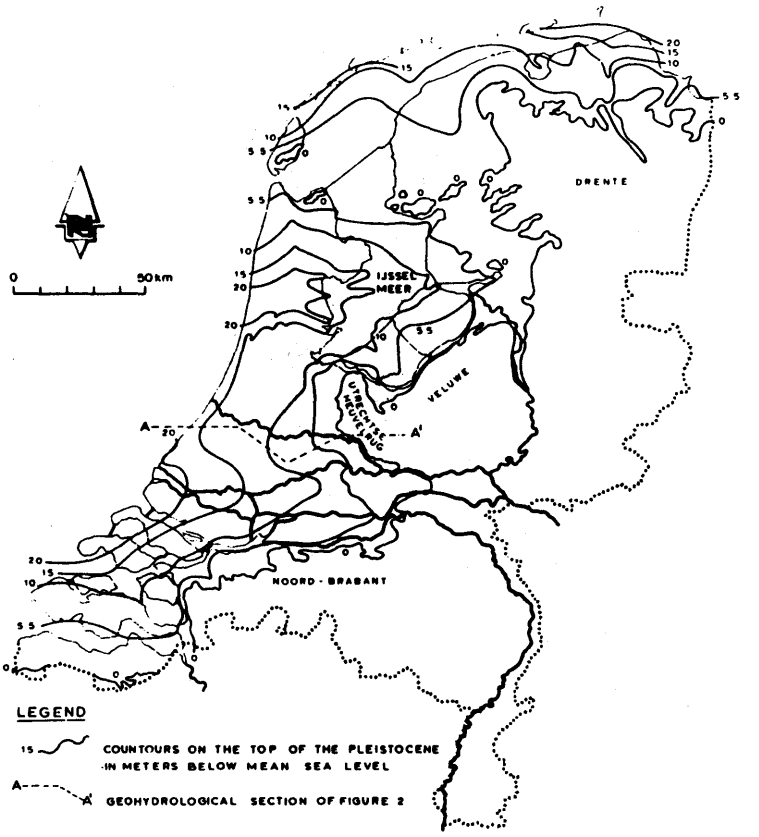
0
50km
DRENTE
IJSSEL MEER
VELUWE
UTRECHTSE HEUVELRUG
NOORD - BRABANT
A
A'
LEGEND
COUNTOURS ON THE TOP OF THE PLEISTOCENE IN METERS BELOW MEAN SEA LEVEL
GEOHYDROLOGICAL SECTION OF FIGURE 2

Figure 2

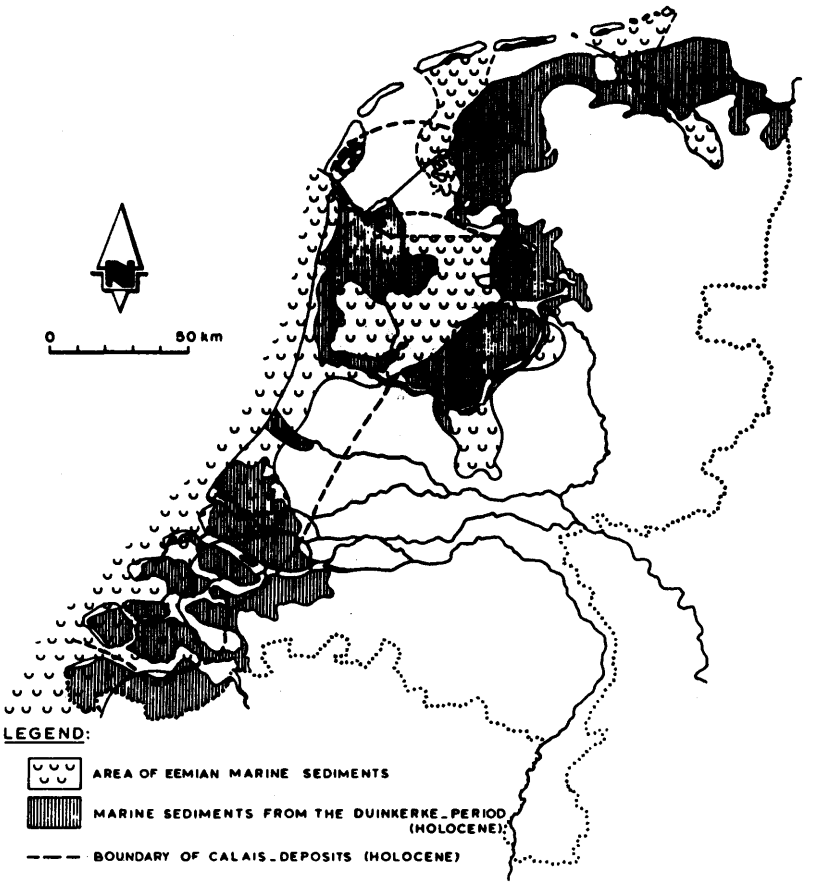
0
50 km
LEGEND:
AREA OF EEMIAN MARINE SEDIMENTS
MARINE SEDIMENTS FROM THE DUINKERKE_PERIOD (HOLOCENE)
BOUNDARY OF CALAIS_DEPOSITS (HOLOCENE)

Figure 3

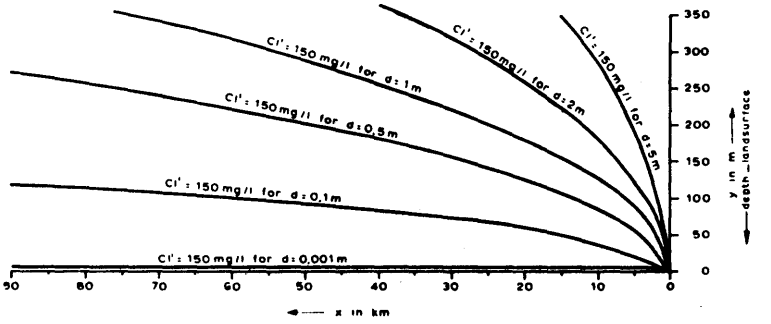

Figure 4

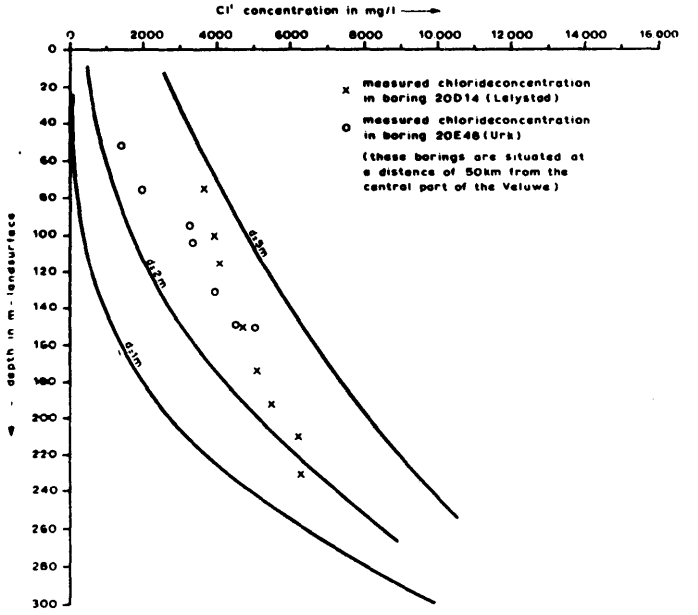

Figure 5

Figure 6

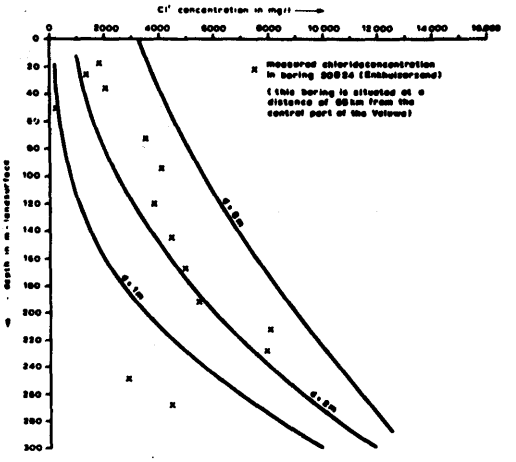

Figure 7

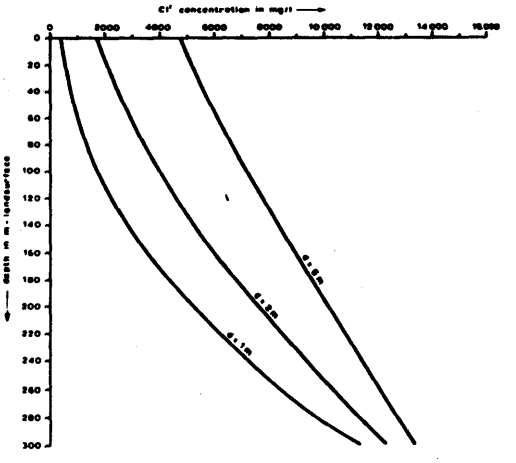

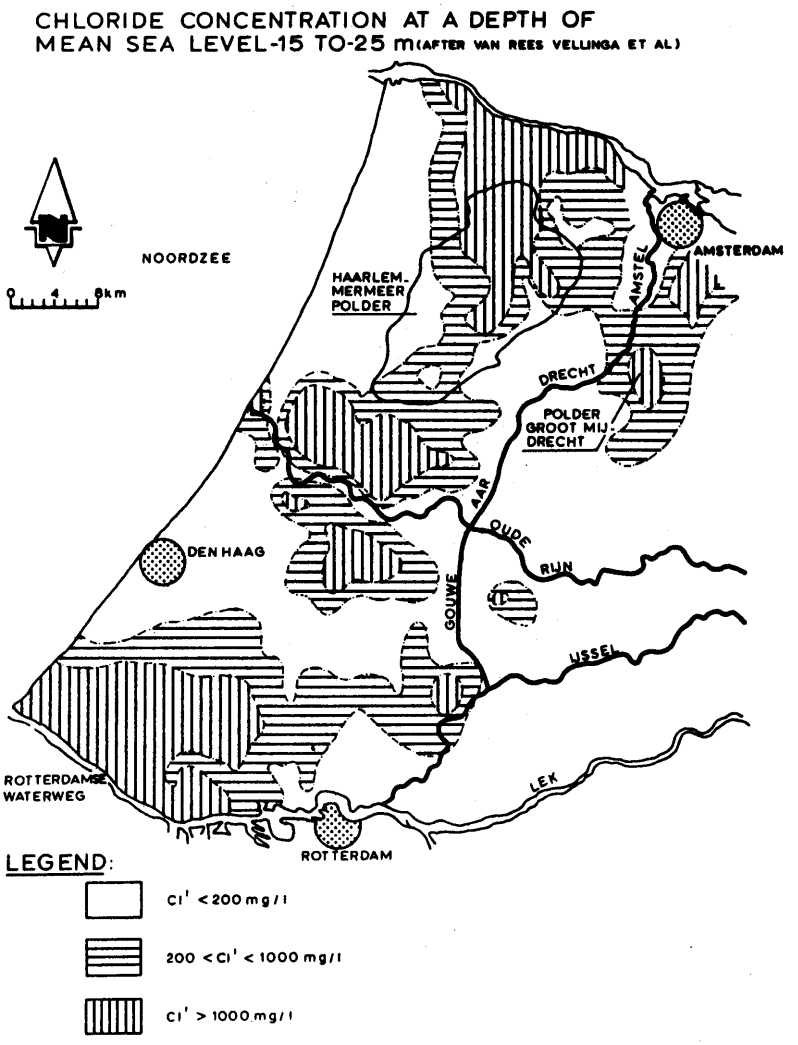
CHLORIDE CONCENTRATION AT A DEPTH OF
MEAN SEA LEVEL-15 TO-25 m (AFTER VAN REES VELLINGA ET AL)
NOORDZEE
0 4 8km
HAARLEM-
MERMEER
POLDER
AMSTEL
AMSTERDAM
DRECHT
POLDER
GROOT MIJ-
DRECHT
AAR
OUDE
RIJN
GOUWE
IJSSEL
DEN HAAG
ROTTERDAMSE
WATERWEG
LEK
ROTTERDAM
LEGEND:
Cl' < 200 mg/l
200 < Cl' < 1000 mg/l
Cl' > 1000 mg/l

Figure 8

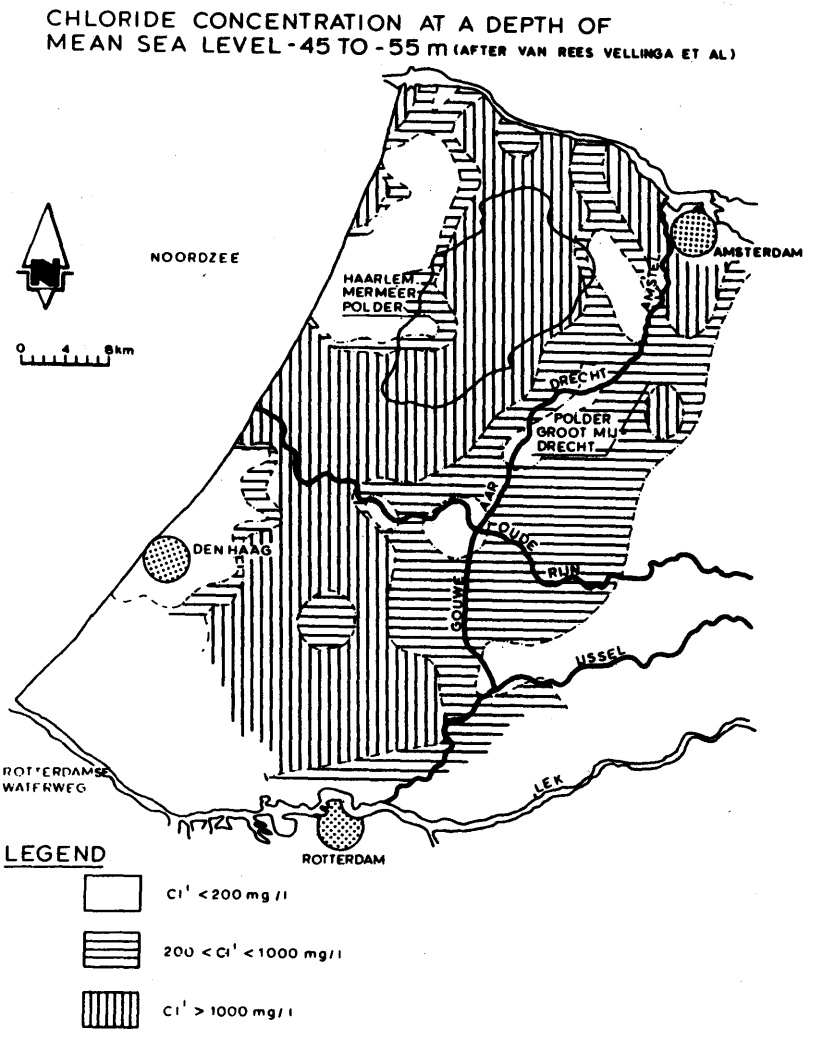
CHLORIDE CONCENTRATION AT A DEPTH OF
MEAN SEA LEVEL -45 TO -55 m (AFTER VAN REES VELLINGA ET AL)
NOORDZEE
0 4 8km
HAARLEM-
MERMEER-
POLDER
AMSTERDAM
AMSTEL
DRECHT
POLDER
GROOT MU
DRECHT
DEN HAAG
LEK
OUDE
RIJN
GOUWE
IJSSEL
ROTTERDAMSE
WATERWEG
LEK
ROTTERDAM
LEGEND
Cl' < 200 mg/l
200 < Cl' < 1000 mg/l
Cl' > 1000 mg/l

Figure 9

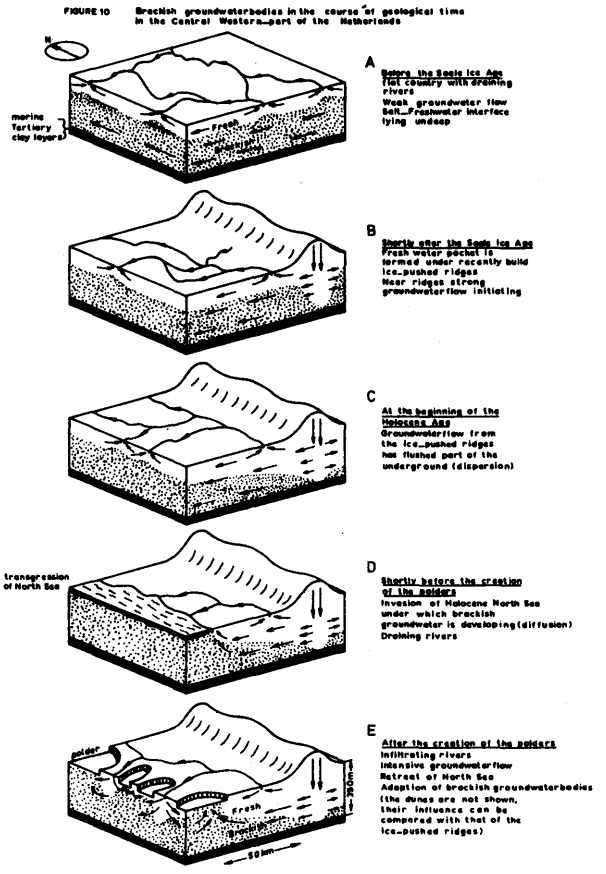
FIGURE 10 Brackish groundwaterbodies in the course of geological time in the Central Western part of the Netherlands
N
marine Tertiary clay layer
fresh
brackish
salt
A
Before the Saale Ice Age
Flat country with draining rivers
Weak groundwater flow
Salt–Freshwater interface lying undeep
B
Shortly after the Saale Ice Age
Fresh water pocket is formed under recently build ice-pushed ridges
Near ridges strong groundwaterflow initiating
C
At the beginning of the Holocene Age
Groundwaterflow from the ice-pushed ridges has flushed part of the underground (dispersion)
transgression of North Sea
D
Shortly before the creation of the polders
Invasion of Holocene North Sea under which brackish groundwater is developing (diffusion)
Draining rivers
polder
fresh
brackish
salt
250m
50km
E
After the creation of the polders
Infiltrating rivers
Intensive groundwaterflow
Retreat of North Sea
Adaption of brackish groundwaterbodies
(the dunes are not shown, their influence can be compared with that of the ice-pushed ridges)

Figure 10

5.3. PROCESSES ACCOMPANYING THE INTRUSION OF SALT WATER

C.A.J. APPELO & W. GEIRNAERT

SUMMARY

Salt-water intrusion and conversely refeshening of water-bearing strata are often accompanied by cation-exchange processes in which $CaCl_2$ or $NaHCO_3$ type water is formed. In the refreshening process $CaCO_3$ solution also takes place. On salinization the deposition of $CaCO_3$ is prevented by simultaneously occurring sulphate reduction.

In various parts of The Netherlands no clear manifestation is found of these cation-exchange processes; on a Piper-diagram analyses plot on the mixing line between $CaHCO_3$ and NaCl type water.

Equilibrium between cations in the salinization or refreshening front and exchangeable cations of the aquifer material was calculated using the Gapon equation. Whether cation exchange is visible in water analyses depends on Cation Exchange Capacity (CEC) of the sediments and concentrations in water. In a refreshening process, the pore volume needs to be flushed a number of times before water composition is unaffected by cation exchange; sea water intrusion gives faster salinization of a fresh aquifer with the same CEC. Mixed water is generally limited to situations where the pore volume has been flushed a number of times by the same water. These above processes are discussed with reference to a borehole in the western Netherlands, where the CEC of soil samples has been determined and compared with groundwater analyses.

1. INTRODUCTION

Glaciation induced sea-level changes in the Pleistocene period have caused alternations of transgressions and regressions in most coastal basins. During periods of low sea-level erosion took place and coarse material was deposited, these sediments being covered by marine clays in the interglacial periods. The aquifers also experienced different phases of salinization and of refreshing.

The last glacial period (Weichselian) and the rapid Holocene sea-level rise still decisively influence the fresh-salt distribution in coastal areas. Infiltration of sea water and the replacement of salt- by fresh water are generally accompanied by cation-exchange processes, which in turn can be used for reconstructing the events which caused an often complex fresh-salt distribution in groundwater bodies.

2. CATION-EXCHANGE PROCESSES

In cation-exchange processes the solid phase of the aquifer interacts with the groundwater. The negative charge of clay minerals, due to substitutions in the lattice, is balanced by adsorption of cations from the groundwater. Absorbed cations are in equilibrium with the ions in solution according to:

$$Na^+ + K^+\text{-clay} \rightleftarrows Na^+\text{-clay} + K^+$$

with the equilibrium constant K being given by:

$$K = \frac{[Na^+\text{-clay}] \cdot [K^+]}{[K^+\text{-clay}] \cdot [Na^+]}$$

The brackets indicate "activity" of the species, i.e. moles/l for the ion in solution, and mequivalents of the absorbed ion/100 g soil.

Cations of higher charge are preferred in exchange reactions, but ion size can also be decisive. Ca is about 1,2 times stronger adsorbed than Mg. Specific adsorption of K results from the good fit of K in the interlayer space of clay minerals and the ion is about 5 times stronger adsorbed than Na.

The definition of an exchange equation is generally easy for exchange between ions of the same charge, but is difficult for ions of differing charge. In the latter case, definition of the exchanger-phase becomes an important, still unresolved problem. BOLT (1967), also BOLT & BRUGGENWERT (1976), suggests use of the Gapon-equation for Na/Ca-exchange when detailed information on the exchanging material is lacking. This equation is also commonly used in irrigation practice for estimating the Exchangeable Sodium Ratio (ESR) in soils. For Na/Ca-exchange the Gapon-equation reads:

$$\frac{[Na\text{-clay}]}{[Ca\text{-clay}]} = K_G \cdot \frac{[Na^+]}{\sqrt{[Ca^{2+}]}}$$

where K_G is the Gapon-constant (≈ 0.5 $(mol/l^{-1/2})$). It should be noted that VAN DER MOLEN (1958) found a certain discrepancy for Dutch soils when using this equation, and as such it must be considered as only an approximation when describing the equilibrium between a solution and the aquifer solid material.

Equilibrium will be disturbed when composition of the solution changes. When sea-water infiltrates an aquifer containing fresh water, Na ions present in sea-water will be exchanged against Ca ions adsorbed on the clays. Sea-water thus becomes $CaCl_2$-type water. The reverse process occurs when fresh water replaces salt water in an aquifer. The fresh water will then change into $NaHCO_3$-type water. Fig. 1 shows composition of the groundwater at an intrusion and replacement front as calculated from the Gapon-formula. It is evident that an increase of Ca in the salinization front is limited, since calcite will be deposited. In the refreshing process decrease of Ca will lead to a renewed dissolution of $CaCO_3$. Ca may then be further exchanged for Na, and HCO_3^- increases to often high values.

2.1. Observed water qualities

The reactions are visible in a number of water analyses plotted in the Piper-diagram of fig. 2. Groundwater analyses are from Zeeland and Western Brabant in The Netherlands, where inundations have often occurred in the past centuries. A mixing line is drawn on the Piper-diagram to represent conservative mixing of sea-water and fresh water. The mark given with each plotted point is directed towards the location on this mixing line based on chloride content of the water samples.

It is clear from fig. 2 that reactions with $CaCO_3$ occur upon refreshing of the aquifer, but are less for salinization. In fact, it seems that water composition evolves in a direction opposite to that which would be expected for an exchange of Na for Ca accompanied by $CaCO_3$-deposition. It is possible that $CaCO_3$-deposition (though occurring) is masked (as a reaction) in the Piper-diagram by SO_4-reduction, since it lowers the % [SO_4 + Cl]. SO_4 reduction also produces CO_2 by:

$$SO_4^{2-} + 2CH_2O \rightarrow S^{2-} + 2CO_2 + 2H_2O.$$

When S^{2-} precipitates with Fe into FeS or FeS_2 (pyrite), the CO_2 can make the water agressive towards $CaCO_3$, so that $CaCO_3$ deposition is actually prevented. Sulfate reduction may still be active in the intruded sea-water analyses plotted in fig. 2, since many of the samples are from shallow depth, taken after the great flood of 1953. Table 1 illustrates some typical examples of $CaCl_2$-type and $NaHCO_3$-type groundwater.

However such a clear manifestation of the cation-exchange process is not always found. In various parts of The Netherlands where refreshening and salinization are taking place analyses plot on the mixing line between $CaHCO_3$ and NaCl type water. This cannot originate from a lack of exchangeable cations since the lithology of formation is not different.

2.2. "Mixed-water"

Cation exchange is dependent on the amount of cations to be exchanged in water and the available cations at exchange sites of the solid aquifer material. For a relatively low CEC of 0,1 meq/100 g used in fig. 1, the fresh-water composition is little affected (less than 10 % of Na- and Ca-concentrations) when 3 pore volumes have flushed the aquifer. For sea-water on the other hand, less than 1/10 of a pore volume is sufficient to salinize the exchange complex of a fresh-water aquifer with the same CEC. This low CEC of 0,1 meq/100 g has been found in coarse sandy Pleistocene sediments in The Netherlands Veluwe area, and is used here to obtain an indication of minimum effects of cation exchange. With an increase in silt content or organic material, CEC increases. Values of 0,5 to 2 meq/100 g have been found in the sandy Pleistocene aquifers, leading to more prolonged exchange effects than shown in fig. 1.

A substantial intrusion of sea- or fresh water must show a compositional change from the intrusion front to inner zones which are not affected by cation exchange. Mixing of water from a spasmodic sea-water intrusion with residing fresh water gives water with an intermediate chloride concentration, but also with signs of cation exchange as in Zeeland and Western Brabant, provided that the CEC's of sediments are large enough. "Mixed water" with a composition that falls on the mixing line given in the Piper-diagram is limited to the situation where the pore volume has been flushed a number of times by the same water.

Flushing situations with brackish water can be expected in estuaries where inundations take place with regular intervals, or at salt-/fresh-water interfaces where groundwater flow is active. These are the environments among others, where "mixed water" is presently observed: under polders directly north of the Nieuwe Waterweg (the Rhine estuary west of Rotterdam), and the fresh-/salt-water interface under the Wadden island Ameland. Typical analyses are shown in table 1.

Table 1. Groundwaters showing "mixed-water" composition, and composition influenced by cation exchange ("$CaCl_2$" and "$NaHCO_3$"-types). Values in mmoles/l.

sea-water		mixed water		$CaCl_2$ water		$NaHCO_3$ water		fresh water
pH	8,22	7,5	7,2	6,91	6,6	8,7	8,3	7,37
Na	485	24,5	54,3	341	124			0,48
K	10,6	0,82	1,42	2,8	2,4	40	2,0	0,05
Mg	55,1	2,93	7,1	27,9	30,7	2,8	1,1	0,07
Ca	10,7	3,04	7,86	39,6	47,2	0,7	0,65	1,31
Cl	566	27,2	73,0	440	271	25,6	1,4	0,73
HCO_3	2,4	9,03	15,3	7,0	3,8	14,4	4,0	2,48
SO_4	29,3	0,07	0	18,8	4,7	2,7	0,2	0,11
% sea-water		5	13	78	48	5	0	0
Location		Ameland		48E	48H	48E	48A	49A
(RID code)				45-1	35-1	69-1	3-3	48-1

In the two analyses given, Na and Mg are within 5 % of concentrations expected from conservative mixing of fresh and sea-water based on Cl-concentrations. Ca and HCO_3 have increased however, as a result of calcite dissolution activated by reduction of sulphate.

3. POLDER GROOT MIJDRECHT

An example of using cation-exchange processes to obtain paleo-hydrological information can be given for the Polder Groot Mijdrecht.

In this polder in the western part of The Netherlands (fig. 3), upconing of salt groundwater due to upward seepage has already been studied by GEIRNAERT (1971). A new deep borehole of The Netherlands Geological Survey could be used for taking undisturbed soil samples. The samples were taken with a coring device under the (hollow) drill bit preventing contamination with the drilling fluid.

A hydrological schematization of this borehole is given in fig. 5 and shows covering layers of Holocene age, water-bearing strata of fluvial Pleistocene sediments and a hydrological base at the change to marine deposits (Maassluis Formation). In the western Netherlands the Holocene is of marine origin, with the transition to fluvial sedimentation lying on the eastern border of the polder. In the aquifer to the west of the polder Groot Mijdrecht covered by marine Holocene deposits, $NaHCO_3$-type groundwater is found showing that the aquifer was subjected to a salinization phase and is now in the process of refreshening.

In the polder Groot Mijdrecht, however, upconing of salt groundwater occurs which is of mixed-water type. This upconing is related to the difference in water level (about 3 m) between the polder canals and lake level at the eastern polder border.

Since the Holocene and the Maassluis Formation are the only marine sediments found in the area, the salinization of the aquifer must have occurred at the onset and during Holocene transgression.

The new borehole was located on the eastern flank of the salt-water cone. It was equipped with 5 piezometer tubes from which water samples were taken on different occasions. The cation-exchange complex was determined from 8 soil samples (fig. 4). Borehole-water analyses fit the regional picture. Water from the bordering lake is found to a depth of 80 m, indicating deep infiltration and groundwater flow towards the polder. Samples 3, 4 and 5 show mixed water. The Cl concentration in sample 5 at a depth of 270 m was 83 meq/l, and is surprisingly lower than the 181 meq/l found in sample 4 at a depth of 240 m. Water sample 3 has a composition that is almost exactly comparable with those taken at shallow depth in other parts of the polder. The soil samples show different compositions. The exchange complex is compared with water compositions in table 2, using the Gapon equation. Soil samples S1 and S2 are in equilibrium with water samples W1 and W2. Soil sample S3 is somewhat "saltier" (contains relatively too much Na) when compared with water samples W3 and W4. Samples S4 to S7 are from the marine Maassluis and Oosterhout formations, but show a fresh-water composition; only the (saltier) sand sample S4 is in equilibrium with water samples W3 and W4.

Table 2. Comparison of water composition and exchange complex of Groot Mijdrecht samples with a Gapon-type equation.

water sample & ratio (*) $\frac{([Ca] + [Mg])}{[Na]}$		soil sample & ratio $\frac{[Na]}{([Ca] + [Mg])}$		K_G (**)
W1	7,94	S1 (sand)	0,04	0,32
		S2 (sand)	0,048	0,38
W2	7,76	S2 (sand)	0,048	0,37
		S3 (sand)	2,15	16,7
		S3 (sand)	2,15	1,9
W3	0,883	S4 (clay)	0,24	0,21
		S5 (sand)	0,52	0,46
		S5 (sand)	0,52	0,46
W4	0,887	S6 (clay)	0,061	0,054
		S7 (clay)	0,102	0,09
		S5 (sand)	0,52	0,34
W5	0,657	S6 (clay)	0,061	0,04
		S7 (clay)	0,102	0,07

(*) [] denotes activity in water (moles/l), or meq/100 g.

(**) $K_G \approx 0,5$ (moles/l)$^{-1/2}$. Deviations point to non-equilibrium: a lower value to salinization, a larger value to freshening of the aquifer.

3.1. Groundwater-flow pattern

By combining the water analyses and adsorption complex a picture emerges of flow patterns in the Groot Mijdrecht polder (fig. 5). Seepage occurs from the eastern lakes towards the low-lying polders. This lake water penetrates to depths of at least 80 m, and in amounts which are sufficiently large to flush the adsorption complex and bring it to equilibrium with the lake water.

Sample S3 at a depth of 75 m, does not fit this picture however, and still has too much Na. It may be that the sandy layer from which the sample is obtained is shielded by clay, and therefore not affected by the different lake water quality. The exchange complex is also too salt for the deeper water, and might represent a still older (more Na-rich) situation.

Mixed water is found beneath the lake water, and also in central parts of the polder at shallower depth. This water has Cl-concentrations of 150 - 160 meq/l, and suggests former salt-water intrusions in the fluviatile deposits. Beneath the "mixed water", a chloride inversion (lowering) is evident in marine formations at a depth of 280 m.

The adsorption complex of these layers at present has a fresh-water composition, thus showing that refreshing of the marine Maassluis formation has taken place. This may have occurred during deposition of the overlying fluviatile deposits.

The CEC's for sand and clay material of the aquifers vary from 0,5 to 20 meq/100g. If the sandy aquifer has on average 0,5 to 1 meq/100 g CEC, the pore volume needs to be flushed 2 to 3 times before the water composition becomes constant, and within 10 % of the measured, mixed concentration in which no cation exchange is visible. The chloride concentration is very uniformly 150 - 160 meq/l in the mixed water (water sample W3 and older samples at shallow depth in the polder).

This might be obtained by mixing through dispersion of original water and a single pulse of intruded water. The amount of flushing, needed to equilibrate the exchange complex, is a number of pore volumes, however. It seems therefore, that the mixed water is a remnant of a brackish flow through the aquifer that was sufficiently continuous to give one water type to a depth of at least 120 m, and also flush the pore volume 2 to 3 times. This flow of large brackish-water volumes means that the fluviatile (Pleistocene) aquifer became totally saline during the Holocene transgression. The existing variation in salt, fresh and brackish water is thus relatively young, and the result of groundwater flow induced by polder reclamation at different levels over past centuries.

In the marine Maassluis formation clay layers have a fresher composition than sandy layers. Water sample W5 has lost Ca in return for Na, indicating that this water freshens the aquifer. Comparison with the exchange complex of clayey samples S6 and S7 points to salinization however, with a calculated value of $K_G \approx 0,05$ (table 2). This cannot be explained with the sample obtained in the present investigation. Reactions in the Maassluis formation will be more complex, since this formation was subjected to at least one refreshening and salinization phase more than the overlying fluviatile deposits.

4. CONCLUSIONS

In the subsurface of The Netherlands alternating fresh-, salt- and brackish-water types are found. In the western part of the country these are the result of sea-level changes in Pleistocene and Holocene times. Indications of past and present flow patterns can be obtained from cation-exchange reactions which are reflected in water composition. A sea-water intrusion front shows $CaCl_2$-type water, while refreshening gives $NaHCO_3$-water. The exchange reactions are accompanied by other reactions, notably dissolution of $CaCO_3$ and reduction of SO_4. Mixed water may be found behind the front when sufficient water has flushed the aquifer to equilibrate the exchange complex.

The comparison of water samples with the exchange complex of soil samples obtained from a borehole in the polder Groot Mijdrecht suggest that the fluviatile Pleistocene aquifer was completely salinized during the Holocene transgression. The present pattern of water types indicates large water flows from the Vinkeveensche Plassen (lake) east of the polder, and slower refreshening from higher lying polders lying more to the west. In groundwater originating from the lake, cation exchange is no longer apparent and the water is in equilibrium with the

exchange complex. In the western part there is still $NaHCO_3$-water present at the fresh/salt boundary, indicating a lesser flow.

The water types can be explained by the present distribution of land surface and groundwater levels, with salt water "bleeding out" of the deep lying polder (VAN DAM, 1976); the rate of "bleeding" depends on local conditions. In the lake to the east of the polder deep sandpits have been dug which permit the rapid infiltration of large amounts of water (ENGELEN, 1981). The polders to the west have a Holocene clay layer which impedes the fresh-water flow towards the polder Groot Mejdrecht. The distribution of water types in the upper fluviatile aquifer is therefore relatively young and is the result of polder reclamation at different levels in the past few centuries. This confirms the qualitative genetic model proposed by DE VRIES (1981) based on Holocene landscape evolution.

ACKNOWLEDGEMENTS

The authors would like to thank Prof. I. Simmers for editing the english text. Discussion of data from borehole 31E176 in the polder Groot Mijdrecht is based on a report by J. van Wieringen and G. Willemsen (1981).

REFERENCES

BOLT, G.H. (1967). Cation-exchange equations used in soil science - a review. Neth. J. Agric. Sci. 15, 81-103.

BOLT, G.H. & BRUGGENWERT, M.G.M. (1976). Soil chemistry - part A. Amsterdam: Elsevier.

DE VRIES, J.J. (1981). Fresh and salt groundwater in the dutch coastal area in relation to geomorphological evolution. Geol. Mijnb. 60, p. 363-368.

ENGELEN, G.B. (1981). A systems approach to groundwater quality. In: Quality of groundwater (W. VAN DUYVENBOODEN et al. (eds.)), p. 1-25, Amsterdam: Elsevier.

GEIRNAERT, W. (1971). Het optreden van kationen-uitwisseling in grondwater. H_2O 4, p. 118-127.

VAN DAM, J.C. (1976). Partial depletion of saline groundwater by seepage. J. Hydrol. 29, p. 315-339.

VAN DER MOLEN, W.B. (1958). The exchangeable cations in soils flooded with sea water. 's-Gravenhage: Staatsdrukkerij.

VANWIERINGEN, J. & WILLEMSEN, G. (1981). Kationenuitwisseling in het grondwater onder de polder Groot Mijdrecht. Inst. Aardwet. VU, intern rapport.

FIGURES

Fig. 1: Change in water composition by cation exchange in the intrusion front: fresh water in salt aquifer and salt water in fresh aquifer. Composition change is shown as a function of passed pore volumes, using the Gapon formula and zero selectivity for Ca/Mg-exchange.

Fig. 2: Piper plot showing compositions of groundwater from Zeeland and Western Brabant, The Netherlands, in which cation exchange is visible. Mark at plotted points is directed towards position on mixing line based on Cl concentration of the groundwater sample.

Fig. 3: Location of new borehole in the polder Groot Mijdrecht with groundwater potentiometric surface.

Fig. 4: Lithology of the new borehole 31E176, showing lithology and ion percentages in water and soil samples.

Fig. 5: Profile over the polder Groot Mijdrecht with groundwater-flow pattern.

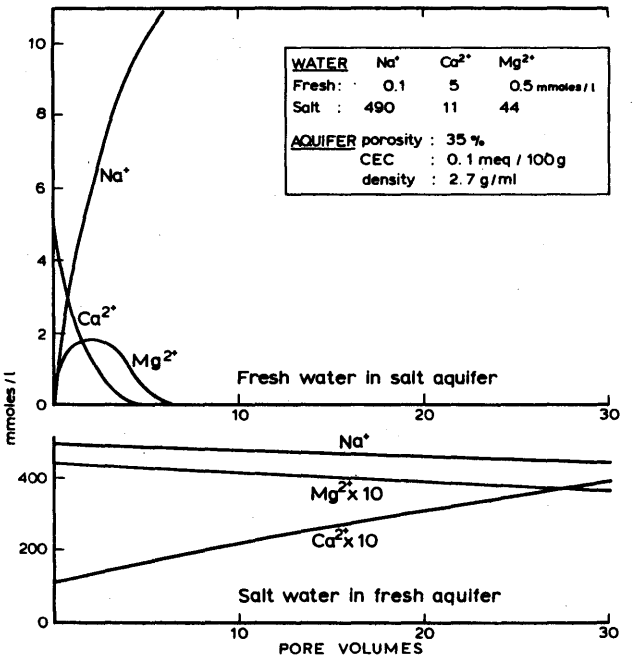

Figure 1

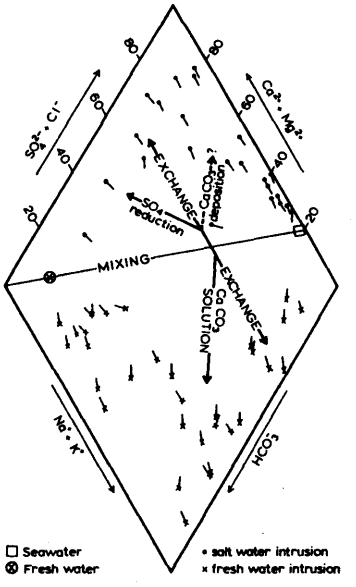

Figure 2

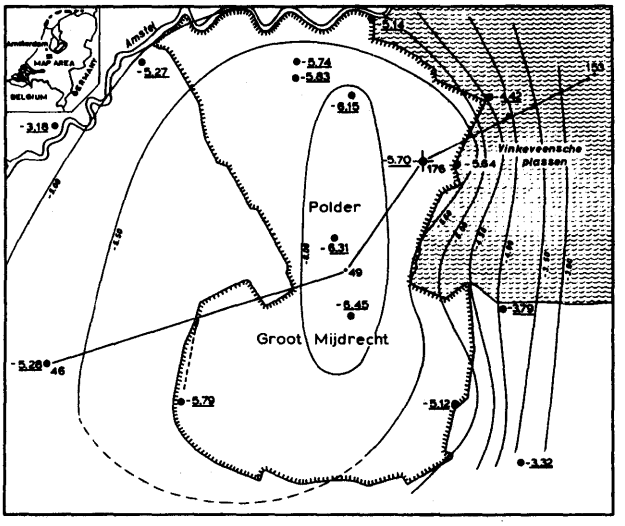

Legend

- Polder Groot Mijdrecht
- new borehole 31 E 176
- test well with piezometric level in m below msl at a depth of around 25 m
- countours of piezometric surface in m below msl
- section (fig.5)
- lake

Figure 3

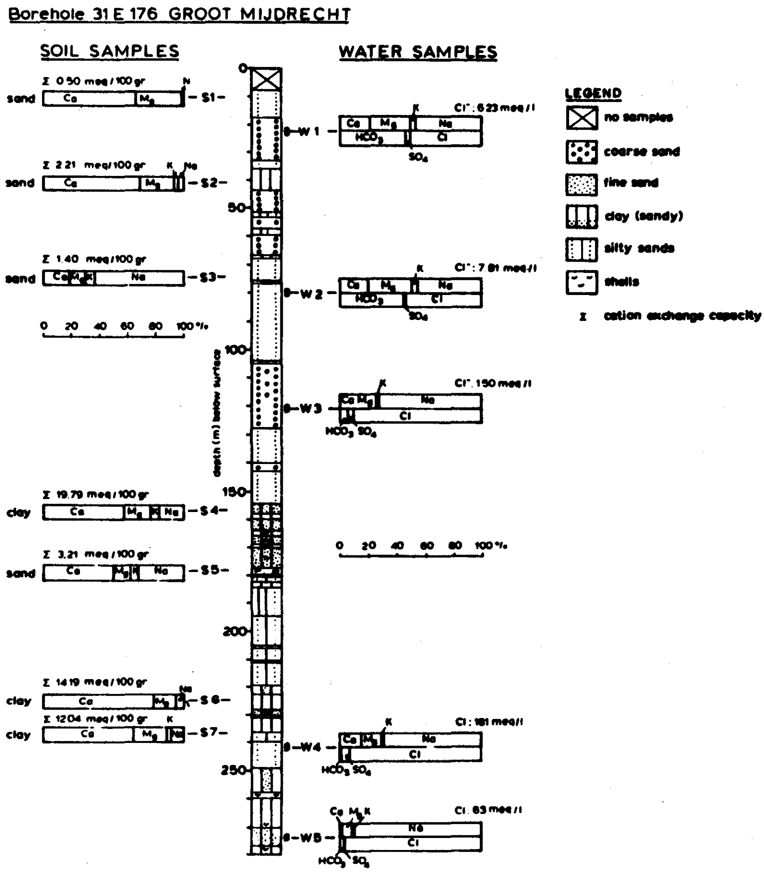

Borehole 31 E 176 GROOT MIJDRECHT
SOIL SAMPLES
WATER SAMPLES
Σ 0.50 meq/100 gr
sand
S1
Σ 2.21 meq/100 gr
sand
S2
Σ 1.40 meq/100 gr
sand
S3
0 20 40 60 80 100 %
Σ 19.79 meq/100 gr
clay
S4
Σ 3.21 meq/100 gr
sand
S5
Σ 14.19 meq/100 gr
clay
S6
Σ 12.04 meq/100 gr
clay
S7
depth (m) below surface
0
50
100
150
200
250
W1
Cl⁻: 6.23 meq/l
W2
Cl⁻: 7.81 meq/l
W3
Cl⁻: 150 meq/l
W4
Cl: 181 meq/l
W5
Cl: 83 meq/l
0 20 40 60 80 100 %
LEGEND
no samples
coarse sand
fine sand
clay (sandy)
silty sands
shells
Σ cation exchange capacity

Figure 4

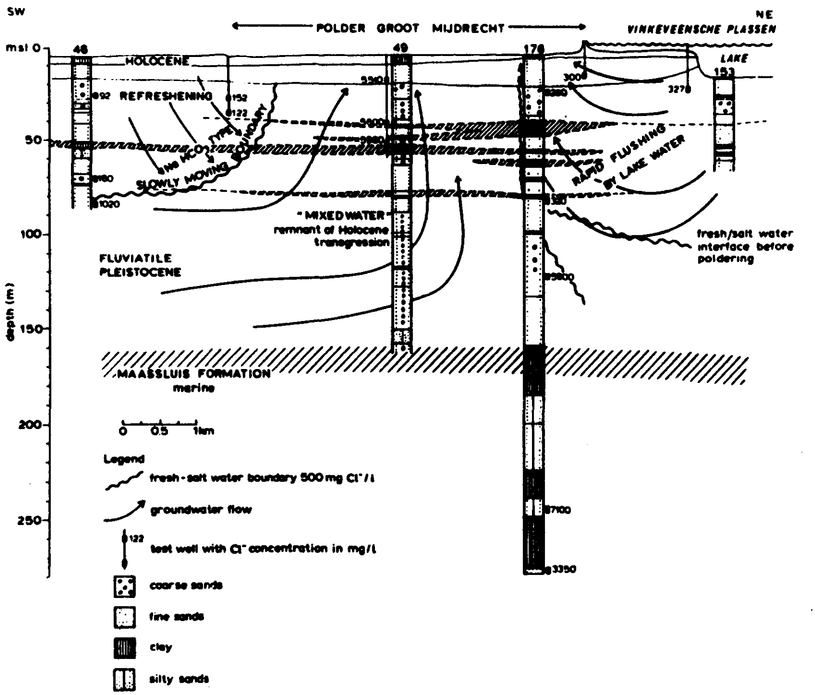
SW
NE
POLDER GROOT MIJDRECHT
VINKEVEENSCHE PLASSEN
LAKE
msl 0
50
100
150
200
250
depth (m)
46
49
178
153
HOLOCENE
REFRESHENING
SLOWLY MOVING
BOUNDARY
RAPID FLUSHING BY LAKE WATER
"MIXED WATER"
remnant of Holocene transgression
FLUVIATILE PLEISTOCENE
fresh/salt water interface before poldering
MAASSLUIS FORMATION
marine
92
152
122
180
1020
5300
300
3270
320
5800
7100
3350
0 0.5 1km
Legend
fresh-salt water boundary 500 mg Cl⁻/l
groundwater flow
test well with Cl⁻ concentration in mg/l
coarse sands
fine sands
clay
silty sands

Figure 5

5.4. PERMEABILITY DECREASE IN COASTAL AQUIFERS DUE TO WATER-ROCK INTERACTION

L.C. GOLDENBERG

SUMMARY

Sea-water and fresh groundwater were made to flow through columns filled with sediments from a "good aquifer" that contain 5 % or less clay minerals.

Hydraulic conductivity (H.C.) decreased very sharply whenever sea-water was flushed by fresh groundwater. The extent of the decrease reached 10^{-1} to 10^{-3} of the orginal H.C.. Subsequent flushing with sea-water restored H.C. only slightly, if at all.

Similar results were obtained when using artificial mixtures of analytically pure sand and montmorillonite. But, illite-sand and kaolinite-sand mixtures were not influenced by the type of the water.

The model that explains the H.C. decrease is based on the formation of water-clay-gel configurations that behave as practically rigid particles and clog the bottlenecks between adjacent pores.

Examination of the hydrological situation of parts of Israel's coastal aquifer yields results similar to these obtained in the laboratory.

1. INTRODUCTION

Hydrological processes characterizing sandy coastal aquifers are the subject of research of this paper. The role of the water-rock interaction in those processes is emphasized related to the behaviour of very minute amounts of clay minerals in a sea-water/fresh-groundwater interface environment.

The analysis, simulation and management of coastal aquifers are usually based on two assumptions: a) Aquifer parameters, especially hydraulic conductivity (H.C.), remain constant throughout the time-span under consideration, and b) the sea-water/fresh-water interface is a movable boundary, modified by the effects of diffusion and hydrodynamic dispersion (BACHMAT & CHETBOUN (1974), KAPULER (1978), MERCER & FAUST (1980), VOLKER et al. (1982).

However, observations in the Israel coastal aquifer contradict these assumptions, and models based on them appear to be inaccurate. Expected intrusion of sea-water over extensive areas near the coastline, where depressions appeared due to intensive pumping, are generally not monitored. At any rate, it is certain that this intrusion is by far not as massive as predicted.

This paper is focussed on the properties of the interface system, and contributes to elucidation of this apparent contradiction. Laboratory experiments were conducted to find out the role of different components of this aquifer zone.

The experimental results indicate that, in sandy coastal aquifers containing a minute amount of montmorillonite, the water-rock interaction may cause a

rapid and very drastic decrease of hydraulic conductivity. In extreme cases such amounts of clay may transform the assumed movable boundary between sea-water and fresh water into a practically fixed one.

2. MATERIALS AND METHODS

The sediments tested were uncontaminated samples taken from research boreholes in Israel's coastal aquifer near Ashdod and near Askelon, wave-washed sands, dune sand (situated 4000 m inland), and pure quartz sand (supplied by B.D.H.). The samples were characterized by grain-size analysis, X-ray analysis for mineralogical composition, permeability and porosity.

The waters used were Mediterranean sea-water, water from the Ashdod aquifer (Table 1), as well as various mixtures of $CaCl_2$ and NaCl solutions of different ionic strength.

Table 1. Chemical analysis of water (in meq/l).

	Na^+	K^+	Ca^{+2}	Mg^{+2}	Cl^-	HCO_3^-	SO_4^{-2}	E.C. (µS/cm)
Aquifer water from Ashdod (1)	3,8	0,1	2,6	2,0	4,6	3,4	0,4	780
Mediterranean sea water (2)	530,0	11,0	22,8	107,3	615,0	2,2	60,0	48.500

(1) Analyses done in the chemical laboratory, Israel Geological Survey, at author's request.

(2) NADLER et al. (1980).

The dispersion of clays was demonstrated by a series of microphotographs. Natural sediments, as well as artificial mixtures of sand and clay, were examined for the effects caused by the passage of various types of fluid by using a petrographic microscope equiped with a camera.

The experimental set-up consisted of: 1) columns equiped with electrodes, which allowed monitoring of the electrical conductivity of the system; 2) calibrated vessels, for introducing and collecting the influent and the effluent.

Small modifications of the experimental set-up were made in the course of the experiments (GOLDENBERG et al., 1983 a).

3. SUMMARY OF EXPERIMENTS AND FIELD OBSERVATIONS

3.1. A series of experiments with sediments from the Israeli coastal aquifer and with artificial mixtures of pure sand and clay reveal that aquifers stay "good" when sea-water, or fresh groundwater, flows through alone. But, when the type of water changes the permeability decreases, arriving in some experiments

at values of one tenth, in others at one thousandth, or even less, relative to their original value (table 2 and fig. 1). During these experiments, in some cases when displacement of saline water by fresh water took place, a cyclic behaviour of H.C. and E.C. was observed. It appeared as an increase in the E.C. values in the columns, which was closely followed by an increase of the H.C. (GOLDENBERG et al., 1983 a). Introduction of a dilute NaCl solution into the sediment rapidly reduced the H.C. by about 3 orders of magnitude (fig. 1, B).

Table 2. Darcy's K-coefficient range of values.

Sample Identification	K-coefficient value	
	maximum value cm/sec	minimum value cm/sec
Zikim N116 6,0 - 6,45 m	$1,63 \cdot 10^{-2}$	$3,33 \cdot 10^{-5}$
Zikim N116 12,0 - 12,45 m	$3,30 \cdot 10^{-3}$	$1,17 \cdot 10^{-4}$
Zikim N113 13,5 - 13,95 m	$4,83 \cdot 10^{-3}$	$4,80 \cdot 10^{-4}$
Zikim N116 36,0 - 36,45 m	$3,77 \cdot 10^{-3}$	$1,36 \cdot 10^{-4}$
Zikim N116 48,0 - 48,26 m	$1,84 \cdot 10^{-3}$	$2,1 \cdot 10^{-4}$
Wadi Soreq Sand	$1,78 \cdot 10^{-3}$	$1,16 \cdot 10^{-6}$

3.2. The matrix components of the aquifer were analyzed in order to establish which of them is responsible for the H.C.-decrease phenomenon. Experiments conducted on various sediments certainly point to the clay fraction as being the responsible one (GOLDENBERG et al., 1983 b). Studies conducted with different types of clay mineral (kaolinite, illite and montmorillonite) show the following results:

a) 1,5 % of montmorillonite in the mixture allows an undisturbed sea water flow. Above this amount, the influence of this type of clay on the H.C. is (fig. 2):

$$K = KO \cdot \exp(-0,85 \cdot C) \quad \text{(eq. 1)}$$

(R: $\log K:C = -0,98$ [0,0063]).

K = hydraulic conductivity (cm/sec),
C = % of clay in the mixture,
R = coefficient of linear regression,
KO = value of K when C = 0 found by linear extrapolation.

b) The H.C. decrease is influenced by illite and kaolinite in sand mixtures to an extent of about one half of that of the montmorillonite:

$$K = KO \cdot \exp(-0,43 \cdot C) \quad \text{(eq. 2)}$$

c) When flushing the sea water by fresh groundwater the system became activated and the H.C. of the sand-montmorillonite mixtures drastically decreased. This was also observed in natural sediments collected from the coastal aquifer. When 3 % and 7,5 % of clay were present, the H.C. decreased drastically to 10^{-6} and 10^{-7} cm/sec respectively. The second value is approximately the experimentally detectable limit. The relation between the clay content and the H.C. value is:

$$K = KO*\exp(-3{,}036*C) \quad \text{(eq. 3)}$$

(R: log K:C = - 0,949)

3.3. a) The shoreward movement of saline water was examined in the Israeli coastal aquifer.

The analyses show: water levels were depressed below sea level over extensive areas near the coast for long periods, but sea water intrusion became a problem only in Tel-Aviv region (hydrological strips 29-32); there, depressions of 4 to 11 m below sea level, at 2 km distance from the shore, were created for a period of 10 - 15 years (fig. 3). Some minor intrusions only were also proved in the Emeq Hefer area.

b) In order to push the interface seawards by creating hydrostatic pressure of high-quality water against the saline water, the pumping in this zone was drastically reduced, or even totally stopped. Fresh groundwater has been introduced, but the T.D.S. content of the water in this zone is still high, about 500 - 2000 mg-Cl/l, as in the last period of intensive exploitation.

c) Introduction of high-quality water in sea-water contaminated wells resulted in rapid head development, without a large quantity of water entering the aquifer.

3.4. Microphotographs of sediments in contact with sea-water and fresh water consecutively, clearly show that a thin coating of clay on sand and intragranular clay packets expand to a large size.

3.5. Dolomite formation is another aspect of the water-rock interaction in the interface zone. Using a scanning electron microscope and x-ray diffractometer, horizons of protodolomite were detected, coinciding with interface zones of different ages. It was found that protodolomite crystals, reaching a size up to 50 µm, were created in voids between the previously existing grains (MAGARITZ et al., 1980). This continuous process of dolomite precipitation in the diffusion zone might also have some effect on the decrease of permeability of coastal aquifers by reducing their pore space.

4. DISCUSSION

1) The relevant processes are summarized in fig. 4.
In stage 1 only one kind of water flows through channels formed by pores of varying size, the clay fraction is in a flocculated state and forms more or less dense packets that coat the grains of the sediment and fill a small part of the pore space. If fresh water flows through the pores flocculation is maintained by the prevalence of Ca ions. If sea-water flows through the pores flocculation is maintained by the high ionic strength. In either case the system remains in a stable, unactivated state.

In stage 2 the type of water is changed and the system becomes activated. If the saline water is displaced by fresh groundwater a dilution occurs, arriving at a threshold value at which the clay fraction is induced towards deflocculation. The clay becomes very reactive, and is partly transformed into small gel droplets with a certain resistance to shearing stress. They float with the flowing water until they become lodged in bottle necks between pores.

As a consequence H.C. of the sediment quickly decreases by a factor of 10^{-4} to 10^{-3}. The system may be said to be in an unstable activated state.

In this stage a cyclic flow behaviour appears under certain conditions, related to the H.C. and E.C. behaviour. Because of different flow velocities, inclusions of the previous type of water are formed. Along their borders gel walls are sometimes formed, and they disappear under certain conditions.

In state 3 connections between pores are, to a large extent, blocked, and permeability has decreased to a very small value. This condition is being characterized by a large "resistance" to changes. This fact means that the process is a practically irreversible one. Even if sea water is made to flow through the pores its interaction with gel droplets proceeds at a very slow rate due to the blocking of passages. The system may be said to be in an activated stable state.

2) One may use the C-factor which appears in the equation given by DAVIS & DE WIEST (1966) for the hydraulic conductivity coefficient (K) in Darcy's law to explain both the field and laboratory results. Hydraulic conductivity (H.C.) can be expressed, by dimensional reasoning, as:

$$K = C * d^2 + \gamma/\mu \quad \text{(eq. 4)}$$

where C is a non-dimensional parameter characterizing connectivity, d^2 is the representative cross-section area of an average pore, γ and μ are specific weight and dynamic viscosity of water, respectively. (In many textbooks d is defined as "average grain size" and C is assumed to refer to a packing parameter as well as to connectivity. The above definition is better suited to our present purpose).

One may argue that the process described above can be interpreted as leading to reduction of the factor C(connectivity).

5. CONCLUSIONS

a) The sea-water/fresh-water interface in a coastal aquifer necessarily shifts on a quasi-geologic time scale due to climatic changes and eustatic changes of the sea level. In an aquifer containing 3 % or more montmorillonite these shifts create a zone of strongly reduced permeability that impedes subsequent shifts of the interface.

An additional fact that acts in the same direction is the existence of a certain amount of suspended matter in the seaward-flowing groundwater. The inorganic fraction of this matter arrives at the interface zone almost in an activated form of pre-gel droplets, contributing to the lowering of the H.C. value. A simulation that ignores this almost impermeable boundary necessarily yields wrong predictions.

b) Attempts to push the interface seaward by artificial recharge of fresh water are likely to clog the aquifer. According to accepted theory, the saline-water front is believed to be pushed seawards, the reality is quite different. Thus, such attempts to push the interface seaward by injection of fresh water in the zone of mixing defeat their own purpose.

c) An interesting scientific ramification concerns the possible transport of fresh water across the interface zone into the sea: it may be assumed that along portions of a sea-water/fresh-groundwater zone the droplets of gel in the pore space form a semi-permeable membrane. This may cause an equilibrium state between the output of fresh water and the head in the two sides of the interface. Quantities of fresh water may be transferred to the sea due to osmotic pressure. The inverse situation may also occur in certain conditions, and quantities of "distilled water" may enter the fresh water part of the aquifer after "desalinization". However, at present, these are only hypotheses.

The above mentioned finding may have great hydrological importance. It may be inferred that fundamental laws regarding the behaviour of aquifers in the interface zone, such as the Ghyben-Herzberg rule, may not be valid, or valid with some modifications. If the passage of fresh water to the sea may be modified by such processes, as small movements of the interface are, one is led to believe that many aquifers may be obstructed in a larger or a smaller measure due to it. Thus, one may state that the interface region behaves as a "bottle neck" for the aquifer system.

ACKNOWLEDGEMENTS

This presentation was made possible thanks to the Goldsmith Prize of the Israeli National Committee of Hydrology Section of I.U.G.G..

I am most grateful to the Goldsmith family.

REFERENCES

BACHMAT, Y. & CHETBOUN, G. (1974). Seawater encroachment in the Coastal Plain of Israel during the period 1958 - 1971. Jerusalem: Ministry of Agr. Water Commission, Hydrological Service.

DAVIS, S.N. & DE WIEST, R.J. (1966): Hydrogeology, London: J. Wiley.

GOLDENBERG, L.C., MAGARITZ, M. & MANDEL, S. (1983 a). Experimental Investigation on irreversible changes of hydraulic conductivity on the seawater-freshwater interface in coastal aquifers. W.R.R., 19(1), 77.

GOLDENBERG, L.C., MAGARITZ, M., AMIEL, A.J. & MANDEL, S. (1983 b). Changes in hydraulic conduvtivity of laboratory sand-clay mixtures caused by a seawater-freshwater interface. I. of Hydrology, (in press), 1983.

ISAAR, A. (1968). Geology of the Central Coastal Plain of Israel. Israel J. of Earth-Sciences 17.

KAPULER, I. (1978). Computation of required quantities of water in the coastal aquifer for a stable situation (in Hebrew), Tahal.

MAGARITZ, M., GOLDENBERG, L., KAFRI, U. & ARAD, A. (1980). Dolomite formation in the seawater-freshwater interface. Nature 287, 622.

MERCER, J.W. & FAUST, C.R. (1980). Groundwater modelling: mathematical models. Ground Water 18, 212.

SCHWARTZ, J., BLANK, D., KAPULER, I. & EVRON, M. (1978). The Tahal use of mathematical models for groundwater, (part a), Tahal, T.A. (in Hebrew).

VOLKER, R.E. & RUSHTON, K.R. (1982). An assessment of the importance of some parameters for seawater intrusion in aquifers and comparison of dispersive and sharp-interface modelling approaches. J.of Hydrology 56, 239.

WATER COMMISSIONER (1975). The Hydrological Service Cross-sections of groundwater levels and pumpage in Coastal Aquifer, 1951 - 1968. Jerusalem (in Hebrew).

PARK, S.C. & O'CONNOR, G.A. (1980). Salinity effects on H.C. properties of soils. Soil Sci. 130, 167-173.

VAN OLPHEN, H. (1966). Clay colloid chemistry. New York: Wiley.

FIGURES

Fig. 1: Permeability decrease in sands.

Fig. 2: H.C. decrease in sand-clay mixtures.

Fig. 3: Hydrological situation in Tel-Aviv region.

Fig. 4: The conceptual approach.

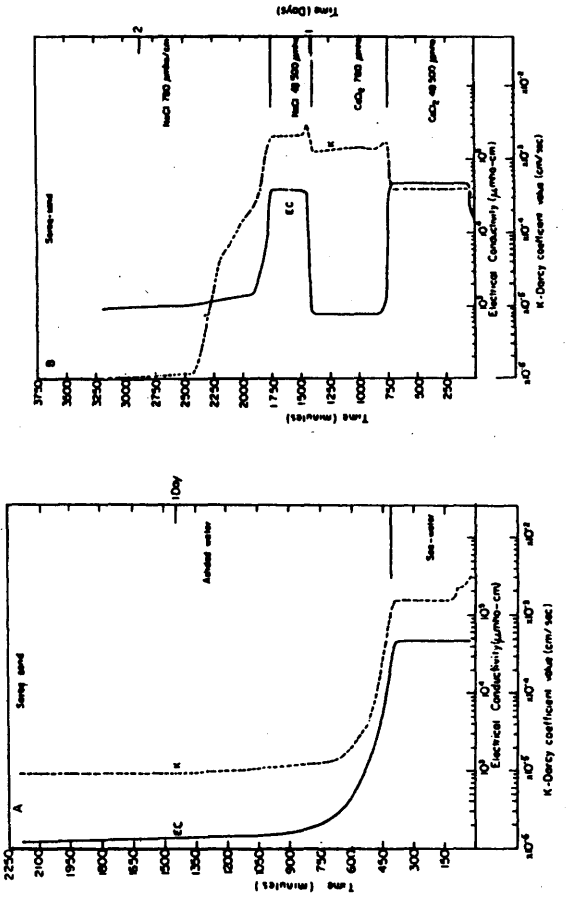
Time (Days)
Sandy-sand
NaCl 780 ppm/cm
NaCl 49 500 ppm
CaCl2 780 ppm
CaCl2 49 500 ppm
EC
K
Electrical Conductivity (μmho-cm)
K-Darcy coefficient value (cm/sec)
Time (minutes)
B
Sandy sand
10dy
Added water
Sea-water
A

Figure 1

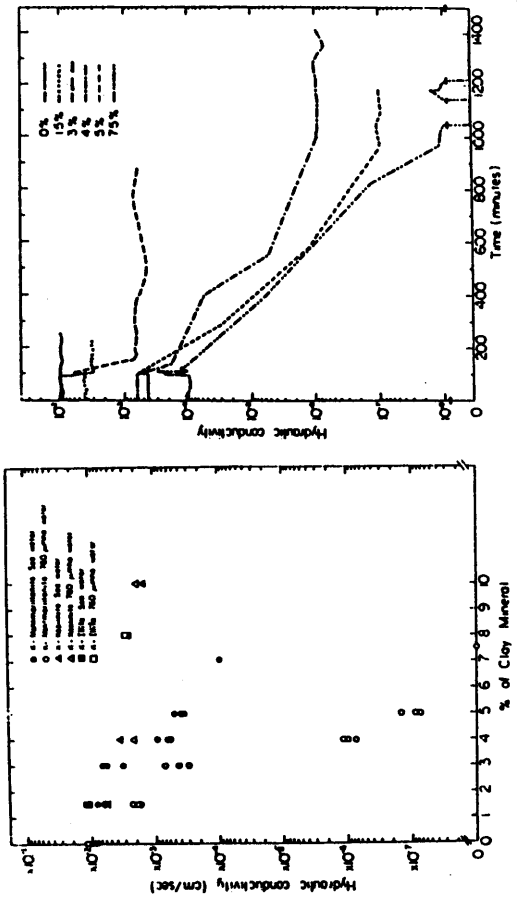
0%
15%
3%
4%
5%
75%
Hydraulic conductivity
Time (minutes)
0
200
400
600
800
1000
1200
1400
Hydraulic conductivity (cm/sec)
% of Clay Mineral
0
1
2
3
4
5
6
7
8
9
10

Figure 2

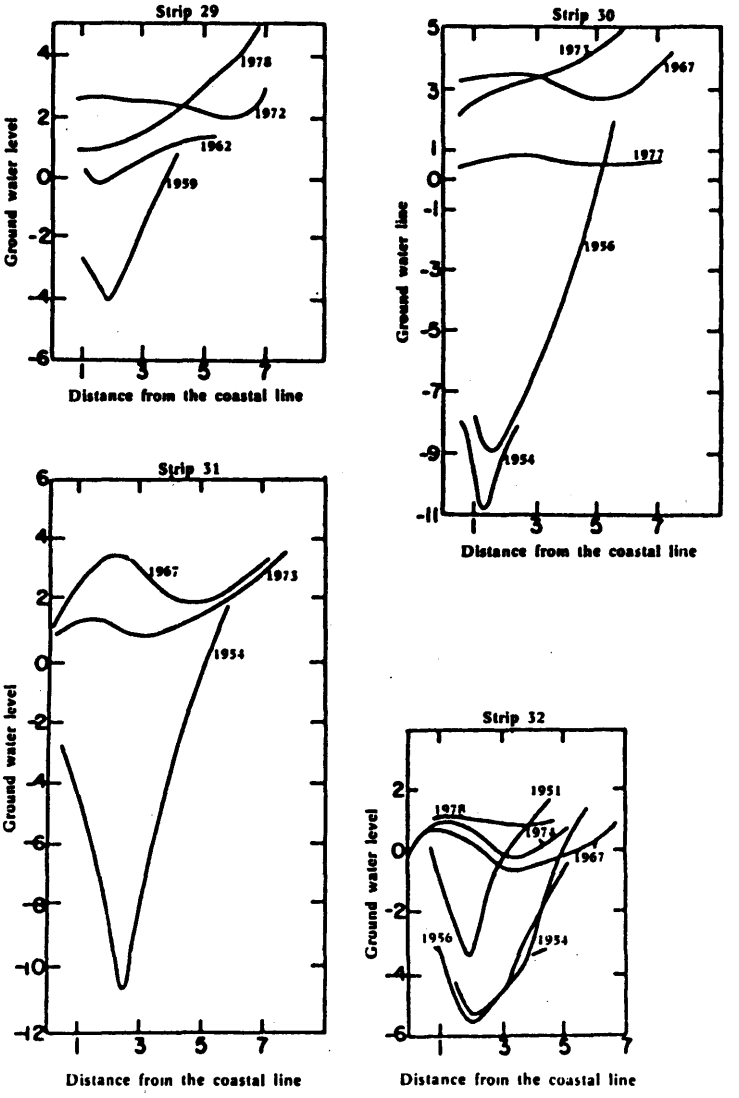
Strip 29
Ground water level
1978
1972
1962
1959
Distance from the coastal line
Strip 30
1973
1967
1977
1956
1954
Ground water line
Distance from the coastal line
Strip 31
1967
1973
1954
Ground water level
Distance from the coastal line
Strip 32
1951
1978
1974
1967
1956
1954
Ground water level
Distance from the coastal line

Figure 3

STAGE 3
Stable activated stage.
"bad aquifer"
STAGE 2
The activation stage
gel formation occur s
Temporary H.C. and E.C.
changes; entrapment of
the previous type of water
STAGE 1
Stable unactivated stage
"good aquifer"

Figure 4

5.5. MIXING PHENOMENA DUE TO SEA-WATER INTRUSION FOR THE INTERPRETATION OF CHEMICAL AND ISOTOPIC DATA OF DISCHARGE WATER IN THE APULIAN COASTAL CARBONATE AQUIFER (SOUTHERN ITALY)

M.D. FIDELIBUS & L. TULIPANO

ABSTRACT

The chemical and isotopic features of waters drained from coastal springs, through which groundwaters of the Apulian karst, carbonate and coastal aquifer flow into the sea, turn out to be mostly affected by mixing phenomena between fresh- and sea-water intrusion waters. Some chemical parameters allow intruding sea-water to be differentiated in the areas considered, depending, above all, on the different residence time in the aquifer of sea-water origin.

Through the isotopic characteristics of mixed water with reference to the isotopic composition of sea-origin groundwater, one is able to trace the original isotopic composition of feeding waters.

From the whole of such information and further data likely to be used as environmental tracers, one is able to obtain more reliable data on the flow system of groundwaters and intruding sea-water on the basis of coastal discharge.

1. EVOLUTION OF CHEMICAL CHARACTERISTICS IN UNDERGROUND SEA-WATER WITH REFERENCE TO DIFFERENT RESIDENCE TIME IN THE AQUIFER

The coastal aquifer of Apulia, made up by Mesozoic limestones and dolomitic limestones, generally permeable by fissuring and karst phenomena, represents an all important pattern in the study of a series of phenomena connected with sea-water intrusion (COTECCHIA, 1977). In the southern part of the region (Salento peninsula) a control network, made up by a series of observation wells (fig. 1), allows sampling of groundwater from different depths, covering the whole range from fresh to salt water.

Chemical features of waters flowing into the aquifer result in simple mixing, in various proportions, between fresh groundwater and intruding sea-water found in the same observation well.

Such a verification permits one to estimate concentration values of single ionic species referring to the same salinity (40 g/l) for the different underground salt waters, thus allowing a more reliable comparison.

The most remarkable differentiations in such waters can be ascribed to Ca^{++} and Mg^{++} contents while the other main constituents prove to be little changed.

The lines representing fresh-water/salt-water mixing (fig. 2 and 3), reconstruct Ca^{++} and Mg^{++} concentration trends relative to the salinity for each observation well. They also allow the determination of the rMg/rCa ratio value in fresh waters (groundwaters), brackish waters (transition zone) and salt water (intruding sea-water) related to the same well (fig. 4). Underground salt waters

then turn out to be characterized by ratio values ranging from 6 (SI3 well) to 2 (Ta well).
The change in such a ratio is partly due to dolomitization phenomena of carbonate rocks, the degree of which may be bound to the different residence times of salt water in the aquifer (TULIPANO & FIDELIBUS, 1984). However, $CaCO_3$ dissolution and precipitation phenomena do bring about changes in the rMg/rCa ratio as well, in relation to the increase or decrease in Ca^{++} concentration value (HANSHAW et al., 1971).

By analyzing minor constituents, Sr^{++}, with respect to the above karst phenomena, may be thought of as being a conservative ion in the carbonate-dissolution process (HARRIS & MATTHEWS, 1968). Such an ionic species occurs in groundwaters and brackish waters according to the degree of mixing.

However, its content turns out to be very different in underground salt waters; concentration values of some 7 mg/l, which are similar to those of sea-water, are found in the SI3 well, while, in underground salt water of the observation wells, concentrations become higher, up to a max. value of some 19 mg/l, peculiar to TA well.

This ionic species, variably occurring in the carbonate rocky matrix, passes into solution together with Ca^{++} during dissolution steps, but the different concentrations reached in underground sea-waters, above all in those showing very close Ca^{++} concentrations, may lead to the conclusion that not only are they to be connected with the occurrence of steps of dissolution, but also of those of precipitation. These latter would preferably involve Ca^{++} ions keeping Sr^{++} ions in solution. This way underground waters of sea origin, undergoing numerous and alternate events relating to karst phenomena, may show their effects in the high Sr^{++} values, as a proof of steps of dissolution reaching a higher degree than that revealed by Ca^{++} contents, which undergoes precipitation too, as assumed.

By such premises, the investigation of mutual variations in Mg^{++}, Ca^{++} and Sr^{++} contents, represented for each underground salt water in fig. 5, is likely to give useful information on the evolution that intruding sea water has undergone in the different areas. The progressive decrease in Mg^{++} contents, starting from max. values peculiar to present or recently intruded sea-waters (such as SI3 waters coming under an area of a tested salt-water recycling) and the simultaneous increase in Ca^{++} contents, indicate the occurrence of dolomitization phenomena.

However, the increase of Ca^{++} contents proves to be higher, in most cases, than dolomitization processes only would allow. The degree of such Ca^{++} surplus against the increase by dolomitization only appears irregularly variable, unless it is reviewed through the evaluation of its Sr^{++} content increase. Once the value of content in the parent rock is known, the ratio between Sr^{++} content increase and Ca^{++} surplus is able to supply an evaluation of Ca^{++}

content acquired during processes of dissolution and possibly lost by consecutive precipitations (fig. 6).

However, from a qualitative standpoint it is also possible to give an explanation of data: when for instance, facing considerable increases in Sr^{++} content, it seems there is nothing but a Ca^{++} quantity equal to that resulting from dolomitization (LR well). Conversely it may be asserted that dissolution processes have taken place, but the mighty precipitation phenomena have cancelled out the effect.
In the light of what has been said, a hypothesis about intruding sea-water circuits may be put forward.

By considering the south-western area of the Salento Peninsula, a meaningful change of chemical features, which have been presented so far, can be noticed moving toward the Adriatic shoreline starting from SI3 well, penetrating intruding sea-water. The rMg/rCa value ratio becomes lower and lower in the area under study, reaching a minimum value in underground sea-water at the SR well, next to the Adriatic coast, where dolomitization action seems to have reached a maximum.

Going from the Ionian Sea to the Adriatic Sea, Sr^{++} contents also indicate changes in the degree of dissolution processes, induced by underground salt water.
The permeability features along the Ionian coast justify the fact that the areas considered are affected by present day intrusion.

Miocene formations, often impervious, outcropping along wide stretches of the Adriatic coast, act as a barrier against sea-water intrusion. As such in view of hydrogeological knowledge and salt-content distribution in groundwaters, what has been asserted so far should lead one to assume that intruding sea-waters, occurring throughout the middle area of the Salento peninsula, undergo a slow recycling by sea-water seeping through the mainland mostly from the Ionian coast.
Such a recycling is indeed favoured by groundwater pumping which, at present, drains remarkable quantities of waters contaminated by underground salt water.

2. IDENTIFICATION OF THE CHARACTERISTICS IN UNDERGROUND SALT WATER DRAINED BY MIXING FROM COASTAL SPRINGS

The discharge into the sea of groundwaters throughout the area in question takes place by means of a series of coastal springs, generally draining brackish waters. These result from fresh groundwaters, from recharge areas and the mixing of underground salt water.
The main springs, as far as flow rate is concerned, are concentrated in type.

Fig. 1 shows the location of some of them, representing hydrogeologically different situations. Of the Adriatic coastal springs, all those emerging NW of Brindisi are directly fed by the main hydrogeological system made up by limestones of the Cretaceous, in which the groundwater floats on intruding sea-water; the one examined South of Brindisi (Idume spring) is fed by a shallow aquifer made up by Neogene-Quaternary calcarenites with an impermeable marly calcarenite layer at the base, transgressive on the Cretaceous formation. Sea-water intrusion, moving from the Adriatic coast to the hinterland, affects only shallow aquifers, while, as previously said, salt water in the deep aquifer seems to have nothing to do with present sea waters. On the Ionian side, the Taranto spring group and the Chidro and Boraco springs are examples of conspicuous concentrated discharges fed by the Mesozoic aquifer. Such springs gush forth from discontinuities in the clayey Pliocene-Quaternary layer, transgressive on Cretaceous formations along the whole coastal strip stretching from Taranto to some 10 km east of the Chidro spring.

By considering the fact that the main features in underground salt water, resulting from dolomitization and dissolution processes, are fully shown in the Mg^{++} vs. Sr^{++} diagram, the salt-water component of brackish water drained from each spring may be easily related to one of the possible types of underground salt water in the aquifer, by comparing their concentrations in the above mentioned ions with the trend of the mixing lines obtained from each observation well. Fig. 7 shows that the Adriatic coastal springs generally display a salt-water component which may be ascribed to quite a recent intrusion, while those of the Ionian coastal ones seem to be mixed with sea-waters having a more complex history.

3. PROVENANCE OF THE FRESH-WATER COMPONENT IN THE BRACKISH COASTAL SPRING WATERS

The results of our studies enable us to put forward some hypotheses about underground-water history. Such waters proved to be differentiated, above all, by their different residence times in the aquifer.

Absolute-age evaluations by means of the C-14 method, carried out on some previously examined intruding sea-waters, confirm the differentiations which have been found (COTECCHIA et al., 1977). Conversely, the stable isotope compositon does not, and that is why it becomes a reference point in tracing back the primary isotopic features of the fresh-water component, when underground waters are mixed with water of sea origin.

The samples taken at different depths, in some previously considered observation wells, show the mixing effect in their isotopic compositions. The change in stable isotope contents as a function of salinity, permits the extrapolation of isotopic characteristics of fresh groundwaters (0,3 - 0,5 g/l).

The δD - $\delta^{18}O$-diagram in fig. 8 shows isotopic characteristics of the fresh-water component deduced from values peculiar to samples of mixed water which have been taken in each observation well.
The resulting values thus prove to be correlated to isotopic data concerning some fresh spring waters, absolutely not contaminated by the sea, which were sampled in the Salento.
Obviously, this methodology is also useful for determining the provenance of fresh-water components in the brackish coastal spring waters.

The isotopic-content evaluation of such a fresh-water component was carried out by assuming that the mixing process occurred with sea-waters slightly differentiated isotopically speaking.
The available information relates to isotopic differentiations which occur during replenishment processes.

By way of example, in fig. 9 the isotopic characteristics of the fresh-water component concerning the springs of the Salento, are compared with those pertaining to another spring group (Trani spring group in Murgia area) deriving its replenishment from higher zones than the region under examination (fig. 1).
In this way, the differentiation between the examined waters is fully demonstrated.

On the one hand, trends comparable to evaporation lines link groundwaters to each other, thus connecting them to replenishment areas, topographically similar in height, but with a different infiltration percentage of replenishment rains. On the other hand, intercept values on the meteoric line, considered as representative for the whole studied region, show different average characteristics of replenishing rain waters: enriched values differentiate waters replenishing the Salento as compared with the depleted values of waters replenishing the adjacent Murgia.

REFERENCES

COTECCHIA, V. (1977). Studies and investigations on Apulian groundwaters and intruding sea-waters (Salento Peninsula). Quad. Inst.Ricerca Acque C.N.R. 20.

COTECCHIA, V., MAGRI, G. & TAZIOLI, G.S. (1974). Isotopic measurements in research on seawater ingression in the carbonate aquifer of the Salentine Peninsula, Southern Italy. In: Isotope Techniques in groundwater hydrology 1974, Vienna: I.A.E.A., 445-463.

FIDELIBUS, M.D. & TULIPANO, L. (1985). Determination of the isotopic characteristics of the waters feeding the coastal aquifers of the Murgia and Salento (Apulia - Southern Italy), deduced from an examination of the isotope contents of groundwaters mixed with waters of marine origin. Proc. V Int. Symp. on Ground., November, 1985 Taormina.

HANSHAW, B.B., BACK, W. & DEIKE, R.G. (1971). A geochemical hypothesis for dolomitization by ground water. Econ. Geol. 66, 710-724.

HARRIS, W.H. & MATTHEWS, R.K. (1968). Subaerial diagenesis of carbonate sediments: efficiency of the solution-reprecipitation process. Science 160, 77-79.

TULIPANO, L. & FIDELIBUS, M.D. (1984). Geochemical characteristics of Apulian coastal springs water (Southern Italy) related to mixing processes of ground waters with sea water having different residence time into the aquifer. 5th Int. Conf. on Water Resources Planning and Man., 1984, Athens, pp.2.55-2.67.

FIGURES

Fig. 1: Location of observation wells and springs under examination.

Fig. 2: Ca^{++} concentration vs. TDS relationships.

Fig. 3: Mg^{++} concentration vs. TDS relationships.

Fig. 4: rMg/rCa ratio vs. TDS relationships.

Fig. 5: Ca^{++}, Mg^{++} and Sr^{++} concentrations of salt groundwaters and sea-water.

Fig. 6: Variations of Ca^{++}, Mg^{++} and Sr^{++} contents in salt groundwaters referred to sea-water.

Fig. 7: Mg^{++} and Sr^{++} contents of brackish spring waters compared with those evaluated for mixed groundwater in the observation wells.

Fig. 8: Stable isotope contents of the waters sampled in observation wells and trend of mixing.

Fig. 9: Classification of spring waters on the basis of theoretical isotope composition of the relative fresh-water components.

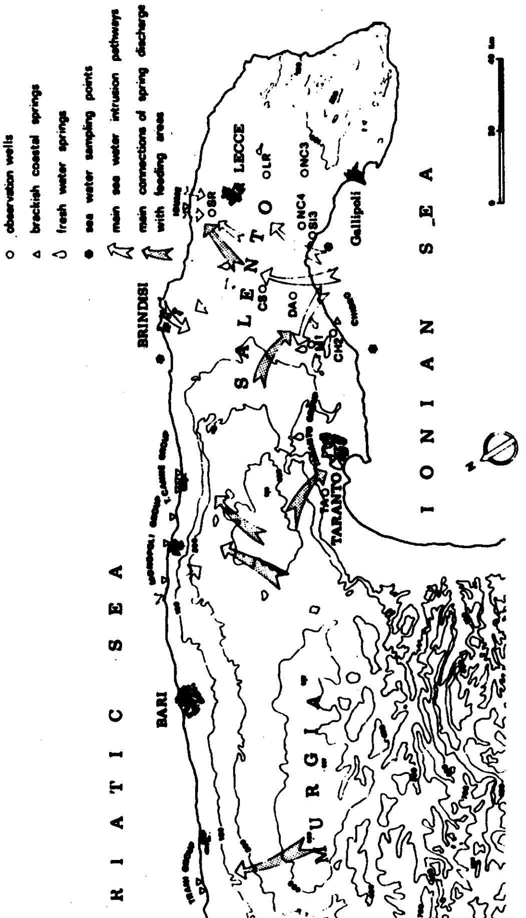
observation wells
brackish coastal springs
fresh water springs
sea water sampling points
main sea water intrusion pathways
main connections of spring discharge with feeding areas
ADRIATIC SEA
IONIAN SEA
BARI
BRINDISI
LECCE
TARANTO
Gallipoli
MURGIA
SALENTO

Figure 1

Figure 2

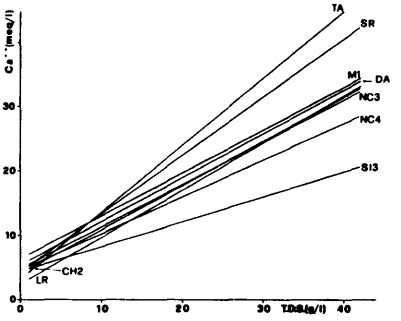

Figure 3

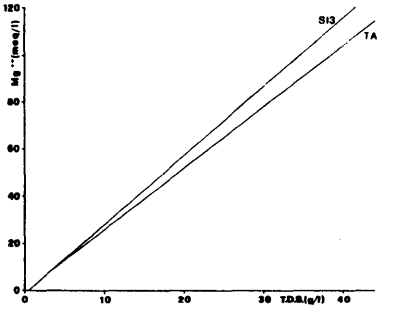

Figure 4

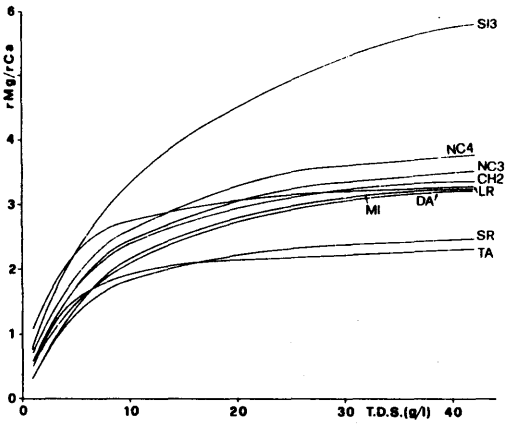

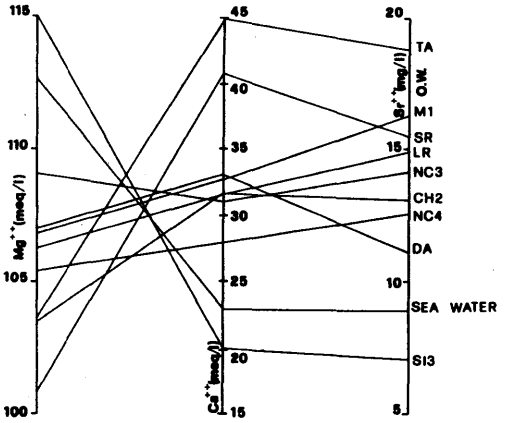

Figure 5

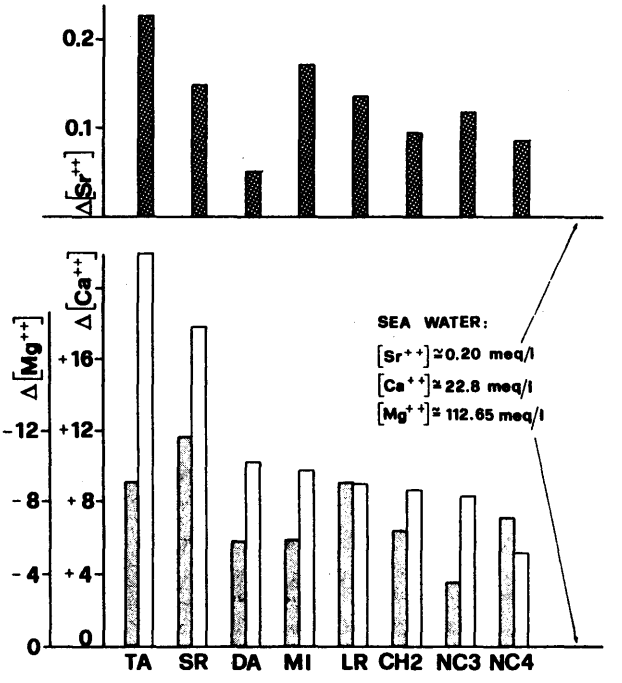

Figure 6

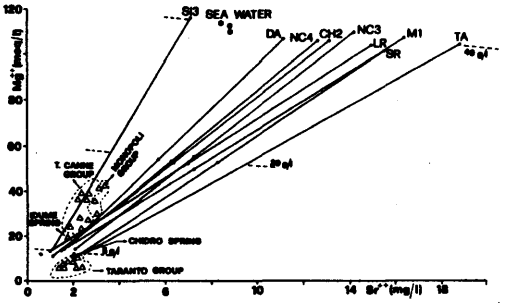

Figure 7

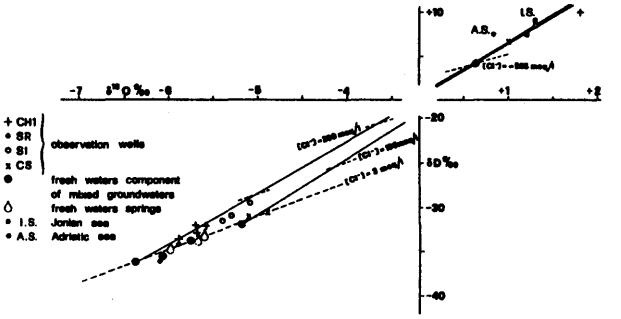

Figure 8

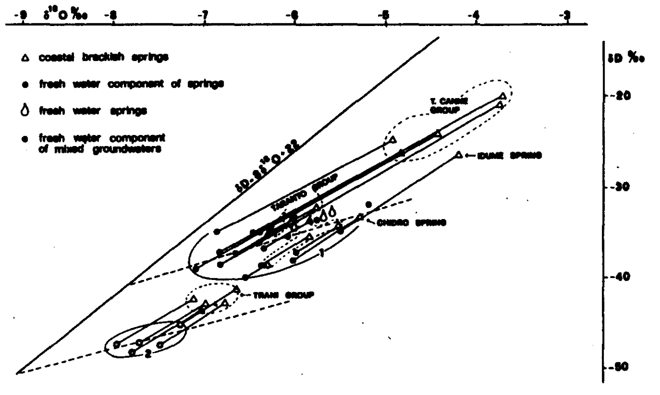

-9 δ18O ‰ -8 -7 -6 -5 -4 -3
δD ‰
-20
-30
-40
-50
coastal brackish springs
fresh water component of springs
fresh water springs
fresh water component of mixed groundwaters
T. CANNE GROUP
IDUME SPRING
TARANTO GROUP
CHIDRO SPRING
TRANI GROUP
1
2

Figure 9

5.6. A NEW HYDROCHEMICAL CLASSIFICATION OF WATER TYPES: PRINCIPLES AND APPLICATION TO THE COASTAL-DUNES AQUIFER SYSTEM OF THE NETHERLANDS

P.J. STUYFZAND

ABSTRACT

The hydrochemical classification system presented here combines excellent features of existing classifications with new, strongly diagnostic criteria for subdivision. This results in an easier identification of cation-exchange phenomena, e.g. due to salt- or fresh-water intrusion, and in the applicability to a broader spectrum of hydrochemical environments. A hierarchical structure, high flexibility and logical coding guarantee an easy handling of a sophisticated system. As an example, the areal distribution of water types in the coastal dunes near Castricum, North Holland is discussed, focussing upon cation exchange due to fresh- and salt-water intrusion.

1. INTRODUCTION

MATTHESS (1982) summarizes approximately 10 different systems of classification of natural water types. His selection constitutes only the top of an iceberg. Are there more inventors than adherants? Apparently, each system lacks a subdivision, which is subtle (diagnostic) and logical enough to satisfy a large group of users.
The method presented here combines several excellent features of other classifications with new, strongly diagnostic criteria for subdivision. The first version (STUYFZAND, 1985) had been developed specifically for groundwaters in coastal, calcareous-sand aquifer systems with cation-exchange phenomena due to fresh- or salt-water intrusion. The present, second version has been extended with subdivisions useful for non-calcareous systems, e.g. those suffering from acidification or from the excessive application of manure c.q. fertilizers. Therefore, the classification can be applied to water in any hydrological compartment and in most geochemical systems.
Examples of application of the classification will be given for the aquifer system near Castricum, in the coastal-dune area of the Western Netherlands.

I hope of course, that this classification will also be applied elsewhere in the world. Eventual failures or additions and suggestions for perfection will be received with pleasure.
These will be remedied c.q. incorporated and then published in a next version.

2. THE CLASSIFICATION SYSTEM

2.1. General aspects

The determination of a water type implies the successive determination of the main type, type, subtype and class of the water sample. This hierarchical structure is elucidated in fig. 1.

Each of the four levels of subdivision contributes to the total code (and name) of the water type, as shown in fig. 2. With 6 main types, 11 types, 16 subtypes and 3 classes the theoretical maximum number of water types amounts to 3168. Of course many water types do not exist in nature, which reduces the total number to a few hundred. Clearly, in complex situations the total number of water types might still be confusingly and unnecessarily high. In that case several water types or even classification units should form a so called association.

Guidelines to form sensible associations as well as further differentiations are given in section 2.6.

2.2. Main types

The chloride content determines the main type, as indicated in table 1. The boundaries are based upon:

- the drinking-water standard (150 mg l^{-1}) in the European Community;
- the upper boundary of most meteoric recharge water in The Netherlands (< 300 mg l^{-1});
- boundaries reported by DGV-TNO in geophysical surveys of the fresh-salt interface of groundwater in The Netherlands (150 and 1000 mg l^{-1});
- the upper Cl-concentration of normal sea-water (close to 20,000 mg l^{-1});
- the Cl-concentration (10,000 mg l^{-1}) of a fifty-fifty mixture of fresh water and sea-water.

Table 1. Division in main types on the basis of chloride concentration.

Main type	code	Cl^- mg l^{-1}	Main type	code	Cl^- mg l^{-1}
fresh	F	$\leq$ 150	brackish-salt	B_s	10^3 - 10^4
fresh-brackish	F_b	150 - 300	salt	S	10^4 - $2,10^4$
brackish	B	300 - 10^3	hyperhaline	H	> $2,10^4$

2.3. Types

Each main type is further subdivided into a maximum of 11 types (table 2), according to the total hardness (mainly Ca + Mg) in mmol l^{-1}. The upper boundary of each type is defined by:

$$\text{upper boundary type } X = 2^X$$

where X is an integer between -1 and 9.

Table 2. Subdivision of main types into types on the basis of total hardness (mainly Ca + Mg).

type no.	type name	code	total hardness mmol l^{-1}	natural occurrence
-1	very soft	*	0 - 1/2	F
0	soft	0	1/2 - 1	F F_b B
1	moderately hard	1	1 - 2	F F_b B B_s
2	hard	2	2 - 4	F F_b B B_s
3	very hard	3	4 - 8	F F_b B B_s
4	extremely hard	4	8 - 16	F_b B B_s S
5	extremely hard	5	16 - 32	B_s S H
6	extremely hard	6	32 - 54	B_s S H
7	extremely hard	7	64 - 128	S H
8	extremely hard	8	128 - 256	H
9	extremely hard	9	$\geq$ 256	H

2.4. Subtypes

Cation and anion preponderate in the ion balance determines more or less traditionally, through their combination, the name of a water type (here "subtype"). However, in this classification the cation or anion with the highest meq l^{-1} does not necessarily determine the name.
First the strongest geohydrochemical family is determined both for cat- and anions, e.g. the [Al + H + Fe + Mn] - and [SO_4 + NO_3 + NO_2] - family. Then, the strongest member of both families is chosen to form the combination. Fig. 3 and table 3 help to clarify the subdivision of types into subtypes.
The theoretical maximum number of subtypes amounts to 9 x 6 = 54. So far only 16 subtypes have been discovered, namely those cited in table 3.

2.5. Classes

Each subtype is subdivided into 3 classes (table 4) according to a new parameter: the sum of Na, K and Mg in meq l^{-1} corrected for a contribution of sea salt, abbreviated as:

$$\{Na + K + Mg\}\ corr = [Na + K + Mg]\ measured - 1{,}061\ Cl$$

The factor 1,061 is equal to {(Na + K + Mg)/Cl} in meq l^{-1} for mean ocean water (RILEY & SKIRROW, 1965).

Table 3. Determination of 16 hitherto discovered subtypes. Σk = sum cations; Σa = sum anions.

subtypes	conditions, in strict order, in meq l^{-1}
NaCl	$(Na+K+NH_4) > 1/2\ \Sigma k$; $(Na+K) > NH_4$; $Na > K$; $Cl > 1/2\ \Sigma a$
$NaSO_4$	as NaCl, however $(SO_4+NO_3+NO_2) > 1/2\ \Sigma a$; $SO_4 > (NO_3+NO_2)$
$NaHCO_3$	as NaCl, however $(HCO_3+CO_3) > 1/2\ \Sigma a$; $HCO_3 > CO_3$
NaMix	as NaCl, however Cl and $(SO_4+NO_3+NO_2)$ and (HCO_3+CO_3): $< 1/2\ \Sigma a$
KNO_3	as NaCl, however $K \geqq Na$; $(SO_4+NO_3+NO_2) > 1/2\ \Sigma a$; $(NO_3+NO_2) \geqq SO_4$
NH_4SO_4	as $NaSO_4$, however $NH_4 \geqq Na+K$
CaCl	$(Na+K+NH_4) \leqq 1/2\ \Sigma k$; $(Ca+Mg) > (Al+H+Fe*Mn)$; $Ca > Mg$; $Cl > 1/2\ \Sigma a$
$CaSO_4$	as CaCl, however $(SO_4+NO_3+NO_2) > 1/2\ \Sigma a$; $SO_4 > (NO_3+NO_2)$
$CaNO_3$	as $CaSO_4$, however $(NO_3+NO_2) \geqq SO_4$
$CaHCO_3$	as CaCl, however $(HCO_3+CO_3) > 1/2\ \Sigma a$; $HCO_3 > CO_3$
CaMix	as CaCl, however Cl and $(SO_4+NO_3+NO_2)$ and (HCO_3+CO_3): $< 1/2\ \Sigma a$
MgCl	as CaCl, however $Mg \geqq Ca$
$MgHCO_3$	as $CaHCO_3$, however $Mg \geqq Ca$
MgMix	as CaMix, however $Mg \geqq Ca$
$AlSO_4$	$(Na+K+NH_4) \leqq 1/2\ \Sigma k$; $(Al+H+Fe*Mn) \geqq (Ca+Mg)$; $(Al+H) \geqq (Fe+Mn)$; $Al > H$; $(SO_4+NO_3+NO_2) > 1/2\ \Sigma a$; $SO_4 > (NO_3+NO_2)$
$FeSO_4$	as $AlSO_4$, however $(Fe+Mn) > (Al+H)$ and $Fe > Mn$

It is assumed that all Cl-ions originate from the sea (ERIKSSON, 1952), that fractionation of the major constituents of sea-water upon spraying can be neglected (DUCE & HOFFMAN, 1976; VERMEULEN, 1977) and that Cl behaves conservatively.

The class boundaries at $\pm \sqrt{1/2}$ Cl form a compromise between the expected analytical errors and a meaningful genetic differentiation of water types.

Salt-/fresh-water intrusion and {Na+K+Mg} corr.

Salt-groundwater in- and extrusion generally bring about the following cation-exchange reaction, at least in The Netherlands (VAN DER MOLEN, 1957; STUYFZAND, 1985 in prep.):

Table 4. Subdivision of subtypes into classes according to {Na+K+Mg} corrected for sea salt.

class	code	condition (meq L^{-1})
{Na+K+Mg} deficit[1]	-	{Na+K+Mg} corr < $-\sqrt{1/2\ Cl}$
{Na+K+Mg} equilibrium	φ	$-\sqrt{1/2\ Cl} \leq$ {Na+K+Mg} corr $\leq +\sqrt{1/2\ Cl}$
{Na+K+Mg} surplus[2]	+	{Na+K+Mg} corr > $\sqrt{1/2\ Cl}$

1 = often indicating a (former) salt water intrusion.
2 = often indicating a (former) fresh water encroachment.

$$Ca^{++} + \{\alpha Na,\ \beta K,\ (1 - 1/2\alpha - 1/2\beta)Mg\text{-clay} \rightarrow [Ca]\text{-clay} + \alpha Na^{+} + \beta K^{+} + (1 - 1/2\alpha - 1/2\beta)Mg^{++},$$

if clay forms the exchanger and with $0 \leq \alpha + \beta \leq 2$.

With fresh-water encroachment, Ca expels the formerly adsorbed Na-, K- and Mg-ions from the exchanger. The above reaction proceeds consequently from the left to the right, causing a significant {Na+K+Mg} surplus. With salt-water intrusion the reverse takes place.

Na, K and Mg do not always ad- or desorb simultaneously during salt- respectively fresh-water intrusion. In the case of $MgHCO_3^-$-water e.g., mainly Mg and K have been desorbed, as the more easily desorbable Na was already exchanged against Ca at an earlier stage (WITT & WIT, 1982; STUYFZAND, 1985).

Under ideal circumstances, which prevail in The Netherlands, {Na + K + Mg}- corr thus determines the sign and quantifies the (total) cation-exchange reaction, induced by a (former) change in the position of the fresh-salt interface.

Serious complications occur when (a) minerals containing Na, K and/or Mg, like feldspars and dolomite, dissolve; (b) biomass mineralizes, (c) manure/fertilizer is leached; (d) minerals transform with an uptake of Na, K and/or Mg, e.g. during dolomitization; (e) new minerals, containing Na, K and/or Mg form; and (f) biomass is synthesized.
Complications a-c can cause a {Na + K + Mg} surplus, whereas complications d-f can create a {Na + K + Mg} deficit.

2.6. Flexibility: association and differentiation

The classification provides a high flexibility to cope with the needs to simplify or to further differentiate, whenever a situation is too complex resp. too monotonous.

In coastal, calcareous aquifers with salt-water intrusion, the association of the main types F + F_b into F, B + B_s into B and of the "types" 4-9 into one category (extremely hard) or even the omission of all "types" can be advantageous.
A further differentiation can be useful, when groundwaters within one classification unit but with a different origin occupy one aquifer system, e.g. autochtonous, infiltrated atmospheric water and artificially recharged, allochtonous surface waters. The latter can be coded with e.g. an "R" before position 1 (main type) in fig. 2, or at position 1 when the Cl-content falls within one main type.

3. APPLICATION TO THE COASTAL DUNES NEAR CASTRICUM

Under the coastal dunes and adjacent shallow polders near Castricum (fig. 4), a fresh-water lens is floating on intruded North Sea-water. The areal distribution of water types is given in cross section AA' (fig. 5) and BB' (fig. 6) and in a horizontal section at about 25 m - Ordnance Datum (fig. 7).
The applied associations and differentiation are repeated in fig. 5 - 7. For stylistic purposes the symbol "φ", pointing at {Na + K + Mg} equilibrium, is omitted at the end of the coding. The total hardness of all water types (also omitted in the coding) is $\geq$ 2 mmol l^{-1} (type $\geq$ 2).

Clearly, the artificially recharged Rhine water (since 1957) is penetrating the deep aquifer between 50 and 90 m-OD through erosional gaps in the glacial till at 40 - 50 m-OD (fig. 5).
In general, water types with a {Na + K + Mg} surplus, which points here exclusively at a fresh-water encroachment, fringe the fresh-water lens:

a) at the bottom, because of a slow extension of the fresh-water lens with depth as a reaction to the strong widening of the coastal-dune belt between 950 and 650 years B.P. (ZAGWIJN, 1984);

b) on the inland side, because the eastward fresh-water flow had been extended as a consequence of the reclamation of marshland east of the dunes, particularly in the deep Schermer polder in 1635 (fig. 5);

c) on the sea-side, by a restoration of the westward fresh-water flow since 1957. Artificial recharge reversed a strong lateral salt-water intrusion due to excessive groundwater extraction for drinking-water supply (1930 - 1956).

It follows from fig. 5 and 7 that during an actual fresh-water intrusion, monitoring at one site would ideally reveal the successive passage of water types S-$NaCl^+$, B-$NaCl^+$, B-$NaHCO_3^+$ (eventually), F-$NaHCO_3^+$, F-$MgHCO_3^+$, F-$CaHCO_3^+$ and finally F-$CaHCO_3$φ.
In a snapshot these water types are found in that order in zones from the fresh-water intrusion front towards the hinterland, long ago freed from salt.

Especially in the southern area, water types with a strong {Na + K + Mg} deficit up to -62 meq l^{-1}, viz. B-NaCl- and S-NaCl-, are found below water types with a strong {Na + K + Mg} surplus up to +16 meq l^{-1} (fig. 6). Their presence correlates with a strong salt-water intrusion since 1865 due to excessive groundwater extraction and the strongly draining North Sea Canal 1 - 2 km south of the investigated area. For the whole area, shown in fig. 4 and studied in detail by STUYFZAND (1985), a three-dimensional plexi-glass demonstration model has been constructed and described by ENGELEN et al. (1986).

4. ACKNOWLEDGEMENTS

The research was financed by the Free University of Amsterdam (Institute for Earth Sciences, Dept. of Hydrology) and by the Netherlands Waterworks Testing and Research Institute KIWA. I wish to thank Prof. Dr. G.B. Engelen for his beneficial review.

REFERENCES

DUCE, R.A. & HOFFMANN, E.J. (1976). Chemical fractionation at the air/sea interface. Ann. Rev. Earth Planet. Sci. 4, 187-228.

ENGELEN, G.B., STUURMAN, R.J., STUYFZAND, P.J. & ROOSMA, E. (1986). A three-dimensional plexi-glass demonstration model of the hydrology, chemical groundwater types and flow systems in the coastal dunes near Castricum, The Netherlands. Proc. 9th SWIM, 193-197.

ERIKSSON, E. (1952). Composition of atmospheric precipitation; II. Sulfur, chloride, iodine compounds. Bibliography. Tellus 4, 280-303.

MATTHESS, G. (1982). The properties of groundwater, 406 p. - New York: John Wiley.

MOLEN, W.H. van der (1958). The exchangeable cations in soils flooded with sea water. Ph.D. Thesis, Wageningen, 167 pp.

RILEY, J.P. & SKIRROW, G. (1965). Chemical Oceanography. London/New York: Academic Press.

STUYFZAND, P.J. (1985). Hydrochemistry and Hydrology of the coastal dunes between Egmond and Wijk aan Zee. KIWA report SWE-85-012 (in Dutch), 205 p.

STUYFZAND, P.J. in prep. Hydrochemistry and hydrology of the coastal dune area of the Western-Netherlands. Ph.D. Thesis, Free Univ. Amsterdam, Instit. Earth Sci. (in English).

VERMEULEN, A.J. (1977). Immission research with rain gauges: experimental setup, experiences and results. Report Prov. Water Dept., Section Env. Hyg., (in Dutch), 109 pp.

WITT, H. & WIT, K.E. (1982). The salinization process in the subsoil of North Holland. Instit. Land & Water Manag. Res., Wageningen. ICW Note 1323, (in Dutch), 34 pp.

ZAGWIJN, W.H. (1984). The formation of the younger dunes on the west coast of the Netherlands (AD 1000-1600). Geol. & Mijnbouw 63, 259-268.

FIGURES

Fig. 1: The hierarchical structure of the classification system, with four levels of subdivision. The number of subdivisions within types, subtypes and classes is merely a theoretical maximum, because many combinations do not occur in nature.

Fig. 2: Coding and deciphering of a water type in 10 positions. The example is called "a fresh, moderately hard calciumbicarbonate water with a {Na+K+Mg}-surplus". This surplus is often due to a (former) freshwater intrusion.

Fig. 3: Subdivision of types into subtypes on the basis of the proportional share of main constituents in the sum of cations (left) and anions (right) in meq l^{-1}. First the strongest geohydrochemical families at the corners of each triangle are determined, e.g. the [Al + H + Fe + Mn]- and [SO_4 + NO_3 + NO_2]-family. Then the strongest (couple) within a family is chosen, e.g. [Al + H] and SO_4, and subsequently the strongest within a couple, e.g. Al. The combination of e.g. Al and SO_4 gives the subtype, here $AlSO_4$. The couples within a family have been set in brackets. The strongest members of a family, which have been discovered hitherto, have been placed in the proper fields within the triangles.

Fig. 4: Location map of the coastal dunes (dotted area) near Castricum and of the hydrochemical sections AA' and BB'.

Fig. 5: Hydrochemical cross section AA' (fig. 4), extended with the Lake of Alkmaar and a deep polder (modified after STUYFZAND, 1985). F = Cl $\leq$ 300 mg l^{-1} ; B = 300 < Cl $\leq$ 10.000 mg l^{-1}; total hardness omitted; R = fresh, artificially recharged Rhine water.

Fig. 6: Hydrochemical cross section BB' (fig. 4), after STUYFZAND (1985). F = Cl $\leq$ 300 mg l^{-1}; B = 300 < Cl $\leq$ 10.000 mg l^{-1}; total hardness omitted.

Fig. 7: Areal distribution of water types at 25 metres below mean sea level in the coastal dunes and adjacent shallow polders near Castricum (after STUYFZAND, 1985) F = Cl $\leq$ 300 mg l^{-1}; B = 300 < Cl $\leq$ 10.000 mg l^{-1}; total hardness omitted; B = 300 < Cl $\leq$ 10.000 mg l^{-1}; total hardness omitted; R = fresh, artificially recharged Rhine water.

TABLES

Table 1: Division in main types on the basis of chloride concentration.

Table 2: Subdivision of main types into types on the basis of total hardness (mainly Ca + Mg).

Table 3: Determination of 16 hitherto discovered subtypes. Σk = sum cations; Σa = sum anions.

Table 4: Subdivision of subtypes into classes according to {Na + K + Mg} corrected for sea salt.

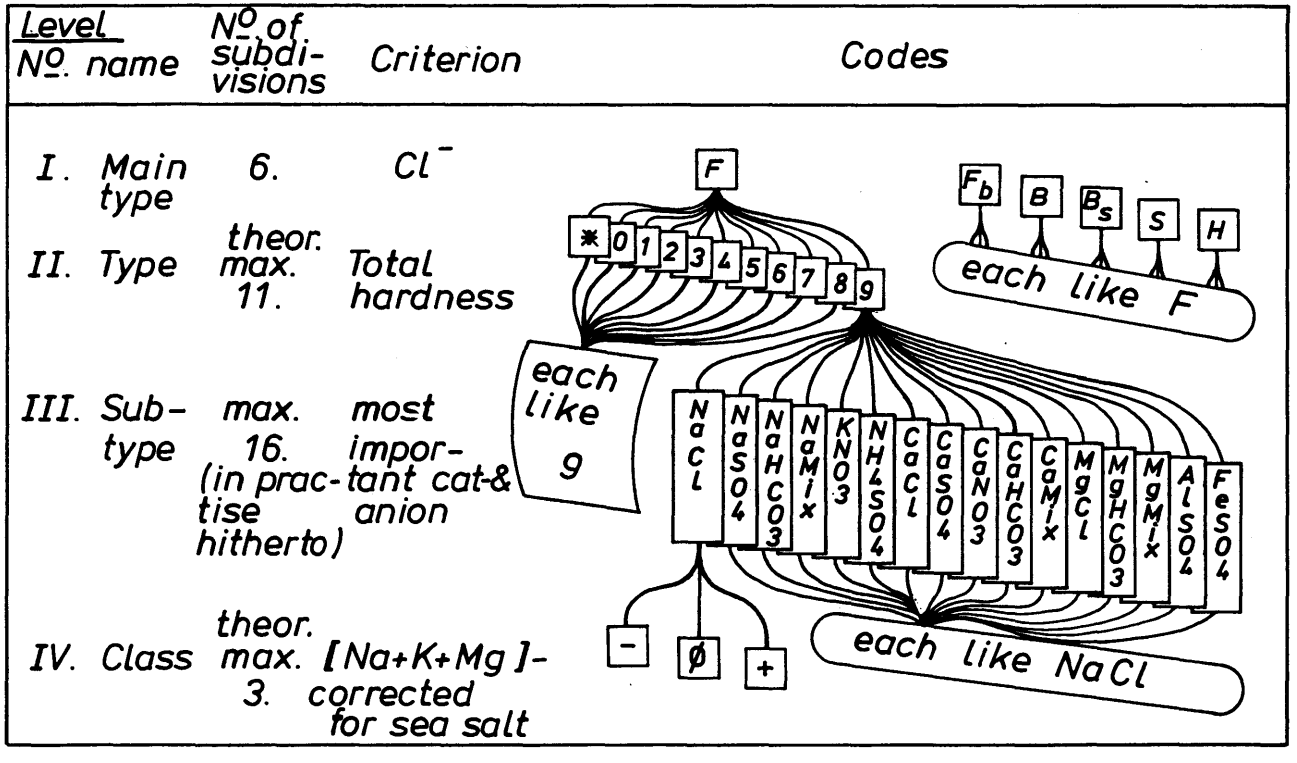
Level No. name
No. of subdivisions
Criterion
Codes
I. Main type
6.
Cl⁻
II. Type
theor. max. 11.
Total hardness
III. Sub-type
max. 16. (in practise hitherto)
most important cat-& anion
IV. Class
theor. max. 3.
[Na+K+Mg]- corrected for sea salt
F
* 0 1 2 3 4 5 6 7 8 9
each like 9
Fb B Bs S H
each like F
NaCl NaSO4 NaHCO3 NaMix KNO3 NH4SO4 CaCl CaSO4 CaNO3 CaHCO3 CaMix MgCl MgHCO3 MgMix AlSO4 FeSO4
each like NaCl
- ø +

Figure 1

2 4 6 8 10
F l - C a H C O 3 +
subdivision level
IV
class
for sea salt corrected
[Na+K+Mg] significantly
positive, i.e. > +√0,5 Cl (meq. L-1)
III
subtype
most important cation (Ca) and
anion (HCO3), in meq. L-1
separator
II
type
total hardness type 1 = 1–2 mmol
Ca+Mg L-1 (moderately hard)
I
main type
Chloride ≤ 150 mg L-1 (Fresh)

Figure 2

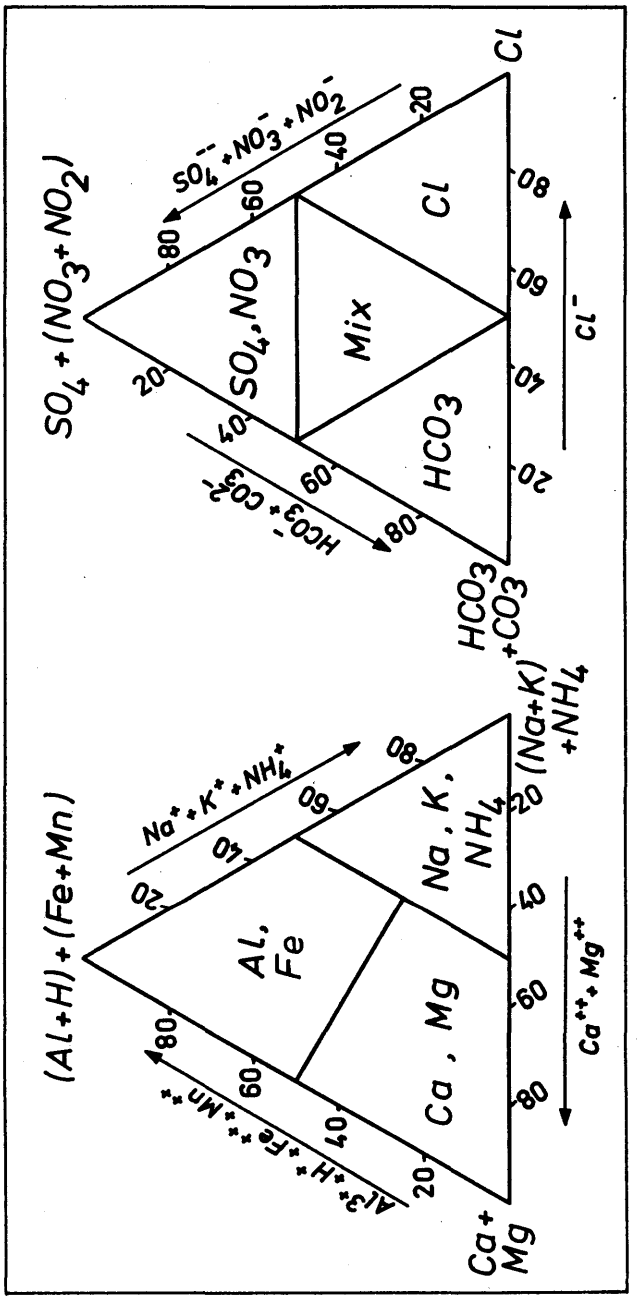
$SO_4 + (NO_3 + NO_2)$
Cl
$HCO_3 + CO_3$
$(Al+H)+(Fe+Mn)$
$(Na+K)+NH_4$
$Ca+Mg$
SO_4, NO_3
Cl
Mix
HCO_3
Al, Fe
Ca, Mg
Na, K, NH_4
$SO_4^{--} + NO_3^- + NO_2^-$
$HCO_3^- + CO_3^{--}$
Cl^-
$Na^+ + K^+ + NH_4^+$
$Al^{3+} + H^+ + Fe^{++} + Mn^{++}$
$Ca^{++} + Mg^{++}$

Figure 3

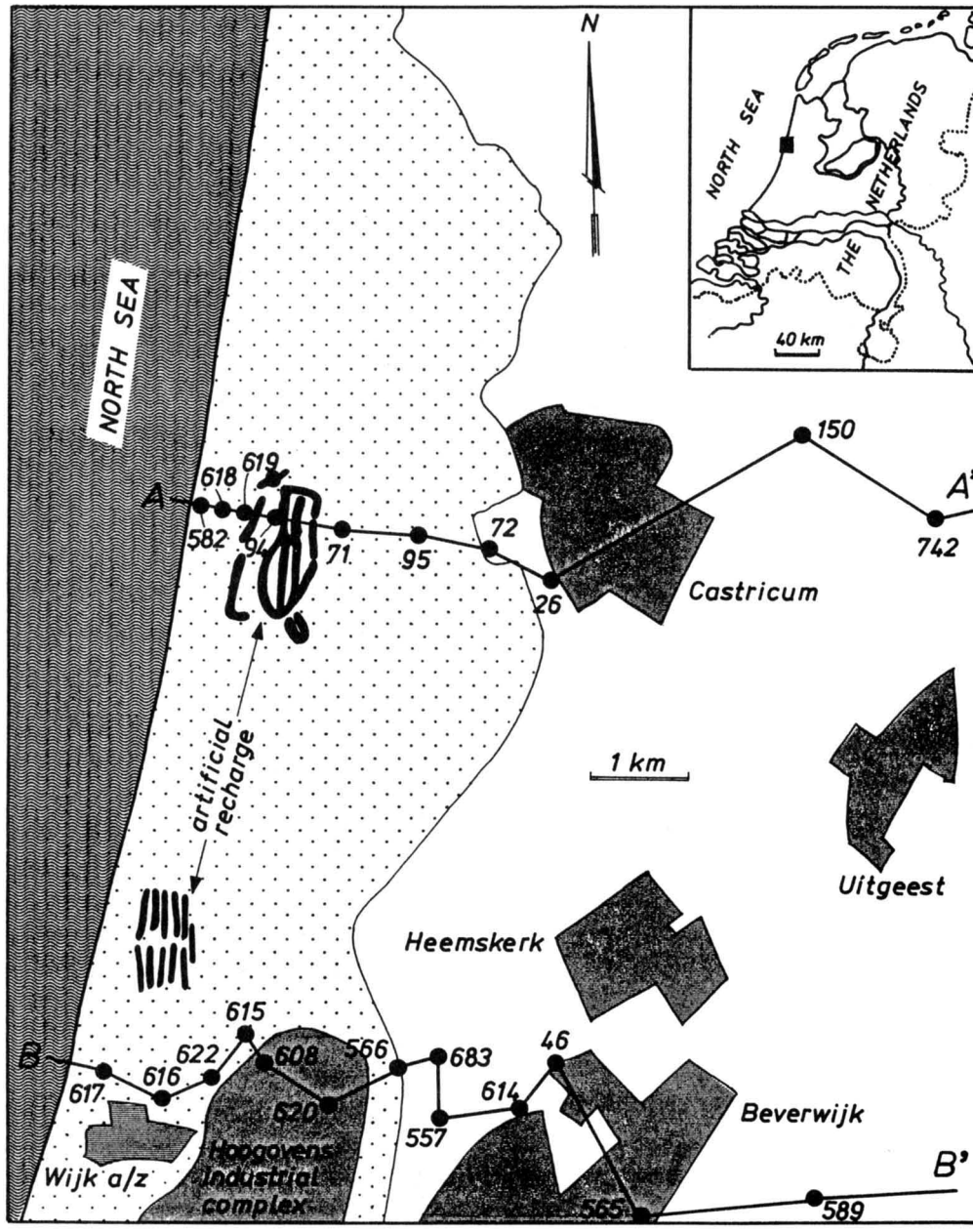
N
NORTH SEA
THE NETHERLANDS
40 km
NORTH SEA
A
A'
618
619
582
94
71
95
72
26
150
742
Castricum
artificial recharge
1 km
Uitgeest
Heemskerk
B
B'
615
622
608
566
683
46
617
616
620
614
557
Beverwijk
Wijk a/z
Hoogovens industrial complex
565
589

Figure 4

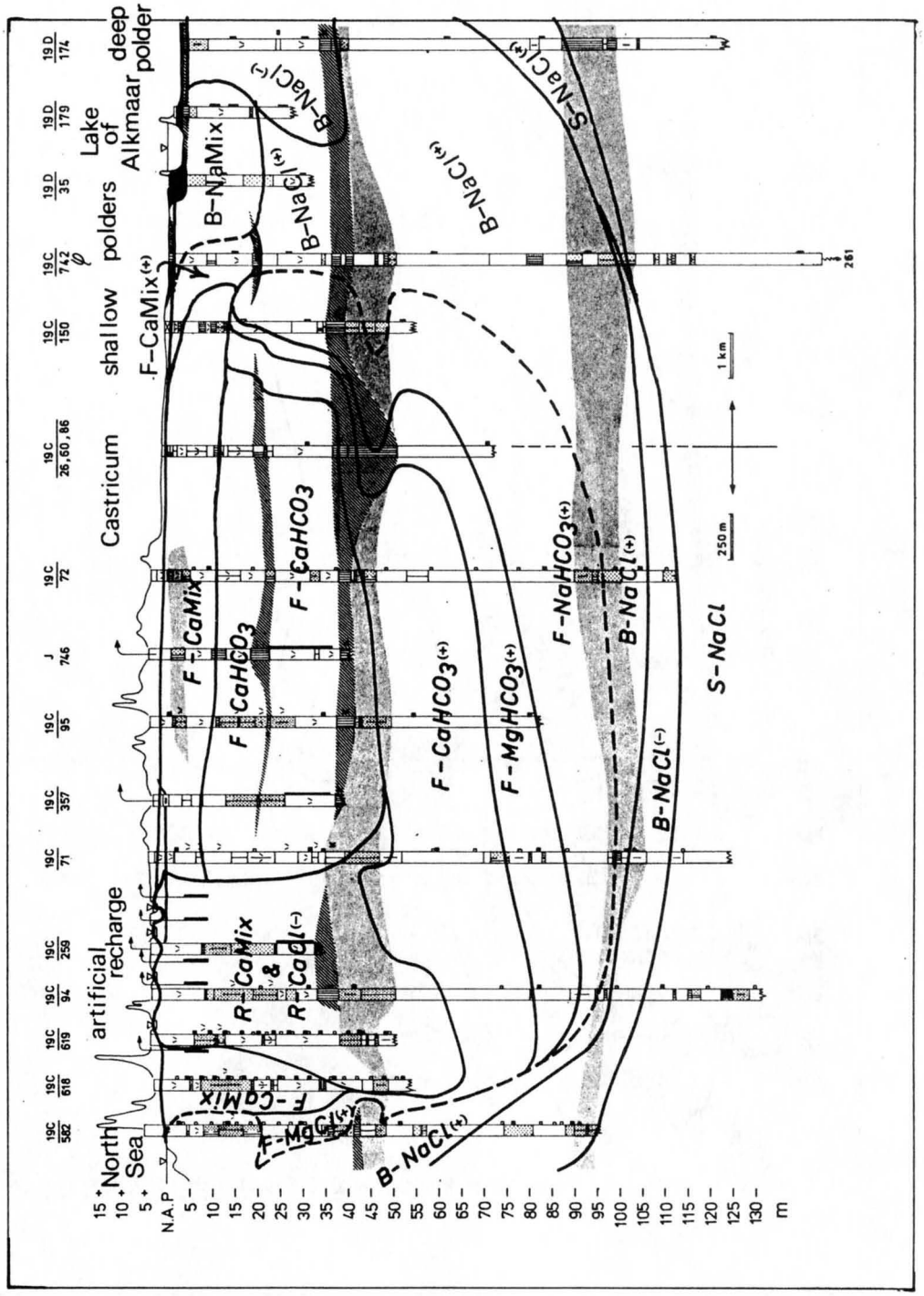
deep polder
Lake of Alkmaar
shallow polders
Castricum
artificial recharge
North Sea
F-CaMix
B-NaMix
B-NaCl(-)
B-NaCl(+)
F-CaHCO3
F-CaHCO3(+)
F-MgHCO3(+)
F-NaHCO3(+)
S-NaCl
S-NaCl(+)
F-MgCl(+)
1 km
250 m
NAP
m

Figure 5

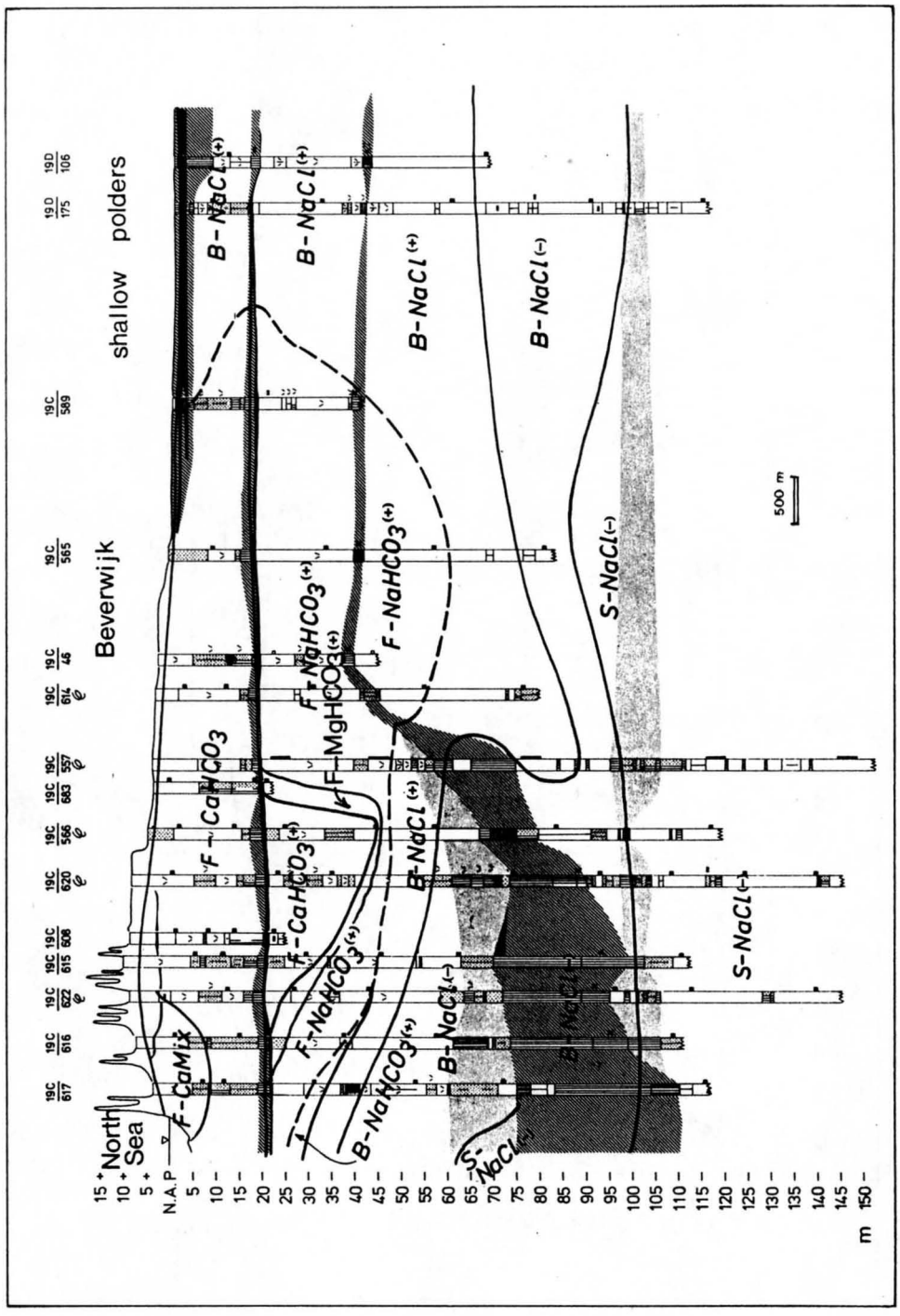
shallow polders
Beverwijk
North Sea
N.A.P
m
500 m
B-NaCl(+)
B-NaCl(-)
F-CaMix
F-CaHCO3
F-NaHCO3(+)
F-MgHCO3(+)
S-NaCl(-)

Figure 6

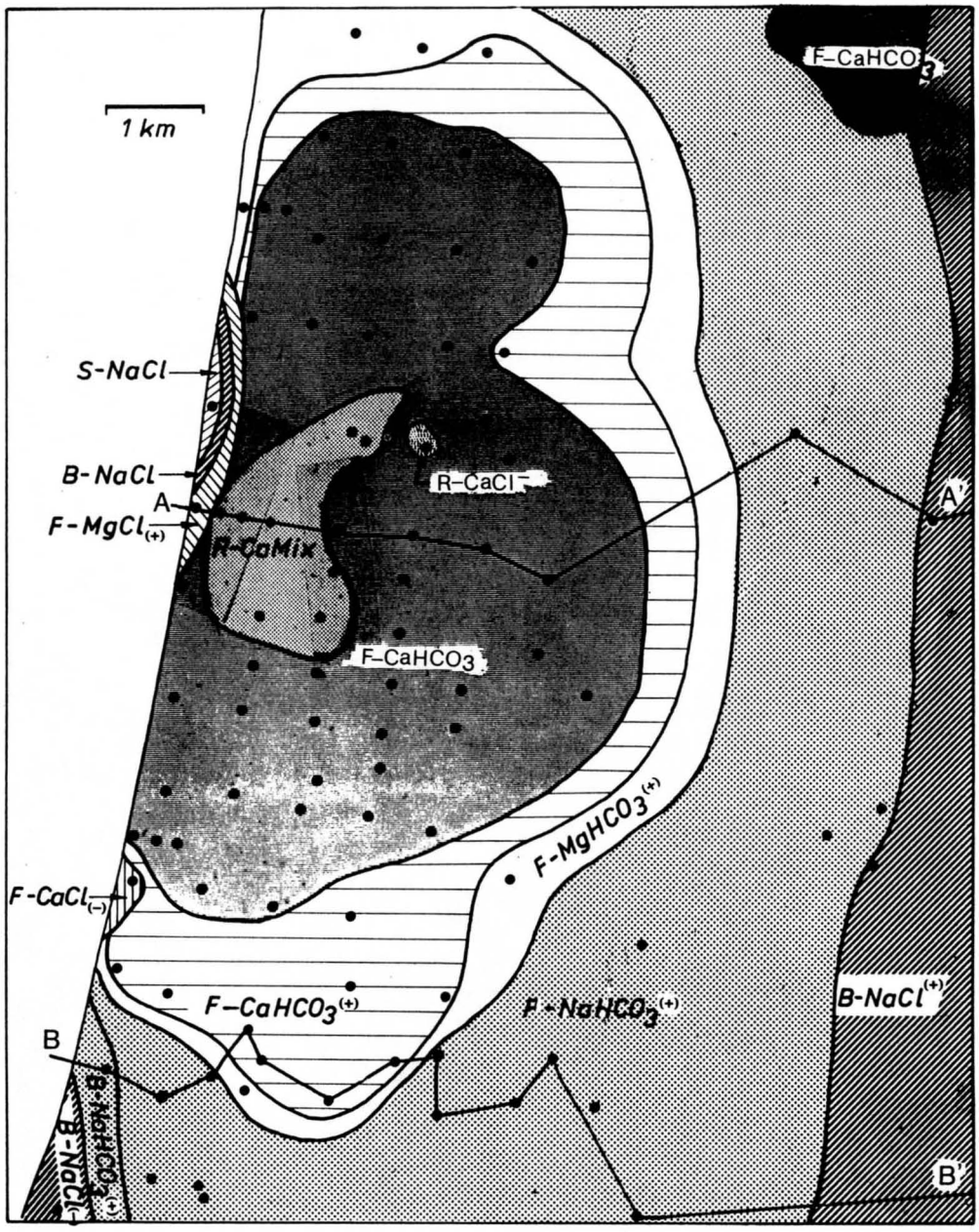
1 km
S-NaCl
B-NaCl
A
F-MgCl(+)
R-CaMix
R-CaCl
F-CaHCO3
F-CaHCO3
A'
F-MgHCO3(+)
F-CaCl(-)
F-CaHCO3(+)
F-NaHCO3(+)
B-NaCl(+)
B
B-NaHCO3(+)
B-NaCl
B'

Figure 7

5.7. SALT-WATER ENCROACHMENT IN THE WESTERN BELGIAN COASTAL PLAIN

I. BOLLE, L. LEBBE & W. de BREUCK

SUMMARY

In the western part of the Belgian coastal plain the water quality in the unconfined aquifer has been investigated. A correlation between the total dissolved solids, the Cl^--content and the resistivity of the water has been established. The resistivity logging in the area has been calibrated by taking the lithostratigraphy and the hydrochemistry into account. A resistivity profile through the shore, the young dunes, the polders, the old dunes and the low polders was obtained by logging a series of borings along a north-south line. By means of this resistivity profile the distribution of the water-quality groups can be described.

1. INTRODUCTION

The depth of the fresh-/salt-water interface in the unconfined aquifer of the Belgian coastal area has been mapped by means of resistivity surveying and borings (DE BREUCK et al., 1974).

Salt water was defined as having a total dissolved solids content exceeding 1500 mg/l. The resistivity of the fresh-water layer ranges between 50 and 12 Ωm and the resistivity of the saline layer between 2,5 and 1,5 Ωm (De BREUCK & De MOOR, 1969, 1973).
A part of the map is shown in fig. 1.

Since then a more detailed study has been carried out in the western part of the coastal area. It comprised a detailed investigation of the lithostratigraphy by cable-tool drilling and grain-size analyses, the hydrochemistry by extensive chemical analyses of water samples from different depths and locations, and the resistivity of the formation and the groundwater by resistivity-logging techniques.

By means of long normal logging in boreholes, drilled by the rotary method, a resistivity profile over a length of 5 km and a depth of 30 m was obtained. The resistivity profile has been interpreted in terms of water mineralization and lithostratigraphy.

2. LITHOSTRATIGRAPHY

A series of boreholes has been drilled by a cable tool. Samples have been taken every half metre. Thus a lithostratigraphical section could be drawn along a line, stretching from the beach 3 km landwards (fig. 1). Grain-size analyses of every layer have been made.

The lithostratigraphical section (fig. 2) shows the following features.

The unconfined aquifer is bounded below by the Eocene clay substratum (layer 1[1]). The undulating top of this clay occurs between -24,5 and -31,5[2]. Layer 2 consists of medium to coarse medium sands with shells; its thickness varies between 6 and 12 m, its upper boundary being located between -15,5 and -18,5; this layer does not occur in the borings 117DB7 and 193DB6.

In the southern part of the area layer 2 is covered by a complex of sand, silt and clay. Two facies can be distinguished: a silty and a clayey one. In boring 117DB7 when layer 2 is absent the clayey facies lies on the Eocene clay and occurs between the levels -17,3 and -26,8. In the borings 117DB8 and 117DB6 the silty facies lies on layer 2; it attains a thickness of only 3 to 4 m between the levels -18 and -14. In borings 117DB15 and 117DB6 this layer is reduced to silt lenses at level -16. In boring 193DB5 the clayey facies gradually changes into the layer 2.

In the borings 193DB6 and 193DB7 layer 3 lies upon a very heterogeneous deposit of sand, clay and silt with organic matter. The Tertiary clay substratum has not been attained at these locations. Layer 4 is a rather homogeneous layer of well sorted medium to fine sands. It lies upon layer 2 or layer 3. The basis of this layer is located between the levels -14,5 and -17,5; the top between +1 and +3. Lenses of different composition can occur: lenses 4.1, 4.2, 4.3 and 4.4 contain fine sand and silt, lenses 4.5 and 4.6 shell-bearing medium sand.

A clay-silt-sand complex (layer 5) overlies layer 4 throughout the area. Its top lies at +4 and reaches the surface in the polder area. Four facies can be distinguished: a clay or a clay-silt layer (facies 5.1) between 0,2 m and 1,0 m thick rests upon silty sands and sometimes upon peat; facies 5.2 mainly consists of silty fine sand with silt and clay lenses (less than 0,1 thick); in most cases, a humus-bearing or peaty soil is found on top; facies 5.3 occurs under the dunes in the northern part of the area and is formed by well-sorted fine sand; facies 5.4 occurs under the fore-dunes and the back-shore in the eastern part; it is formed by a layer of pale, rubiginous shell and shell debris.

Layer 6 consists of well-sorted fine medium sands (layer 6). It occurs in the dunes from the surface to the level +4. Within this layer brown bands of light humus-bearing sands occur at several levels. Beach sands are less well sorted and finer than dune sands.

3. HYDROCHEMICAL STUDY

Some of the boreholes have been equipped with a screen over the whole depth of the aquifer. In these boreholes resistivity measurements were made. In other boreholes several piezometers at different depths were installed. These piezometers have a one-metre long screen surrounded by a gravel pack sealed by a clay cover.

(1) Indication of the layers in the lithostratigraphical profile (fig. 2).

(2) TAW Datum level of the second general leveling (National Geographical Institute, Belgium).

A series of shallow piezometers were also drilled. The piezometers not only served for hydraulic-head measurements but also for the collection of groundwater samples.

The analysis of the water samples consisted of the determination in the field of turbidity, smell, taste, temperature of the water and the air, and measurements in the laboratory of temperature, resistivity, pH, dry residue, ash rest, hardness (carbonate and non-carbonate), alkalinity, free carbon dioxide, silica, organic constituents, sodium, potassium, calcium, magnesium, ferrous and ferric iron, ammonia, hydrogen chloride, sulphate, nitrate, bicarbonate, carbonate, phosphate, and hydroxyl iron.

Some two hundred water samples have been analyzed. An empirical relationship between the resistivity of water at 11°C (average temperature of the aquifers) and the total dissolved solids has been established:

$$\rho_w = \frac{12{,}000}{TDS} \qquad (1)$$

where ρ_w is the resistivity of the water at 11°C in Ωm;
TDS is the total dissolved solids in mg/l.

It was found that the relation between the chloride content and the total dissolved solids content was very poor for fresh water (TDS < 1600 mg/l).

For the brackish- and salt-water samples (TDS > 1600 mg/l), a simple relation could be established:

$$Cl^-\text{-content} = 0{,}54 \times TDS \qquad (2)$$

where Cl^--content is the chloride content in mg/l,
TDS is the total dissolved solids in mg/l.

This relation enables one to extend the table of the water-quality groups of G. De MOOR & W. De BREUCK (1969) to the limits for the resistivities at 11°C and for Cl^--content (table 1).

Table 1. Water quality groups.

Water quality group	Appreciation of water quality	Total dissolved solids (mg/l)	Resistivity at 11°C (in Ωm)	Cl^--content (in mg/l)
G	very fresh	< 200	> 60	-
W	fresh	200 - 400	60 - 30	-
V	moderately fresh	400 - 800	30 - 15	-
F	weakly fresh	800 - 1600	15 - 7,5	-
A	moderately brackish	1600 - 3200	7,5 - 3,75	860 - 1720
B	brackish	3200 - 6400	3,75 - 1,88	1720 - 3440
C	very brackish	6400 - 12800	1,88 - 0,94	3440 - 6880
S	moderately salt	12800 - 25600	0,94 - 0,47	6880 - 13760
Z	salt	> 25600	< 0,47	> 13760

4. RESISTIVITY LOGGING OF FULLY SCREENED WELLS

In fully screened wells the resistivity of the water was measured by a resistivity cell. The resistivity of the surrounding sediments was determined by a normal device with an electrode separation AM of 1 m. The influence of the well screen thus being minimal a good value of the horizontal resistivity of the sediments was obtained. As a first approximation the quality of the water in the well was assumed to be the same as that of the pore water in the sediments. This is especially true when the water quality does not vary much over the entire thickness of the aquifer. This is the case in well 117DB9 in the dune area (fig. 3). The variation of the resistivity of the sediment is mainly due to the variation of the formation factor. The latter varies from 2,5 in fine-grained sediments of layer 4 to 3,3 in the coarser-grained sediments of layer 2.

In the polder area the assumption that the water in the well has the same quality as the pore water in the surrounding sediments does not always hold. This is proved by sequential measurements in well 193DB5 (fig. 5). The first measurement 193DB5EBM1 was done at the end of the discharge period 1976, the second 193DB5EBM2 at the end of the following recharge period. The two resistivity loggings of the surrounding sediment, ρ_t, do not differ very much. This is not the case for the resistivity of water ρ_w in the well. At the end of the recharge period the water in the upper part of the well has a higher resistivity. The transition zone between fresh and salt water has narrowed and sunk. This can be explained by the higher hydraulic head in the upper part of the aquifer than in the lower part at the end of the recharge period. The sequential measurements of ρ_t also indicate that the transition zone in the sediments does not visibly move.

This phenomenon has already been mentioned by J.F. POLAND & R.H. MORRISON (1940). From resistivity measurements in wells in stratified deposits they conclude that the circulation in a well under non-pumping conditions is ordinarily controlled

by difference in head rather than by difference in density. For the determination of the exact quality of the water-producing layers they proposed to make resistivity logs in the well, first in non-pumping conditions and then during pumping. It may be necessary to pump a contaminated well for a considerable time before the intruded aquifers are completely flushed out. A similar phenomenon was also described by K.R. RUSHTON (1980) in the vicinity of an abstraction well.

Apart from this exception one can assume the ratio ρ_t/ρ_w to be roughly equal to the formation factor. In the study area the formation factor thus varies between 2 in the very silty fine sands and 5 in the medium to coarse medium shell-bearing sands.

In most of the cases the formation factor varies around the average value 2,7. Taking this mean value into account, sediment resistivities can be predicted for different water qualities.

Table 2. Resistivities of sediments filled with pore water of different quality.

Resistivity group	Appreciation of water quality	Total dissolved solids (mg/l)	Resistivity of the water at 11°C	Resistivity of sediments (11°C)
G'	very fresh	< 200	> 60	> 160
W'	fresh	200 - 400	60 - 30	160 - 80
V'	moderately fresh	400 - 800	30 - 15	80 - 40
F'	weakly fresh	800 - 1600	15 - 7,5	40 - 20
A'	moderately brackish	1600 - 3200	7,5 - 3,75	20 - 10
B'	brackish	3200 - 6400	3,75 - 1,88	10 - 5
C'	very brackish	6400 - 12800	1,88 - 0,94	5 - 2,5
S'	moderately salt	12800 - 25600	0,94 - 0,47	2,5 - 1,25
Z'	salt	> 25600	< 0,47	> 1,25

5. RESISTIVITY LOGGING OF UNCASED BOREHOLES

Along a north-south line from the beach over the polders, over the old dunes to the low polders, uncased boreholes have been logged. The drilling mud consisted of a suspension of organic additives that degrade with time. Because of the small borehole diameter (about 100 mm) the resistivity measured with the long normal device (AM = 1 m) was similar to the one measured in a fully screened well (Ø 80 mm). The resistivities thus measured approximate the horizontal resistivities of the surrounding sediments. This was confirmed by field measurements in a screened well and in a borehole (Ø 100 mm) not far distant. The data of both series of measurements can thus be combined.

6. RESISTIVITY PROFILE

The results of the resistivity logging on the shore, young dunes, polders, old dunes and low polders are represented in a resistivity profile (fig. 6). Seven resistivity groups can be distinguished. This resistivity profile provides a picture of the distribution of the quality groups in the unconfined aquifer. The water quality in the unsaturated zone and impermeable substratum was not studied.

In some places resistivity groups and water-quality groups do not coincide. Two explanations can be given. In the first place, the formation factor may differ from the average value of 2,7. This is confirmed from the bore log. In the second place the resistivity may abruptly change, as in the case of a sharp interface. Water samples taken over a limited length of a screened well and short normal measurements show that the long normal measurements tend to enlarge the transition zone on the resistivity profile (fig. 4).

Under the shore a salt-water lens floats upon the fresh groundwater which flows from the dunes in the direction of the sea. The salt water infiltrates on the backshore and the upper part of the foreshore. Under the lower part of the foreshore salt water flows upwards resulting in a seepage. The fresh water below the salt water gradually takes up more salts when it flows towards the sea. Under the low-water line a brackish water foot can occur in the lower part of the aquifer, as mentioned by L. LEBBE (1981).

In the young dunes fresh water infiltrates. The chloride content of the rain, as measured during a period of thirty months, was approximately 12,0 mg/l. The mean chloride content of 27 samples of fresh water in the young dunes was 32,5 mg/l. Hence one can conclude that about 40 % of the rain infiltrates in the young dunes (L. LEBBE, 1978). This value was confirmed by calculation of the potential evapotranspiration from hydrometeorological data after the PENMAN method (1952) and by a balance of the unsaturated zone after the method of THORNTHWAITE MATHER (1955).

The young dunes can be subdivided into two parts. In the northern part they rest on old dune deposits and in the southern part they lie on old tidal flat deposits. Here the fresh-water lens reaches the impermeable substratum. This lens is older in the northern than in the southern part. As a consequence the water is less mineralized in the north (TDS, 200 - 500 mg/l) than in the south (TDS, 400 - 800 mg/l). Near the impermeable substratum the fresh water has a higher salt content. In the southern part the lens of resistivity group F is not only due to the increasing mineralization of the pore water but also to the smaller formation factor (2,1 in well 117DB6) of the finer sediments.

Under the polder area fresh water rests upon salt water. The fresh water has a higher salt content than the fresh water of dunes and belongs to the water-quality group F. Between the fresh and the salt water the transition zone of brackish water attains an average thickness of 12 m. Under the ditches an upconing of

brackish water can be seen. The ditch at the foot of the young dunes drains much of the groundwater which flows from the dunes to the polders. This results in an important vertical groundwater flow, which brings brackish water just under the water table. the upconing of brackish water is less conspicuous at the edge of the old dunes in the south.

Under the old dunes a fresh-water lens is present. In the upper part of the aquifer the resistivity is rather small. This is due to a low value of the formation factor of the clay, silt and peat deposits just below the dune sands. The asymmetrical shape of the fresh-water lens can be explained by the different drainage levels of the polders in the north and the low polders in the south. The drainage level in the polder is two metres higher than in the low polders. In the old dunes fresh water infiltrates. Because of the different drainage levels the largest part of the fresh water flows to the low polders. Only a small part flows towards the polders in the north. In the lower part of the aquifer under the old dunes the fresh-water head is at its lowest near the low polders. This explains the presence of fresh water in the deepest parts of the aquifer under the old dunes where the downward vertical flow is maximal.

In the deep polders seepage of salt water occurs. An important vertical flow is directed upwards in the vicinity of the large ditch close to the old dunes. The water just below the water table is moderately salt to very brackish. The higher resistivity in the lower part of the aquifer is due to fine sediments (very silty fine sand). In the case of very salt pore water the formation factor tends to increase with decreasing grain size (L.N. DAKHNOV, 1962).

7. CONCLUSIONS

Field observations and laboratory measurements show that the average value of the formation factor is 2,7. Resistivity logging of a line of borings thus provide a 5 km section through the coastal area showing the water-quality distribution. This distribution can be explained in terms of the topography, the geological history and the groundwater flow.

REFERENCES

DAKHNOV, L.N. (1962). Geophysical well logging. Quart. Colorado School Min. 57, 1-445.

DE BREUCK, W. & DE MOOR, G. (1969). The water-table aquifer in the Eastern Coastal Area. Bull. Int. Ass. Sci. Hydrol. 14, 137-155.

DE BREUCK, W. & DE MOOR, G. (1973). De kwartaire resistiviteitsprofileringen en voorbeelden van toepassing bij het hydrogeologisch onderzoek. Belgisch Comite voor Ingenieursgeologie, Publ. 24, 1-18.

DE BREUCK, W., DE MOOR, G., MARECHAL, R. & TAVERNIER, R. (1974). Diepte van het grensvlak tussen zoet en zout water in de freatische taag van het Belgisch kustgebied (1963 - 1973). SWIM 4, annex-map, scale 1/100.000.

DE MOOR, G. & DE BREUCK, W. (1969). De freatische waters in het Oostelijk Kustgebied en in de Vlaamse Vallei. Natuurwet. Tijdschr. 51, 3-68.

LEBBE, L.C. (1978). Hydrogeologie van het duingebied ten westen van De Panne. 164 p., Gent: Geol. Inst. Rijksuniv. Gent (Dr. Thesis) (unpubl.).

LEBBE, L.C. (1981). The subterranean flow of fresh and salt water underneath the western Belgian beach. Proceedings of Seventh Salt Water Intrusion Meeting. Uppsala. Sver. Geol. Under. Rap. Meddel. 27, 193-219.

PENMAN, H.L. (1952). The physical bases of irrigation control. Proc. 13th int. horticult. Congr. London 2, 913-924.

POLAND, J.F. & MORRISON, R.B. (1940). An electrical resistivity-apparatus for testing well-waters. Trans. Amer. Geophysical Union 21, 35-46.

RUSHTON, K.R. (1980). Differing positions of saline interface in aquifers and observation boreholes. Journ. Hydrol. 48, 185-189.

THORNTWAITE, C.W. & MATHER, J.K. (1955). The water balance. Publ. in Climatol. 8(1), 104.

FIGURES

Fig. 1: Location of lithostratigraphical (dashed) and resistivity (full) profiles.

Fig. 2: Lithostratigraphical profile: 1. medium to coarse medium sands; 2. medium sands; 3. fine sands; 4. slightly silt-bearing fine sands; 5. silt-bearing fine sands; 6. silt; 7. peat; 8. shells; 9. humus; 10. gravel; 11. clay.

Fig. 3: Resistivity logs 117DB9EBM1 and EBM2.

Fig. 4: Resistivity logs 193DB5EBM1 and EBM2.

Fig. 5: Resistivity log 193SB13.

Fig. 6: Resistivity profile De Panne-Adinkerke-De Moeren.

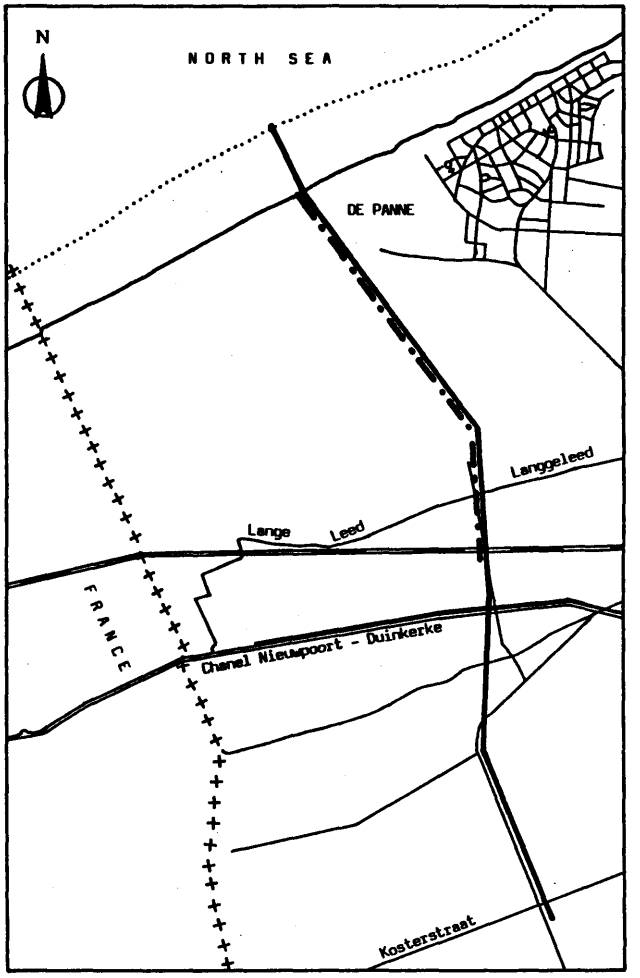
N
NORTH SEA
DE PANNE
Langgeleed
Lange Leed
FRANCE
Kanaal Nieuwpoort - Duinkerke
Kosterstraat

Figure 1

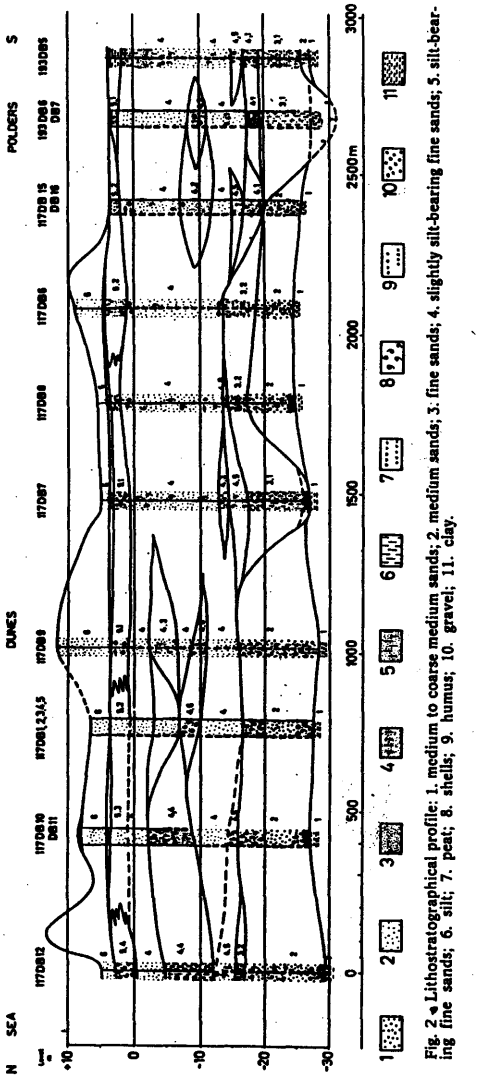

Fig. 2. Lithostratographical profile: 1. medium to coarse medium sands; 2. medium sands; 3. fine sands; 4. slightly silt-bearing fine sands; 5. silt-bearing fine sands; 6. silt; 7. peat; 8. shells; 9. humus; 10. gravel; 11. clay.

Figure 2

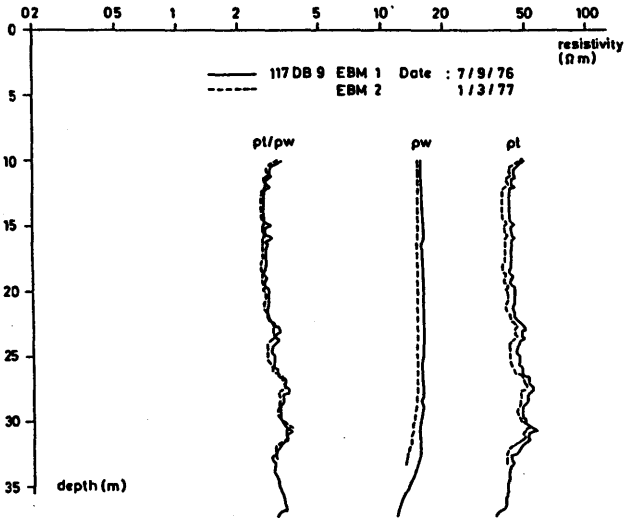
0.2
0.5
1
2
5
10
20
50
100
resistivity (Ω m)
117 DB 9 EBM 1 Date : 7/9/76
EBM 2 1/3/77
ρt/ρw
ρw
ρt
0
5
10
15
20
25
30
35
depth (m)

Figure 3

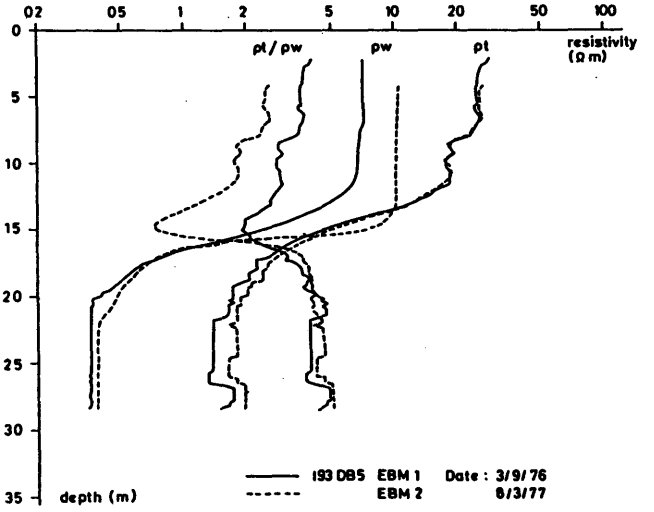

Figure 4

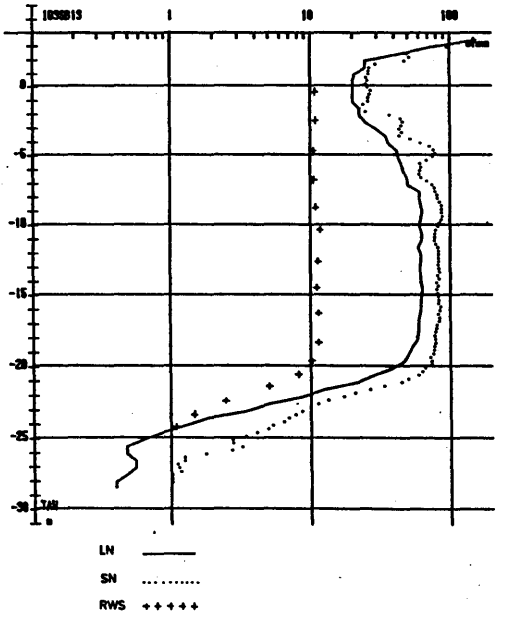

Figure 5

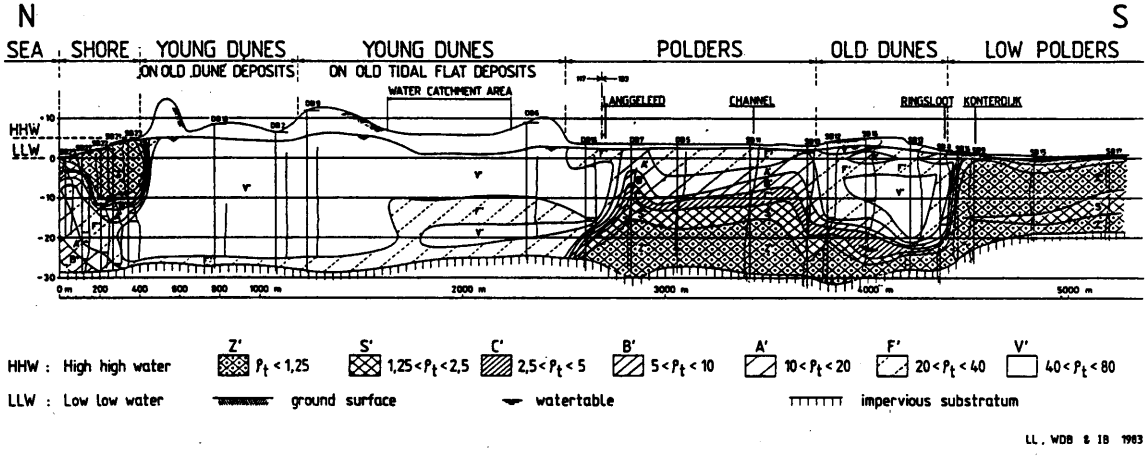
N
S
SEA
SHORE
YOUNG DUNES
ON OLD DUNE DEPOSITS
YOUNG DUNES
ON OLD TIDAL FLAT DEPOSITS
WATER CATCHMENT AREA
POLDERS
LANGGELEED
CHANNEL
OLD DUNES
RINGSLOOT
KONTEROLK
LOW POLDERS
HHW
LLW
0 m
200
400
600
800
1000 m
2000 m
3000 m
4000 m
5000 m
HHW : High high water
LLW : Low low water
Z' Pt < 1,25
S' 1,25 < Pt < 2,5
C' 2,5 < Pt < 5
B' 5 < Pt < 10
A' 10 < Pt < 20
F' 20 < Pt < 40
V' 40 < Pt < 80
ground surface
watertable
impervious substratum
LL . WDB & IB 1983

Figure 6

THEME 6

GEOPHYSICAL INVESTIGATIONS

6

GEOPHYSICAL INVESTIGATIONS

6.0. INTRODUCTION

P. MEISER

Saline groundwater occurs in almost all coastal areas in the world. Permeable rocks in coastal regions act as aquifers and provide a hydraulic connection between the inland groundwater and the sea water.

Knowledge of the location of the interface between saline and fresh groundwater is of far-reaching importance for the supply of drinking water for the population of coastal regions and islands. Therefore, it is not in the least surprising that for safeguarding the water supply in coastal regions methods have been sought which allow the identification of the interface between fresh water and sea water in the rock body without expensive drilling.

Electrical methods have proved to be particularly well suited for this purpose, since the electric resistivity of the aquifer is very strongly influenced by the ions dissolved in the groundwater.

On the basis of the values observed in the coastal region of northern Germany, the following ranges of resistivity may be assumed:

dry dune sand (above groundwater)	200 - 2000 ohm·m
gravelly sand filled with fresh groundwater	45 - 130 ohm·m
gravelly sand filled with brackish water	10 - 45 ohm·m
gravelly sand filled with saline water	3 - 10 ohm·m

However, it must be pointed out that also silt and clay contained in the gravelly sand may reduce the resistivity of a groundwater aquifer; this means that the low resistivities determined by geoelectric sounding methods do not necessarily indicate the presence of saline groundwater. Therefore, data from drillholes and drillhole logging (electrologs and gammalogs) are necessary which allow the rock resistivities determined by surface measurements to be correlated with the hydrogeological structure.

Electrical sounding methods are divided into direct current methods and alternating current methods. The latter allow the inductive coupling between the transmitter and the rock body and may therefore also be applied using a helicopter or a plane.

The large number of electrical methods offered by various companies differ with respect to the arrangement of the transmitter and receiver, the source of the

transmitted energy (natural or artificial fields), the type of transmitted current (direct or alternating current at various frequencies), and the type of coupling (direct, ac, or inductive).

Electrical resistivity methods (direct current method after Schlumberger or Wenner) have gained special importance because they are particularly well suited for solving hydrogeological problems. During the last few decades, these methods have been applied with great success, mainly in the coastal regions but also on islands, to determine the location of the interface between fresh water and saline water and to estimate the amount of fresh water available.

Two electrodes are used to induce direct current of defined intensity into the ground. The distribution of the electric potential at the surface is then recorded between the two electrodes.

The apparent electrical resistivity ρ_s of the subsurface can be determined on the basis of the voltage I, the tension U and a geometric factor K. A log-log plot of these resistivity values as a function of half of the distance between the electrodes (AB/2) is then made. This plot is evaluated by comparison with theoretical curves. Thus, a picture of the thickness and true resistivities of the individual rock beds is obtained.

An idea of the location of the freshwater-saline water interface and the shape of the freshwater occurrence may be derived from the interpretation of the curves obtained from geoelectrical soundings made within an area. This is of considerable importance for estimating the amount of freshwater that is available.

The advantage of these direct-current methods compared with the inductive alternating-current methods is mainly the precision with which the hydrogeological parameters are determined. The alternating current methods, in general, allow only a qualitative evaluation of the results.

Electromagnetic methods can be used to conduct a quick, general survey of large regions, even in inaccessible areas.

The method should always be chosen according to the task at hand. A combination of two or more methods is sometimes appropriate.

6.1. GEOELECTRICAL SURVEY IN THE POLDER "GROOT MIJDRECHT"

R.H. BOEKELMAN

ABSTRACT

The salinization of the suboil, especially in the western part of The Netherlands, has a detrimental influence on agriculture and horticulture. From previous investigations it is known that 75 % of the chloride load of polders in western Holland is due to seepage from the subsoil.

In this report the results of field-work in the polder "Groot Mijdrecht" are presented.

Groot Mijdrecht is a low polder - polder level 6,5 m below M.S.L. - causing a strong upconing of saline groundwater.

By means of geoelectrical investigations the position of the interface (zone) between fresh and saline groundwater has been determined.

The first results show a small gradient of the interface on the west side and a rather steep gradient in the eastern part of the polder. The latter is caused by a higher polder level of the bounding 'Vinkeveense polder'.

It has also been proved that saline groundwater is reaching the surface in the middle of the polder.

1. INTRODUCTION

Salinization of the subsoil in The Netherlands, especially in the low western part, has a detrimental effect on agri- and horticulture. This effect is enforced by all kinds of measures of man, i.e. reclamation of lakes, necessitating lowering of the water level and thus, the potential difference between deeper saline groundwater and polder level initiates seepage of saline groundwater. Sandpits are another cause of salinization as the impermeable layers are disturbed or taken away causing a strong salinization of the surface water.

Wells for industrial use or for drinking-water supply are also causing upconings of saline groundwater. In order to be able to predict changes in the groundwater system and to prevent unwanted effects caused by the measures mentioned above the Water Management Group of the University of Technology started to develop models (van DAM, 1976; Ten HOORN, 1979).

Apart from this field-work was also initiated to establish the present state of salinization in a certain area and if possible to compare this with results obtained by model calculations. The area which was chosen is a deep polder in the western part of Holland, Groot Mijdrecht (fig. 1). The polder is situated about 20 km south of Amsterdam and is about 20 km^2 in size. Reclamation of this former lake took place a century ago. The polder level is - 6,50 m. Fig. 2 shows polder Groot Mijdrecht with surrounding polders and polder levels.

In the east:	Vinkeveen	2,01 m below m.s.l.
In the north:	Ronde Hoep	2,47 m below m.s.l.
In the west:	1st, 2nd, 3rd polders of Mijdrecht	5,65 m below m.s.l.
In the south:	Wilnis	5,97 m below m.s.l.

Especially from the east side a strong seepage can be expected because of a 4,5 m difference in polder levels.

Also because of the lower polder level the saline groundwater is upconing according to the Badon Ghijben/Herzberg relation, causing saline seepage to the polder, which can be demonstrated by groundwater samples.

2. GEOLOGY OF THE SURVEY AREA

The deepest formations known from borings are marine layers of Tertiary age, the so called Oosterhout Formation, consisting of fine silty sands with shells intersected by clay layers (fig. 3). On top of these Pliocene layers, the oldest Pleistocene formation - the Maassluis formation - was deposited, also of marine origin, consisting of rather fine sands with clay layers. The first major non-marine formation, the Tegelen Formation was deposited by the rivers Rhine and Meuse. It consists mainly of sand with occasional clay layers. The most important aquifer in the area is the coarse sand of the Harderwijk Formation with a thickness of about 50 m. In the southern part of the polder it is overlain by the Kedichem Formation, rather thick clay layers and fine sands. In the northern part the Formation of Urk and Sterksel covers the Harderwijk Formation with coarse sands and occasional loam and fine-sand layers. During the Saalian glacial period the Drenthe Formation was deposited, consisting of rather coarse sands. During this glacial period the ice-pushed ridges were also created, with material from the Urk and Sterksel Formation, which nowadays acts as an important infiltration area. In the Weichselian glacial period layers of fine sand of eolian origin were deposited, some 10 m thick. The top of the subsoil is of Holocene age (thickness 5 - 10 m) and consists of clay, sand and peat layers of marine origin.

The distribution of saline and brackish water in the subsoil is not only due to the geological history, but is also affected by the flow of fresh groundwater from the infiltration areas - hills of Utrecht and Veluwe - which causes hydrodynamical dispersion. Molecular diffusion of chlorine ions is another important process which can explain the present distribution of saline and brackish groundwater (MEINARDI, 1974; VOLKER, 1961).

3. INVESTIGATIONS

A geoelectrical survey was carried out in order to obtain an impression of the present state of the salinization of the subsoil of 'Groot Mijdrecht'. Initially

a density of 5 soundings/km^2 was adopted, but already from previous investigations it was known that a higher density was necessary, especially in the eastern part of the polder because of a rather steep fresh-/salt-water interface.

Three cross-sections have been investigated (fig. 2), in all some 45 soundings. The first one was carried out by a student with technical assistance from the Water Management Group (LEENEN, 1978). During the autumn of 1978 the cross-sections in the north were investigated and by the end of 1981 enough material will be available to finish the inventory investigations. For the geoelectrical survey a 400 Watt D.C. instrument has been used. The soundings were carried out according to the Schlumberger arrangement, with current electrode spacings ranging from 3 - 600 m. In order to diminish the effects of - electrically - non-horizontal layers, e.g. a steep fresh-/salt-water interface, the line along which the electrodes were spaced was kept as close as possible perpendicular to the expected slope of the interface.

4. RESULTS

The first cross-section investigated is situated in the middle narrow part of the polder (fig. 2).

The sounding curves (fig. 4) represent the apparent specific resistivities as a function of half of the current electrode spacings.

At the east side of the polder (curve 2) rather high resistivity values are found even at long spacings. Westward the apparent resistivity values are diminished at greater L/2 values, interpreted as a rising interface between fresh and saline/brackish groundwater. At locations 7 and 12 the fresh water has disappeared and the apparent resistivity values are rather constant for all L/2 values. The soundings in the western part of this cross-section (fig. 5) show a similar effect. Here again the saline water is rising towards the centre of the polder.

As can be seen from the graphs 18, 16 and 14 (fig. 5) the interface in the western part rises less compared to the eastern part of this cross-section. Another difference from the west to the east of the cross-section, are the apparent resistivity values at long electrode spacings which are 3 - 4 Ω m in the west indicating saline groundwater, whereas in the eastern part these values are 10 Ω m, indicating brackish water. At locations 20 and 19 there is no further indication of the presence of fresh water in the subsoil.

Cross-section II in the north of the polder shows the same tendency (fig. 6). Again starting at the east side the first few graphs do not show saline groundwater, but from graph 24 apparent resistivity values for long electrode spacings tend to approximate 3 - 4 Ω m, indicating saline water.

Fig. 6 also shows the upconing of the brackish/saline groundwater as proven by westward increasing resistivity values at successively shorter spacings. The west side of this cross-section again shows a less steep upconing (curves 36 to 27) as can be seen in fig. 7. The saline groundwater comes closest to the surface at sounding 27.

The soundings along the dike in the very north of the polder do not differ essentially from the soundings of fig. 8, only the position of the saline groundwater seems to show up slightly deeper.

Especially for small electrode spacings considerable changes in apparent specific resistivity values can be noticed. This effect is due to the local situation of alternating peats, sands and clays of the Holocene layers. Secondly, the apparent resistivity values at long electrode spacings in general approximate values between 3 - 4 Ω m, indicating saline groundwater (Cl^--content 4000 mg/l), with the exception of the soundings in the eastern part of the cross sections, where values of 10 Ω m are found. The saline groundwater could not be proved here due to the limitations of the measuring device. Longer electrode spacings would have been necessary. To obtain more quantitative information the sounding curves have been interpreted using an 8-layer computer program, the results of which are shown for the first cross section (fig. 8). More layers have been distinguished but because of simplicity, only four layers are given here.

The Holocene top layer has a wide range of specific resistivity values (2,3 - 52 Ω m). Below a sandy layer with resistivity values between 35 and 40 Ω m, layers containing fresh pore water can be distinguished. A layer with resistivities between 9 and 12 Ω m represents the brackish zone, whereas the zone with saline groundwater is indicated by specific resistivity values of 3,3 - 6 Ω m. As can be seen in fig. 8, the saline groundwater reaches the surface between soundings 20 and 10. The zone with fresh and brackish pore water is shallow (< 20 m) in the western part of the cross-section and disappears in the direction of the centre of the polder, whereas at the east side a very thick fresh water zone (≈ 85 m) and also a thick brackish zone are demonstrated. This can be explained by the small differences in polder levels between the bounding polders in the western part and, on the contrary, great differences in the eastern part. This implies a great difference in groundwater flow from the bounding polders - est. 0,15 mm/day from the west, 3,1 mm/day from the east - which consequently affects the thickness of the brackish zone. It also explains the eastward decrease in specific resistivity values viz. 3,3 - 5,7 Ω m. The specific resistivity cross-sections in the north show a similar tendency (fig. 9) of a slowly rising interface from the west towards the centre of the cross-section. At the border of the polder the interface shows up at ≈ 40 m below the surface at sounding 27, at a minimum value of 22 m, here in the sandy Holocene top layer. The saline groundwater does not reach the surface in this cross-section. The slope of the interface is steeper from the north than the west, due to a greater difference in polder levels.

In the area where from previous investigations the flow towards the polder is known to be maximal, a relatively thick fresh water zone has been found (KRUIJK, 1963).

In the eastern part a thick fresh water zone of up to 90 m at the border is noticeable which strongly decreases in a western direction. A thick brackish zone can also be observed here. Although the thickness could not be determined accurately, it is less than in the cross-section in the centre of the polder.

An unexpected effect can be noticed in the east side of cross-section I which is shown in fig. 10. Here the interpretations of several soundings show an increase of specific resistivity with depth, whereas a decrease - due to higher salinity - is expected, as the lithology is very likely to be uniform. This effect has also been noticed in previous investigations (van DAM, 1960). A possible explanation of this effect might be the occurrence of mixing of saline groundwater from the west side and water from the brackish zone from the east side, which is supported by the trend of the specific resistivity values as found. Another cause of this effect might be the method used. The interpretation of the sounding curves assumes 'electrically' horizontal layers and, especially in the area with a steep interface, this assumption is not correct.

5. DISCUSSIONS

For comparison, results of WIT (1974) are shown in fig. 11 which presents chloride contour lines as determinated from samples of the upper groundwater.

The results from our investigations in the western part of the first cross-section fit well into this picture, with Cl^--contents varying between 4000 and 5000 mg/l. However, in the eastern part, according to our results the contour lines have to be moved westward. The lack of sampling points in this area can explain the difference.

The cross-sections in the north also fit well. The presence of saline groundwater is demonstrated at sampling point 8. Just north of this location the geoelectrical survey gave a maximum rise of the interface.

The Cl^--contents in the western and eastern part of the cross-section resemble our findings.

For deeper layers only a few data are available from a regional geoelectrical survey by Rijkswaterstaat (van DAM, 1960). At location 47, at a depth of 33 m below m.s.l., a Cl^--content of 5180 mg/l was found, formation resistivity 4,0 Ω m, At a depth of 56 m below m.s.l. 5220 mg Cl^-/l, formation resistivity 3,0 Ω m. In the first cross-section, at location 4, a Cl^--content of 5370 mg/l showed up at a depth of 17,7 m below m.s.l., in a formation with a specific resistivity of 3,5 Ω m.

These specific resistivity values are in good accordance with the values found in the present survey.

The University of Leiden carried out investigations concerning ion exchange in groundwater (GEIRNAERT, 1971). From these investigations fig. 12 and fig. 13 are borrowed, which give an east-west cross-section of the western part of Holland. 'Groot Mijdrecht' is situated in the eastern part.

In the figures different types of groundwater are distinguished, according to their origin:

- Ca $(HCO_3)_2$-water (Δ), which is actually infiltrated rainwater;
- $NaHCO_3$-water (o), found in marine sediments if the saline water is superseded by fresh water, or if saline water has intruded continental sediments and then again has been superseded by fresh water;
- NaCl-water (□), water of sea-water composition, e.g. with high chlorine content;
- $CaCl_2$-water (◇), formed if saline water intrudes sediments which have been in contact with fresh water;
- mixed-water (x), mixture of the first two with the latter two types of water.

Originally $Ca(HCO_3)_2$-water was found near the infiltration area, the hills of Utrecht and Veluwe. In the direction of flow towards the sea $NaHCO_3$-water was formed, where the pore water of marine sediments was superseded by fresh water.

After the reclamation of 'Groot Mijdrecht' the salt water was upconing as fig. 12 shows, thus splitting the $NaHCO_3$-zone.

At the eastern and western borders of the polder mixed NaCl- and $Ca(HCO_3)_2$-waters are found. At the west-side this appeared to be rather narrow, whereas at the eastside of the polder a wide zone with mixed water was observed. These findings also support the results of the geoelectrical survey.

6. CONCLUSIONS

For inventory investigations concerning salinization geoelectrical sounding can be very helpful. The results of the survey in 'Groot Mijdrecht' so far show a strong salinization in the centre of the polder, with a sharp rising interface between fresh and brackish/saline groundwater in the east. A thick transitional zone is also demonstrated.

In the west the interface is rising slowly and a shallow transitional zone is found. In the north the situation lies between those extremes. In order to predict a possible steady-state situation, the survey should be repeated.

An interesting subject for further research is to investigate the composition and origin of the transitional zones, e.g. by well-logging and using isotope techniques.

REFERENCES

DAM, J.C. VAN (1960). Het kwelonderzoek in de Horstermeerpolder. Den Haag: Rijkswaterstaat.

DAM, J.C. VAN (1964). Geo-elektrisch onderzoek Randgebied Zuid Flevoland. Den Haag: Rijkswaterstaat.

DAM, J.C. VAN (1976). Partial depletion of saline groundwater by seepage. J. Hydrol. 29, 315-339.

GEIRNAERT, W. (1971). Het optreden van kathionenuitwisseling in groundwater. H_2O 6, 118-127.

HOORN, W.H.C. TEN (1981). Some calculations concerning the fresh water-salt water interface in the subsoil. Geol. Jb. C 29.

KRUIJK, K.H. (1963). Groot Mijdrecht, Hydrologisch onderzoek. Utrecht: Provinciale Waterstaat.

LEENEN, J.D. (1978). Geo-elektrisch onderzoek naar de verzilting van de polder Groot Mijdrecht. Engin. Thes. Univ. Technol., Delft.

MEINARDI, C.R. (1974). The origin of brackish groundwater in the lower parts of the Netherlands. Leidschendam: Dutch Nat. Inst. Water Supply.

RIJKS GEOLOGISCHE DIENST (1975). Geologie Provincie Utrecht. Haarlem: Rijks Geol. Dienst.

VOLKER, A. (1961). Source of brackish groundwater in Pleistocene formations beneath the Dutch Polderland. Econ. Geol.

WIT, K.E. (1974). Hydrologisch onderzoek in Midden-West-Nederland. Institute for Land and Water Management Research (I.C.W. Wageningen, Nota 782.

FIGURES

Fig. 1: Location of Groot Mijdrecht in the western part of The Netherlands.

Fig. 2: Polder-levels; profiles.

Fig. 3: Schematic geological section of the underground in the Groot Mijdrecht area.

Fig. 4: Geoelectrical sounding curves of the eastern part of cross-section 1.

Fig. 5: Geoelectrical sounding curves of the western part of cross-section 1.

Fig. 6: Geoelectrical sounding curves of the eastern part of cross-section II.

Fig. 7: Geoelectrical sounding curves of the western part of cross-section II.

Fig. 8: Resistivity Profile I - Geoelektrisch Onderzoek Polder Groot Mijdrecht-

Fig. 9: Resistivity Profiles II, III - Geoelektrisch Onderzoek Polder Groot Mijdrecht.

Fig. 10: Resistivity Profile I - East - Geoelektrisch Onderzoek Polder Groot Mijdrecht.

Fig. 11: Chlorine contents (mg/l) in the groundwater near surface. Contour lines after WIT (1974).

Fig. 12: Groundwater types of western Holland, E-W cross-section (after GEIRNAERT, 1971).

Fig. 13: Location of the cross-section of fig. 12 (after GEIRNAERT, 1971).

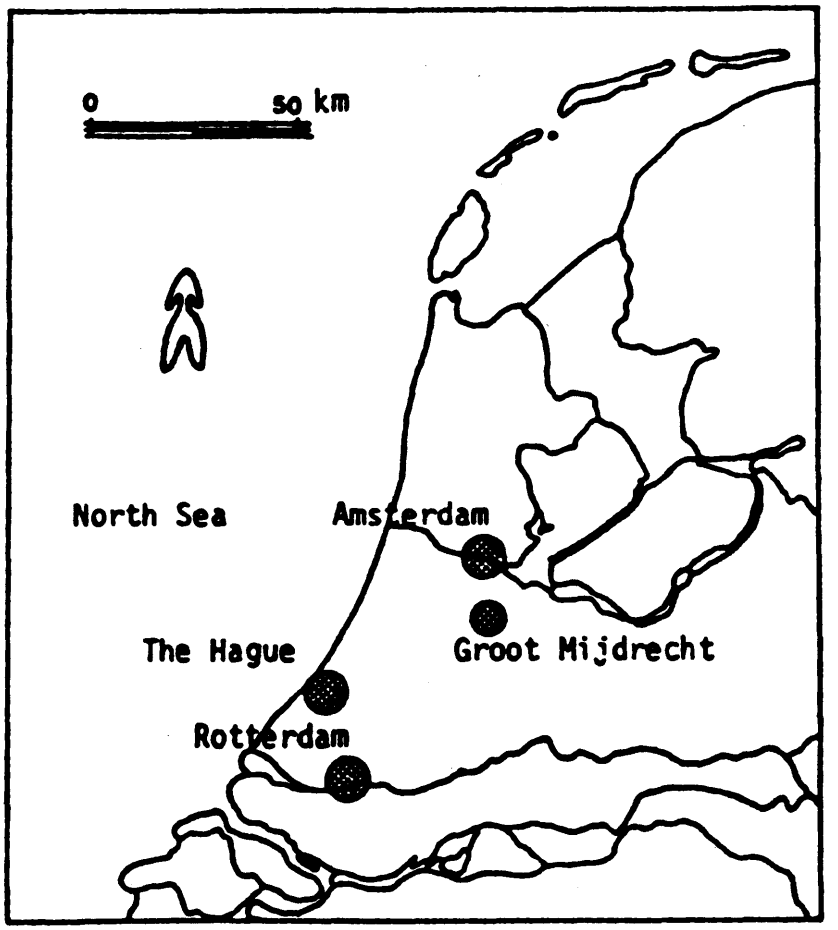

Figure 1

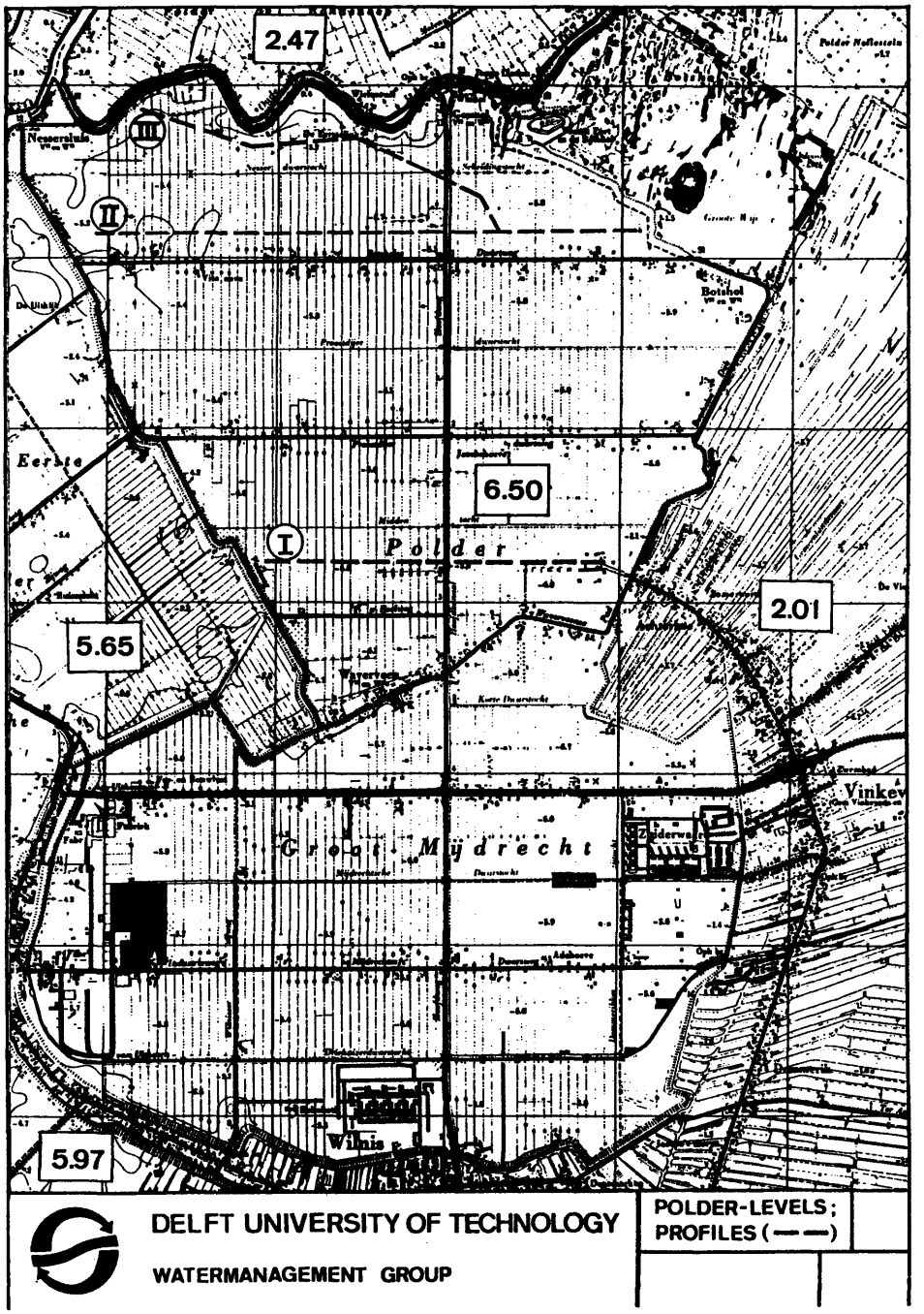
2.47
6.50
2.01
5.65
5.97
Polder
Groot Mijdrecht
Botshol
Vinkeveen
Wilnis
DELFT UNIVERSITY OF TECHNOLOGY
WATERMANAGEMENT GROUP
POLDER-LEVELS;
PROFILES (——)

Figure 2

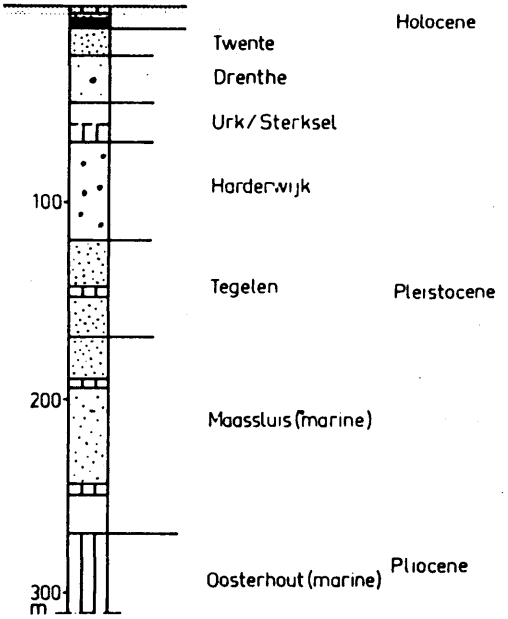

Figure 3

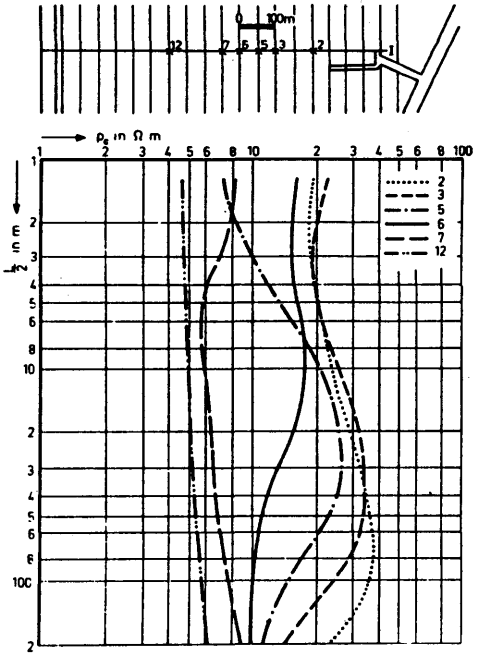

Figure 4

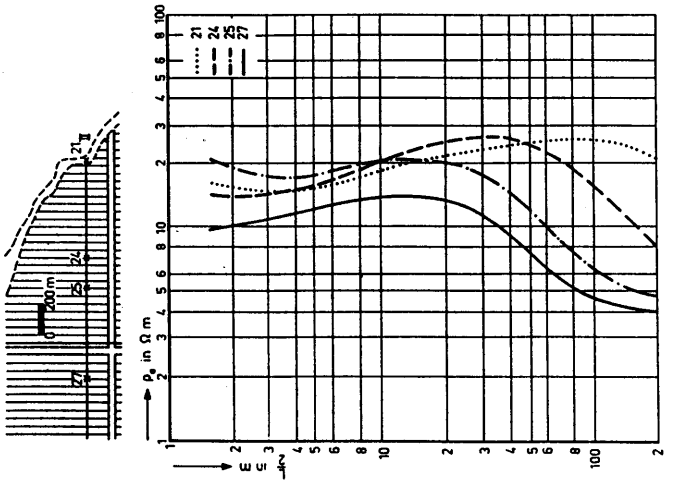

Figure 6

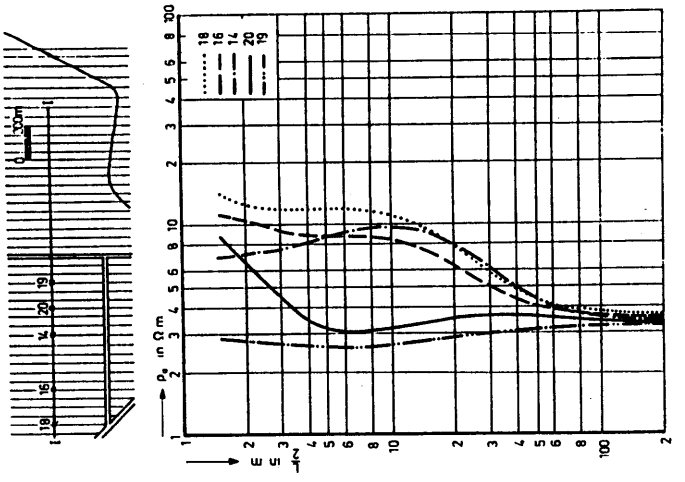

Figure 5

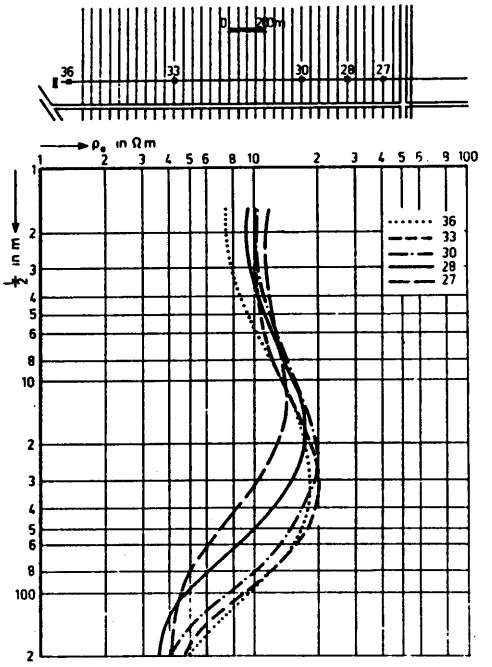

Figure 7

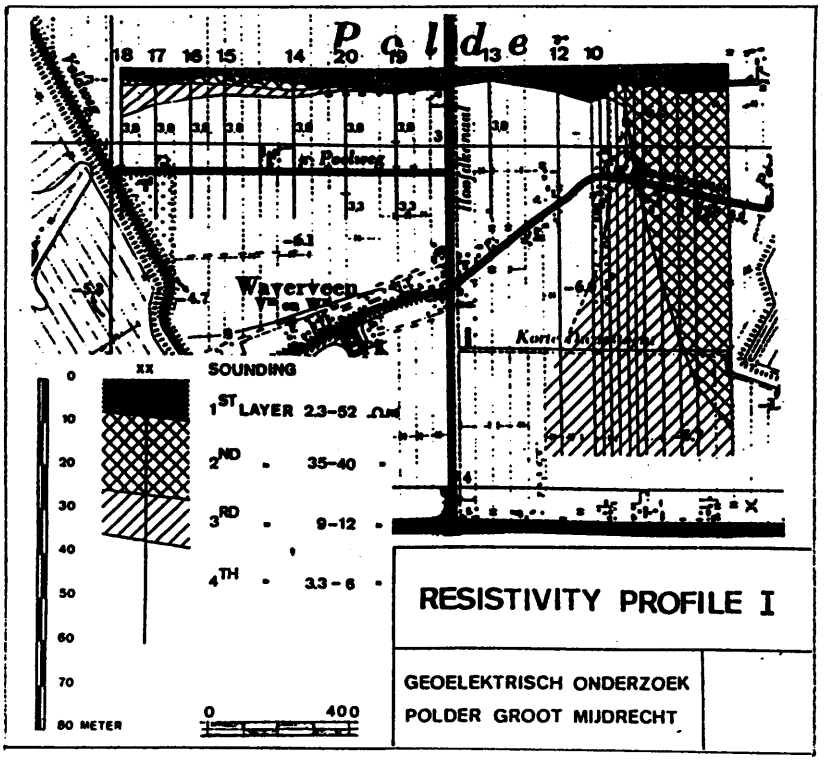

Figure 8

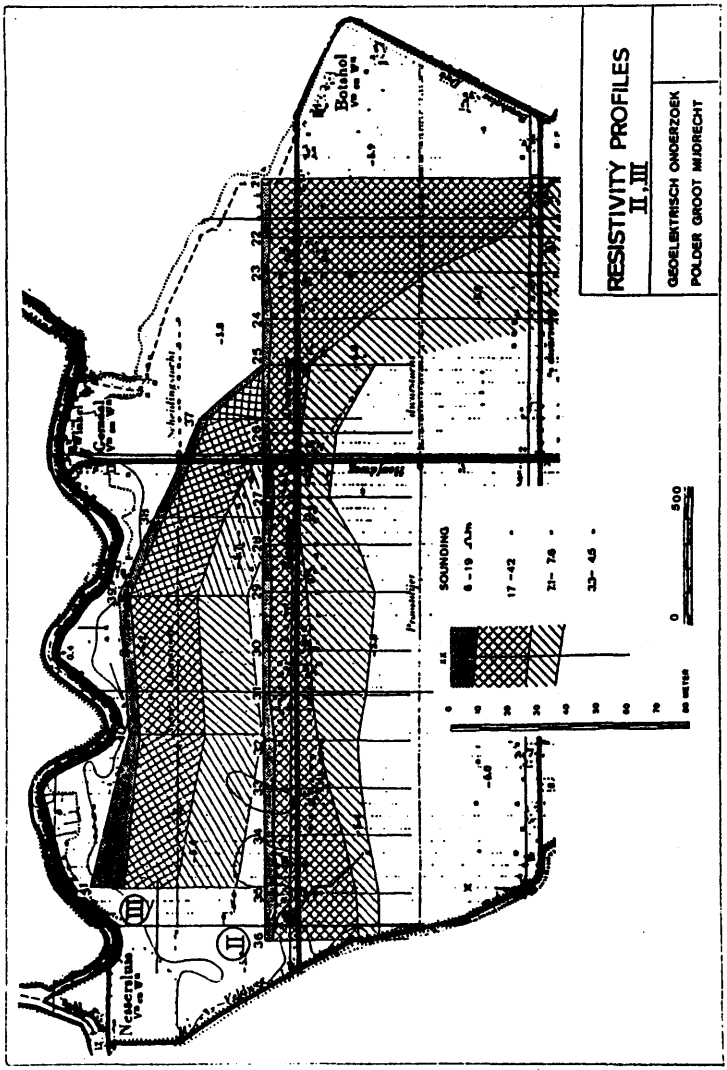
RESISTIVITY PROFILES
II, III
GEOELEKTRISCH ONDERZOEK
POLDER GROOT MIJDRECHT
SOUNDING
0
500

Figure 9

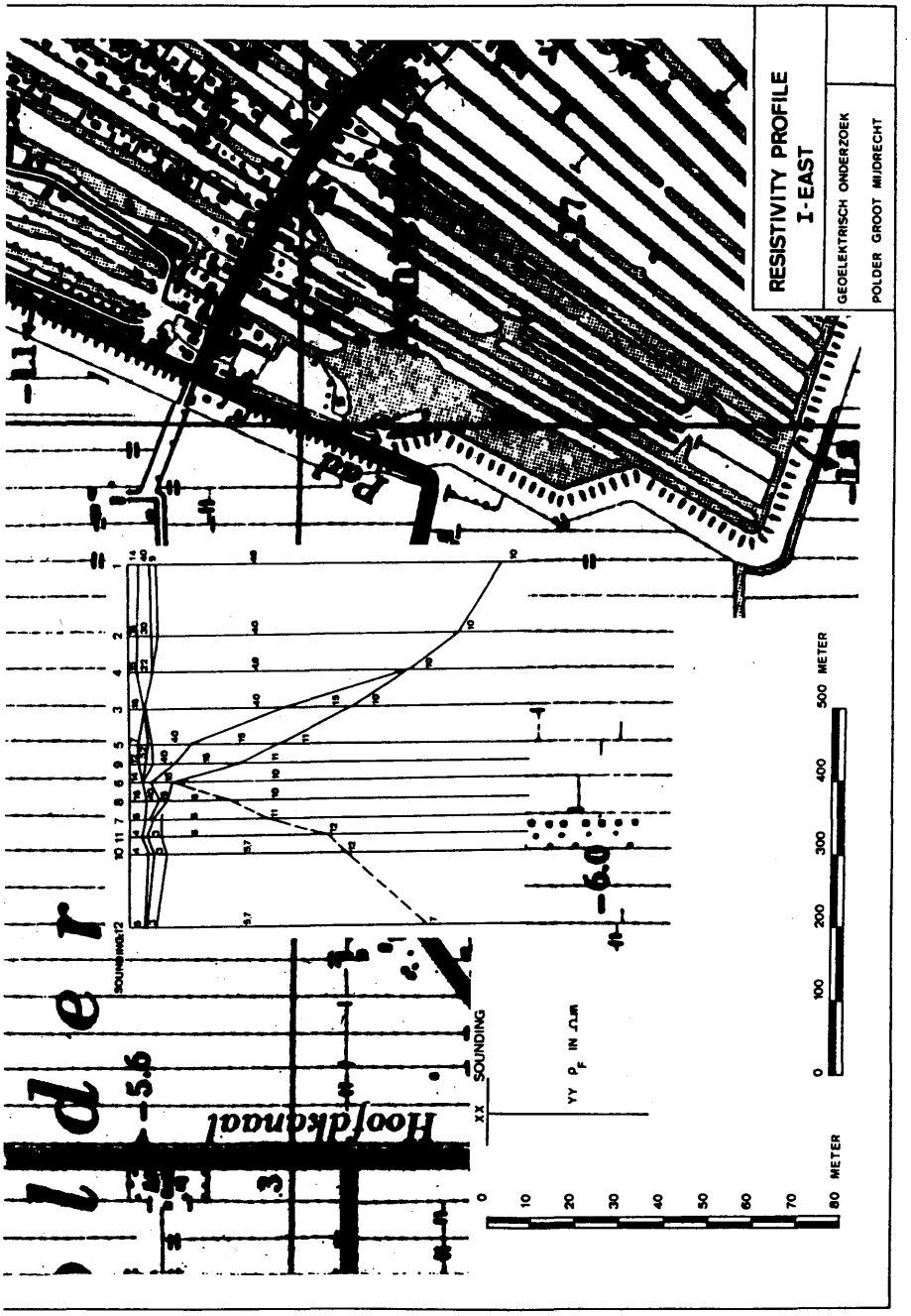
RESISTIVITY PROFILE
I - EAST
GEOELEKTRISCH ONDERZOEK
POLDER GROOT MIJDRECHT
Hoofdkanaal
-5.6
-6.0
SOUNDING
XX
YY
0 10 20 30 40 50 60 70 80 METER
0 100 200 300 400 500 METER

Figure 10

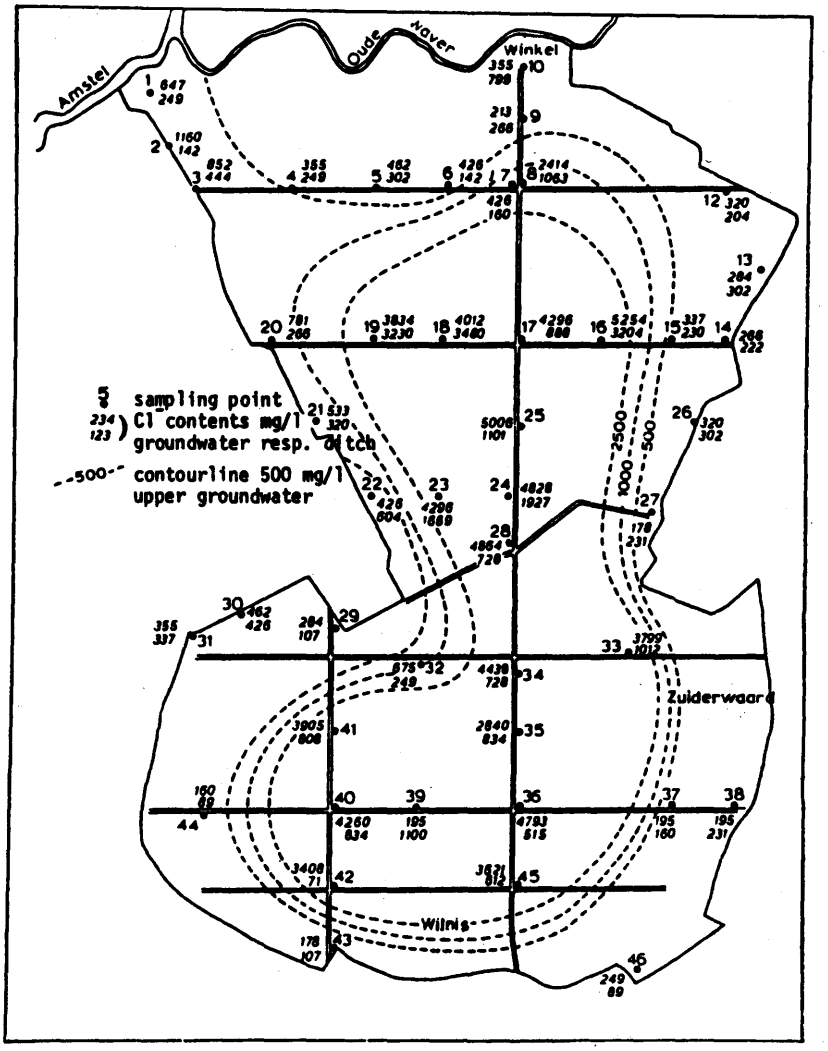
Amstel
Oude Haver
Winkel
Zuiderwaard
Wilnis
sampling point
Cl contents mg/l
groundwater resp. ditch
contourline 500 mg/l
upper groundwater

Figure 11

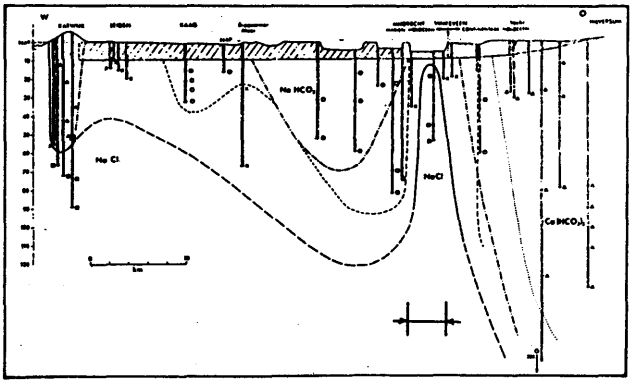

Figure 12

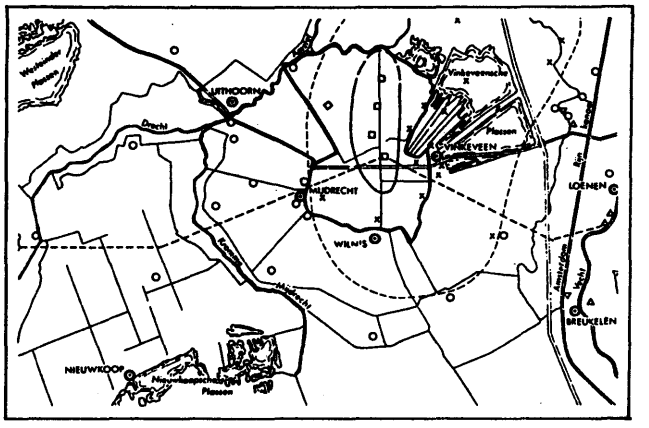

Figure 13

6.2. LOCATING THE FRESH-/SALT-WATER INTERFACE ON THE ISLAND OF SPIEKEROOG BY AIRBORNE EM RESISTIVITY/DEPTH MAPPING

K.P. SENGPIEL & P. MEISER

ABSTRACT

A test survey was flown on 4 July 1978 over the eastern part of the island of Spiekeroog with the helicopter of the BGR. The purpose was to test the applicability of new interpretation procedures for data from the "Dighem-II" electromagnetic (EM) measuring system for hydrogeological problems. The results of the resistivity/depth mapping show that the lateral and vertical extent of a known freshwater lens may be located indirectly by mapping the surface of the salt water intrusion below it. Thus, a technique for rapidly determining the location of the freshwater/salt water interface in large areas below medium to poorly conducting cover is available.

1. INTRODUCTION

The BGR has been testing a combined helicopter-borne measuring system for use in prospecting for mineral deposits since 1976. This has been done within the framework of a research project of the Federal Minister for Research and Technology. The system includes three instruments for geophysical measurements:

1. an electromagnetic transmitter-receiver (Dighem-II) for determining the conductivity distribution in the subsurface,
2. a proton magnetometer (G 803), and
3. a gamma-ray spectrometer (Exploranium DiGRS 3001).

Although it is planned to use this measuring system primarily for prospecting for solid mineral resources, there are good reasons for also testing its use for solving hydrogeological problems.

This is especially the case for the Dighem-II equipment, since among the geophysical methods, chiefly the electrical methods have been successfully applied in the field of hydrogeology.

The Dighem-II system normally operates with a frequency of about 900 Hz and responds especially to zones of low electrical resistivity in the subsurface (with values between 0,5 and 50 Ohm·m). Such resistivities are very often encountered in hydrogeology, e.g. sands containing saline water (about 1 Ohm·m), clays (3 to 20 Ohm·m), fresh water (20 - 50 Ohm·m), etc.

Airborne electromagnetic measurements were tested in France and Canada as early as 1965 for their applicability in the field of hydrogeology (BAUDOUIN et al., 1967; COLLETT, 1967). Although very modern and efficient equipment (Input) was used, the results obtained were not convincing enough due to an evaluation procedure that was too simple for airborne geophysical methods to become common hydrogeological practice.

A new starting point for investigations was provided for the BGR when the development of an airborne resistivity/depth mapping method was completed (SENGPIEL et al., 1979). This method has been used for the interpretation of data measured with the Dighem system since 1978. It seems to be particularly well suited for the determination of the fresh-/salt-water boundary in the subsurface.

A test area was selected on which information concerning the location of the fresh-water/saline-water boundary is already available, i.e. the eastern half of Spiekeroog Island.

The results of the airborne test surveys with the Dighem-II system are described and discussed in the following.

2. PLANNING AND IMPLEMENTATION OF THE SURVEY

The location of the survey area can be seen in fig. 1. Eighteen N-S profiles were flown in the eastern half of the island with a nominal spacing of 100 m and a length of about 2 km. Additionally, two check profiles were flown from east to west. The total profile length is 40 km, the surveyed area 4 km^2.

The survey was made on 4 July 1978 starting from Wilhelmshaven airport (distance to Spiekeroog 36 km). Total flying time was 1,2 hours. The island has a flat topography; the dunes are up to 19 m above sea level.

3. MEASURING SYSTEM

- General Description

The data are recorded simultaneously during the flight on the three instruments that make up the measuring system. In analog form on paper and in digital form on magnetic tape, the electromagnetic data are recorded every 0,5 second, the magnetic and gamma-ray-spectrometer data every second.

- Electromagnetic System

The first Dighem-II electromagnetic system was commissioned by the BGR from Dighem Ltd., Toronto, Canada. It was installed in the BGR helicopter with the rest of the equipment in June/July 1976. The most conspicuous part of the Dighem-II system is a 10-m-long cylinder-shaped unit (50 cm in diameter) trailing from the helicopter on a 50-m-long cable. In the front part of the unit there are two transmitter coils, one with a vertical axis, the other with a horizontal axis, that generate an alternating electromagnetic field of slightly differing frequency close to 900 Hz.

During the survey flight with the unit about 30 m above ground, this magnetic field penetrates the earth where it generates eddy currents. The higher the electric conductivity of the subsurface, the stronger the eddy currents. The intensity of these currents depends also on shape and location of the conducting body with respect to the direction of the inducing fields. The strength of the induced magnetic field is recorded relative to the strength of the transmitted field as measured by three receiver coils oriented perpendicularly to each other at the rear end of the trailing unit (bird). The signals are split into two time components (inphase and quadrature) during the further processing depending on the phase of the transmitted field. Theoretically, 12 values (2 transmitters (T_1, T_2) x 3 receivers (R_1, R_2, R_3) x 2 time components) are available for evaluation.

For evaluation by the resistivity/depth mapping method, however, only the amplitude and phase of the combinations T_1R_1 or T_2R_2 are required.

In addition to these values, man-made (e.g. 50 Hz high-voltage power lines) and atmospheric disturbances are recorded both with analog and digital methods in the so-called Sferics channel.

- Magnetometer, Gamma-ray Spectrometer

A detailed description of the magnetometer and the gamma-ray spectrometer is not given here since data obtained with these measuring systems are not discussed in this paper.

- Radar Altimeter

The radar altimeter installed in the helicopter (Sperry, model AA-200) shows the altitude above ground or, if there are woods, the altitude above the tree tops within the range of 0 - 2.500 feet; the range from 0 to 500 feet is exaggerated. Within this range the indicator can be read to the nearest 5 feet. According to the manufacturer, the accuracy between 100 and 500 feet is $\pm$ 5 %. The altitude is recorded both in analog and digital form.

- Flight-path Camera

The flight-path camera was specially made by Geocam in Toronto, Canada. It is operated with a 35 mm film drawn over a 0,025 mm-wide opening at constant speed. Thus, a continuous film of the flight path is made by the camera, which is installed in the floor of the helicopter. The flight path is much easier to reconstruct from this "strip film" than from film consisting of a number of individual pictures. The objective used has a focal length of 17 mm. Accordingly, at an altitude of 250 feet, the film shows an about 100 m-wide strip of ground.

- Recording of the Data

All measurements by the various instruments are collected in a signal-distribution box. From there they are transferred via switches to the two 8-channel analog recorders or to the "Data Acquisition System" where they are recorded digitally on magnetic tape. The switches of the signal-distribution box allow great freedom in selecting which channel is to be used for recording any particular signal.

The data is recorded on an 8-channel chart recorder R 800 produced by the Barringer Co. in Toronto, Canada, with heated needles on wax paper. The width of the paper for each channel is 40 mm, the velocity of the paper is about 2 mm/sec.

The data arriving at the input of the "Data Acquisition System" are sampled twice a second (conversion of parallel data into serial data) before they are recorded on magnetic tape on a 9-track tape recorder, product of the Kennedy Co., USA, with a density of 800 bpi.

- Time Markers

In order to be able to correlate the measured data to their locations in the field, time markers are set at specific intervals on the film, the chart and the magnetic tape. For this purpose a pulse is generated in the "Data Acquisition System" after each 20 reading cycles, i.e. every 10 sec. These pulses are counted by the intervalometer. Their numbers are recorded on the magnetic tape after every reading.

4. EVALUATION AND REPRESENTATION OF THE DATA

- Reconstruction of the Flight path

The reconstruction of the flight path is based on the time marks (fids) which appear every 10 sec on the film of the flight path (and on the other data-storage media). The location represented by these fids is determined by comparing the flight-path film with air-photo maps, scale in this case 1 : 5.000, and then marked on these maps. The flight path is normally represented by straight-line strips of about 300 m length. Higher (slower) flight velocity increases (decreases) the fid interval.

The co-ordinates of the fid locations are digitized and recorded on magnetic tape. Any section of the flight path can then be drawn on suitable maps by computer.

- Maps Used for Registering the Data

Air-photo maps, scale 1 : 5.000, serve as basis for representing the data obtained in this area. Flight paths and data are plotted on these maps, partly by computer. A simplified form of these maps is contained in the Appendices.

- The Resistivity/Depth Mapping (RDM) Method

Using an electromagnetic measuring system with only one transmitter frequency, two values can be obtained, i.e. amplitude and phase of the induced magnetic field. Two parameters of a simple conductivity model can be calculated from these measured values. With the resistivity/depth mapping method, the resitivity ρ and the distance h between the probe and upper boundary of a conductive homogeneous half-space (SENGPIEL & RICHTER, 1975; FRASER, 1978; SENGPIEL et al., 1979) can be determined for each pair of these values. As the flight altitude H of the bird is known from the radar measurements, the depth p of the upper boundary of the half-space below the surface of the earth can be calculated from the difference between h and H.

Fig. 2 shows the relationship of the parameters ρ and h to the amplitude and phase (or its tangent).

It is obvious that low specific resistivities of the subsurface generate considerably larger amplitudes than high resistivites. For example, a large conductive area at 61 m depth with ρ = 1 Ohm·m gives a much stronger response to the probe (i.e. an amplitude of 110 ppm) than a conductor at only 30 m depth with ρ = 200 Ohm·m (A = 18 ppm). Accordingly, mainly areas of low resistivities (ρ < 50 Ohm·m) can be located in the subsurface with a transmitter frequency of 900 Hz.

The subsurface only seldom corresponds to the simple conductivity model that is used. Therefore, the parameters calculated using the RDM method are designated as <u>apparent</u> resistivity (in the following called w) or as <u>apparent</u> depth (p). The conversion of the values amplitude and phase into the parameters w and p is advantageous for a number of reasons (FRASER, 1978; SENGPIEL, 1981), e.g. the significantly lower dependence of w and p on flight altitude.

In the following, a theoretical example is used to investigate the significance of the values w and p if the resistivity distribution in the subsurface is not homogeneous. For this purpose, a two-layer-case model is used with ρ_1 = 100 Ohm·m, ρ_2 = 1 Ohm·m and a variable thickness d of the overlying strata. This model corresponds approximately to the sequence: fresh-water filled sand above salt-water bearing sand. The calculation is made in two steps:

1) Determination of amplitude and phase above a horizontally layered half space using a computer program by SINHA & COLLETT (1973) which was converted into HPL by S. GREINWALD.

2) Conversion of these values into w and p with an (unpublished) algorithm by FRASER (1975).

The results are shown in fig. 3 for a two-layer case with increasing thickness d of the cover layers (abscissa).

It is quite conspicuous that for d < 30 m, resistivity and depth of the substratum are given rather accurately by w and p, i.e. the overlying strata appear to be transparent. For larger values of d, w increases and reaches 100 Ohm·m, the resistivity of the overlying strata, at ≈ 170 m. At the same time, p ≈ 0, i.e. the good-conducting substratum no longer gives a response. In this case, d corresponds to the "penetration depth" (or "skin depth") δ, a parameter frequently used in electromagnetics, which for f = 900 Hz can easily be calculated from

$$\delta = 16{,}8 \cdot \sqrt{\rho} \qquad (\rho \text{ in Ohm·m})$$

and yields δ = 168 m in this case.

Fig. 3 demonstrates that the apparent depth p does not increase indefinitely with increasing d, but reaches a maximum (of 40 m) already at d = 60 m and then decreases. This ambiguity of p as a function of d, however, can be eliminated if the corresponding resistivities w are also considered: in the example in fig. 3 the values of p for w < 6 Ohm·m are on the rising limb of the curve, where they represent a serviceable measure for the depth of the substratum. The threshold value w_M for this limiting case for p can be determined for two-layer cases with ρ_1, ρ_2 with the following empirical formula (for f = 900 Hz):

$$w_M = 1{,}5 \cdot \rho_2 + \sqrt{\frac{\rho_1 - \rho_2}{5}}$$

The value of w_M need not be determined very precisely to yield an adequate boundary between usable and fictious values of p as shown by the example in fig. 3.

It can be demonstrated (e.g. FRASER, 1978) that in two-layer cases with $\rho_2 \ll \rho_1$, the apparent depth p is always negative as long as d < δ. Although no information on the depth of a stratigraphic boundary can be obtained from p in this case, it may be concluded that the overlying stratum is better conducting than the substratum.

From these and other (SENGPIEL, 1981) theoretical examples it can be derived that a good-conducting substratum, e.g. salt-water bearing sands, can be located not only by the apparent resistivity w, but that also its depth beneath the earth's surface can be described approximately by p. Consequently, the electromagnetic resistivity/depth mapping method yields somewhat more information than mapping with direct-current geoelectric methods using constant distances between the electrodes. Moreover, due to the rate of measurement (2 per sec.), i.e. a distance between measuring points of about 14 m, the grid of measuring points for this airborne survey is denser than is usual for a ground survey.

- Data Processing

Only the data (0° - 90° phase) from the horizontal coil system T_2R_2 (frequency about 900 Hz) were used for the resistivity/depth mapping method. The evaluation is based on the data recorded on magnetic tape. It is almost completely computerized and is carried out in the following steps:

- determination of the sensitivity using a calibration curve;
- conversion of the measured voltage (mV) into ppm of the strength of the transmitter field at the receiver;
- determination of the absolute zero level (AZL) and zero point drift during flights at altitudes H > 300 m outside the survey area;
- calculation of the amplitudes relative to AZL;
- slight to medium smoothing of the data, depending on their amplitude;
- conversion of all pairs of values to specific resistivity w and depth p for the assumed model of a homogeneous, conducting subsurface (according to FRASER, 1975);
- labelling of uncertain resistivity values and fictitious depth values;
- subtraction of the flight altitude as measured by radar from the calculated depth values;
- control plot of the measured and calculated data (for each profile);
- read-in of the flight-path co-ordinates (after digitization);
- assignment of the co-ordinates to each measurement;
- determination of the points of intersection of the given isolines with the flight paths;
- determination of the locations where maximum and minimum values were measured;
- computerized plotting of the data from the two preceding steps and the flight paths, including the identification of uncertain or fictitious values.

On the basis of this plot an isoline map is drawn by hand for the (apparent) specific resistivity w and the (equivalent) depth p on air-photo maps, scale 1 : 5000.

5. HYDROGEOLOGY OF SPIEKEROOG ISLAND

Only few of the wells on the island penetrate the Holocene sediments. From the data obtained in a drillhole sunk near the administration office of the health resort of Spiekeroog, the following profile can be derived:

Holocene 0	- 3,5 m fine-grained sand ("dune sand")	
	- 19,8 m fine- to medium-grained sand ("tidal sand") with thin silt layers	
Pleistocene	- 30,0 m medium- to coarse-grained sand partly with fine gravel	Saalian glaciation
	- 30,2 m clay (?Lauenburger clay)	Elsterian glaciation
	- 44,7 m medium-grained sand to fine gravel	
Pliocene	- 60,2 m clay and fine-grained sand (basin silt)	
	- 80,0 m fine- to medium-grained sand	

In general it can be assumed that Holocene sediments, primarily sandy becoming increasingly silty with depth, occur down to about 20 m depth; below that, there are Pleistocene to Pliocene sands of differing grain-size mixtures down to about 100 m with occasional intercalations of clays and silts at various levels. The sands are highly permeable. They are, however, mostly filled with highly saline groundwater as can be seen from geoelectric-resistivity measurements (Schlumberger array).

In the Holocene sands there is an unconfined aquifer draining to the sea. In the Pleistocene sands there is a lower layer with confined groundwater.

The average annual rainfall on Spiekeroog Island is 700 mm. Assuming a seepage (infiltration) factor of 0,5, the groundwater recharge rate must be about 0,8 million m^3/yr.

6, DISCUSSION OF THE RESULTS

The depth contours of the bottom of the fresh-water bearing sands were plotted on a map of the eastern part of Spiekeroog Island (fig. 4); this was done on the basis of a geoelectric survey by the Geological Survey of Lower Saxony in September 1969, reported by RÜLKE. The depths are given relative to sea level; the depth contours for the apparent depth p (fig. 6), however, were calculated from the earth's surface, most of which is 2 to 10 m above m.s.l.

In addition, the following remarks should be made about the depth contour map in fig. 4.

1) Twenty-seven geoelectric soundings (no. 20 to 46) were made in the area represented in this map. The evaluation of the results yielded a three-layer case for most of the area (RÜLKE, 1969): a high-resistivity cover layer, several metres thick (500 - 9000 Ohm·m, dry sands); a layer up to 50 m thick with 100 to 160 OHm·m (fresh-water bearing sands); and a substratum with 5 Ohm·m (containing salt water). Locally, an intercalation of 20 to 60 Ohm·m and varying thickness (e.g. 30 m thickness in sounding 46,

NW of the Hermann Lietz School) is encountered between the substratum and the fresh-water lens. This intercalated layer is interpreted as a silt or clay layer or as brackish water (RÜLKE, 1969, p. 5). The bottom of the fresh-water layer is therefore assumed at the upper edge of this intercalation. These are the depth values on the map in fig. 4.

2) The depth contours of the northern and eastern boundary of the fresh-water lens were determined by extrapolation and are therefore uncertain. The northernmost and easternmost sounding sites are along the path 100 to 150 m inland parallel to the northern edge of the island. The path then turns southward (towards the Hermann Lietz school). The southern boundary could not be traced because it crosses a built-up area (RÜLKE).

The results of the test survey with the helicopter are represented in figs. 5 and 6.

Fig. 5 shows the contour-lines of the apparent resistivity w in Ohm·m. First, it must be stated that only low resistivities $w \leq 7.5$ Ohm·m occur. This is to be expected (see fig. 3) if there is a widely distributed salt-water bearing layer of sand at depth with a very low true resistivity ($\rho < 2$ Ohm·m). It is not possible to determine the boundary of a fresh-water lens only on the basis of the resistivity map, since primarily the resistivity of the good-conducting layer is indicated here. It is, however, conspicuous that the fresh-water lens is surrounded by a zone of slightly higher resistivites ($3{,}4 < w < 7{,}5$) which in fig. 5 is between the adjoining isolines $w = 3{,}2$ Ohm·m. There are only a few possibilities to explain this bounding zone of w values:

a) the good-conducting layer is at an extremely great depth below this zone, i.e. > 50 m (see fig. 3);

b) there is a transition zone of resistivity in the cover layer of the area immediately outside the fresh-water lens.

Assumption a) cannot be correlated with the hydrogeological model of the island nor is it confirmed by the calculated depths in fig. 6.

Case b) was studied theoretically. A two-layer case with constant thickness $d_1 = 20$, 30 or 40 m and constant $\rho_2 = 1{,}5$ Ohm·m was assumed and the resistivity ρ_1 of the cover layer was varied from 1 to 400 Ohm·m. The values of w and p were calculated as a function of ρ_1. The results are presented in fig. 7. Indeed, a maximum is to be seen in each of the curves of w; this maximum is at $w = 3{,}1$, 4,9 and 7,2 Ohm·m for thickness of the cover layer $d_1 = 20$, 30, and 40 m, respectively. The corresponding true resistivities of the cover layer are $d_1 =$ 6, 10 and 14 Ohm·m. Paradoxically, the w decreases again for higher values of ρ_1. Due to the increase of ρ_1, the cover layer becomes increasingly "transparent" for the electromagnetic fields, so that w begins to approximate the true resistivity of the substratum (1,5 Ohm·m).

The resistivity maxima observed along the zone of fig. 5 range from 3,4 to 7,5 Ohm·m, which means that they correspond well with the theoretical values in fig. 7. Consequently, the resistivity distribution shown in fig. 5 can be explained as follows:

The inner contour line w = 3,2 approximately defines the boundary of the fresh-water lens. There, the true resistivities of the cover layer are sufficiently high (100 to 160 Ohm·m) that mainly the resistivity and the depth of the intruded salt water (i.e. good-conducting layer) are recorded. Outside the inner contour w = 3,2 there is an area with a continual decrease in the true resistivity ρ_1 in the up to 40 m-thick cover layer. Brackish water with a salt concentration increasing in the direction to the sea is assumed in this zone. According to the values of w (fig. 5), this zone corresponds approximately to the beach area on the north side of the island; in the south it is much wider and includes about one third of the island.

The lateral extent of the fresh-water lens as found by the resistivity-mapping project corresponds to a large extent to the extrapolation given in fig. 4. However, certain differences must be expected, since the ground survey and the airborne survey were done nine years apart.

The contour map of the apparent depths (fig. 6) shows very distinctly the depression of the good-conducting layer, i.e. the upper edge of the salt water below the fresh-water lens. This boundary is identical with the bottom of the fresh-water lens only if any intercalations present, e.g. clay, are thin. According to the data in figs. 3 and 7, the depth of the good-conducting layer as given in fig. 6 is somewhat too small, since the resistivity of the cover layers is mostly not high enough. The results of fig. 6 do not differ very much from those obtained during the geoelectric survey in 1969 (fig. 4).

The depth contour p = 20 m corresponds generally to w = 3,2 Ohm·m and thus also represents approximately the lateral extent of the fresh-water lens. Neither the theoretical curves p of fig. 7 nor the depth contours of fig. 6 show a maximum in the resistivity transition zone of the cover layer and therefore support assumption b). This also means that the calculated depths p for the transition zone, e.g. for p > 20 m, do not indicate the bottom of the fresh-water lens, but only the approximate upper edge of the salt-water bearing good-conducting layer below the zone of brackish water; it must be assumed that the calculated values of p are a little too low (according to fig. 3).

7. CONCLUSIONS

The electromagnetic-test survey of Spiekeroog Island carried out with the helicopter of the BGR in combination with the resistivity/depth mapping method yielded the following results:

1) Both the lateral extent and the bottom of a known fresh-water lens up to 60 m thick were determined by a method using a combination of the parameters apparent resistivity w and apparent depth p. This method is based mainly on the determination of the depth of the good-conducting layer, i.e. the upper edge of the salt-water bearing sands below the fresh-water lens.

2) Although a measurement with only one transmitter frequency was used, it was possible to draw conclusions for a multilayer case (e.g. the existence of a transition zone of resistivity in the cover layer around the fresh-water lens) by the combined use of the parameters w and p, which for the assumed model of a homogeneous half-space can be calculated directly from the measured values.

   It is assumed that this up to 40 m-thick zone is filled with brackish water with a salt concentration increasing in the direction away from the fresh-water lens.

3) If electromagnetic methods by helicopter are to be applied in the field of hydrogeology, it is recommended that multi-frequency systems be used and the data be evaluated on the basis of multi-layer cases. However, considering the measuring rate of the airborne systeme, 72 multi-layer cases would have to be calculated per line-kilometre or 7200 per flight hour.

   Simple and fast conversion methods for multi-layer cases have not yet been developed. Moreover, the requirements with respect to the quality of the data would have to be increased considerably in order to obtain sufficiently reliable data (i.e. less drift and better signal-to-noise ratio).

4) Because a rather large area can be rapidly surveyed (flight speed = 100 km/h) and because the data can be rapidly processed by computer, the use of a helicopter for an electromagnetic survey is also suitable for reconnaissance surveys of the hydrogeology of large areas. In addition to the salt-water/fresh-water interface studied here, other not too complicated conductivity distributions can also be studied, e.g. clay layers in fresh-water bearing sand, fresh-water occurrences in dry sands, etc.

ACKNOWLEDGEMENT

The authors wish to express their appreciation to the Federal Minister for Research and Technology for providing the necessary funds for the survey and the evaluation of the data obtained within the framework of the research project NTS-6 "Equipping and testing of a helicopter for geophysical surveys". Thanks are also due to the helicopter team of the BGR, to Dr. H. GERHARDY, Mrs. J. NOWAK (Dipl.-Ing), Mr. H. KRÖNING and Mr. E.-G. KIND (Dipl.-Math.) for their encouragement and co-operation during acquisition, processing and interpretation of the data.

REFERENCES

BAUDOUIN, P., DUROZOY, G. & UTARD, M. (1967). Etude par prospection électromagnétique aérienne d'un contact eau douce - eau salée dans le delta du Rhône. In: Mining and Groundwater Geophysics/1967, Rep. geol. Surv. Canada 26, 626-637.

COLLET, L.S. 1967). Resistivity mapping by electromagnetic methods. In: Mining and Groundwater Geophysics/1967, Rep. Geol. Surv. Canada 26, 615-624.

FRASER, D.C. (1975). The Dighem Interpretation Manual. Toronto, Dighem Limited (Not publ.).

FRASER, D.C. (1978). Resistivity mapping with an airborne multicoil electromagnetic system. Geophysics 43, 144-172.

RÜLKE, O. (1969). Bericht über die geoelektrische Untersuchung auf der Insel Spiekeroog 1969. Arch. NLfB 5191 (Hannover).

SENGPIEL, K.P. (1979). Airborne EM combined resistivity and depth mapping in mineral and groundwater exploration. Vortrag 49th int. Meeting der SEG; New Orleans.

SENGPIEL, K.P. (1981). Airborne EM combined resistivity and depth mapping. (To be published in Geophysics).

SENGPIEL, K.P. & RICHTER, P. (1975). Aerogeophysikalische Detailvermessung im Gebiet Pitangui, Minas Gerais, Brasilien. Ber. Arch. BGR 075305 (Hannover).

SINHA, A.K. & COLLETT, L.S. (1973). Electromagnetic fields of oscillating magnetic dipoles placed over a multilayer conducting earth. G.S.C. paper 72 - 25 (Ottawa).

FIGURES

Fig. 1: Location of the test area on the Island of Spiekeroog.

Fig. 2: Amplitude and phase of the induced magnetic field in relation to distance (h) and resistivity (ρ) of a conducting halfspace (after FRASER, 1978).

Fig. 3: Apparent resistivity w, depth p, and field amplitude above two-layer-cases with variable thickness d_1 of upper layer for the Dighem-II system (coil separation = 7,98 m, frequency = 900 Hz).

Fig. 4: Island of Spiekeroog: depth contours of the bottom of the fresh-water lens in m below sea level as inferred from 26 d.c. depth soundings on the ground (after RÜLKE, 1969).

Fig. 5: Contour lines of the apparent resistivity w in Ohm·m from the helicopter survey with the Dighem-II system.

Fig. 6: Contour lines of the apparent depth p in m below earth surface from the helicopter survey with the Dighem-II system.

Fig. 7: Apparent resistivity w and depth p above two-layer cases with variable resistivity ρ_1 and for three values for the thickness d_1 of the top-layer. The resistivity of the substratum is 1,5 Ohm·m.

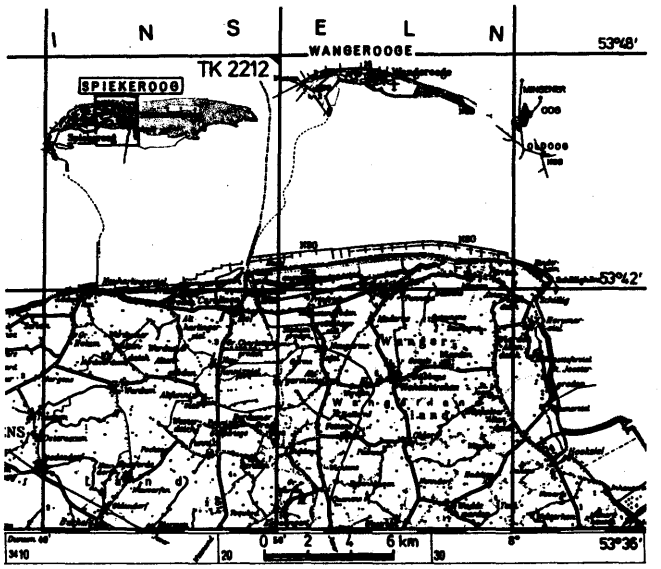

Location of the test area on the island of Spiekeroog.

Figure 1

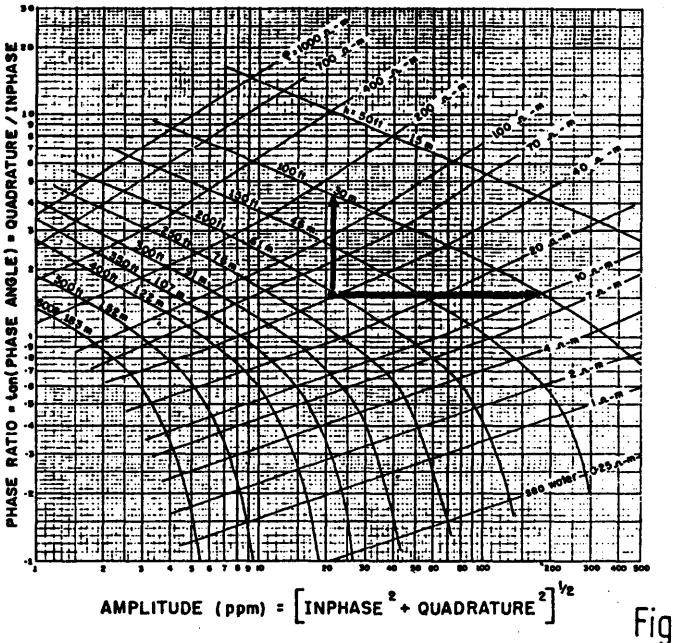

Figure 2

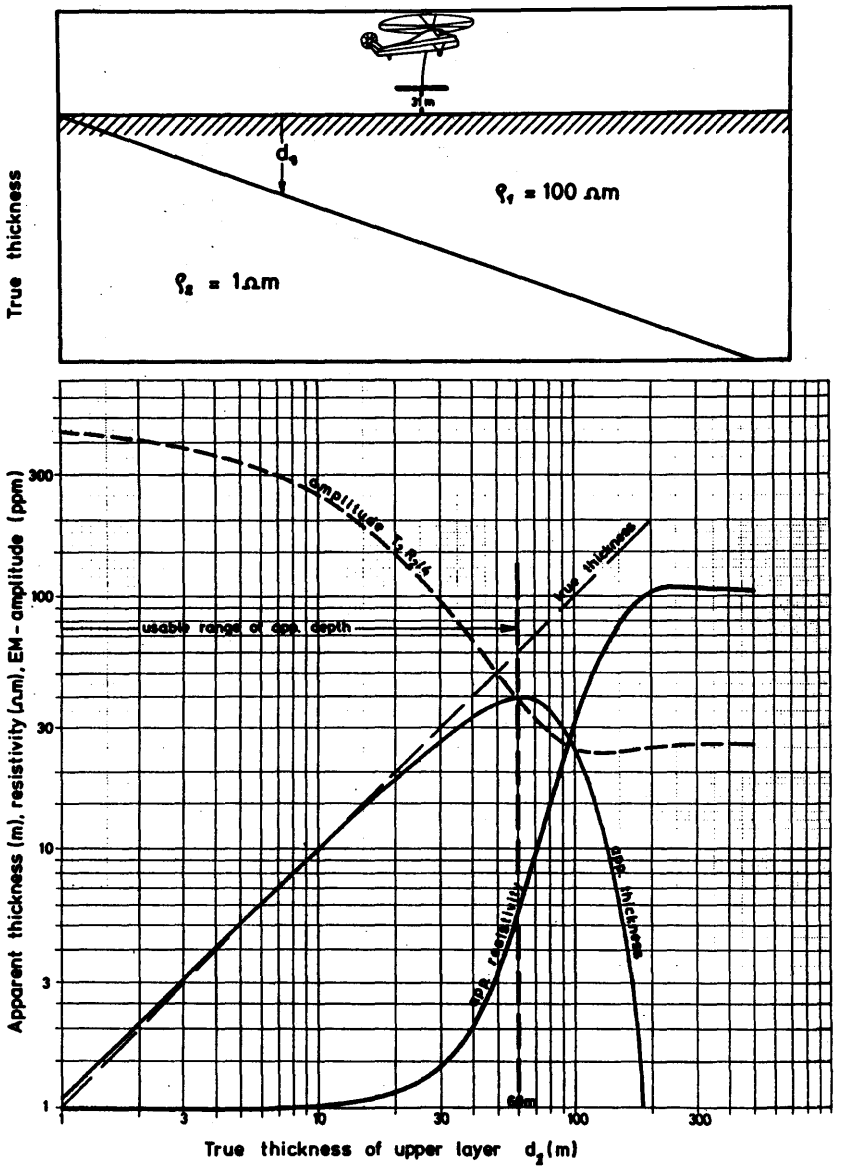
True thickness
31m
d_1
ρ_1 = 100 Ωm
ρ_2 = 1Ωm
Apparent thickness (m), resistivity (Ωm), EM - amplitude (ppm)
300
100
30
10
3
1
amplitude $\propto h^{-4}$
usable range of app. depth
true thickness
app. resistivity
app. thickness
3
10
30
100
300
60m
True thickness of upper layer d_1 (m)

Figure 3

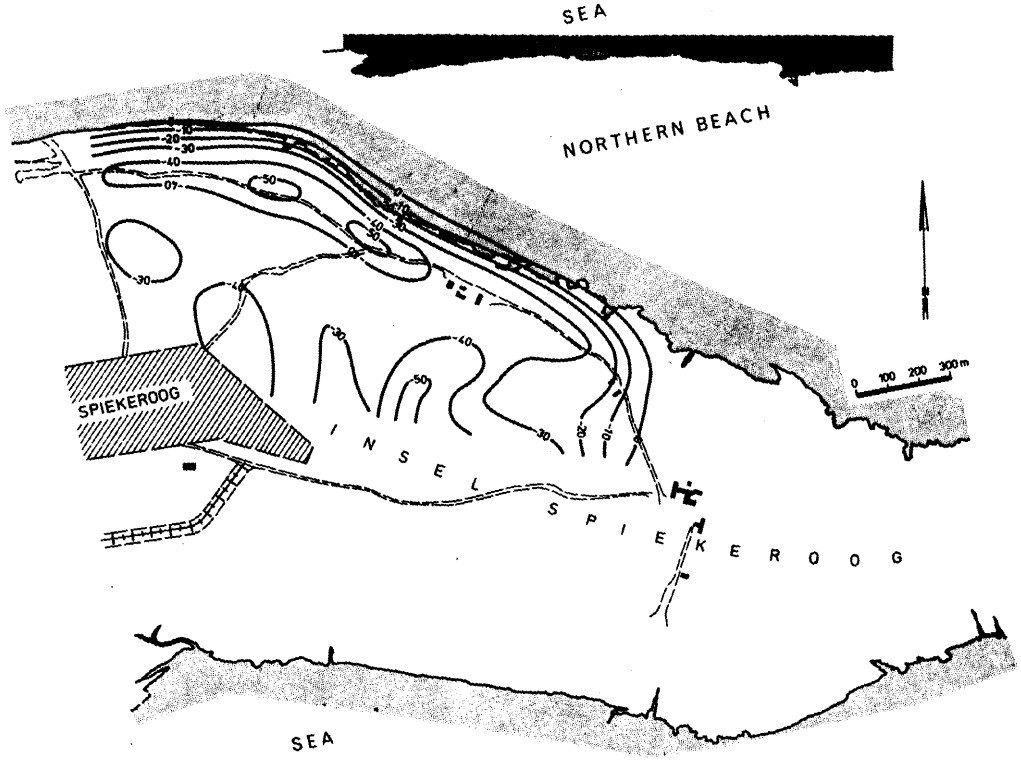
SEA
NORTHERN BEACH
SPIEKEROOG
INSEL SPIEKEROOG
0 100 200 300m
SEA

Figure 4

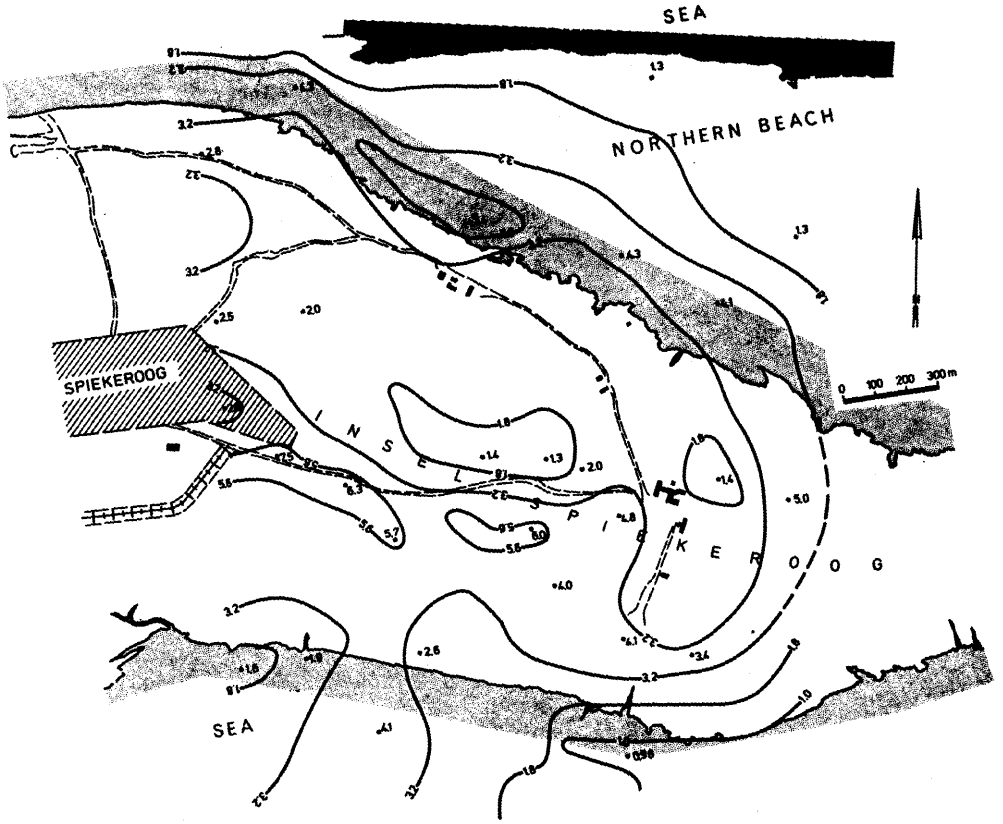
SEA
NORTHERN BEACH
SPIEKEROOG
INSEL
SPIEKEROOG
SEA
0 100 200 300m

Figure 5

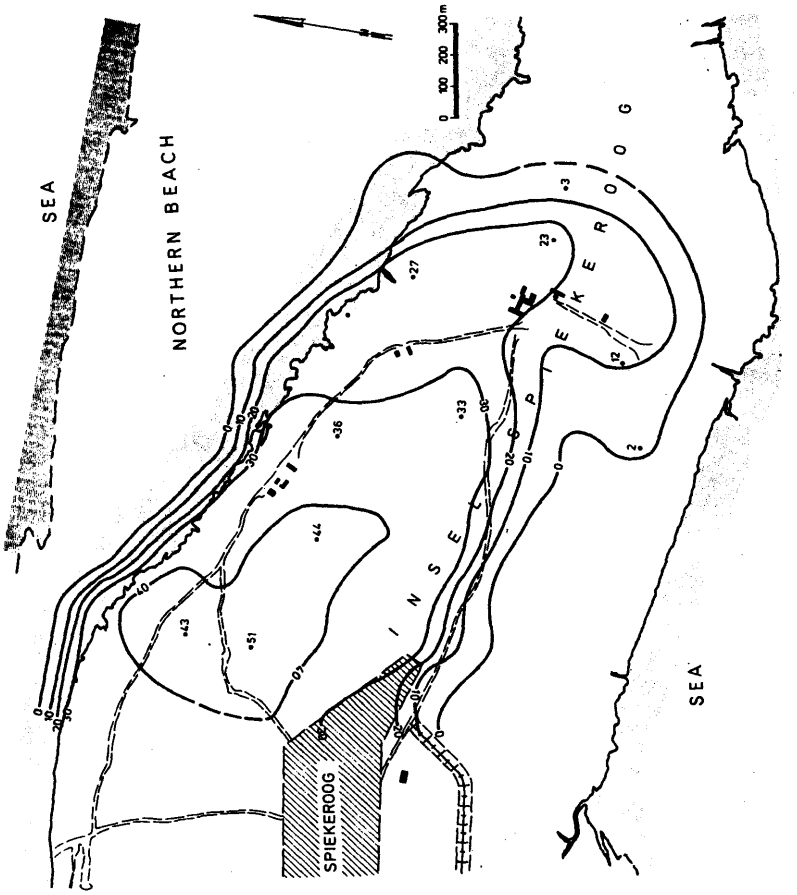
SEA
NORTHERN BEACH
0 100 200 300m
SPIEKEROOG
I N S E L
S P I E K E R O O G
SEA

Figure 6

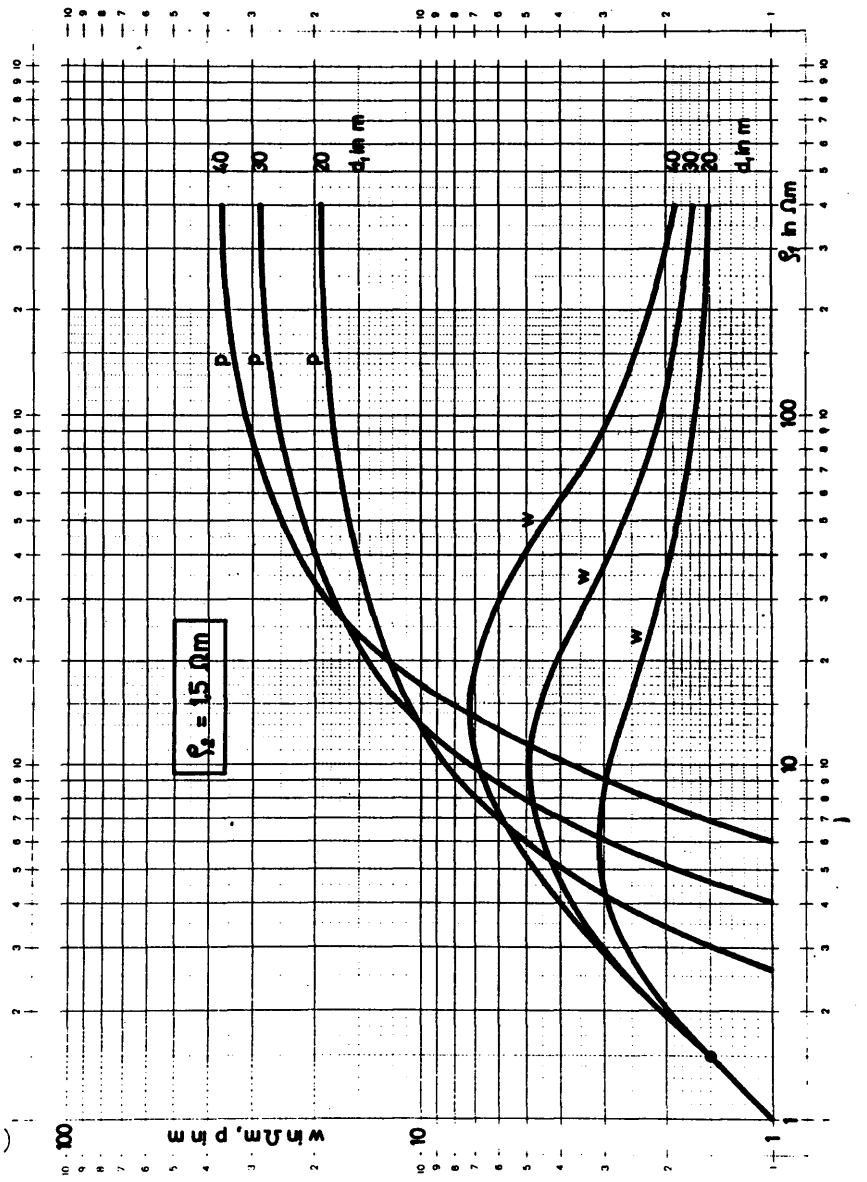

Figure 7

6.3. EVALUATION OF GROUNDWATER SALINITY FROM WELL LOGS AND CONCLUSIONS ON FLOW VELOCITIES

K. FIELITZ & W. GIESEL

ABSTRACT

Groundwater conductivity was evaluated from resistivity and porosity logs applying the formation-factor concept. From the conductivity the density of highly saline waters with a main content of sodium chloride was calculated. These data were used in combination with density data from water samples to derive the three-dimensional density distribution in the sedimentary cover of a salt dome. An aquifer directly on top of the salt dome exhibited nearly plane surfaces of equal density. From the vertical density gradient and the inclination of these planes the relative change of the Darcy-velocity in relation to the depth was evaluated.

During an investigation of fresh- and saline-groundwater flow in unconsolidated sediments we had to deal with two problems:

- first, to calculate continuous profiles of groundwater conductivity and density from borehole measurements,
- second, to apply the density data to the evaluation of groundwater flow.

In the region of the study the saline water originates from the solution of salt at a salt dome. Water of very different salt content, ranging from fresh water to saturated salt solution, is found.
In this case the density differences are, of course, extreme, but the methods used may be applied to coastal aquifers in a similar way.

The sediments of the investigated area consist of sands, clays and silt of mainly Quaternary age and mainly glacial or glaciofluvial origin.

The available data were: a pumped-water sample and water-level data from each observation well and the following well logs: gamma ray log, focussed electric log, induction electric log, spontaneous potential density log, and caliper log.

We tried to derive continuous profiles of groundwater conductivity by evaluating the formation resistivity from the focussed electric log or the induction log and calculating the water resistivity by use of formation factors.

For the determination of formation factors we first tested the applicability of the Archie formula.

Testing is possible at points where water samples are available. Fig. 1 shows a plot of the formation factor versus the porosity of the formation. The formation-factor values were calculated by dividing the formation resistivity R_o by the water resistivity R_w of samples.

The data were restricted to water samples of low resistivity. Only in this case is the quotient R_o/R_w equal to the true formation factor.

The porosity was evaluated from the density log data. The points are scattered around the drawn curve, which represents the Archie relation after inserting the Humble coefficient and exponent (D.W. HILCHIE, 1978).

There are considerable deviations from the curve, but the application of the formula will obviously provide better results than the assumption of a constant formation factor.

Consequently the application of the Archie-Humble relation, which was derived primarily for oil field formations, to unconsolidated Quaternary sediments is justified, as long as there is no better method.

In groundwater with large variations of salinity the difference between true and apparent formation factors has also to be taken into account (M. RINK & J.R. SCHOPPER, 1974).

The apparent formation factor F_o is defined as the quotient R_o/R_w, while the true formation factor F_o is the limit of R_o/R_w for R_w approaching zero.

Fig. 2 shows the apparent formation factor F_o in relation to the water resistivity R_w. These are data of sand aquifers of the investigated area. The water resistivities are measured values of pumped-water samples.

F_o decreases with increasing water resistivity. This is an effect described by different authors (M. RINK & J.R. SCHOPPER, 1974; H. REPSOLD, 1976), with respect to laboratory and field measurements of sand resistivities.

It may be explained as follows: the conductivity is made up of two parts: one which is proportional to the conductivity of the electrolyte, and one which is independent of the conductivity of the electrolyte. The latter results from ionizing forces at the pore surfaces. We call the corresponding resistivity R_i - the resistivity related to the internal surface of the porous material. R_i is big for coarse and clean sands, and it is small for silt and clay.

We thus have two characteristic values for a formation, defining its resistivity in relation to water resistivity: the true formation factor F_o and the internal-surface resistivity R_i.

While F_o may be approximately calculated from well-log data, as mentioned above, only average R_i values for certain regions or formations may be estimated. So, for instance, the two curves of fig. 2 represent R_i-values of 300 Ohm.m or 60 Ohm.m respectively, which were found to be the best average values for sands from different periods of sedimentation.

Based on these considerations we use the formula of fig. 3 for calculating the water resistivity R_w.

The electrical conductivity of the formation is expressed as the sum of the conductivities, which is proportional to the conductivity of the water plus the constant conductivity related to the internal surface. The latter conductivity is divided into two terms, since R_i-values of sand and clay are different, and the clay content may be derived from the gamma ray log. The first of the two terms contains the internal-surface resistivity of clay and is assumed to be proportional to the clay content V_{c1}. The second term contains the internal surface resistivity of sand of the respective formation and is assumed to be proportional to $1-V_{c1}$.

R_o is evaluated from an Induction electric log or focussed electric log, the porosity $\emptyset$ from the density log, and the clay content from the gamma ray log.

This is, of course, an approximate formula, which tries to make use of the measured parameters as well as possible. If conductivity profiles are calculated, the results have to be observed critically and rechecked at any point where a water sample is available.

We applied the formula mainly in the case of brackish and salt water. In this case the first term of the sum is dominant, the estimation of R_i is not critical and errors are mainly due to the application of the Archie formula.

In the case of fresh water in silty sands the application of the formula is problematic, because R_i depends on the grain size and silt content.

A computer program was used to calculate conductivity profiles from the well-log data, which were recorded on digital tape.

Fig. 4 shows an example of a plot of groundwater conductivity. The conductivity is plotted on a logarithmic scale as mS/cm.

It increases from 1 mS/cm at 80 m depth to 70 mS/cm at the bottom of the borehole. The water-bearing formations are medium sand to coarse sand and silty sand.

For the study of saline-water flow the density is needed. Its calculation from conductivity data is possible if the ion content is roughly known. In our case we could simply use the conductivity/density relation of sodium chloride, because this was the dominating salt in solution.

The calculated density profiles were used for two different purposes. The first is illustrated in fig. 5. Two piezometer wells of different depth in an aquifer with water of varying density are shown. The formula gives the average Darcy-velocity $v_{1,2}$ between filters F_1 and F_2 · K_f is the permeability, h_1 and h_2 the piezometric levels (assuming fresh water of density ρ_o in the piezometer pipes), and $\rho(z)$ the density of the groundwater.

The integral term is a correction taking account of the excess hydrostatic pressure caused by the increased density of the salt water.

The equation holds only if both wells are so close together that the density may be regarded as a function of z only.

Fig. 6 shows a computed density profile at the left and the corresponding excess hydrostatic pressure at the right. The pressure unit is metres fresh-water column. The filter positions of two wells are marked by points F_1 and F_2.

The result is that 25 cm of fresh-water column have to be subtracted from the piezometric level of well No. 2 (with filter F_2) before calculating the hydraulic potential difference between the two wells. From the potential difference the local-flow velocities may be determined.

The procedure works sufficiently well as long as the water is not very salty and the vertical distance of the piezometer filters is not too big. In that case the correction term may be much bigger than the resulting potential difference and the accuracy of the calculation is no longer sufficient.

If enough boreholes with borehole measurements and water samples are available, information on saline-water flow may be got by analyzing the distribution of water density in vertical sections.

Fig. 7 shows a section through a mainly sandy aquifer at about 120 to 250 m depth and on top of a salt dome.
The aquifer is separated from that above it by silt and clay layers.

The inclined lines are lines of equal density. They mark water densities of 1050, 1100, and 1150 kg/m³ respectively. The plotted density data were evaluated from measurements of 16 water samples and borehole measurements for 11 wells.

A transition zone about 30 m thick is observed, where the density increases from below 1050 kg/m³ to that of a saturated solution.

The fresh water above the drawn section flows from the left to the right. The inclination of the transition zone is reasonable and resembles the appearance of a salt-/fresh-water boundary at the coast.

In this study it was essential to determine the flow velocities in and around the transition zone.

We used the equation shown in fig. 8 (J. BEAR, 1979). This defines the difference in velocities above and below a density discontinuity in relation to the density contrast and the inclination of the interface. ρ_o is the fresh-water density and k_f the permeability coefficient at $\rho = \rho_o$. This is a general equation, which includes the Ghyben-Herzberg relation as a special case.

Regarding the density lines of fig. 7 as discontinuities, the differences of velocities above and below each discontinuity may be calculated if a permeability value is assumed.

The velocities will decrease from top to bottom in the shown example, and it is obvious that the flow velocity of the nearly saturated water at the left of the section will be close to zero, since no salt-saturated water can enter from the left.

Starting from here (point 1) the velocities above this point may be calculated step by step. The resulting velocities are shown in fig. 7. The length of the arrows is proportional to the Darcy-velocity. The velocities above the transition zone are 4 to 5 m/year.

Assuming the simplified case of a constant potential gradient above the transition zone and a constant permeability, velocities may also be estimated at other points.
These velocity data are verified by velocities measured by a tracer technique.

The velocity data, particularly those at the right end of the section, enabled us to estimate the amount of salt per year which is transported away from the salt dome.

The method of determining flow velocities discussed here may seem to be quite indirect. However, in this case of high-salinity groundwater the direct determination of potential gradients is difficult, because the evaluation of piezometric levels leads to quite serious errors.

On the other hand, the analysis of the density distribution derived from many sample- and well-logging data has the advantage of giving an overall picture of the existing flow pattern.

REFERENCES

BEAR, J. (1979). Hydraulics of Groundwater. New York: McGraw Hill.

HILCHIE, D.W. (1978). Applied Open Hole Log Interpretation. Golden (Colorado): Hilchie Inc..

REPSOLD, H. (1976). Über das Verhalten des Formationsfaktors in Lockersedimenten bei schwach mineralisierten Porenwässern. Geol. Jahrb. E 9, 19-34.

RINK, M. & SCHOPPER, J.R. (1974). Interface conductivity and its implications to electric logging. SPWLA, Transactions of the Third European Formation Evaluation Symposium, London, 1974.

FIGURES

Fig. 1: Formation factor versus porosity. The data refer to Quaternary sands of glacial origin.

Fig. 2: Apparent formation factor in relation to water resistivity. The data refer to Quaternary sands of glacial origin and varying silt content.

Fig. 3: Formula for calculation of groundwater resistivity from well-log data (model of parallel conductances).

Fig. 4: Computed log of groundwater conductivity.

Fig. 5: Piezometers in groundwater of varying density ρ. Fresh water with density ρ_o assumed in the piezometers, $v_{1,2}$ = Darcy-velocity, μ = salt-water viscosity, μ_o = fresh-water viscosity.

Fig. 6: Computed logs of water density and excess hydrostatic pressure. F_1 and F_2 are filter positions of two boreholes.

Fig. 7: Section through aquifer on top of a salt dome, density and velocity of saline groundwater.

Fig. 8: Velocity discontinuity at an interface between waters of different density.

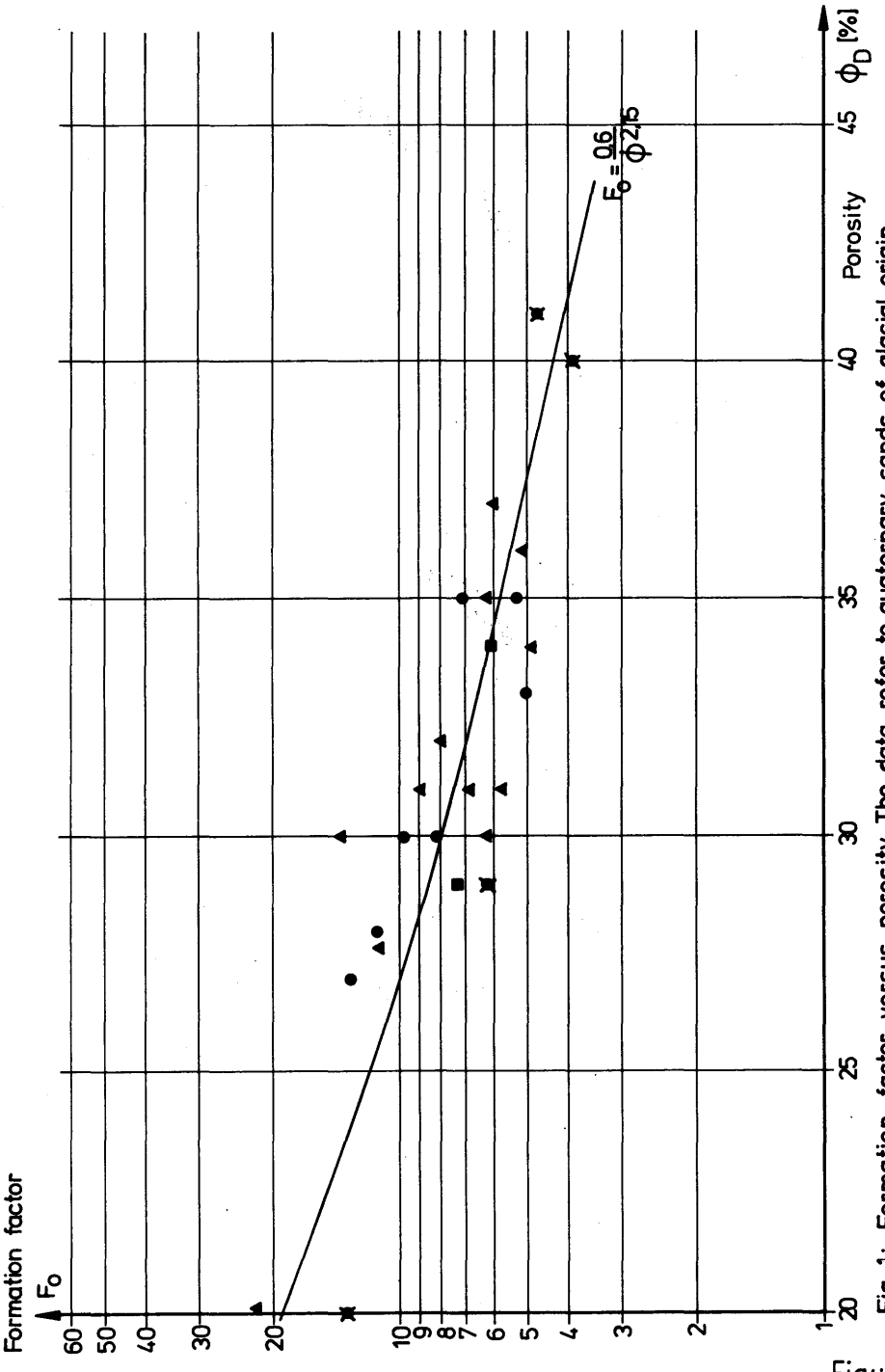

Fig. 1: Formation factor versus porosity. The data refer to quaternary sands of glacial origin.

Figure 1

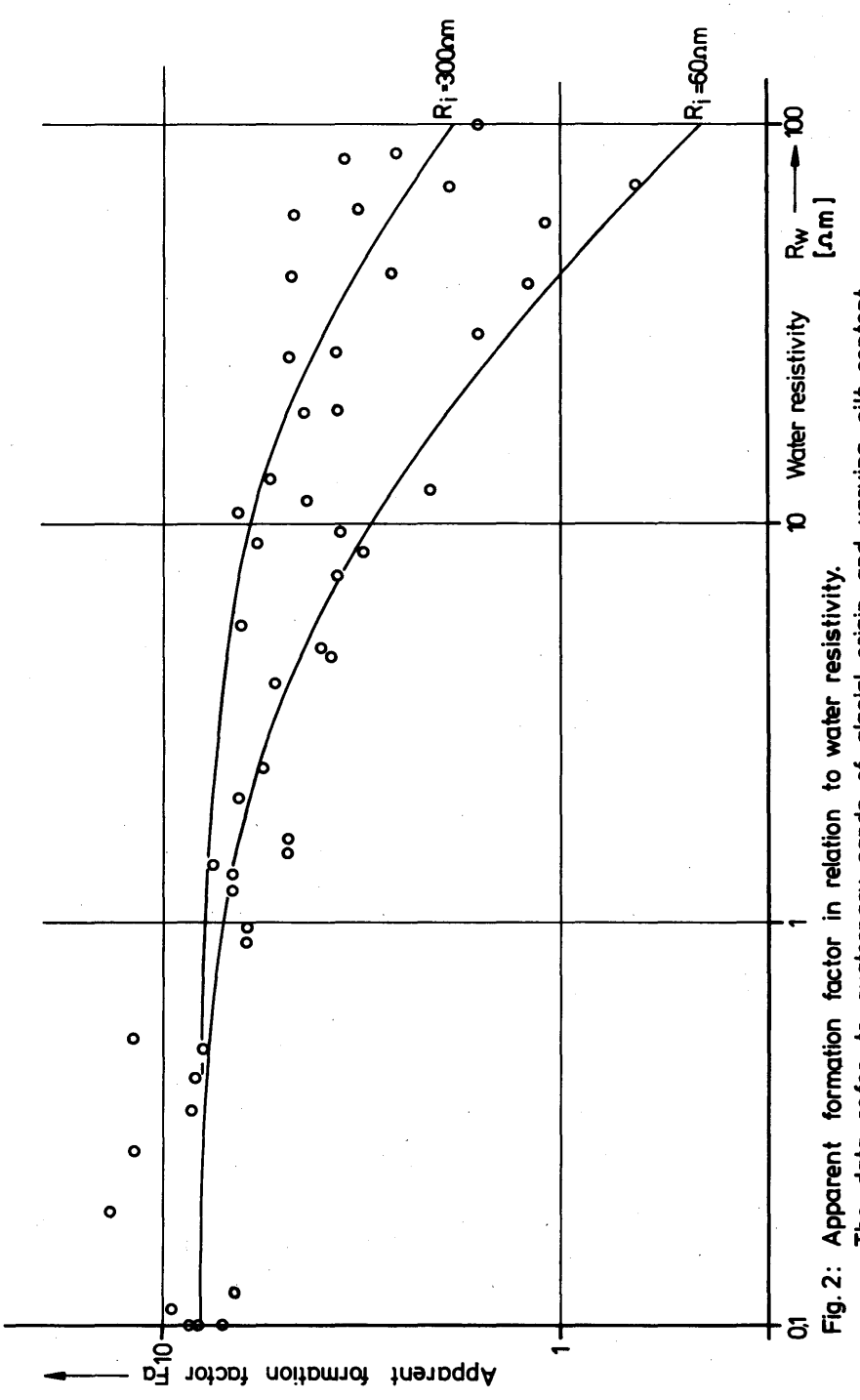

Fig. 2: Apparent formation factor in relation to water resistivity.
The data refer to quaternary sands of glacial origin and varying silt content.

Figure 2

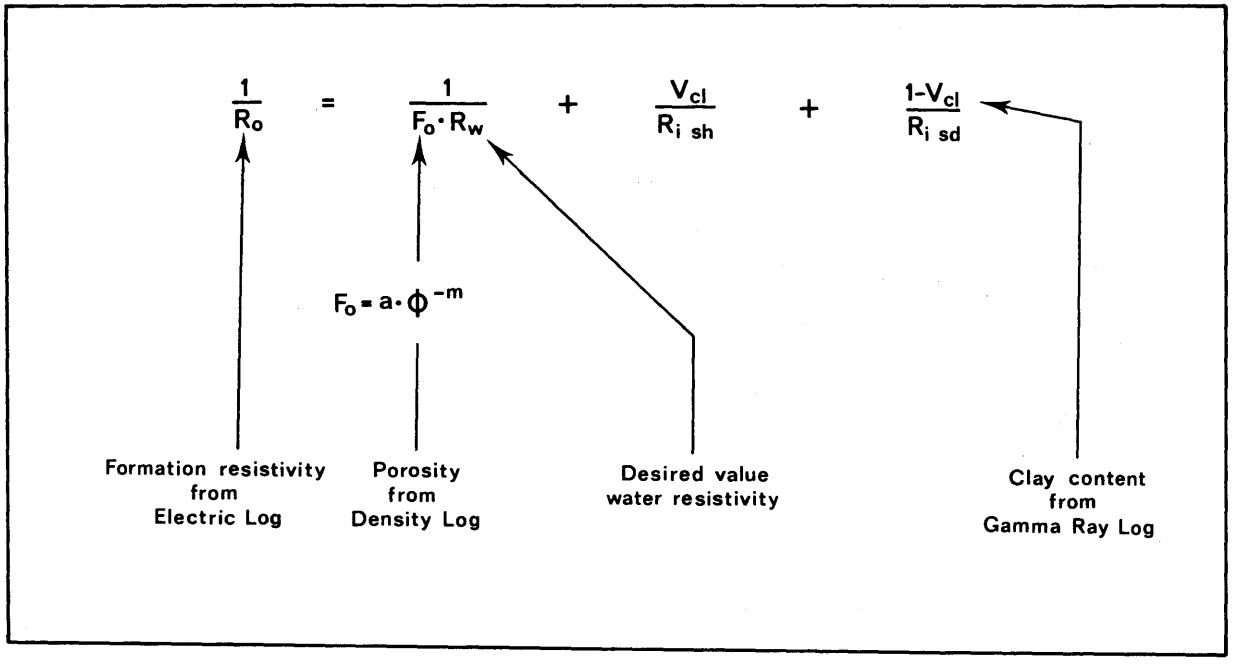

Fig.3 : Formula for calculation of groundwater resistivity from well log data (model of parallel conductances).

Figure 3

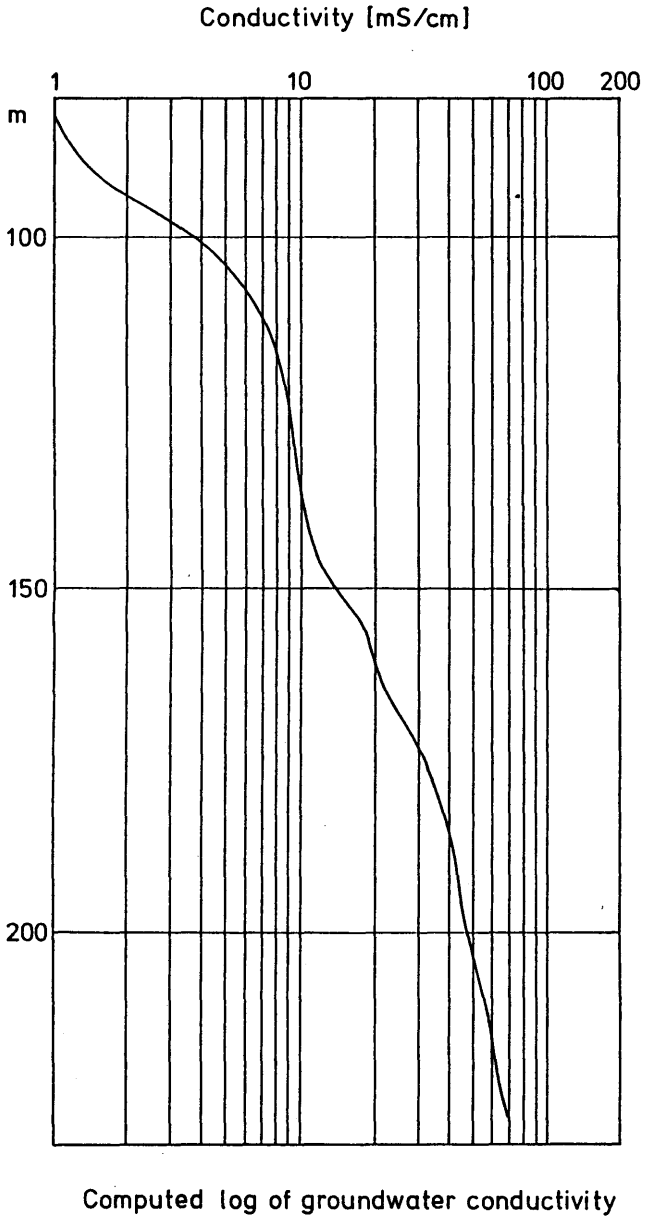
Conductivity [mS/cm]
1
10
100
200
m
100
150
200
Computed log of groundwater conductivity

Figure 4

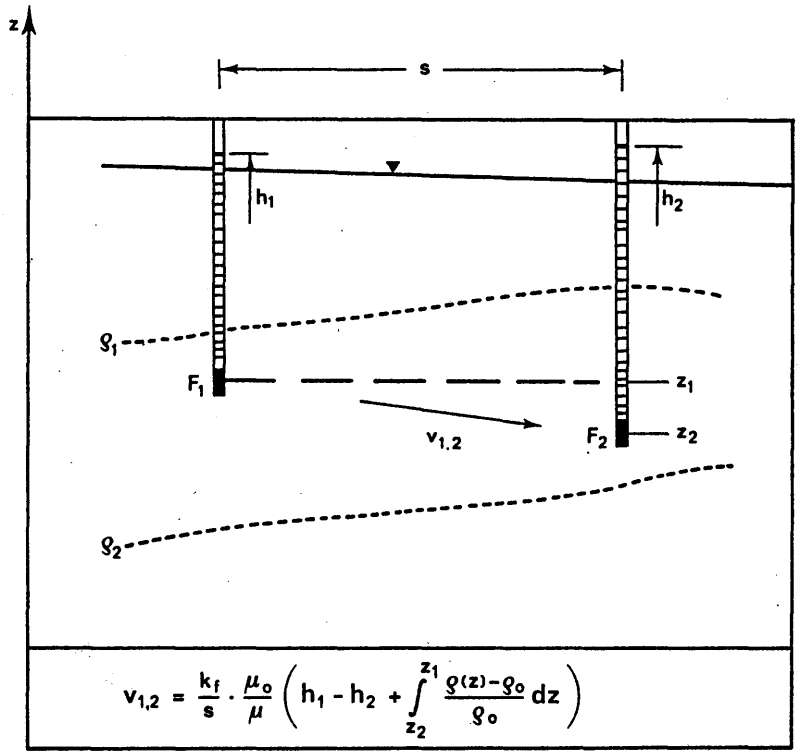

Piezometers in groundwater of varying density ϱ. Fresh water with density ϱ_o assumed in the piezometers; $v_{1,2}$ = Darcy-velocity, μ = salt-water viscosity, μ_o = fresh-water viscosity.

Figure 5

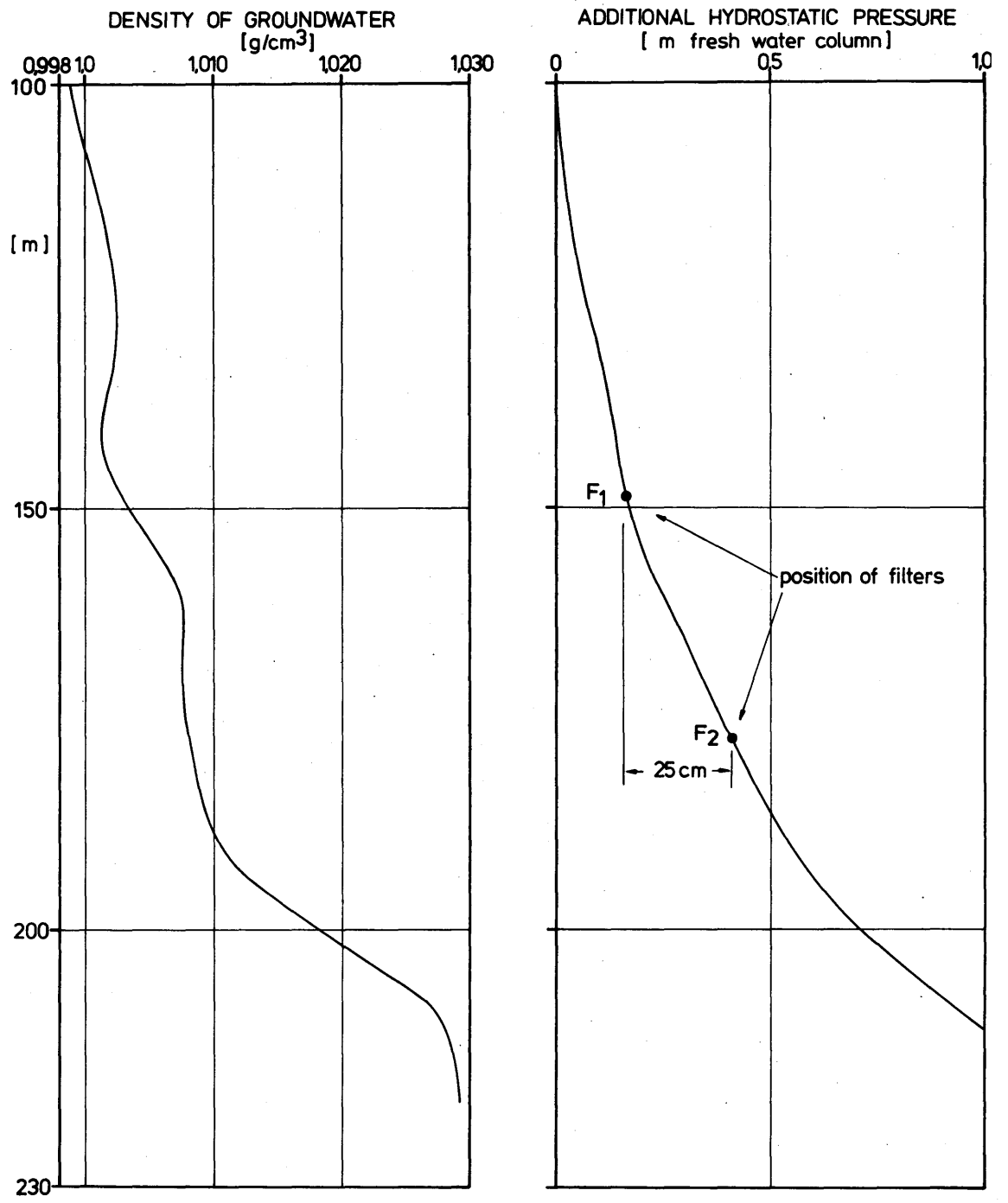

Figure 6 **Computed logs of water density and excess hydrostatic pressure. F_1 and F_2 are filter positions of two boreholes.**

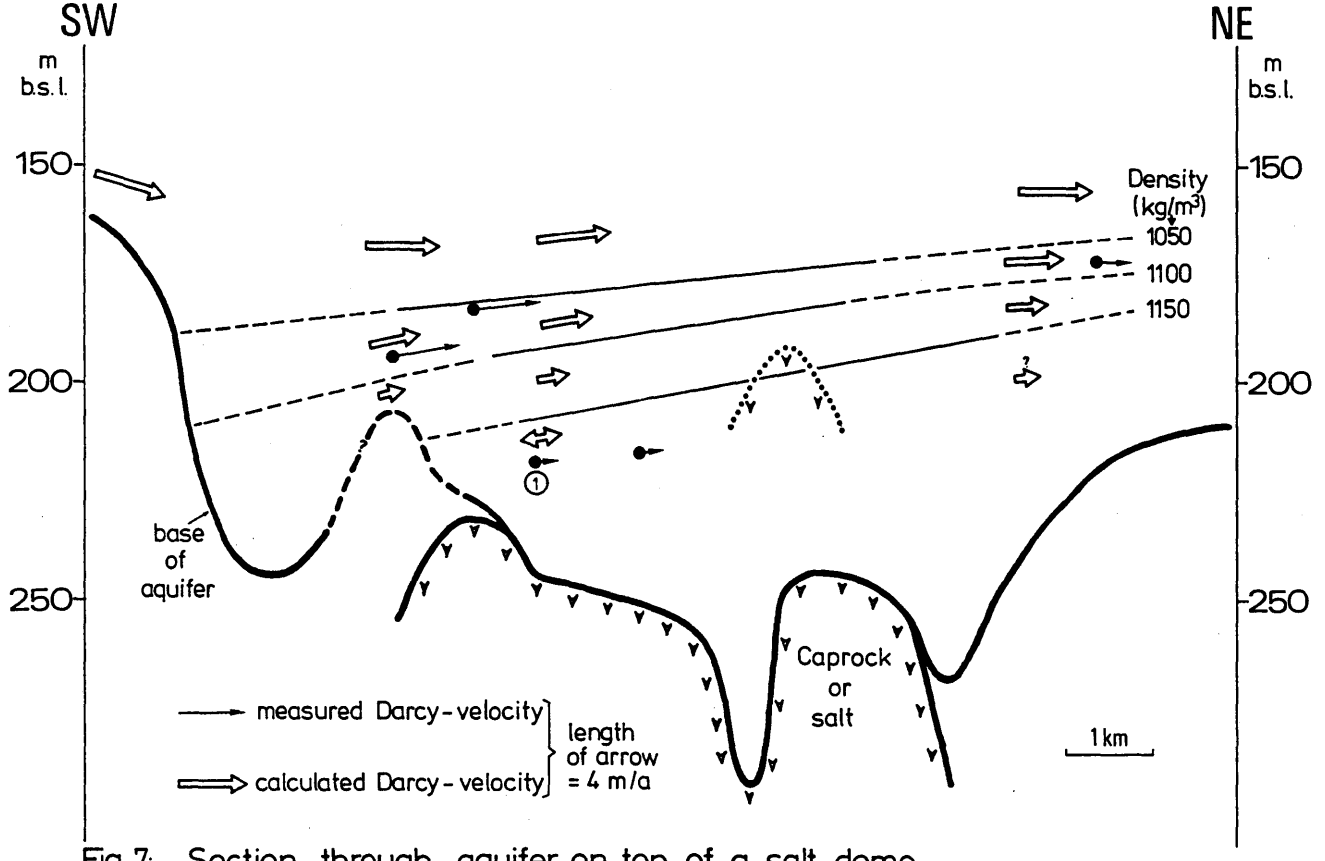

Fig. 7: Section through aquifer on top of a salt dome, density and velocity of saline groundwater

Figure 7

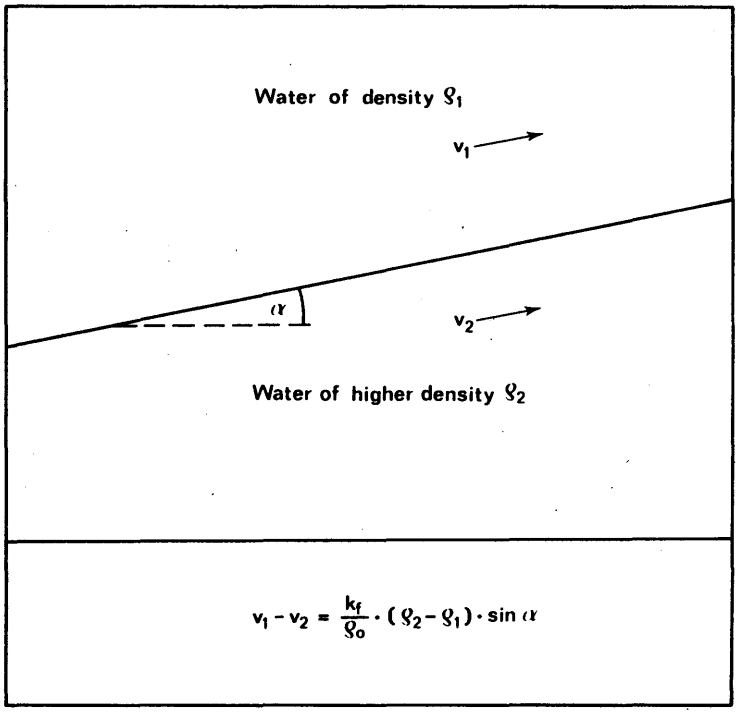

: Velocity discontinuity at an interface between waters of different density

Figure 8

6.4. HYDROGEOLOGICAL AND GEOPHYSICAL INVESTIGATIONS FOR EVALUATING SALT-INTRUSION PHENOMENA IN SARDINIA

G. BARBIERI, G. BARROCU & G. RANIERI

ABSTRACT

In the region of Muravera, south-east coast of Sardinia, the trend of salt-intrusion phenomena has been studied for more than two years through systematic hydrogeological, hydrochemical and geophysical investigations. Water level and chlorine content measurements have been compared with the results of resistivity and induced-polarization (I.P.) vertical soundings. In particular, a close relationship has been established between salinity, resistivity and recharge potential and as a result the extent and depth of the fresh-, brackish- and salt-water bodies have been defined in extent detail.

1. INTRODUCTION

A systematic geophysical investigation has been carried out, involving resistivity and chargeability soundings, in order to verify the evolution of sea-intrusion phenomena already studied in the delta plain of the river Flumendosa on the south-east coast of Sardinia (BARBIERI et al., 1984). The object of the investigation was to integrate existing information on the coastal plain of the river Flumendosa, with particular regard to stratigraphy.

The geophysical survey was designed to check the reliability of geoelectrical methods used in studying salt-intrusion phenomena by comparing results with data obtained from hydrogeological observations.

2. GEOLOGY

The geological formations of the coastal plain shown in fig. 1 are, from top to bottom:

- eolian deposits and coastal dunes,
- recent alluvium, mostly sandy with layers of gravel, silt and clay (Holocene),
- terraced alluvial deposits well-cemented with Paleozoic silty, sandy gravels and ancient alluvial fans, now inactive, bordering the slopes of the Paleozoic schist and granite hills to the west of the plain (Pliocene-Pleistocene),
- granite and schisty sandstone bedrock (Paleozoic).

No wells have been drilled down to the bedrock. The thickness of the overlying alluvium is presumed to be more than 100 m at least in the central plain.

3. HYDROGEOLOGY

The plain is crossed by the river Flumendosa and its former outlets, now inactive. Up to a few years ago, before the river was dammed upstream, these outlets drained a surface aquifer recharged by frequent devastating floods.

Two main aquifers have been identified in the delta plain. A phreatic aquifer, with a water table a few metres below the surface level, has been studied by direct observations via a network of 30 productive wells excavated down to a depth of 4 - 5 m. They are representative of more than 300 wells surveyed throughout the plain.
The contour lines in fig. 2 a represent the water table in March 1984, after recharging by winter rainfall and before overpumping for irrigation began.

The contour lines in fig. 2 b clearly show the water table drawdown below sea level in areas of citrus groves in July 1984, when the natural recharge was nil and water demand for irrigation was at its peak. At that time, as indicated by the flow lines, wells were draining water from the beds of the river Flumendosa and its former outlets, in direct connection with the sea.

The recent alluvium is highly permeable. Transmissivity and storativity have been calculated, using the Theis, Jacob and Chow methods, as $2,4 \times 10^{-4}$ - $4,2 \times 10^{-3}$ m^2/s and S = 0,13 respectively. Yields are strongly affected by well characteristics, and range from as little as 3 up to 200 l/sec.

Hydrochemical analysis of water samples from the wells revealed the salt content in the surface groundwater in the coastal zone. Isochlore contour lines in fig. 3 a and 3 b indicate the trend of salt intrusion from June 1983 to October 1985.

The underlying confined aquifer is exploited by only a few boreholes drilled upstream from the plain down to depths of 50 m for drinking-water supply. A maximum yield of 30 l/sec has been measured with transmissivity $T = 1,3 \times 10^{-2}$ m^2/sec and storativity S = 0,48.

4. GEOPHYSICAL INVESTIGATIONS

For the purpose of defining the shape and size of the salt-intrusion wedge, a resistivity and IP survey was carried out via 26 Schlumberger soundings using an Austral Y842 transmitter, a Scintrex IPR 10 receiver and an 8 Hp generator for the field survey. Steel stakes and copper-copper sulphate porous pots were used as current and potential electrodes respectively and the charging-discharging time was fixed at 4 seconds.

Measurements were repeated in June 1983 and October 1985, before and after heavy rainfall, in order to study relationships between phreatic groundwater and resistivity or chargeability.

A resistivity map of the water table at 3 m below the surface for 1983 is given in fig. 4 a. Low-resistivity values (< 2 Ohm·m) have been observed near the mouth of the river Flumendosa. Furthermore, a marked inflexion of the isoresistivity lines along the former outlets of the river Flumendosa delineates critical areas where brackish-water intrusion had been detected with direct hydrogeological observations.
The area delineated by the 5 Ohm·m resistivity line protrudes even further inland along the former outlets.

I.P. methods have been used for a long time in groundwater investigations as reported, among others, by VACQUIER et al. (1957), BODMER et al. (1968), OGILIVY & KUZMINA (1972) and PATELLA (1973). According to ROY & ELLIOT (1980), salt and fresh water may be distinguished through combined chargeability and resistivity measures.

In the Flumendosa delta plain vertical resistivity soundings have been integrated with chargeability measurements repeated in June 1983 and October 1985. Figs. 5 and 6 show the apparent chargeability map for AB/2 = 5 m and AB/2 = 45 m. These values may be referred to the phreatic and the confined aquifer respectively.

The relationship between true resistivity calculated at 3 m below the surface and the salinity of water samples collected at the same depth is shown in fig. 7 a. The relationship is linear up to a resistivity of 50 Ohm·m and negative exponential for higher values. The maximum permissible salt contents for drinking-water and citrus-grove irrigation water are also indicated in order that the resistivity maps might provide pointers for optimum development of soil and water resources. Peak resistivity was observed near a canal excavated to protect the town of Muravera from floods and to drain the area.

A salinity-chargeability relationship has been obtained using the apparent chargeability values calculated with AB/2 = 5 m, that, in the case at hand, refers to a layer about 3 m deep. The relationship is non-linear with negative values for $[Cl]^-$ > 1080 mg/l and maximum values coincide with low concentrations (fig. 7 b). A relative maximum is given for contents of $[Cl]^-$ at 500 - 1000 mg/l.

This result does not appear to entirely agree with the findings of ROY & ELLIOT (1980) who claim that salty-water zones are identified by a simultaneous decrease in resistivity and chargeability. In reality the discrepancy is only apparent and can probably be put down to the variability of the salinity-chargeability relationship which is strongly affected not only by groundwater salt content but also by the lithology of the aquifer. The relationship found allows one to distinguish zones with different salinity. Negative and positive zones show areas with salt and fresh water respectively.
The evolution of the salt-intrusion phenomenon with time and depth is clearly evidenced in figs. 5 and 6.

The electrostratigraphic sections constructed from the resistivity data are given in fig. 8. Sections A, B and C are parallel and section D perpendicular to the

coastline. Different layers have been interpreted by extrapolating to depth the relationships between chlorine content and resistivity or apparent chargeability.

5. CONCLUSIONS

The relationship between salinity and resistivity or chargeability has been studied on the basis of the results of hydrogeological and hydrochemical investigations. In the case under study the areas of higher salinity are characterized by low resistivity and negative I.P.

The correlation found for the phreatic aquifer has been extrapolated to depth. In this way the stratigraphy of the region has been defined as well as the spatial and temporal development of sea-water intrusion.

REFERENCES

BARBIEREI, G., BARROCU, G., POLEDRINI, C. & URAS, G. (1983). Salt intrusion phenomena in the south east coast of Sardinia. Geol. Appl. Idrogeol. 18, 315-323.

BARBIERI, G. & BARROCU, G. (1984). Consequences of overexploiting coastal aquifers in areas of touristic development in south eastern Sardinia (Italy). 5th International Conference on Water Resources Planning and Management "Water in the year 2000". 1-4 October, 1984. 1-12 (preprints).

BODMER, R., WARD, S.H. & MORRISON, H.F. (1968). Induced electrical polarization and groundwater. Geophys. 33, 805-821.

OGILIVY, A.A. & KUZMINA, E.N. (1972). Hydrogeologic and engineering-geologic possibilities for employing the method of induced potentials. Geophys. 37, 839-861.

PATELLA, D. (1973). A new parameter for the interpretation of induced polarization field prospecting (time-domain). Geophys. Prosp. 21, 315-329.

ROY, K.K. & ELLIOT, H.M. (1980). Resistivity and I.P. survey for delineating saline water and fresh water zones. Geoexpl. 18, 145-162.

VASQUIER, V., HOLMES, C.R., KINTZINGER; R.P. & LAVERGNE; M. (1957). Prospecting for ground water by induced electrical polarization. Geophys. 22, 660-687.

FIGURES

Fig. 1: Geological sketch map of the delta plain of the river Flumendosa. Holocene: 1. sands; 2. loose alluvium; Pliocene-Pleistocene: 3. cemented alluvium; Paleozoic: 4. schisty sandstones.

Fig. 2: Water-table contour lines of phreatic aquifer (cm a.s.l.). a) March 1984; b) July 1984. Observation wells (o).

Fig. 3: Isochlore contour lines of phreatic aquifer (Cl^- mg/l). a) June 1983; b) October 1985. Observation wells (o).

Fig. 4: Resistivity map at depth of 3 m(Ohm·m). V.E.S. centres (.).
a) June 1983; b) October 1985.

Fig. 5: Apparent chargeability map AB/2 = 5 m (mV.s/V) V.E.S. centres (.).
a) June 1983; b) October 1985.

Fig. 6: Apparent chargeability map AB/2 = 45 m (mV.s/V) V.E.S. centres (.).
a) June 1983; b) October 1985.

Fig. 7: a) resistivity-chlorine relationship,
b) apparent chargeability-chlorine relationship.

Fig. 8: Electrostratigraphic and hydrogeological sections.

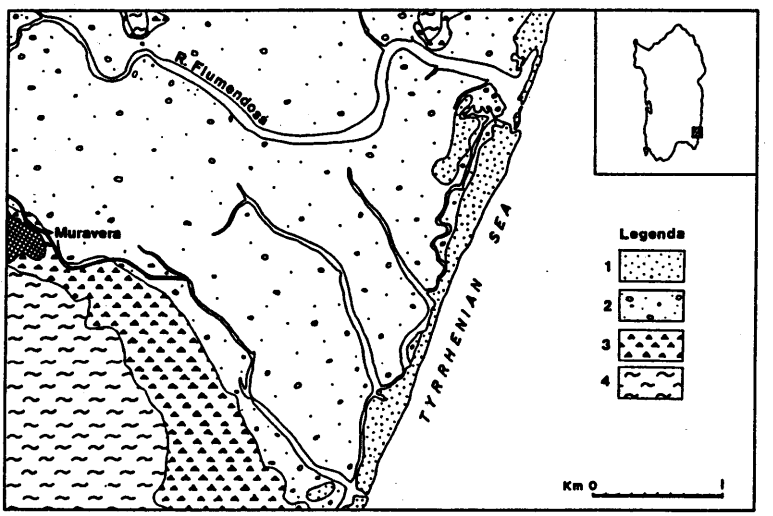

Figure 1

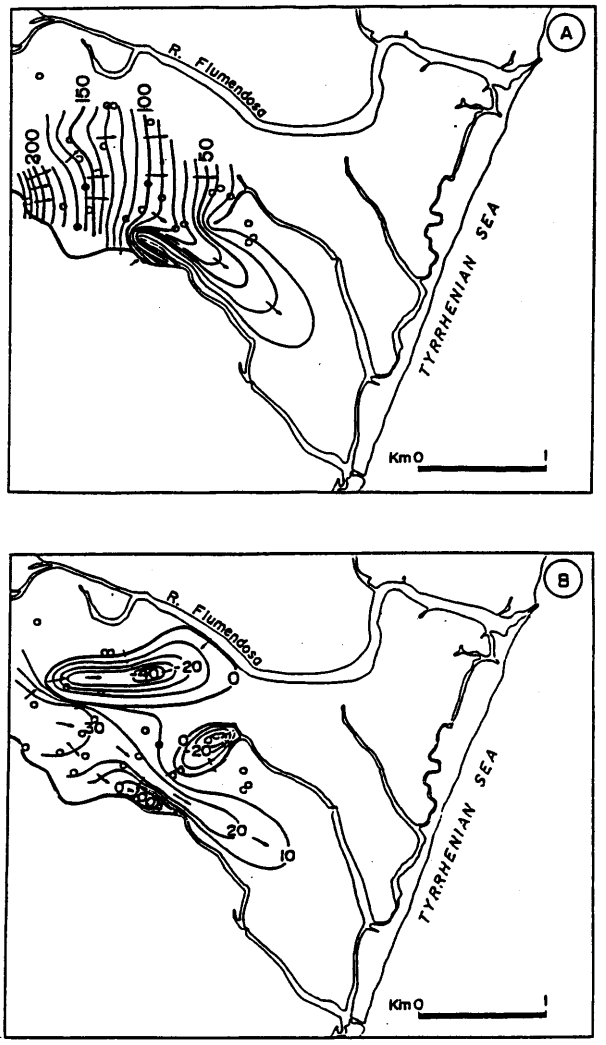
A
R. Flumendosa
200
150
100
50
TYRRHENIAN SEA
Km 0
1
B
R. Flumendosa
30
20
0
10
TYRRHENIAN SEA
Km 0
1

Figure 2

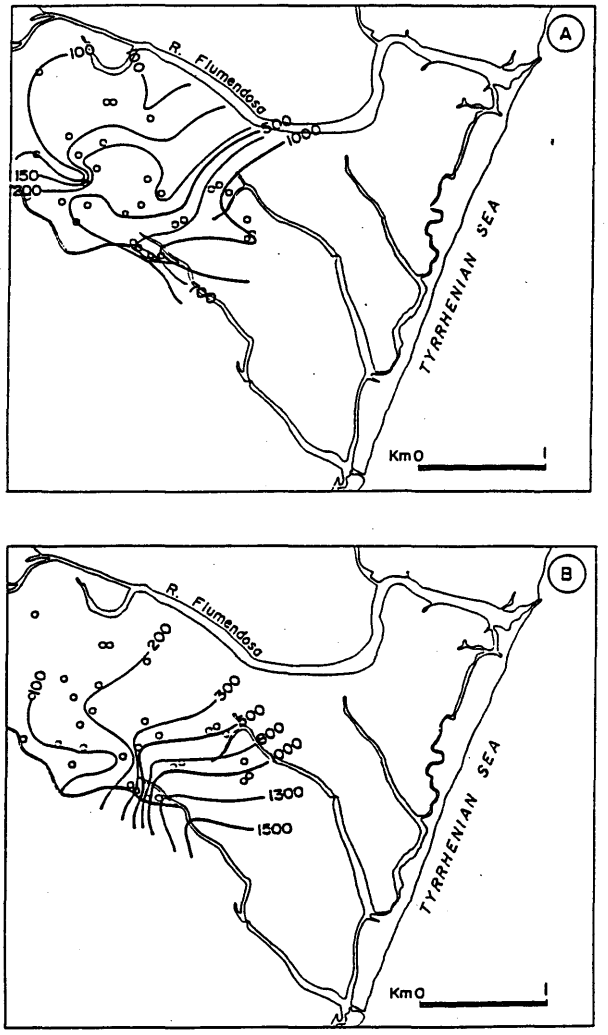
A
R. Flumendosa
100
50
150
200
500
1000
700
TYRRHENIAN SEA
Km 0
1
B
R. Flumendosa
200
300
500
800
900
1000
1300
1500
TYRRHENIAN SEA
Km 0
1

Figure 3

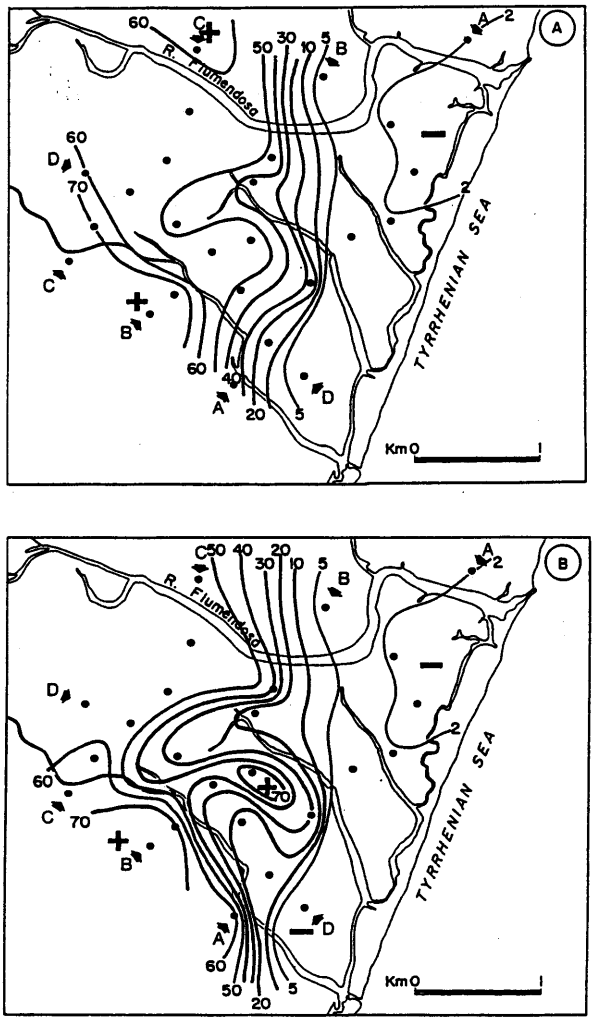

Figure 4

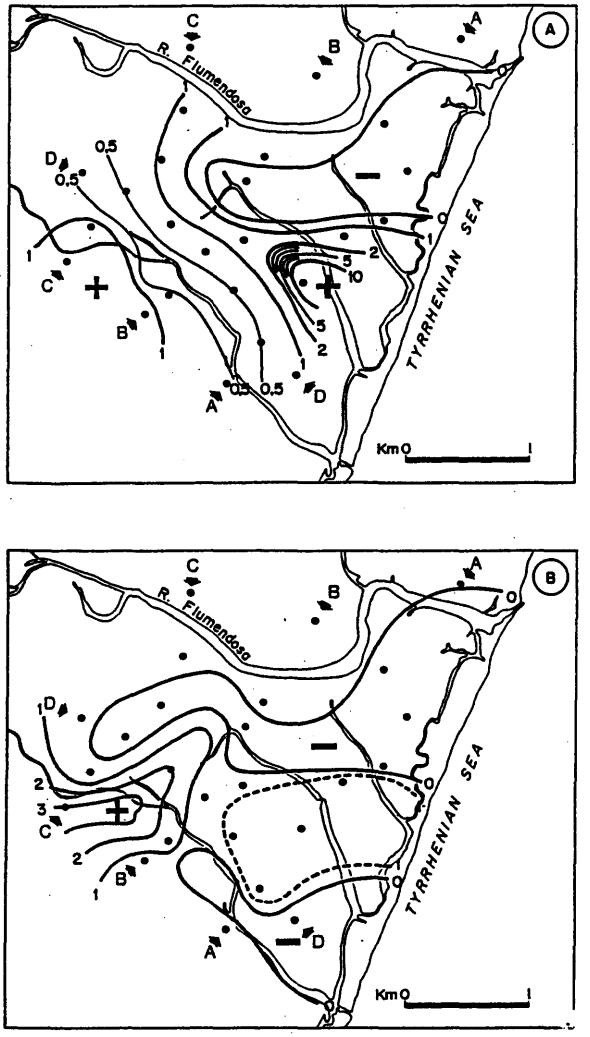

Figure 5

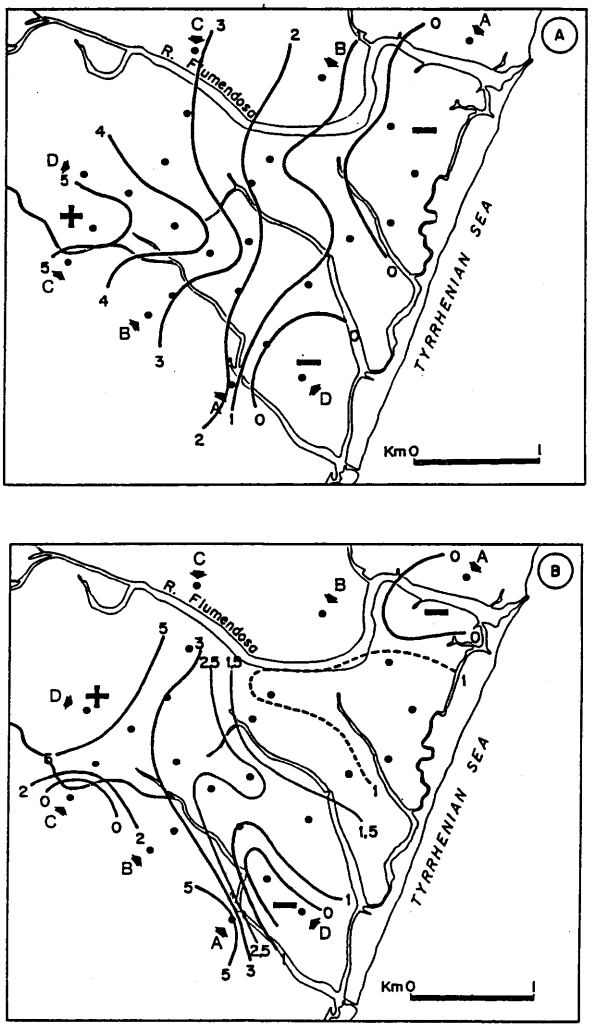
A
R. Flumendosa
TYRRHENIAN SEA
Km 0 1
B
R. Flumendosa
TYRRHENIAN SEA
Km 0 1

Figure 6

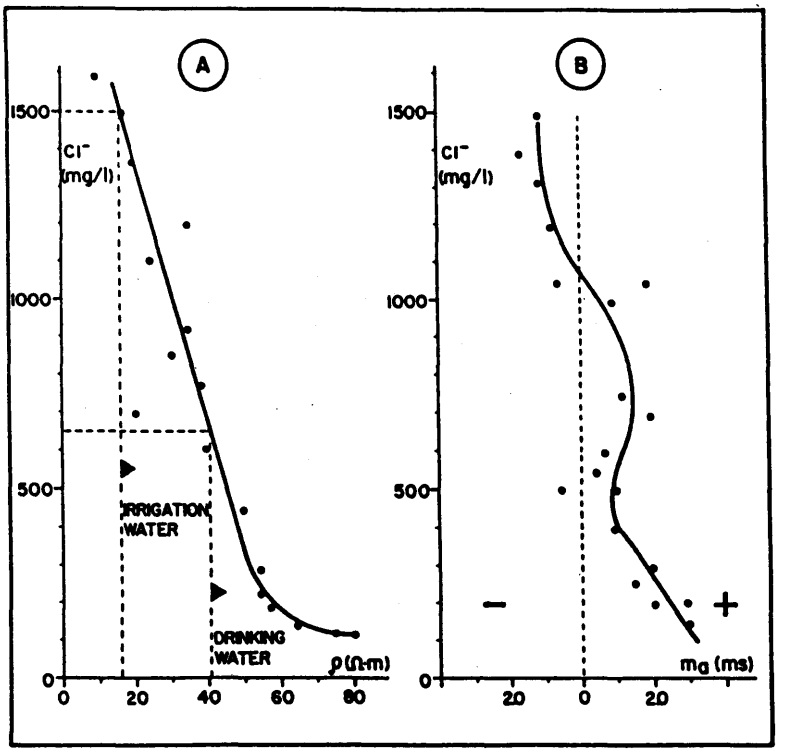
A
B
1500
1000
500
0
Cl⁻
(mg/l)
IRRIGATION
WATER
DRINKING
WATER
ρ(Ω·m)
0
20
40
60
80
mg (ms)
20
0
20
−
+

Figure 7

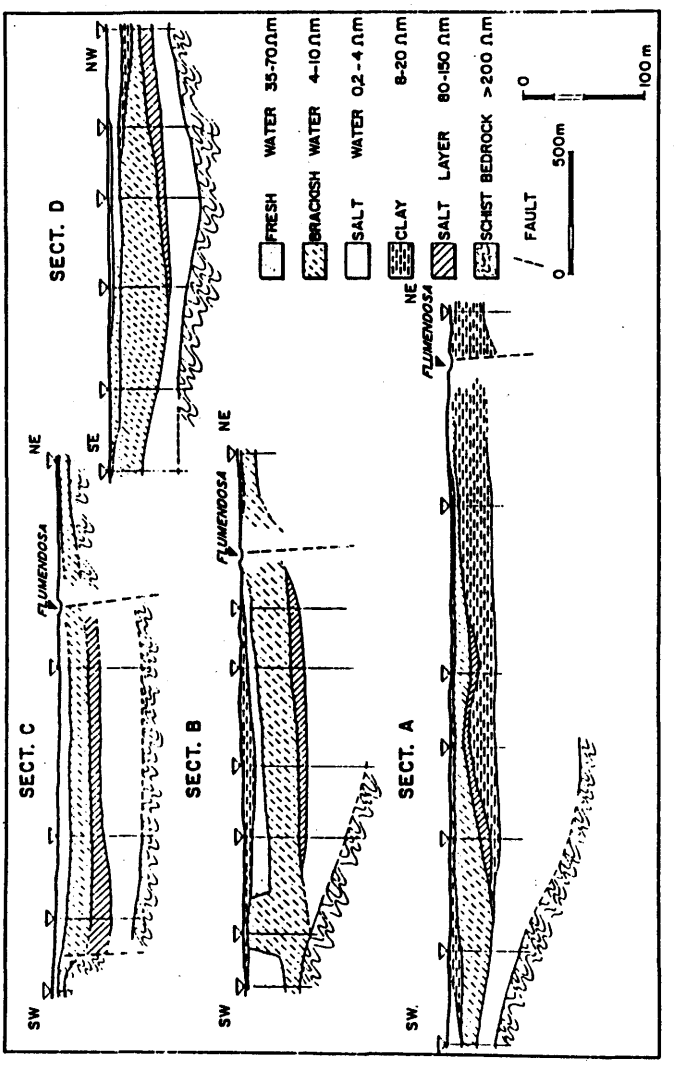
SECT. D
NW
SE
SECT. C
NE
SW
FLUMENDOSA
SECT. B
NE
SW
FLUMENDOSA
SECT. A
NE
SW
FLUMENDOSA
FRESH WATER 35-70 Ωm
BRACKISH WATER 4-10 Ωm
SALT WATER 0.2-4 Ωm
CLAY 8-20 Ωm
SALT LAYER 80-150 Ωm
SCHIST BEDROCK >200 Ωm
FAULT
0
500m
0
100 m

Figure 8

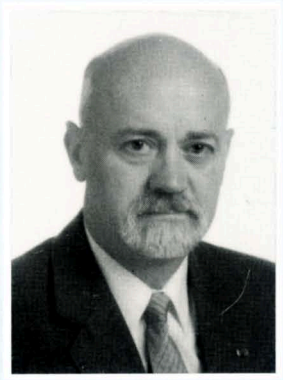

Prof. Dr. W. De Breuck

Although the phenomenon of salt-water intrusion in aquifers is well known the behavious of the interface between salt and fresh water in changing conditions is far more difficult to predict. Changing hydrogeologic conditions can only be understood by thorough field investigations supported by an extensive hydrochemical analysis and mathematical modeling.

Salt-water encroachment is not just a subject for mere scientific study. The description of the phenomenon and the understanding of its evolution in time and space in natural and man-made conditions provide the means to optimize the management of fresh water in coastal asuifers and to safeguard it from depletion and contamination.

In the low countries, especially the Netherlands and the coastal regions of Germany the salinization of aquifers has been recognized as a fundamental problem at the end of the previous century. HERZBERG in Germany and BADON-CHYBEN in the Netherlands were the first to propase the theory on the relationship between fresh and salt water in an aquifer.

In 1968 researchers of the three North Sea countries joined in an informal meeting to exchange investigation results. This meeting was to become the first of a series of biannual symposia, during which scientists interested in this field of hydrologie research exchanged experiences and results. Subsequent salt-water intrusion meetings, shortened SWIM, were to be attended by an ever increasing group of representatives from countries of the North Sea and the Mediterranean Sea. The proceedings of the meetings were available to only a limited number of researchers who attended these meetings.

In 1983 the International Association of Hydrogeologists by creating a commission on coastal aquifers recognized the importance of hydrogeologic research of coastal aquifers. In this context the association thought it to be useful to present a selection of the previous SWIM proceedings to a world wide audience.

ISSN 0936-3912
ISBN 3-922705-92-8

Verlag Heinz Heise GmbH & Co KG, P.O.B. 610407, D-3000 Hannover 61, Germany